Gurbinder Kaur *Editor*

Clinical Applications of Biomaterials

State-of-the-Art Progress, Trends, and Novel Approaches

Springer

Clinical Applications of Biomaterials

Gurbinder Kaur
Editor

Clinical Applications of Biomaterials

State-of-the-Art Progress, Trends, and Novel Approaches

Springer

Editor
Gurbinder Kaur
School of Physics and Materials Science
Thapar University
Patiala, India

ISBN 978-3-319-56058-8 ISBN 978-3-319-56059-5 (eBook)
DOI 10.1007/978-3-319-56059-5

Library of Congress Control Number: 2017939632

Printed on acid-free paper

This Springer imprint is published by Springer Nature
The registered company is Springer International Publishing AG
The registered company address is: Gewerbestrasse 11, 6330 Cham, Switzerland

A
Dedication to every individual of
My Alma Mater
“Thapar University”
&
“Virginia Tech”
who motivated me to change my
dreams into realities

Acknowledgments

During my journey of book writing, there are many people who have knowingly and unknowingly helped me in the successful completion of this project. At this overwhelming moment of accomplishment, first of all I am indebted to *Dr. O. P. Pandey, Dr. B. Chudasama*, *Dr. Gary Pickrell, Dr. Kulvir Singh,* and *Dr. N. Sriranganathan* whose understanding, encouragement, and personal attention have always provided decisive and energetic support. *Dr. Pandey* was the one who stood by me during my struggling days and is among one of the strongest pillars of my career. Without his support, I would have never been able to accomplish most of the milestones of my career. I have never seen a dedicated and hard working supervisor like *Dr. Chudasama* who can come forward for his students all the time and never leave any stone unturned so as to make them reach the zenith. *Dr. Singh* has given rational freedom to his students so that they can add wings to their imagination. *Dr. Gary Pickrell* and *Dr. N. Sriranganathan* provided the most conducive and comfortable environment to me during my stay in the USA and are superb mentors. I am short of words for all of them as they are an indispensable part of my journey and cannot be amputated. I feel honored to be able to work as a Post-Doc under such talented supervisors who have big souls to accommodate every aspect of their students. Their diligence, persistence, and vitality are highly admirable.

All the faculties and staff of Physics Department (Guru Nanak Dev University), SPMS (Thapar University) and MSE (Virginia Tech, USA) are acknowledged who never turned me down whenever I approached for any help. I cannot forget the very supportive and cordial attitude of *Dr. Manoj Sharma*, HOD, SPMS, who is always ready to help his students. This truly depicts his excellent administrative qualities. I cannot forget the support provided by *Dr. S.S. Sekhon* during the toughest phase of my life. His motivation and zeal for hard work has enlightened my path always. I am so grateful to the UGC, New Delhi, for the financial assistance provided to me [F.15-1/2013-14/PDFWM-2013-14-GE-PUN-14803 (SA-II)] during the course of my work.

A very special thanks to *Dr. John Mauro*, who is a brilliant scientist, a dedicated mentor, extraordinary human being, and a wonderful friend! His perfection and

promptness inspired me to think big. He has always endowed me with the "out of box" thinking.

This book gradually emerged amid the friendships that provided their most lasting lessons. It is a pleasure to mention my good friends especially from *Functional Materials lab* and *Ceramic Research lab,* who made my working atmosphere very conducive.

Finally my most personal source of gratitude is my husband, my true soul mate *Dr. Vishal Kumar* who is my enduring strength. Thanks for erasing the word nightmare from the dictionary of my life. During every downhill of my life, he was the one who lifted up my spirits and helped me in innumerable ways. It is only and only due to him that I could put in lots of working hours tirelessly. Honestly, he sheltered me through every thick and thin situation and took the entire burden off my shoulders. He was full of patience and support during the time when my work schedule became too hectic. This book would not have been possible at all without him. He was more concerned about my important schedules and kept on reminding me about it along with my diet chart!

Dear mom and dad, I have let so many years pass without thanking you both. But you haven't let a single second pass without loving me unconditionally. I am highly thankful to my *parents-in-law and parents* for their support, encouragement, care, understanding, and creation of a pleasant atmosphere for me. Especially my father-in-law *Sh. Surinder Kumar* and my father *Sh. Harbhajan Singh,* the strong pillars of my career who have always motivated me to fly high and change dreams into realities. I am very lucky to have wonderful in-laws' family for whom I am more of a daughter. I doubt that I will ever be able to convey my appreciation fully, but I owe them my eternal gratitude.

Besides this, above all, thanks to the *almighty* beneath the blue sky for bestowing me with his precious blessings! With every passing day, I start believing in you more and more as you have filled my life with wonderful things, which I could never ever think about. Thanks for protecting me, sheltering me, and blessing me in the best ways!

Dr. Gurbinder Kaur

Contents

1 How Did Bioactive Glasses Revolutionize Medical Science? A Tribute to Larry Hench 1
Gurbinder Kaur, John C. Mauro, Vishal Kumar, Gary Pickrell, and Francesco Baino

2 Variation in Properties of Bioactive Glasses After Surface Modification 35
Vojislav Stanić

3 Apatites for Orthopedic Applications 65
Berna Kankilic, Eda Ciftci Dede, Petek Korkusuz, Muharrem Timuçin, and Feza Korkusuz

4 Calcium Phosphate Cements for Medical Applications 91
Fatma Ozdemir, Iain Evans, and Oana Bretcanu

5 Calcium Orthophosphate-Based Bioceramics and Its Clinical Applications 123
Sergey V. Dorozhkin

6 Nanostructured Calcium Phosphates for Drug, Gene, DNA and Protein Delivery and as Anticancer Chemotherapeutic Devices 227
Andy H. Choi, Innocent J. Macha, Sibel Akyol, Sophie Cazalbou, and Besim Ben-Nissan

7 Synthesis and Functionalization of Mesoporous Bioactive Glasses for Drug Delivery 257
F. Branda

8 Bioactive Glass/Polymer Composites for Drug Delivery 287
Telma Zambanini, Roger Borges, and Juliana Marchi

9 Restorative Dental Glass-Ceramics: Current Status and Trends 313
Maziar Montazerian and Edgar Dutra Zanotto

10 Bioactive Glass-Based Composites for Cranioplasty Implants 337
Arnab Mahato and Biswanath Kundu

11 Antibacterial Properties of Bioactive Glasses 357
Muhammad Akram and Rafaqat Hussain

12 Development of URIST™ a Multiphasic rhBMP-2 Bone Graft Substitute 383
Sean A.F. Peel, Aileen J.J. Zhou, Hanje Chen, and Cameron M.L. Clokie

13 Development and In Vitro Analysis of a New Biodegradable PLA/Hydroxyapatite (HAp) Composite for Biomedical Applications 411
Innocent J. Macha, Besim Ben-Nissan, Andy Choi, and Sophie Cazalbou

14 Biomaterials for Cell Encapsulation: Progress Toward Clinical Applications 425
Gurbinder Kaur, Francesco Baino, John C. Mauro, Vishal Kumar, Gary Pickrell, Nammalwar Sriranganathan, and Steven Grant Waldrop

Index 459

Editor Biography

Gurbinder Kaur Dr. Gurbinder Kaur holds her B.Sc. (Hons. Physics) and M.Sc. (Hons. Physics) from Guru Nanak Dev University, Amritsar. She moved to Thapar University, Patiala to pursue her research work in the field of solid oxide fuel cells (SOFC) and received her doctorate in 2012. Her Ph.D. dissertation was based on "Investigations on interfacial interaction of glass sealants with electrolytes and interconnect for solid oxide fuel cells (SOFC)." She has three other books on "Solid Oxide Fuel Cell Components: Interfacial compatibility of SOFC glass seals" (Springer, NY), "Bioactive glasses: potential biomaterials for future therapy"(Springer, Germany) and "Modern Physics" by McGraw Hill Pvt. Ltd. She also carried her research in the field of Biomedical Enginnering and Bioglasses. She is recipient of fellowship under the RFSMS scheme of University Grants Commission (UGC). She also received fellowship under Women-Scientist Scheme, DST, New Delhi from 2010 to 2012. After completing her Doctorate, she moved to Virginia Tech, USA to work as a Post-Doctoral Fellow with Dr. Gary Pickrell. She is a recipient of Post-doc Scholarship from UGC, New Delhi for pursuing research work in the field of bioglasses. She works on a variety of different materials and applications including high temperature energy materials, bioactive materials and optical materials.

Contributors

Muhammad Akram Dr. Muhammad Akram Ch has his Ph.D. in Chemistry under the supervision of Prof. Dr. Rafaqat Hussain from University Teknologi Malaysia. His current research interest focuses on the Continuous Microwave Flow Synthesis and Microwave Assisted Synthesis of nanostructured materials, including biomaterials and photocatalytic materials. His work also involves the study of properties and applications of nanostructured material.

Sibel Akyoll Assoc. Prof. Sibel Akyoll received a Ph.D. in Immunology/ Physiology Sciences (in 2004) cum laude, from the University of Istanbul Cerrahpasa Medical Faculty after her master degree of Immunology (in 1992) and Physiology (in 1995). After a 2 year post-doc at the University of Louisville, Department of Obstetrics, Gynecology & Immunology (2004–2006), she joined the faculty in the Department of Physiology Cerrahpasa Medical Faculty University of Istanbul (Turkey). She established first Cytokines and their receptors Immunology Research Laboratory in University of Istanbul, Cerrahpasa Medical Faculty. She is currently Assoc. Professor and the Group Leader/director of the Immunology Research Laboratory and Departmant of Physiology Cerrahpasa Medical Faculty. Her research interests encompass a wide variety of issue including

properties of biomaterials and implants, reproductıve ımmunology, neurosurgery immunology, haematology, menopause and andropause. She is a fellow of the American Society for Reproductive Immunology(ASRI), The Australasian Society for Immunology(ASI) and Turkish Society of Physiological Sciences. She was awarded 14th Turkish Society of Physiological Sciences in 1996, Second Prize in the Young Researchers and The Society for Free Radical Research in 1999, First Prize in the Young Researchers and 38th National Congress of Physiological Sciences in 2012, Second Prize in the Young Researchers, National BSE-Science-Art Award and the University of Istanbul Scientific Research Award in 2016.

Francesco Baino Francesco Baino is an Assistant Professor in the Department of Applied Science and Technology, Politecnico di Torino (Italy). He received his M.S. in Biomedical Engineering and Ph.D. in Materials Science and Technology from Politecnico di Torino in 2006 and 2010, respectively. Dr. Baino has published more than 70 peer-reviewed journal articles and 10 book chapters, and is author of 4 patents. His current research interests include bioceramics, bioactive glasses and composite biomaterials for tissue engineering and medical implants, as well as processing and testing of advanced ceramics.

Besim Ben-Nissan Prof. Ben-Nissan has MSC degree in Ceramic Engineering and a Ph.D. in Mechanical and Biomedical Engineering, both from UNSW Australia. Over the last three decades, Professor Ben-Nissan has worked and contributed to the biomedical materials and implant design, production and analysis of various advanced ceramics, nanocoated sol-gel developed thin films, biomedical materials orthopaedic and dental implant design, slow drug delivery and finite element analysis of material structures. He has successfully developed materials for implant technology (bioactive materials), bone graft production and bio-composites, and conducted investigative research on biomechanics (jaw bone, knee and hip joints), reliability and implant design (modular zirconia ceramic knee prosthesis, femoral head and taper stresses and bionic eye). He has expertise in zirconia and hydroxyapatite bioceramics, transformations and measurement of micro-mechanical stresses in ceramics and biomaterials. He is involved in consulting work related to various patent litigations in biomaterials and medical devices related to orthopaedic implants. His current research involves calcium

phosphates, nanocoatings, bioactive bone grafts and biomimetics approach in slow drug delivery. Since year 2000 he has published over 190 fully refereed papers in journals, and a book and 35 book chapters. He is the editor of the Journal of the Australasian Ceramic Society. He was awarded by the Australian Ceramic Society a prestigious award for his "sustained contribution to the Ceramics Research & Development and Education in Australia". And his research on hydroxyapatite nanocoatings received "The Future Materials Award".

Roger Borges BSc. Roger Borges has a sandwich degree in Science and Technology received by the Federal University of ABC (Brazil) and the University of Idaho (USA). He is currently a Master of Science student in Nanoscience and Advanced Materials, and member of the Research Group in Functional Biomaterials, Regenerative Medicine, Tissue Engineering and Biotechnology (BioMMR), which is headed by Dr. Marchi. He has experience with biocompatible glasses, mainly those glasses for application in dentine hypersensitivity and treatment of cancer.

F. Branda Francesco Branda is Full Professor of Chemistry at the University "Federico II" of Naples. The initial research activity was in the synthesis and physicochemical characterization of glasses and glass-ceramics produced through melt-quenching or sol-gel route when he got a large experience on bioactive glasses. More recently he is applying his experience in sol-gel chemistry to the synthesis of functionalized mesoporous particles and in-situ preparation of hybrid and nanostructured composites.

Oana Bretcanu Dr. Oana Bretcanu is a lecturer in Biomaterials at the School of Mechanical and Systems Engineering of Newcastle University, UK. Her research is focused on synthesis and characterisation of advanced ceramics, glass-ceramics and composites for bone and cartilage tissue engineering, surface functionalisation and drug delivery systems. She is currently involved in a variety of research projects related to magnetic biomaterials.

Sophie Cazalbou Her research activities mainly concern the formulation, shaping and characterization of new bioactive biomaterials (mainly used as bone substitutes), capable of releasing in vivo active substances (ions, molecules, proteins)

She is currently interested in developing new minerals and composite biomaterials in supercritical CO2. This process of "green chemistry" opens new perspectives in the synthesis and development of highly reactive ceramic with controlled architecture. She is working on the following areas:

Formulation of Biologically active biomaterials (coatings, ceramics, cements, composites ...)

Formulation of biomaterials used as delivery systems for active substances (antibiotics, anti-inflammatories, growth factors, biologically active ions, bisphosphonates ...),

Influence of microstructure on the properties of transport through the pore space (transport of active species, biological fluids and cells)

Theory of percolation used as preformulation element.

Hanje Chen Hanje Chen obtained his M.Sc. from Brock University and has spent over 25 years working in regenerative medicine. Prior to starting his own company, ViaBiotech (China), Hanje was a scientist at Induce Biologics.

Andy H. Choi Dr. Andy Choi is an early career researcher who received his Ph.D. from the University of Technology Sydney (UTS) in Australia in 2004 on the use of computer modelling and simulation known as finite element analysis (FEA) to examine the biomechanical behavior of implants installed into a human mandible. After completing his Ph.D., he expanded his research focus from FEA to sol-gel synthesis of multifunctional calcium phosphate nano coatings and nano composite coatings for dental and biomedical applications. In late 2010, Dr. Choi was successfully awarded the internationally competitive Endeavour Australia Cheung Kong Research Fellowship Award and undertook post-doctoral training at the Faculty of Dentistry of the University of Hong Kong, focusing on the application of FEA in dentistry and the development of calcium phosphate nano-bioceramics. He served as an Editorial Board Member for Oral Health and Dentistry (OHDE), Austin Journal of Dental Applications (ISSN: 2381–9049), Journal of Dental and Oral Health (ISSN: 2369–4475), JSM Dental Surgery, Dentistry and Oral Medicine, Remedy Open Access Journal, and SciTz Dentistry: Research & Therapy.

Cameron M.L. Clokie Cameron Clokie received his DDS and Ph.D. from McGill University. He practiced as an oral and maxillofacial surgeon for more than 30 years, including a term serving as Professor and Head of Oral and Maxillofacial Surgery at the University of Toronto.

In 2008 Sean Peel and Cameron Clokie founded Induce Biologics, where Sean serves as the Chief Scientific Officer and Cameron serves as the Chief Executive Officer and clinical advisor.

Eda Çiftci Dede Eda Çiftci Dede is a biologist who has M.Sc. degree from the department of Nanotechnology and Nanomedicine at Hacettepe University.

Sergey V. Dorozhkin Sergey V. Dorozhkin received his MSc in chemical engineering with honors in 1984 from Moscow Institute of Chemical Technology, Moscow, Russia, and his Ph.D. in chemistry in 1992 from the Research Institute of Fertilizers, Moscow, Russia. From 1992 to 1994 he worked as a senior researcher at the same institute, and from 1994 to 1996 he worked as a biotechnologist at a Swiss-Russia joint venture. From 1996 to 2004 he held five postdoctoral positions in France, Portugal, Germany and Canada where he worked on various aspects of calcium orthophosphates. Dr. Sergey V. Dorozhkin has authored more than 70 research papers, about 20 reviews, 15 book chapters and three monographs.

Iain Evans Dr. Iain Evans is a senior lecturer in the School of Mechanical and Systems Engineering at Newcastle University, UK, having previously worked extensively in industry. His current research involves mechanical characterisation of biomaterials for bone and dental implants and the development of reliable and reproducible testing methods for mechanical, electrical and thermal properties of biomaterials.

Rafaqat Hussain Dr. Rafaqat is currently working as a professor in the Department of Physics at the COMSATS Institute of Information Technology. His research focuses on synthesizing novel bio-ceramic materials for orthopedic applications. Special attention is paid to parting unique properties such as antibacterial, magnetic and special optical properties to bioceramics to make them more versatile.

Berna Kankiliç Berna Kankılıç is a biomedical engineer who has M.Sc. and Ph.D. degrees from department of Biotechnology at Middle East Technical University.

Feza Korkusuz Feza Korkusuz is an Orthopedist M.D. Professor at the department of Sport Medicine at Medical School, Hacettepe University.

Petek Korkusuz Petek Korkusuz is a Professor in the department of Histology and Embryology at Medical School, Hacettepe University.

Vishal Kumar Dr. Vishal Kumar completed his M.Tech. (Materials Science and Engineering) from Thapar University, Patiala in 2007. He was awarded his Ph.D. in 2010 on the topic" Study of SiO_2- B_2O_3 based glasses and glass ceramics as sealants". He has been granted scholarships by funding agencies like CSIR and DST, New Delhi to pursue his research work. He was awarded Fulbright fellowship by USIEF to pursue his research on glasses with Dr. Kathy Lu in Virginia Tech, Blacksburg, USA. His objective was "Study and development of materials for increasing the power generation efficiency of Solid Oxide Fuel Cells (SOFC)".

Biswanath Kundu Dr. Biswanath Kundu is presently working as Scientist at CSIR-Central Glass and Ceramic Research Institute, Kolkata, India. His research area covers the fields of biomedical materials, their characterization, coating on medical implants, scaffolds, granules, drug delivery systems, etc. He has published more than 40 SCI papers with 5 book chapters and 2 patents in his credit. He is also the recipient of many prestigious awards of India.

Innocent J. Macha Dr. Innocent Macha has over 10 years experience in teaching and research in the area of engineering materials, biomaterials, drug delivery implants and thin film. His thrust for multidisciplinary research has made him shift fields from polymer chemistry to materials and medical technology. In his Ph.D., Dr. Macha specifically involved in using bioresorbable composite materials (PLA, Bioglass, β-TCP, HAp) and coating technology to deliver and control the drugs release. He is the author of 12 articles, 3 book chapters and 3 conference papers.

Arnab Mahato Mr. Arnab Mahato is presently a Ph.D. scholar at CSIR-Central Glass and Ceramic Research Institute, Kolkata, India, and is actively doing his research on the development and characterization of different inorganic bio-composite materials suitable for cranioplasty reconstruction. He has published many articles on bioactive glass based materials with different biomedical applications.

Juliana Marchi Prof. Dr. Juliana Marchi is a Materials Engineer and Associate Professor in the Centre for Humanities and Natural Sciences at the Federal University of ABC (UFABC, Brazil). She is Ph.D. in Nuclear Technology (University of Sao Paulo, Brazil), and has been working with biomaterials since her Post-Doc studies in calcium phosphates bioceramics at the University of Erlangen-Nurnberg (Germany). Dr. Marchi is also a Researcher Professor in the Graduate Program in Nanoscience and Advanced Materials, besides being Associate Researcher in the Biomaterials Research Group at the Nuclear and Energy Research Institute (IPEN, Brazil), and an active member of the Brazilian Ceramic Society. Dr. Marchi has a wide experience in materials science and engineering (processing and characterization of materials), as well as the development of biomaterials aiming different applications, such as bone and cartilaginous tissue regeneration, dentine hypersensitivity and treatment of cancer. She is the head of the Research Group in Functional Biomaterials, Regenerative Medicine, Tissue Engineering and Biotechnology (BioMMR).

John C. Mauro John C. Mauro is Senior Research Manager—Glass Research at Corning Incorporated. John earned a B.S. in Glass Engineering Science (2001), B.A. in Computer Science (2001), and Ph.D. in Glass Science (2006), all from Alfred University. He joined Corning Incorporated in 1999 and is currently a world-recognized expert in fundamental and applied glass science, statistical mechanics, computational and condensed matter physics, thermodynamics, and the physics of topologically disordered networks. John is a Fellow of the American Ceramic Society and has received numerous awards for his research. John is the author of over 165 peer-reviewed publications and has 60 U.S. patent applications, including 20 granted patents.

Maziar Montazerian Maziar Montazerian received his Ph.D. degree in Materials Science and Engineering from Iran University of Science and Technology in 2015. He is currently a post-doctoral fellow at Centre for Research, Technology and Education in Vitreous Materials (CeRTEV), Federal University of São Carlos (UFSCar), Brazil. He intends to develop novel bioactive glasses/glass-ceramics for biomedical applications. His research work also encompasses rigorous tests, improvement or development of nucleation and growth models for glasses. He has published seven refereed articles, three review papers, one book chapter and eight international conference papers.

Fatma Ozdemir Fatma Ozdemir graduated in Genetics and Bioengineering from Yeditepe University Istanbul, Turkey and completed her MSc in Biomedical Engineering at the School of Mechanical and Systems Engineering at Newcastle University, UK. She is currently a Ph.D. student working on the development of bone cements for orthopaedic applications.

Sean A.F. Peel Sean Peel received his Ph.D. from the University of Toronto and has spent 20 years working in innovative companies developing tissue regeneration products.

Gary Pickrell Gary Pickrell is Professor, Department of Materials Science and Engineering, and the Rolls Royce Professor of Surface Engineering and Sensor Instrumentation. He is also the Director of the Nano-Bio Materials Laboratory at Virginia Tech, and the Associate Director of the Center for Photonics Technology in the Electrical and Computer Engineering Department, the largest academic fiber optic sensor research group dedicated to applications of sensors in harsh industrial environments. He also serves as the VT Director of Surface Engineering for the Commonwealth Center for Advanced Manufacturing, a partnership including Rolls Royce, Siemens, Canon, Sulzer Metco, Aerojet, Chromalloy, Newport News Shipbuilding, Virginia Tech, UVA, VSU, and the State of Virginia, among others.

His current research is focused on surface engineering, plasma spray coatings, random-hole optical fibers and optical fiber sensors, nanomedicine, nanotechnology, nanobiotechnology, glass, ceramic, and various other aspects of Materials Science and Engineering. Industrially, he has worked on the development of ceramic matrix and metal matrix porous infiltration preforms for 3–3 composite manufacturing.

Nammalwar Sriranganathan Dr. Sriranganathan is the Professor of Microbiology Virginia Maryland College of Veterinary Medicine, Virginia Tech, Blacksburg.

The goal of his research is to improve the bioavailability of poorly water-soluble therapeutic agents including peptide nucleic acid (PNAs), by use of the novel concept of amorphous nanoparticles for the treatment of disease caused by intracellular pathogens. His long-term research effort has been focused on the development of vaccines against brucellosis in animals and humans. The current USDA approved vaccine against bovine brucellosis, *B. abortus RB51,* was developed in our laboratories. As the Faculty-in-Charge of CDC approved Biosafety level-3 laboratory during 2000 through 2010, he was responsible for training new faculty and graduate students involved in research with Bioterrorism agents like *Brucella abortus*, *B. melitensis, B. suis*, *Yersinia pestis*, *Francisella thularensis*, and *Burkholderia mallei*. He has extensive experience building and actively participating in interdisciplinary teams from within as well as between Universities. He was the Director of an Animal Challenge core of a highly successful NIH Program Project grant of Dr. Mizel from Wake Forest University 2004–2009.

Vojislav Stanić Vojislav Stanić was born in Banja Luka, Yugoslavia. He graduated at Faculty of Chemistry, University in Belgrade, Serbia. He received his Ph.D. degree in technology from the Faculty of Technology and Metallurgy, University of Belgrade. He has worked at the Vinca Institute of Nuclear Sciences, University of Belgrade.

Muharrem Timuçin Muharrem Timuçin is a Professor in the department of Metallurgical and Materials Engineering at Middle East Technical University.

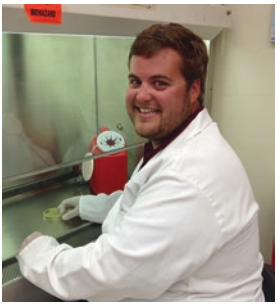

Steven Grant Waldrop Steven Grant Waldrop is a native of South Carolina and obtained his Bachelor's of Science from Ferrum College, where he majored in Biology and Pre-Professional Sciences with a Chemistry minor. He was also a graduating member of the Boone Honor's Society, along with many other prestigious accolades. Steven now is attending the Virginia-Maryland College of Veterinary Medicine at Virginia Tech in Blacksburg, Virginia. He is a member of the Biomedical and Veterinary Science's dual degree program, where he is working towards his Ph.D. in infectious diseases and immunology, along with his Doctorate of Veterinary Medicine. With many years of experience in both the fields of microbiology and veterinary medicine, Steven Grant Waldrop plans to follow a government career combining the two fields after the completion of his degrees in 2022.

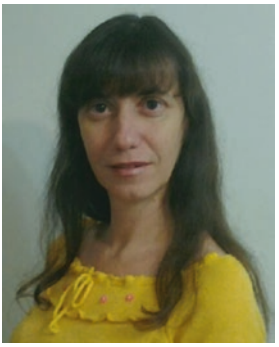

Telma Zambanini M.Sc. Telma Zambanini is a Speech Therapist graduated at the Federal University of the State of Sao Paulo (UNIFESP, Brazil) and Biomedical Engineer graduated at the Federal University of ABC (UFABC, Brazil). She pursues a Master Degree in Nanoscience and Advanced Materials received by the UFABC, and is a current Ph.D. student in the same graduate program. M.Sc. Zambanini has experience with computational simulation of materials, and is currently working on a project for development of hybrid systems (hydrogels + biocompatible glasses) for treatment of cancer. She is also member of the Research Group in Functional Biomaterials, Regenerative Medicine, Tissue Engineering and Biotechnology (BioMMR), which is headed by Dr. Marchi.

Edgar Dutra Zanotto Edgar D. Zanotto is a Professor of Materials Science and Engineering and Director of the Center for Research, Technology and Education in Vitreous Materials (CeRTEV - www.certev.ufscar.br) at the Federal University of São Carlos, Brazil. His main research interests refer to dynamic processes in inorganic glass-forming liquids (diffusion, viscous flow, crystal nucleation and growth, crystallization and glass-forming ability). He has been working for 40 years in this field. He is an editor of the Journal of Non-Crystalline Solids, and member of both Brazilian and São Paulo State Academy of Sciences, National Academy of Engineering, The World Academy of Sciences, World Academy of Ceramics, and Fellow of the Society of Glass Tech and American Ceramic Society.

Aileen J.J. Zhou Aileen Zhou obtained her Ph.D., under the supervision of Drs Peel and Clokie, at the University of Toronto in 2014. After graduating, Aileen joined Induce Biologics as a Regulatory Scientist.

Chapter 1
How Did Bioactive Glasses Revolutionize Medical Science? A Tribute to Larry Hench

Gurbinder Kaur, John C. Mauro, Vishal Kumar, Gary Pickrell, and Francesco Baino

Abstract Biomaterials influence human lives through their versatile medical applications and very promising future. A large number of pharmaceutical firms and manufacturing companies are investing in the production, development, and commercialization of new biomaterial products. The biomaterials industry is a large contributor to the overall market for medical technology, resulting in approximately $42 billion in annual sales with an anticipated growth rate of ~15–18% over the succeeding years. The rapid growth of this large industry is a direct result of its positive influence on the quality of human life. Biomaterials have already opened a large range of medical devices for the skin, bone and dental repair, artificial arteries, limb replacements, nerve guidance tubes, mechanical heart valves, stents, and pacemakers, all of which can increase the quality and length of life for people around the globe. Bioactive glasses are excellent examples of biomaterials for clinical applications owing to their high biocompatibility, bioactivity, and flexibility in compositional design and properties. The invention of Bioglass® by Prof. Larry Hench magnificently revolutionized the medical industry. Following this breakthrough, many research groups have actively engaged in developing different bioactive glasses and implementing them for scaffold generation, tissue engineering, ophthalmology, cranioplasty implants, angiogenesis, wound healing, and cardiovascular applications. The present chapter focuses on the various applications of bioactive

G. Kaur (✉)
School of Physics and Materials Science, Thapar University, Patiala, India
e-mail: gkapds@gmail.com

J.C. Mauro
Science and Technology Division, Corning Incorporated, Corning, New York 14831, USA

V. Kumar
Sri Guru Granth Sahib World University, FatehGarh Sahib, Punjab, India

G. Pickrell
Department of Material Science and Engineering, Holden Hall, Virginia Polytechnic Institute and State University, Blacksburg, VA 24060, USA

F. Baino
Institute of Materials Physics and Engineering, Applied Science and Technology Department (DISAT), Politecnico di Torino, Corso Duca degli Abruzzi 24, 10129 Torino, Italy

G. Kaur (ed.), *Clinical Applications of Biomaterials*,
DOI 10.1007/978-3-319-56059-5_1

glasses in medicine and is dedicated to the founder of this research field, Prof. Larry Hench (Prof. Larry Hench passed away on December 16, 2015, in Florida (USA), after spending his life for biomaterials research), who carried key invaluable contributions to biomaterials science and industry. The trails set by him will always be guiding researchers in this field.

Keywords Bioactive Glass • Porous Scaffolds • Dental Materials • Ophthalmology • Bone Tissue Repair • Angiogenesis • Wound Healing

1.1 Introduction

Biomaterials have been an indispensable component of various applications in cardiovascular stents/valves, wound healing, cranioplasty implants, dental restorations, orthopedics, and tissue engineering applications [1–6]. Over the past several decades, biomaterials have been the object of intensive research and development by scientists in both industry and academia. Biomaterials have unique properties, such as bioactivity, tissue-like mechanical properties, osteoinduction/osteogenesis/osteoconduction capability, cytocompatibility, and/or biodegradation [7–11]. In the 1960s, the first generation of biomaterials was established with the main aim of obtaining a blend of chemical and physical properties to match those of the host tissue as closely as possible, thereby yielding minimal or no cytotoxic response [12–15]. The main dictum followed for designing first-generation biomaterials was "inertness," in the attempt to avoid any foreign body reaction or biological rejection. Molecular biology, which took the first steps in the 1970s, carried a great contribution to the areas of biomaterials and biomedical engineering, especially when combined with the advancing fields of genomics and proteomics. During the 1980s and 1990s, the focus of research moved toward the development of bioactive materials that could stimulate suitable biological response, especially at the biomaterial/host tissue interface. The last 10 years have been an innovative period for the development of biomaterials as the progress of molecular biology has laid a strong foundation for understanding concepts such as degradation kinetics, biocompatibility, and synthesis techniques. This research has brought unprecedented understanding of biomimetic and smart biomaterials, which can simulate nature's hierarchical structures.

Bioactive glasses and ceramics are especially promising materials for clinical applications due to their high biocompatibility, bioactivity, and flexibility of compositions and properties. In 1969, Larry Hench invented the first bioactive glass known as Bioglass® 45S5 [16–18], which was FDA-approved and commercialized for clinical use since the 1980s. Bioceramics are typically characterized by a polycrystalline or noncrystalline (in the case of glass) microstructure, possess high hardness and brittleness, and often exhibit elastic moduli comparable to that of human bone. Crystalline ceramics like ZrO_2 and Al_2O_3 are used as acetabular liners/artificial femoral heads owing to their excellent mechanical strength and high durability

[19–21]. Al_2O_3 is of high clinical interest for biological fixation [20, 21]. High-purity Al_2O_3 (>99.5%) was the first bioceramic to be used clinically for dental implants and load-bearing hip prostheses. Small amount of magnesia can be added to Al_2O_3 for aiding sintering and limiting grain growth process during sintering.

Bioceramics and especially bioactive glasses have found interesting applications in tissue engineering, which is a rapidly emerging multidisciplinary field targeting the development of biological replacements to substitute, restore, and regenerate defective tissues. Cells, growth-stimulating signals, and porous scaffolds are the building blocks of the tissue-engineering approach to regenerative medicine. Scaffolds act as 3-D tissue-like constructs on which cells can grow for allowing tissue repair or regeneration and are therefore regarded as the backbone of tissue engineering [22–26]. The nature of biomaterial processing techniques and composition deeply influences the scaffold structure. 3-D scaffolds play a vital role by providing a substrate for the attachment and proliferation of cells to form an extracellular matrix and should facilitate nutrient diffusion and metabolic waste removal [27–30]. Pore characteristics should be suitable to allow cell migration, proliferation, and vascularization. In addition, scaffolds should possess adequate mechanical properties for providing mandatory biomechanical support during the tissue regeneration process. Since stress is produced in the physiological environment, the scaffolds must also provide strong mechanical interlocking at the tissue-implant interface. Therefore, a careful balancing between mechanical strength and total pore volume is required. Scaffolds may possess macro- (>50 μm), micro- (1–10 μm), or nanoporosity, thereby creating a hierarchically porous construct. Macroporosity supports osteogenesis, whereas surface microporosity promotes cell adhesion and can stimulate cell differentiation [31–33]. Microporous CaP materials have been used as a drug carrier, especially for vancomycin, heparin, and BMP-2 loading with bone growth factors. To maximize the diffusion process and ion exchange rate, pore interconnectivity must be close to 100% with interconnection size of at least 100 μm.

The greatest criterion while selecting materials for scaffold fabrication is accomplishing the required biocompatibility and maintaining controlled degradation kinetics such that the regenerated host tissue progressively replaces the volume occupied by the initial scaffold [34–36]. However, researchers have a large variety of choices when selecting scaffolds for tissue engineering, including typically glasses, ceramics, or polymeric biomaterials processed in a porous form that provide the structural support for cell attachment followed by tissue development. Accounting for the aging process, there is also a strong need for uninterrupted functioning of the biomaterials over a prolonged duration.

Although many research groups have reported applications of bioactive ceramics for bone regeneration and prosthetics, significantly less attention has been paid to their application in the regeneration of soft tissues. Some recent studies have demonstrated the ability of bioactive glasses to enhance angiogenesis and promote neocartilage formation during in vitro cultures [37–40]. These properties are vital for numerous applications such as soft tissue wound healing. For the regeneration of soft tissues, soft biomaterials with elastomeric behavior are desirable. This explains the need for studying blends of bioactive ceramics with thermoplastic materials,

which exhibit behavior ranging from the glassy to elastomeric states, thereby covering a wide range of mechanical properties obtained in body tissues [41–48]. Several researchers have proposed that the incorporation of a bioresorbable and biocompatible polymer in hydroxyapatite/bioactive glass scaffolds can improve the toughness of the construct [45–50]. Improved mechanical properties for polymer-based scaffolds loaded with bioactive glass or hydroxyapatite particles have also been obtained, attributed to the presence of a stiff second phase dispersed in a soft polymer matrix [41–50]. This can also contribute to enhance the osteointegration of the scaffold with the surrounding bone: in fact, cells seeded on bioactive glass/hydroxyapatite-filled polymer-based scaffolds show improved in vitro growth along with osteogenic differentiation compared to the unfilled counterparts.

After the invention of 45S5 Bioglass®, many research groups worldwide have actively engaged in the development of different bioactive glasses and implementation for 3-D scaffold generation, tissue engineering, ophthalmology, cranioplasty implants, angiogenesis, wound healing, and cardiovascular applications. The degree of bioactivity in glass is aided by designing compositions with a silica content up to 60 mol.%, a high CaO/P_2O_5 ratio, and generally high levels of sodium and calcium. From the biological point of view, the addition of magnesium to the glass tends to bond calcium and fluorine for bone generation [51–53]. Zinc has the ability to enhance protein synthesis in the bone tissues, promotes bone formation, and can modify bioactivity; therefore, it is also sometimes used in the glass composition design [54–56]. The current chapter discusses and emphasizes several diverse applications of bioactive glasses.

1.2 Bioactive Glasses in 3-D Porous Scaffolds

The past two decades have seen great progress from interdisciplinary efforts to fabricate and develop synthetic scaffolds incorporating a wide range of materials including ceramics, polymers, and composites. As mentioned earlier, an ideal scaffold material for synthetic bone grafts should be osteoconductive, osteoinductive, and promote osteointegration [22–30]. If resorbable, the scaffold could be exploited to deliver therapeutic agents (e.g., anti-infectives, osteogenic growth factors) and/or stem cells, with a degradation rate matching that of new bone formation. The common ceramic/polymer composite scaffold compositions are given in Table 1.1.

Among various materials, synthetic bioresorbable polyesters, such as polylactones and polylactides, have attracted a great deal of attention for scaffold fabrication due to their biodegradability, biocompatibility, and tunable properties [40, 43, 57, 58]. However, these polymers lack essential bioactive properties to allow bonding to bone as well as adequate proliferation and differentiation of cells. The addition of phosphate or silicate-based bioactive fillers has been explored to improve the bioactivity of bioresorbable synthetic polymers for regenerating hard and soft tissues. Calcium phosphate ceramic scaffolds are also excellent candidates for 3-D scaffolds, offering many design options [59–62].

Table 1.1 Ceramic/polymer composite scaffolds [1–22]

Ceramic	Polymer	Porosity (%)	Pore size (μm)
Hydroxyapatite (HAp)	Chitosan/gelatin	–	300–500
HAp	PLGA-collagen	87	350–430
HAp	Collagen	49–85	30–300
HAp	PCL	85–90	150–200
45S5 Bioglass®	PLA	–	50–200
β-TCP	Poly(propylene fumarate) (PPF)	65–75	150–300
HAp-βTCP	Chitosan	–	300–600
β-TCP	PLA	80–90	125–150

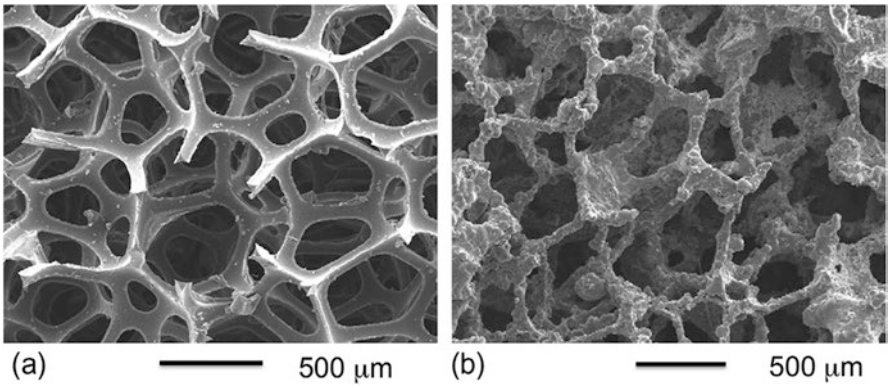

Fig. 1.1 SEM images of the (**a**) polyurethane foam template and (**b**) porous glass scaffold after pyrolysis of the polymeric template and sintering of the glass particles [63]

For an ideal scaffold, 60–80 vol.% of interconnected porosity with macropore diameters in the range of 150–500 μm are desired. Bioceramic and bioactive glass scaffolds with 3-D open-cell structures are usually prepared by the polymer foam replication technique, in which the polymer sponge is coated with a well-dispersed ceramic (or glass) slurry [24–30, 63]. The coated foam is then slowly dried and burnt-out, resulting in an open-cell ceramic construct as shown in Fig. 1.1. Foaming, gel casting, and the addition of the thermally removable porogens are some other fabrication techniques for producing open-cell bioactive glass scaffolds [63]. Ceramic and glass scaffold production techniques may result in shrinkage, phase transformation, and crystallization, since firing or sintering is required in the final step. Bioactive glasses can play an efficient role here since their chemical composition is tunable to widen the sintering window, thereby allowing full sintering to occur before the onset of the crystallization**.**

The biological properties of scaffolds, i.e., the response of cells and tissues to the implanted material, are of utmost importance in view of the clinical outcome of the device. These issues are briefly discussed here with special reference to porous ceramics and bioactive glasses. Osteoinduction is the chemical stimulation of

human mesenchymal stem cells into bone-forming osteoblasts, thereby inducing osteogenesis. It is also the ability of a material to form bone in an ectopic site. It is postulated that osteoinductivity results from the combination of macro- and microporosity capable of trapping and concentrating the growth factors directly involved in mesenchymal stem cell differentiation into an osteoblastic lineage. Surface and bulk chemistry of the crystalline phases play a major role in osteoinduction. The hydroxyapatite crystalline structure comprises highly exchangeable sites, where both cationic and anionic substitutions can take place [64–66]. Sr^{2+}, Mg^{2+}, and Si^{4+} are the most widely studied of the major dopants in hydroxyapatite; Sr^{2+} promotes osteogenesis; Mg^{2+} enhances angiogenesis; and Si^{4+} induces angiogenesis and aids the mineralization processes [51–53, 67–71]. Furthermore, the osteoinductive properties of ceramics can be synergistically enhanced by the permutation of the dopants. Certain calcium phosphate ceramics (CPC) are also osteoinductive in nature [72]. Bioactive glasses have also been doped with the therapeutic elements mentioned above in the effort to impart special properties and improve the clinical outcome [63].

Osteoconduction is a highly desirable property for a synthetic bone graft substitute, implying that new bone can grow onto a surface. Osteointegration is the formation of a chemical bond between the bone and the surface of an implanted material without the formation of fibrous tissues. Scaffolds are designed to biodegrade over time, thereby promoting osteointegration by wettability, nanotopography, surface charge, microporosity, and hemocompatibility. Microporosity and nanotopography can be designed and tailored through thermal treatment by adjusting temperature, heating rate, or time duration, but wettability and surface charge are not easy to tailor in ceramic materials.

Cytokines, stem cells, growth factors, and anti-infectives are some essential factors required for successful bone formation. The naturally occurring angiogenic and osteoinductive molecules present in the body can be easily adsorbed by ceramic scaffolds, thereby enhancing bone formation. For improved bone formation, many of these molecules are pre-loaded on ceramic and glass scaffolds before implantation. Platelet-derived growth factor (PDGF-BB), bone morphogenetic proteins (e.g., BMP-2, BMP-7), human growth hormone (hGH), platelet-rich plasma (PRP), transforming growth factor beta-3 (TGF-β3), and fibroblast growth factor-2 (FGF-2) are some of the osteogenic factors delivered by ceramic scaffolds for orthopedic and dental applications [1, 63, 73, 74]. An efficient delivery system is important because it regulates the release of the growth factor in a controlled manner within the infected site. To avoid any damage to biological activity by the heat, osteogenic molecules are added to ceramic scaffolds after sintering. Coating of growth factor over the scaffold surface is favored over simple adsorption, since the latter approach is often associated with a burst release of growth factor. The biological effects of growth factors depend on the release kinetics; a stable, consistent release is highly desired. To optimize the delivery of growth factor, some researchers have encapsulated the biomolecule inside a polymer coating that was deposited over the ceramic or glass scaffold. The application of a polymer as an outer layer can improve the ability of the ceramic scaffold to act as an osteogenic drug delivery vehicle.

Composite shell scaffolds have been synthesized by Gentile et al. [75] using CaO-rich bioactive glass (BGCa/Mix) and commercial hydroxyapatite coated with bioresorbable gelatin that incorporated drug-loaded polyurethane nanoparticles to imitate the natural bone structure and obtain in vitro release of indomethacin (IDMC). The composite scaffold is made up from 70 wt.% of BGCa/Mix (grain size below 45 μm) and 30 wt.% of commercial hydroxyapatite powders mixed together. The sintered porous scaffolds are then impregnated with 5 wt.% of drug (IDMC) loaded in polyurethane nanoparticles followed by surface coating of scaffold with gelatin for drug delivery. The polymeric coating slows down the process of drug release (up to 7 days) by entrapping IDMC, which is delivered by the nanoparticles in the gelatin-swollen network. Results of the MTT test to assess cell viability and ALP (alkaline phosphatase) activity for all of the prepared scaffolds showed an increase of cell viability during the cell incubation period. Cell adhesion did not show any significant differences among samples after 24 h of incubation. The in vitro drug release tests showed a 65–70% release of IDMC during the first week of incubation, which helps in preventing postoperative infections and inflammation after scaffold implantation in vivo. It was also shown that the drug-loaded polymeric nanoparticles did not affect the ALP activity of the osteoblasts seeded on the composite scaffolds. According to Idowu et al. [11], scaffold mineral content increases the stiffness, which modulates cell interaction with the substrate and is an important feature for osteoblast differentiation. Therefore, biomimetic-coated composite scaffolds of desired porosity, pore size, and mechanical properties are important for bone tissue regeneration and having therapeutic potential.

Polymers such as polylactides and polylactones are both biodegradable and biocompatible, making them suitable for tissue engineering. Specifically, poly(L-lactide) (PLLA), poly(ε-caprolactone) (PCL), and poly(L-lactide/ε-caprolactone) (PLCL) having up to 90% porosity have been extensively investigated as scaffold materials [76–78]. Researchers are currently working on bioresorbable polymers that incorporate inorganic bioactive particles (typically hydroxyapatite or bioactive glass) for their effect on the mechanical properties and cell behavior, as demonstrated by in vitro studies of adhesion of adipose-derived stem cells (ADSCs) and their cytocompatibility [76–82].

PCL-based scaffolds incorporating bioactive glass or hydroxyapatite as a second phase are able to withstand high deformation, making them suitable candidate for soft tissue engineering applications, where the elastomeric behavior of materials is beneficial [79–82]. Furthermore, the incorporated bioactive glass can facilitate both angiogenesis and neocartilage formation and contribute in promoting the regeneration of soft tissues.

Silicate glass-ceramics and glasses can achieve high bioactivity and offer the ability to stimulate new bone formation by activating genes in osteoblast cells. The use of bioactive glass material as a drug delivery system is also currently being studied in detail. Previous studies by Yagmurlu et al. [83] and Zhang et al. [84, 85] mainly focused on biopolymers and reported the inability of polymeric materials to chemically bond with bone, making them unsuitable for bone repair. Researchers are also

focusing on mesoporous glass materials as a drug delivery system. New formulations of bioactive glass as porous scaffolds for drug delivery and their ability to treat infections in vitro are also being assessed [86–90].

Drug release mechanisms and the kinetics of glass scaffold dissolution in different media have also been studied by fitting the release data from Korsmeyer–Peppas (Eq. 1.1), Higuchi (Eq. 1.2), and Hixon–Crowell (Eq. 1.3) models as shown below [86–90]:

$$\left(A_t / A_\infty\right) = k_{KP} t^n \tag{1.1}$$

$$A_t = k_H t^{0.5} \tag{1.2}$$

$$\left(AR_t\right)^{1/3} = k_{HC} t \tag{1.3}$$

Here, A_t represents the amount of drug released at time t; AR_t denotes the amount of unreleased drug at time t; A_∞ denotes the amount of drug released in the limit of infinite time; k_H, k_{HC}, and k_{KP} are the release constants for the Korsmeyer–Peppas, Higuchi, and Hixon–Crowell models, respectively. In (1.1), "n" represents the exponent indicative of the release mechanism.

1.3 Bioactive Glasses in Dental Materials

In addition to treatment of various bone diseases, bioactive glasses are also applied as dental materials. Various research groups are studying bioactive glasses for use in dentistry because alveolar bone loss occurs similarly to normal bone. In this regard, bioactive glasses are often being studied in combination with anti-osteoporotic drugs, since these favor apatite formation and increased bioactivity [91–96].

The application of bioactive glasses in combination with bisphosphonates has been investigated for bone defects, as a result of their use as a filling material during surgery. Rosenqvist et al. [94] proposed that the favorable effects of bioactive glass on bone is promoted by bisphosphonates. A strong bone-glass interaction is indicated due to enhanced ion exchange and formation of an apatite layer while treating periodontal disease. Bioactive glass has also been used in combination with clodronate for dental applications. The surface hydroxyapatite formation and the level of bioactivity of the glass depend on the amount of clodronate used and the size of the bioactive particles. For anterior/posterior teeth, dental composite resins are commonly used as restorative materials. Materials such as hydroxyapatite or 45S5 Bioglass® with biodegradable polymers are used to fabricate composite materials and scaffolds; an overview of compositions is given in Table 1.1 [91–96]. Collagen and PLGA generally exhibit great biocompatibility and biodegradability; however, if PLGA degrades too quickly and in large quantities, it can produce an acidic environment. Therefore, incorporation of a ceramic (glass) phase

can contribute to increase the stability of the material upon contact with biological fluids and to reduce pH fluctuations.

A large number of people are affected by the acid released during fermentation of dietary sugars by plaque bacteria. With regard to the hydroxyapatite constituents, due to undersaturation of saliva and plaque fluids, demineralization of enamel can be induced. These enamel ions can be remineralized with the use of remineralizing agents such as Na_2F, phosphorus, calcium phosphate, etc. or naturally at a slow rate. Highly organized hierarchical microstructures, consisting of 20–25 nm thick and 50–70 nm wide carbonated hydroxyapatite nanocrystals, impart high hardness and strength to the dental enamel. For the treatment of early human dental enamel caries lesions, Bakry et al. [95, 96] used a paste consisting of 45S5 Bioglass® and phosphoric acid. This well-known glass has exceptional ability to bond with soft connective tissues as well as with bone, and it has many similarities to hard tissues found in oral and internal body environments. In an aqueous acidic medium, calcium, sodium, and phosphate crystals are leached out of glass by mixing 45S5 Bioglass® powder with an aqueous solution of 50% phosphoric acid. On the other hand, calcium and phosphate ions are released when enamel comes in contact with acidic gel. Finally, phosphate ions, which are released from the enamel and 45S5 Bioglass®, react with calcium ions to produce acidic calcium–phosphate salts (i.e., brushite, $CaHPO_4{\cdot}2H_2O$). Recent studies have found that a paste consisting of 50% phosphoric acid and 45S5 Bioglass® forms an "interaction layer" to block dentinal tubule orifices, thus acting as a potential candidate for curing dentin hypersensitivity lesions.

Applications of bioactive glasses in dentistry have been reviewed by Jones [63], and the interested reader is referred to this comprehensive publication.

1.4 Bioactive Glasses in Ophthalmology

Some striking features of biocompatible glass and glass-ceramics, such as relative ease of processing, transparency to visible light, and the ability to stimulate cell activity and tissue regeneration, have made them appropriate for use in ocular surgery (Table 1.2) [97–102]. Bioactive glasses have been successfully used for orbital floor defect treatment, with postoperative X-ray analysis demonstrating desirable results (Fig. 1.2). Specifically, S53P4 glass having weight composition 53% SiO_2, 20% CaO, 4% P_2O_5, and 23% Na_2O has been clinically used for the repair of orbital bone fractures. Kinnunen et al. [98] utilized melt-derived S53P4 glass plates in human patients; after surgery, none of the patients showed implant-related postoperative complications, and better clinical outcomes were reported as compared to conventional cartilage grafts.

S53P4 glass implants were studied by Aitasalo et al. [99] in 36 patients, with the results showing no foreign body reaction in the soft tissue or bone; also, no implant extrusion/displacement, hemorrhage, or infection after 1 year of implantation were

Table 1.2 Role of bioactive glasses in ophthalmology [97–102]

Type of device and glass	Type of recipient	Application	Outcome
Porous skirt, bioactive glass	In vitro tests with cells	Keratoprosthesis	Positive results with keratocytes
Titanium coated with bioactive A/W glass-ceramic	Animal	Keratoprosthesis	Tested in rabbits; titanium coated with a glass-ceramic layer was used to fix the prosthesis to the host corneal tissue
Disk, bioactive glass-ceramic	Animal	Keratoprosthesis	Material found unsuitable after testing in rabbits
Porous sphere, glass-ceramic	Animal	Orbital implant	Tested in rabbits with promising results
Bioverit I and II, bioactive glass	Animal	Keratoprosthesis	Tested as materials for the porous skirt in rabbits
Ceravital, bioactive glass	Human	Keratoprosthesis	Risk of resorption, unsuitable for use
Aesthetic shells, glass	Human	Ocular prosthesis	High brittleness; glass was replaced by PMMA for making artificial eyes
Hollow sphere, glass	Human	Orbital implant	Used in nineteenth century and before the Second World War, now declared unsuitable
Transparent lens (optical core), glass	Human	Keratoprosthesis	Used in the "champagne cork" prosthesis
Glass plates, S53P4 glass	Human	Orbital floor repair	Slow resorption, good osteointegration

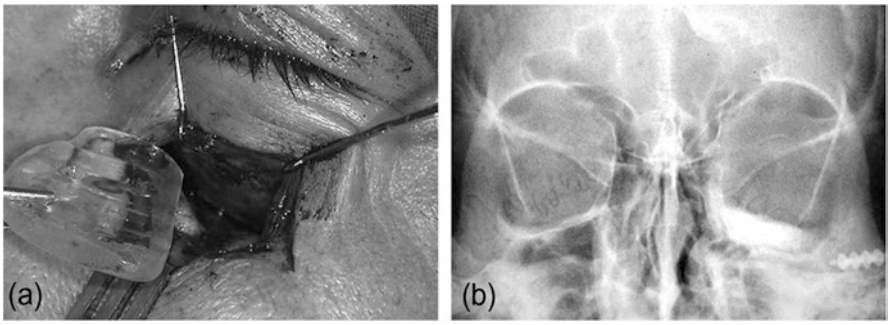

Fig. 1.2 Bioactive glasses for orbital floor repair: (**a**) inserting the glass implant beneath the eye and (**b**) postoperative X-ray analysis indicating that the eyes are on the same height and the implant was well biointegrated in the host orbital bone [63]

observed. New bone growth around implanted S53P4 plates was also revealed by tomographic scans. The results for orbital floor reconstruction, with the use of stainless steel templates for S53P4 glass, are shown by Peltola et al. [101] by choosing the precise glass plate that can fit in the defect margins and surrounding orbit bone

anatomy with maximum accuracy. After 2 years, there was new bone formation on the glass surface with no signs of implant-related infection, displacement, or extrusion and no foreign body reaction. As S53P4 glass is biocompatible, bioactive, and biodegradable, it can be a promising and reliable solution for orbital floor reconstruction. If shape and size of glass implant are carefully selected, then high-quality functional and aesthetic results can be obtained.

Bioactive glasses and ceramics have also been employed for the fabrication of artificial corneas. To produce the optical part of keratoprosthesis (the transparent core), conventional soda–lime–silicate glass can be used; however, in recent times, for the fabrication of the prosthetic skirt, some bioactive glass compositions have been investigated to improve biointegration of the device in host tissue. To initiate the biocolonization of the porous skirt, penetration of biological fluids from the host tissue is required; hence, the skirt materials must possess a hydrophilic nature. Bioactive glasses and ceramics can effectively fulfill this criterion, since after contacting with aqueous solutions, they can expose hydroxyl groups and have good water wettability.

If there is ingrowth of conjunctival or corneal epithelium into the anterior chamber, then keratoprostheses can suffer from extrusion of the prosthesis, infections, secondary glaucoma, or growth of a retroprosthetic membrane. To solve this issue, Linnola et al. [100] recommended an apatite/wollastonite (A/W) glass-ceramic coating. The challenge offered here was to find a material that could increase the fixation of the prosthesis to the corneal tissue before the epithelium grows inward, thus preventing these complications. These corneal prostheses have been investigated in vivo and comprised an optic part consisting of transparent PMMA supported by a flange made up of bare or A/W glass-ceramic-coated titanium. Glass-ceramic coatings were an effective strategy to delay the corneal epithelium ingrowth, since when these surface-modified prostheses were implanted in rabbit corneas, they prevented any significant inward growth of epithelium in the areas where the A/W glass-ceramic was deposited.

Bioactive glasses have also been experimented to manufacture spherical porous orbital implants [97]; early in vivo tests in animal models suggest promising applications.

1.5 Bioactive Glasses for Bone Tissue Repair

Bone healing is a spontaneous process that occurs naturally, but the natural healing process may need assistance as a result of critical traumatic injuries, tumor resections, or bone cancers. Hence, osteoconductive, osteoinductive, and osteogenic materials are necessary for the bone reconstruction. High compressive strength and biodegradation of 3-D porous scaffolds comprising polymer/ceramic composites make them promising candidates in tissue engineering [103–111]. Tumorlike lesions have been treated with TricO$_s$ (Biomatlante, Vigneux de Bretagne, France) granules, which is a biphasic calcium phosphate with 40% β-TCP and 60%

hydroxyapatite [63, 111]. Segmental tibial defects in sheep can be reconstructed by using composite scaffolds made from aliphatic polyesters and tricalcium phosphate.

The major structural components of the extracellular matrix (ECM) of various connective tissues is collagen. The collagen promotes cellular events such as adhesion, migration, proliferation, and differentiation and is the primary focus for the cartilage implant. The most promising clinical materials for cartilage repair are chondrocyte-laden collagen I membranes and hydrogels. Collagen hydrogels can take desirable shapes and cause limited inflammatory reactions.

Presently there is steady increase in the clinical need for biomaterials that promote bone growth as well as regeneration. During replacement of normal tissue, a biomaterial should exhibit bioactive nature along with an optimum degradation rate without causing any inflammation. Many efforts have been made to restore normal functions of the skeletal system with a variety of bone substitute materials that, however, still have some disadvantages. From a general viewpoint, it is very important for a biomaterial to obtain favorable responses from cells or tissues in a particular situation. Any implantable device must be proven safe through in vitro and in vivo experiments followed by early clinical trials before it is definitely approved for medical application. Taking into account the need for bone replacement materials, bioactive and biocompatible glasses have been developed, as they can control gene transcription through glass dissolution products and also get resorbed by a combination of cellular mechanisms and chemical dissolution, enhancing bone generation. Although bioactive glasses have been a highly active area of research, only a few bioactive glasses are available as implant materials for clinical use. Currently silica-based melt-quenched glass compositions are being studied as substitutes for bone graft in orthopedics and dentistry for hard tissue repair. The high Na_2O content in many bioactive glasses may be a limitation for a number of reasons, including the sudden increase of pH associated to the release of Na^+ ions upon contact with biological fluids and risk of cytotoxicity. There is a need to design low alkali content silicate glasses for obtaining excellent bioactive properties, controlled chemical dissolution, high mechanical strength, and good sintering ability. Bioactive glasses in the $CaO–MgO–SiO_2$ system have been doped with P_2O_5, Na_2O, CaF_2, and B_2O_3 to obtain Q_2 (Si)-dominated silicate glass network for their applications in human biomedicine. These glasses can stimulate osteoblast proliferation in cell culture medium and induce remarkable biomineralization upon immersion in simulated body fluid, while avoiding toxicity or any other negative effects in the functionality of cells. These bioactive glass particulates have also been used in the treatment of jaw–bone defects of adult humans in the age group 19–60 year over a period of 8 months (Fig. 1.3) [104–106]. The clinical trials showed that the glasses demonstrated a hemostatic effect as they formed a cohesive mass with patient's blood. The grafting procedure needs to be improved using other bioactive glass compositions or biodegradable organic composites in order to avoid unwanted loss of glass particulates.

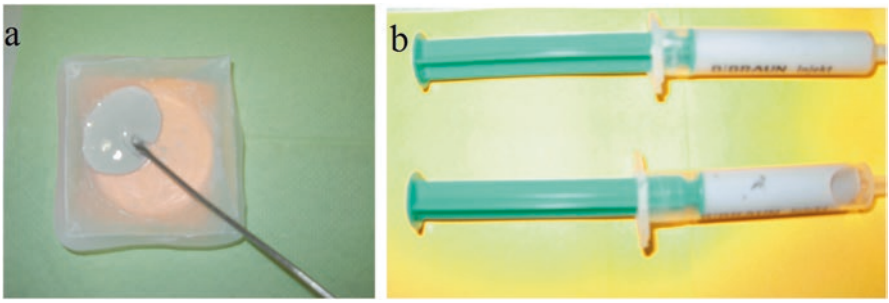

Fig. 1.3 Injectable biomedical glasses: (**a**) bioactive glass particulate-based paste and organic carrier, (**b**) experimental paste-filled standard syringe [104]

1.6 Bioactive Glasses and Angiogenesis

Following the original 45S5 Bioglass®, two other compositions that have received widespread attention are 13–93 and S53P4, owing to their excellent clinical outcomes. Apart from the regeneration of calcified tissues, glasses have also been studied for soft tissue repair requiring angiogenesis and wound healing capabilities as well [112–131]. Hard-soft tissue interfaces, particularly in bioactive glass/polymer composites, have been investigated widely; furthermore, the surface modification of bioactive glasses has been done to enhance their bioactivity/biocompatibility. Due to the "hard" physical characteristics of bioactive glasses, they have been studied more for hard tissue applications, and less attention has been paid to soft tissue interactions. Angiogenesis is the mechanism of formation of new blood vessels and is vital for the formation of granulation tissue as well as for promoting the wound healing mechanism. Various growth factors such as vascular endothelial growth factor (VEGF), TGF-β, and fibroblast growth factor (FGF) regulate angiogenesis. VEGF increases the capillary numbers in a given site and hence acts as a major contributor to the angiogenesis [112–118]. Due to increased blood flow at the affected area, VEGF is unregulated with muscle contraction causing increased mRNA production of VEGF receptors. Matrix metallic proteinase (MMP) inhibition prevents new capillaries from forming because they degrade the protein, which keeps the vessel walls solids, thereby allowing the endothelial cells to escape into interstitial matrix resulting in sprouting angiogenesis.

For the regeneration process to occur, neovascularization is an essential criterion so that the growing cells are provided with oxygen and nutrients. Hence, the angiogenic potential of bioactive materials is receiving great attention for tissue engineering applications. Angiogenesis is a process that can take place during normal tissue regeneration as well as during the pathogenic conditions such as malignant tumors/cancer. Angiogenesis forms the basis of tissue engineering, and hence the mass transport and oxygenation mechanics need to be regulated [112].

Bioactive glasses like 45S5 Bioglass®, 4555F, and 52S4.6 have been used for in vitro investigations on hamsters, chickens, mice, and rats, whereas disk-shaped

bioactive glasses were implanted subcutaneously and intramuscularly in the peritoneal cavity of mammals (like dogs) [118–131]. The results indicated tissue growth and adhesion around the implants, and the autopsy results indicated no inflammatory response of the host tissue. Gatti et al. [39] implanted glass granules of size ~300 μm in the dorsal muscle and under dorsal skin of rabbits. In addition to this, the defects were created surgically in sheep jaw, and glass granules were implanted into them to understand the hard/soft tissues interaction with the glass. After 2 and 3 months from excision in rabbits and sheep, respectively, it could be seen that the bioactive glass granules and their surroundings exhibited almost similar morphology, indicating that the nature of reactions are independent of the implantation site and tissue type.

Wilson et al. [113] have performed wide in vivo and in vitro experiments to study the 45S5 Bioglass® cytocompatibility and toxicity when in contact with various soft tissues. Gorustovich et al. [114] provided a broad review of the in vitro/in vivo effects of glasses on angiogenesis. Keshaw et al. [38] studied the angiogenic growth factor release from CCD-18Co normal colon fibroblast human cells encapsulated in alginate beads with 45S5 Bioglass®. The alginate beads containing 0.01% and 0.1% 4555 Bioglass® released higher VEGF compared to pure polymer control after 3, 6, 9, and 17 days post-encapsulation. VEGF is an endothelial cell-specific mitogen and is involved in pathological and physiological angiogenesis. For the same concentrations, fibroblasts culture revealed an increase of cell proliferation on the bioactive glass-coated surfaces. For the alginate beads containing 0.1% 45S5 Bioglass®, a significant increase in the endothelial cells was observed, attributed to the presence of VEGF and other angiogenic factors in optimum concentration. It must be noted that the concentration of 45S5 Bioglass® should be optimized, i.e., if 45S5 Bioglass® content is quite high, then VEGF secretion reduces, most likely due to the cytotoxic effects. The alginate beads containing 0.01–0.1% 4555 Bioglass® lysed with EDTA, yielded high VEGF as compared to the beads with 0–1% 4555 Bioglass® glass. Day [116] found the stimulation of angiogenesis and angiogenic growth factor using 45S5 Bioglass®, too. For the 45S5 Bioglass® coating of 0.03125–0.625 mg/cm^2 in tissue culture wells with human intestinal fibroblasts, enhanced amount of VEGF could be observed. To assess the effect on angiogenesis of growth factors secreted from fibroblasts in response to 45S5 Bioglass®, an in vitro model of human angiogenesis was used. It was observed that 45S5 Bioglass® stimulates fibroblasts to secrete growth factors thereby causing a significant increase in angiogenesis. Significant increase in the number of endothelial tubules and tubule junctions could be observed within the conditioned media obtained from fibroblasts cultured on the 4555 Bioglass®. The number of endothelial tubules, tubule length, and tubule junctions were reduced as compared to control endothelial cells due to the presence of 20 μM suramin, an angiogenesis inhibitor.

The studies done by Day [116] also demonstrated that small quantities of bioactive glass could stimulate the expression of VEGF and hence enhance in vitro angiogenesis, although it is not clear whether other angiostatic factors are also released. A complex network of interconnected tubules and tubule branching could be seen in

the presence of 45S5 Bioglass® (in vitro). These tubules mimic the essential stages for the angiogenesis, involving cell migration, proliferation, anastomosis, and vessel branching.

Leach et al. [117] coated VEGF secreting polymeric scaffolds with 45S5 Bioglass®. VEGF enhances osteoconductivity via biomineralization, and localized VEGF delivery has been beneficial for bone regeneration as the neovascularization promoted osteoblast migration and bone turnover. Porous scaffolds made of poly(lactide-co-glycolide) for the localized protein delivery were surface-coated with 45S5 Bioglass® (up to 0.5 ± 0.2 mg of glass were deposited). Mitogenic effect could be seen on the human microvascular endothelial cells (HMVEC) by the VEGF released from bioactive glass coated and non-coated scaffolds. After day 6, the bioactive glass coated blank scaffolds could support enhanced HMVEC proliferation, but this was not detectable by day 9, probably due to complete dissolution of the material. After 10 days, the proliferation values decreased for VEGF-releasing scaffolds along with mitogenicity comparable to VEGF-secreting uncoated scaffold. It suggests that with the material degradation, the bioactive glass coating contribution is decreasing upon seeding the scaffolds with HMVECs. Differences in alkaline phosphatase activity could not be observed between the scaffolds at different time points. The bioactive glass-coated scaffolds were implanted in cranial defects in Lewis rats. VEGF-releasing scaffolds have higher neovascularization in the defect (117 ± 20 vessel/cm^2) as compared to bioactive glass-coated scaffolds (66 ± 8 vessel/cm^2). Robust angiogenic response could be seen by the coated scaffolds lacking VEGF, in the studies conducted on a similar model by Murphy et al. [118]. Bone mineral density results indicated that the prolonged VEGF delivery from polymeric substrates improved the maturation of newly formed bone. With VEGF-releasing scaffolds, a slight increase in the newly formed bone within the defect could be seen as compared to bioactive glass-coated scaffolds.

Day [116] assessed the effect of 45S5 Bioglass® on VEGF secretion using a rat fibroblast cell line (208F). Enzyme-linked immunosorbent assay (ELISA) of media collected from the fibroblasts grown for 24 h on surfaces coated with 45S5 Bioglass® particles (via a suspension of 45S5 Bioglass® in distilled and deionized water) yielded increased VEGF concentration. The same group conducted similar studies on PLGA disks containing different concentrations of 45S5 Bioglass® with particle size <5 μm. Increased VEGF secretion was observed upon culturing fibroblasts L929 on PLGA disks with 0.01–1% 45S5 Bioglass® particles. The results of Day and Keshaw [38, 116] revealed that endothelial cell proliferation was increased by conditioned medium collected capable of inducing proliferation. Bovine aortic endothelial cells (BAECs) were also plated on zinc-doped 45S5 bioactive glass: a significantly higher proliferation of BAECs could be seen on 5% ZnO-containing glasses as compared to 20% ZnO-containing glass and control 45S5 Bioglass®. The high rate of dissolution for the 20% ZnO-containing glasses causes pH changes and hence affects the cell proliferation.

Leu et al. [119] found a dose-related proliferative response of endothelial cells cultured with 45S5 Bioglass®-loaded collagen toward the soluble products of the constructs. The collagen sponges loaded with 1.2 mg of 45S5 Bioglass® particles

yielded the highest proliferative cell response, whereas considerable inhibition of endothelial cell proliferation could be observed for the sponges loaded with 12 mg of glass. In addition to this, the endothelial cells exposed to 1.2 and 0.12 mg 45S5 Bioglass® demonstrated higher VEGF mRNA secretion after 72 h of exposure. Leu et al. [119] also explored the pro-angiogenic potential of 45S5 Bioglass® by analyzing its tubule generating ability within co-culture of endothelial cells and fibroblasts. The stimulation of co-cultures was done with conditioned medium from 45S5 Bioglass®-treated rat aortic rings during a test similar to endothelial proliferation assay, and a dose-related tubule formation response to 45S5 Bioglass® could be seen. The highest number of tubules was seen in the presence of 1.2 mg of 45S5 Bioglass®, whereas no tubule formation over the collagen sponges could be seen for 6, 0.12, and 0.6 mg 45S5 Bioglass®-loaded sponges.

Durand et al. [120] studied the angiogenic effects of ionic dissolution products released from boron-doped 45S5 bioactive glass (45S5.2B: 45% SiO_2, 23.5% Na_2O, 23.5% CaO, 6% P_2O_5, and 2% B_2O_3, wt.%). 45S5.2B composition was also reported to enhance the bone formation upon implantation into the intramedullary canal of rat tibiae. In addition to this, the human umbilical vein endothelial cells (HUVECs) possess greater migratory and proliferative response, enhanced secretion of pro-angiogenic cytokines (IL-6 and bfGF), and higher tubule formation capacity upon stimulation from the ionic dissolution products of 45S5.2B glass. The ELISA test done to determine the endogenous levels of integrin α_ν β_3 in the chorioallantoic membrane (CAM) of quail embryos revealed that upon treatment (2 days) with ionic dissolution products from bioactive glass 4555.2B, the levels of expression are 2.5–3-fold higher than those treated with Hank's balanced salt solution (HBSS). Moreover, greater expression of β_3 subunit of integrin α_ν β_3 was seen in the Western Blot test. No significant differences of CAM treated with HBSS +4555.2B/bFGF or HBSS +4555.2B on the vascular density could be observed when compared to negative control (HBSS) even after 5 days of treatment. The CAM treated with 4BSS + 4555.2B and 4BSS + 4555.2B/bFGF showed a higher vascular density of 30% and 73%, respectively, comparable to the response observed with HBSS + bFGF. The authors further investigated the effect of boron concentration on the angiogenic activity in the CAM treated with HBSS enriched with the 4555.2B dissolution products. For the boron concentrations of 5, 50, and 150 μM, the corresponding CAM yielded greater vascular density as compared to the control HBSS after 5 days of treatment (Fig. 1.4). For the HBSS containing 50 or 150 μM borate, no significant differences in the angiogenic response could be seen after 2 or 5 days of treatment. The study of Durand et al. [120] confirmed that the ionic dissolution products did not induce any angiogenic response and hence did not affect the normal development of the embryonic quail CAMs vasculature. This could be due to the smaller contact area of CAM with the scaffolds causing insufficient ion release. Boron in the form of H_3BO_3 activates the mitogen-activated protein kinase (MAPK) signaling pathway to enhance cell proliferation and growth at low concentrations and inhibits them at higher concentrations. Angiogenesis involves vascular growth factors and extracellular matrix interacting molecules like integrins. α_ν β_3, a heterodimer integrin, is expressed at low levels on quiescent endothelial cells in vivo but is upregulated during vascular remodeling and angiogenesis.

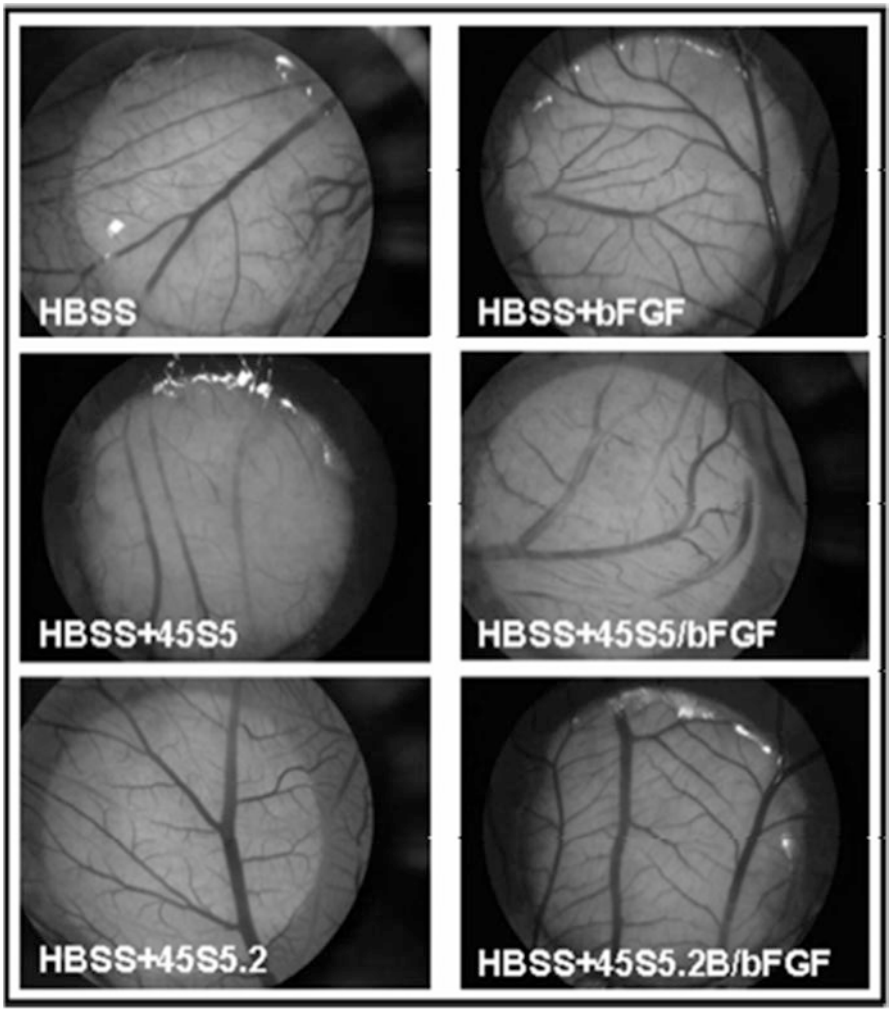

Fig. 1.4 The angiogenic response of CAM to 45S5.2B bioactive glass, 5 days after treatment [120]

Ghosh et al. [121] evaluated the biological response of a bioactive glass block with composition 43.7% SiO_2, 19.2% CaO, 5.46% P_2O_5, 9.4% B_2O_3, and 22.24% Na_2O (wt.%) upon implantation in the radius bone of Bengal goats. After a 3-month implantation, a well-formed vascularization and bone tissue ingrowth could be seen, directly integrating with the neighboring bone. This group also worked on the same experimental model with glass composition 58.6 SiO_2, 23.66% CaO, 3.38% P_2O_5, 3.78% B_2O_3, 1.26% TiO_2, and 9.32% Na_2O (wt.%) and found the establishment of vascular supply and angiogenesis across the bone defects. Andrade et al. [122] evaluated the angiogenic and inflammatory response of bioactive glass-coated

collagen scaffolds upon subcutaneous implantation in mice. It was observed that the hemoglobin (Hb) content extracted from implants was higher in glass-coated collagen implants compared to the glass-free group after 14 days of implantation. No inflammatory response associated with the glass-coated collagen samples could be observed in the presence of Hb, as revealed by the control group. Gerhardt et al. [112] investigated the angiogenic effect of bioactive glass by comparing composite PDLLA/45S5 Bioglass® scaffolds with plain PDLLA samples and obtained a marked increase in the VEGF release by fibroblasts cultured on PDLLA/glass composites compared to the polymeric control. The in vivo experiments on a rat model confirmed enhanced vascularization and higher percentage of blood vessel formation, as shown by the stereological examination.

Lin et al. [123] demonstrated that no systemic cytotoxicity could be observed upon subcutaneous implantation of 13-93B3 glass (53 wt% B_2O_3) microfibers in rats, even when a high amount of glass (up to 1,120 mg/animal) was used. This study suggested that the controlled release of borate ions could represent a promising strategy to enhance neovascularization in regenerative medicine.

Mahmood et al. [124] demonstrated the relation between glass porous matrix and in vivo vascularization. A fiber-based bioactive glass scaffold (composition 32.24% CaO, 9.26% P_2O_5, 41% SiO_2, 17.5% Al_2O_3 wt.%) was used in combination with recombinant human bone morphogenetic protein–2 (rhBMP – 2). Vascularization was evaluated by mRNA expression of KDR and Flt-1, two VEGF receptors. The scaffolds were designed in two shapes, i.e., bundle-shaped and porous ball constructs. The receptors, KDR and Flt-1, did not express for the subcutaneously implanted bundle-shaped scaffolds after 2–4 weeks of implantation in rats, but the same receptors expressed in porous ball scaffolds under the same conditions. The histology results also revealed that after 2–4 weeks of subcutaneous implantation of the scaffolds, higher bone formation could be seen for porous ball constructs compared to the bundle-shaped scaffolds. rhBMP-2 was found to promote vascularization and also to induce bone formation.

1.7 Bioactive Glasses in Wound Healing

Whereas extensive studies have been conducted on bioactive glasses and other biomaterials (metallic implants, polymers, polymer/bioactive glass composites) for hard-tissue repair, fewer studies are available on the use of bioactive glass in soft tissue applications such as wound healing. Nevertheless, the wound healing capability of bioactive glasses has been demonstrated by different experiments. For example, application of cottony fibrous bioactive borate glass promoted scarless healing roughly over a period of 7 months as shown in Fig. 1.5.

Bioactive glass-ceramics with varying chitosan-to-gelatin ratios (C/G ratio) were synthesized by Ma et al. [125] as fibrous membranes for applications in wound dressing (30% SiO_2, 27% CaO, 20% B_2O_3, 4% P_2O_5, 1.5 CuO, 1% ZnO, 3% K_2O, 9% Na_2O, wt.%) using an electro-spinning technique. These nanofibrous constructs

Fig. 1.5 Application of cottony fibrous bioactive borate glass to deep chronic wounds (lower leg of a 70-year-old shown here) promotes scarless healing. Time lapse from bottom left to right is roughly 7 months (Photo courtesy of Peggy Taylor/Phelps, County Regional Medical Center (Photos)/Steven Jung/MO-SCI (Micrograph))

comprise open pores having dimensions of several micrometers. The presence of beads can be observed in the fiber body with the increase in C/G ratio from 1/19 to 5/15 in the starting solutions, likely due to aggregation. These glass nanofibers were synthesized via the sol-gel method. The increasing bioactive glass (BG) content limits the fixing of bioactive glasses in the porous network of the fiber matrix. The tensile strength of BG-based mats is very high, and with the addition of 15% BG, the average elongation ratio of mats can be increased up to 150%, making them suitable for biomedical applications. The human body has large amounts of collagen (insoluble structural fiber), which yields gelatin under controlled hydrolysis. Cross-linking of the gelatin-based dressings is useful for improving the structural and thermal stabilities in contact with biological fluids. There was no tenderness or adverse response of the host tissue even after 2 weeks of implantation of G/C – 15% BG and G/C – 0% BG mats in rats, signifying their high biocompatibility (Fig. 1.6). However, the degradation of the G/C-15% BG and G/C – 0% BG mats were noticeable after 4 weeks of implantation. Two factors, i.e., the release of inorganic

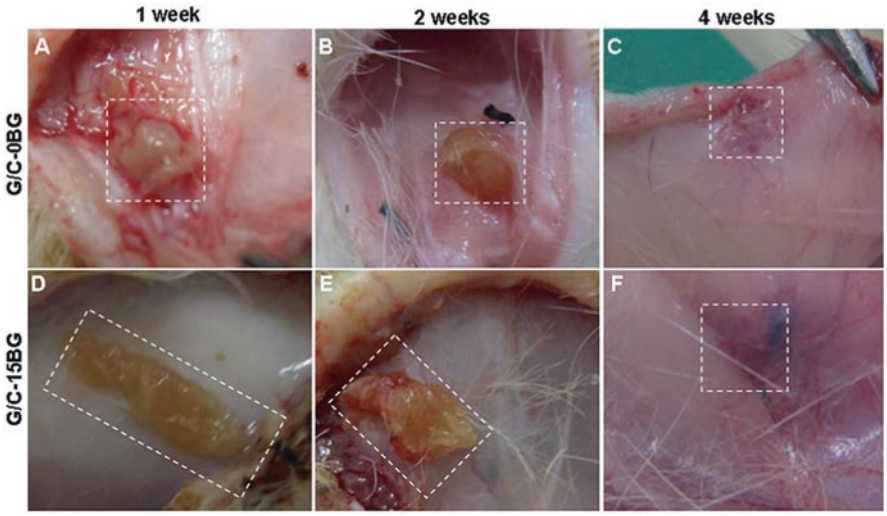

Fig. 1.6 (**a–f**) Wound healing upon implanting G/C-xBG in subcutaneous tissue of rats [125]

ion products via BG dissolution and the beneficial G/C functions on the wound site, are responsible for the bioactive potential of G/C – BG mats. Due to these two aspects, there is improvement in cellular signaling, and, at the same time, the nanofibrous network containing BG provides reformed surface properties and antibacterial activities, which prove favorable for the anti-adhesion on wet wounds.

The wound repair in the worst cases of diabetic patients on small scale using 13-93B3 glass nanofibers in the range of 300 nm–5 μm has also been studied [126]. Accelerated healing of the wounds along with marked decrease in scar tissue formation could be observed as compared to congenitally treated wounds. Nanoporous bioactive glass (n-BGS) containing silver were investigated for its antibacterial dressings and hemostatic properties as compared to the bioactive glass not containing nanopores (BGS). n-BGS exhibits higher surface area compared to the BGS, which results in its higher water absorption efficacy. n-BGS released Ag^+ ions quickly, although the concentration of silver in solution was the same even after 24 h of incubation in phosphate-buffered solution (PBS). For n-BGS with 0.02 wt.% silver concentration, the highest antibacterial rate of 99% could be attained for the *Escherichia coli* after 12 h incubation time. n-BGS and BGS particles were useful to treat the impaired femoral arteries and veins of male New Zealand white rabbits. n-BGS has considerably lower clotting times in both prothrombin time (PT) and activated partial thromboplastin time (APTT) in vitro. Hence, silver-doped n-BGS accelerates clotting, is responsible for bactericidal effect, and promotes hemorrhage control.

Due to abnormalities in immune function, neuropathic, vascular, biochemical diabetic wounds are very problematic. Patients having diabetes have reduced wound

healing chances because of due high blood glucose levels. A better option for curing such diabetic wounds could be bioactive glass-containing ointments. In this regard, Cong et al. [127] worked on wound healing in diabetic rats by using Yunnan Baiyao (YB), a renowned Chinese herbal medicine as hemostatic agent, and 45S5 Bioglass® on the diabetic wound. Yunnan Baiyao helps release of platelet constituents along with improving surface glycoprotein expression on platelets under stimulated conditions, which is responsible for shortening clotting/bleeding times in rabbits and rats. The remedial effects of bioactive glass and Yunnan Baiyao ointments were successfully observed on wounds in diabetic rats. Better results were exhibited by Group 6 containing 5% Yunnan Baiyao compared to any other ointment.

Lin et al. [128] worked on making Vaseline-based ointments for the treatment of superficial injuries in diabetic rats with 18 wt.% of 58S glass (SGBG-58S), nanoscale 58S, and melt-derived 45S5 glass powders. The Vaseline-based ointment and bioactive glass were applied on the full-thickness wounds directly. The presence of bioactive glass, especially SGBG – 58S, accelerated the wound healing. On the other hand, the wounds that were still open for the control group took a little longer time for the healing. An increased proliferation of fibroblasts could be seen along with granulation tissues and formation of new capillary for the bioactive glass-treated ointments, and, at day 7, immunohistochemical assays showed the VEGF presence in all tissues. The animals that were treated with bioactive glass ointments exhibited no adverse reaction or inflammatory response. Also, the wound healing results confirmed rapid healing of wounds with the sol-gel-derived glasses as compared to melt-quenched-derived 45S5 glass, which was attributed to the larger surface area of the sol-gel glasses.

Yang et al. [129] gave complete assessment of hydroxyapatite conversion and cell-glass interactions for both dynamic and static modes during in vitro tests. Nano-/microfibers of 45S5, 13-93B3, and 1605 (6% Na_2O, 12% K_2O, 5%MgO, 20% CaO, 4% P_2O_5, 51.6% B_2O_3, 0.4% CuO, 1% ZnO, wt.%) bioactive glasses were used to study the effect on the human fibroblast skin line (CCL-10) as well as on wound healing. The structure of the fibers obtained was smooth with small amount of fine structures such as flakes and whiskers. The 45S5 glass fibers possessed eroded/porous inner structures. For the 13-93B3 fibers, polished surface fiber morphology with porous granule network underlying the surface layers was observed. Borate-based 1605 glass fibers exhibited roughened surface and protruded spherical structures. Under high magnification, eroded fiber surfaces and hollowed cross-sections could be seen. Furthermore, the fibers had an undesirable effect on cell viability at high dosages. With respect to 45S5 and 1605 glasses, high cell proliferation was detected for the dosages of $\leq$750 μg/ml and $\leq$250 μg/ml, respectively. Both the treatment time and fiber dosage affected cell viability. It was observed that better viability was provided by the fiber dosage <200 μg/ml than the control. The cell proliferation was stimulated by 35–40% using 45S5 and 13-93B3 glasses, even after 1 h of soaking, if the fibers were pre-soaked with serum-free cell culture medium. The partial conversion of fibers was able to reduce the cytotoxicity, which was attributed to the rapid uplifting rate of dissolved calcium and boron,

along with better surface elemental deposition. Dynamic control group fibers offered high cell viabilities as compared to the static control. Although silicate 45S5 glass fibers possessed broader dosage range for positive cell proliferation, borate-based fibers were able to elicit higher cell viabilities compared to the silicate glass fibers. Under static mode, there was observed negative impact on the cell migration in all fiber-treated groups, with the higher effect in the case of borate glasses. The creation of new tissue around the wound can be due to cell migration and keratinocyte/fibroblast proliferation. This mechanism of tissue repairing could be seen in the presence of 45S5, 13-93B3, and 1605 glasses, along with the effect of fiber stimulation on cell proliferation and migration abilities.

Gillette et al. [130] experimented the effect of bioactive glass particulates (<20 μm) on open wounds that were surgically created in nine dogs. To better study and control the bioactive glass-treated wound, the wounds were made bilaterally. A small amount of slurry comprising bioactive glass and blood was prepared and then applied to the wounds. Most of the mixture stayed in the internal area of the wound, while a small amount of the slurry lied between the edges of wound. There was no significant difference observed in the breaking strength of healed skin in all the samples after 5 days of application, but there was an increase in breaking strength of healed cutaneous/subcutaneous trunci in treated wounds as compared to control wounds. Furthermore, in addition to this, there was no inflammatory response of the host tissue.

Li et al. [131] studied how 45S5 Bioglass® can promote wound healing by affecting gap function connexin 43-mediated endothelial cell behavior. The behavior of all endothelial cells is correlated to gap junctional cell-to-cell communications as connexin 43 (C×43) plays a vital role in determining the fate of endothelial cells along with cell-to-cell communications for angiogenesis and wound healing. C×43 is the most universal connexin in the skin located in dermal appendages, fibroblasts as well as cutaneous vasculature. C×43 antisense, C×43 mimetic peptides, and C×43 hemichannels play imperative role in the wound healing. 45S5 Bioglass® (BG) extracts at ratios of 1/8, 1/16, 1/32, 1/64, 1/128, 1/256, and 1/512, respectively, were diluted for BG 1/8 and BG 1/16, and it was found that the proliferation of HUVECs was suppressed as compared to the medium alone. Under hypoxia conditions, almost 80% of HUVECs cultured in BG 1/128 ion extracts remained sustainable, and the survival was the same as that of the non-hypoxic conditions. Only 65% cells remain alive for BG 1/152, indicating that BG at appropriate concentration could protect HUVECs exposed to hypoxic conditions. After 1 day of culture with HUVECs, the culture media containing BG 1/64, BG 1/128, and BG 1/256 loose the bFGF, VEGF, and KDR gene expression. Immunofluorescence staining gave more positive results for in KDR HUVECs cultured in BG 1/64, BG 1/128, BG 1/256 as compared to the cell cultures in BG 1/32 and BG/512. The KDR expression in HUVECs cultured with BG 1/64, BG 1/128, and BG 1/256 were advanced compared to the control results as shown in Fig. 1.7. C×43 expression of HUVECs cultured in BG 1/64 and BG 1/128 for 7 days was much higher compared to the cells cultured in endothelial medium alone BG 1/32 and BG 1/512. For the wound treated with BG, the granulation tissue formation could be seen in the form

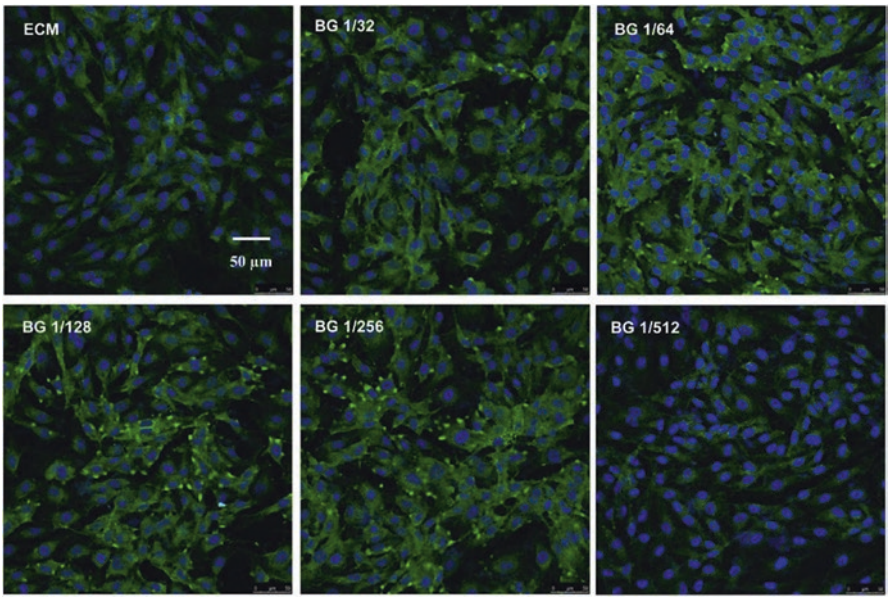

Fig. 1.7 KDR protein expression and localization in HUVECs cultured with different media for 3 days [131]

of vascularized endodermis (beginning at day 6). After 12 days of implantation, the granulation tissue was much more organized, but no neoepidermis formation could be seen for the untreated wound although eschar and noticeable granulation tissue formation could be seen as depicted in Fig. 1.8. C×43 expression could be seen after 2 days of operation in control and BG-treated wounds. After 12 days of operation, the highest C×43 expression could be seen for the BG-treated wounds compared to the untreated ones.

Rai et al. [132] fabricated poly(3-hydrony-octanoate) composite forms with nanosized bioactive glass (nBG) for wound dressing. With increasing proportion of glass nanoparticles, the toughness was increased with enhanced polymer wettability along with decreased clotting time of citrated whole blood. Increased cell proliferation could be seen when human keratinocytes were cultured on the composite films, which can be attributed to the increased surface area of the nBG. Zhao et al. [133] fabricated copper-doped (0–3 wt.% CuO) 13-93B3 microfibers for wound dressing. Copper is considered to be a vital component of angiogenic response attributed to the fact that it stabilizes the expression of hypoxia-inducible factor (HIF-1α), thereby simulating hypoxia and hence playing a fundamental role in the recruitment and differentiation of the cells as well as blood vessel formation. The release of Cu^{2+} also stimulates the expression of pro-angiogenic factors such as transforming growth factor – β (TGF-β), etc. Hence, Cu^{2+} ions boost implant vascularization when it is used in combination with the VEGF and bFGF. It was observed that after 7 days of cell culture, Cu-doped microfibers increased the proliferation of

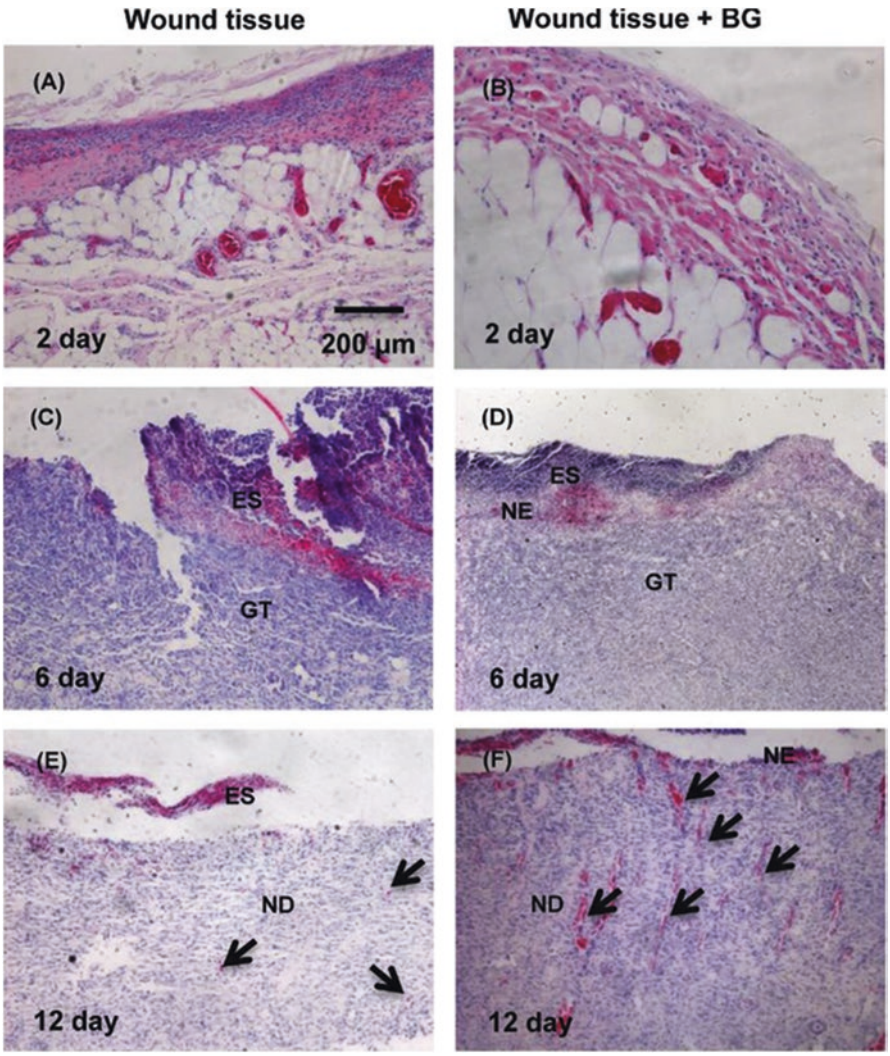

Fig. 1.8 HE staining of tissue samples after rat excision wounds treated with or without BG powder for 2 days (**a**, **b**), 6 days (**c**, **d**), and 12 days (**e**, **f**). *ND* neodermis, *ES* eschar, *GT* granulation tissue, *NE* neoepidermis; the *arrows* indicate a clearly defined lumen containing red blood cells [131]

HUVECs compared to the cells cultured on the ionic dissolution product of Cu-free microfibers. HUVECs incubated with the ionic dissolution product of Cu-doped microfibers generated elongated and tubelike structures (after incubating on the matrigel substratum for 12 h). On the contrary, there was incomplete or sparse tubular network formation when HUVECs were treated with the ionic dissolution product of Cu-free microfibers. As the content of CuO is increased in fibers, VEGF,

bFGF, and PDGF gene expression for fibroblasts incubated in the ionic dissolution products of microfibers enhances, which indicates the pro-angiogenic potential of the bioactive glass microfibers. The wound size decreased over the healing period for all the groups; the smallest wound was observed in the 3Cu-BG group. The wound was closed by day 14 after treatment with 3Cu-BG. For the quantification of wound size, the following equation was used:

$$\%\ Wound\ size\ reduction = \left[\left(A_o - A_t\right)/A_o\right] \times 100 \tag{1.4}$$

where A_o and A_t are the wound areas initially and at each time point, respectively. A higher density of blood vessels was observed in the defects treated with 3Cu–BG microfibers compared to the untreated or BG microfiber-treated wounds. There were extensive collagen deposition and thick wavy collagen fibers in wound areas when treated with BG microfibers as compared to the untreated defects. The 3Cu-BG microfiber-treated wound exhibited the highest amount of collagen fibers arranged in an orderly fashion, which is similar to the normal skin. For both 3Cu-BG and BG, there was accelerated formation of hair follicles and sebaceous glands after 14 days of surgery. All these results showed that the Cu-doped borate bioactive glass microfibers are favorable candidates for wound dressing.

1.8 Bioactive Glass in Bone Tissue Regeneration

The early 1990s marked the emergence of bioactive glasses prepared via the sol-gel technique. In contrast to bioactive glasses prepared by melt-quenching, these do not require high processing temperatures. In addition, they exhibit better bone bonding rates because of increased nanoporosity and higher surface area, which also improves their resorption/degradation properties. In some recent investigations, the SiO_2–CaO–P_2O_5–MgO-based quaternary sol-gel bioactive glass system has shown its ability to support the growth of human fetal osteoblastic cells (hFOB) [134–138]. This material is nontoxic and compatible in segmental bone defects created in vivo in a goat model. Another important requirement for a sol-gel system is to have antimicrobial properties, and sol-gel systems having SiO_2–CaO–P_2O_5 as main constituents actually show antimicrobial activity against *Escherichia coli* with addition of Ag_2O (up to 3 wt.%), without producing any detrimental effect on the bioactivity. Sol-gel glasses were found to elicit an antibacterial effect against Streptococcus mutants, too, and were extensively studied for bone tissue engineering applications [139–146].

Imparting bioactivity to other functional materials by preparing composites is another high-end application of bioactive sol-gel glasses. A typical example is the induction of in vitro bioactivity in acrylic polymers [144–146]. Work has also been done for osteointegration of magnetic seeds with the help of SiO_2–CaO–P_2O_5-based sol-gel [147–149]. These types of materials have been synthesized using bioceramics

with magnetic iron oxides, which have low bioactivity. Magnetic hyperthermia treatment against potential metastasis is provided with the help of magnetic glass, and they are also helpful in strengthening the bone site after surgery extirpation of the osseous tumor. The bioactive behavior of biocompatible hydroxyapatite can also be improved by the addition of sol-gel glasses, the inclusion of which facilitates osteointegration of permanent and biocompatible implants.

In the case of sol-gel glasses, incorporation of biological and organic molecules and even cells within silica matrices is relatively easy since processing for these glasses generally occurs at room temperature. Another advantage of this technique is the generation of highly ordered mesoporous materials, which have tremendous potential as drug delivery systems. The synthesis route of mesoporous bioactive glass (MBG) involves three main steps, i.e., gelling, drying, and surfactant calcinations, ultimately producing glasses with higher surface area and porosity compared to conventional sol-gel glass. This is the main reason for their fast and intense bioactivity [142–154]. A typical $58SiO_2$–$36CaO$–$6P_2O_5$ (mol.%) MBG exhibits intense Ca^{2+} release when soaked in SBF, resulting in the growth of an amorphous calcium phosphate (ACP) layer onto its surface. This material exhibits a CaP–OCP–HCA maturation with the final product almost equal to the mineral phase of bones in vertebrates.

MBG-85 (3D cubic mesostructural arrangement) is a mesoporous glass with high silica content, $85SiO_2$–$9CaO$–$6P_2O_6$ (mol.%), which develops a nanocrystalline carbonated hydroxyapatite surface layer within 1 h after being soaked in SBF, and when it comes in contact with vitronectin- and fibronectin-containing medium, it adsorbs large amount of serum proteins. It has been observed that biodegradation of MBGs release ionic dissolution products that are biocompatible, and in vitro testing has indicated favorable behavior of fibroblasts, osteoblasts, and lymphocytes in the presence of these materials. Preparation of scaffolds for bone tissue engineering or in situ implantation is currently being done using these materials [152–154]. Mesoporous materials have also been proposed as platforms for the controlled release of drugs and growth factors, thereby opening new perspectives for the local therapy and targeted treatment of a wide range of pathologies [152, 153].

1.9 Future Prospects

Many investigations have been carried out on bioactive glasses based on the 45S5 Bioglass® during the last 40 years. Recent studies on borate glasses have shown that they are biocompatible in small animals but have also addressed concerns about potential toxicity for cells and tissues. Borate- and borosilicate-based bioactive glasses are currently being used for many different experimental applications in tissue engineering. In vivo studies in small animals have been very successful to eradicate bone infections and to restore diseased or damaged bone to its natural state. However, the repair of large bone defects resulting from infected prosthetic implants still needs additional research and development. Some reports have shown that

bioactive glasses can stimulate osteogenesis and promote angiogenesis, implying their future use for the applications related to soft tissue repair. During the biodegradation of the glass, ions are released that have beneficial effect on angiogenesis, osteogenesis, and chondrogenesis. The controlled degradation rate and conversion to hydroxyapatite-like materials help bioactive glasses to form bonds to both hard and soft tissues, thereby enhancing new bone formation. As bioactive glasses are inherently brittle, future research aims at how to improve the design and processing of bioactive glass scaffolds, especially in load-bearing conditions, so as to improve their mechanical reliability. Mechanical properties have always been a limiting factor with both melt-derived and sol-gel glasses. Organic–inorganic hybrid materials, which exhibit bioactive behavior and easy pliability, are being explored as an attempt to overcome this drawback. In the future, for controlling the implant–tissue interface, more sophisticated systems can be developed that address bone tissue regeneration rather than just bone substitution. Finally, there are many other important factors that could play a key role in the development of osteoregenerative bioactive glasses and on which future research should focus, such as the fine control of their chemical composition and the doping with therapeutic metallic ions, the added value of local drug release (for example through an ordered mesoporosity), the careful design of macroporosity and 3-D architecture of glass scaffolds, and the incorporation of osteogenic agents like BMPs.

References

1. Kaur G. Bioactive glasses: potential biomaterials for future therapy. Heidelberg: Springer; 2017.
2. Kaur G, Pandey OP, Singh K, Homa D, Scott B, Pickrell G. A review of bioactive glasses: their structure, properties, fabrication, and apatite formation. J Biomed Mater Res A. 2013;102:254–74.
3. Williams DF. Definitions in biomaterials. In: Progress in biomedical engineering, 4. Amsterdam: Elsevier; 1987.
4. Shah R, Sinanan ACM, Knowles JC, Hunt NP, Lewis MP. Craniofacial muscle engineering using a 3-dimensional phosphate glass fibre construct. Biomaterials. 2005;26:1497–505.
5. Chen QZ, Harding SE, Ali NN, Lyon AR, Boccaccini A. Biomaterials in cardiac tissue engineering: ten years of research survey. Mater Sci Eng R-Rep. 2008;59:1–37.
6. Shin H, Jo S, Mikos AG. Biomimetic materials for tissue engineering. Biomaterials. 2003;24:4353–64.
7. Kaur G, Pickrell G, Sriranganathan N, Kumar V, Homa D. Review and the state of the art: sol-gel or melt quenched bioactive glasses for tissue engineering. J Biomed Mater Res B Appl Biomater. 2016;104(6):1248–75.
8. Arcos D, Regí MV. Sol–gel silica-based biomaterials and bone tissue regeneration. Acta Biomater. 2010;6:2874–88.
9. Albrektsson T, Johansson C. Osteoinduction, osteoconduction and osseointegration. Eur Spine J. 2001;10:S96–101.
10. Minardi S, Corradetti B, Taraballi F, et al. Evaluation of the osteoinductive potential of a bio-inspired scaffold mimicking the osteogenic niche for bone augmentation. Biomaterials. 2015;62:128–37.
11. Park J. Bioceramics: properties, characterizations, and applications. New York: Springer; 2008.

12. Rahaman, et al. Bioactive glass in tissue engineering. Acta Biomater. 2011;7:2355–73.
13. Thamaraiselvi TV, Rajeswari S. Biological evaluation of bioceramic materials – a review. Trends Biomater Artif Organs. 2004;18:9–17.
14. Chevalier J, Gremillard L. Ceramics for medical applications: a picture for the next 20 years. J Eur Ceram Soc. 2009;29:1245–55.
15. Hench LL, West JK. The sol-gel process. Chem Rev. 1990;90:33–72.
16. Hench LL, Wilson J. Introduction to bioceramics. Singapore: World Scientific; 1993.
17. Hench LL, Polak JM. Third generation biomaterials. Science. 2002;295:1014–7.
18. Hench LL, Splinter RJ, Allen WC, Greenlee TK. Bonding mechanisms at the interface of ceramic prosthetic materials. J Biomed Mater Res. 1972;2:117–41.
19. Hench LL. Biomaterials: a forecast for the future. Biomaterials. 1998;19:1419–23.
20. Ramakrishna S, Meyer J, Wintermantel E, Leong KW. Biomedical applications of polymer-composite materials: a review. Comp Sci Tech. 2001;61:1189–224.
21. Williams DF. Consensus and definitions in biomaterials, advances in biomaterials. Amsterdam: Elsevier Science; 1988. p. 11–6.
22. Hench LL. Bioceramics: from concept to clinic. J Am Ceram Soc. 1991;74:1487–510.
23. Ducheyne P, Qiu Q. Bioactive ceramics: the effect of surface reactivity on bone formation and bone cell function. Biomaterials. 1999;20:2287–303.
24. Lu HH, El-Amin SF, Scott KD, Laurencin CT. Three-dimensional, bioactive, biodegradable, polymer-bioactive glass composite scaffolds with improved mechanical properties support collagen synthesis and mineralization of human osteoblast-like cells in vitro. J Biomed Mater Res. 2003;64A:465–74.
25. Kim S-S, Ahn KM, Park MS, Lee J-H, Choi CY, Kim B-S. A poly(lactide coglycolide)/hydroxyapatite composite scaffold with enhanced osteoconductivity. J Biomed Mater Res. 2007;80A:206–15.
26. Day RM, Boccaccini AR, Shurey S, Roether JA, Forbes A, Hench LL, Gabe S. Assessment of polyglycolic acid mesh and bioactive glass for soft tissue engineering scaffolds. Biomaterials. 2004;25:5857–66.
27. Griffith LG. Emerging design principles in biomaterials and scaffolds for tissue engineering. Ann N Y Acad Sci. 2002;961:83–95.
28. Chen QZ, Rezwan K, Armitage D, Nazhat SN, Boccaccini AR. The surface functionalization of 45S5 bioglass®-based glass-ceramic scaffolds and its impact on bioactivity. J Mater Sci-Mater Med. 2006;17(11):979–87.
29. Boccaccini AR, Blaker JJ, Maquet V, Day RM, Jéróme R. Preparation and characterisation of poly(lactide-co-grycolide) (PLGA) and PLGA/bioglass W composite tubular foam scaffolds for tissue engineering applications. Mater Sci Eng C. 2005;25:23–31.
30. Hoppe A, Guldal NS, Boccaccini AR. A review of the biological response to ionic dissolution products from bioactive glasses and glass-ceramics. Biomaterials. 2011;32:2757–74.
31. Sepulveda P, Jones JR, Hench LL. Bioactive sol-gel foams for tissue repair. J Biomed Research A. 2002;49:340–8.
32. Chen QZ, Liang SL, Wang J, Simon GP. Manipulation of mechanical compliance of elastomeric PGS by incorporation of halloysite nanotubes for soft tissue engineering applications. J Mech Behav Biomed Mater. 2011;4:1805–18.
33. Kaur G, Pickrell G, Kimsawatde G, Allbee H, Sriranganathan N. Synthesis, cytotoxicity, and hydroxypatite formation in 27-Tris-SBF for sol-gel based CaO-P2O5-SiO2-B2O3-ZnO bioactive glasses. Sci Rep. 2014; doi:10.1038/srep0439.
34. Kaur G, Sharma P, Kumar V, Singh K. Assesment of in-vitro bioactivity of SiO_2-BaO-ZnO-B_2O_3-Al_2O_3 glasses: an optico-analytical approach. Mater Sci Eng C. 2012;32(7):1941–7.
35. Levenberg S, Langer R. Advances in tissue engineering. Curr Top Dev Biol. 2004;61:113–34.
36. Huang R, Pan J, Boccaccini AR, Chen QZ. A two-scale model for simultaneous sintering and crystallization of glass-ceramic scaffolds for tissue engineering. Acta Biomater. 2008;4:1095–103.

37. Karageorgiou V, Kaplan D. Porosity of 3D biomaterial scaffolds and osteogenesis. Biomaterials. 2005;26:5474–91.
38. Keshaw H, Forbes A, Day RM. Release of angiogenic growth factors from cells encapsulated in alginate beads with bioactive glass. Biomaterials. 2005;26:4171–9.
39. Gatti AM, Valdre G, Andersson OH. Analysis of the in vivo reactions of a bioactive glass in soft and hard tissue. Biomaterials. 1994;15:208–12.
40. Tian H, Tang Z, Zhuang X, Chen X, Jing X. Biodegradable synthetic polymers: preparation, functionalization and biomedical application. Prog Polym Sci. 2012;37:237–80.
41. Zhang Q, Lin D, Yao S. Review on biomedical and bioengineering applications of cellulose sulfate. Carbohydr Polym. 2015;132:311–22.
42. Nettles DL, Chilkoti A, Setton LA. Applications of elastin-like polypeptides in tissue engineering. Adv Drug Deliv Rev. 2010;62:1479–85.
43. Gunatillake PA, Adhikari R. Biodegradable synthetic polymers for tissue engineering. Eur Cells Mater. 2003;5:1–16.
44. Joseph DB. Biomedical engineering fundamentals. 3rd ed. Boca Raton: CRC press; 2006.
45. Gijpferich A. Mechanisms of polymer degradation and erosion. Biomaterials. 1996;17: 103–4.
46. Puppi D, Chiellini F, Piras AM, Chiellini E. Polymeric materials for bone and cartilage repair. Prog Polym Sci. 2010;35:403–40.
47. Ochubiojol EM, Rodrigues A. Starch: from food to medicine. In: Scientific, health and social aspects of the food industry (InTech); 2012.
48. Agrawal CM, Athanasiou KA, Heckman JD. Biodegradable PLA/PGA polymers for tissue engineering in orthopaedica. Mater Sci Forum. 1997;250:115–28.
49. Nelson JF, Stanford HG, Cutright DE. Evaluation and comparison of biodegradable substances as osteogenic agents. Oral Surg. 1977;43:836–43.
50. Temenoff JS, Mikos AG. Injectable biodegradable materials for orthopaedic tissue engineering. Biomaterials. 2000;21:2405–12.
51. Darby WJ. In: Prasad AS, Oberleas D, editors. Trace elements in human health and disease, vol. 1. New York: Academic; 1976. p. 17.
52. Chandra RK. Micronutrients and immune functions: an overview. Ann N Y Acad Sci. 1990;587:9–16.
53. Soetan KO, Olaiya CO, Oyewole OE. The importance of mineral elements for humans, domestic animals and plants: a review. Afr J Food Sci. 2010;4:200–22.
54. Yamaguchi M. Role of zinc in bone formation and bone resorption. J Trace Elem Exp Med. 1998;11:119–35.
55. Lang C, Murgia C, Leong M, Tan L-W, Perozzi G, Knight D, Ruffin R, Zalewski P. Anti-inflammatory effects of zinc and alterations in zinc transporter mRNA in mouse models of allergic inflammation. Am J Phys Lung Cell Mol Phys. 2007;292:L577–84.
56. Cousins RJ. A role of zinc in the regulation of gene expression. Proc Nutr Soc. 1998;57: 307–11.
57. Gunatillake P, Mayadunne R, Adhikari R. Recent developments in biodegradable synthetic polymers. Biotechnol Annu Rev. 2006;12:301–47.
58. Kohane DS, Langer R. Polym Biomater Tissue Eng Pediatr Res. 2008;63:487–91.
59. B.B. Nissan, Advances in calcium phosphate biomaterials, Springer series in biomaterials science and engineering. Springer; 2014. p. 535.
60. Hayakawa S, Tsuru K, Iida H, Ohtsuki C, Osaka A. MAS-NMR studies of Apatite Formation on 50CaO·50SiO2 Glass in a simulated body fluid. Phys Chem Glasses. 1996;37(5): 188–92.
61. Mandel S, Cuneyt Tas A. Brushite ($CaHPO_4{\cdot}2H_2O$) to octacalcium phosphate ($Ca8(HPO_4)2(PO_4)4{\cdot}5H_2O$) transformation in DMEM solutions at 36.5 °C. Mater Sci Eng C. 2010;30:245–54.
62. Ryu H-S, Youn H-J, Hong KS, Chang B-S, Lee C-K, Chung S-S. An improvement in sintering property of b-tricalcium phosphate by addition of calcium pyrophosphate. Biomaterials. 2002;23:909–14.

63. Jones JR. Review of bioactive glass: from Hench to hybrids. Acta Biomater. 2013;9: 4457–86.
64. Porter AE, Patel N, Skepper JN, Best SM, Bonfield W. Comparison of in vivo dissolution processes in hydroxyapatite and silicon-substituted hydroxyapatite bioceramics. Biomaterials. 2003;24:4609–20.
65. JunWang Y, Lai C, Wei K, Chen X, Ding Y, Wang ZL. Investigations on the formation mechanism of hydroxyapatite synthesized by the solvothermal method. Nanotechnology. 2006;17: 4405–12.
66. Gross KA, Berndt CC, Herman H. Amorphous phase formation in plasma-sprayed hydroxyapatite coatings. J Biomed Mater Res. 1998;39:407.
67. Ragel CV, Vallet-Regi M, Rodriguez-Lorenzo LM. Preparation and in vitro bioactivity of hydroxyapatite/solgel glass biphasic material. Biomaterials. 2002;23:1865–72.
68. Tardei C, Grigore F, Pasuk I, Stoleriua S. The study of Mg2+/Ca2+ substitution of β -tricalciumphosphate. J Optoelectr Adv Mater. 2006;8(2):568–71.
69. Schwarz K. A bound form of silicon in glycosaminoglycans and polyuronides. Proc Natl Acad Sci U S A. 1973;70:1608–12.
70. Marie PJ, Ammann P, Boivin G, Rey C. Mechanisms of action and therapeutic potential of strontium in bone. Calcif Tissue Int. 2001;69:121–9.
71. Wong CT, Chen QZ, Lu WW, Leong JCY, Chan WK, Cheung KMC, Luk KDK. Ultrastructural study of mineralization of a strontium-containing hydroxyapatite (Sr-HA) cement in vivo. J Biomed Mater Res A. 2004;70A:428–35.
72. Denrya I. Liisa T. Kuhn design and characterization of calcium phosphate ceramic scaffolds for bone tissue engineering. Dent Mater. 2016;32:43–53.
73. Chan BP, Leong KW. Scaffolding in tissue engineering: general approaches and tissue-specific considerations. Eur Spine J. 2008;17(Suppl 4):467–79.
74. Jaklenec A, Hinckfuss A, Bilgen B, Ciombor DM, Aaron R, Mathiowitz E. Sequential release of bioactive IGF-I and TGF-b1 fromPLG microsphere-based scaffolds. Biomaterials. 2008;29:1518–25.
75. Gentile P, Bellucci D, Sola A, Matt C, Cannillo V, Ciardelli G. Composite scaffolds for controlled drug release: role of the polyurethane nanoparticles on the physical properties and cell behavior. J Mech Behav Biomed Mater. 2015;44:53–60.
76. Larrañaga A, Diamanti E, Rubio E, Palomares T, Alonso-Varona A, Aldazabal P, Martin FJ, Sarasua JR. A study of themechanical properties and cytocompatibility of lactide and caprolactone based scaffolds filled with inorganic bioactive particles. Mater Sci Eng C. 2014;42: 451–60.
77. Bellucci D, Sola A, Cannillo V. Bioactive glass-based composites for the production of dense sintered bodies and porous scaffolds. Mater Sci Eng C Mater Biol Appl. 2013;33:2138–51.
78. Williams JM, Adewunmi A, Schek RM, Flanagan CL, Krebsbach PH, Feinberg SE, et al. Bone tissue engineering using polycaprolactone scaffolds fabricated via selective laser sintering. Biomaterials. 2005;26:4817–27.
79. Schwartz I, Robinson BP, Hollinger JO, Szachowicz EH, Brekke J. Calvarial bone repair with porous D,L-polylactide. Otolaryngol Head Neck Surg. 1995;112:707–13.
80. Blaker J, Maquet V, Jérome R, Boccaccini AR, Nazhat SN. Mechanical properties of highly porous PDLLA/bioglass composite foams as scaffolds for bone tissue engineering. Acta Biomater. 2005;1:643–52.
81. Kikuchi M, Koyama Y, Yamada T, Imamura Y, Okada T, Shirahama N, et al. Development of guided bone regeneration membrane composed of [beta]-tricalcium phosphate and poly(–lactide-coglycolide-co-caprolactone) composites. Biomaterials. 2004;25:5979–86.
82. Ma PX. Tissue engineering. In: Kroschwitz JI, editor. Encyclopedia of polymer science and technology, vol. 12. New York: Wiley; 2004. p. 261–91.
83. Yagmurlu MF, Korkusuz F, Guersel I, Korkusuz P, Ors U, Hasirci V. Sulbactam-cefoperazone polyhydroxybutyrate-co-hydroxyvalerate (PHBV) local antibiotic delivery system: in vivo effectiveness and biocompatibility in the treatment of implant-related experimental osteomyelitis. J Biomed Mater Res. 1999;46:494–503.

84. Zhang X, Wyss UP, Pichora D, Goosen MF. Biodegradable controlled antibiotic release devices for osteomyelitis: optimization of release properties. J Pharm Pharmacol. 1994;46: 718–24.
85. Zhang X, Wyss UP, Pichora D, Goosen MFA. Amechanistic study of antibiotic release from biodegradable poly (d, 1-lactide)cylinders. J Control Release. 1994;31:129–44.
86. Kaur G, Pickrell G, Pandey OP, Singh K, Chudasama BN, Kumar V. Combined and individual doxorubicin/vancomycin drug loading, release kinetics and apatite formation for the CaO-CuO-P_2O_5- SiO_2- B_2O_3 mesoporous glasses. RSC Adv. 2016;6:51046–56.
87. Wu, Chang J. Interface Focus. 2012;2:292–306.
88. Massaro M, Colletti CG, Noto R, Riela S, Poma P, Guernelli S, Parisi F, Milioto S, Lazzara G. Int J Pharm. 2015;478:476–85.
89. Massaro M, Amorati R, Cavallaro G, Guernelli S, Lazzara G, Milioto S, Noto R, Poma P, Riela S. Colloids Surf B: Biointerfaces. 2016;140:505–13.
90. Soundrapandiana C, Mahatob A, Kundu B, Datta S, Sac B, Basu D. Development and effect of different bioactive silicate glass scaffolds: in vitro evaluation for use as a bone drug delivery system. J Mech Behav Biomed Mater. 2014;40:1–12.
91. Murphy WL, Peters MC, Kohn DH, Mooney DJ. Sustained release of vascular endothelial growth factor from mineralized poly(lactide-co-glycolide) scaffolds for tissue engineering. Biomaterials. 2000;21(24):2521–7.
92. Baino F, Novajra G, Miguez-Pacheco V, Boccaccini AR, Vitale-Brovarone C. Bioactive glasses: special applications outside the skeletal system. J Non-Cryst Solids. 2016;432:15–30. doi:10.1016/j.jnoncrysol.2015.02.015.
93. Miguez-Pacheco V, Hench LL, Boccaccini AR. Bioactive glasses beyond bone and teeth: emerging applications in contact with soft tissues. Acta Biomater. 2015;13:1–15. doi:10.1016/j.actbio.2014.11.004.
94. Rosenqvist K, Airaksinen S, Vehkamäki M, Juppo AM. Evaluating optimal combination of clodronate and bioactive glass for dental application. Int J Pharm. 2014;468:112–20.
95. Bakry AS, Takahashi H, Otsuki M, Sadr A, Yamashita K, Tagami J. CO_2 laser improves 45S5 bioglass interaction with dentin. J Dent Res. 2011;90(2):246–50.
96. Bakry AS, Takahashid H, Otsukie M, Tagamie J. Evaluation of new treatment for incipient enamel demineralization using 45S5 bioglass. Operat Dent Mater. 2014;30:314–20.
97. Baino F, Vitale-Brovarone C. Bioceramics in ophthalmology. Acta Biomater. 2014;10: 3372–97.
98. Kinnunen I, Aitasalo K, Pollonen M, Varpula M. Reconstruction of orbital fractures using bioactive glass. J Cranio-Maxillofac Surg. 2000;28:229–34.
99. Aitasalo K, Kinnunen I, Palmgren J, Varpula M. Repair of orbital floor fractures with bioactive glass implants. J Oral Maxillofac Surg. 2001;59:1390–6.
100. Linnola RJ, Happonen RP, Andersson OH, Vedel EA, Yli-Urpo U, Krause U, et al. Titanium and bioactive glass-ceramic coated titanium as materials for keratoprosthesis. Exp Eye Res. 1996;63:471–8.
101. Peltola M, Kinnunen I, Aitasalo K. Reconstruction of orbital wall defects with bioactive glass plates. J Oral Maxillofac Surg. 2008;66:639–46.
102. Chirila TV. An overview of the development of artificial corneas with porous skirts and the use of PHEMA for such an application. Biomaterials. 2001;22:3311–7.
103. Renghini C, Giuliani A, Mazzoni S, Brun F, Larsson E, Baino F, et al. Microstructural characterization and in vitro bioactivity of porous glass ceramic scaffolds for bone regeneration by synchrotron radiation X-ray microtomography. J Eur Ceram Soc. 2013;33:1553–65.
104. Tulyaganova DU, Reddy AA, Siegelc R, Ionescud E, Riedeld R, Ferreira JMF. Synthesis and in vitro bioactivity assessment of injectable bioglass-organic pastes for bone tissue repair. Ceram Int. 2015;41:9373–82.
105. Tulyaganov DU, Agathopoulos S, Valerio P, Balamurugan A, Saranti A, Karakassides MA, Ferreira JM. Synthesis, bioactivity and preliminary biocompatibility studies of glasses in the system CaO–MgO–SiO2–Na2O–P2O5–CaF2. J Mater Sci Mater Med. 2011;22:217–27.

106. Tulyaganov DU, Makhkamov ME, Urazbaev A, Goel A, Ferreira JMF. Synthesis, processing and characterization of a bioactive glass composition for bone regeneration. Ceram Int. 2013;39:2519–26.
107. Fu Q, Saiz E, Rahaman MN, Tomsia AP. Bioactive glass scaffolds for bone tissue engineering: state of the art and future perspectives. Mater Sci Eng C. 2011;31:1245–56.
108. Bellucci D, Cannillo V, Sola A. Calcium and potassium addition to facilitate the sintering of bioactive glasses. Mater Lett. 2011;65:1825–7.
109. Idowu B, Cama G, Deb S, DiSilvio L. In vitro osteoinductive potential of porous monetite for bone tissue engineering. J Tissue Eng. 2014;5:1–14.
110. Thomson RC, Yaszemski MJ, Power JM, Mikos AG. Hydroxyapatite fiber reinforced poly(α-hydroxy ester) foams for bone regeneration. Biomaterials. 1998;19:1935–43.
111. Roether JA, Boccaccini AR, Hench LL, Maquet V, Gautier S, Jérome R. Development and in vitro characterization of novel bioresorbable and bioactive composite materials based on polylactide foams and bioglassfor tissue engineering applications. Biomaterials. 2002;23:3871–8.
112. Gerhardt L-C, Widdows KL, Erol MM, Burch CW, Sanz-Herrera JA, Ochoa I, et al. The pro-angiogenic properties of multi-functional bioactive glass composite scaffolds. Biomaterials. 2011;32(17):4096–108.
113. Wilson J, Pigott GH, Schoen FJ, Hench LL. J Biomed Mater Res. 1981;15(6):805–17.
114. Gorustovich AA, Roether JA, Boccaccini AR. Effect of bioactive glasses on angiogenesis: a review of in vitro and in vivo evidences. Tiss Eng B Rev. 2010;16(2):199–207. doi:10.1089/ten.TEB.2009.0416.
115. Li H, Chang J. Bioactive silicate materials stimulate angiogenesis in fibroblast and endothelial cell co-culture system through paracrine effect. Acta Biomater. 2013;9(6):6981–91.
116. Day RM. Bioactive glass stimulates the secretion of angiogenic growth factors and angiogenesis in vitro. Tissue Eng. 2005;11(5):768–77. doi:10.1089/ten.2005.11.768.
117. Kent Leach J, Kaigler D, Wang Z, Krebsbach PH, Mooney DJ. Coating of VEGF-releasing scaffolds with bioactive glass for angiogenesis and bone regeneration. Biomaterials. 2006;27(17):3249–55. doi:10.1016/j.biomaterials.2006.01.033.
118. Murphy WL, Simmons CA, Kaigler D, Mooney DJ. Bone regeneration via a mineral substrate and induced angiogenesis. J Dent Res. 2004;83:204–10.
119. Leu A, Leach JK. Pharm Res. 2008;25:1222.
120. Haro Durand L, Vargas GE, Romero NM, Vera-Mesones R, Porto-López JM, Boccaccini AR, Gorustovich A. Angiogenic effects of ionic dissolution products released from a boron-doped 45S5 bioactive glass. J Mater Chem B. 2015;3(6):1142–8. doi:10.1039/C4TB01840K.
121. Ghosh SK, Nandi SR, Rumdu B, Datta S, De DK, Roy SR, Baseu D, Biomed J. Mater Res Part B. 2008;86B:217.
122. Andrade AL, Andrade SP, Domingues RZ, Biomed J. Mater Res B. 2006;79B:122.
123. Lin Y, Brown RF, Jung SB, Day DE, Biomed J. Mater Res A. 2014;102:4491–9.
124. Mahmood J, Takita H, Ojima Y, Kobayshi M, Kohgo T, Kubole Y. J Biochem. 2001;129:163.
125. Ma W, Yang X, Ma L, Wang X, Zhang L, Yang G, et al. Fabrication of bioactive glass-introduced nanofibrous membranes with multifunctions for potential wound dressing. RSC Adv. 2014;4(104):60114–22. doi:10.1039/C4RA10232K.
126. Wray P. Cotton candy that heals. Am Ceram Sec Bull. 2011;90.4:24–31.
127. Cong M, Lin C, Chen X. Enhanced healing of full-thickness diabetic wounds using bioactive glass and Yunnan baiyao ointments. J Wuhan Univ Technol Mat Sci Ed. 2014;29(5):1063–70. doi:10.1007/s11595-014-1044-y.
128. Lin C, MaO C, Jhang J, Li Y, Chen X. Healing effect of bioactive glass moment on full thickness skin wounds. Biomed Mater. 2012;7(4):045017.
129. Yang Q, Chen S, Shi H, Xiao H, Ma Y. In vitro study of improved wound-healing effect of bioactive borate-based glass nano−/micro-fibers. Mater Sci Eng C. 2015;55:105–17. doi:10.1016/j.msec.2015.05.049.

130. Gillette RL, Swaim SF, Sartin EA, Bradley DM, Coolman SL. Am J Vet Res. 2001;62(7): 1149–53.
131. Li H, He J, Yu H, Green CR, Chang J. Bioglass promotes wound healing by affecting gap junction connexin 43 mediated endothelial cell behavior. Biomaterials. 2016;84:64–75. doi:10.1016/j.biomaterials.2016.01.033.
132. Rai R, Boccaccini AR. ATP Conf Proc. 2010;1255:126–8.
133. Zhao S, Li L, Wang H, Zhang Y, Cheng X, Zhou N, et al. Wound dressings composed of copper-doped borate bioactive glass microfibers stimulate angiogenesis and heal full-thickness skin defects in a rodent model. Biomaterials. 2015;53:379–91. doi:10.1016/j.biomaterials.2015.02.112.
134. Yunos DM, Bretcanu O, Boccaccini A. Polymer– bioceramic composites for tissue engineering scaffolds. J Mater Sci Mater Med. 2008;43:4433–42.
135. Domingues ZR, Cortes ME, Gomes TA, Diniz HF, Freitas CS, Gomes JB, Faria AMC, Sinisterra RD. Bioactive glass as a drug delivery system of tetracycline and tetracycline associated with β-cyclodextrin. Biomaterials. 2004;25:327–33.
136. Czarnobaj K. Preparation and characterization of silica xerogels as carriers for drugs. Drug Deliv. 2008;15:485–92.
137. Merchant HA, Shoaib HM, Tazeen J, Yousuf RI. Once- daily tablet formulation and in vitro release evaluation of cefpodoxime using hydroxypropyl methylcellulose: a technical note. AAPS Pharm Sci Tech. 2006;7
138. Bang H-G, Kim S-J, Park S-Y. Biocompatibility and the physical properties of bio-glass ceramics in the Na2O–CaO– SiO2–P2O5 system withCaF2 and MgF2 additives. J Ceram Proc Res. 2008;9:588–90.
139. Xia W, Chang J. Well-ordered mesoporous bioactive glasses (MBG): a promising bioactive drug delivery system. J Control Release. 2006;110:522–30.
140. Kundu B, Soundrapandian C, Nandi SK, Mukherjee P, Dandapat N, Roy S, Datta BK, Mandal TK, Basu D, Bhattacharya RN. Development of new localized drug delivery system based on ceftriaxone-sulbactam composite drug impregnated porous hydroxyapatite: a systematic approach for in vitro and in vivo animal trial. Pharm Res. 2010;27:1659–76. Leng, Y., Xin, R.,
141. Noble L, Gray AI, Sadiq L, Uchegbu IF. A non-covalently cross-linked chitosan based hydrogel. Int J Pharm. 1999;192:173–82.
142. Catauro M, Raucci MG, De Gaetano F, Marotta A. Antibacterial and bioactive silver-containing Na2O_CaO_2SiO2 glass prepared by sol–gel method. J Mater Sci Mater Med. 2004;15:831–7.
143. Ragel CV, Vallet-Regí M. In vitro bioactivity and gentamicin release from glass–polymer-antibiotic composites. J Biomed Mater Res. 2000;51:424–9.
144. Arcos D, Ragel CV, Vallet-Regi M. Bioactivity in glass/PMMA composites used as drug delivery system. Biomaterials. 2001;22:701–8.
145. Ladrón de Guevara S, Ragel CV, Vallet-Regí M. Bioactive glass–polymer materials for controlled release of ibuprofen. Biomaterials. 2003;24:4037–43.
146. Arcos D, Peña J, Vallet-Regí M. Influence of a SiO2–CaO–P2O5 sol–gel on the bioactivity and controlled release of a ceramic/polymer/antibiotic mixed materials. Chem Mater. 2003;15:4132–8.
147. Arcos D, del Real RP, Vallet-Regí M. A novel bioactive and magnetic biphasic material. Biomaterials. 2002;23:2151–8.
148. Ruiz E, Serrano MC, Arcos D, Vallet-Regí M. Glass–glass ceramic thermoseeds for hyperthermic treatment of bone tumours. J Biomed Mater Res. 2006;79A:533–43.
149. Serrano MC, Portoles MT, Pagani R, Sáez de Guinoa J, Ruíz-Fernández E, Arcos D, et al. In vitro positive biocompatibility evaluation of glass–glass ceramic thermoseeds for hyperthermic treatment of bone tumours. Tissue Eng. 2008;14:617–27.
150. Ragel CV, Vallet-Regí M, Rodríguez-Lorenzo LM. Preparation and in vitro bioactivity of hydroxyapatite/solgel-glass biphasic material. Biomaterials. 2002;23:1865–72.

151. Vallet-Regí M, Rámila A, Padilla S, Muñoz B. Bioactive glasses as accelerators of the apatites bioactivity. J Biomed Mater Res. 2003;66:580–5.
152. Vallet-Regí M. Revisiting ceramics for medical applications. Dalton Trans. 2006;44: 5211–20.
153. Vallet-Regí M, Balas F, Arcos D. Mesoporous materials for drug delivery. Angew Chem Int Ed. 2007;46:7548–58.
154. López-Noriega A, Arcos D, Izquierdo-Barba I, Sakamoto Y, Terasaki O, Vallet-Regí M. Ordered mesoporous bioactive glasses for bone tissue regeneration. Chem Mater. 2006;18: 3137–44.

Chapter 2
Variation in Properties of Bioactive Glasses After Surface Modification

Vojislav Stanić

Abstract Surface modification is one of the most effective ways to improve properties of biomaterials for specific applications in medicine, dentistry, pharmacology, and biotechnology. The surface properties of biomaterials play a significant role in the interaction with the surrounding tissues. This chapter is mainly focused on bioactive silicate glasses, in the following three aspects: (1) ion doping glass, (2) covalent modification of a bioactive glass's surfaces by silanes, and (3) biological surface functionalization of bioactive glass. The incorporation of various ions in the structure of bioactive glasses can improve their bioactivity, stimulating effects on osteogenesis, angiogenesis, and antibacterial activity. The goal of covalent modification by silanes is to improve the interaction with the surrounding bone tissue, to enhance dispersion stability of inorganic particles in various liquids, or to act as anchors for the immobilization of drugs. Biological functionalization of bioactive glasses can improve their bone integration.

Keywords Bioactive glasses • Biomaterials • Surface modification • Silinization • Bone

2.1 Introduction

Bioactive glasses have been widely investigated as biomaterials in medicine and stomatology for hard tissue substitution. Hench and co-workers first made bioactive silicate glasses by melt quenching of chemical composition: 45% SiO_2, 24.5% CaO, 24.5% Na_2O, and 6% P_2O_5 in weight percent, denoted Bioglass® 45S5 [1]. Bioactive materials are surface active and form a stable bond with round hard and soft tissues: muscle and tendons (Class A) or to hard tissues only (Class B) [2, 3]. Class A biomaterials such as bioactive glasses showed rapid bonding to the bone and enhanced bone proliferation. Most calcium-phosphate biomaterials such as synthetic hydroxyapatite are an example of a Class B material; the bonding rate to the bone is slow

V. Stanić (✉)
University of Belgrade, Vinca Institute of Nuclear Sciences,
P.O. Box 522, 11001 Belgrade, Serbia
e-mail: voyo@vin.bg.ac.rs

G. Kaur (ed.), *Clinical Applications of Biomaterials*,
DOI 10.1007/978-3-319-56059-5_2

with no enhancement of bone proliferation. Surfaces of bioactive glasses represent the site of interaction with the surrounding living tissues and are therefore crucial to enhance their biological performance. The bioactivity of a glass is usually evaluated by its ability to form a hydroxycarbonate apatite (HCA) layer on its surface upon immersion in SBF. HCA is very similar to the mineral component of the bone; its presence on the glass surface promotes further attachment of biomolecules, cells, and tissue growth factors, which then favor the development of bonds with surrounding tissues and the creation of new tissue. The bioactivity of glasses depends on its network structure, chemical composition, particle size, surface area, and textural properties (pore size, pore volume, pore structure) and various organic compounds present in their composites. The surface modification of bioactive glasses should be viewed in several aspects: improving bioactivity; binding of biomolecules; binding, proliferation, and differentiation of cells; delivery of drugs, cytotoxicity; antimicrobial properties, and diagnosis, monitoring, and control of disease.

The mechanism of bonding silicate bioactive glasses to the bone has been attributed to the formation of a carbonate-substituted hydroxy apatite (HCA)-like layer on the glass surface in contact with the body fluid. The mechanism of HCA layer formation on bioactive glasses has been widely studied in vitro [4–6]. This process is complex and can be simplified to be shown through sequence of various stages (Table 2.1).

Some of these stages are played out partly in parallel, such as 6 and 7 with stages 3–5 [7]. The initial stages (1 and 2) involve the partial dissolution of the bioactive glass after contact with the body fluid or simulated body fluids (SBF), with substitutions of Na + and Ca2+ with H+ ions and the pH increase of solution (Eq. 2.1) [4, 7].

$$\mathrm{Si-ONa + H^{+}_{(aq)} \rightarrow Si-OH + Na^{+}_{(aq)}} \tag{2.1}$$

Table 2.1 Stages of interfacial reactions between bioactive glass and surrounding bone tissue

LogT (hour)	Surface reaction stages	
	1 and 2	Exchange of Na^+ ions with H^+ ions leads to formation of silanol groups (Si–OH)
		Network dissolution: formation of Si–OH groups and release of $Si(OH)_4$
	3	Polycondensation of silanol groups
1	4	Formation of amorphous $CaO–P_2O_5$
2	5	Crystallization of hydroxycarbonate apatite (HCA)
10	6	Adsorption of biological moieties in HCA layer
	7	Action of macrophages
20	8	Attachment of osteoblast stem cells
	9	Differentiation and proliferation of osteoblasts
	10	Generation of matrix
	11	Crystallization of matrix and growth of the bone
100	12	Proliferation of the bone

As a result, this leads to network degradation by breaking the Si–O–Si bonds, formation of Si–OH groups, and release of $Si(OH)_4$ and larger silicate fragments (stage 2, Eq. 2.2).

$$Si-O-Si+H_2O \rightarrow Si-OH+Si-OH \tag{2.2}$$

The continuous formation of silanol groups results (three stages) in their polycondensation and formation of a porous silica-rich layer. Fourth, creating an amorphous $CaO–P_2O_5$-rich film with a low Ca/P atomic ratio on the surface of the silica-rich layer results from the liberated Ca^{2+} and PO_4^{3-} ions from the glass and from a solution. The silica-rich layer has high density of surface silanol (Si–OH) groups, which are essential as nucleation centers for the precipitation of calcium phosphate. The formation of an amorphous calcium silicate and an amorphous calcium phosphate is the result of electrostatic interactions between the Si–OH groups on the glass surface and the calcium and phosphate ions in a solution [4]. The bioactivity of Na-free and P-free silicate glasses comes from the hydrated silica-rich layer [6, 8, 9]. Fifth, the amorphous calcium phosphate further increased its Ca/P atomic ratio, incorporating OH− and CO_3^{2-} anions from the solution and crystallized into hydroxycarbonate apatite (HCA). The crystallization of amorphous calcium phosphate into crystalline HCA can be explained by the increase in its stability. Apatite minerals are the most thermodynamically stable and have a lower solubility in water than any other calcium phosphates [10, 11]. In parallel with chemical reactions in the HCA layer, cellular stages 6–12 occur, such as action of macrophages, adsorption, and desorption of proteins, growth factors, and collagen which triggers proliferation and differentiation of cells and the creation of osteoblasts, thus encouraging bone growth on the surface glass [12]. Osteoblast cells create an extracellular matrix, which mineralizes to form a nanocrystalline mineral and collagen on the surface of the glass implant, while the degradation and conversion of the glass continue over time [12, 13]. These stages are very complex and not fully clarified.

2.2 Glass Structure

Bioactive glasses (BG) are built from glass formers, network modifiers, and intermediate oxides. The primary glass formers (network formers) in bioactive glasses are silica (SiO_2), boric acid (B_2O_3), and phosphoric oxide (P_2O_5), which can form single-component glasses. The generic name of glass is generally derived from its network former. Bioactive silicate glasses are amorphous solids. The basic building unit of silicate glasses is the SiO_4 tetrahedron in a network, which is interconnected in a network through Si–O–Si bonds, commonly referred to as bridging oxygen atoms [14]. These tetrahedra are commonly referred to as Q^n units, where "n" represents the number of bridging oxygens per tetrahedron (Fig. 2.1).

The network modifiers (Na^+, K^+, Ca^{2+}, etc.) provoke, during the synthesis, the disruption of the continuity of the glassy network, due to the breaking of some of

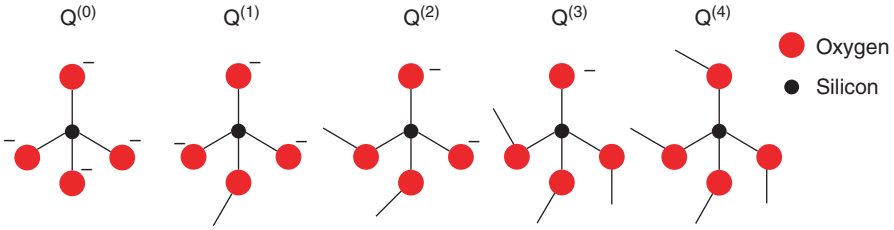

Fig. 2.1 Silica tetrahedral sites of silicate glasses

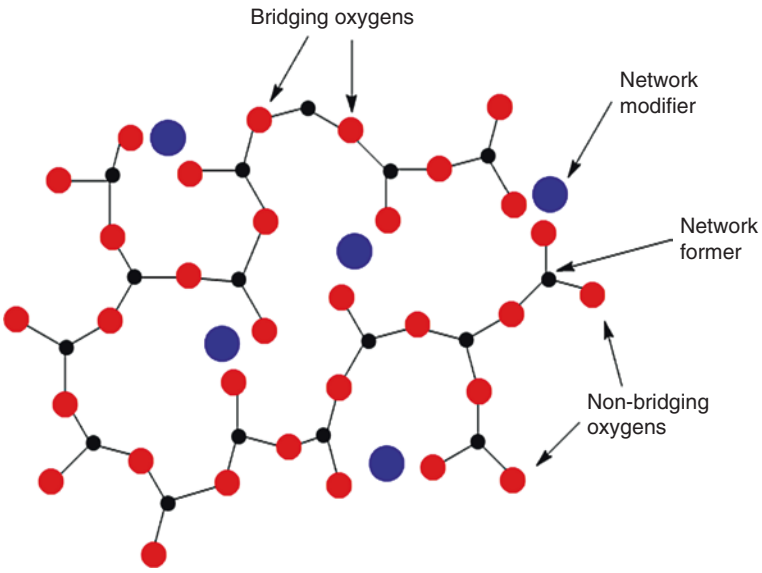

Fig. 2.2 2D presentation of random glass network modifiers and network formers

the Si–O–Si bonds leading to the formation of non-bridging oxygen groups (Fig. 2.2). The properties of bioactive silicate glasses are, to a large extent, influenced by a portion of non-bridging oxygen atoms. Network modifiers are often necessary to modify the properties of the glass. The intermediate oxides (ZnO and MgO) can act as typical network formers and modifiers [14].

Borate Bioactive Glasses

The major glass former in bioactive borate glasses is B_2O_3 and possesses a more complex structure due to a greater number of building blocks [15]. Some structural elements of borate glasses are shown in Fig. 2.3 [15, 16]. Borate glass structure can be built of trigonal planar BO_3 and/or tetrahedral BO_4 units. Adding metal oxides to borate glass comes to the crossing of planar into tetrahedral units, resulting in a higher degree of network connectivity. Non-bridging oxygen atoms are formed when the content of metal-doped ions is high.

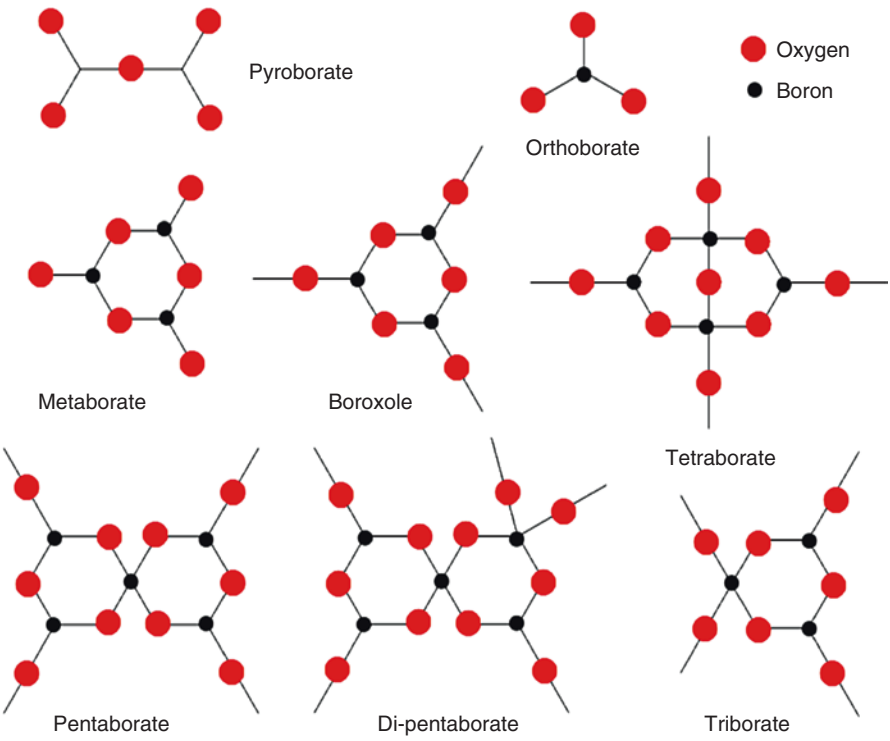

Fig. 2.3 The network units of borate glasses

Borate glasses are very reactive and have lower chemical durability; hence, they can convert faster and more completely to hydroxyapatite (HAp) in an aqueous phosphate solution, when compared to silica counterparts. Huang et al. [17] studied the formation of HAp, in a dilute phosphate solution, during the conversion of partial and full replacement of SiO_2 content in 45S5 glass with B_2O_3. The glasses with higher B_2O_3 content produced a more rapid conversion to HAp and a lower pH value of the phosphate solution. The borate glass was fully converted to HAp in less than 4 days, while silicate and borosilicate compositions were partially converted after 70 days and contained residual SiO_2 in a Na-depleted core. The borate glasses, unlike silicate glasses, form HCA directly on the surface without forming a borate-rich layer. For the borosilicate glasses, a conversion mechanism is similar to that of silicate 45S5 glass. A similar study was performed subsequently by Fu et al. [18] for 13–93 bioactive glass. This study showed the conversion rate of the scaffolds to HAp in the SBF increased with the B_2O_3 content of the glass. In vitro studies showed that on the surface of some borate glasses comes to attachment, proliferation, and differentiation of cells, while in vivo they are reported to enhance tissue infiltration [19–24]. Brown et al. [25] reported that glasses with higher B_2O_3 content showed an increase conversion rate to HAp, but also resulted in a greater inhibition of cell proliferation under static culture conditions. Boron compounds such as borax and

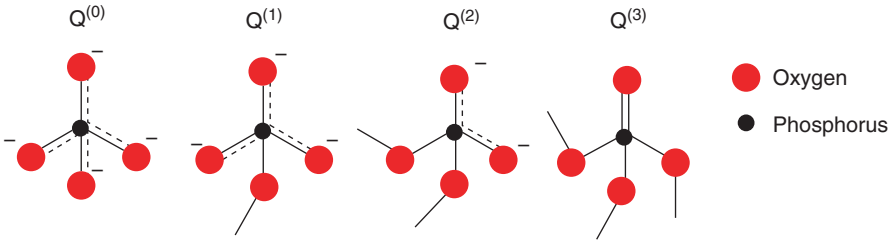

Fig. 2.4 Phosphate tetrahedral sites that can exist in phosphate glasses

boric acid in high concentrations are toxic [26]. The borosilicate scaffolds containing 12.5 wt% B_2O_3 showed cytocompatibility to a stromal cell line (ST2) [27].

Phosphate Bioactive Glasses

Phosphate glasses consist of P_2O_5 as the network former oxide and CaO and Na_2O as modifiers. The chemical composition of phosphate glasses is similar to the inorganic phase of the bone. These glasses have great potential as biomaterials because they are completely biodegradable and nontoxic [28]. Compared to silicate glasses, phosphate glasses have relatively poor chemical durability which durability limits their use in tissue engineering [29]. The solubility of phosphate glasses decreases with the increase of CaO content [30]. The basic building blocks of glasses are the P-tetrahedra, similar to those in silicate glasses [31]. The tetrahedra in the glass structure are interconnected through covalent bridging to form various phosphate anions (Fig. 2.4).

2.3 Ion-Doped Bioactive Silicate Glasses

In recent years, bioactive glasses are modified with a variety of trace elements such as Cu, Zn, Sr, and others. Many of these ions are essential or nonessential. Many nonessential metal ions are used for therapeutic purposes or are subject to various biological examination. These ions in bioactive glasses can cause changes in the crystal structure, specific surface, thermal stability, morphology, solubility, and chemical and biological properties. These trace elements have been found to play absolutely vital roles in the formation, growth, and repair of the bone.

Various studies have also demonstrated that the addition of trace elements to bioactive glasses materials can lead to controlled degradation and increase in mechanical strength of the materials and positively influence the biological response. Incorporation of various metallic dopants into the structure of bioactive glass (BG) can be made predominantly by methods of direct synthesis and sorption of ions from the solution. Doping of metal ions into the structure of BG by direct synthesis provides a greater amount and a more uniform distribution of ions over the entire volume.

The most common methods for the production of bioactive glass materials are melt-quenching routes and the sol-gel technique. The schematic illustration of melt-quenching and of sol-gel processes is shown in Fig. 2.5.

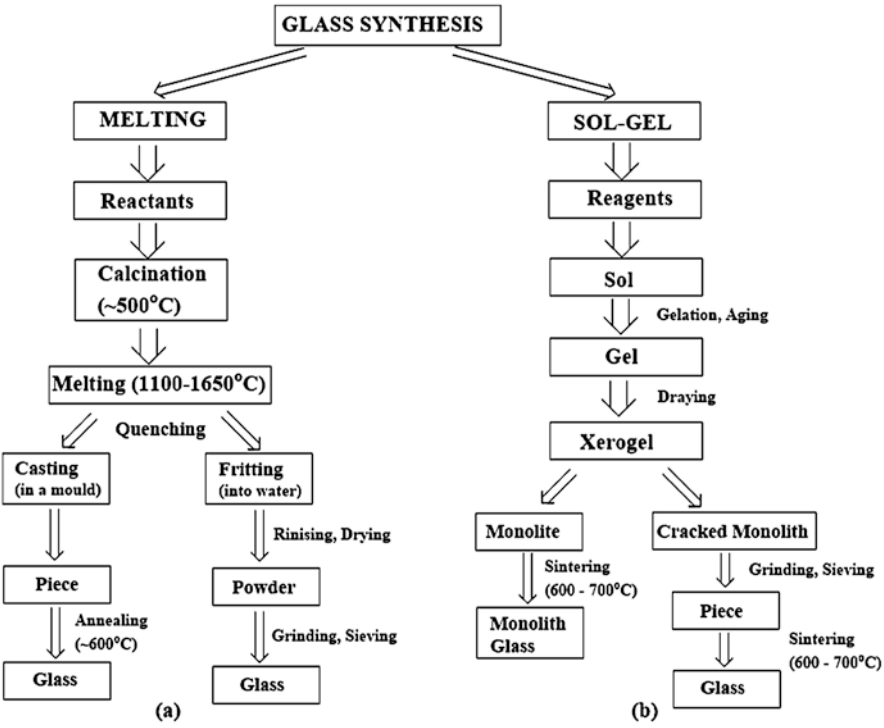

Fig. 2.5 Schematic view of the preparation route for (**a**) melt quench and (**b**) sol-gel bioactive glasses

The melt-quenching method is based on melting a heterogeneous reactant mixture in a specified molar ratio. The reaction mixture calcined at about 500 °C to remove moisture, which is adsorbed onto the precursor materials or may be formed by dehydration of hydroxides [15, 32]. Additionally, there comes to the release of gases caused by decomposition of the possibly present precursors: carbonate, nitrate, and sulfate. Oxides are mainly used as precursors. The melting temperature (1,100–1,650 °C) is above the glass transition temperature (Tg) of the target bioactive glasses, to afford a viscous state. The Tg of the BG is lower than its crystallization temperature (Tc) at which that leads to the formation of glass-ceramics. The glasses are often melted twice in order to increase homogeneity. In order to prevent evaporation of individual components: alkalis, boron, phosphorus, and fluorides, melting is carried out in covered crucibles [2]. The molten glass is then cast into a preheated graphite or steel molds to make bulk implants or is immersed in water which is used for quenching. The sol-gel method is most applied in the synthesis of bioactive glasses. This method may prepare materials in various forms: nanoparticles, thin film coatings, microporous, monoliths, and aerogel materials. Sol-gel process involves the transition of the colloidal solution (sol) into a solid phase (gel). Gel can be described as a three-dimensional solid skeleton surrounded by a liquid phase,

where both phases are continuous and nanometer dimensions. The gelation process is achieved by reactions of hydrolysis (Eq. 2.3) and condensation (Eqs. 2.4 and 2.5).

$$M(OR)n + xH_2O = M(OR)n - x(OH)x + xROH \tag{2.3}$$

$$-M-OH + HO-M- = -M-O-M- + H_2O \tag{2.4}$$

$$-M-OH + R-O-M- = -M-O-M- + R-OH \tag{2.5}$$

These reactions can occur very slowly at ambient temperatures so that they are added to acidic or basic catalysts for their acceleration. The gelation phase is followed by a drying process, in which the solvent is removed from the gel and forms a solid, porous matrix called xerogel. The resulting xerogel is heat-treated in order to obtain the final product. Annealing process frequently leads to agglomeration and coarsening of nanoparticles. The properties of the obtained material are affected by many factors that influence the rate of hydrolysis and condensation, such as pH value, temperature, reaction time, concentration of reagents, the type and concentration of the catalyst, temperature, and time of aging and drying. The advantages of the sol-gel method are the low-temperature processing, the purity and homogeneous distribution of the components, higher porosity and specific surface area values, and the possibility of particle size control [33]. Increasing the specific surface area and pore volume of bioactive glasses greatly accelerates its dissolution and HCA formation on the surface and therefore enhances the bioactive behavior. The porosity of ~90% and pore size of >100 μm are desirable, as well as high pore interconnectivity being important for the formation of bone tissue, enabling the migration and proliferation of osteoblasts and mesenchymal cells, vascularization, and nutrient delivery to the newly formed tissue [34, 35]. In addition, the porous surface promotes mechanical coupling between the implanted biomaterial and the surrounding natural bone, providing greater mechanical stability in critical areas. The comparative studies of gel-derived and melt-quenched glasses showed that the synthesis technique causes differences in the texture and the glass structure [36, 37]. The sol-gel-derived glasses showed more polymerized structure and higher porosity and specific surface area values, enhancing the solubility. The rate of HCA formation is higher for the sol-gel-prepared glasses, and they exhibit bioactivity with a content of higher than 90% of SiO_2 [38]. Bioactivity at melt-derived glasses is present with a content of up to 60% of SiO_2.

2.3.1 Flourine-Doped Bioactive Glass

Fluoride ions are not natural constituents of bones, but in vivo it is mainly associated with calcified tissue, the bone, and teeth, replacing the hydroxyl groups in hydroxyapatite phase producing its partial conversion into fluorapatite [39, 40]. Compared to pure hydroxyapatite, fluorapatite has a much higher physic-chemical stability, such as an increased resistance to dissolution by acid [41]. Dental caries is one of the most

widespread bone diseases. Acidogenic bacteria are the main cause of dental caries, where the fermentation of sugars and starches in food accumulated on the surface of teeth can lead to the formation of organic acids, which then cause demineralization, and can lead to complete destruction of teeth [42]. The ability of fluorine ions to stabilize the apatitic structure against demineralization by acid is a useful way in preventing tooth degradation. Fluoride-doped biomaterials in an acidic environment, upon dissolution, lead to the release of fluorine ions, which act as an antimicrobial agent [43, 44]. Liu et al. [45] reported that the F-doped BG significantly inhibited the growth of periodontal pathogens, *A. actinomycetemcomitans* and *P. gingivalis*, the antibacterial activity being dependent on the F^- content of the BG. Low concentrations of fluoride ions are not toxic to humans, but high concentrations are toxic and can lead to enamel fluorosis [46]. The fluoride glasses have good biological compatibility because they do not cause a hemolysis reaction and have no toxicity to cells and living animals [47]. Liu et al. reported that alkaline phosphatase activity, cell number, collagen formation, bone-like mineral nodules, and osteogenic gene expression of MC3T3-E1 cells were significantly promoted in low fluoride – BG-conditioned medium [45]. Currently, fluoride is one of the most common anticaries agents present as primary components in toothpaste and mouthwash [47, 48].

Fluoride ions in a bioactive glass increase the polymerization of the silicate network binding for modifiers (CaO and Na_2O) from the siliceous matrix and reduce its reactivity and bioactivity [49, 50]. The high fluoride-content glasses in melt-derived glass SiO_2–P_2O_5–CaO–Na_2O mainly form calcium fluorite (CaF_2) in SBF, while the formation of apatite is reduced compared to the fluoride-free composition [51]. With the increase in P_2O_5 content in fluoride-containing glasses comes the increase in glass degradation and ion release and favors the formation of fluorapatite (FAP) rather than CaF_2. FAP formation occurred more rapidly (within 6 h) with increased phosphate content in the glass, compared to 3 days for low phosphate-content glasses.

2.3.2 Magnesium-Doped Bioactive Glass

Magnesium is an essential element that is needed for a broad variety of physiological functions.

It is a cofactor for many enzymes, stabilizes the structures of DNA and RNA, and is important for the metabolism of Ca, K, P, Zn, Cu Fe, Na, Pb, and Cd [52–55]. Magnesium ions have a significant role in bone formation, enhance osteoblast cell activity, and inhibit osteoclasts [56]. Several investigations showed that the effect of long-term magnesium-deficient diets cause osteopenia and the inhibition of growth of the bone [54, 57, 58]. The effect of magnesium ions on the structure of a bioactive glass is questionable; they can act as modifiers [59] or as an intermediate oxide, partially entering the silicate network as MgO_4^{2-} tetrahedral units [60, 61]. Zhao et al. [60] have illustrated when MgO content in the bioactive glass surpasses 10 mol%; then a part of Mg ions enter the silicate structure as a network former. Watts et al. [61] suggested that magnesium oxide acts more as an intermediate oxide than as a

modifier, with a proportion of 86% of MgO acting as a network-modifying cation while up to 14% entering the silicate network as tetrahedral MgO_4 species. The presence of magnesium in the glasses increases the surface area and porosity [62, 63]. In contrast, Ma et al. [64] reported that the presence of MgO (0–20 mol%) in glass composition (SiO_2–CaO–P_2O_5–MgO) has little influence on its textural properties.

Some in vitro results indicate that magnesium ions in bioactive glasses delay apatite formation [62, 64–66], while others suggest that it does not effect on mineralization [24]. Ma et al. investigated the effects of the substitution of MgO (0–20 mol%) for CaO on sol-gel-derived glass degradation and bioactivity. The studies of in vitro showed that the rate of glass degradation gradually decreases with the increase of MgO, and the formation of an apatite layer on glass surface is retarded. The retardation in the formation of the layer on the surface of glass could be attributed with the decrease of the solubility of the glass and influence of the Mg^{2+} leached to the solution. Leached Mg^{2+} ions from a glass into the solution are considered as an inhibitor of calcium-phosphate crystallization and are marked as a delay to the transformation of amorphous calcium phosphates to more stable apatite phases [65, 66]. Moya et al. [67] reported that a glass of nominal composition (wt%) 54.5 SiO_2, 12.0 Na_2O, 4.0 K_2O, 15.0 CaO, 8.5 MgO, and 6.0 P_2O_5 found that the role of Mg^{2+} in the formation of Ca–P-rich layer was insignificant.

Numerous in vitro studies showed that Mg-doped bioactive glasses have better results in terms of cell adhesion, proliferation, and differentiation of osteoblasts cells than controlled samples [68–71]. Bioactive glass containing 5 mol% of MgO (SiO_2–CaO–P_2O_5–MgO) has been shown to enhance differentiation of human fetal osteoblastic cells (hFOB 1.19) [68]. This bioactive glass did not induce any signs of toxicity after 48 h with L929 mouse fibroblast cells. Bioactive glass scaffolds (SiO_2–CaO–P_2O_5) doped with MgO at different concentrations of up to 2.25 mol.% were demonstrated a higher proliferation and ALP activity of mesenchymal stem cells (MSCs) than controls: scaffold without doping and hydroxyapatite after 14 days of culture [69]. The MSCs on the scaffolds with 2.25 mol.% Mg show the highest MSC proliferation and ALP activity among those of the Mg-doped scaffolds. Balamurugan et al. [70] reported that SiO_2–CaO–MgO–P_2O_5 bioactive glass with 13 mol% MgO has the ability to support the growth of human osteoblast-like cells (MG63) and to promote osteoblast differentiation by stimulating the expression of alkaline phosphatase activity. Bioactive glasses SiO_2–CaO–P_2O_5–MgO doped with MgO (0, 10, and 20 mol%) did not show cytotoxicity to human gastric adenocarcinoma cells and antibacterial activity [71]. The presence of MgO in the glass composition increases the formation of the apatite layer, whereas when compared with base glass, the formation of HAp layer decreases when the concentration of MgO increases above 10%. The bioactive glass with 10% MgO had the highest specific surface area and solubility.

There are a few investigations focusing on the in vivo behavior of Mg-containing bioactive glasses [72–74]. Bioactive glass based on the SiO_2–P_2O_5–CaO–Na_2O–K_2O–Al_2O_3 system with the addition of 1–3 mol% of MgO has been prepared by melt technique as implants are embedded in the muscle and bone of white rabbits [72]. This bioactive glass elicits a favorable response both in the muscle and bone; a gradual degradation process leads to disruption and partial resorption of the

material, and a tight apposition is promoted with the newly formed bone. Implants did not produce any adverse inflammatory response in the muscle at any time.

Tamura et al. [73] reported that histological examination of rat tibiae showed that two types of bioactive bone cement containing either $MgO–CaO–SiO_2–P_2O_5–CaF_2$ (4.6 mol% MgO) or glass-ceramic powder, incorporated in bone defects, formed direct contact with the bone.

A bioactive study of 26 glasses in system $Na_2O–K_2O–MgO–CaO–B_2O_3–P_2O_5–SiO_2$ in vivo showed that glasses that contained 4–30 mol% alkali oxides, 14–30 mol% alkaline earth oxides, and <59 mol% SiO_2 can create links with bone tissue [74]. Glasses which contain potassium and magnesium (0–7.8 mol% MgO) bind to the bone in a similar way as other glasses that bind to bone.

2.3.3 Strontium-Doped Bioactive Glass

Strontium (Sr) is an important trace element in the human body and has a significant impact on bone metabolism. Its compounds strontium ranelate and strontium chloride are currently used to treat osteoporosis [75–78]. In vitro and in vivo studies showed that a low dose of strontium ions promotes bone formation and osteoblast replication while inhibiting bone resorption by osteoclasts. In contrast, high doses of strontium may induce skeletal abnormalities [76]. Sr ions exhibit cariostatic properties depending on their concentration, predominantly in the presence of fluoride [79]. Liu et al. reported that Sr-doped BG showed antimicrobial activity against subgingival bacteria, *A. actinomycetemcomitans* and *P. gingivalis* and that it depends on the amount on the percentage of strontium in the glasses [46]. Incorporation of strontium ions in a bioactive glass may be an effective way to deliver a steady supply of strontium ions to a bone defect site and in this way speed up the recovery of the patient.

The effect of strontium ions on the structure of several bioactive glasses has been reported. Substitution of strontium for calcium does not lead to significant structural changes, but there is a small expansion of the glass network. The density of the glasses increased with strontium substitution, while the oxygen density decreased [80, 81]. Expansion of the glass network was associated with the characteristics of metal ions. Strontium has a higher ionic radius and lower ionic field strength (r = 0.127 nm; I = 0.24) compared to the calcium ion (r = 0.106 nm; I = 0.35). Calcium and strontium ions were found to preferentially distribute in glass around phosphorus ions [46, 81, 82]. Glasses with a high content of silica showed a slight decrease in solubility, building Sr-substituted apatite layers, and bioactivity with increasing concentrations of strontium ions [80, 83–85]. The bioactive glasses with a higher content of phosphates exhibit greater solubility and bioactivity with increasing strontium content [83, 86].

Several studies have reported the enhancing effects of strontium-doped BG on osteogenesis in vitro using different cell sources, demonstrating their potential for bone tissue regeneration.

Strontium-doped BG promotes osteoblast proliferation and activity and decreases osteoclast activity and resorption [87, 88]. The concentration of Sr is a critical parameter for its increasing effect on cell proliferation. Bioactive glass containing little amounts of SrO (<5 mol%) has higher proliferation and alkaline phosphatase activity of the rat osteoblastic cells than samples without Sr and with its high dose [84]. Zhang et al. [89] showed that 5 mol% Sr significantly increased the proliferation and osteogenic differentiation of bone marrow stromal cells in a concentration-dependent manner. Sr-doped BG 64S with 5% Sr accelerates the differentiation of mesenchymal stem cells but not proliferation [90].

The available studies in vivo show that strontium-doped BG scaffolds can successfully regenerate bone defects [88, 89, 91–94]. Gorustovich et al. [91] reported that new lamellar bone had formed along the surface of both 45S5 and 45S5.6Sr BG particles within 4 weeks. Studies that were performed by Zhang et al. [89] have shown that the incorporation of Sr into mesoporous bioactive glass (MBG) scaffolds significantly stimulated new bone formation in osteoporotic bone defects when compared to MBG scaffolds alone. Recently, Zhao et al. [92] reported that Sr–MBG scaffolds had good osteogenic capability and stimulated new blood vessel formation in critical-sized rat calvarial defects within 8 weeks. Zhang et al. [88] have done a study on the immune response affected by Sr–BG. The results showed that Sr−BG in vivo initiated a less severe immune response and had an improved effect on bone regeneration than BG, which corresponded with the in vitro evaluation.

2.3.4 Silver-Doped Bioactive Glass

Orthopedic implant infections are significant because of their morbidity and usually require the removal or replacement of installed materials [95]. Incorporation of antimicrobial agents such as antibiotics, fluorine, and biocide metal ions in the implant biomaterial alone proved to be very successful in the prophylaxis [96]. Silver ions have expressed an oligodynamic effect with a minimal development of microorganism's resistance [97–99]. Bioactive glasses doped with small amounts of silver ions showed a broad spectrum of antimicrobial activity [100, 101]. Low concentrations of silver ions in BG are not toxic, but high concentrations can cause cytotoxicity. The Ag-doped borate bioactive glasses containing 0.75 and 1 wt% Ag were not toxic to the mouse MC3T3 osteoblasts and L929 fibroblast cells, whereas the glass containing 2 wt% Ag was toxic [101, 102]. Phetnin and Rattanachan reported that Ag-doped silicium glasses exhibited anticancer properties against human liver cancer HepG2 cells [103]. Silver-containing bioactive glasses are mostly obtained by a sol-gel technique because of the homogenous product. The melt-quenching technique is not suitable for the synthesis of Ag-doped BG, because homogeneity and reproducible of the product cannot be provided [104]. Modification of the surface of the bioactive glass with silver using techniques of ion exchange may be done in two different ways: in molten salts and in an aqueous solution [105]. The amount of Ag within the glass was reported to be very low (up to 0.66 wt.% Ag/glass), but its concentration

within the glass surface layer was high. Addition of silver ions into the BG structure induced lower bioactivity as a result of lower solubility and surface area [106]. The release of silver ions from glasses in SBF is slow compared with the dissolution of other constituents. There are several important factors which limit the dissolution of AgBG and release of silver ions. Replacing calcium with silver ions in the bioactive glass structure increases glass network connectivity as a result of reducing the number of non-bridging oxygen groups, which are essential for the solubility [107].

The formation of the HCA or HCA/AgCl layer on the glass surface can be limited or even stop the dissolution and release of silver ions. Released Ag ions in the AgBG surface layer can interact with phosphate and chloride ions (SBF), building a silver phosphate compound and difficult soluble AgCl (Ksp = 1.8 × 10–10 at 25 °C) [105]. Apatite materials can incorporate silver ions into the structure during its formation, or they can be absorbed from the solution. Silver ions may have a strong stimulatory effect on the formation of carbonate apatite [99]. The increase in the amount of silver (3%) in a BG leads to the formation of secondary phases: quartz and metallic silver, which reduce the BG transformation into HCA [107]. The textural characteristics of AgBG also play an important role; a higher surface area is favorable for obtaining a higher dissolution rate of glasses and therefore a higher bioactivity. Some studies have reported that with the increase silver content in a BG, there occurs a progressive decrease of the surface area and pore volume and the progressive broadening of the pores distribution [108, 109].

2.3.5 Copper-Doped Bioactive Glass

Copper is an essential trace metal found in all living organisms and is necessary for a lot of biological processes. It is an angiogenic agent because it increases the expression of pro-angiogenic and growth factors (VEGF, bFGF, TNF-α, and IL-1β), enhances the in vivo angiogenesis, and stimulates the human endothelial cell proliferation [110–112]. Insufficient amounts of copper in a diet can cause a reduction of bone mineral density [113]. Copper ions in vitro diminished the proliferation rate of mesenchymal stem cells but increase their ability to differentiate into osteogenic lineage [114]. Previous studies suggested that Cu^{2+} ions could enhance cell activity and proliferation of osteoblastic cells and inhibit osteoclast activity [115, 116]. Copper and its compounds are highly significant as antimicrobial agents in the prevention of postoperative infections [117, 118]. Incorporation of Cu into BG may offer an alternative route for sustained delivery of Cu ions. The in vitro bioactivity of Cu-doped glasses was dependent on the concentration of Cu^{2+} ion incorporated which decreased the formation of apatite at higher concentrations [119, 120]. Cu^{2+} ions acted as network modifiers and disrupted the silicate network of BG [121]. Its effect on the network is inferior to Mg^{2+} and Zn^{2+} ions (Cu < Mg < Zn) [124]. The effect of Cu on the textural properties and microstructure of the doped glass matrices depended on their compositions. Bejarano et al. [120] reported that the incorporation of CuO increased the surface area and pore volume of 58S BG

($60SiO_2$–$36CaO$–$4P_2O_5$), whereas an opposite effect was observed in NaBG ($60SiO_2$–$25CaO$–$11Na_2O$–$4P_2O_5$).

In vitro and in vivo studies reported that Cu–BG scaffolds release Cu^{2+} ion and stimulate processes such as angiogenesis as well as osteogenesis. Li et al. [122] reported that the composite of Cu–BG nanocoatings on a natural eggshell membrane can stimulate angiogenesis and neoepidermis formation during wound healing process. The composite containing 5 mol% Cu stimulated proangiogenesis by improving the vascular endothelial growth factor (VEGF) and hypoxia-inducible factor (HIF)-1a protein secretion. In a previous study, Wu et al. [123] also found that Cu–BG scaffolds (1, 2, and 5% Cu) significantly enhance hypoxia-like tissue reaction leading to the coupling of angiogenesis and osteogenesis. Furthermore, Cu–MBG scaffolds showed a sustained release of ibuprofen. Studies by Lin et al. [124] have demonstrated that Cu–BG (13–93) scaffolds with 0.4 and 0.8 wt.% CuO did not have a significant effect on the response of pre-osteoblastic MC3T3–E1 cells in vitro and on angiogenesis and osteogenesis in rat calvarial defects at 6 weeks post-implantation. The scaffold with the highest dopant concentration of 2.0 wt.% CuO significantly enhanced angiogenesis in the fibrous tissue that infiltrated the scaffolds and significantly reduced osteogenesis as a result of cytotoxic effects of high concentrations of copper.

Copper-doped BG materials showed antibacterial activity in suppressing some bacterial pathogens involved in postsurgical infections, such as *S. aureus*, *S. mutans*, *E. coli,* and *P. aeruginosa* [123, 125–128].

2.3.6 Zinc-Doped Bioactive Glass

Zinc is an essential trace element to the structure of biomolecules and function of metabolism. It plays a physiologically important role in bone metabolism, formation, and resorption [129, 130]. Zinc deficiency results in a retardation of bone growth, indicating that the element is required for the growth, development, and maintenance of healthy bone [131]. Excess zinc may have adverse and serious effects on health such as reduced bone formation, anemia, hypertension at rats, as well as systemic cytotoxicity [132–135].

The possibility of incorporating Zn^{2+} ions in bioactive glasses has received special interest lately, and several formulations of bioactive glasses doped with ZnO have been recently obtained, both by melting and sol-gel techniques [136–141]. ZnO in the structure of bioactive glass might act as divalent network modifier and/or network former depending on the composition and its content. Several studies based on experimental and computational approaches have shown that Zn^{2+} ions in BG adopt a tetrahedral coordination (ZnO_4^{2-}) and so act as a weak tetrahedral network former and participate in the copolymerization with the Si tetrahedra units [136, 137]. Zinc ions in the presence of sufficient amounts of alkali ions act as a network former. Conversely, if there are insufficient alkaline ions, the zinc ion will be a network modifier [138]. Haimi et al. [139] reported that ZnO in BG (Na_2O,

K_2O, MgO, CaO, B_2O_3, TiO_2, ZnO, P_2O_5, and SiO_2) acts both as network former and network modifier [142]. The addition of Zn^{2+} ions to silicate and phosphosilicate glasses enhances its chemical durability and improves the thermal and mechanical strength of BG [138, 140]. The textural properties such as the surface area, pore volume, and pore size diameter of the scaffolds progressively decreased with the increasing concentration of Zn^{2+} ions in BG [136, 141]. These changes can be associated with the structural role played by Zn^{2+} species in the glass network. Zinc has been found to have a great influence on the growth kinetics of HCA in SBF [140, 142–145]. The increasing Zn content in BG leads to a decrease in the solubility of glasses. Srivastava et al. [140] reported that there is no effect on the formation of HCA layer by addition of 1% of ZnO by weight in 45S5 bioactive glass, but increasing the ZnO content more than 1% decreases the formation of HCA layer. Zinc ions potently inhibit the growth of hydroxyapatite crystals [118, 146]. It has been recognized that ZnO retards the crystal nucleation of HCA during the initial periods of in vitro bioactivity studies in SBF, but apatite growth still takes place within a few hours to a few days of immersion. The bioactivity and biocompatibility of Zn-doped BG materials were not only strongly associated with the apatite forming ability but also related with the release of zinc ions, which have a stimulatory effect on bone cells' proliferation and differentiation. Zinc ions must be released slowly from the BG because its elevated concentrations can have harmful effects. Uncontrolled fast release of Zn^{2+} ions from BG can create negative effects on the growth of new bone tissue and have a cytotoxic effect. Aina et al. [143] reported that 45S5 glasses with a zinc content of 5 wt% showed reduced solubility and bioactivity (monitored by HCA formation) in relation to the parent glass, while the endothelial cell adhesion on the surface thereof was the best. The sample with 20 wt% Zn has completely inhibited the growth of HCA. Balamurugan et al. [147] reported that BG with 5 wt% ZnO showed proliferation and differentiation of osteoblast rat's cells. In contrast, another study reported that BG scaffolds with 0–5% ZnO had no effect on proliferation and osteogenesis of human adipose stem cells (hASCs) [139].

Several studies have reported that Zn-doped BG exhibits antimicrobial activity as an important feature in the prevention of postoperative infections [141, 148, 149].

2.3.7 Cobalt-Doped Bioactive Glass

Cobalt is an essential trace element and is a constituent of several enzymes and vitamin cyanocobalamin (vitamin B12) [150, 151]. The investigation of cobalt materials in bone tissue engineering implants and as anticancer and antimicrobial agents is a broad area attracting increasing attention [152–156]. Highly vascularized bone tissue is essential for successful clinical application of engineered implants. Cobalt ions can stimulate angiogenesis via inducing hypoxic conditions and activate the hypoxia-inducible factor-1 (HIF-1) in mesenchymal stem cells and subsequently activate HIF-α target genes including VEGF, EPO, and p21 [157–159]. Hypoxia can also create a potentially lethal environment and limit cellular respiration and growth

[160]. High doses of cobalt may be cytotoxic and genotoxic and can cause cancer [161]. Hence, for applications in bone tissue engineering, a BG matrix is needed for the controlled release of Co^{2+} ions into a physiological environment. In this context, BG matrix has been shown to be suitable carriers for therapeutic ions [162]. Cobalt doped BG is bioactive and, in SBF, develops a hydroxycarbonate apatite layer on the surfaces [163–165]. Cobalt ions ware present in both the silicate and phosphate phases of the BG and formed Si–O–Co and P–O–Co linkages [165]. It plays a concentration-dependent role in the glass network, acting as network modifier at 1 wt% and a network former at ≥5 wt% [163]. The results indicated that the doping of CoO in 45S5 bioactive glass and glass-ceramics enhanced its density, compressive, bending strength, and elastic properties [163, 165]. Several studies have shown positive effects of the addition of Co^{2+} ions to BG scaffolds in angiogenesis and osteogenesis. Mesoporous bioactive glass (MBG) scaffolds showed that low amounts of Co (<5%) incorporated into MBG scaffolds had no significant cytotoxicity and that their incorporation significantly enhanced VEGF protein secretion, hypoxia-inducible factor HIF-1α expression, and bone-related gene expression in BMSCs, and also that the Co–MBG scaffolds support BMSC attachment and proliferation [166]. Another study showed that 1393 BG with 1 wt.% of CoO was biocompatible with osteoblast-like cells and endothelial cells which showed slightly stimulating effects on osteoblast-like cells, while the addition of 5 wt.% of CoO was cytotoxic to both cell types [167]. A recent study has shown that incorporation of CoO (0.5 mol%) in the BG significantly promotes osteogenic activity of human osteosarcoma cells without any cytotoxicity effect [164].

2.4 Silanization: Covalent Modification of a Bioactive Glass's Surfaces by Silanes

Silanization is an effective covalent coating method to modify material surfaces that are rich in hydroxyl groups, such as bioactive glasses, hydroxyapatite, titania, and many other metal oxide surfaces [168, 169]. The goal of silanization is to form bonds across the interface between the inorganic components and organic molecules or biomolecules in order to improve the interaction with the surrounding bone tissue and to enhance dispersion stability of inorganic particles in various liquids or as anchors for the immobilization of drugs. The mechanism of the silanization of inorganic materials is well studied [170, 171]. The reaction conditions such as nature and concentration of the alkoxysilane, solvent type, temperature, and reaction time must be carefully controlled to prevent the forming of a thick polymerized silane network on the surface. The resulting chemical bonds between alkoxysilane and the surface of a material can be hydrolyzed in some conditions. Silanol groups from hydrolyzed silicon alkoxides are able to condense with the hydroxyl groups present on the material surface, while the alkyl chain bears the functional group such as amino, chloro, carboxyl, epoxide, thiol, vinyl, cyanide, or phenyl that can be exploited for further functionalization [172–174]. The amino ($-NH_2$) groups are

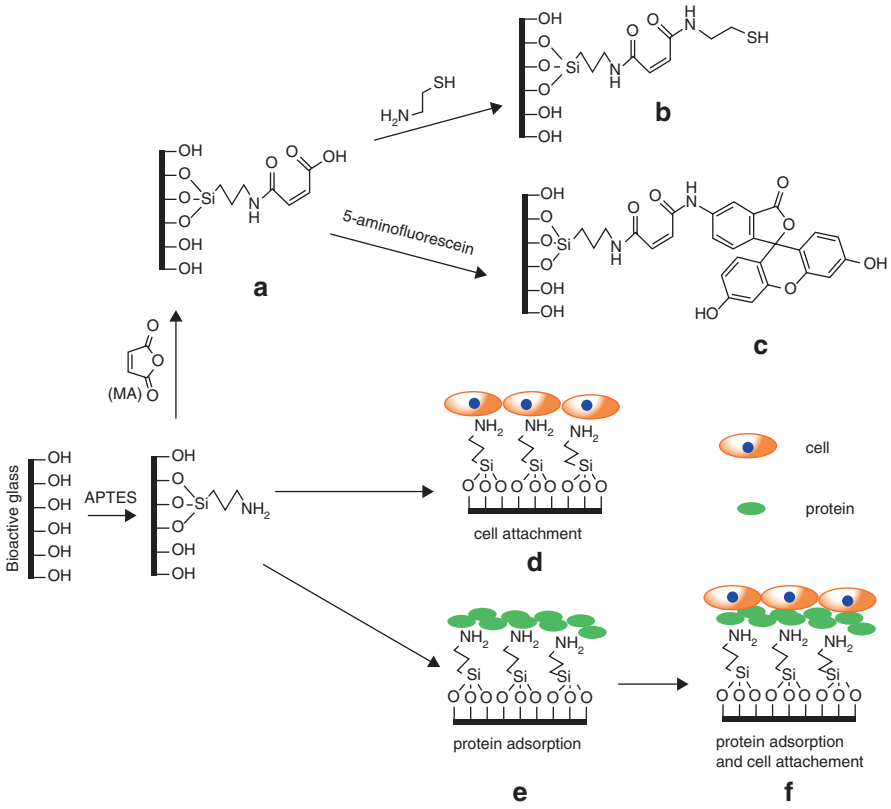

Fig. 2.6 Synthetic procedure for the preparation of APTS-BG-MA (**a**); synthesis of the APTS-BG-MA and cysteamine conjugate (**b**); synthesis of the APTS-BG-MA and 5-aminofluorescein conjugate (**c**); models for cell binding (**d**, **f**) and protein adsorption (**e**, **f**)

responsible for the covalent bonding and electrostatic interactions with negatively charged groups present on a variety of molecules such as DNA and proteins. The capability of biomaterials to adsorb proteins on their surface can affect cell adhesion and their growth. The 3-aminopropyltriethoxysilane (APTES) is one of the most frequently used silanes for the modification of different materials in many in vitro and in vivo biological studies (Fig. 2.6). Surface modification with APTES can be done during the synthesis of BG [175] or adsorption from solution [176, 177]. The highest calcination temperature of 150 °C is used in order to avoid the decomposition of the $-CH_2-CH_2-CH_2-NH_2$ chains of APTS molecules inserted during the synthesis [175]. In vitro tests indicated that APTES on a bioactive glass surface does not reduce its bioactivity [175, 178, 179]. Chen et al. [12] reported that the APTES layers themselves do not influence the kinetics of structural and chemical changes of the 45S5 Bioglass®-derived glass-ceramic material in SBF, while the aqueous treatment involved during the surface modification plays a key role in speeding up these changes. Zhang et al. [180] described the synthesis of mesoporous bioactive

glass (MBG) and its functionalization with APTES (N-MBG) and triethoxysilylpropyl succinic anhydride (TESPSA) (C-MBG). In vitro studies showed that all samples could significantly promote the proliferation and osteogenic differentiation of rabbit bone marrow stromal cells; the effect was greatest with N-MBG. In vivo results demonstrated that N-MBG could promote higher levels of bone regeneration compared with MBG and C-MBG. Amino groups present on the surface are likely to have a significant role in improving cell proliferation and differentiation. The type of charge and hydrophilicity of functional groups can influence protein and cell adhesion by changing the hydrophilicity-hydrophobicity of surfaces [181]. The amino groups are less hydrophilic than carboxyl groups present on the surface of the C-MBG sample [180]. Consequently, surfaces containing amino groups exhibit hydrophilic-hydrophobic balance, which is beneficial for cell adhesion. Composites consisting of polymers such as polylactide (PLA) and bioactive glasses have been developed as bone-repairing devices because of their bioactivity and biodegradability [182, 183]. The APTES proved successful for surface modification of BG as a coupling agent for improving the interface between PLLA and BG particles [184]. The APTES-treated glass particles without agglomeration are uniformly dispersed into the polymer phase compared to non-treated glass. The bending strength, bending modulus, and shearing strength of PLLA/BG-APS composites were all higher than those of unmodified composites. The acid anhydride reagents and glutaraldehyde (GA) are the most common used heterobifunctional cross-linker molecules for derivatization of the $-NH_2$ in the $-COOH$ groups (Fig. 2.6). Aina et al. [175] described derivatization of APTES-functionalized 25SG423 glass with maleic or cis-aconitic anhydrides and then conjugation with cysteamine and 5-aminofluorescein, used as model molecules to simulate a drug (Fig. 2.6a–c).

Degradation studies have shown that total release of conjugates from composites occurs only in an acid solution (pH 4.5), whereas at physiological pH (7.4) in conditions close to neutrality, a slow release of these organic molecules has been observed. The use of GA as a protein coupling agent allows the control of protein release kinetics and almost completely maintains the native protein structure [185–187]. The surface functionalization of the BG substrate with APTES and GA does not induce significant conformational changes in the methemoglobin and 5-methylaminomethyl-uridine forming enzyme structure [186, 187]. The GA also improved the stability of hemoglobin attachment and induces its polymerization on the surface of Ag-doped BG [188].

2.5 Biological Surface Functionalization of Bioactive Glass

Biological functionalization of bioactive glasses can be described as the attachment (immobilization) of biological species such as proteins, cells, and other biomolecules to material surfaces. Biomolecules can be bound to the surface of the materials by the weak physical interaction (electrostatically and Van der Waals forces) and/or chemical bonds (covalent and ionic). Physical and chemical immobilization may occur on

the surface at the same time; a primary layer of molecules may be physically adsorbed on top of an underlying chemisorbed layer. Chemical immobilization is highly selective and occurs only between certain adsorptive and adsorbent species, for example, salinization (Sect. 2.3). Many physicochemical characteristics of materials may affect the binding biomolecules, for example, chemical composition, dissolution behavior or pH, degree of crystallization, microstructure, hydrophobicity, z-potential, surface roughness, surface reactivity, particle sizes, etc. [189]. Surface functionalization of bioactive glasses with the proteins can improve their bone integration. The interactions of cells and tissues with biomaterials are the main condition for its survival and function in the human body. Biomaterials applied in most cases remain a long-term contact with local cells and tissues at the site of installation by entering into contact with them. The interaction of cells with biomaterials starts the moment when tissue comes into contact with biomaterial elements, first, through the adsorption of proteins on the surface of biomaterials in a very short time (<1 s). The formation of a protein monolayer on almost the entire surface of the implant is played for several seconds to minutes [190]. The type, amount, and conformation of adsorbed proteins on the surface are important for adhesion, proliferation, and differentiation of cells, and they can be an important factor in controlling the next bioprocess on the implant [189, 191]. Chemical composition of biomaterial surfaces can greatly influence the absorption of proteins. A calcium-phosphate surface on bioactive glass plays an important role in enhancing protein attachment. El-Ghannam et al. [192] reported that the amount of serum proteins adsorbed to the calcium-phosphate surface-modified porous 45S5 bioactive glass was significantly higher than that to the unmodified porous bioactive glass. Porous stoichiometric hydroxyapatite bound significantly higher amount of total proteins than the amount adsorbed to the bioactive glass substrates. The surface-modified porous bioactive glass selectively adsorbed higher amounts of fibronectin from serum than the hydroxyapatite or unmodified bioactive glass. BG in vivo showed a more intense bioactive effect than HAp [193]. The greater bioactive effect (i.e., bone bonding) of BG compared to hydroxyapatite was due to its ability to concentrate active proteins on its surface [192, 194]. Fibronectin is one of the most abundant extracellular matrix glycoproteins that adsorbs to biomaterials, mediating cell adhesion. In vitro, other proteins such as vitronectin, laminin, and collagen have been shown to be involved in cell adhesion [195]. On the contrary, albumin from the plasma can be used to "passivate" surfaces preventing cell adhesion and greatly reducing the acute inflammatory response to the material [196, 197]. Metal ions in the structure of BG can increase or decrease adsorption of proteins on its surface. High content of 8 mol% Ag_2O in bioactive glasses ($CaO–SiO_2–P_2O_5$) contributes to the improvement of its protein binding capability [198]. Silver ions in the particle surface of biomaterial particles can form bonds with proteins primarily through thiol-containing amino acids [199]. Rosengrena et al. [200] reported that two bioactive glass-ceramics, AP40 and RKKP, exhibit good absorption capacity to apolipoprotein J, fibrinogen, and fibronectin from human plasma. The presence of La or Ta in bioactive glass-ceramics decreased the adsorption of proteins. The proteins adsorbed on the surface of the glass act as promoters or inhibitors of the formation of apatite. The fibrinogen adsorbed on the BG surfaces induces a growing of the

apatite-like layer [201]. The presence of serum proteins delayed apatite precipitation for fluoride-containing glasses, while Bioglass 45S5, despite a considerably higher phosphate content, formed only amorphous calcium phosphate [202]. The cells are primarily associated with proteins as the main coating than to the actual surface of biomaterials [203, 204]. Cells adhered to the adsorbed proteins on biomaterial surface through integrins, a family of heterodimeric calcium-dependent membrane receptor proteins [191]. The role of fibronectin for in vitro cell adhesion on BG surfaces has been highlighted by several authors [190, 192]. Adherent cells on the surface in the absence of fibronectin are only spread 5%, but the expansion of the increased is close to 100% if the fibronectin adsorbed to the surface of the previously [190]. Osteogenic cell (MC3T3-El) adhesion to porous 45S5 BG glass treated to form a dual layer of calcium-phosphate and serum protein was significantly higher than adhesion to porous hydroxyapatite with adsorbed serum protein [192]. Hydroxyapatite adsorbed the greatest amount of total protein, while BG demonstrated selectivity. The calcium-phosphate surface on BG plays an important role in the selective concentration of fibronectin required to promote the accumulation of cells [192, 204].

Acknowledgment This work was supported by the Ministry of Education Science and Technological Development of the Republic of Serbia (Project III43009).

References

1. Hench LL, Splinter RJ, Greenlee TK, et al. Bonding mechanisms at the interface of ceramic prosthetic materials. J Biomed Mater Res. 1971;2:117–41.
2. Hench LL. Chronology of bioactive glass development and clinical applications. New J Glass Ceram. 2013;3:67–73.
3. Hench LL. Sol-gel materials for bioceramic. Curr Opin Solid State Mater Sci. 1997;2: 604–10.
4. Takadama H, Kim HM, Kokubo T, et al. Mechanism of biomineralization of apatite on a sodium silicate glass: tem-edx study in vitro. Chem Mater. 2001;13:1108–13.
5. Itälä A, Ylänen HO, Yrjans J, et al. Characterization of microrough bioactive glass surface: surface reactions and osteoblast responses in vitro. J Biomed Mater Res. 2002;62:404–11.
6. Ebisawa Y, Kokubo T, Ohura K, et al. Bioactivity of CaO·SiObased glasses: in vitro evaluation. J Mater Sci Mater Med. 1990;1:239–44.
7. Filho OP, LaTorre GP, Hench LL, et al. Effect of crystallization on apatite-layer formation of bioactive glass 45%. J Biomed Mater Res. 1996;30:509–14.
8. Goel A, Kapoor S, Rajagopal RR, et al. Alkali-free bioactive glasses for bone tissue engineering: a preliminary investigation. Acta Biomater. 2012;8:361–72.
9. Brito AF, Antunes B, dos Santos F, et al. Osteogenic capacity of alkali-free bioactive glasses. In vitro studies. J Biomed Mater Res B. 2016; doi:10.1002/jbm.b.33771.
10. Dorozhkin SV. Calcium orthophosphates (CaPO4): occurrence and properties. Prog Biomater. 2016;5:9–70.
11. Raicevic S, Stanic V, Kaludjervoic-Radoicic T, et al. Theoretical assessment of calcium arsenates stability: application in the treatment of arsenic contaminated waste. Mater Sci Forum. 2007;555:131–6.
12. Ducheyne P, Qiu Q. Bioactive ceramics: the effect of surface reactivity on bone formation and bone cell function. Biomaterials. 1999;20:2287–303.

13. Hench LL, Polak JM. Third-generation biomaterials. Science. 2002;295:1014–7.
14. Brauer DS. Bioactive glasses – structure and properties. Angew Chem Int Ed. 2015;54:4160–81.
15. Schubert U, Hüsing N. Synthesis of inorganic materials, 2nd, revised and updated edition. Weinheim: Wiley-VCH, 2005.
16. Affatigato M, Feller S, Schue AK, et al. Studies of oxide glass structure using laser ionization time of flight mass spectrometry. J Phys Condens Matter. 2003;15:S2323–34.
17. Huang W, Day DE, Kittiratanapiboon K, et al. Kinetics and mechanisms of the conversion of silicate (45S5), borate, and borosilicate glasses to hydroxyapatite in dilute phosphate solutions. J Mater Sci Mater Med. 2006;17:583–96.
18. Fu Q, Rahaman MN, Fu H, et al. Silicate, borosilicate, and borate bioactive glass scaffolds with controllable degradation rate for bone tissue engineering applications. I. Preparation and in vitro degradation. J Biomed Mater Res A. 2010;95:164–71.
19. Wiederhorn SM, Chae Y-H, Simon CG, et al. Cell adhesion to borate glasses by colloidal probe microscopy. Acta Biomater. 2011;7:2256–63.
20. Bi L, Rahaman MN, Day DE, et al. Effect of bioactive borate glass microstructure on bone regeneration, angiogenesis, and hydroxyapatite conversion in a rat calvarial defect model. Acta Biomater. 2013;9:80158026.
21. Wu C, Miron R, Sculean A, et al. Proliferation, differentiation and gene expression of osteoblasts in boron-containing associated with dexamethasone deliver from mesoporous bioactive glass scaffolds. Biomaterials. 2011;32:7068–78.
22. Gu Y, Huang W, Rahaman MN, et al. Bone regeneration in rat calvarial defects implanted with fibrous scaffolds composed of a mixture of silicate and borate bioactive glasses. Acta Biomater. 2013;9:9126–36.
23. Gorustovich AA, JMP L'o, Guglielmotti MB, et al. Biological performance of boron-modified bioactive glass particles implanted in rat tibia bone marrow. Biomed Mater. 2006;1:100–5.
24. Fu Q, Rahaman MN, Bal BS, et al. Silicate, borosilicate, and borate bioactive glass scaffolds with controllable degradation rate for bone tissue engineering applications. II. In vitro and in vivo biological evaluation. J Biomed Mater Res A. 2010;95:172–9.
25. Brown RF, Rahaman MN, Dwilewicz AB, et al. Effect of borate glass composition on its conversion to hydroxyapatite and on the proliferation of MC3T3-E1 cells. J Biomed Mater Res A. 2009;88:392–400.
26. Landolph JR. Cytotoxicity and negligible genotoxicity of borax and borax ores to cultured mammalian cells. Am J Ind Med. 1985;7:31–43.
27. Balasubramanian P, Grünewald A, Detsch R, et al. Ion release, hydroxyapatite conversion, and cytotoxicity of boron-containing bioactive glass scaffolds. Int J Appl Glas Sci. 2016;7:206–15.
28. Hoppe A, Güldal NS, Boccaccini AR, et al. A review of the biological response to ionic dissolution products from bioactive glasses and glass-ceramics. Biomaterials. 2011;32:2757–74.
29. Neel EAA, Pickup DM, Valappil SP, et al. Bioactive functional materials: a perspective on phosphate-based glasses. J Mater Chem. 2009;19:690–701.
30. Ahmed I, Lewis M, Olsen I, et al. Phosphate glasses for tissue engineering: part 1. Processing and characterisation of a ternary-based P_2O_5–CaO–Na_2O glass system. Biomaterials. 2004;25:491–9.
31. Brow RK. Review: the structure of simple phosphate glasses. J Non-Cryst Solids. 2000;263–264:1–28.
32. Kaur G, Pickrell G, Sriranganathan N, et al. Review and the state of the art: sol–gel and melt quenched bioactive glasses for tissue engineering. J Biomed Mater Res B. 2016;104:1248–75.
33. Lucas-Girot A, Mezahi FZ, Mami M, et al. Sol-gel synthesis of a new composition of bioactive glass in the quaternary system SiO_2-CaO-Na_2O-P_2O_5: comparison with melting method. J Non-Cryst Solids. 2011;357:3322–7.
34. Perez RA, Mestres G. Role of pore size and morphology in musculo-skeletal tissue regeneration. Mater Sci Eng C. 2016;61:922–39.

35. Bellucci D, Cannillo V, Sola A, et al. Macroporous bioglass1-derived scaffolds for bone tissue regeneration. Ceram Int. 2011;37:1575–85.
36. Dziadek M, Zagrajczuk B, Jelen P, et al. Structural variations of bioactive glasses obtained by different synthesis routes. Ceram Int. 2016;42:14700–9.
37. Qiu D, Martin RA, Knowles JC, et al. A comparative study of the structure of sodium borophosphates made by sol–gel and melt-quench methods. J Non-Cryst Solids. 2010;356:490–4.
38. Li R, Clark AE, Hench LL, et al. An investigation of bioactive glass powders by sol-gel processing. J Appl Biomater. 1991;2:231–9.
39. Kannan S, Rocha JHG, Agathopoulos S, et al. Fluorine-substituted hydroxyapatite scaffolds hydrothermally grown from aragonitic cuttlefish bones. Acta Biomater. 2007;3:243–9.
40. Eanes ED, Reddi AH. The effect of fluoride on bone mineral apatite. Metab Bone Dis Relat Res. 1979;2:3–10.
41. Eslami H, Solati-Hashjin M, Tahriri M, et al. The comparison of powder characteristics and physicochemical, mechanical and biological properties between nanostructure ceramics of hydroxyapatite and fluoridated hydroxyapatite. Mater Sci Eng C. 2009;29:1387–98.
42. Komori R, Sato T, Takano-Yamamoto T, et al. Microbial composition of dental plaque microflora on first molars with orthodontic bands and brackets, and the acidogenic potential of these bacteria. J Oral Biosci. 2012;54:107–12.
43. Stanić V, Dimitrijević S, Antonović DG, et al. Synthesis of fluorine substituted hydroxyapatite nanopowders and application of the central composite design for determination of its antimicrobial effects. Appl Surf Sci. 2014;290:346–52.
44. Stanić V, Radosavljević-Mihajlović AS, Živković-Radovanović V, et al. Synthesis, structural characterisation and antibacterial activity of Ag^{+}-doped fluorapatite nanomaterials prepared by neutralization method. Appl Surf Sci. 2015;337:72–80.
45. Liu J, Rawlinsona SCF, Hillb RG, et al. Fluoride incorporation in high phosphate containing bioactive glasses and in vitro osteogenic, angiogenic and antibacterial effects. Dent Mater. 2016;32:e221–37.
46. Browne D, Whelton H, O'Mullane D, et al. Fluoride metabolism and fluorosis. J Dent. 2005;33:177–86.
47. Diamanti I, Koletsi-Kounari H, Mamai-Homata E, Vougiouklakis G, et al. In vitro evaluation of fluoride and calcium sodium phosphosilicate toothpastes, on root dentine caries lesions. J Dent. 2011;39:619–28.
48. Christie JK, Pedone A, Menziani MC, et al. Fluorine environment in bioactive glasses: ab initio molecular dynamics simulations. J Phys Chem B. 2011;115:2038–45.
49. Lusvardi G, Malavasi G, Menabue L, et al. Fluoride-containing bioactive glasses: surface reactivity in simulated body fluids solutions. Acta Biomater. 2009;5:3548–62.
50. Brauer DS, Karpukhina N, MD O'D, et al. Fluoride-containing bioactive glasses: effect of glass design and structure. Acta Biomater. 2010;6:3275–82.
51. Mneimne M, Hill RG, Bushby AJ, et al. High phosphate content significantly increases apatite formation of fluoride-containing bioactive glasses. Acta Biomater. 2011;7:1827–34.
52. Cowan JA. Structural and catalytic chemistry of magnesium-dependent enzymes. Biometals. 2002;15:225–35.
53. Hartwig A. Role of magnesium in genomic stability. Mutat Res/Fund Mol Mech Mutagen. 2001;475:113–21.
54. Johnson S. The multifaceted and widespread pathology of magnesium deficiency. Med Hypotheses. 2001;56:163–70.
55. He LY, Zhang XM, Liu B, et al. Effect of magnesium ion on human osteoblast activity. Braz J Med Biol Res. 2016;49:e5257.
56. Janning C, Willbold E, Vogt C, et al. Magnesium hydroxide temporarily enhancing osteoblast activity and decreasing the osteoclast number in peri-implant bone remodeling. Acta Biomater. 2010;6:1861–8.
57. Belluci MM, Schoenmaker T, Rossa-Junior C, et al. Magnesium deficiency results in an increased formation of osteoclasts. J Nutr Biochem. 2013;24:1488–98.

58. Bernick S, Hungerford GF. Effect of dietary magnesium deficiency on bones and teeth of rats. J Dent Res. 1965;44:1317–24.
59. Oliveira JM, Correia RN, Fernandes MH, et al. Effects of Si speciation on the in vitro bioactivity of glasses. Biomaterials. 2002;23:371–9.
60. Zhao Y, Song M, Liu J, et al. Characteristics of bioactive glass coatings obtained by pulsed laser deposition. Surf Interface Anal. 2008;40:1463–8.
61. Watts SJ, Hill RG, O'Donnell MD, et al. Influence of magnesia on the structure and properties of bioactive glasses. J Non-Cryst Solids. 2010;356:517–24.
62. Perez-Pariente J, Balas F, Vallet-Regi M, et al. Surface and chemical study of SiO_2 P_2O_5 CaO MgO bioactive glasses. Chem Mater. 2000;12:750–5.
63. Ma J, Chen CZ, Wang D, et al. Textural and structural studies of sol–gel derived SiO_2–CaO–P_2O_5–MgO glasses by substitution of MgO for CaO. Mater Sci Eng C. 2010;30:886–90.
64. Ma J, Chen CZ, Wang DG, et al. Effect of magnesia on the degradability and bioactivity of sol–gel derived SiO_2–CaO–MgO–P_2O_5 system glasses. Colloids Surf B Biointerfaces. 2010;81:87–95.
65. Vallet-Regí M, Salinas AJ, Román J, et al. Effect of magnesium content on the in vitro bioactivity of CaO-MgO-SiO_2-P_2O_5 sol-gel glasses. J Mater Chem. 1999;9:515–8.
66. Dietrich E, Oudadesse H, Lucas-Girot A, et al. In vitro bioactivity of melt-derived glass 46S6 doped with magnesium. J Biomed Mater Res. 2009;88A:1087–96.
67. Moya JS, Tomsia AP, Pazo A, et al. In vitro formation of hydroxyapatite layer in a MgO-containing glass. J Mater Sci Mater Med. 1994;5:529–32.
68. Saboori A, Rabiee M, Moztarzadeh F, et al. Synthesis, characterization and in vitro bioactivity of sol-gel-derived SiO_2–CaO–P_2O_5–MgO bioglass. Mater Sci Eng C. 2009;29:335–40.
69. Wang X, Li X, Ito A, et al. Synthesis and characterization of hierarchically macroporous and mesoporous CaO–MO–SiO_2–P_2O_5 (M = Mg, Zn, Sr) bioactive glass scaffolds. Acta Biomater. 2011;7:3638–44.
70. Balamurugan A, Balossier G, Michel J, et al. Sol gel derived SiO_2-CaO-MgO-P_2O_5 bioglass system—preparation and in vitro characterization. J Biomed Mater Res B. 2007;83:546–53.
71. Prabhu M, Kavitha K, Manivasakan P. Synthesis, characterization and biological response of magnesium-substituted nanobioactive glass particles for biomedical applications. Ceram Int. 2013;39:1683–94.
72. Merolli A, Leali PT, Guidi PL, et al. Comparison in in-vivo response between a bioactive glass and a non-bioactive glass. J Mater Sci Mater Med. 2000;11:219–22.
73. Tamura J, Kawanabe K, Kobayashi M, et al. Mechanical and biological properties of two types of bioactive bone cements containing: MgO-CaO-SiO_2-P_2O_5-CaF_2, glass and glass-ceramic powder. J Biomed Mater Res. 1996;30:85–94.
74. Brink M, Turunen T, Happonen RP, et al. Compositional dependence of bioactivity of glasses in the system Na_2O-K_2O-MgO-CaO-B_2O_3-P_2O_5-SiO_2. J Biomed Mater Res. 1997;37:114–21.
75. Reginster JY, Seeman E, De Vernejoul MC, et al. Strontium ranelate reduces the risk of non-vertebral fractures in postmeno-pausal women with osteoporosis: treatment of peripheral osteoporosis (TROPOS) study. Endocrinol Care. 2005;90:2816–22.
76. Marie PJ, Ammann P, Boivin G, et al. Mechanisms of action and therapeutic potential of strontium in bone. Calcif Tissue Int. 2001;69:121–9.
77. Morohashi T, Sano T, Yamada S. Effects of strontium on calcium metabolism in rats. I. A distinction between the pharmacological and toxic doses. Jpn J Pharmacol. 1994;64:155–62.
78. Huang M, Hill RG, Rawlinson SCF. Strontium (Sr) elicits odontogenic differentiation of human dental pulp stem cells (hDPSCs): a therapeutic role for Sr in dentine repair? Acta Biomater. 2016;38:201–11.
79. Curzon MEJ. The relation between caries prevalence and strontium concentrations in drinking water, plaque, and surface enamel. J Dent Res. 1985;64:1386–8.
80. Liu J, Rawlinson SCF, Hill RG, et al. Strontium-substituted bioactive glasses in vitro osteogenic and antibacterial effects. Dent Mater. 2016;32:412–22.

81. Fredholm YC, Karpukhina N, Law RV, et al. Strontium containing bioactive glasses: glass structure and physical properties. J Non-Cryst Solids. 2010;356:2546–51.
82. Xiang Y, Du J. Effect of strontium substitution on the structure of 45S5 bioglasses. Chem Mater. 2011;23:2703–17.
83. Dziadeka M, Zagrajczuk B, Menaszek E, et al. Gel-derived SiO_2–CaO–P_2O_5 bioactive glasses and glass-ceramics modified by SrO addition. Ceram Int. 2016;42:5842–57.
84. Lao J, Nedelec JM, Jallot E, et al. New strontium-based bioactive glasses: physicochemical reactivity and delivering capability of biologically active dissolution products. J Mater Chem. 2009;19:2940–9.
85. Hesaraki S, Gholami M, Vazehra S, et al. The effect of Sr concentration on bioactivity and biocompatibility of sol–gel derived glasses based on CaO–SrO–SiO_2–P_2O_5 quaternary system. Mater Sci Eng C. 2010;30:383–90.
86. Du J, Xiang Y. Effect of strontium substitution on the structure, ionic diffusion and dynamic properties of 45S5 bioactive glasses. Ceram Int. 2016;42:5842–57.
87. Arepalli SK, Tripathi H, Hira SK, et al. Enhanced bioactivity, biocompatibility and mechanical behavior of strontium substituted bioactive glasses. Mater Sci Eng C. 2016;69:108–16.
88. Gentleman E, Fredholm YC, Jell G, et al. The effects of strontium-substituted bioactive glasses on osteoblasts and osteoclasts in vitro. Biomaterials. 2010;31:3949–56.
89. Zhang Y, Wei L, Chang J, et al. Strontium-incorporated mesoporous bioactive glass scaffolds stimulating in vitro proliferation and differentiation of bone marrow stromal cells and in vivo regeneration of osteoporotic bone defects. J Mater Chem B. 2013;1:5711–22.
90. Wu X, Meng G, Wang S, et al. Zn and Sr incorporated 64S bioglasses: material characterization, in-vitro bioactivity and mesenchymal stem cell responses. Mater Sci Eng C. 2015;52:242–50.
91. Gorustovich AA, Steimetz T, Cabrini RL, et al. Osteoconductivity of strontium-doped bioactive glass particles: a histomorphometric study in rats. J Biomed Mater Res A. 2010;92:232–7.
92. Zhao S, Zhang J, Zhu M, et al. Three-dimensional printed strontium-containing mesoporous bioactive glass scaffolds for repairing rat critical-sized calvarial defects. Acta Biomater. 2015;12:270–80.
93. Wei L, Ke J, Prasadam I, et al. A comparative study of Sr-incorporated mesoporous bioactive glass scaffolds for regeneration of osteopenic bone defects. Osteoporos Int. 2014;25:2089–96.
94. Zhang Y, Wei L, Wu C, et al. Periodontal regeneration using strontium-loaded mesoporous bioactive glass scaffolds in osteoporotic rats. PLoS One. 2014;9:e104527.
95. Campoccia D, Montanaro L, Arciola CR. The significance of infection related to orthopedic devices and issues of antibiotic resistance. Biomaterials. 2006;27:2331–9.
96. Mozafari M, Moztarzadeh F. Silver-doped bioactive glasses: what remains unanswered? Interceram. 2013;62:423–5.
97. Silver S, Phung LT, Silver G, et al. Silver as biocides in burn and wound dressings and bacterial resistance to silver compounds. J Ind Microbiol Biotechnol. 2006;33:627–34.
98. Stanić V, Janaćković D, Dimitrijević S, et al. Synthesis of antimicrobial monophase silver-doped hydroxyapatite nanopowders for bone tissue engineering. Appl Surf Sci. 2011;257:4510–8.
99. Stanić V, Radosavljević-Mihajlović AS, Živković-Radovanović V, et al. Synthesis, structural characterisation and antibacterial activity of Ag^+-doped fluorapatite nanomaterials prepared by neutralization method. Appl Surf Sci. 2015;337:72–80.
100. Bellantone M, Williams HD, Hench LL, et al. Broad-spectrum bactericidal activity of Ag2O-doped bioactive glass. Antimicrob Agents Chemother. 2002;46:1940–5.
101. Verné E, Di Nunzioa S, Bosettib M. Surface characterization of silver-doped bioactive glass. Biomaterials. 2005;26:5111–9.
102. Luo SH, Xiao W, Wei XJ. In vitro evaluation of cytotoxicity of silver-containing borate bioactive glass. J Biomed Mater Res Part B. 2010;95:441–8.
103. Phetnin R, Rattanachan ST. Preparation and antibacterial property on silver incorporated mesoporous bioactive glass microspheres. J Sol-Gel Sci Technol. 2015;75:279–90.
104. Bunetel L, Wers E, Novella A, et al. In vitro chemical and biological effects of Ag, Cu and Cu + Zn adjunction in 46S6 bioactive glasses. Mater Res Express. 2015;2:095402.

105. Nezafati N, Moztarzadeh F, Hesaraki S, et al. Surface reactivity and in vitro biological evaluation of sol gel derived silver/calcium silicophosphate bioactive glass. Biotechnol Bioprocess Eng. 2012;17:746–54.
106. Rabiee SM, Nazparvar N, Azizian N, et al. Effect of ion substitution on properties of bioactive glasses: a review. Ceram Int. 2015;41:7241–51.
107. Shirkhanzadeh M, Azadegan M. Formation of carbonate apatite on calcium phosphate coating containing silver ions. J Mater Sci Mater Med. 1998;9:385–91.
108. Delben JRJ, Pimentel OM, Coelho MB. Synthesis and thermal properties of nanoparticles of bioactive glasses containing silver. J Therm Anal Calorim. 2009;97:433–6.
109. Vulpoi A, Baia L, Simon S, et al. Silver effect on the structure of SiO_2-CaO-P_2O_5 ternary system. Mater Sci Eng C. 2012;32:178–83.
110. Saghiri MA, Asatourian A, Orangi J, et al. Functional role of inorganic trace elements in angiogenesis – part II: Cr, Si, Zn, Cu, and S. Crit Rev Oncol Hematol. 2015;96:143–55.
111. Nasulewicz A, Mazur A, Opolski A, et al. Role of copper in tumor angiogenesis—clinical implications. J Trace Elem Med Biol. 2004;18:1–8.
112. Hu G. Copper stimulates proliferation of human endothelial cells under culture. J Cell Biochem. 1998;69:326–35.
113. Smith BJ, King JB, Lucas EA, et al. Skeletal unloading and dietary copper depletion are detrimental to bone quality of mature rats. J Nutr. 2002;132:190–6.
114. Rodríguez JP, Rios S, Gonzales M, et al. Modulation of the proliferation and differentiation of human mesenchymal stem cells by copper. J Cell Biochem. 2002;85:92–100.
115. Ewald A, Kappel C, Vorndran E, et al. The effect of Cu(II)-loaded brushite scaffolds on growth and activity of osteoblastic cells. J Biomed Mater Res. 2012;A100:2392–400.
116. Zhang JC, Huang JA, Xu SJ, et al. Effects of Cu^{2+} and pH on osteoclastic bone resorption in vitro. Prog Nat Sci. 2003;13:266–70.
117. Borkow G, Gabbay J. Copper as a biocidal tool. Curr Med Chem. 2005;12:2163–75.
118. Stanić V, Dimitrijević S, Antić-Stanković J, et al. Synthesis, characterization and antimicrobial activity of copper and zinc-doped hydroxyapatite nanopowders. Appl Surf Sci. 2010;256:6083–9.
119. Li X, Wang X, He D, et al. Synthesis and characterization of mesoporous CaO–MO–SiO_2–P_2O_5 (M= Mg, Zn, Cu) bioactive glasses/composites. J Mater Chem. 2008;18:4103–9.
120. Bejarano J, Caviedes P, Palza H, et al. Sol–gel synthesis and in vitro bioactivity of copper and zinc-doped silicate bioactive glasses and glass-ceramics. Biomed Mater. 2015;10:025001.
121. Hoppe A, Meszaros R, Stähli C, et al. In vitro reactivity of Cu doped 45S5 Bioglass® derived scaffolds for bone tissue engineering. J Mater Chem B. 2013;1:5659–74.
122. Li J, Zhai D, Lv F, et al. Preparation of copper-containing bioactive glass/eggshell membrane nanocomposites for improving angiogenesis, antibacterial activity and wound healing. Acta Biomater. 2016;36:254–66.
123. Wu C, Zhou Y, Xu M, et al. Copper-containing mesoporous bioactive glass scaffolds with multifunctional properties of angiogenesis capacity, osteostimulation and antibacterial activity. Biomaterials. 2013;34:422–33.
124. Lin Y, Xiao W, Bal BS, et al. Effect of copper-doped silicate 13–93 bioactive glass scaffolds on the response of MC3T3-E1 cells in vitro and on bone regeneration and angiogenesis in rat calvarial defects in vivo. Mater Sci Eng C. 2016;67:440–52.
125. Miola M, Verné E. Bioactive and antibacterial glass powders doped with copper by ion-exchange in aqueous solutions. Materials. 2016;9:405.
126. Ye J, He J, Wang C, et al. Copper-containing mesoporous bioactive glass coatings on orbital implants for improving drug delivery capacity and antibacterial activity. Biotechnol Lett. 2014;36:961–8.
127. Palza H, Escobar B, Bejarano J, et al. Designing antimicrobial bioactive glass materials with embedded metal ions synthesized by the sol–gel method. Mater Sci Eng C. 2013;33:3795–801.
128. Popescu RA, Magyari K, Vulpoi A, et al. Bioactive and biocompatible copper containing glass-ceramics with remarkable antibacterial properties and high cell viability designed for future in vivo trials. Biomater Sci. 2016;4:1252–65.

129. Brandao-Neto J, Stefan V, Mendonca BB, et al. The essential role of zinc in growth. Nutr Res. 1995;15:335–58.
130. Hadley KB, Newman SM, Hunt JR, et al. Dietary zinc reduces osteoclast resorption activities and increases markers of osteoblast differentiation, matrix maturation, and mineralization in the long bones of growing rats. J Nutr Biochem. 2010;21:297–303.
131. Park JHY, Grandjean CJ, Antonson DL, et al. Effects of isolated zinc deficiency on the composition of skeletal muscle, liver and bone during growth in rats. J Nutr. 1986;116:610–7.
132. Salgueiro MJ, Zubillaga M, Lysionek A, et al. Zinc as an essential micro nutrient: a review. Nutr Res. 2000;20:737–55.
133. Gonzales GF, Gasco M, Tapia V, et al. High serum zinc and serum testosterone levels were associated with excessive erythrocytosis in men at high altitudes. Endocrine. 2011;40:472–80.
134. Aina V, Perardi A, Bergandi L, et al. Cytotoxicity of zinc-containing bioactive glasses in contact with human osteoblasts. Chem Biol Interact. 2007;167:207–18.
135. Kasai M, Miyazaki T, Takenaka T, et al. Excessive zinc intake increases systemic blood pressure and reduces renal blood flow via kidney angiotensin II in rats. Biol Trace Elem Res. 2012;150:285–90.
136. Aina V, Bonino F, Morterra C, et al. Influence of the chemical composition on nature and activity of the surface layer of Zn-substituted sol-gel (bioactive) glasses. J Phys Chem C. 2011;115:2196–210.
137. Linati L, Lusvardi G, Malavasi G, et al. Qualitative and quantitative structure-property relationships analysis of multicomponent potential bioglasses. J Phys Chem B. 2005;109:4989–98.
138. Wers E, Oudadesse H. Thermal behaviour and excess entropy of bioactive glasses and Zn-doped glasses. J Therm Anal Calorim. 2014;115:2137–44.
139. Haimi S, Gorianc G, Moimas L, et al. Characterization of zinc-releasing three-dimensional bioactive glass scaffolds and their effect on human adipose stem cell proliferation and osteogenic differentiation. Acta Biomater. 2009;5:3122–31.
140. Srivastava AK, Pyare R. Characterization of ZnO substituted 45S5 bioactive glasses and glass—ceramics. J Mater Sci Res. 2012;1:207–20.
141. Atkinsona I, Anghela EM, Predoana L, et al. Influence of ZnO addition on the structural, in vitro behavior and antimicrobial activity of sol–gel derived $CaO–P_2O_5–SiO_2$ bioactive glasses. Ceram Int. 2016;42:3033–45.
142. Goel A, Kapoor S, Tilocca A, et al. Structural role of zinc in biodegradation of alkali-free bioactive glasses. J Mater Chem B. 2013;1:3073–82.
143. Aina V, Malavasi G, Pla AF, et al. Zinc-containing bioactive glasses: surface reactivity and behaviour towards endothelial cells. Acta Biomater. 2009;5:1211–22.
144. Ouis MA. Effect of ZnO on the bioactivity of hench's derived glasses and corresponding glass-ceramic derivatives. Silicon. 2011;3:177–83.
145. Du RL, Chang J, Ni SY, et al. Characterization and in vitro bioactivity of zinc-containing bioactive glass and glass-ceramics. J Biomater Appl. 2006;20:341–60.
146. Kanzaki N, Onuma K, Treboux G, et al. Inhibitory effect of magnesium and zinc on crystallization kinetics of hydroxyapatite (0001) face. J Phys Chem B. 2000;104:4189–94.
147. Balamurugan A, Balossier G, Kannan S, et al. Development and in vitro characterization of sol–gel derived $CaO–P_2O_5–SiO_2–ZnO$ bioglass. Acta Biomater. 2007;3:255–62.
148. Esteban-Tejeda L, Prado C, Cabal B, et al. Antibacterial and antifungal activity of ZnO containing glasses. PLoS One. 2015; doi:10.1371/journal.pone.0132709.
149. Baghbani F, Moztarzadeh F, Mozafari M, et al. Production and characterization of a Ag- and Zn-doped glass-ceramic material and in vitro evaluation of its biological effects. J Mater Eng Perform. 2016;25:3398–408.
150. Arfin SM, Kendall RL, Hall L, et al. Eukaryotic methionyl aminopeptidases: two classes of cobalt-dependent enzymes. Proc Natl Acad Sci U S A. 1995;92:7714–8.
151. Brown KL. Chemistry and enzymology of vitamin B12. Chem Rev. 2005;105:2075–149.
152. Bose S, Roy M, Bandyopadhyay A, et al. Recent advances in bone tissue engineering scaffolds. Trends Biotechnol. 2012;30:546–54.

153. Morcellia SR, Bulla ÉS, Terra WS, et al. Synthesis, characterization and antitumoral activity of new cobalt(II)complexes: effect of the ligand isomerism on the biological activity of the complexes. J Inorg Biochem. 2016;161:73–82.
154. Singh D, Kumar K, Kumar R, et al. Template synthesis and characterization of biologically active transition metal complexes comprising 14-membered tetraaza macrocyclic ligand. J Serb Chem Soc. 2010;75:217–28.
155. Vučković G, Stanić V, Sovilj SP, et al. Cobalt(II) complexes with aromatic carboxylates and N-functionalized cyclam bearing 2-pyridylmethyl pendant arms. J Serb Chem Soc. 2005;70:1121–9.
156. Vučković TSB, Miodragović ZM, et al. High-spin binuclear Co(II) complexes with a pendant octaazamaclocycle and carboxylates. J Serb Chem Soc. 2007;72:1295–308.
157. Peters K, Schmidt H, Unger R, et al. Paradoxical effects of hypoxia-mimicking divalent cobalt ions in human endothelial cells in vitro. Mol Cell Biochem. 2005;270:157–66.
158. Chachami G, Simos G, Hatziefthimiou A, et al. Cobalt induces hypoxia-inducible factor-1α expression in airway smooth muscle cells by a reactive oxygen species- and PI3K-dependent mechanism. Am J Respir Cell Mol Biol. 2004;31:544–51.
159. Pacary E, Legros H, Valable S, et al. Synergistic effects of CoCl(2) and ROCK inhibition on mesenchymal stem cell differentiation into neuron-like cells. J Cell Sci. 2006;119:2667–78.
160. Amellem O, Pettersen EO. Cell inactivation and cell cycle inhibition as induced by extreme hypoxia: the possible role of cell cycle arrest as a protection against hypoxia-induced lethal damage. Cell Prolif. 1991;24:127–41.
161. Mobasheria A, Proudman CJ. Cobalt chloride doping in racehorses: concerns over a potentially lethal practice. Vet J. 2015;205:335–8.
162. Azevedo MM, Jell G, O'Donnell MD, et al. Synthesis and characterization of hypoxia-mimicking bioactive glasses for skeletal regeneration. J Mater Chem. 2010;20:8854–64.
163. Hoppe A, Jokic B, Janackovic D, et al. Cobalt-releasing 1393 bioactive glass-derived scaffolds for bone tissue engineering applications. ACS Appl Mater Interfaces. 2014;6:2865–77.
164. Kargozar S, Lotfibakhshaiesh N, Ai J, et al. Synthesis, physico-chemical and biological characterization of strontium and cobalt substituted bioactive glasses for bone tissue engineering. J Non-Cryst Solids. 2016;449:133–40.
165. Vyas VK, Kumar AS, Singh SP, et al. Effect of cobalt oxide substitution on mechanical behaviour and elastic properties of bioactive glass and glass ceramics. Trans Indian Ceram Soc. 2016;75:12–9.
166. Wu C, Zhou Z, Fan W, et al. Hypoxia-mimicking mesoporous bioactive glass scaffolds with controllable cobalt ion release for bone tissue engineering. Biomaterials. 2012;33:2076–85.
167. Hoppe A, Brandl A, Bleiziffer O, et al. In vitro cell response to co-containing 1393 bioactive glass. Mater Sci Eng C. 2015;57:157–63.
168. Qiu ZY, Chen C, Wang XM, et al. Advances in the surface modification techniques of bone-related implants for last 10 years. Regener Biomater. 2014;1:67–79.
169. RussoL TF, Lupo C, et al. Carbonate hydroxyapatite functionalization: a comparative study towards (bio)molecules fixation. Interface Focus. 2014;4:20130040.
170. Brzoska JB, Azouz IB, Rondelez F, et al. Silanization of solid substrates: a step toward reproducibility. Langmuir. 1994;10:4367–73.
171. HowarterJA,YoungbloodJP.Optimizationofsilicasilanizationby3-aminopropyltriethoxysilane. Langmuir. 2006;22:11142–7.
172. ParedesV,SalvagniE,Rodríguez-CastellonE,etal.Studyontheuseof3-aminopropyltriethoxysilane and 3-chloropropyltriethoxysilane to surface biochemical modification of a novel low elastic modulus Ti–Nb–Hf alloy. J Biomed Mater Res B. 2015;103:495–502.
173. Toworfe GK, Composto RJ, Shapiro IM, et al. Nucleation and growth of calcium phosphate on amine-, carboxyl- and hydroxyl-silane self-assembled monolayers. Biomaterials. 2006;27:631–42.
174. Zucca P, Sanjust E. Inorganic materials as supports for covalent enzyme immobilization: methods and mechanisms. Molecules. 2014;19:14139–94.

175. Aina V, Magistris C, Cerrato G, et al. New formulation of functionalized bioactive glasses to be used as carriers for the development of ph-stimuli responsive biomaterials for bone diseases. Langmuir. 2014;30:4703–15.
176. Verne E, Vitale-Brovarone C, Bui E, et al. Surface functionalization of bioactive glasses. J Biomed Mater Res A. 2009;90:981–92.
177. Ferraris S, Vitale-Brovarone C, Bretcanu O, et al. Surface functionalization of 3D glass–ceramic porous scaffolds for enhanced mineralization in vitro. Appl Surf Sci. 2013;271:412–20.
178. Vernè E, Ferraris S, Cassinelli C, et al. Surface functionalization of Bioglass® with alkaline phosphatase. Surf Coat Technol. 2015;264:132–9.
179. Chen QZ, Rezwan K, Francon V, et al. Surface functionalization of Bioglass®-derived porous scaffold. Acta Biomater. 2007;3:551–62.
180. Zhang X, Zeng D, Li N, et al. Functionalized mesoporous bioactive glass scaffolds for enhanced bone tissue regeneration. Sci Rep. 2016;6:19361.
181. Sperling C, Fischer M, Maitz MF, et al. Blood coagulation on biomaterials requires the combination of distinct activation processes. Biomaterials. 2009;30:4447–56.
182. Lu HH, El-Amin SF, Scott KD, et al. Three-dimensional, bioactive, biodegradable, polymer–bioactive glass composite scaffolds with improved mechanical properties support collagen synthesis and mineralization of human osteoblast-like cells in vitro. J Biomed Mater Res A. 2003;64:465–74.
183. Zhou Z, Liu L, Liu Q, et al. Effect of surface modification of bioactive glass on properties of poly-L-lactide composite materials. J Macromol Sci B. 2012;51:1637–46.
184. Roether JA, Boccaccini AR, Hench LL, et al. Development and in vitro characterisation of novel bioresorbable and bioactive composite materials based on polylactide foams and bioglass for tissue engineering applications. Biomaterials. 2002;23:3871–8.
185. Ducker RE, Montague MT, Leggetta GJ, et al. A comparative investigation of methods for protein immobilization on self-assembled monolayers using glutaraldehyde, carbodiimide, and anhydride reagents. Biointerphases. 2008;3:59–65.
186. Gruian C, Vanea E, Simon S, et al. FTIR and XPS studies of protein adsorption onto functionalized bioactive glass. Biochim Biophys Acta. 2012;1824:873–81.
187. Gruian C, Vulpoi A, Steinhoff HJ, et al. Structural changes of methemoglobin after adsorption on bioactive glass, as a function of surface functionalization and salt concentration. J Mol Struct. 2012;1015:20–6.
188. Gruian C, Vulpoi A, Vane E, et al. The attachment affinity of hemoglobin toward silver-containing bioactive glass functionalized with glutaraldehyde. J Phys Chem B. 2013;117:16558–64.
189. Wang K, Zhou C, Hong Y, et al. A review of protein adsorption on bioceramics. Interface Focus. 2012;2:259–77.
190. Eskin SG, Horbett TA, McIntire, Mitchell RN, Ratner BD, Schoen FJ, Yee A. Some background concepts. In: Ratner BD, editor. Biomaterials science: an introduction to materials in medicine. 2nd ed. San Diego: Elsevier/Academic Press; 2004. p. 237–46.
191. Hynes RO. Integrins: versatility, modulation, and signaling in cell adhesion. Cell. 1992;69:11–25.
192. El-Ghannam A, Ducheyne P, Shapiro M, et al. Effect of serum proteins on osteoblast adhesion to surface-modified bioactive glass and hydroxyapatite. J Orthop Res. 1999;17:340–5.
193. Schepers E, de Clercq M, Ducheyne P, et al. Bioactive glass particulate material as a filler for bone lesions. J Oral Rehabil. 1991;18:439–52.
194. Higuchi A, Ling QD, Hsu ST, et al. Biomimetic cell culture proteins as extracellular matrices for stem cell differentiation. Chem Rev. 2012;112:4507–40.
195. Ballet T, Boulange L, Brechet Y, et al. Protein conformational changes induced by adsorption onto material surfaces: an important issue for biomedical applications of material science. Bull Pol Acad Sci Tech Sci. 2010;58:303–15.
196. Sousa SR, Lamghari M, Sampaio P, et al. Osteoblast adhesion and morphology on TiO2 depends on the competitive preadsorption of albumin and fibronectin. J Biomed Mater Res A. 2008;84:281290.

197. Vulpoi A, Gruian C, Vanea E, et al. Bioactivity and protein attachment onto bioactive glasses containing silver nanoparticles. J Biomed Mater Res A. 2012;100:1179–86.
198. Liau SY, Read DC, Pugh WJ, et al. Interaction of silver nitrate with readily identifiable groups: relationship to the antibacterial action of silver ions. Lett Appl Microbiol. 1997;25:279–83.
199. Rosengren A, Oscarsson S, Mazzocchi M, et al. Protein adsorption onto two bioactive glass-ceramics. Biomaterials. 2003;24:147–55.
200. Magyari K, Baia L, Vulpoi A, et al. Bioactivity evolution of the surface functionalized bioactive glasses. J Biomed Mater Res B. 2015;103:261–72.
201. Shah FA, Brauer DS, Hill RG, et al. Apatite formation of bioactive glasses is enhanced by low additions of fluoride but delayed in the presence of serum proteins. Mater Lett. 2015;153:143–7.
202. Boyan BD, Hummert TW, Dean DD, et al. Role of material surfaces in regulating bone and cartilage cell response. Biomaterials. 1996;17:137–46.
203. Anselme K. Osteoblast adhesion on biomaterials. Biomaterials. 2000;21:667–81.
204. García AJ, Ducheyne P, Boettiger D, et al. Effect of surface reaction stage on fibronectin-mediated. J Biomed Mater Res. 1998;40:48–56.

Chapter 3
Apatites for Orthopedic Applications

Berna Kankilic, Eda Ciftci Dede, Petek Korkusuz, Muharrem Timuçin, and Feza Korkusuz

Abstract The complex nature of the bone complicates its reconstruction and arises the use of biomaterials for this purpose. The materials should have similar properties with the bone and can be used in different application. Particularly, beta-tricalcium phosphate (β-TCP) and hydroxyapatite (HAp) are biocompatible, bioactive, and osteoconductive materials having similar properties with the bone. In this review, the applications of tricalcium phosphate and hydroxyapatite in orthopedics are given in terms of graft, carrier, and coating materials.

Keywords Bone • Orthopedics • Tissue engineering • Biomaterials • Calcium phosphates • Tricalcium phosphate • Hydroxyapatite • Bone graft • Carrier systems • Coating • Osteoconductivity

B. Kankilic
Middle East Technical University, Graduate School of Natural and Applied Sciences, Department of Biotechnology, Çankaya, Ankara, Turkey
e-mail: uysalberna@yahoo.com

E.C. Dede
Hacettepe University, Graduate School of Science and Engineering, Department of Bioengineering, Beytepe, Ankara, Turkey
e-mail: eda.ciftci.hu@gmail.com

P. Korkusuz
Hacettepe University, Faculty of Medicine, Department of Histology and Embryology, Sıhhıye, Ankara, Turkey
e-mail: petek@hacettepe.edu.tr

M. Timuçin
Middle East Technical University, Faculty of Engineering, Department of Metallurgical and Materials Engineering, Çankaya, Ankara, Turkey
e-mail: timucin@metu.edu.tr

F. Korkusuz (✉)
Hacettepe University, Faculty of Medicine, Department of Sports Medicine, Sıhhıye, Ankara, Turkey
e-mail: feza.korkusuz@gmail.com

G. Kaur (ed.), *Clinical Applications of Biomaterials*,
DOI 10.1007/978-3-319-56059-5_3

3.1 Introduction

A bone is a tissue that supports and protects the organs, provides motility, stores minerals, and produces red and white blood cells. From the biological perspective, the natural bone matrix is a combination of organic/inorganic composite materials and consists of a naturally occurring polymer (type I collagen) and a biological mineral (apatite) [1]. The organic compartment, type I collagen, gives flexibility, while inorganic compartment, apatite, gives the rigidity to the tissue [2].

Due to its complexity, reconstruction of bone tissue is not an easy process. As trauma, surgery, infection, and tumors disrupt the bone structure, researchers seek for substitute materials to fulfill the gap. There are several different materials that can be used for this purpose. Biomaterials are a class of engineering materials, which can be used in animal body tissue replacements, reconstructions, and regenerations, without long-term adverse effects [3]. The development of biomaterials and manufacturing techniques broadened the diversity of applications of various biocompatible materials. These include bioceramics, biopolymers, metals, and biocomposites. Bioceramics are compatible ceramic materials classified as bioglasses, alumina, zirconia, and calcium phosphates (CaPs) [4]. CaPs are the most frequently used materials in this area as their compositions are too similar with the natural bone. They are used in bone defects, to support cell proliferation, migration, and differentiation. They can be used as drug carriers to eradicate bone infections and implant coating materials to enhance bone adhesion. They are biocompatible, osteoconductive materials and have high protein affinity [5]. Beta-tricalcium phosphates (β-TCP) and hydroxyapatite are the most well-known CaPs, as they are used in various bone tissue engineering applications.

3.2 What Is Beta-Tricalcium Phosphate (β-TCP)?

β-TCP can be synthesized by several different methods including sol-gel procedures, solid-state reaction, microwave irradiation, wet chemical method, hydrothermal synthesis, mechanochemical synthesis, combustion synthesis, and electrochemical deposition [6]. The material can be characterized by using scanning electron microscopy (SEM) (Fig. 3.1) and x-ray diffraction (XRD) (Fig. 3.2). The stoichiometric β-TCP has 1.5 Ca/P ratio in vivo; hydroxyapatite can be formed on the surface of β-TCP as a result of β-TCP/body fluid interaction [7].

Beta-tricalcium phosphate (β-TCP) has many advantages to be used in orthopedic applications. These are its:

- Biocompatibility
- Bioactivity
- Osteoconductivity
- High resorption rate [9]

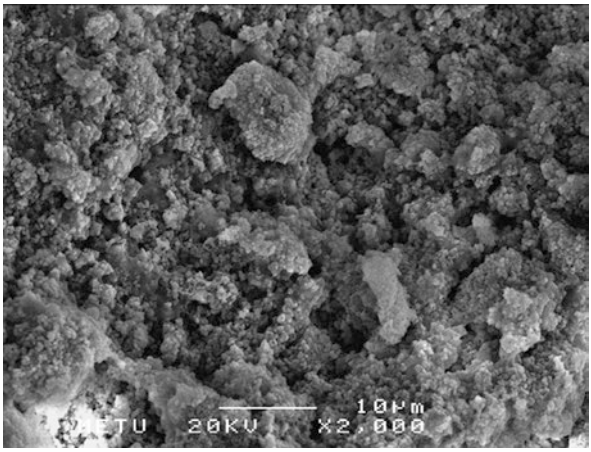

Fig. 3.1 Scanning electron micrograph of the vancomycin-containing PLLA/ β-TCP composite showed the porous structure of the surface that is composed of β-TCP and vancomycin powder [8]

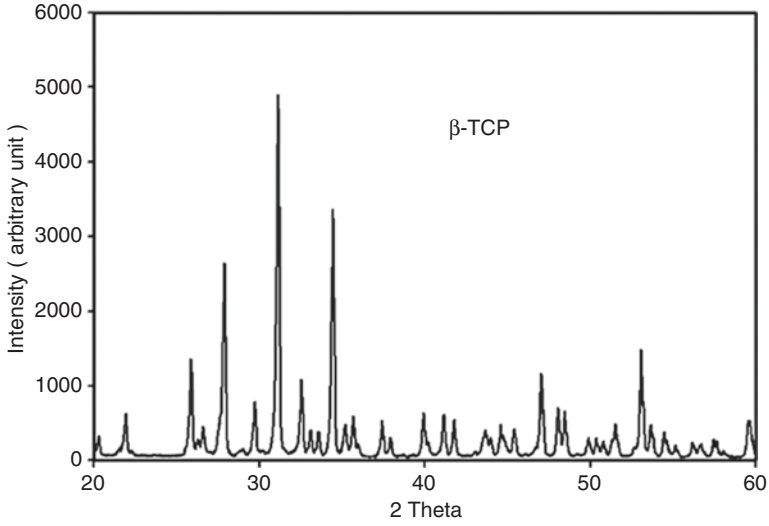

Fig. 3.2 The powder XRD pattern of the β-TCP showing typical calcium phosphate peaks [8]

Due to its resorption, it can be replaced by new tissue as it degrades [10]. Researchers found that β-TCP improves osteosynthesis and forms an interface for the bone [11].

Besides these advantages, β-TCP also has some disadvantages. Firstly, due to its poor mechanical properties, it cannot resist against fatigue. Secondly, it is absorbed more rapidly than new formed tissue. Finally, despite its osteoconductivity, it does not show any osteogenicity or osteoinductivity [12].

3.2.1 Orthopedic Applications of β-TCP

As we previously mentioned, β-TCP can be used as bone substitutes, carrier systems, and coating material due to its advantages. In order to avoid its disadvantages, it can be also used with other biomaterials as composites. In this part, we will review the applications of β-TCP in orthopedic field.

3.2.1.1 Grafts as Bone Substitutes or Fillers

Zhang et al. fabricated gelatin/β-TCP nanofibers with different β-TCP contents using electrospinning. The purpose of the study was to evaluate the physicochemical-biological correlation of nanofibers according to its calcium ion release and its compatibility with human osteoblast-like cells. They characterized the nanocomposites with various methods like scanning electron microscopy (SEM) and Fourier transform infrared spectroscopy (FTIR) and found that proliferation and differentiation of the cells were increased parallel with the content of β-TCP nanoparticles [13].

In the study conducted by Damlar et al., three different commercial β-TCP bone grafts were evaluated in pig bone defect model. Bone grafts had <50 μm, 1–5 μm, and 1–5 μm micropores, respectively. Five bone defects were made with burr, and three defects were filled with the commercial bone grafts, while one defect was filled with autogenous bone graft as positive control, and the last defect was filled with blood clot as negative control. When compared with negative control, histomorphometric results showed that bone grafts with smaller micropore sizes contributed in healing. The graft with higher micropore size showed no sign of healing. Authors suggested that not the chemical structure but also physical structure of materials had major roles in clinical applications [14].

Cao et al. fabricated three-dimensional composite scaffolds from β-TCP and polyglycolic acid (PGA) with 3:1 and 1:1 weight ratio. They characterized the composites and compared them with hydroxyapatite in vivo according to their biodegradation, biocompatibility, and osteogenesis. According to results, new bone formation began 14 days after the surgery, and composite with highest TCP weight ratio had the highest bone mineral density and biodegradation rate [15].

Daculsi et al. developed polymer/β-TCP composites with two different β-TCP contents (10 and 24 w-%) to evaluate the effect of bioceramic content on bone formation. The composites were evaluated in long-term rabbit bone model at weeks 24, 48, and 76 weeks by using micro-computed tomography (CT), SEM, and light microscopy. The composites did not show any foreign body reaction at week 76, and higher β-TCP-containing composite showed the highest bone in-growth [11].

Lee et al. conducted a study to compare β-TCP/hydroxyapatite (HAp) composite with a commercial bone graft. The macroporosities of the composite and commercial bone graft were 83 % and 69 %, respectively. The materials were implanted into 8 mm diameter defects in Sprague-Dawley rat's cranials, and histomorphometric analysis was conducted at weeks 4 and 8. The composite showed better bone formation than the commercial bone graft, and it had higher bone volume for both weeks [16].

The other studies using β-TCP as bone graft were summarized in Table 3.1.

Table 3.1 Studies using β-TCP as bone graft material

Ref	Material	Aim	Methods	Results
[17]	20 µl recombinant human bone morphogenetic protein-2 (rhBMP-2)-treated PLA/nano β-TCP composite scaffolds with different weight ratios (PLA/10 nano β-TCP, PLA/30 nano β-TCP, PLA/30 micro β-TCP, PLA/50 nano β-TCP)	Examine the influence of β-TCP in the degradation of the scaffold and evaluate the new bone formation in vivo at weeks 2, 4, and 8	Scaffolds were characterized with XRD, SEM, transmission electron microscopy (TEM), and compression test machine. Immunohistochemical analysis was conducted for in vivo studies	In vitro results indicated that nano TCP minimizing the acidity caused by the PLA degradation more than micro TCP and enhanced the osteoconductivity of the scaffolds. PLA/30 nβ-TCP and PLA/10 nβ-TCP scaffolds exhibited better mechanical properties than PLA/50 nβ-TCP scaffolds. On the other hand, PLA/30 nβ-TCP and PLA/50 nβ-TCP scaffolds exhibited similar osteogenesis. Since ideal scaffold has to have similar mechanical properties with natural bone, authors concluded that PLA/30 nano β-TCP was a promising scaffold for bone regeneration
[18]	PLLA/β-TCP composite scaffolds	Preparation of composite scaffolds without using any residual organic solvent	Composite scaffolds were fabricated using a novel technique comprising powder mixing, compression molding, low-temperature treatment, and particulate leaching. Scaffolds were characterized with SEM. Proliferation of osteoblast cells seeded on scaffolds was evaluated with methylthiazol tetrazolium (MTT) assay, and their differentiation potential was evaluated with alkaline phosphatase (ALP) assay. The expression of genes specified for osteogenicity like ALP, osteocalcin, and type I collagen was determined with real-time polymerase chain reaction (PCR)	The scaffold had interconnected porous structure with a porosity of 70 %. Osteoblast cells proliferated on scaffolds for 14 days. Proliferation and ALP activity rate were statistically significant than control group. Gene expressions of ALP, osteocalcin, and type 1 collagen was upregulated. The results showed that this scaffold preparation method can be useful for bone tissue engineering

(continued)

Table 3.1 (continued)

Ref	Material	Aim	Methods	Results
[19]	Alginate/TCP scaffold	Fabricate alginate/TCP scaffolds for bone tissue engineering with power printing. TCP powder used in fabrication consisted of 60:40 ratio of α:β-tricalcium phosphate, and alginate weight percents were 0, 2.5, 5, and 7.5 %	The scaffolds were characterized with SEM, XRD, and micro-CT. Mechanical properties were defined with universal testing machine. Biocompatibility of the scaffolds was evaluated by WST assay using osteoblastic cell line MG63	The results showed that scaffold with 2.5 wt.% alginate had the best mechanical properties with uniformly distributed alginate-TCP network. MG63 cells proliferated on every scaffold group for 7 days. Authors concluded that alginate/TCP scaffold with 2.5 wt.% alginate powder will be a promising material to be used in bone tissue engineering

3.2.1.2 Carrier for Drug Delivery

Generally, due to its slow degradation, β-TCP is a material of choice for carrier systems. But disadvantages of β-TCP can be an obstacle mainly in orthopedic field in order to provide good mechanical properties. For this purpose, β-TCP is used with polymers as composite to minimize the disadvantages.

In the study conducted by Kankilic et al., vancomycin-containing poly-L-lactic acid (PLLA)/β-TCP composites were developed and characterized to control methicillin-resistant *Staphylococcus aureus* (MRSA) in vitro. Vancomycin-free composites were used as negative control, and in another group composites were dip coated with PLLA to extend the vancomycin release. Coated composites released vancomycin for 6 weeks, and vancomycin-containing composites were susceptible to MRSA at day 4. Based on cell adhesion and proliferation assays, all study groups were compatible with mesenchymal stem cells (MSCs) and osteosarcoma cells (SaOS-2) at days 3 and 7 [8].

In the other study by the same group, same vancomycin-containing composites were used to control implant-related osteomyelitis (IRO) in rat model. IRO model was established by MRSA inoculation into the tibial defect with titanium particles. Infection model was verified by radiographical analysis after 3 weeks. Sham operation was also undertaken and used as control group. After the implantation of composites, radiological and histological scores were quantified with microbiological findings on weeks 1 and 6. IRO was resolved in vancomycin-containing composites, and MRSA was only isolated from vancomycin-free composites. New bone was formed in all the PLLA/β-TCP groups at weeks 1 and 6 according to histomorphometric results [20].

Ahola et al. developed poly(L-lactide-co-caprolactone) (PLCL)/β-TCP composites with 8 wt. % rifampicin for the treatment of osteomyelitis. The β-TCP contents were 0, 50, and 60 wt. %, respectively. They found that ceramic content positively effecting the drug release. All composites were susceptible to *Pseudomonas aeruginosa* [21].

Makarov et al. fabricated 40 vol. % β-TCP/polylactic acid (PLA) nanocomposites containing 1 wt. % vancomycin consolidated at room temperature or 120 °C. Composites released 90% of their drug content at the end of 5 weeks. Mechanical analysis showed that the composites consolidated at high temperature had better mechanical properties. According to microbiological experiments, high and very high MRSA concentrations were eradicated by the end of 7 days [22].

Xie et al. used a fine-spinning technology to produce poly (L-lactide-co-glycolide) (PLGA)-TCP composite containing osteopromotive molecule, icaritin. The composites were characterized with SEM and porosity was defined with micro-CT. Compression test was performed for mechanical properties. High-performance liquid chromatography (HPLC) was used to quantify the icaritin release. Biocompatibility of the composites was evaluated with bone marrow-derived MSCs and intramuscular implantation. As a result of sustainable icaritin release, biocompatible composite was developed [23].

The other studies using β-TCP as carrier material were summarized in Table 3.2.

Table 3.2 Studies using β-TCP as carrier material

Ref	Material	Aim	Methods	Results
[24]	β-TCP and polycaprolactone (PCL)-coated β-TCP powder for the delivery of bovine serum albumin (BSA). β-TCP powders had 100 nm, 550 nm, and 1850 nm particle sizes	Investigate the release behavior of BSA by changing particle size, BSA concentration, and surface modification	The powders were used as plain or they were coated with PCL solution. They were characterized with field emission SEM (FESEM) and FTIR spectrometry. Three different BSA concentrations (1, 3, and 5 mg/ml in deionized water) were used for protein loading. BSA release was evaluated with BCA assay	XRD analysis of TCP samples indicated that only β-phase peaks were present. Comparing the FTIR spectra of all particulate systems before and after BSA loading, there was no extra peak due to chemical interaction between particles and protein. This is the sign of physical adsorption of BSA on particulate systems. The majority of samples showed no more than 50 % release, except the 550 nm particles demonstrated 100 % release. PCL coating showed no significant ability to attenuate burst release in phosphate-buffered saline (PBS)
[25]	Ceftriaxone-sulbactam impregnated porous β-TCP delivery system	Develop highly interconnected porous ceftriaxone-sulbactam containing β-TCP scaffolds to treat chronic osteomyelitis	Stoichiometric β-TCP powder was used with combination of two drugs ceftriaxone and sulbactam in 2:1 ratio (named as CSF). Scaffolds were characterized, and release studies were conducted at 37 °C with PBS and simulated body fluid (SBF). In vivo studies were performed in experimental rabbit tibial osteomyelitis model and histological analysis was undertaken	Samples had 60–65 % porosity with average pore size of 55 μm. CFS release from β-TCP implants was faster in SBF than PBS. Further, both the results of in vitro and in vivo drug elution after 42 days showed that release was higher than minimum inhibitory concentration of CFS against *S. aureus*. The histological findings suggested that there was only a minimal reaction toward biomaterial and gradual new bone formation in the area
[26]	Vancomycin impregnated biodegradable gelatin sponge containing different contents of β-TCP	Eliminate osteomyelitis with vancomycin-containing scaffolds	Scaffolds with 0:10, 1:10, 3:10, and 5:10 β-TCP:gelatin ratio was prepared and characterized. In vivo drug controlled release and antibacterial properties were determined with Kirby-Bauer (K-B) disc diffusion test in Sprague-Dawley rats	The scaffold with 5:10 ratio had burst effect and released vancomycin only for 21 days, while the release in the scaffolds with 1:10 and 3:10 ratios continued until day 42. The release in the scaffolds with 0:10 ratio was extended to 56 days

[27]	Vancomycin and clindamycin impregnated β-TCP plugs	Impregnate microporous β-TCP plugs with different antibiotic solutions and to determine their release behavior	Antibiotics were impregnated into scaffold by drop, dip, and stream coating, and the concentrations were 40, 80, and 120 mg/mL. Antibiotic release was determined by capillary zone electrophoresis and disc diffusion method	Approximately 89 % of vancomycin and 90 % of clindamycin were released from the plugs after 24 h regardless of the impregnation method. Six days later, antibiotics were completely released, but only the concentrations released within 3 days had antimicrobial activity
[28]		Investigate the osteogenic properties of BMP-2 combined with β-TCP scaffolds in both intramuscular and bone defects in rabbits	Chemical etching was performed to increase the surface area of the scaffolds, and scaffolds were characterized. 30 and 15 μg of BMP-2 were impregnated into scaffolds and, respectively, implanted into the back muscles and into femoral (condyle and diaphysis) defects of rabbits for 4 weeks along with the blanks. Histomorphometric analysis was performed for new bone formation	The blank implants did not show any new bone formation, while all BMP-2-loaded implants showed new bone formation with the presentation of osteoblasts and osteocytes in fibrous tissue. The amount of newly formed bone distributed within the pores was 4.4 ± 3.8 %. For femoral defect implantations, new bone was formed regarding the type of scaffold. Bone formation was independent of the femoral implantation site. In condyle defects, loaded and blank scaffolds resulted in new bone formation of, respectively, 33 ± 12 and 26 ± 7 %, while it was 32 ± 9 and 20 ± 8 % in diaphysis defects, respectively

3.2.1.3 Coating Materials for Implants

Metals used as mechanical support in orthopedic field are typically inert and have poor biocompatibility. In order to increase their biocompatibility, metals are usually coated with biocompatible materials. Due to the biocompatibility, bioactivity, and osteoconductivity, implants can be coated with single β-TCP or its composites.

Mina et al. deposited six different chitosan/β-TCP coating on stainless steel substrates with different weight percentages: $\beta\text{-TCP}_{100\ \%}\text{-Ch}_{0\ \%}$, $\beta\text{-TCP}_{95\ \%}\text{-Ch}_{5\ \%}$, $\beta\text{-TCP}_{90\ \%}\text{-Ch}_{10\ \%}$, $\beta\text{-TCP}_{75\ \%}\text{-Ch}_{25\ \%}$, $\beta\text{-TCP}_{65\ \%}\text{-Ch}_{35\ \%}$, and $\beta\text{-TCP}_{50\ \%}\text{-Ch}_{50\ \%}$. The coating was characterized by using XRD and dispersive x-ray analysis (EDX) and electrochemical impedance spectroscopy (EIS). Biocompatibility was assessed with primary Chinese hamster ovary (CHO) cells. They found that chitosan concentrations up to 25 % were cytotoxic to only 5–10% of CHO cells, and chitosan weight concentration changed the arrangement of the b-TCP crystal lattice [29].

Chen et al. coated porous polycaprolactone scaffolds with hyaluronic acid/β-TCP matrix. MSCs were cultured on scaffolds with and without coating to investigate proliferation and osteogenic differentiation. On day 4, hyaluronic acid/β-TCP coating increased the expression of alkaline phosphatase and collagen type I. Uniform cell matrix and calcium deposition was observed with SEM. As a result, hyaluronic acid/β-TCP coating improved biocompatibility and osteoconductivity of the scaffolds [30].

Chai et al. coated Mg alloy (Mg-3AI-1Zn) with β-TCP by phosphating. Cell culture studies conducted and revealed that SaOS-2 cells significantly adhered and proliferated on β-TCP-coated alloys. Bone morphogenetic protein-2 (BMP-2) was highly expressed in these cells. The alloys were implanted into the femur of Wistar rats, and at weeks 1, 4, and 12, pathological and histological examinations were undertaken. New bone formation was observed at week 1 and matured at week 4. Uncoated alloys degraded 33%, while coated alloys only degraded 17% at week 12 [31].

3.3 What Is Hydroxyapatite (HAp)?

Another commonly used apatite in the orthopedics is hydroxyapatite (HAp). HAp, the main inorganic material in natural bone, has been used widely for orthopedic applications [32]. It is clinically used to conduct bone regeneration and improves implant integration. HAp is a biocompatible material that is extensively used in the replacement and regeneration of bone tissue. In nature, nanostructured HAp is the main component present in hard body tissues [33]. Furthermore, it is obtained by some different way synthetically [34–36]. Hydroxyapatite has hexagonal rhombic cage structure and its ideal Ca/P ratio is 10/6. Typical XRD spectrum determines the atomic and molecular structure of HAp crystals shown below (Figs. 3.3 and 3.4).

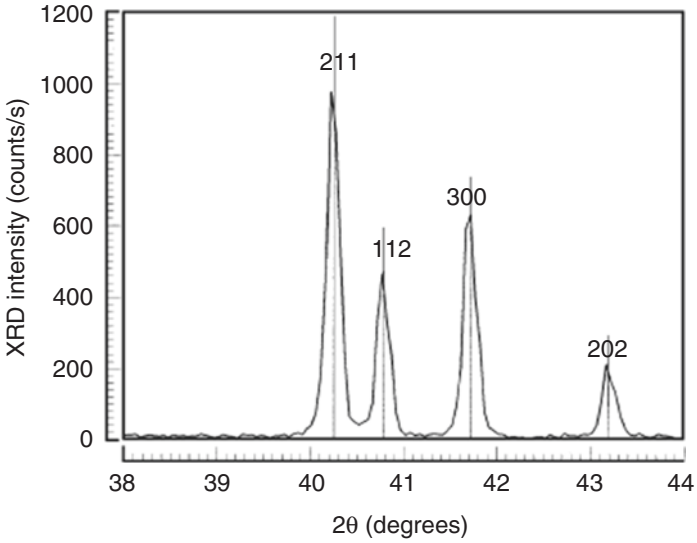

Fig. 3.3 Typical experimental powder XRD spectrum of HAp sample [37]

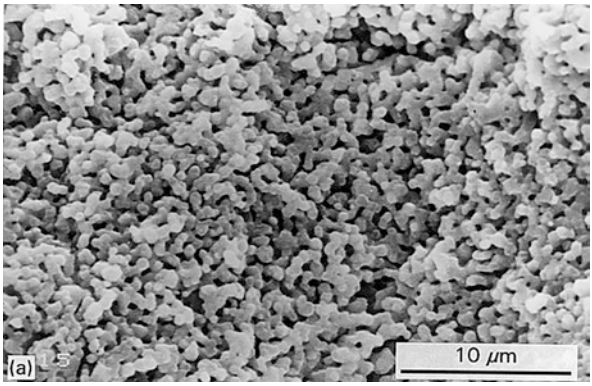

Fig. 3.4 Scanning electron micrograph of HAp powders [37]

Hydroxyapatites have many advantages that support to the use of orthopedic applications:

- Biodegradability
- Biocompatibility
- Osteoinduction
- Osteoconduction
- Nontoxicity
- Noninflammatory

Besides these advantages, the disadvantages of HAp ceramics such as fragility, inelasticity, and irritability have been overcome by using them as a composite with

various materials. The HAp composites have also these advantages together with additive advance by other materials. One of the studies that proving these features, HAp combined with boron trace element and biocompatibility, differentiation, and proliferation potential of this composite was tested with bone marrow-derived mesenchymal stem cells (MSCs). Human bone marrow-derived MSC's phenotype was assessed using scanning and transmission electron microscopy after combining with B-n-HAp and n-HAp. Cell adhesion and proliferation potential of these ceramics were examined with the real-time cell analysis (xCELLigence, Roche Applied Science and ACEA Bioscience, USA) system, and adipogenic/osteogenic differentiation was analyzed with morphological and quantitative methods. MSC's adhesion and proliferation rates (cell index, 4.50) were higher than controls (cell index, 4.00). Adipogenic and osteogenic differentiation potential of MSCs remained unchanged in the presence of B-n-HAp ceramics. In conclusion, B-n-HAp stimulates MSC's adhesion, proliferation, and differentiation and has a potential to regenerate bone tissue [38] (Figs. 3.5 and 3.6).

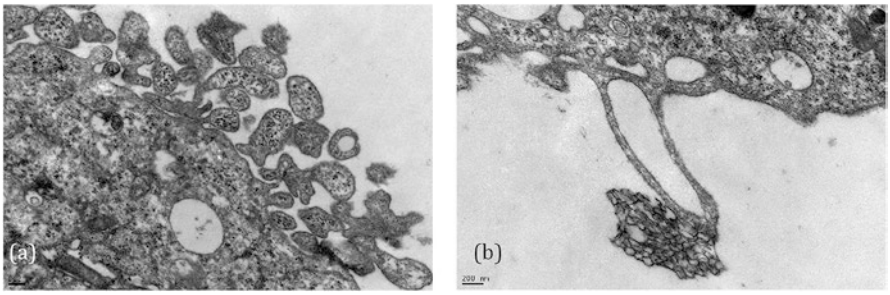

Fig. 3.5 MSCs taking ceramic nanoparticles by their cytoplasmic projections. Numerous cell projections in (**a**) and one projection taking up the ceramic in (**b**) was observed. (Figure courtesy of Petek Korkusuz MD, PhD)

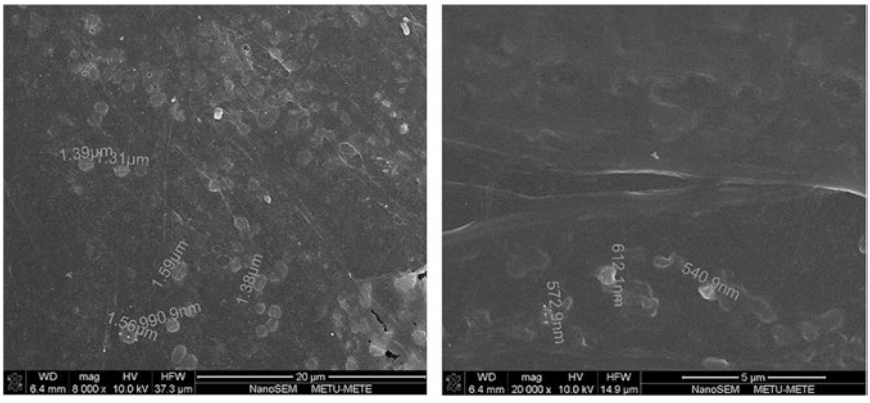

Fig. 3.6 Scanning electron micrographs show MSC's secreting extracellular matrix with the ceramics. Note the size of nanostructure particles on the pictures yerine; Scanning electron micrographs show MSCs secreting extracellular matrix near the ceramics. Note the size of nano structured particles. (Figure courtesy of Petek Korkusuz MD, PhD)

Basically HAp has three different usages for orthopedic applications:

- Carrier for drug delivery (genes, antibiotics, antiresorptives, etc.)
- Coating materials for implants
- Grafts as bone substitutes or fillers

3.3.1 Orthopedic Applications of HAp

3.3.1.1 Carrier for Drug Delivery

Hydroxyapatite composites are used as the controlled drug delivery systems in the treatment of bone tumors and osteomyelitis due to their pore structures and biocompatibility [39]. In one of the research studies about HAp drug delivery systems, a multiple biomimetic design was developed to improve the osteogenesis capacity of composite scaffolds consisting of hydroxyapatite nanoparticles (HAp) and silk fibroin (SF) by Ding et al. In this study, bone morphogenetic protein-2 (BMP-2) was loaded in the SF scaffolds and HAp to tune BMP-2 release. In vitro studies showed the preservation of BMP-2 bioactivity in the composite scaffolds, and programmable sustained release was achieved through adjusting the ratio of BMP-2 loaded on SF and HAp. In vitro and in vivo osteogenesis studies demonstrated that the composite scaffolds showed improved osteogenesis capacity under suitable BMP-2 release conditions, significantly better than that of BMP-2-loaded SF-HAp composite scaffolds reported previously. Therefore, these biomimetic SF-HAp nanoscaled scaffolds with tunable BMP-2 delivery provide preferable microenvironments for bone regeneration [40]. In another study, Parent et al. evaluated a porous hydroxyapatite implant as biocompatible bone substitute and vancomycin delivery system to prevent postoperative infections. They impregnated with optimized conditions insured a high antibiotic loading (up to 2.3 ± 0.3 mg/m^2), with a complete in vitro release obtained within 1–5 days. Additionally, the bacteriostatic and bactericidal effects of vancomycin were retained after loading on hydroxyapatite, as demonstrated after challenge with a *Staphylococcus aureus* strain. At the end of this study, their results demonstrate the efficacy of these hydroxyapatite bone substitutes for local delivery of vancomycin in the context of bone infection [41].

There are different research studies about HAp as the carrier for drug delivery systems in the following table (Table 3.3).

3.3.1.2 Coating Materials for Implants

HAp ceramics are mostly applied on prostheses as a surface coating and clinically used to conduct bone regeneration and improve implant integration. Nano (n)-HAp expands the surface area for cell adhesion and may improve bone regeneration and

Table 3.3 Literature scan for hydroxyapatite as the carrier for drug delivery systems (from 2014 to 2017)

Ref	Composite material	Aim	Methods	Results
[42]	Antibacterial chitosan (CS)-coated nanoHAp (nHAp)/polyamide66 (PA66) porous bone scaffold	Describe new drug-loaded coating scaffold applied in infection therapy during bone regeneration	CS containing antibacterial berberine was coated on a nHAp/PA66 scaffold to realize bone regeneration together with antimicrobial properties	The bactericidal test confirms a strong antibiotic effect of the delivery system, and the minimum inhibitory concentration of the drug is 0.02 mg/ml. In vitro biological evaluation demonstrates that the coating scaffolds act as a good matrix for MG63 adhesion, crawl, growth, and proliferation, suggesting that the antibacterial delivery system has no cytotoxicity
[43]	Zn^{2+}/Mg^{2+} doped hydroxyapatite (HAp)-bovine serum albumin (BSA) nanoparticles (NPs)	Study BSA-HAp nanocarriers to achieve controlled release kinetics of BSA protein and investigated the role of Mg and Zn in controlling the protein release from HAp nanocarriers	The amount of BSA uptake by doped and undoped HAp NPs and subsequent release of BSA from NPs were investigated	BSA release rate from Zn doped HAp NPs was found to be the highest, whereas undoped HAp NPs released BSA at the slowest rate. This study showed that the protein release rate from HAp NPs can be controlled by the addition of suitable dopants and doped HAp-based NP systems can be used in bone growth factor and drug release study
[44]	Dexamethasone (Dex)-loaded hydroxyapatite (HAp)	Investigate whether Dex-loaded HAp (Dex/HAp) enhances bone regeneration in rat calvarial defects	HAp was loaded with Dex and then characterized using SEM and drug release study. The bone regeneration ability of Dex/HAp was investigated in a rat critical size bone defect using digital mammography, multislice spiral computed tomography (MSCT) imaging, and histological analysis	According to digital mammography and MSCT, Dex/HAp showed the highest bone regeneration in rat bone defects compared to those received drug-free HAp. Histological studies confirmed these data and showed osteointegration to the surrounding tissue

[45]	PTHrP (107–111) loading into gelatin-glutaraldehyde biopolymer-coated HAp (HAp_{Glu}) scaffolds	Evaluate whether PTHrP (107–111) loading into gelatin-glutaraldehyde biopolymer-coated HAp (HAp_{Glu}) scaffolds would produce an optimal biomaterial for tissue engineering applications	HAp_{Glu} scaffolds with and without PTHrP (107–111) were implanted into a cavitary defect performed in both distal tibial metaphysis of adult rats. Animals were sacrificed after 4 weeks for histological, microcomputerized tomography and gene expression analysis of the callus	Bone healing occurred only in the presence of PTHrP (107–111)-containing HAp_{Glu} implant, related to an increase in bone volume/tissue volume and trabecular thickness, cortical thickness, and gene expression of osteocalcin and vascular cell adhesion molecule 1, but a decreased gene expression of Wnt inhibitors, SOST, and dickkopf homolog 1. The autonomous osteogenic effect of the PTHrP (107–111)-loaded HAp_{Glu} scaffolds was confirmed in mouse and human osteoblastic cell cultures
[46]	Nanostructured composite (collagen, hydroxyapatite nanoparticles) layer with antibiotics (vancomycin hydrochloride)	Develop a resorbable, nanostructured composite (collagen, hydroxyapatite nanoparticles) layer with the controlled elution of antibiotics (vancomycin hydrochloride)	High-performance liquid chromatography was used so as to characterize the in vitro release rates of the vancomycin and its crystalline degradation antibiotically inactive products over a 21-day period	The modification of collagen with hydroxyapatite nanoparticles does not negatively influence the sustainable release of vancomycin. The balance of vancomycin and its degradation products was observed after 14 days of incubation

tissue integration. In one of our study, we compared the osseointegration of titanium (Ti)-based Küntscher nails (K-nails) and plates with modified nanostructured and hydroxyapatite-coated surfaces in a rat femur model. Both surface modifications significantly improved cell proliferation and alkaline phosphatase (ALP) activity as compared to the control (non-modified Ti implants). The controls and modified nails and plates were implanted in the femur of 21 male Sprague-Dawley rats. The implants, with surrounding tissues, were removed after 10 weeks, and then mechanical tests (torque and pullout) were performed, which showed that the modified K-nails exhibited significantly better osseointegration than the controls. Histological examinations of the explants containing plates showed similar results, and the modified plates exhibited significantly better osseointegration than the controls. Surface nanostructuring of commercially available titanium-based implants by a very simple method – anodization – seems to be a viable method for increasing osseointegration without the use of bioactive surface coatings such as hydroxyapatite [47]. In a different paper, Eto et al. evaluated the potential issues of total hip arthroplasty (THA) with an Ag-HAp-coated implant. In this prospective interventional study, they performed THA with this implant in 20 patients and investigated the effects of silver and HAp coating. This was the first clinical study of Ag-HAp-coated implants in THA. They reported that their Ag-HAp-coated implants markedly improved patients' activities of daily living without causing any adverse reactions attributable to silver in the human body. Ag-HAp is expected to reduce postoperative infections and prevent decreased quality of life in patients undergoing prosthetic arthroplasty, thus leading to more favorable outcomes [48]. In another study that is a systemic review, Patel et al. investigated HAp-coated versus uncoated external fixator and determine benefits in terms of pin loosening, infection, and loss of reduction/malunion. A systematic literature search using PubMed, EMBASE, OVID SP, Cochrane database, ClinicalTrials.gov website, and the references of the studies identified was undertaken on 26th August 2014. Comparative trials investigating HAp-coated versus uncoated external fixation pins were identified. Primary outcome measures included pin loosening and infection. Secondary outcome measures included loss of reduction/malunion. At the end of the study, they reported that HAp coating of external fixator pins improves bone fixation and reduces loosening in patients undergoing prolonged fixation procedures, such as leg lengthening, but the influence on infection and malunion is not clear [49].

There are different types of HAp coatings at the following table (Table 3.4).

3.3.1.3 Grafts as Bone Substitutes or Fillers

Autogenous bone grafts also named as autografts are widely used due to their osteoinductive and osteoconductive features. However, there are some disadvantages of autogenous grafts that are the development of wound complications in the area of grafting, the prolongation of the operation time, and the inability to obtain

Table 3.4 Literature scan for hydroxyapatite as the coating materials for implants (from 2014 to 2017)

Ref	Composite material	Aim	Methods	Results
[50]	Two kinds of CeO_2-incorporated hydroxyapatite coatings (HAp-10Ce and HAp-30Ce) were prepared via plasma spraying technique and the effects of osteogenic activity of mesenchymal stem cell and macrophage polarization was assessed	Examine the incorporation of CeO_2 into HAp coating regulates osteogenic activity of bone mesenchymal stem cell (BMSC) and macrophage polarization	Two kinds of CeO_2-incorporated HAp coatings were prepared via plasma spraying technique. The effects of CeO_2 addition on the osteogenic activity of BMSCs and the related mechanism were investigated. Besides, the effects of CeO_2 incorporation on the inflammatory response mediated by macrophage were also examined	An increase in CeO_2 content in the HAp coatings resulted in better osteogenic behaviors of BMSCs in terms of cell proliferation, alkaline phosphatase (ALP) activity and mineralized nodule formation. RT-PCR and Western blot analysis suggested that the incorporation of CeO_2 may promote the osteogenic differentiation of BMSCs through the Smad-dependent BMP signaling pathway, which activated Runx2 expression and subsequently enhanced the expression of ALP and OCN. The incorporation of CeO_2 in HAp coatings can be a valuable strategy to promote osteogenic responses and reduce inflammatory reactions
[51]	Porous and cytocompatible silicon carbide (SiC) ceramics derived from wood precursors and coated with bioactive hydroxyapatite (HAp) and HAp-zirconium dioxide (HAp/ZrO_2) composite	Evaluate the potential of porous and cytocompatible silicon carbide (SiC) ceramics derived from wood precursors and coated with bioactive HAp and HAp/ZrO_2 composite to use at application in engineering of bone implants due to their excellent mechanical and structural properties	Biomorphic SiC ceramics have been synthesized from wood using a forced impregnation method. The SiC ceramics have been coated with bioactive HAp and HAp/ZrO2 using effective gas detonation deposition (GDD) approach. The surface morphology and cytotoxicity of SiC ceramics as well as phase composition and crystallinity of deposited coatings were analyzed. The XRD and FTIR studies revealed the preservation of crystal structure and phase composition of in the HAp coating, while addition of ZrO2 to the initial HAp powder resulted in significant decomposition of the final HAp/ZrO2 coating and formation of other calcium phosphate phases	Phase composition and crystallinity of deposited coatings analyses showed that the porosity and pore size of SiC ceramics depend on initial wood source. At the end of this study, they reported that porous and cytocompatible bio-SiC ceramics with bioactive coatings show a great promise in construction of light, robust, inexpensive, and patient-specific bone implants for clinical application

(continued)

Table 3.4 (continued)

Ref	Composite material	Aim	Methods	Results
[52]	Hydroxyapatite (HAp) coating layer on polyetheretherketone (PEEK)	Evaluate cold-spray coating of HAp on a three-dimensional PEEK implant and its biocompatibility by in vitro and in vivo minipig model	They used cold-spray coating method to form a thick layer of HAp on the topographically complex PEEK substrates with periodic ridges on the surface and implanted in iliac bone defects of mini pigs, which is known to be similar with human body system. In addition, PEEK cage for clinical usage was coated with HAp and inserted in the lumbar intervertebral disc space of minipig	They observed higher ALP activity, calcium production, and BSP production of human bone marrow-derived mesenchymal stem cells on the HAp-coated PEEK implants than the bare PEEK group in in vitro test. In addition, two-dimensional histological analysis and three-dimensional micro-CT analysis demonstrated that implantation of complex shape of HAp-PEEK hybrid implant in in vivo mini pig model resulted in sufficient biocompatibility and osseointegration for further clinical applications
[53]	Zn-, Mg-, and Sr-substituted hydroxyapatite-coated (Zn-HAp-coated, Mg-HAp-coated, Sr-HAp-coated) titanium implants	Confirm the different effects of the fixation strength of Zn-, Mg-, Sr-substituted hydroxyapatite-coated (Zn-HAp-coated, Mg-HAp-coated, Sr-HAp-coated) titanium implants via electrochemical deposition in the osteoporotic condition	Twelve weeks after bilateral ovariectomy, all animals (female Sprague-Dawley rats) were randomly divided into four groups: group HAp, group Zn-HAp, group Mg-HAp, and group Sr-HAp. Afterwards, all rats from groups HAp, Zn-HAp, Mg-HAp, and Sr-HAp received implants with hydroxyapatite containing 0 %, 10 % Zn ions, 10 % Mg ions, and 10 % Sr ions. Implants were inserted bilaterally in all animals until death at 12 weeks. The bilateral femurs of rats were harvested for evaluation	All treatment groups increased new bone formation around the surface of titanium rods and push-out force; group Sr-HAp showed the strongest effects on new bone formation and biomechanical strength. Additionally, there are significant differences in bone formation, and push-out force was observed between groups Zn-HAp and Mg-HAp

adequate grafts. Most patients suffer of pain at the autograft removal site. Superficial nerve damage, hematoma, and infection can be other complications related to autograft obtainment. At this point, an approach to the development of alternative grafts could be needed. Because of its osteoconductive feature, HAp is more effectively used as different forms of grafts for bone fractures, disorders, and diseases. At the study of Yoshii et al., they investigated the efficacy and safety of synthetic porous hydroxyapatite (HAp) combined with local vertebral bone graft for use in anterior cervical corpectomy and fusion (ACCF) for the treatment of patients with ossification of the posterior longitudinal ligament (OPLL). Since 2006, 25 OPLL patients underwent ACCF using HAp blocks (HAp group). Hydroxyapatite blocks with 40 % porosity were used for the one-level ACCFs, and HAp blocks with 15% porosity were used for the two-level ACCFs. Clinical and radiological evaluation was performed with a minimum of 2-year follow-up. Outcomes were compared with those of 25 OPLL patients who underwent ACCFs using auto-fibula grafts at the authors' institution before 2006 (FBG group). Based on the results of this study, ACCF using HAp is a safe and efficacious method for the treatment of patients with OPLL as an alternative to conventional ACCF using autologous fibula bone grafting [54]. In another study, Uemura et al. clinically and radiologically evaluated the availability, osteoconductivity, and resorption of a novel unidirectional porous hydroxyapatite (UDPHAp) used as an artificial substitute for open-wedge high tibial osteotomy. In this study, seven patients (two men and five women aged 34–72 years) who underwent OWHTO and were followed up for more than 12 months were retrospectively studied. After the osteotomy, the gap created was filled with UDPHAp. Radiography and computed tomography (CT) were performed, and gap healing was assessed postoperatively. They reported that short-term results for OWHTO using UDPHAp were satisfactory. Clinical improvement of JOA scores was seen, besides osteogenesis was progressing in and around the artificial bone grafts [55] (Table 3.5).

3.4 Conclusion

As a conclusion, β-TCP and HAp are bioactive, biocompatible, osteoconductive materials that can be used as graft, carrier, or coating materials in orthopedic applications. Due to the disadvantages of calcium phosphates, they should be used with other materials like polymers or metals, especially in load-bearing applications. Their similar chemical properties make them good candidates for orthopedic applications.

Table 3.5 Literature scan for hydroxyapatite as the grafts as bone substitutes or fillers (from 2014 to 2017)

Ref	Composite material	Aim	Methods	Results
[56]	Interconnected porous hydroxyapatite ceramics (IP-HAp)	Examine whether IP-HAp could be used as bone substitute for implant treatment in reconstructive surgery	They assessed if surround of the titanium surface placed into granular or block-type IP-HAp can observe new bone formation in a rabbit bone defect model. Subsequently, osseointegration and stability of titanium implant inserted into block-type IP-HAp were investigated in a rabbit onlay graft model	Direct contact between new bone and the surface of the titanium in granular- or block-type IP-HAp was found in a rabbit bone defect. Further, new bone formation was found in direct contact with the implant surface in the block-type IP-HAp in an onlay graft model, and the implant stability quotient (ISQ) values were significantly increased after surgery. Therefore, IP-HAp may be a useful material for implant treatment in reconstructive surgery strategies
[57]	Biodegradable coralline hydroxyapatite/calcium carbonate (HApCC) composite	Characterize this HApCC to assess its capacity for conductive osteogenesis and to observe its clinical performance as a bone substitute for bone augmentation after skeletal tumor removal	Powder x-ray diffraction (XRD), scanning electron microscopy (SEM), and energy-dispersive x-ray spectroscopy (EDX) were used to characterize HApCC. The osteogenic potential of this graft material was investigated in the present study after incorporation of HApCC together with hMSCs in vitro and following implantation in immunodeficient mice in vivo. A preliminary clinical study was also performed in 16 patients to investigate the extent of bone regeneration following augmentation of bone stock with HApCC after skeletal tumor resection	In conclusion, HApCC appears to be an excellent biodegradable bone graft material. It biointegrates with the host, is osteoconductive and biodegradable, and can be an attractive alternative to autogenous grafts

[58]	HAp granules derived from cuttlefish bone (CB-HAp)	Evaluate the cellular biocompatibility and bone formation properties of CB-HAp granules for use as a bone graft substitute	In this study, HAp granules were prepared from raw CB by using a hydrothermal reaction. The formation of HAp from CB was confirmed by scanning electron microscopy and x-ray diffraction analysis. The bioactivity of the CB-HAp granules was evaluated both in vitro and in vivo	Results show that CB-HAp is nontoxic and that CB-HAp granules supported improved cell adhesion, proliferation, and differentiation compared to stoichiometric synthetic HAp granules. Furthermore, in vivo bone defect healing experiments show that the formation of bone with CB-HAp is higher than that with pure HAp. These results show that CB-HAp granules have excellent potential for use as a bone graft material
[59]	Injectable ceramic biphasic bone substitute CERAMENT™/BONE VOID FILLER	Assess the potential of a novel injectable bone substitute CERAMENT™/BONE VOID FILLER in supporting the initial reduction and preserving alignment of the joint surface until fracture healing	From June 2010 through May 2011, adult patients presenting with acute, closed, and unstable tibial plateau fractures which required both grafting and internal fixation were included in a prospective study with percutaneous or open reduction and internal fixation (ORIF) augmented with an injectable ceramic biphasic bone substitute CERAMENT™/BONE VOID FILLER (BONESUPPORT™, Lund, Sweden) to fill residual voids. Clinical follow-up was performed at 1, 3, 9, and 12 months and any subsequent year, including radiographical analysis and Rasmussen system for knee functional grading	The joint alignment was satisfactory and maintained within a range of 2 mm, with an average of 1.18 mm. The mean Rasmussen knee function score was 26.5, with 14 patients having an excellent result and the remaining 10 with a good result. It can be concluded that radiological and clinical outcome was satisfactory and obtained in all cases without complications. This injectable novel biphasic hydroxyapatite and calcium sulfate ceramic material is a valuable armamentarium in the treatment of trauma where bone graft is required

(continued)

Table 3.5 (continued)

Ref	Composite material	Aim	Methods	Results
[60]	Carbonated hydroxyapatite (CHAp) granules and polysaccharide polymer (β-1,3-glucan)	Study the potential application in orthopedics as a filler of bone defects of a novel elastic hydroxyapatite-based composite of high surgical handiness	The biomaterial was composed of CHAp granules and β-1,3-glucan. Cylinders of 4 mm in diameter and 6 mm in length were implanted into bone cavities created in the proximal metaphysis of tibiae of 24 New Zealand white rabbits. 18 sham-operated animals were used as controls. After 1, 3, or 6 months, the rabbits were euthanized; the bones were harvested and subjected to analysis	Radiological images and histological sections revealed integration of implants with bone tissue with no signs of graft rejection. Peripheral quantitative computed tomography (pQCT) indicated the stimulating effect of the biomaterial on bone formation and mineralization. Densitometry (DXA) analysis suggested that biomineralization of bones was preceded by bioresorption and gradual disappearance of porous ceramic granules. The findings suggest that the CHAp-glucan composite material enables regeneration of bone tissue and could serve as a bone defect filler

References

1. Chu PK, Liu X. Biomaterials fabrication and processing handbook. Boca Raton: CRC Press; 2008.
2. Kankilic B. Analysis of the effects of vancomycin containing bioceramic/polymer composites on biofilm prevention, biocompatibility and osteogenic modification of mesenchymal stem cells. Thesis of Philosophy of Doctorate in Biotechnology, Middle East Technical University, Ankara Turkey, September 2015.
3. Nath S, Basu B, Sinha A. A comparative study of conventional sintering with microwave sintering of hydroxyapatite synthesized by chemical route trends. Biomater Artif Organs. 2006;19(2):93–8.
4. Thamaraiselvi TV, Rajeswari S. Biological evaluation of bioceramic materials – a review. Trends Biomater Artif Organs. 2004;18(1):9–17.
5. Amy J, Johnson W, Herschler BA. A review of the mechanical behavior of CaP and CaP/polymer composites for applications in bone replacement and repair. Acta Biomater. 2011;7(1): 16–30.
6. Mehdikhani B, Borhani GH. Synthesis nano bio-ceramic powder β-Ca2P2O7. J Ceram Process Res. 2015;16(3):308–12.
7. Mirhadi B, Mehdikhani B, Askari N. Synthesis of nano-sized β-tricalcium phosphate via wet precipitation. Proc Appl Ceram. 2011;5(4):193–8.
8. Kankilic B, Bayramli E, Kilic E, Dagdeviren S, Korkusuz F. Vancomycin containing PLLA/b-TCP controls MRSA in vitro. Clin Orthop Relat Res. 2011;469:3222–8.
9. Kannan S, Goetz-Neunhoeffer F, Neubauer J, Pina S, Torres PMC, Ferreira JMF. Synthesis and structural characterization of strontium -and magnesium-co-substituted b-tricalcium phosphate. Acta Biomater. 2010;6:571–6.
10. Dessi M, Borzacchiello A, Mohamed THA, Abdel-Fattah WI, Ambrosio L. Novel biomimetic thermosensitive b-tricalcium phosphate/chitosan-based hydrogels for bone tissue engineering. J Biomed Mater Res Part A. 2013;101A:2984–93.
11. Daculsi G, Goyenvalle E, Cognet R, Aguado E, Suokas EO. Osteoconductive properties of poly(96L/4D-lactide)/beta-tricalcium phosphate in long term animal model. Biomaterials. 2011;32:3166–77.
12. Bin Liu PD, Deng-xing Lun MSC. Current application of b-tricalcium phosphate composites in orthopaedics. Orthop Surg. 2012;4:139–44.
13. Zhang X, Cai Q, Liu H, Zhang S, Wei Y, Yang X, Lin Y, Yang Z, Deng X. Calcium ion release and osteoblastic behavior of gelatin/beta-tricalcium phosphate composite nanofibers fabricated by electrospinning. Mater Lett. 2012;73:172–5.
14. Damlar I, Erdogan O, Tatli U, Arpag OF, Gormez U, Ustun Y. Comparison of osteoconductive properties of three different b-tricalcium phosphate graft materials: a pilot histomorphometric study in a pig model. J Craniomaxillofac Surg. 2015;43:175–80.
15. Cao H, Kuboyama N. A biodegradable porous composite scaffold of PGA/β-TCP for bone tissue engineering. Bone. 2010;46:386–95.
16. Lee JH,Ryu MY, Baek H, Lee K, Seo JH, Lee HK. Fabrication and evaluation of porous beta-tricalcium phosphate/hydroxyapatite (60/40) composite as a bone graft extender using rat calvarial bone defect model. Sci World J. 2013;2013:481789. 9.
17. Cao L, Duan PG, Wang HR, Li XL, Yuan FL, Fan ZY, Li SM, Dong J. Degradation and osteogenic potential of a novel poly(lactic acid)/nano-sized b-tricalcium phosphate scaffold. Int J Nanomedicine. 2012;7:5881–8.
18. Zhao XF, Li XD, Kang YQ, Yuan Q. Improved biocompatibility of novel poly(L-lactic acid)/b--tricalcium phosphate scaffolds prepared by an organic solvent-free method. Int J Nanomedicine. 2011;6:1385–90.
19. Castilho M, Rodrigues J, Pires I, Gouveia B, Pereira M, Moseke C, Groll J, Ewald A, Vorndran E. Fabrication of individual alginate-TCP scaffolds for bone tissue engineering by means of powder printing. Biofabrication. 2015;7:015004.

20. Kankilic B, Bilgic E, Korkusuz P, Korkusuz F. Vancomycin containing PLLA/β-TCP controls experimental osteomyelitis in vivo. J Orthop Surg Res. 2014;9:114.
21. Ahola N, Veiranto M, Männistö N, Karp M, Rich J, Efimov A, Kellomäki M. Processing and sustained in vitro release of rifampicin containing composites to enhance the treatment of osteomyelitis. Biomatter. 2012;2(4):213–25.
22. Makarov C, Berdicevsky I, Raz-Pasteur A, Gotman I. In vitro antimicrobial activity of vancomycin-eluting bioresorbable β-TCP-polylactic acid nanocomposite material for load-bearing bone repair. J Mater Sci Mater Med. 2013;24(3):679–87.
23. Xie XH, Wang XL, Zhang G, He YX, Leng Y, Tang TT, Qin L. Biofabrication of a PLGA–TCP-based porous bioactive bone substitute with sustained release of icaritin. J Tissue Eng Regen Med. 2015;9(8):961–72.
24. Vahabzadeh S, Edgington J, Bose S. Tricalcium phosphate and tricalcium phosphate/polycaprolactone particulate composite for controlled release of protein. Mater Sci Eng C. 2013;33(7):3576–82.
25. Kundu B, Nandi SK, Roy S, Dandapat N, Soundrapandian C, Datta S, Basu D. Systematic approach to treat chronic osteomyelitis through ceftriaxone–sulbactam impregnated porous β-tri calcium phosphate localized delivery system. Ceram Int. 2012;38(2):1533–48.
26. Zhou J, Fang T, Wang Y, Dong J. The controlled release of vancomycin in gelatin/b-TCP composite scaffolds. J Biomed Mater Res Part A. 2012;100A:2295–301.
27. Seidenstuecker M, Mrestani Y, Neubert RH, Bernstein A, Mayr HO. Release kinetics and antibacterial efficacy of microporous β-TCP coatings. J Nanomater. 2013;2013:13.
28. Sohier J, Daculsi G, Sourice S, De Groot K, Layrolle P. Porous beta tricalcium phosphate scaffolds used as a BMP-2 delivery system for bone tissue engineering. J Biomed Mater Res A. 2010;92(3):1105–14.
29. Mina A, Caicedo HH, Uquillas JA, Aperador W, Gutiérrez O, Caicedo JC. Biocompatibility behavior of β–tricalcium phosphate-chitosan coatings obtained on 316L stainless steel. Mater Chem Phys. 2016;175:68–80.
30. Chen M, Le DQ, Kjems J, Bünger C, Lysdahl H. Improvement of distribution and osteogenic differentiation of human mesenchymal stem cells by hyaluronic acid and β-tricalcium phosphate-coated polymeric scaffold in vitro. Bio Res Open Access. 2015;4(1):363–73.
31. Chai H, Guo L, Wang X, Gao X, Liu K, Fu Y, Yang K. In vitro and in vivo evaluations on osteogenesis and biodegradability of a β-tricalcium phosphate coated magnesium alloy. J Biomed Mater Res A. 2012;100(2):293–304.
32. Fox K, Tran PA, Tran N. Recent advances in research applications of nanophase hydroxyapatite. ChemPhysChem. 2012;13:2495–506.
33. Zakaria SM, Sharif Zein SH, Othman MR, Yang F, Jansen JA. Tissue Eng, Part B Rev. 2013;19(5):431–41.
34. Chavan PN, Bahir MM, Mene RU, Mahabole MP, Khairnar RS. Study of nanobiomaterial hydroxyapatite in simulated body fluid: formation and growth of apatite. Mater Sci Eng B. 2010;168:224–30.
35. Akram M, Ahmed R, Shakir I, et al. Extracting hydroxyapatite and its precursors from natural resources. J Mater Sci. 2014;49:1461.
36. Wu S-C, Hsu H-C, Hsu S-K, Chang Y-C, Ho W-F. Synthesis of hydroxyapatite from eggshell powders through ball milling and heat treatment. J Asian Ceramic Soc. 2016;4(1):85–90.
37. Tas CA, Korkusuz F, Timucin M, Akkas N. (1997). An investigation of the chemical synthesis and high-temperature sintering behaviour of calcium hydroxyapatite (HA) and tricalcium phosphate (TCP) bioceramics. J Mater Sci Mater Med. 1997;8(2):91–6.
38. Çiftci E, Kose S, Korkusuz P, Timucin M, Korkusuz F. Boron containing nano hydroxyapatites (B-n-HAp) stimulate mesenchymal stem cell adhesion, proliferation and differentiation. Key Eng Mater. 2015;631:373–8.
39. Korkusuz F, Korkusuz P. Use of hydroxyapatite ceramics in orthopedics. Acta Orthop Traumatol Turc. 1997;31:63–7.
40. Ding Z, Fan Z, Huang X, Lu Q, Xu W, Kaplan DL. Silk-hydroxyapatite nanoscale scaffolds with programmable growth factor delivery for bone repair. ACS Appl Mater Interfaces. 2016;8(37):24463–70.

41. Parent M, Magnaudeix A, Delebassée S, Sarre E, Champion E, Viana Trecant M, Damia C. Hydroxyapatite microporous bioceramics as vancomycin reservoir: antibacterial efficiency and biocompatibility investigation. J Biomater Appl. 2016;31(4):488–98.
42. Huang D, Zuo Y, Zou Q, Zhang L, Li J, Cheng L, Shen J, Li Y. Antibacterial chitosan coating on nano-hydroxyapatite/polyamide66 porous bone scaffold for drug delivery. J Biomater Sci Polymer Edition. 2011;22(7):931–44.
43. Dasgupta S, Banerjee SS, Bandyopadhyay A, Bose S. Zn- and Mg-doped hydroxyapatite nanoparticles for controlled release of protein. Langmuir. 2010;26:4958–64.
44. Tavakoli-darestani R, Manafi-rasi A, Kamrani-rad A. Dexamethasone-loaded hydroxyapatite enhances bone regeneration in rat calvarial defects. A Mol Biol Rep. 2014;41:423. doi:10.1007/s11033-013-2876-9.
45. Lozano D, Sánchez-Salcedo S, Portal-Núñez S, Vila M, López-Herradón A, Ardura JA, Mulero F, Gómez-Barrena E, Vallet-Regí M, Esbrit P. Parathyroid hormone-related protein (107-111) improves the bone regeneration potential of gelatin–glutaraldehyde biopolymer-coated hydroxyapatite. Acta Biomater. 2014;10:3307–16.
46. Suchı T, Šupová M, Klapková E, Hornı L, Rıglová S, Žaloudková M, Braun M, Sucharda Z, Ballay R, Veselı J, Chlup H, Denk F. The sustainable release of vancomycin and its degradation products from nanostructured collagen/hydroxyapatite composite layers. J Pharm Sci. 2016;105:1288e1294.
47. Sirin HT, Vargel I, Kutsal T, Korkusuz P, Piskin E. Ti implants with nanostructured and HA-coated surfaces for improved osseointegration. Artif Cells, Nanomed Biotechnol. 2016;44(3):1023–30. doi:10.3109/21691401.2015.1008512.
48. Eto S, Kawano S, Someya S, Miyamoto H, Sonohata M, Mawatari M. First clinical experience with thermal sprayed silver oxide-containing hydroxyapatite coating implant. J Arthroplast. 2016; doi:10.1016/j.arth.2015.12.034.
49. Patel A, Ghai A, Anand A. Clinical benefit of hydroxyapatite-coated versus uncoated external fixation: a systematic review. Int J Orthod. 2016;183(3):581–590. 2313–1462. doi:10.17554/j.issn.2313-1462.2016.03.163.
50. Li K, Shen Q, Xie Y, You M, Huang L, Zheng X. Incorporation of cerium oxide into hydroxyapatite coating regulates osteogenic activity of mesenchymal stem cell and macrophage polarization. J Biomater Appl. 2016;31(7):1–15.
51. Gryshkov O, Klyui NI, Temchenko VP, Kyselov VS, Chatterjee A, Belyaev AE, Lauterboeck L, Iarmolenko D, Glasmacher B. Porous biomorphic silicon carbide ceramics coated with hydroxyapatite as prospective materials for bone implants. Mater Sci Eng C. 2016;68:143–52.
52. Lee JH, Jang HL, Lee KM, Baek H-R, Jin K, Noh JH. Cold-spray coating of hydroxyapatite on a three-dimensional polyetheretherketone implant and its biocompatibility evaluated by in vitro and in vivo minipig model. J Biomed Mater Res Part B Appl Biomater. 2017;105:647–57.
53. Tao ZS, Zhou WS, He XW, Liu W, Bai BL, Zhou Q, Huang ZL, Tu KK, Li H, Sun T, Lv YX, Cui W, Yang L. A comparative study of zinc, magnesium, strontium-incorporated hydroxyapatite-coated titanium implants for osseointegration of osteopenic rats. Mater Sci Eng C. 2016;62:226–32.
54. Yoshii T, Hirai T, Sakai K, Sotome S, Enomoto M, Yamada T, Inose H, Kato T, Kawabata S, Okawa A. Anterior cervical corpectomy and fusion using a synthetic hydroxyapatite graft for ossification of the posterior longitudinal ligament. Orthopedics. 2016; doi:10.3928/01477447-20161208-02.
55. Uemura K, Kanamori A, Aoto K, Yamazaki M, Sakane M. Novel unidirectional porous hydroxyapatite used as a bone substitute for open wedge high tibial osteotomy. J Mater Sci Mater Med. 2014;25:2541–7. doi:10.1007/s10856-014-5266-5.
56. Minami M, Takechi M, Ohta K, Ohta A, Ninomiya Y, Takamoto M, Fukui A, Tada M, Kamata N. Bone formation and osseointegration with titanium implant using granular- and block-type porous hydroxyapatite ceramics (IP-CHA). Dent Mater J. 2013;32(5):753–60.

57. Fu K, Xu Q, Czernuszka J, Triffitt JT, Xia Z. Characterization of a biodegradable coralline hydroxyapatite/calcium carbonate composite and its clinical implementation. Biomed Mater. 2013;8(6):065007. doi:10.1088/1748-6041/8/6/065007.
58. Kim BS, Kang HJ, Yang SS, Lee J. Comparison of in vitro and in vivo bioactivity: cuttlefish-bone-derived hydroxyapatite and synthetic hydroxyapatite granules as a bone graft substitute. Biomed Mater. 2014;9(2):025004. doi:10.1088/1748-6041/9/2/025004.
59. Iundusi R, Gasbarra E, D'Arienzo M, Piccioli A, Tarantino U. Augmentation of tibial plateau fractures with an injectable bone substitute: CERAMENTTM. Three-year follow-up from a prospective study. BMC Musculoskelet Disord. 2015;16:115.
60. Borkowski L, Pawłowska M, Radzki RP, Bieńko M, Polkowska I, Belcarz A, Karpiński M, Słowik T, Matuszewski Ł, Ślósarczyk A, Ginalska G. Effect of a carbonated HAP/β-glucan composite bone substitute on healing of drilled bone voids in the proximal tibial metaphysis of rabbits. Mater Sci Eng C Mater Biol Appl. 2015;53:60–7.

Chapter 4
Calcium Phosphate Cements for Medical Applications

Fatma Ozdemir, Iain Evans, and Oana Bretcanu

Abstract This chapter presents an overview of calcium phosphate cements (CPCs) used for medical applications. The hardening mechanism and the two types of CPCs apatite and brushite, are discussed. A description of the main properties (and testing methods) of CPCs such as setting time, cohesion time, mechanical properties and injectability and different strategies adopted to improve them are reported. The chapter includes a description of the preparation steps of a typical cement before implantation in the bone defect and some examples of current medical applications and limitations of CPCs.

Keywords Calcium phosphate • Apatite cement • Brushite cement • Setting time • Cohesion • Injectability

4.1 Introduction

According to the Cambridge dictionary, a cement is a binder, a material that *'sticks things together'* [1]. Earliest references are to construction materials where cements were used to join stone or bricks. These early applications share common elements with modern medical cements although the materials and properties are considerably more predictable. When mixed with water, cements sets over a defined period of time, becoming hard, which is usually an irreversible process. During setting, the mixture of cement and water will change from a liquid or viscous state to a solid phase [2].

Calcium phosphate cements (CPCs) are mixtures of one or more calcium phosphate (CPs) powders with water or aqueous solutions that can set at room or body temperature. Having a ceramic structure, CPCs are brittle, being used only for non-loadbearing applications. Due to their similarity with biological hydroxyapatite (HAp), the mineral phase of natural bones and teeth, CPCs have found several applications as fillers for bone fractures or bone defects, for craniomaxillofacial, dental

F. Ozdemir • I. Evans • O. Bretcanu (✉)
Newcastle University, School of Mechanical and Systems Engineering, Newcastle upon Tyne, UK
e-mail: oana.bretcanu@newcastle.ac.uk

G. Kaur (ed.), *Clinical Applications of Biomaterials*,
DOI 10.1007/978-3-319-56059-5_4

and orthopaedics applications. CPCs can easily be moulded or injected into irregular cavities of the bone tissue, restoring the structure and functions of the bone and stimulating new bone formation [3].

The first documented attempt to use CP as a bone substitute was in 1920 when tricalcium phosphate was implanted into small defects in animals to promote new bone regenerations. In 1951, hydroxyapatite (HAp) was used for the first time on rats and guinea pigs. These were the first trials to formulate suitable bone substitutes that could promote new bone formations [4]. It was only in 1970s that HAp and other CPs were synthesised and used as granules or in block form for clinical applications. Since then the interest in these ceramic materials continuously increased due to the significant potential for implants following disease and surgery [5].

The first CPC was a dental cement made at ambient or body temperature via a hardening process. It was developed by LeGeros and other scientists working for the American Dental Association who in 1976 reported a possible dental restoration material [6]. The composition of this cement was further investigated by Brown and Chow in the early 1980s [4, 7]. The first patent for a self-setting CPC was obtained by Brown and Chow in 1983 [8].

In 1996 the Food and Drug Administration (FDA) approved the use of CP bone cements for repairing craniofacial defects [9]. Since then different CPCs with varying compositions of the powder and liquid components have been developed and commercialised.

4.2 Calcium Phosphates

Calcium phosphates used for bone cements are calcium salts of orthophosphoric acid H_3PO_4. Table 4.1 shows the most common calcium phosphates, their atomic Ca/P ratio and pH stability range in aqueous solution at 25 °C. As can be seen in Table 4.1, decreasing the Ca/P ratio results in the compounds becoming more acidic.

Synthetic hydroxyapatite (HAp) has a structure similar to the inorganic part of the teeth and bone. It is highly crystalline, has low solubility and it is more stable thermodynamically than calcium-deficient hydroxyapatite (CDHA), which is similar to biological apatite. CDHA is typically highly amorphous (has low crystallinity) and has a higher surface area than HAp, due to its nanosized structure, being more reactive than HAp, and thus, more soluble than HAp.

Amorphous calcium phosphate (ACP) is the nanometric phase that can initially precipitate from a highly supersaturated calcium phosphate solution and then transform into more stable crystalline phases such as octacalcium phosphate (OCP) or HAp. ACP is highly amorphous and contains about 15–20% of water, mostly in the lattice interstices [12].

Monocalcium phosphate monohydrate (MCPM) is the most acidic calcium phosphate, and it is stable at pH values lower than 2. It has the highest solubility in water.

Table 4.1 Most common calcium phosphate compounds

Name	Formula [10]	Acronym	Ca/P	pH stability[a] [11]
Tetracalcium phosphate (mineral hilgenstockite)	$Ca_4(PO_4)_2O$	TTCP	2.0	Less stable than CDHA, DCPD or OCP in water at pH 7.4
Hydroxyapatite	$Ca_{10}(PO_4)_6(OH)_2$	HAp	1.67	>4.0
Amorphous calcium phosphate	$Ca_xHy(PO_4)_z\ nH_2O$, n = 3–4.5; 15–20% H_2O	ACP	1.0–2.2	4.0–8.0
Calcium-deficient hydroxyapatite	$Ca_{10\text{-}x}(HPO_4)_x(PO_4)_{6\text{-}x}(OH)_{2\text{-}x}$, x∈(0–1) x = 0 → HAp x = 1 → $Ca_9(HPO_4)(PO_4)_5(OH)$	CDHA	1.5–1.67	5.0–10.0
α-Tricalcium phosphate	α-$Ca_3(PO_4)_2$	α-TCP	1.5	6.0–8.0 more stable than DCPD but less than CDHA
β-Tricalcium phosphate (mineral whitlockite)	β-$Ca_3(PO_4)_2$	β-TCP	1.5	6.0–8.0 more stable than α-TCP
Octacalcium phosphate	$Ca_8(HPO_4)_2(PO_4)_4{\cdot}5H_2O$	OCP	1.33	6.5–8.0
Dicalcium phosphate dihydrate (mineral brushite)	$CaH(PO_4){\cdot}2H_2O$	DCPD	1.0	2.0–4.0
Dicalcium phosphate anhydrous (mineral monetite)	$CaH(PO_4)$	DCPA	1.0	2.0–4.0
Monocalcium phosphate monohydrate	$Ca(H_2PO_4)_2{\cdot}H_2O$	MCPM	0.5	<2.0

[a]pH stability range in aqueous solution at 25 °C

Dibasic calcium phosphate anhydrous (DCPA) is less soluble than dicalcium phosphate dihydrate (DCPD). DCPA is stable at very low pH (pH < 2), while DCPD is stable at pH < 4.2. Under physiological conditions, both structures are metastable and tend to transform into a more stable apatite structure [11]. Natural minerals with DCPA and DCPD compositions are named monetite and brushite, respectively.

α-Tricalcium phosphate (α-TCP) is the high-temperature polymorphic form of tricalcium phosphate (TCP). β-Tricalcium phosphate (β-TCP) is the low-temperature polymorphic form of TCP, which is stable at room temperature. It is less soluble than α-TCP but more soluble than hydroxyapatite. Thermodynamically, the most stable structure of β-TCP is the mineral whitlockite, a calcium-magnesium phosphate [11]. Under physiological conditions, α-TCP transforms into a more stable apatitic structure.

Tetracalcium phosphate (TTCP) is the most basic CP, and it has the highest Ca/P atomic ratio (2:1), higher than stoichiometric HAp. Under physiological conditions, TTCP can transform into a more stable apatitic structure (HAp or CDHA).

Octacalcium phosphate has a lower solubility than DCPD. Under physiological conditions, OCP can transform into HAp.

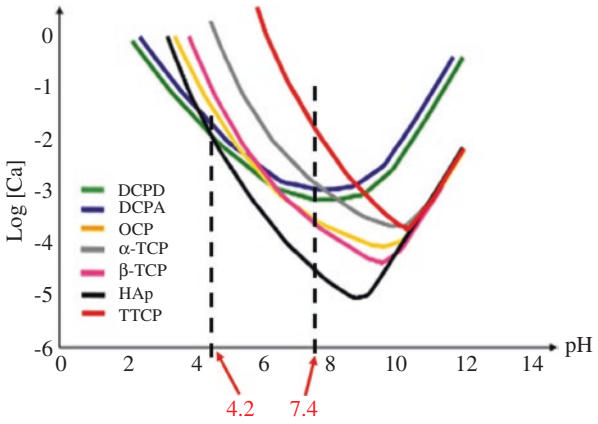

Fig. 4.1 Solubility of common calcium phosphates as a function of pH at 25 °C (Modified from [13, 14])

4.3 Calcium Phosphate Solubility

Solubility of CPs in water depends on the pH and temperature. The solubility of the most common CP compounds dissolved in acidic or basic aqueous solution at 25 °C is presented in Fig. 4.1. Solubility is expressed as $\log_{10}$ of calcium concentration. A higher concentration of calcium ions dissolved in aqueous solution indicates a higher solubility of that compound. Decreasing the pH from neutral towards acidic values increases the solubility of these compounds.

At pH values above 4.2, HAp has the lowest solubility, and it will precipitate. At pH lower than 4.2, DCPD has the lowest solubility, and it will precipitate. Therefore HAp is the phase that is the least soluble at pH $\geq$ 4.2 or the most thermodynamically stable at pH $\geq$ 4.2, while DCPD phase is the least soluble at pH < 4.2 (or the most stable at pH < 4.2).

At physiological pH values (7.4), the most stable phase (the least soluble) is HAp, while the least stable (the most soluble) is TTCP.

4.4 Required Properties of Calcium Phosphate Cements

CPCs are synthetic materials that can be used to fill bone cavities or defects. They consist of two components, a powder and a liquid, that are mixed to form a paste, which can be injected or placed into a bone defect. This paste will then set and harden inside the body (self-setting) [3], and the time necessary for the paste to become hard is defined as the setting time. This critical behaviour will be discussed in detail later, together with other important properties and assessments (see Sect. 4.7), to ensure correct application in varied surgical procedures.

CPCs used for medical applications should have the following general characteristics:

- Low cost
- Simple handling requirements
- Easy to prepare
- Mouldable or injectable so they can fill bone defects of irregular shapes
- Maintain good cohesion to avoid ingress of body fluids
- Radiopaque to be readily identified on X-rays images
- Easy to sterilise
- Degradable with a degradation rate similar to bone tissue regeneration
- Non-toxic in original form or as products of degradation
- Biocompatible
- Bioactive
- Have appropriate stability in body fluids at different pH
- Have appropriate macro- and micro-porosity to allow tissue regeneration
- Have mechanical properties similar to bone, to withstand mechanical loads and allow rapid mechanical stabilisation of the bone tissue after implantation
- Have a working time of about 1–5 min to allow for relevant implantation techniques
- Have a setting time less than 15 min, to allow for wound closure and maintain a minimum time in the operational room

CPC formulations consider the development of cements with *'an optimum balance between resorbability, porosity and mechanical properties'* [3].

4.5 Setting Process of Calcium Phosphate Cements

The setting process starts by mixing the powder and liquid components. During mixing, the powder particles start to dissolve into the liquid. During dissolution, the reagents begin to release Ca^{2+} and PO_4^{3-} ions, increasing the concentration of these ions in the solution. At the interface between powder and liquid, the solution becomes supersaturated, and the nucleation of new phases takes place on the surface of the powder reagents. These new phases continue to grow as long as the powder reagents continue to dissolve. Thus, during this dissolution-precipitation process, more soluble (less stable) CP phases will dissolve, whereas the less soluble (more stable) CP phases will precipitate [15]. The dissolution-precipitation process depends on the pH. As shown in Fig. 4.1, the most stable phase at low pH ($pH < 4.2$) is DCPD, while for higher pH values ($pH \geq 4.2$), HAp (or CDHA) is the most thermodynamically stable. Therefore, the principal end products of the setting reaction are apatite or brushite.

Nucleation and growth of the new phases occur immediately after the dissolution of the powder reagents. The setting reaction depends on both thermodynamic and reaction kinetic factors [3]. As new phases (HAp, CDHA or DCPD) precipitate at the interface between the reagent powder and liquid, their crystals will grow simultaneously from the supersaturated solution at different sites. This forms a network of needles or plates

Table 4.2 Most common chemical reactions for in vitro CPC formation [2, 16]

Chemical reaction	Reaction type
β-TCP (or α-TCP, CDHA or HAp) + MCPM (or H_3PO_4) → DCPD	Acid base
β-TCP (weak base) + MCPM (weak acid) + H_2O → DCPD	Acid base
CDHA (weak base) + H_3PO_4 (acid) + H_2O → DCPD	Acid base
TTCP (weak base) + DCPA (weak acid) → HAp or CDHA	Acid base
ACP + H_2O → CDHA + nH_2O	Hydrolysis
β-TCP (or α-TCP) + H_2O → CDHA	Hydrolysis
TTCP+ H_2O → CDHA + $Ca(OH)_2$	Hydrolysis

that interpenetrate, entangle and interlock, forming a hardened cement. In time, this entangled network of crystals becomes denser, increasing the mechanical properties of the cement. At the end of this stage, the cement has set, becoming hard. The setting mechanism of the CPCs can be simplified as described in the following stages:

1. Dissolution of the powder component particles and formation of a supersaturated solution close to the interface
2. Precipitation of HAp, CDHA or DCPD
3. Entanglement of HAp, CDHA or DCPD crystals, resulting in a hardened cement

Formation of other intermediate CPs such as OCP or ACP, before precipitation of HAp, and formation of CDHA or DCPD are also possible. The change in volume and heat generation during setting is typically negligible [16, 17].

Depending on the composition of the powder and liquid components, there are two types of setting reactions that can occur during CPC hardening: acid base and hydrolysis. During acid-base reactions, a relatively basic CP reacts with an acid or a relatively acidic CP to produce a neutral product [16]. Typical acid-base reactions are shown in Table 4.2. During hydrolysis, a metastable CP such as α-TCP, β-TCP, TTCP, ACP, etc. hydrolyses in an aqueous solution, forming a more stable compound, generally CDHA [16]. The cement in this case has only one phase, as only one CP compound undergoes hydrolysis. Examples of hydrolysis reactions are presented in Table 4.2.

All chemical reactions illustrated in Table 4.2 take place in vitro. In vivo studies showed the formation of a small percentage of carbonated HAp, which does not occur in vitro[16].

Setting reactions could last more than 10 h although generally within 6 h, 80% of final reaction products are obtained [16].

4.6 Types of Calcium Phosphate Cements

CPCs are obtained by chemical reactions between a powder and a liquid component. Depending on the main reaction product that results at the end of the chemical reactions, there are two types of CPCs: apatite (HAp or CDHA) type and brushite (DCPD) type. These two reaction products depend on the pH. At pH ≥ 4.2, HAp is formed, while at pH < 4.2, brushite is produced.

4.6.1 Apatite Cements

Apatite cements have HAp or CDHA phase as the end product of the setting reaction. They can be obtained by both setting reactions (acid base or hydrolysis). Due to their similarity with natural bones and teeth, apatite cements are highly biocompatible, being better osteointegrated than brushite cements. Under physiological conditions HAp has the lowest solubility (see Fig. 4.1), making the apatite cements more stable than brushite cements. Due to the low solubility of HAp, apatite cements have higher viscosity and lower injectability than brushite cements [15]. Generally, apatite cements have longer setting times than brushite cements. They can be applied as a dough, an easily mouldable paste [16].

Apatite cements generally have higher mechanical properties than brushite cements due to their lower solubility [16]. Some examples of commercial apatite bone cements are given in Table 4.3.

Table 4.3 Compositions of commercial apatite CPCs [2, 3]

Commercial name	Composition	Manufacturer	End product (reaction type)
Biobone	Powder: 50% ACP+ 50% DCPD Solution: buffered saline solution	Merck	Apatite (acid base)
BoneSource	Powder: TTCP (73%), DCPA (27%) Solution: H_2O, mixture of Na_2HPO_4 and NaH_2PO_4	Stryker	Apatite (acid base)
Calcibon	Powder: α-TCP (61%), DCPA (26%), $CaCO_3$ (10%), CDHA (3%) Solution: H_2O, Na_2HPO_4	Biomet	Apatite (acid base)
KyphOsTM	Powder: α-TCP (77%), $Mg_3(PO_4)_2$ (14%), $MgHPO_4$ (4.8%), $SrCO_3$ (3.6%) Solution: H_2O, $(NH_4)_2HPO_4$ (3.5 M)	Medtronic	Apatite (hydrolysis)
Cementek	Powder: α-TCP (38%), TTCP (49%), Na glycerol-phosphate Solution: $Ca(OH)_2$, H_3PO_4	Teknimed	Apatite (acid base)
Cementek LV	Powder: α-TCP (38%), TTCP (49%), Na glycerol-phosphate, dimethyl siloxane Solution: $Ca(OH)_2$, H_3PO_4	Teknimed	Apatite (acid base)
Norian SRS (Skeletal Repair System)	Powder: α-TCP (85%), $CaCO_3$ (12%), MCPM (3%) Solution: H_2O, Na_2HPO_4	Synthes	Apatite (acid base)
Norian CRS	Powder: α-TCP (85%), $CaCO_3$ (12%), MCPM (3%) Solution: H_2O, Na_2HPO_4	Synthes	Apatite (acid base)

4.6.2 *Brushite Cements*

Brushite cements have DCPD phase as the final setting reaction product. As can be seen in Table 4.2, all brushite cements are obtained by acid-base setting reactions. According to Fig. 4.1, DCPD can precipitate at pH values lower than 4.2. Therefore, during acid-base setting reactions, brushite cements are acidic, the pH varying between 2.0 and 4.0 (see Table 4.1). DCPD solubility decreases with the increase of pH (Fig. 4.1). Slight increase of the solution pH will promote DCPD precipitation, accelerating the setting time. It is thus expected that more basic reagents (of the setting reaction) with higher solubility could move the pH towards the right side of the graph, leading to faster setting times. Therefore, considering the setting reaction of MCPM reagent (weak acid), the setting time will decrease when more soluble bases are used as reagents. Hence, as β-TCP has a higher solubility than HAp, the mixture of β-TCP and MCPM will have a faster setting time when compared to HAp and MCPM mixture [16].

As DCPD has a higher solubility than HAp under physiological conditions (Fig. 4.1), the brushite cements are more degradable than apatite cements. This faster degradation will lower the mechanical properties in vivo. Setting time could be modified by changing the liquid to powder ratio (LPR) or using certain additives in the liquid or solid phase. These additives can inhibit the nucleation and growth of brushite crystals, increasing the setting time [3].

DCPD is a metastable phase and can transform into apatite in vivo [15]. Generally, brushite cements have shorter setting time, less injectability and weaker mechanical strength than apatite cements [4]. Some examples of commercial brushite bone cements are given in Table 4.4.

Table 4.4 Compositions of commercial brushite CPCs [3]

Commercial name	Composition	Manufacturer	End product (reaction type)
ChronOsTM Inject	Powder: β -TCP (73%), MCPM (21%), $MgHPO_4 \cdot 3H_2O$ (5%), $MgSO_4$ (<1%), $Na_2H_2P_2O_7$ (<1%) Solution: H_2O, sodium hyaluronate (0.5%)	DePuy	Brushite (acid base)
Eurobone	Powder: β -TCP (98%), $Na_4P_2O_7$ (2%) Solution: H_2O, H_3PO_4 (3 M), H_2SO_4 (0.1 M)	FH orthopaedics	Brushite (acid base)
VitalOs	*Component 1* β -TCP (1.34 g) $Na_2H_2P_2O_7$ (0.025 g) H_2O, salts (0.05 M, pH 7.4 PBS solution) *Component 2* MCPM (0.78 g) $CaSO_4 . 2H_2O$ (0.39 g) H_2O, H_3PO_4 (0.05 M)	Produits Dentaires	Brushite (acid base)

4.7 Properties of Calcium Phosphate Cements

CPCs are biocompatible, bioactive, osteoconductive (stimulating bone ingrowth into the implant) and bioresorbable. Bioactivity is the ability of the implant to form a chemical bond with the bone tissue by precipitation of CDHA on the surface of the implant in contact with physiological fluids. As calcium phosphate is naturally radiopaque, all CPCs are thus radiopaque, being visible on X-ray images as soon as they are injected and until they are resorbed and substituted by newly formed bone.

The critical properties of CPCs are explained in the following paragraphs.

4.7.1 Setting Time

In the ISO 18531 draft, setting time is defined as the *'time required from the start of powdered agent and liquid agent blending until hardening of the cement'* [18]. Setting time is an important property of CPCs as it provides guidance to the surgeons when they need to implant the cement. The surgeon should have enough time to inject or place the dough/paste inside the defect, before it becomes too hard due to complete setting. If the setting time is too short, the paste becomes hard too soon, and the surgeon will not have enough time to implant it. If the setting time is too long, the paste may be too liquid (low viscosity), and the surgeon must wait unnecessarily before closing the wound. Clearly, long setting times are inefficient, while short setting times potentially affect the progress and success of the operation.

An optimal setting time will allow the surgeon to place the cement, which will continue to harden inside the body, so that it maintains the desired shape. Setting time is measured from the first moment of mixing the powder and liquid components until the paste becomes hard, at which point it will have the appropriate mechanical properties. At the end of the setting time, the wound can be closed, without significant risk of structural failure of the implant.

The setting process depends on the cement composition, LPR, pH, temperature, particle size of powder component and other additives that can be added to the liquid or solid components.

The LPR is generally expressed in ml/g (vol/wt). Increasing this ratio could increase the setting time, as the time necessary to achieve saturation of the solution will increase. If the LPR is too low, the setting process could be inhibited, as there is not enough liquid phase to dissolve the entire amount of solid powder.

The solubility of the powder components depends on the pH and temperature and affects the setting time as noted earlier. Due to the 'V shape' of the solubility/pH curves of the CPs seen in Fig. 4.1, increasing or decreasing the solution pH will change the powders' solubility. The temperature in the operating theatre is typically 18–25 °C and could influence the powder's solubility. The setting time will be shorter at higher temperatures, and the cement will set faster in the body at 37 °C than at room temperature.

Another factor that can influence the setting time is the particle size of the powder component. Small particles have a higher specific surface area and are more reactive than larger particles, as more area is in contact with the liquid. This leads to reduction in setting time. Conversely larger particles will need more time to dissolve, increasing the setting time.

Both liquid and solid phases could contain different inorganic or organic additives that can modify the setting time by increasing or decreasing the dissolution ratio or by promoting or inhibiting apatite or brushite nucleation [2].

The powder component contains one or more CP powders. Organic additives such as sodium citrate, sodium glycerophosphate, dimethylsiloxane, sodium carboxymethyl cellulose and hydroxypropyl methyl cellulose or inorganic additives such as $NaHCO_3$, Na_2CO_3, $CaCO_3$, $MgHPO_4$, $MgSO_4$, etc. have been used for the powder component in commercial CPCs to modify the setting time [2].

The liquid component is typically water or a CP aqueous solution, depending on the type of the setting reaction. Inorganic additives such as soluble phosphates (NaH_2PO_4, Na_2HPO_4, $(NH_4)_2HPO_4$), sulphates ($CaSO_4{\cdot}2H_2O$, $NaHSO_4$), sodium silicate, H_3PO_4, $Ca(OH)_2$, NaCl (saline solution) or other salts, such as phosphate buffered solution (PBS, which contains a mixture of salts: NaCl, KCl, Na_2HPO_4, KH_2PO_4), could decrease or increase the pH of the solution, increasing the solubility of the powder component and thus modifying the setting time [2, 3]. Some organic additives such as polyvinylpyrrolidone (PVP), sodium hyaluronate, etc, have been added in the liquid phase of commercial CPCs to control the setting time [2].

The two methods used for measuring the setting time of CPCs, Vicat and Gillmore tests, are adapted from two standard methods. Originally, the Vicat needle (ASTM C191-13 [19]) and Gillmore needles (ASTM C266-15 [20]) were employed for hydraulic cements and concretes used in construction materials. Both methods are based on periodic penetration of a needle of known geometry and weight into the surface of the cement.

4.7.1.1 Vicat Needle

The Vicat apparatus is a relatively simple and reliable device, and a commercial unit is presented in Fig. 4.2. The Vicat needle is made from stainless steel with a diameter of 1 mm and a minimum parallel length of 50 mm. The end of the needle that touches the surface of the cement is flat and perpendicular to the length. The mass supported by the needle tip at the time of measurement is 300 g [19].

After mixing the solid and liquid components, the resulting paste is placed in a conical mould. The Vicat needle is positioned on the surface of the cement paste and allowed to settle into the paste. The Vicat initial setting time is the time in minutes elapsed from the initial contact between the solid and liquid components (since the beginning of their mixing) until a needle penetration of 25 mm is obtained. The Vicat final setting time is the time in minutes elapsed from the initial contact between the solid and liquid components (since the beginning of their mixing) until the first moment when the needle does not mark the cement surface with a complete

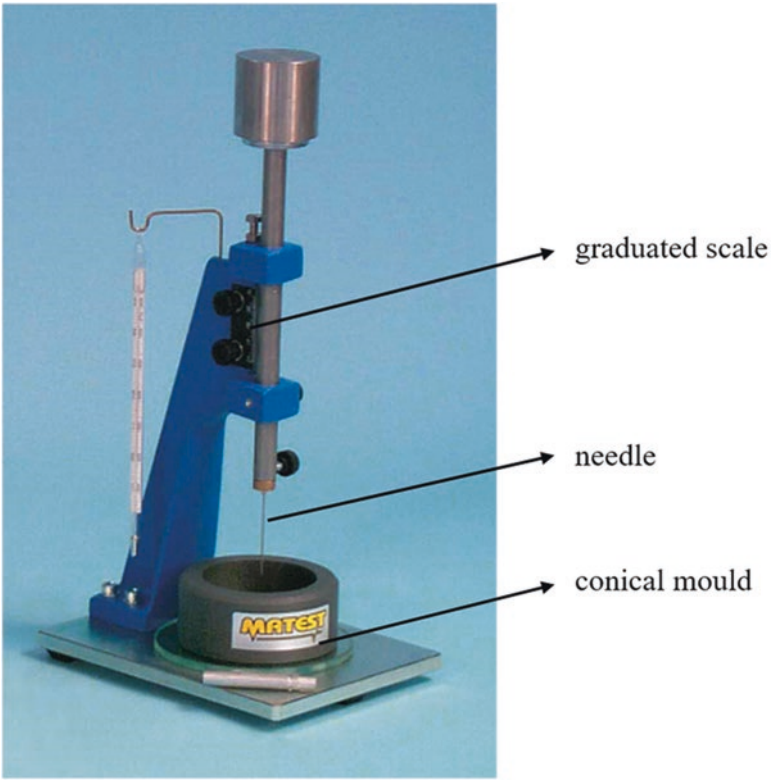

Fig. 4.2 Vicat apparatus [21]

circular impression [19]. Both of these indicators are readily observed but consistency of interpretation is important when comparing results between samples.

4.7.1.2 Gillmore Needle

The Gillmore apparatus shown in Fig. 4.3 has two small cylindrical stainless steel needles: one light and thick (initial needle) and the other one heavier and thinner (final needle). Both needle tips have a length of 4.8 mm and are parallel along this length. The initial needle is used to measure the initial setting time (IST) of the cement. It has a mass of 113.4 g and a tip diameter of 2.12 mm. The final needle is used to measure the final setting time (FST) of the cement. It has a mass of 453.6 g and a tip diameter of 1.06 mm. Both of the needle ends that are in contact with the surface of the cement are flat and perpendicular to the length [20].

After mixing the solid and liquid components, the obtained paste is placed in a conical mould. The draft standard ISO 18531 [18] indicates the following dimensions

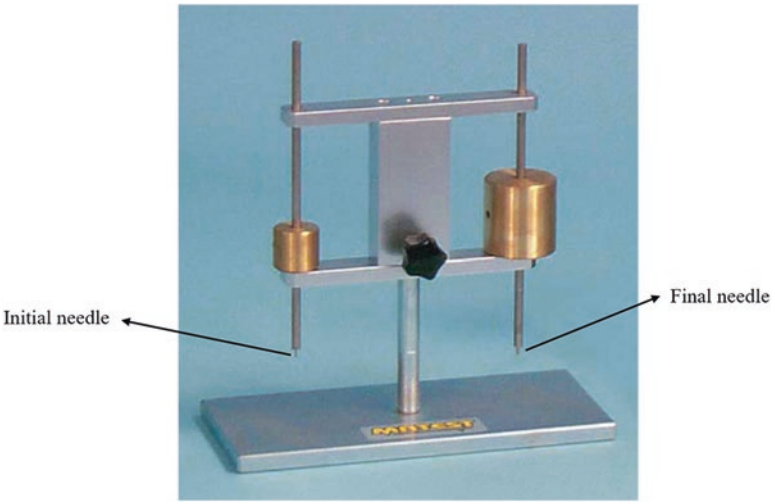

Fig. 4.3 Gillmore apparatus [22]

for this mould: diameter between 7 and 15 mm and height between 3 and 5 mm. The conical mould used for the Gillmore apparatus is smaller than that for the Vicat making the Gillmore test more appropriate, as it requires a smaller volume of paste for testing. The Gillmore test is typically used by commercial manufacturers to determine the setting time of their products.

The Gillmore needles are placed on the surface of the cement paste and allowed to settle into the paste. The Gillmore IST is the time in minutes elapsed from the initial contact between the solid and liquid components (since the beginning of their mixing) until the first moment when the initial needle does not leave a complete circular impression on the paste surface. The Gillmore FST is the time in minutes elapsed from the initial contact between the two paste components (since the beginning of their mixing) until the first moment when the final needle does not leave a complete circular indentation on the paste surface [20]. The clinical significance of the two setting times is related to moment of time when the cement paste can be safely implanted in the patient.

The surgeon must implant the cement before the end of the IST and should close the wound after the end of the FST.

Between IST and FST, the cement paste should not be deformed, as any deformation of the cement paste during the time interval between the two setting times could lead to cement fracture [16]. At the end of the FST, the cement will have become sufficiently hard to resist potential cracking and can be touched without inducing any damage. The wounds or incisions initially created at the beginning of the surgery can thus be closed safely.

The, IST determines the time after which *'no more modifications can be made in the set paste without causing cracking'* [2], while FST determines the moment when it is safe to close the wound.

Typically, IST is between 3 and 8 min, while the FST is less than 15 min, for orthopaedic applications [3, 16]. Generally, mouldable cements have shorter FST than injectable cements. Norian CRS® Fast Set Putty (Synthes), used for cranial defects, is a mouldable cement with FST between 3 and 6 min [3].

4.7.2 Cohesion

During implantation, the cement paste will be in contact with blood and/or body fluids. These fluids could penetrate into the cement and adversely affect its properties [17]. Therefore, it is extremely important that the paste maintains its consistency without breaking into small fragments after mixing the solid and liquid components. This property is called cohesion, and it is defined as the '*ability of a paste to harden in an aqueous environment without releasing loose particles'* [23].

Cohesion time (CT) is the minimum time elapsed after mixing the two cement components until the resultant paste does not disintegrate in aqueous solutions (saline solution, Ringer's solution, simulated body fluid (SBF), etc.) at 37 °C. If the paste disintegrates, the released particles or small fragments could produce tissue inflammation [24] or obstruct blood flow by the formation of blood clots [25].

Typically, the cohesion time is more than 2 min and at least 1 min less than the initial setting time to allow the surgeon to inject the paste within 1 min [2, 16]. The cohesion time can be determined qualitatively by visual inspection.

Different authors have proposed quantitative tests to determine the cement's cohesion based on measuring the percentage of remaining cement [25] or wash-out sediments [24] after partial disintegration in different fluids at 37 °C. After cohesion tests, the stable remaining cement paste is freeze dried, and the amount of dried powder is weighted. The percentage of remaining cement can be calculated with Eq. 4.1 [25]. Similarly, any small fragments washed out during the cohesion test are freeze dried, and the amount of dried sediment is weighed. The percentage of washed-out sediment can be calculated with Eq. 4.2 [24]. The sum of the percentage of remaining cement and sediments should be 100 (%).

$$Remaining\ cement(\%) = \frac{Weight\ of\ freeze-dried\ remaining\ cement}{Initial\ weight\ of\ cement} \times 100 \quad (4.1)$$

$$Wash\ out(\%) = \frac{Weight\ of\ freeze-dried\ sediments}{Initial\ weight\ of\ cement} \times 100 \quad (4.2)$$

The draft standard ISO 18531 [18] suggests a static disintegration test similar to the one above. A cement paste of diameter 4.8 mm and 16.5 mm length (volume about 0.3 ml) is extruded from a syringe (with the inner diameter of 4.8 mm) on a stainless steel wire rack (2 mm grid, 2–4 mm height). The rack is placed into a plastic container with an inner diameter of 50 mm and a volume of approximately 50 ml, which contains 30 ml of physiological saline solution, and is stored at 37 °C for 72 h in an incubator

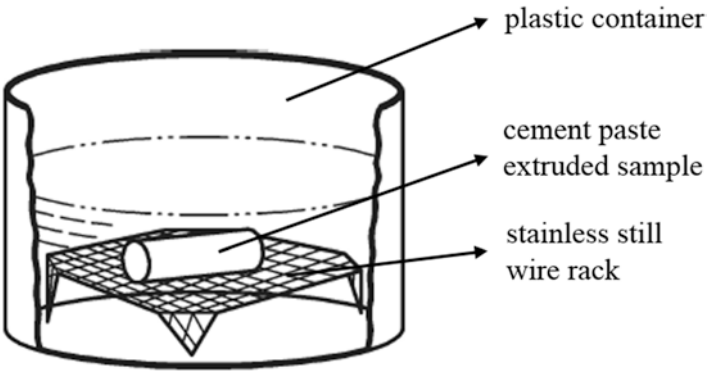

Fig. 4.4 Static disintegration test [18]

(Fig. 4.4). The sample is completely immersed in the saline solution. Any disintegrated cement fragments falling from the wire rack will remain on the bottom of the plastic container. At the end of the incubation period, the remaining cement (solid piece of cement on the rack) and the disintegrated fragments (on the bottom of the container) are carefully collected and dried at 60 °C for 24 h. The percentage of static disintegration SD will be determined with Eq. 4.3, which is similar to Eq. 4.2 of the wash-out percentage.

$$SD(\%) = \frac{Weight\ of\ dried\ sediments}{Weight\ of\ dried\ (sediments + remaining\ \ cement)} \times 100 \qquad (4.3)$$

Cohesion might be enhanced by adding a gelling agent (sodium alginate, chitosan, carboxymethyl cellulose, etc.) into the liquid phase, which could bind the powder particles of the cement paste, increasing the strength of the paste and therefore reducing the erosion caused by the body fluids [11, 17].

Generally the gelling agent increases cohesion but may inhibit the setting reaction. Some gelling agents could form weak bonds with the powder particles and hence increase the cohesion. For example, sodium alginate could react with the CP particles forming calcium alginate, which is insoluble in water, thus minimising the disintegration of the powder particles and improving the cement cohesion [6]. The addition of sodium pyrophosphate or sodium citrate to the powder component will decrease the setting time and will lower the cohesion [3]. Small particle size and low LPR could also reduce the cohesion of the paste [11].

4.7.3 Setting Process Phases

The setting process can be divided into four different phases: mixing, waiting, working (injection or implantation) and setting. Each of these phases has a corresponding time that must be carefully observed and managed in clinical applications

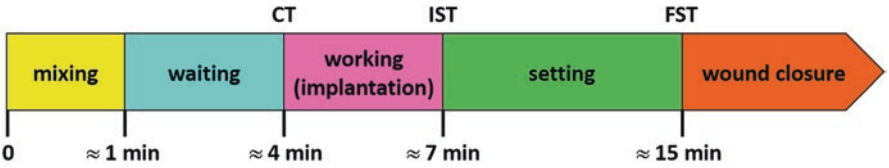

Fig. 4.5 Schematic representation of the setting process phases. *CT* cohesion time, *IST* initial setting time, *FST* final setting time

if predictable results are to be obtained. A schematic representation of these phases is illustrated in Fig. 4.5. The times are measured from the beginning of mixing of the two components. FST should be a maximum of 15 min for efficient surgical procedures, as noted earlier.

The *mixing time* represents the time taken to fully integrate the powder and liquid components and typically takes about 1 min. During the *waiting phase* (typically lasting a few min), the cement paste achieves a suitable viscosity for implantation or handling, without the risk of particle disintegration. The end of the waiting time generally corresponds to the CT. At the end of the waiting period, the paste can be injected or placed into the bone defect. This phase is referred as the *working phase*, when the cement can be manipulated and inserted into the bone cavity. The *cement must be implanted before the end of the working phase.* Initial setting time, IST, marks the end of the working phase. *Working time* is the interval between the CT and IST and is typically 2–4 min. During the *setting phase*, the paste's viscosity increases, and the cement continues to harden. The duration of this phase is the interval between the IST and FST, typically 6–7 min. No modification or deformation of the cement paste should be made during the setting phase, to avoid the formation of the cracks as noted earlier. At the end of the setting phase, marked by FST, the wound can be closed.

ChronOS™ Inject Bone Void Filler is an injectable brushite cement which has an IST of 6 min and a FST of 12 min. The manufacturer (DePuy Synthes) reported the following setting phases: mixing phase 1 min, waiting phase 2 min, implantation phase 3 min and setting phase 6 min. At the end of the working time, it is recommended to *'leave chronOS Inject Bone Void Filler undisturbed for 6 min*' and to *'avoid touching chronOS Inject Bone Void Filler in this phase'* [26].

4.7.4 Cement Preparation Protocol

The mixing process is crucial for correct application of the cement, and commercial products are generally provided with a suitable sterile kit. High viscosity cements are typically mixed in a bowl and applied as a dough, while low viscosity cements are generally applied through a syringe. The main steps for preparation of the cement before implantation are described below, using the guidelines of two commercial cements produced by Stryker®: HydroSet™ (lower viscosity, fast setting, injectable paste) and BoneSource® (higher viscosity, longer setting, mouldable paste).

4.7.4.1 HydroSet™ Preparation Steps

HydroSet is an easily injectable apatite cement that is used for craniomaxillofacial, trauma and orthopaedic applications. HydroSet is sold in a kit presented in Fig. 4.6. Each package contains one syringe with the liquid component, one bowl with the powder component, one delivery syringe, one cannula and one spatula. The powder component contains a mixture of dicalcium phosphate dihydrate, tetracalcium phosphate and trisodium citrate. The liquid component is an aqueous solution of sodium phosphate and polyvinylpyrrolidone. Sterilisation is carried out using ethylene oxide and gamma irradiation [27].

This cement *'acts only as a temporary support and it is not intended to provide structural support during the healing process'* [26]. The cement can be implanted via a syringe or manually, depending on the clinical need. It was designed to set quickly once implanted under normal physiological conditions, has good cohesion and can be drilled and tapped to accommodate the placement of provisional hardware (K-Wires, plates, screws) as required by the surgical procedure [26].

HydroSet recommended use is *'to fill bone voids or gaps of the skeletal system (i.e., extremities, craniofacial, spine, and pelvis)'* that have been caused by traumatic injury or have been surgically created. HydroSet is indicated only for bone defects *'that are not intrinsic to the stability of the bone structure'* [26].

The main steps in the preparation of this cement are shown in Fig. 4.7. The liquid is first added to the bowl containing the powder component, ensuring that all the liquid is uniformly distributed throughout the powder. The two components are mixed for 45 s (*mixing phase*), until a homogeneous paste is achieved (Fig. 4.7a). At the end of the mixing time, the paste can be transferred into the delivery syringe

Fig. 4.6 HydroSet delivery kit [26]

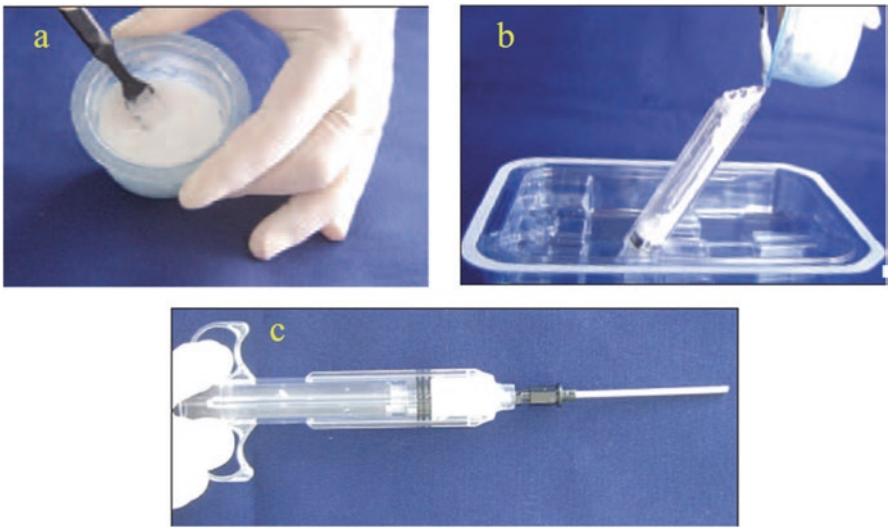

Fig. 4.7 HydroSet preparation steps [26]. (**a**) Mixing the cement paste, (**b**) transferring the paste into the delivery syringe and (**c**) cannula attached to the delivery syringe

using a spatula and the kit provided (Fig. 4.7b). The supplied cannula can be then attached to the delivery syringe (Fig. 4.7c). The loading process corresponds to the *waiting phase* and should be completed within 2 min and 30 s. The *injection time* is approximately 2 min before the material begins to set (initial setting time). Material manipulation must stop after 4 min and 30 s (initial setting time). Setting time may vary between 8 and 10 min from the start of mixing, depending on the ambient and product temperatures. The recommended operating and storage room temperatures should be between 18 and 22 °C. Between IST and FST, the material should be *'left undisturbed, until it sets completely'*. At the end of the setting time, the wound can be closed [26]. If orthopaedic equipment (plates, needles, screws, etc.) are required before the wound closure, it is recommended to wait about 12 min before using them instead of only 10 min [26].

The entire setting process for HydroSet is presented in Fig. 4.8. The times shown are evaluated considering the temperatures in the storage and operating rooms between 18 and 22 °C.

4.7.4.2 BoneSource® BVF Preparation Steps

BoneSource was the first commercially available bone cement approved for craniofacial surgery applications such as repair of cranial burr hole defects (maximum area of 25 cm^2 or a maximum dimension of 5 cm), cranial defects and facial skeletal augmentation [27]. BoneSource is an apatite cement that can be applied for reconstructive surgery, trauma surgery and bone defects.

BoneSource is provided in a kit presented in Fig. 4.9. Each package contains a syringe with the liquid component, a bowl with the powder component and a spatula

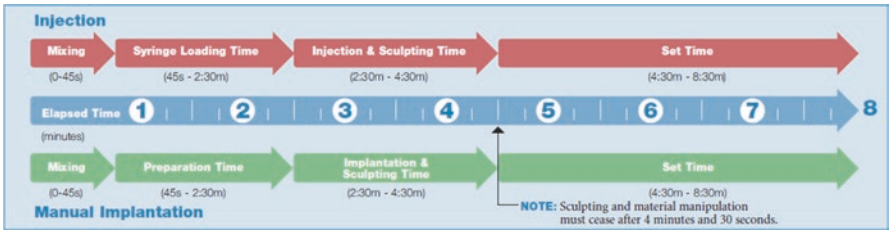

Fig. 4.8 Schematic representation of the HydroSet setting process [26]

Fig. 4.9 BoneSource delivery kit [28]

[28]. The powder component contains a mixture of dicalcium phosphate anhydrous and tetracalcium phosphate. The liquid component is an aqueous solution of sodium hydrogen phosphates and sodium dihydrogen phosphate (Table 4.3). The LPR mixing ratio is 1:4 ml/g [27]. The setting time is approximately 20–25 min, and the cement will continue to harden in the body for about 4–6 h. A dry implant site is mandatory for this cement to achieve the appropriate setting [29].

The main steps for the preparation of this cement are shown in Fig. 4.10. The contents of the syringe is emptied into the powder in the mixing bowl (Fig. 4.10a). The two components are mixed vigorously to ensure that all of the liquid has been distributed uniformly throughout the powder (Fig. 4.10b). Total mixing time may

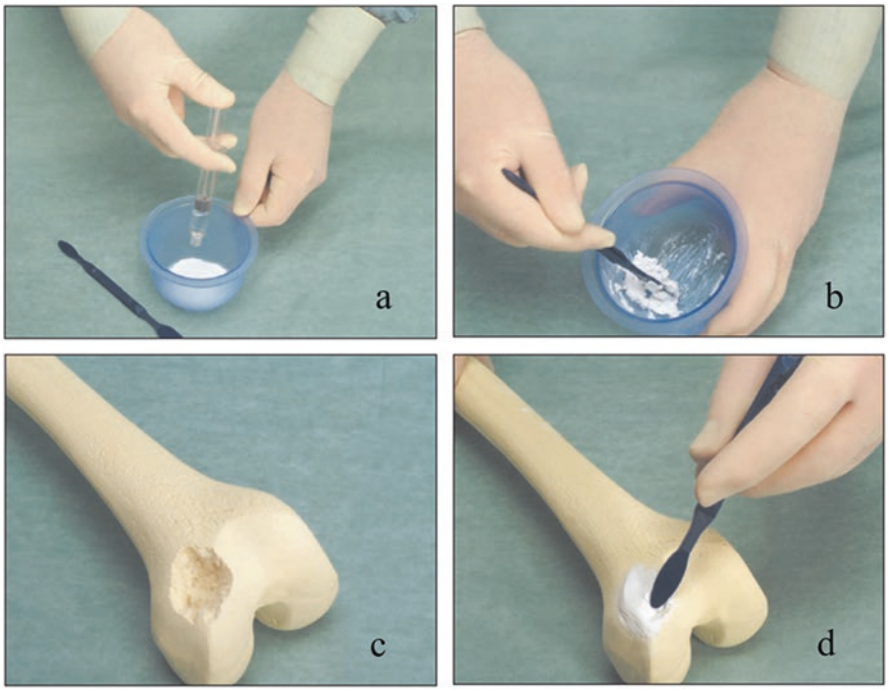

Fig. 4.10 BoneSource preparation steps [28]. (**a**) Adding the liquid component in the bowl with the powder component, (**b**) mixing the cement paste, (**c**) dried defect and (**d**) implanting the paste into the defect

vary between 30 and 60 s, until a homogeneous paste is achieved [28]. The paste can be further kneaded manually (between fingers), within 5 min, to achieve a homogeneous liquid phase dispersion and the desired consistency prior to application. Before application of the cement, the implant site should be dried by removing any active bleeding or excessive body fluids (Fig. 4.10c). At the end of the mixing time, the paste can be applied to the dried bone defect using the spatula or by hand (Fig. 4.10d). After application of the paste, surgical sponges and suction should be used to remove any excessive wound fluid [27, 28]. The cement paste will harden in approximately 20 min [27].

4.7.5 Injectability

For minimally invasive surgical procedures, CPCs are injected into the bone cavity or defects, such as spine fractures, via a cannulated needle [30]. Cement injectability, or the ability of the cement paste to keep its homogeneity (without solid/liquid phase separation or demixing) when it is extruded through a syringe needle, is

crucial. If demixing occurs, the liquid phase may be expelled while the solid phase remains in the syringe [30].

Injectability depends on the type of syringe, needle size and injection rate, as well as particle size, LPR and additives. Smaller particle size and different organic additives (sodium alginate, chitosan, polysaccharides, lactic acid, glycerol, hydroxymethylcellulose, polyvinyl alcohol) that can bind the powder particles can improve injectability [17].

Very high viscosity pastes have poor injectability, as the applied force needs to be very high to extrude the cement through a narrow needle/nozzle. The needle diameter depends on the clinical application which may preclude the use of larger diameter needles.

Very low viscosity pastes are often associated with the *'filter-pressing'* phenomenon, where the needle (nozzle) acts as a 'filter paper' and 'filters' the paste, only allowing the liquid to be ejected from the syringe [17]. The liquid can flow faster than the solid as the mixture passes through the needle and the solid particles accumulate at the needle/nozzle. This phenomenon of solid/liquid phase separation has been observed for different commercial CPCs, limiting their clinical applications [30]. Very low viscosity cements could 'leak' in vivo, leading to surgical complications such as occlusion and pulmonary embolism [31].

An optimal viscosity for the cement paste could be obtained by modifying the LPR. Higher LPR will decrease the paste viscosity and could increase the injectability, but might affect the mechanical properties of the hardened cement. An optimum LPR should be used to balance these properties [2, 6].

Injectability could be increased by addition of a gelling agent to the liquid component. The gelling agent could also increase the cohesion but it will inhibit the dissolution-precipitation reaction, increasing the setting time. Low viscosity cement pastes are generally injectable. High viscosity cement pastes are typically applied as a dough [16].

A typical syringe with a cannulated needle used for the CPC extrusion is shown in Fig. 4.11.

As there is no standard method for measuring the injectability of CPCs, different techniques are reported in the literature. All these methods measure the amount of cement extruded through a syringe relative to the total mass of the cement in the syringe.

A typical technique used for assessing injectability measures the percentage weight of extruded cement through a syringe with or without a cannulated needle, by application of force. The injectability is then calculated with Eq. 4.4 [30].

$$Injectability(\%) = \frac{Mass\ of\ extruded\ cement}{Total\ mass\ before\ injection} \times 100 \tag{4.4}$$

Another method calculates CPC injectability by extruding the paste through a nozzle with an internal diameter of 2.3 mm, using a constant force of 100 N. The force is applied 15 min after the cement is inserted into the syringe. Injectability is determined as the percentage of the cement extruded over a time period of 10 s [30, 32].

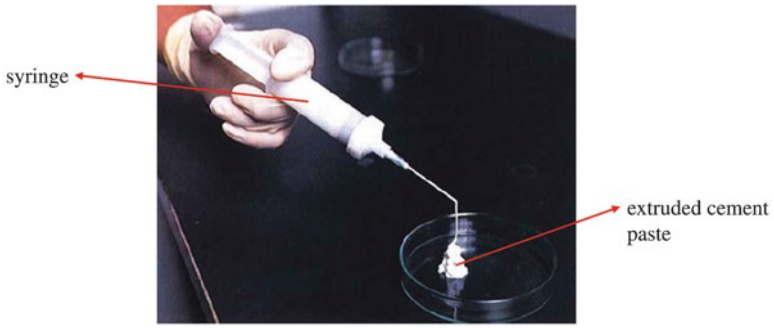

Fig. 4.11 CPCs injected using a syringe [17]

Other authors have extruded the cement through a 0.8 mm internal diameter needle using an universal testing machine with a crosshead speed of 50 mm/min and a maximum force of 300 N [30, 33]. The percentage of the cement extruded through the needle was determined with Eq. 4.5 [33], using the mass of the cement that remained in the syringe.

$$Injectability\left(\%\right) = 100 - \frac{Mass\ of\ remaining\ cement}{Total\ mass\ before\ injection} \times 100 \tag{4.5}$$

4.7.6 Porosity

As CPCs are used for filling bone defects, they should mimic the porous bone structure as far as possible. Ideally, materials should have both macro- (500–1000 μm) and microporosity (<100 μm), with interconnected pores to allow cell attachment, proliferation and differentiation, as well as nutrient diffusion and vascularisation.

Commercial CPCs only have a microporous structure where pores are formed within the nucleation and growth of the new crystals during the setting reaction, by entanglement of the precipitated crystals [17]. Good interconnection of the pores enhances cell migration and diffusion of oxygen and nutrients. The degradability and mechanical properties of CPCs are influenced by cement porosity, pore size and interconnectivity. Porosity could be controlled by modifying the particle size of the powder component, LPR ratio and/or the addition of water soluble porogens. These porogens (NaCl, $NaHCO_3$, sugar or other soluble polymers) will dissolve in biological fluids, creating a porous structure [3]. They should not produce a toxic effect or trigger any inflammatory response in situ.

A typical microstructure of an apatite bone cement (HydroSet™) is illustrated in Fig. 4.12. Entangled apatite crystals form interconnected nano- and micropores that allow body fluids to penetrate the cement.

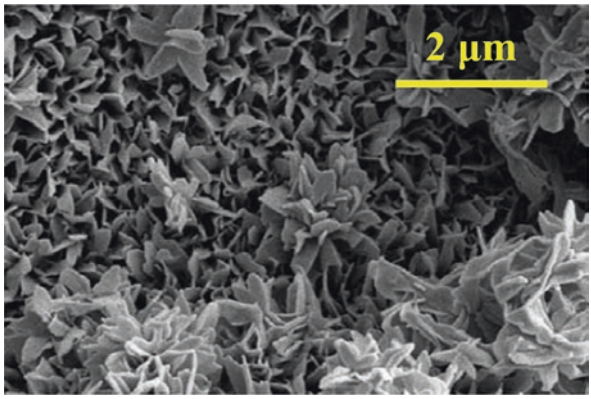

Fig. 4.12 Scanning electron microscope image of HydroSet™ microstructure (magnification 15,000×) (Modified from [26])

One strategy used to create a macroporous structure is to add soluble polymeric fibres to the CPC paste. These fibres could improve the short-term strength of CPCs after implantation and in time will dissolve, creating macropores or macro-channels that will facilitate vascular ingrowth [3]. Resorbable fibres made of polyglycolic and polylactic acids, having a diameter of 300 µm and a length of 8 mm, have been randomly mixed with the CPC paste [34]. The hardened specimens were immersed in saline solution at 37 °C for 2 months. The fibre-reinforced cements maintained their strength for 2–4 weeks after immersion, depending on the dissolution rate of the fibres. They presented higher flexural strength values compared to non-reinforced CPC. Subsequently, macropores and macro-channels were created by the fibres dissolving after 3 months of immersion in saline solution [34].

4.7.7 Mechanical Properties

CPCs are brittle materials with low values of tensile strength (less than 10 MPa [2]) and flexural strength (less than 20 MPa [15]) that can be used only for non-loadbearing applications. The mechanical properties depend on the cement porosity; increasing the porosity will decrease the mechanical properties. Smaller particle size of the powder component will produce cements with lower porosity and higher strength, while the addition of polymeric additives could increase the mechanical properties. Brushite cements are generally weaker than apatite cements due to their higher solubility [16].

As noted earlier, incorporation of resorbable polymeric fibres into the cement paste can increase the short-term strength. Fracture toughness of the fibre-reinforced cements could increase with the volume fraction of fibres [35]. Increasing the cement porosity by adding resorbable fibres in the cement paste will not reduce the short-term strength [34].

Mechanical tests can be performed in dry or wet conditions, by immersion of the samples in aqueous solutions (PBS, SBF, etc.) for a defined time.

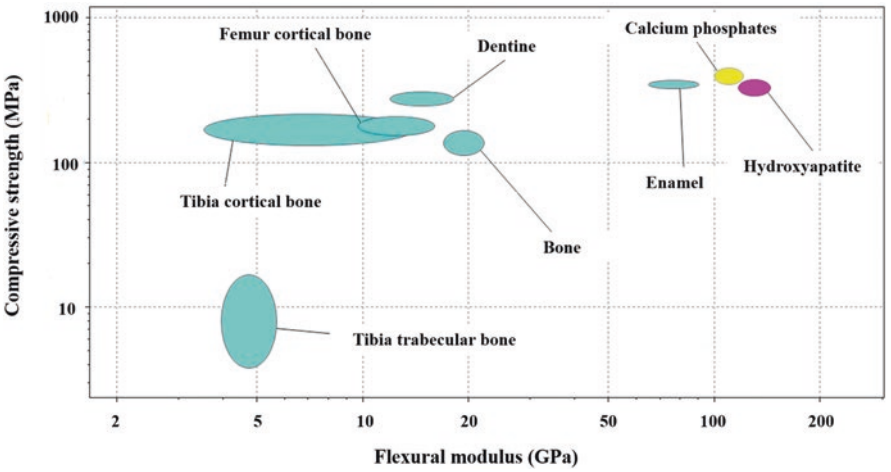

Fig. 4.13 Compressive strength versus flexural modulus

The draft standard ISO 18531 [18] suggests a compression test for measuring the mechanical strength of CPCs. Cylindrical samples with a diameter of 6 mm and height of 12 mm should be kept in polytetrafluoroethylene (PTFE) moulds in distilled water in an incubator at 37 °C for 72 h. At the end of this immersion time, the samples are removed from the PTFE mould and tested at room temperature using an universal testing machine, with a cell load of a minimum 1kN and a crosshead speed of 0.5 mm/min.

Typical compressive strength versus flexural modulus data (CES EduPack 2016 software) is illustrated in Fig. 4.13 for natural bone, dentine, enamel and calcium phosphate ceramics. The software database contains a summary of typical values taken from the literature. It can be seen that there is a wide range of values for these materials, which represent bulk dense materials rather than porous forms. The database does not contain specific data for CPCs.

Calcium phosphate ceramics have compressive strength values similar to natural enamel whilst the values of flexural modulus are typically higher than those of the natural tissue. In Fig. 4.13 above, compressive strength of bulk CP ceramics is between 350 and 450 MPa. Even though the database for CP ceramics indicates a high range of values, commercial CPCs do not have such high mechanical properties due to their porous microstructure.

4.7.8 Bioresorption

Bioresorption of CPCs is related to the solubility of their constitutive phases. Under biological conditions the cements will resorb, being replaced by newly formed bone tissue. Ideally, the resorption rate of the implant should be similar to that of tissue regeneration. During degradation the implant will become more porous, enabling

the development of tissue vascularisation and bone ingrowth into material, restoring the mechanical integrity of the bone tissue. If the implant resorption rate is too fast, the structure might collapse due to reduced mechanical stability induced by increased local porosity. If the implant resorption rate is too slow, the new bone ingrowth will be reduced, diminishing the osteointegration of the implant material.

In vitro bioresorption of CPCs could include both chemical (hydrolysis) and physical process (dissolution) in contact with physiological solutions. In vivo bioresorption of CPCs is mediated by cellular activity of osteoclasts, which will chemically degrade the cement structure. Osteoclasts are the bone-dissolving cells that are responsible for bone resorption. During natural bone remodelling process, osteoclasts remove the old bone tissue by dissolving the bone mineral matrix and breaking down the organic collagen fibres. Osteoclasts create an acidic environment that dissolves the bone mineral matrix. Once the bone mineral has been dissolved, enzymes released by osteoclasts remove the remaining collagen matrix to complete the resorption process.

After in vivo implantation of the CPCs, the acidic environment created by the osteoclasts will increase the solubility of the cements, facilitating their dissolution and promoting bone regeneration. *'Dissolution pits or etched crystals are evidence of osteoclast-mediated degradation'* [2].

Bioresorption is influenced by a number of factors which include cement composition and porosity (pores size, interconnectivity) [11], patient's age, health and sex, anatomical location of the implant [30], defect size, degree level of defect (acute traumatic fractures or only small microfractures), bone quality, etc.

Apatite cements have a slower degradation rate compared to brushite cements. Increasing the porosity of the cement will improve the degradation rate but will reduce the mechanical properties.

For in vitro evaluation of the biodegradation, the specimens are immersed in physiological fluids (SBF, PBS or bovine serum) over a defined period of time. This allows the determination of mass loss percent, pH variation, dissolution rate, amount of ions released in the fluid and mechanical stability at specific time intervals.

In vivo bioresorption is evaluated in animal models and assessed at different time points using histological examination of the explant in order to estimate the rate of new bone ingrowth, the percent and the quality of the new bone, the degree/percent of implant resorption, etc.

4.8 Process Parameters Effect

The effect of process parameters on the main properties of CPCs is illustrated in Table 4.5 where the general trend of increasing or decreasing values is indicated by rising or falling arrows, respectively. Typically, increasing LPR will increase the cohesion, injectability and setting time whilst reducing relevant mechanical properties.

Smaller particle size increases the surface area and hence accelerates the setting reaction. Decreasing the size of particles results in increased injectability and mechanical properties but decreased cohesion. Additives could be included in both

Table 4.5 Effect of process parameters on CPCs properties

Process parameter	Process parameter variation	Injectability	Cohesion	Mechanical properties	Setting time	Porosity	Degradability
LPR	↗	↗	↗	↘	↗		
Particles size	↘	↗	↘	↗	↘	↘	↘
Additives	↗	↗		↗ or ↘	↗ or ↘		
Gelling agent added into the liquid phase	↗	↗	↗	↘	↗		
Additives added into the powder phase	↗		↘		↘		
Porogens	↗			↘		↗	↗
Temperature	↗				↘		

↗ increasing (amount or relevant property), ↘ decreasing (amount or relevant property), *LPR* liquid to powder ratio

liquid and powder components to control the setting time and mechanical properties. Generally, adding a gelling agent into the liquid phase will increase the injectability and cohesion but will reduce the mechanical properties. Additives used in the powder component might reduce cohesion and mechanical properties.

Room and component temperatures affect the solubility of CP powders. Increasing the temperature generally accelerates the setting time. Porogens can be added to the cement composition to increase porosity and pore interconnectivity. This will improve the beneficial in vivo degradability of the cements but will reduce required mechanical properties.

Predictably, it is rarely possible to obtain and maintain all desired properties, from the most basic powder and liquid components through to hardened cements or resorbed materials. There will always be a compromise between desired and achievable properties. The scientist will need to determine an optimum balance between material properties at any stage and process parameters, by deciding the relevant importance of each property for specific applications. This becomes more complicated in-situ, after implantation, as in vivo conditions add further, and often significant and complex, variability.

4.9 Advantages and Disadvantages of Calcium Phosphate Cements

There are many compositions of CPCs which have been continuously developed since the first cement was synthesised in 1980. CPCs are attractive materials due to their range of critical properties, making them suitable for dental, craniofacial and

Table 4.6 Advantages and disadvantages of CPCs

Advantages	Disadvantages
Good bioactivity, being able to form a direct chemical bond with bone tissue Good biocompatibility, no toxicity Good biodegradability, stimulating bone tissue regeneration Good osteoconductivity, allowing ingrowth of new bone Good injectability allowing minimally invasive surgical implantation and the ability to adapt to different bone defect geometry Good mouldability that allows good fitting of complex bone cavities Self-setting ability in physiological environments at the implant site Radiopaque, being visible on X-ray imaging Easy preparation and handling Non-exothermic, non-toxic setting reaction Suitable as drug delivery carriers	Poor mechanical properties that limit their use to only non-loadbearing applications Poor cohesion with potential to disintegrate when in contact with body fluids; potential for inflammatory reaction and embolism Lack of macroporosity which prevents fast bone ingrowth Slow degradation rates, lower than new bone formation rate which might limit natural healing

orthopaedic applications where low stresses are required. Despite the reluctance of some surgeons to use them clinically, because of possible inflammatory reaction and embolism caused by potential poor cohesion, there is still a high demand for CPCs, especially when high tissue regeneration is requested. As their structure is very similar to the mineral bone matrix, CPCs have excellent biological properties that stimulate osteointegration. The main advantages and disadvantages of CPCs are summarised in Table 4.6.

4.10 Medical Applications

Commercial CPCs have been used in a wide range of applications in orthopaedic surgery, trauma surgery, prosthetic revisions, craniomaxillofacial, periodontal and spinal surgery. They help to increase the structural integrity of the surrounding natural bone by rebuilding lost bone mass, filling defects after resection of bone tumours and as augmentation material where cancellous bone should be replaced. They also are useful as bioactive fillers for revision arthroplasty, bone fixation support, filling of congenital defects and similar applications [26, 28, 36, 37].

4.10.1 Vertebral Applications

Vertebral fractures can be extremely painful and may cause significant loss of function and structural stability, reducing the quality of life for patients. Usually, pain killers, bed rest and external bracing are suggested to control and to support natural healing of vertebral fractures [38].

Vertebroplasty and kyphoplasty are two minimally invasive surgical techniques to treat vertebral compression fractures. Vertebroplasty is performed by injection of the cement directly into the fractured vertebral body using cannulated needles. In kyphoplasty techniques, also known as balloon vertebroplasty, the cement is injected into a cavity previously created with an inflatable balloon [31]. To date, these two methods have been preferred since they treat painful fractures, enhance healing and protect the fracture from further deformation.

CPCs cements are indicated for acute traumatic fractures, as they will facilitate new bone ingrowth and vascularisation due to their high bioactivity and osteoconductivity, despite their poor mechanical properties. Compared to polymethylmethacrylate (PMMA) cements, which are generally used for spinal surgery, CPCs are bioactive, and the heat developed during the setting reaction of CPCs is negligible. In contrast, the setting reaction of PMMA cements is highly exothermic, and the methylmethacrylate monomer residues are extremely toxic. Physiologically elevated temperatures (greater than 80 °C) are possible during typical PMMA setting reaction which can cause local tissue necrosis. Similarly, any leakage of the toxic monomer could result in tissue necrosis. Nevertheless, PMMA cements are still preferred by some surgeons due to their higher mechanical properties and higher injectability, even if they are not bioactive, osteoconductive or bioresorbable.

4.10.2 Dental Applications

CPCs have been used for bone void filling and bone regeneration in dental surgery for applications such as filling defects around dental implants, ridge augmentation, sinus floor augmentation and filling complex bone cavities. However, due to their poor mechanical properties, they have been substituted by PMMA dental cements.

4.10.3 Craniofacial Applications

Several commercial cements are recommended for augmentation or restoration of bone contours in the craniofacial skeleton, including frontal, orbital, malar and mental areas. Typically, they are useful for filling cavities less than 25 cm^3, which have a surface area of 4 cm^2 or less. These cements are generally recommended for burr hole voids, orbital rims, craniotomy cuts and surgically created bone defects [39, 40].

4.10.4 Orthopaedic Applications

A range of commercial cements are recommended for metaphyseal cancellous bone defects caused by trauma, benign tumour, surgery, or congenital defects. They can also be applied in reconstruction surgery, such as revisions and reinforcing

osteoporotic bone, and for bone augmentation. The most common indications for clinical use of these cements are distal radius fractures, tibia plateau fractures and calcaneus fractures [26, 28, 36, 37].

4.10.5 Drug Delivery

CPCs have been used successfully for the delivery of drugs directly to the implant site. Unlike PMMA bone cements, the setting reaction of CPCs is not exothermic, so drugs can be loaded within either the liquid or powder phase without affecting their chemical and physical properties. However, during the setting reaction, any of the reagents or final products could interact with the drug and change their properties. The microporous structure of CPCs is adequate as a delivery carrier for different antibiotics, antitumour agents or other biomolecules (growth factors, proteins, etc.) and can be effective for the treatment of bone diseases such as bone tumours and osteoporosis [41, 42].

The drug release kinetics will depend on the solubility of the drug, cement composition, porosity (pores size and interconnectivity) and bioresorption rate of the hardened cement [41, 43].

4.11 Summary

CPCs are bioactive, biocompatible, osteoinductive and bioresorbable materials that can allow and promote bone tissue regeneration. Their structure is similar to the mineral phase of natural bone and teeth, stimulating bone ingrowth and vascularisation within the implant. However, CPCs are brittle, have relatively low mechanical properties, low cohesion and no macroporosity, limiting the clinical applications to non-loadbearing applications. Due to their excellent biological properties, CPCs are used as temporary bone space fillers, dental implants, in maxillofacial reconstruction and spinal surgery.

The main advantages of CPCs is their injectability, making the surgical procedure minimally invasive, and the ability to harden in situ at body temperature, directly at the implantation site. CPCs can be injected or moulded into the bone defect, being able to adapt to very complex shapes and sizes of a wide variety of bone cavities.

CPCs are fabricated by mixing one or more calcium phosphates in a solid form with an aqueous liquid, typically water or sodium phosphate solutions, to form a paste which can harden and set without affecting their surroundings. Thus, CPCs are self-setting materials that can set under physiologic conditions without any heat generation, by a dissolution-precipitation process. During setting, the precipitated crystals interlock, leading to a micro- and nanoporous hardened structure with higher mechanical properties than the original paste. The setting reaction produces

two types of cements: apatite and brushite. Generally, apatite cements have higher mechanical properties than brushite cements due to their lower solubility. Brushite cements have a higher resorption rate and lower setting time when compared to apatite cements. They can transform into a more stable apatite structure in vivo. Process parameters have a complex effect on the properties of the paste and hardened cement. There will always be a compromise between desired and achievable properties. This is further complicated as properties are normally determined in vitro, and in vivo conditions add further unknown variability.

CPCs are developing rapidly with new potential applications that depend upon improved properties and the opportunities that they offer over existing materials and techniques. Whilst carefully controlled for clinical use, this area of medically relevant materials is still not mature. It can be seen from the variety and ad hoc nature of some of the testing and assessment methods that considerable further development is possible, and arguably required, to improve the understanding and use of these biomaterials. With greater understanding and predictability of properties, current limitations can be addressed.

References

1. http://dictionary.cambridge.org/dictionary/english/cement. Last access 16 Jan 2017.
2. Castaño O, Planell JA. Cements (chapter 8). In: Vallet-Regi M, editor. Bio-ceramics with clinical applications. Hoboken: Wiley; 2014. p. 195–248.
3. Cama G. Calcium phosphate cements for bone regeneration (chapter 1). In: Dubruel P, Vlierberghe SV, editors. Biomaterials for bone regeneration: Novel techniques and applications. Burlington: Elsevier; 2014. p. 3–25.
4. Dorozhkin SV. Calcium orthophosphate cements and concretes. Materials. 2009;2(1): 221–91.
5. Bohner M. Calcium orthophosphates in medicine: from ceramics to calcium phosphate cements. Injury Int J Care Injured. 2000;31:S37–47.
6. Ishikawa K. Bioactive ceramics: cements (chapter 1.116). In: Ducheyne P, editor. Comprehensive biomaterials, Metallic, ceramic and polymeric biomaterials, vol. 1. Amsterdam: Elsevier; 2011. p. 267–84.
7. Sanzana ES, Navarro M, Macule F, Suso S, Planell JA, Ginebra MP. Of the in vivo behavior of calcium phosphate cements and glasses as bone substitutes. Acta Biomater. 2008;4(6): 1924–33.
8. Zhang JT, Tancret F, Bouler JM. Fabrication and mechanical properties of calcium phosphate cements (CPC) for bone substitution. Mater Sci Eng C. 2011;31(4):740–7.
9. Xu HHK, Carey LE, Simon CG, Takagi S, Chow LC. Premixed calcium phosphate cements: synthesis, physical properties, and cell cytotoxicity. Dent Mater. 2007;23(4):433–41.
10. Dorozhkin SV. Biphasic, triphasic and multiphasic calcium orthophosphates. Acta Biomater. 2012;8:963–77.
11. Sariibrahimoglu K, Wolke JGC, Leeuwenburgh SCG, Jansen JA. Calcium phosphates (chapter 3). In: Fisher JP, Mikos AG, Bronzino JD, Peterson DR, editors. Tissue engineering: principles and practices. London: CRC Press; 2012. p. 1–22.
12. Zhao J, Yu L, Sun W-b, Zhang H. Amorphous calcium phosphate and its application in dentistry. Chem Cent J. 2011;5:40.
13. Neira MIS. PhD thesis: an efficient approach to the synthesis of a calcium phosphate bonecement and its reinforcement by hydroxyapatite crystals of various particle morphologies, University Santiago de Compostela, Spain, 2008, p. 44

14. Ishikawa K. Bone substitute fabrication based on dissolution-precipitation reactions. Materials. 2010;3:1138–55.
15. Zhang J, Liu W, Schnitzler V, Tancret F, Bouler J-M. Calcium phosphate cements for bone substitution: chemistry, handling and mechanical properties. Acta Biomater. 2014;10: 1035–49.
16. Sergey V. Dorozhkin, calcium orthophosphate cements for biomedical application. J Mater Sci. 2008;43:3028–57.
17. Ishikawa K. Calcium phosphate cement (chapter 7). In: Ben-Nissan B, editor. Advances in calcium phosphate biomaterials. Berlin: Springer; 2014. p. 199–227.
18. Draft BS ISO 18531 Implants for surgery – calcium phosphate bioceramics – characterization of hardening bone paste materials.
19. ASTM C191−13, Standard test methods for time of setting of hydraulic cement by Vicat Needle.
20. ASTM C266–15, Standard test method for time of setting of hydraulic-cement paste by Gillmore Needles.
21. http://matest.com/en/Products/--1/Macro-Category/vicat-apparatus/e055n-vicat-apparatus. Last access on 15 Jan 2017.
22. http://matest.com/en/Products/--1/Macro-Category/vicat-apparatus/e058-gillmore-apparatus-0. Last access on 15 Jan 2017.
23. Bohner M, Doebelin N, Baroud G. Theoretical and experimental approach to test the cohesion of calcium phosphate pastes. Eur Cells Mater. 2006;12:26–35.
24. An J, Wolke JGC, Jansen JA, Leeuwenburgh SCG. Influence of polymeric additives on the cohesion and mechanical properties of calcium phosphate cements. J Mater Sci Mater Med. 2016;27:58.
25. Chen G, Li W, Yu X, Sun K. Study of the cohesion of TTCP/DCPA phosphate cement through evolution of cohesion time and remaining percentage. J Mater Sci. 2009;44:828–34.
26. http://www.stryker.com/en-us/products/Orthopaedics/BoneSubstitutes/Hydroset/index.htm. Last access 15 Jan 2017.
27. Friedman CD, Costantino PD, Takagi S, Chow LC. BoneSource hydroxyapatite cement: a novel biomaterial for craniofacial skeletal tissue engineering and reconstruction. J Biomed Mater Res. 1998;43(4):428–32.
28. http://www.stryker.com/stellent/groups/public/documents/web_prod/023526.pdf. Last access 15 Jan 2017.
29. Seitz IA, Teven CM, Reid RR. Repair and grafting of bone (chapter 21). In: Neligan PC, editor. Plastic surgery, Principles, vol. 1. London/New York: Elsevier; 2013. p. 425–63.
30. O'Hara R, Buchanan F, Dunne N. Injectable calcium phosphate cements for spinal bone repair (chapter 2). In: Dubruel P, Van Vlierberghe S, editors. Biomaterials for bone regeneration: novel techniques and applications. Burlington: Elsevier; 2014. p. 26–61.
31. Verlaan JJ, Oner FC, Dhert WJA. Anterior spinal column augmentation with injectable bone cements. Biomaterials. 2006;27(3):290–301.
32. Jack V, Buchanan V, Dunne FJ. Particle attrition of alpha-tricalcium phosphate: effect on mechanical, handling, and injectability properties of calcium phosphate cements. Proc Inst Mech Eng H-J Eng Med. 2008;222(H1):19–28.
33. Barralet JE, Grover LM, Gbureck U. Ionic modification of calcium phosphate cement viscosity. Part II: hypodermic injection and strength improvement of brushite cement. Biomaterials. 2004;25:2197–203.
34. Xu HHK, Quinn JB. Calcium phosphate cement containing resorbable fibers for short-term reinforcement and macroporosity. Biomaterials. 2002;23(1):193–202.
35. Zuo Y, Yang F, Wolke JGC, Li Y, Jansen JA. Incorporation of biodegradable electrospun fibers into calcium phosphate cement for bone regeneration. Acta Biomater. 2010;6(4):1238–47.
36. http://emea.depuysynthes.com/hcp/biomaterials/products/qs/chronos-inject. Last access 15 Jan 2017.
37. http://www.groupfhortho.com/our-products/bone-substitutes/eurobone-2/. Last access 15 Jan 2017.

38. Low KL, Tan SH, Zein SHS, Roether JA, Mourino V, Boccaccini AR. Calcium phosphate-based composites as injectable bone substitute materials. J Biomed Mater Res. 2010;94(1):273–86.
39. http://www.synthes.com/MediaBin/US%20DATA/Product%20Support%20Materials/Technique%20Guides/MXTGFastPuttyJ4261F.pdf. Last access 15 Jan 2017.
40. https://cmf.stryker.com/products/directinject#. Last access 15 Jan 2017.
41. Ginebra MP, Canal C, Espanol M, Pastorino D, Montufar EB. Calcium phosphate cements as drug delivery materials. Adv Drug Deliv Rev. 2012;64(12):1090–110.
42. Vorndran E, Geffers M, Ewald A, Lemm M, Nies B, Gbureck U. Ready-to-use injectable calcium phosphate bone cement paste as drug carrier. Acta Biomater. 2013;9(12):9558–67.
43. Ginebra MP, Traykova T, Planell JA. Calcium phosphate cements as bone drug delivery systems: a review. J Control Release. 2006;113(2):102–10.

Chapter 5
Calcium Orthophosphate-Based Bioceramics and Its Clinical Applications

Sergey V. Dorozhkin

Abstract Various types of grafts have been traditionally used to restore damaged bones. In the late 1960s, a strong interest was raised in studying ceramics as potential bone grafts due to their biomechanical properties. A bit later, such synthetic biomaterials were called bioceramics. In principle, bioceramics can be prepared from diverse inorganic substances but this review is limited to calcium orthophosphate ($CaPO_4$)-based formulations only, which possess the specific advantages due to the chemical similarity to mammalian bones and teeth. During the past 40 years, there have been a number of important achievements in this field. Namely, after the initial development of bioceramics that was just tolerated in the physiological environment, an emphasis was shifted towards the formulations able to form direct chemical bonds with the adjacent bones. Afterwards, by the structural and compositional controls, it became possible to choose whether the $CaPO_4$-based implants remain biologically stable once incorporated into the skeletal structure or whether they were resorbed over time. At the turn of the millennium, a new concept of regenerative bioceramics was developed and such formulations became an integrated part of the tissue engineering approach. Now $CaPO_4$-based scaffolds are designed to induce bone formation and vascularization. These scaffolds are usually porous and harbor various biomolecules and/or cells. Therefore, current biomedical applications of $CaPO_4$-based bioceramics include bone augmentations, artificial bone grafts, maxillofacial reconstruction, spinal fusion, periodontal disease repairs and bone fillers after tumor surgery. Perspective future applications comprise drug delivery and tissue engineering purposes because $CaPO_4$ appear to be promising carriers of growth factors, bioactive peptides and various types of cells.

Keywords Calcium orthophosphates • Hydroxyapatite • Tricalcium phosphate • Bioceramics • Biomaterials • Grafts • Biomedical applications • Tissue engineering

S.V. Dorozhkin (✉)
Kudrinskaja sq. 1-155, Moscow 123242, Russia
e-mail: sedorozhkin@yandex.ru

G. Kaur (ed.), *Clinical Applications of Biomaterials*,
DOI 10.1007/978-3-319-56059-5_5

5.1 Introduction

One of the most exciting and rewarding areas of the engineering discipline involves development of various devises for health care. Some of them are implantable. Examples comprise sutures, catheters, heart valves, pacemakers, breast implants, fracture fixation plates, nails and screws in orthopedics, various filling formulations, orthodontic wires, total joint replacement prostheses, etc. However, in order to be accepted by the living body without any unwanted side effects, all implantable items must be prepared from a special class of tolerable materials, called biomedical materials or biomaterials, in short. The physical character of the majority of the available biomaterials is solids [1, 2].

From the material point of view, all types of solids are divided into four major groups: metals, polymers, ceramics and various blends thereof, called composites. Similarly, all types of solid biomaterials are also divided into the same groups: biometals, biopolymers, bioceramics and biocomposites. All of them play very important roles in both replacement and regeneration of various human tissues; however, setting biometals, biopolymers and biocomposites aside, this review is focused on bioceramics only. In general, bioceramics comprise various polycrystalline materials, amorphous materials (glasses) and blends thereof (glass-ceramics). Nevertheless, the chemical elements used to manufacture bioceramics form just a small set of the Periodic Table. Namely, bioceramics might be prepared from alumina, zirconia, magnesia, carbon, silica-contained and calcium-contained compounds, as well as from a limited number of other chemicals. All these compounds might be manufactured in both dense and porous forms in bulk, as well as in the forms of crystals, powders, particles, granules, scaffolds and/or coatings [1–3].

As seen from the above, the entire subject of bioceramics is still rather broad. To specify it further, let me limit myself by a description of $CaPO_4$-based formulations only. Due to the chemical similarity to mammalian bones and teeth, this type of bioceramics is used in a number of different applications throughout the body, covering all areas of the skeleton. The examples include healing of bone defects, fracture treatment, total joint replacement, bone augmentation, orthopedics, cranio-maxillofacial reconstruction, spinal surgery, otolaryngology, ophthalmology and percutaneous devices [1–3], as well as dental fillings and periodontal treatments [4]. Depending upon the required properties, different types of $CaPO_4$ might be used. For example, Fig. 5.1 displays some randomly chosen samples of the commercially available $CaPO_4$ bioceramics for bone graft applications. One should note that, in 2010, only in the USA the sales of bone graft substitutes were valued at ~$1.3 billion with a forecast of ~$2.3 billion by 2017 [5]. This clearly demonstrates an importance of $CaPO_4$-based bioceramics.

A list of the available $CaPO_4$, including their standard abbreviations and major properties, is summarized in Table 5.1 [3, 6]. To narrow the subject further, with a few important exceptions, bioceramics prepared from undoped and un-substituted $CaPO_4$ will be considered and discussed only. Due to this reason, $CaPO_4$-based bioceramics prepared from biological resources, such as bones, teeth, corals, etc. [7–16], as well as the ion-substituted ones [17–41] are not considered. The readers interested in both topics are advised to study the original publications.

Fig. 5.1 Several examples of the commercial $CaPO_4$-based bioceramics

5.2 General Knowledge and Definitions

A number of definitions have been developed for the term "biomaterials". For example, by the end of the twentieth century, the consensus developed by the experts was the following: biomaterials were defined as synthetic or natural materials to be used to replace parts of a living system or to function in intimate contact with living tissues [42]. However, in September 2009, a more advanced definition was introduced: "A biomaterial is a substance that has been engineered to take a form which, alone or as part of a complex system, is used to direct, by control of interactions with components of living systems, the course of any therapeutic or diagnostic procedure, in human or veterinary medicine" [43]. The definition alterations were accompanied by a shift in both the conceptual ideas and the expectations of biological performance, which mutually changed in time [44].

In general, the biomaterials discipline is founded in the knowledge of the synergistic interaction of material science, biology, chemistry, medicine and mechanical science and it requires the input of comprehension from all these areas so that potential implants perform adequately in a living body and interrupt normal body functions as little as possible [45]. As biomaterials deal with all aspects of the material synthesis and processing, the knowledge in chemistry, material science and engineering appears to be essential. On the other hand, since clinical implantology is the main purposes of biomaterials, biomedical sciences become the key part of the research. These include cell and molecular biology, histology, anatomy and physiology. The final aim is to achieve the correct biological interaction of the

Table 5.1 Existing calcium orthophosphates and their major properties [3, 6]

Ca/P molar ratio	Compounds and their typical abbreviations	Chemical formula	Solubility at 25 °C, −log(K_s)	Solubility at 25 °C, g/L	pH stability range in aqueous solutions at 25 °C
0.5	Monocalcium phosphate monohydrate (MCPM)	$Ca(H_2PO_4)_2·H_2O$	1.14	~18	0.0–2.0
0.5	Monocalcium phosphate anhydrous (MCPA or MCP)	$Ca(H_2PO_4)_2$	1.14	~17	[a]
1.0	Dicalcium phosphate dihydrate (DCPD), mineral brushite	$CaHPO_4·2H_2O$	6.59	~0.088	2.0–6.0
1.0	Dicalcium phosphate anhydrous (DCPA or DCP), mineral monetite	$CaHPO_4$	6.90	~0.048	[a]
1.33	Octacalcium phosphate (OCP)	$Ca_8(HPO_4)_2(PO_4)_4·5H_2O$	96.6	~0.0081	5.5–7.0
1.5	α-Tricalcium phosphate (α-TCP)	α-$Ca_3(PO_4)_2$	25.5	~0.0025	[b]
1.5	β-Tricalcium phosphate (β-TCP)	β-$Ca_3(PO_4)_2$	28.9	~0.0005	[b]
1.2–2.2	Amorphous calcium phosphates (ACP)	$Ca_xH_y(PO_4)_z·nH_2O$, n = 3–4.5; 15–20% H_2O	[c]	[c]	~5–12[d]
1.5–1.67	Calcium-deficient hydroxyapatite (CDHA or Ca-def HAp)[e]	$Ca_{10-x}(HPO_4)_x(PO_4)_{6-x}(OH)_{2-x}$ (0 < × < 1)	~85	~0.0094	6.5–9.5
1.67	Hydroxyapatite (HAp, HAp or OHAp)	$Ca_{10}(PO_4)_6(OH)_2$	116.8	~0.0003	9.5–12
1.67	Fluorapatite (FA or FAp)	$Ca_{10}(PO_4)_6F_2$	120.0	~0.0002	7–12
1.67	Oxyapatite (OA, OAp or OXA)[f], mineral voelckerite	$Ca_{10}(PO_4)_6O$	~69	~0.087	[b]
2.0	Tetracalcium phosphate (TTCP or TetCP), mineral hilgenstockite	$Ca_4(PO_4)_2O$	38–44	~0.0007	[b]

[a]Stable at temperatures above 100 °C

[b]These compounds cannot be precipitated from aqueous solutions

[c]Cannot be measured precisely. However, the following values were found: 25.7 ± 0.1 (pH = 7.40), 29.9 ± 0.1 (pH = 6.00), 32.7 ± 0.1 (pH = 5.28). The comparative extent of dissolution in acidic buffer is: ACP >> α-TCP >> β-TCP > CDHA >> HAp > FA

[d]Always metastable

[e]Occasionally, it is called "precipitated HAp (PHA)"

[f]Existence of OA remains questionable

artificial grafts with living tissues of a host. Thus, to achieve the goals, several stages have to be performed, such as: material synthesis, design and manufacturing of prostheses, followed by various types of tests. Furthermore, before clinical applications, any potential biomaterial must also pass all regulatory requirements [46].

In any case, biomaterials are intended to interface with biological systems in vivo to evaluate, treat, augment or replace any tissue, organ or function of the body and are now used in a number of different applications throughout the body. Thus, biomaterials are solely associated with the health care domain and must have an interface with tissues or tissue components. One should stress, that any artificial materials those simply are in contact with skin, such as hearing aids and wearable artificial limbs, are not included in the definition of biomaterials since the skin acts as a protective barrier between the body and the external world [1, 2, 47].

The major difference of biomaterials from other classes of materials lays in their ability to remain in a biological environment with neither damaging the surroundings nor being damaged in that process. Therefore, biomaterials must be distinguished from *biological materials* because the former are the materials that are accepted by living tissues and, therefore, they might be used for tissue replacements, while the latter are just the materials being produced by various biological systems (wood, cotton, bones, chitin, etc.) [48]. Furthermore, there are *biomimetic materials*, which are not made by living organisms but have the composition, structure and properties similar to those of biological materials. Concerning the subject of current review, *bioceramics* (or biomedical ceramics) is defined as biomaterials having the ceramic origin. Now it is important to define the meaning of ceramics. According to Wikipedia, the free encyclopedia: "The word *ceramic* comes from the Greek word κεραμικός (*keramikos*), "of pottery" or "for pottery", from κέραμος (*keramos*), "potter's clay, tile, pottery". The earliest known mention of the root "ceram-" is the Mycenaean Greek *ke-ra-me-we*, "workers of ceramics", written in Linear B syllabic script. The word "ceramic" may be used as an adjective to describe a material, product or process, or it may be used as a noun, either singular, or, more commonly, as the plural noun "ceramics". A ceramic material is an inorganic, non-metallic, often crystalline oxide, nitride or carbide material. Some elements, such as carbon or silicon, may be considered ceramics. Ceramic materials are brittle, hard, strong in compression, weak in shearing and tension. They withstand chemical erosion that occurs in other materials subjected to acidic or caustic environments. Ceramics generally can withstand very high temperatures, such as temperatures that range from 1,000 to 1,600 °C (1,800–3,000 °F). Glass is often not considered a ceramic because of its amorphous (noncrystalline) character. However, glassmaking involves several steps of the ceramic process and its mechanical properties are similar to ceramic materials" [49]. Similar to any other type of biomaterials, bioceramics can have structural functions as joint or tissue replacements, be used as coatings to improve the biocompatibility, as well as function as resorbable lattices, providing temporary structures and frameworks those are dissolved and/or replaced as the body rebuilds the damaged tissues [50–53]. Some types of bioceramics feature a drug-delivery capability [54–57].

In medicine, bioceramics is needed to alleviate pain and restore functions of diseased or damaged calcified tissues (bones and teeth) of the body. A great challenge

facing its medical application is, first, to replace and, second, to regenerate old and deteriorating bones with a biomaterial that can be replaced by a new mature bone without transient loss of a mechanical support [1, 2]. Since an average life span of humans is now 80+ years and the major need for spare parts begins at about 60 years of age, the after-effects of the implanted bioceramics need to last, at least, for 20+ years. This demanding requirement of survivability is under conditions of use that are especially harsh to implanted biomaterials: corrosive saline solutions at 37 °C under variable, multiaxial and cyclical mechanical loads. The excellent performance of the specially designed bioceramics that have survived these clinical conditions represented one of the most remarkable accomplishments of research, development, production and quality assurance by the end of the past century [50]. Concerning $CaPO_4$ bioceramics, a surface bioactivity appears to be its the major feature. It contributes to a bone bonding ability and enhances new bone formation [58].

5.3 Bioceramics of $CaPO_4$

5.3.1 History

The detailed history of HAp and other types of $CaPO_4$, including the subject of $CaPO_4$ bioceramics, as well as description of their past biomedical applications might be found elsewhere [59, 60], where the interested readers are referred.

5.3.2 Chemical Composition and Preparation

Currently, $CaPO_4$ bioceramics can be prepared from various sources [7–15]. Nevertheless, up to now, all attempts to synthesize bone replacement materials for clinical applications featuring the physiological tolerance, biocompatibility and a long-term stability have had only a relative success; this clearly demonstrates both the superiority and a complexity of the natural structures [61].

In general, a characterization of $CaPO_4$ bioceramics should be performed from various viewpoints such as the chemical composition (including stoichiometry and purity), homogeneity, phase distribution, morphology, grain sizes and shape, grain boundaries, crystallite size, crystallinity, pores, cracks, surface roughness, etc. From the chemical point of view, the vast majority of $CaPO_4$ bioceramics is based on HAp [62–67], both types of TCP [62, 68–78] and various multiphasic formulations thereof [79]. Biphasic formulations (commonly abbreviated as BCP – biphasic calcium phosphate) are the simplest among the latter ones. They include β-TCP + HAp [80–88], α-TCP + HAp [89–91] and biphasic TCP (commonly abbreviated as BTCP) consisting of α-TCP and β-TCP [92–97]. In addition, triphasic formulations (HAp + α-TCP + β-TCP) have been prepared as well [98–101]. Further details on this topic might be found in a special review [79]. Leaving aside a big subject of DCPD-forming

self-setting formulations [102, 103], one should note that just a few publications on bioceramics, prepared from other types of $CaPO_4$, are available [104–112].

The preparation techniques of various $CaPO_4$ have been extensively reviewed in literature [6, 113–117] where the interested readers are referred to. Briefly, when compared to both α- and β-TCP, HAp is a more stable phase under the physiological conditions, as it has a lower solubility (Table 5.1) and, thus, slower resorption kinetics [118–120]. Therefore, the BCP concept is determined by the optimum balance of a more stable phase of HAp and a more soluble TCP. Due to a higher biodegradability of the α- or β-TCP component, the reactivity of BCP increases with the TCP/HAp ratio increasing. Thus, in vivo bioresorbability of BCP can be controlled through the phase composition [81]. Similar conclusions are also valid for the biphasic TCP (in which α-TCP is a more soluble phase), as well as for both triphasic (HAp, α-TCP and β-TCP) and yet more complex formulations [79].

As implants made of sintered HAp are found in bone defects for many years after implantation (Fig. 5.2, bottom), bioceramics made of more soluble types of $CaPO_4$ [62, 68–112, 121, 122] are preferable for the biomedical purposes (Fig. 5.2, top). Furthermore, the experimental results showed that BCP had a higher ability to adsorb fibrinogen, insulin or type I collagen than HAp [123]. Thus, according to both observed and measured bone formation parameters, $CaPO_4$ bioceramics have been ranked as follows: low sintering temperature BCP (rough and smooth) ≈ medium sintering temperature BCP ≈ TCP > calcined low sintering temperature HAp > non-calcined low sintering temperature HAp > high sintering temperature

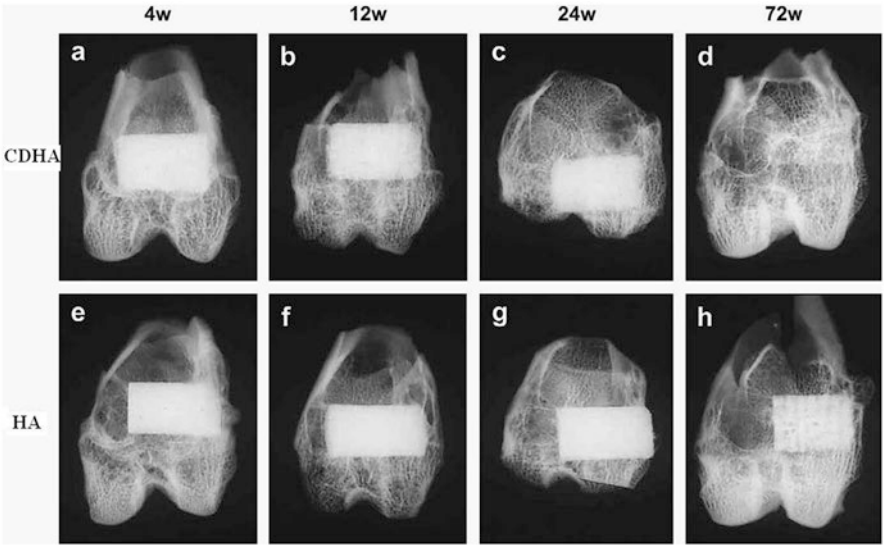

Fig. 5.2 Soft x-ray photographs of the operated portion of the rabbit femur. Four weeks (**a**), 12 weeks (**b**), 24 weeks (**c**) and 72 weeks (**d**) after implantation of CDHA; 4 weeks (**e**), 12 weeks (**f**), 24 weeks (**g**) and 72 weeks (**h**) after implantation of sintered HAp [121]

BCP (rough and smooth) > high sintering temperature HAp [124]. This sequence has been developed in year 2000 and, thus, neither multiphase formulations, nor other $CaPO_4$ have been included.

5.3.3 Forming and Shaping

In order to fabricate bioceramics in progressively complex shapes, scientists are investigating the use of both old and new manufacturing techniques. These techniques range from an adaptation of the age-old pottery techniques to the newest manufacturing methods for high-temperature ceramic parts for airplane engines. Namely, reverse engineering [125, 126] and rapid prototyping [127–129] technologies have revolutionized a generation of physical models, allowing the engineers to efficiently and accurately produce physical models and customized implants with high levels of geometric intricacy. Combined with the computer-aided design and manufacturing (CAD/CAM), complex physical objects of the anatomical structure can be fabricated in a variety of shapes and sizes. In a typical application, an image of a bone defect in a patient can be taken and used to develop a three-dimensional (3D) CAD computer model [130–134]. Then a computer can reduce the model to slices or layers. Afterwards, 3D objects and coatings are constructed layer-by-layer using rapid prototyping techniques. The examples comprise fused deposition modeling [135, 136], selective laser sintering [137–143], laser cladding [144–147], 3D printing and/or plotting [73, 148–162], solid freeform fabrication [163–171] and stereolithography [172–175]. 3D printing and/or plotting of the $CaPO_4$-based self-setting formulations could be performed as well [160, 161]. In the specific case of ceramic scaffolds, a sintering step is usually applied after printing the green bodies. Furthermore, a thermal printing process of melted $CaPO_4$ has been proposed [176], while, in some cases, laser processing might be applied as well [177, 178]. A schematic of 3D printing technique, as well as some 3D printed items are shown in Fig. 5.3 [56]. A custom-made implant of actual dimensions would reduce the time it takes to perform the medical implantation procedure and subsequently lower the risk to the patient. Another advantage of a prefabricated, exact-fitting implant is that it can be used more effectively and applied directly to the damaged site rather than a replacement, which is formulated during surgery from a paste or granular material [164, 178–180].

In addition to the aforementioned modern techniques, classical forming and shaping approaches are still widely used. The selection of the desired technique depends greatly on the ultimate application of the bioceramic device, e.g., whether it is for a hard-tissue replacement or an integration of the device within the surrounding tissues. In general, three types of the processing technologies might be used: (1) employment of a lubricant and a liquid binder with ceramic powders for shaping and subsequent firing; (2) application of self-setting and self-hardening properties of water-wet molded powders; (3) materials are melted to form a liquid and are shaped during cooling and solidification [181–184]. Since $CaPO_4$ are either thermally unstable (MCPM, MCPA, DCPA, DCPD, OCP, ACP, CDHA) or have a

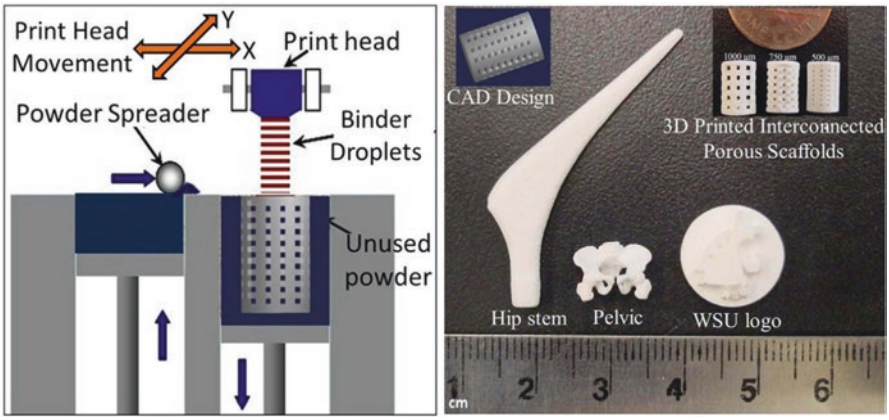

Fig. 5.3 A schematic of 3D printing and some 3D printed parts (fabricated at Washington State University) showing the versatility of 3D printing technology for ceramic scaffolds fabrication with complex architectural features [56]

melting point at temperatures exceeding ~1,400 °C with a partial decomposition (α-TCP, β-TCP, HAp, FA, TTCP), only the first and the second consolidation approaches are used to prepare bulk bioceramics and scaffolds. The methods include uniaxial compaction [185–187], isostatic pressing (cold or hot) [87, 188–195], granulation [196–202], loose packing [203], slip casting [75, 204–209], gel casting [172, 210–218], pressure mold forming [219, 220], injection molding [221–223], polymer replication [224–231], ultrasonic machining [232], extrusion [233–239], slurry dipping and spraying [240]. In addition, to form ceramic sheets from slurries, tape casting [213, 241–245], doctor blade [246] and colander methods can be employed [181–184]. In addition, flexible, ultrathin (of 1 to several microns thick), freestanding HAp sheets were produced by a pulsed laser deposition technique, followed by thin film isolation technology [247]. Various combinations of several techniques are also possible [77, 213, 248–250]. Furthermore, some of these processes might be performed under the electromagnetic field, which helps crystal aligning [205, 208, 251–254]. Finally, the prepared $CaPO_4$ bioceramics might be subjected by additional treatments (e.g., chemical, thermal and/or hydrothermal ones) to convert one type of $CaPO_4$ into another one [231].

To prepare bulk bioceramics, powders are usually pressed damp in metal dies or dry in lubricated dies at pressures high enough to form sufficiently strong structures to hold together until they are sintered [255]. An organic binder, such as polyvinyl alcohol, helps to bind the powder particles altogether. Afterwards, the binder is removed by heating in air to oxidize the organic phases to carbon dioxide and water. Since many binders contain water, drying at ~100 °C is a critical step in preparing damp-formed pieces for firing. Too much or too little water in the compacts can lead to blowing apart the ware on heating or crumbling, respectively [181–184, 189]. Furthermore, removal of water during drying often results in subsequent shrinkage of the product. In addition, due to local variations in water content, warping and even cracks may be

developed during drying. Dry pressing and hydrostatic molding can minimize these problems [184]. Finally, the manufactured green samples are sintered.

It is important to note that forming and shaping of any ceramic products require a proper selection of the raw materials in terms of particle sizes and size distribution. Namely, tough and strong bioceramics consist of pure, fine and homogeneous microstructures. To attain this, pure powders with small average size and high surface area must be used as the starting sources. However, for maximum packing and least shrinkage after firing, mixing of ~70% coarse and ~30% fine powders have been suggested [184]. Mixing is usually carried out in a ball mill for uniformity of properties and reaction during subsequent firing. Mechanical die forming or sometimes extrusion through a die orifice can be used to produce a fixed cross-section.

Finally, to produce the accurate shaping, necessary for the fine design of bioceramics, machine finishing might be essential [132, 181, 256, 257]. Unfortunately, cutting tools developed for metals are usually useless for bioceramics due to their fragility; therefore, grinding and polishing appear to be the convenient finishing techniques [132, 181]. In addition, the surface of bioceramics might be modified by various supplementary treatments [258].

5.3.4 Sintering and Firing

A sintering (or firing) procedure appears to be of a great importance to manufacture bulk bioceramics with the required mechanical properties. Usually, this stage is carried out according to controlled temperature programs of electric furnaces in adjusted ambience of air with necessary additional gasses; however, always at temperatures below the melting points of the materials. The firing step can include temporary holds at intermediate temperatures to burn out organic binders [181–184]. The heating rate, sintering temperature and holding time depend on the starting materials. For example, in the case of HAp, these values are in the ranges of 0.5–3 °C/min, 1,000–1,250 °C and 2–5 h, respectively [259]. In the majority cases, sintering allows a structure to retain its shape. However, this process might be accompanied by a considerable degree of shrinkage [260–262], which must be accommodated in the fabrication process. For instance, in the case of FA sintering, a linear shrinkage was found to occur at ~715 °C and the material reached its final density at ~890 °C. Above this value, grain growth became important and induced an intra-granular porosity, which was responsible for density decrease. At ~1,180 °C, a liquid phase was formed due to formation of a binary eutectic between FA and fluorite contained in the powder as impurity. This liquid phase further promoted the coarsening process and induced formation of large pores at high temperatures [263].

In general, sintering occurs only when the driving force is sufficiently high, while the latter relates to the decrease in surface and interfacial energies of the system by matter (molecules, atoms or ions) transport, which can proceed by solid, liquid or gaseous phase diffusion. Namely, when solids are heated to high temperatures, their constituents are driven to move to fill up pores and open channels between the grains

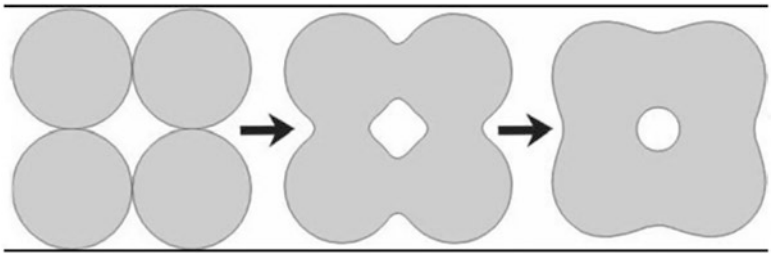

Fig. 5.4 A schematic diagram representing the changes occurring with spherical particles under sintering. Shrinkage is noticeable

of powders, as well as to compensate for the surface energy differences among their convex and concave surfaces (matter moves from convex to concave). At the initial stages, bottlenecks are formed and grow among the particles (Fig. 5.4). Existing vacancies tend to flow away from the surfaces of sharply curved necks; this is an equivalent of a material flow towards the necks, which grow as the voids shrink. Small contact areas among the particles expand and, at the same time, a density of the compact increases and the total void volume decreases. As the pores and open channels are closed during a heat treatment, the particles become tightly bonded together and density, strength and fatigue resistance of the sintered object improve greatly. Grain-boundary diffusion was identified as the dominant mechanism for densification [264]. Furthermore, strong chemical bonds are formed among the particles and loosely compacted green bodies are hardened to denser materials [181–184]. Further knowledge on the ceramic sintering process might be found elsewhere [265].

In the case of $CaPO_4$, the earliest paper on their sintering was published in 1971 [266]. Since then, numerous papers on this subject were published and several specific processes were found to occur during $CaPO_4$ sintering. Firstly, moisture, carbonates and all other volatile chemicals remaining from the synthesis stage, such as ammonia, nitrates and any organic compounds, are removed as gaseous products. Secondly, unless powders are sintered, the removal of these gases facilitates production of denser ceramics with subsequent shrinkage of the samples (Fig. 5.5). Thirdly, all chemical changes are accompanied by a concurrent increase in crystal size and a decrease in the specific surface area. Fourthly, a chemical decomposition of all acidic orthophosphates and their transformation into other phosphates (e.g., $2HPO_4^{2-} \rightarrow P_2O_7^{4-} + H_2O\uparrow$) takes place. Besides, sintering causes toughening [66], densification [67, 267], partial dehydroxylation (in the case of HAp) [67], grain growth [264, 268], as well as it increases the mechanical strength [269–271]. The latter events are due to presence of air and other gases filling gaps among the particles of un-sintered powders. At sintering, the gases move towards the outside of powders and green bodies shrink owing to decrease of distances among the particles. For example, sintering of a biologically formed apatites was investigated [272, 273] and the obtained products were characterized [274, 275]. In all cases, the numerical value of Ca/P ratio in sintered apatites of biological origin was higher than that of the stoichiometric HAp. One should mention that in the vast majority

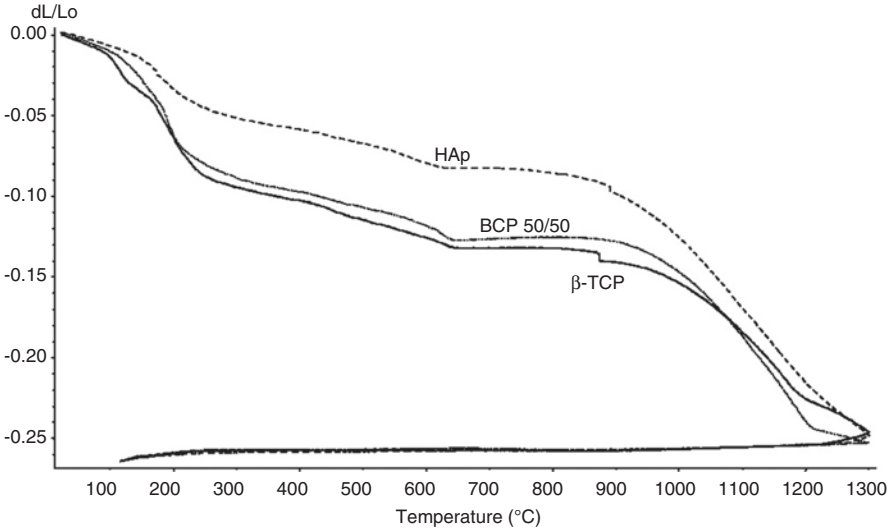

Fig. 5.5 Linear shrinkage of the compacted ACP powders that were converted into β-TCP, BCP (50% HAp + 50% β-TCP) and HAp upon heating. According to the authors: "At 1300 °C, the shrinkage reached a maximum of approximately ~ 25, ~ 30 and ~ 35% for the compacted ACP powders that converted into HAp, BCP 50/50 and β-TCP, respectively" [261]

cases, $CaPO_4$ with Ca/P ratio <1.5 (Table 5.1) are not sintered, since these compounds are thermally unstable, while sintering of non-stoichiometric $CaPO_4$ (CDHA and ACP) always leads to their transformation into various types of biphasic, triphasic and multiphase formulations [79].

An extensive study on the effects of sintering temperature and time on the properties of HAp bioceramics revealed a correlation between these parameters and density, porosity, grain size, chemical composition and strength of the scaffolds [276]. Namely, sintering below ~1,000 °C was found to result in initial particle coalescence, with little or no densification and a significant loss of the surface area and porosity. The degree of densification appeared to depend on the sintering temperature whereas the degree of ionic diffusion was governed by the period of sintering [276]. To enhance sinterability of $CaPO_4$, a variety of sintering additives might be added [277–280].

Solid-state pressureless sintering is the simplest procedure. For example, HAp bioceramics can be pressurelessly sintered up to the theoretical density at 1,000–1,200 °C. Processing at even higher temperatures usually lead to exaggerated grain growth and decomposition because HAp becomes unstable at temperatures exceeding ~1,300 °C [6, 113–117, 281–284]. The decomposition temperature of HAp bioceramics is a function of the partial pressure of water vapor. Moreover, processing under vacuum leads to an earlier decomposition of HAp, while processing under high partial pressure of water prevents from the decomposition. On the other hand, a presence of water in the sintering atmosphere was reported to inhibit densification of HAp and accelerated grain growth [285]. Unexpectedly, an application of a

magnetic field during sintering was found to influence the growth of HAp grains [268]. A definite correlation between hardness, density and a grain size in sintered HAp bioceramics was found: despite exhibiting high bulk density, hardness started to decrease at a certain critical grain size limit [286–288].

Since grain growth occurs mainly during the final stage of sintering, to avoid this, a new method called "two-step sintering" (TSS) was proposed [289]. The method consists of suppressing grain boundary migration responsible for grain growth, while keeping grain boundary diffusion that promotes densification. The TSS approach was successfully applied to $CaPO_4$ bioceramics [78, 86, 290–294]. For example, HAp compacts prepared from nanodimensional powders were two-step sintered. The average grain size of near full dense (>98%) HAp bioceramics made via conventional sintering was found to be ~1.7 μm, while that for TSS HAp bioceramics was ~190 nm (i.e., ~9 times less) with simultaneous increasing the fracture toughness of samples from 0.98 ± 0.12 to 1.92 ± 0.20 MPa $m^{1/2}$. In addition, due to the lower second step sintering temperature, no HAp phase decomposition was detected in TSS method [290].

Hot pressing [288, 295–301], hot isostatic pressing [87, 188, 193, 195] or hot pressing with post-sintering [302, 303] processes make it possible to decrease a temperature of the densification process, diminish the grain size, as well as achieve higher densities. This leads to finer microstructures, higher thermal stability and subsequently better mechanical properties of $CaPO_4$ bioceramics. Both microwave [304–313] and spark plasma [69, 104, 314–323] sintering techniques are alternative methods to the conventional sintering, hot pressing and hot isostatic pressing. Both alternative methods were found to be time and energy efficient densification techniques. Further developments are still possible. For example, a hydrothermal hot pressing method has been developed to fabricate OCP [105], CDHA [324], HAp/β-TCP [298] and HAp [299–302, 325] bioceramics with neither thermal dehydration nor thermal decomposition. Further details on the sintering and firing processes of $CaPO_4$ bioceramics are available in literature [115, 326, 327].

To conclude this section, one should mention that the sintering stage is not always necessary. For example, $CaPO_4$-based bulk bioceramics with the reasonable mechanical properties might be prepared by means of self-setting (self-hardening) formulations (see Sect. 5.5.1 below). Furthermore, the reader's attention is paid on an excellent review on various ceramic manufacturing techniques [328], in which various ceramic processing techniques are well described.

5.4 The Major Properties

5.4.1 Mechanical Properties

The modern generation of biomedical materials should stimulate the body's own self-repairing abilities [329]. Therefore, during healing, a mature bone should replace the modern grafts and this process must occur without transient loss of the

mechanical support. Unluckily for material scientists, a human body provides one of the most inhospitable environments for the implanted biomaterials. It is warm, wet and both chemically and biologically active. For example, a diversity of body fluids in various tissues might have a solution pH varying from 1 to 9. In addition, a body is capable of generating quite massive force concentrations and the variance in such characteristics among individuals might be enormous. Typically, bones are subjected to ~4 MPa loads, whereas tendons and ligaments experience peak stresses in the range of 40–80 MPa. The hip joints are subjected to an average load up to three times body weight (3,000 N) and peak loads experienced during jumping can be as high as ten times body weight. These stresses are repetitive and fluctuating depending on the nature of the activities, which can include standing, sitting, jogging, stretching and climbing. Therefore, all types of implants must sustain attacks of a great variety of aggressive conditions [330]. Regrettably, there is presently no artificial material fulfilling all these requirements.

Now it is important to mention, that the mechanical behavior of any ceramics is rather specific. Namely, ceramics is brittle, which is attributed to high strength ionic bonds. Thus, it is not possible for plastic deformation to happen prior to failure, as a slip cannot occur. Therefore, ceramics fail in a dramatic manner. Namely, if a crack is initiated, its progress will not be hindered by the deformation of material ahead of the crack, as would be the case in a ductile material (e.g., a metal). In ceramics, the crack will continue to propagate, rapidly resulting in a catastrophic breakdown. In addition, the mechanical data typically have a considerable amount of scatter [182]. Alas, all of these are applicable to $CaPO_4$ bioceramics.

For dense bioceramics, the strength is a function of the grain sizes. Namely, finer grain size bioceramics have smaller flaws at the grain boundaries and thus are stronger than one with larger grain sizes. Thus, in general, the strength for ceramics is proportional to the inverse square root of the grain sizes [331]. In addition, the mechanical properties decrease significantly with increasing content of an amorphous phase, microporosity and grain sizes, while a high crystallinity, a low porosity and small grain sizes tend to give a higher stiffness, a higher compressive and tensile strength and a greater fracture toughness. Furthermore, ceramics strength appears to be very sensitive to a slow crack growth [332]. Accordingly, from the mechanical point of view, $CaPO_4$ bioceramics appear to be brittle polycrystalline materials for which the mechanical properties are governed by crystallinity, grain size, grain boundaries, porosity and composition [333]. Thus, it possesses poor mechanical properties (for instance, a low impact and fracture resistances) that do not allow $CaPO_4$ bioceramics to be used in load-bearing areas, such as artificial teeth or bones [50–53]. For example, fracture toughness (this is a property, which describes the ability of a material containing a crack to resist fracture and is one of the most important properties of any material for virtually all design applications) of HAp bioceramics does not exceed the value of ~1.2 $MPa \cdot m^{1/2}$ [334] (human bone: 2–12 $MPa \cdot m^{1/2}$). It decreases exponentially with the porosity increasing [335]. Generally, fracture toughness increases with grain size decreasing. However, in some materials, especially non-cubic ceramics, fracture toughness reaches the maximum and rapidly drops with decreasing grain size. For example, a fracture toughness of

pure hot pressed HAp with grain sizes between 0.2 and 1.2 μm was investigated. The authors found two distinct trends, where fracture toughness decreased with increasing grain size above ~0.4 μm and subsequently decreased with decreasing grain size. The maximum fracture toughness measured was 1.20 ± 0.05 MPa·m$^{1/2}$ at ~0.4 μm [295]. Fracture energy of HAp bioceramics is in the range of 2.3–20 J/m^2, while the Weibull modulus (it is a measure of the spread or scatter in fracture strength) is low (~5–12) in wet environments, which means that HAp behaves as a typical brittle ceramics and indicates to a low reliability of HAp implants [336]. Porosity has a great influence on the Weibull modulus [337, 338]. In addition, that the reliability of HAp bioceramics was found to depend on deformation mode (bending or compression), along with pore size and pore size distribution: a reliability was higher for smaller average pore sizes in bending but lower for smaller pore sizes in compression [339]. Interestingly that three peaks of internal friction were found at temperatures about −40, 80 and 130 °C for HAp but no internal friction peaks were obtained for FA in the measured temperature range; this effect was attributed to the differences of F^- and OH^- positions in FA and HAp, respectively [340]. The differences in internal friction values were also found between HAp and TCP [341].

Bending, compressive and tensile strengths of dense HAp bioceramics are in the ranges of 38–250 MPa, 120–900 MPa and 38–300 MPa, respectively. Similar values for porous HAp bioceramics are substantially lower: 2–11 MPa, 2–100 MPa and ~3 MPa, respectively [336]. These wide variations in the properties are due to both structural variations (e.g., an influence of remaining microporosity, grain sizes, presence of impurities, etc.) and manufacturing processes, as well as they are caused by a statistical nature of the strength distribution. Strength was found to increase with Ca/P ratio increasing, reaching the maximum value around Ca/P ~1.67 (stoichiometric HAp) and decreases suddenly when Ca/P >1.67 [336]. Furthermore, strength decreases almost exponentially with porosity increasing [342, 343]. However, by changing the pore geometry, it is possible to influence the strength of porous bioceramics. It is also worth mentioning that porous $CaPO_4$ bioceramics is considerably less fatigue resistant than dense ones (in materials science, fatigue is the progressive and localized structural damage that occurs when a material is subjected to cyclic loading). Both grain sizes and porosity are reported to influence the fracture path, which itself has a little effect on the fracture toughness of $CaPO_4$ bioceramics [333, 344]. However, no obvious decrease in mechanical properties was found after $CaPO_4$ bioceramics had been aged in the various solutions during the different periods of time [345].

Young's (or elastic) modulus of dense HAp bioceramics is in the range of 35–120 GPa [346, 347], which is more or less similar to those of the most resistant components of the natural calcified tissues (dental enamel: ~74 GPa, dentine: ~21 GPa, compact bone: ~18–22 GPa). This value depends on porosity [348]. Nevertheless, dense bulk compacts of HAp have mechanical resistances of the order of 100 MPa versus ~300 MPa of human bones, diminishing drastically their resistances in the case of porous bulk compacts [349]. Young's modulus measured in bending is between 44 and 88 GPa. To investigate the subject in more details, various types of modeling and calculations are increasingly used [350–354]. For example, the elastic properties of HAp appeared to be significantly affected by the presence of

vacancies, which softened HAp via reducing its elastic modules [354]. In addition, a considerable anisotropy in the stress-strain behavior of the perfect HAp crystals was found by ab initio calculations [351]. The crystals appeared to be brittle for tension along the *z*-axis with the maximum stress of ~9.6 GPa at 10% strain. Furthermore, the structural analysis of the HAp crystal under various stages of tensile strain revealed that the deformation behavior manifested itself mainly in the rotation of PO_4 tetrahedrons with concomitant movements of both the columnar and axial Ca ions [351]. Data for single crystals are also available [355]. Vickers hardness (that is a measure of the resistance to permanent indentation) of dense HAp bioceramics is within 3–7 GPa, while the Poisson's ratio (that is the ratio of the contraction or transverse strain to the extension or axial strain) for HAp is about 0.27, which is close to that of bones (~0.3). At temperatures within 1,000–1,100 °C, dense HAp bioceramics was found to exhibit superplasticity with a deformation mechanism based on grain boundary sliding [320, 356, 357]. Furthermore, both wear resistance and friction coefficient of dense HAp bioceramics are comparable to those of dental enamel [336].

Due to a high brittleness (associated to a low crack resistance), the biomedical applications of $CaPO_4$ bioceramics are focused on production of non-load-bearing implants, such as pieces for middle ear surgery, filling of bone defects in oral or orthopedic surgery, as well as coating of dental implants and metallic prosthesis (see below) [61, 358, 359]. Therefore, ways are continuously sought to improve the reliability of $CaPO_4$ bioceramics. Namely, the mechanical properties of sintered bioceramics might be improved by changing the morphology of the initial $CaPO_4$ [360]. In addition, diverse reinforcements (ceramics, metals or polymers) have been applied to manufacture various biocomposites and hybrid biomaterials [361], but that is another story. However, successful hybrid formulations consisted of $CaPO_4$ only [362–369] are within the scope of this review. Namely, bulk HAp bioceramics might be reinforced by HAp whiskers [363–367]. Furthermore, various biphasic apatite/TCP formulations were tested [362, 368, 369] and, for example, a superior superplasticity of HAp/β-TCP biocomposites to HAp bioceramics was detected [368].

Another approach to improve the mechanical properties of $CaPO_4$ bioceramics is to cover the items by polymeric coatings [370–372] or infiltrate porous structures by polymers [373–375]; however, this is still other story. Further details on the mechanical properties of $CaPO_4$ bioceramics are available elsewhere [335, 336, 376], where the interested readers are referred to.

5.4.2 Electric/Dielectric and Piezoelectric Properties

Occasionally, an interest to both electric/dielectric [304, 377–390] and piezoelectric [391, 392] properties of $CaPO_4$ bioceramics is expressed. For example, a surface ionic conductivity of both porous and dense HAp bioceramics was examined for humidity sensor applications, since the room temperature conductivity was influenced by relative humidity [378]. Namely, the ionic conductivity of HAp has been a subject of research for its possible use as a gas sensor for alcohol [379], carbon

dioxide [377, 386] or carbon monoxide [382]. Electric measurements were also used as a characterization tool to study the evolution of microstructure in HAp bioceramics [380]. More to the point, the dielectric properties of HAp were examined to understand its decomposition to β-TCP [379]. In the case of CDHA, the electric properties, in terms of ionic conductivity, were found to increase after compression of the samples at 15 t/cm^2, which was attributed to establishment of some order within the apatitic network [381]. The conductivity mechanism of CDHA appeared to be multiple [384]. Furthermore, there was an attempt to develop CDHA whisker electrets for biomedical utilization [383].

The electric properties of $CaPO_4$ bioceramics appear to influence their biomedical applications. For example, there is an interest in polarization of HAp bioceramics to generate a surface charge by the application of electric fields at elevated temperatures [393, 394]. The presence of surface charges on HAp was shown to have a significant effect on both in vitro and in vivo crystallization of biological apatite [395–401]. Furthermore, a growth of both biomimetic $CaPO_4$ and bones was found to be accelerated on negatively charged surfaces and decelerated at positively charged surfaces [399–412]. Similar effect was found for adsorption of bovine serum albumin [413]. In addition, the electric polarization of $CaPO_4$ was found to accelerate a cytoskeleton reorganization of osteoblast-like cells [414–417], extend bioactivity [418], enhance bone ingrowth through the pores of porous implants [419] and influence the cell activity [420, 421]. The positive effect of electric polarization was found for carbonated apatite as well [422]. There is an interesting study on the interaction of a blood coagulation factor on electrically polarized HAp surfaces [423]. Further details on the electric properties of $CaPO_4$-based bioceramics are available in literature [304, 387–390, 424–428].

5.4.3 Possible Transparency

Single crystals of all types of $CaPO_4$ are optically transparent for the visible light. As bioceramics of $CaPO_4$ have a polycrystalline nature with a random orientation of big amounts of small crystals, it is opaque and of white color, unless colored dopants have been added. However, in some cases, a transparency is convenient to provide some essential advantages (e.g., to enable direct viewing of living cells, their attachment, spreading, proliferation, and osteogenic differentiation cascade in a transmitted light). Thus, transparent $CaPO_4$ bioceramics (Fig. 5.6) [429] have been prepared and investigated [69, 87, 188, 190, 317–323, 429–438]. They can exhibit an optical transmittance of ~66% at a wavelength of 645 nm [435]. The preparation techniques include a hot isostatic pressing [87, 188, 190, 437], an ambient-pressure sintering [430], a gel casting coupled with a low-temperature sintering [431, 434], a pulse electric current sintering [432], as well as a spark plasma sintering [69, 317–323]. Fully dense, transparent $CaPO_4$ bioceramics are obtained at temperatures above ~800 °C. Depending on the preparation technique, the transparent bioceramics has a uniform grain sizes ranging from ~67 nm [87] to ~250 μm [431] and

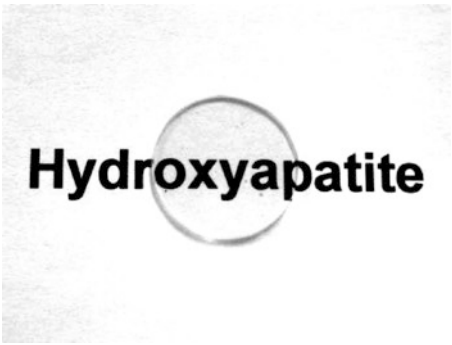

Fig. 5.6 Transparent HAp bioceramics prepared by spark plasma sintering at 900 °C from nano-sized HAp single crystals [429]

always is pore-free. Furthermore, a translucent $CaPO_4$ bioceramics is also known [87, 266, 439–441]. Concerning possible biomedical applications, the optically transparent for the visible light $CaPO_4$ bioceramics can be useful for direct viewing of other objects, such as cells, in some specific experiments [433]. In addition, the transparent for a laser light $CaPO_4$ bioceramics may appear to be convenient for minimal invasive surgery by allowing passing the laser beam through it to treat the injured tissues located underneath. However, due to a lack of both porosity and the big necessity to have see-through implants inside the body, the transparent and translucent forms of $CaPO_4$ bioceramics will hardly be extensively used in medicine except the aforementioned cases and possible eye implants.

5.4.4 Porosity

Porosity is defined as a percentage of voids in solids and this morphological property is independent of the material. The surface area of porous bodies is much higher, which guarantees a good mechanical fixation in addition to providing sites on the surface that allow chemical bonding between the bioceramics and bones [442]. Furthermore, a porous material may have both closed (isolated) pores and open (interconnected) pores. The latter look like tunnels and are accessible by gases, liquids and particulate suspensions [443]. The open-cell nature of porous materials (also known as reticulated materials) is a unique characteristic essential in many applications. In addition, pore dimensions are also important. Namely, the dimensions of open pores are directly related to bone formation, since such pores grant both the surface and space for cell adhesion and bone ingrowth [444–446]. On the other hand, pore interconnection provides the ways for cell distribution and migration, as well as it allows an efficient in vivo blood vessel formation suitable for sustaining bone tissue neo-formation and possibly remodeling [123, 419, 447–453]. Namely, porous $CaPO_4$ bioceramics is colonized easily by cells and bone tissues [447, 452, 454–461]. Therefore, interconnecting macroporosity (pore size >100 μm) [84, 442, 447, 462, 463] is intentionally introduced in solid bioceramics (Fig. 5.7). Calcining of natural

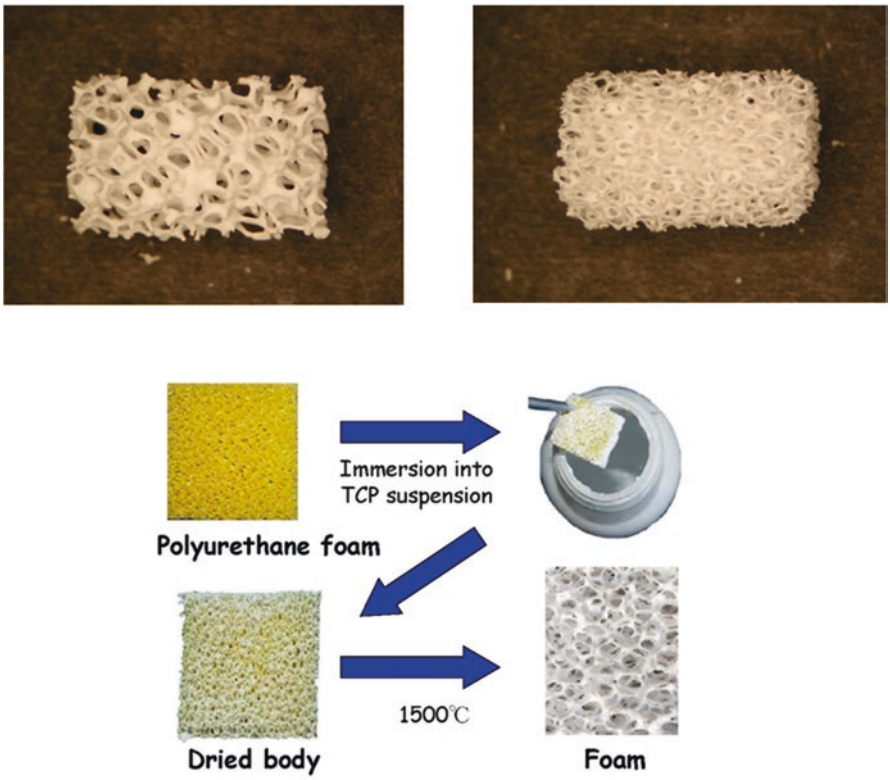

Fig. 5.7 Photographs of a commercially available porous $CaPO_4$ bioceramics with different porosity (*top*) and a method of their production (*bottom*). For photos, the *horizontal* field width is 20 mm

bones appears to be the simplest way to prepare porous $CaPO_4$ bioceramics [7–16]. In addition, macroporosity might be formed artificially due to a release of various easily removable compounds and, for that reason, incorporation of pore-creating additives (porogens) is the most popular technique to create macroporosity. The porogens are crystals, particles or fibers of either volatile (they evolve gases at elevated temperatures) or soluble substances. The popular examples comprise paraffin [464–466], naphthalene [333, 467–469], sucrose [470, 471], $NaHCO_3$ [472–474], NaCl [475, 476], polymethylmethacrylate [74, 477–479], hydrogen peroxide [480–485], cellulose derivatives [64]. Several other compounds [326, 343, 486–497] might be used as porogens either. The ideal porogen should be nontoxic and be removed at ambient temperature, thereby allowing the bioceramic/porogen mixture to be injected directly into a defect site and allowing the scaffold to fit the defect [498]. Sintering particles, preferably spheres of equal size, is a similar way to generate porous 3D bioceramics of $CaPO_4$. However, pores resulting from this method are often irregular in size and shape and not fully interconnected with one another. Schematic drawings of various types of the ceramic porosity are shown in Fig. 5.8 [499].

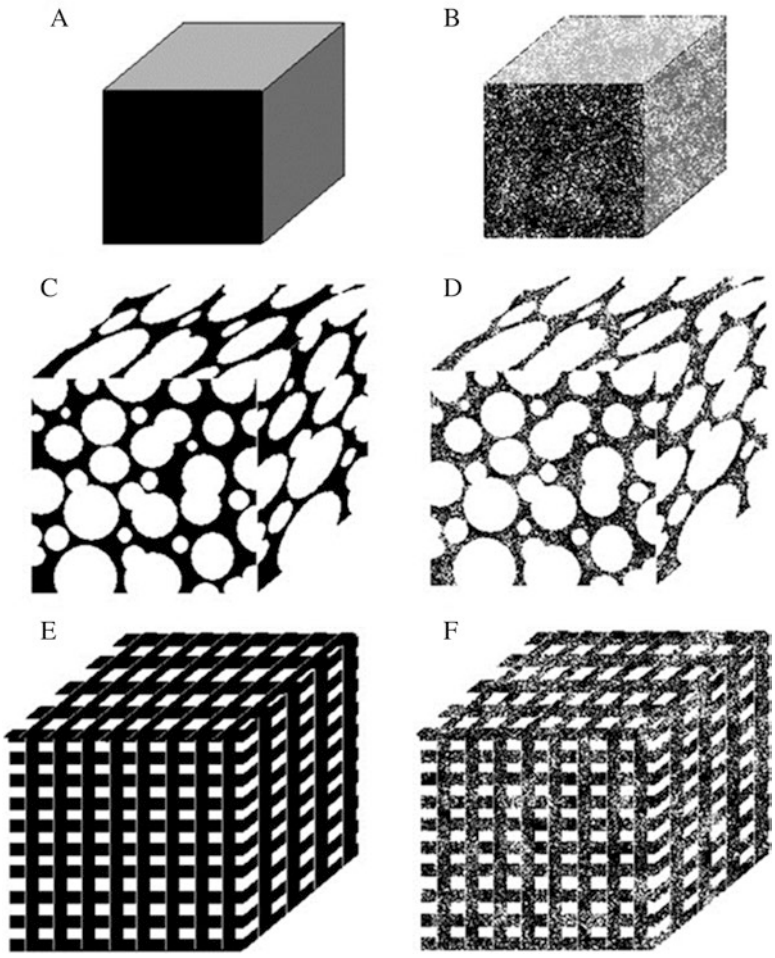

Fig. 5.8 Schematic drawings of various types of the ceramic porosity: (**a**) non-porous, (**b**) microporous, (**c**) macroporous (spherical), (**d**) macroporous (spherical) + micropores, (**e**) macroporous (3D-printing), (**f**) macroporous (3D-printing) + micropores [499]

Many other techniques, such as replication of polymer foams by impregnation [224–226, 229, 500–504] (Fig. 5.7), various types of casting [206, 207, 213, 215, 485, 505–513], suspension foaming [101], surfactant washing [514], microemulsions [515, 516], ice templating [517–520], as well as many other approaches [68, 71, 74, 75, 142, 521–556] have been applied to fabricate porous $CaPO_4$ bioceramics. Some of them have been summarized in Table 5.2 [498]. In addition, both natural $CaCO_3$ porous materials, such as coral skeletons [557, 558] or shells [558, 559], and artificially prepared ones [560] can be converted into porous $CaPO_4$ under the hydrothermal conditions (250 °C, 24–48 h) with the microstructure undamaged. Porous HAp bioceramics can also be obtained by hydrothermal hot pressing. This technique allows solidification of the HAp

Table 5.2 The procedures used to manufacture porous $CaPO_4$ scaffolds for tissue engineering [498]

Year	Location	Process	Apatite from:	Sintering	Compressive strength	Pore size	Porosity	Method of porosity control
2006	Deville et al. Berkeley, CA	HAp + ammonium methacrylate in polytetrafluoroethylene mold, freeze dried and sintered	HAp #30	Yes: 1,300 °C	16 MPa 65 MPa 145 MPa	Open unidirectional 50–150 μm	>60% 56% 47%	Porosity control: slurry conc. Structure controlled by physics of ice front formation
2006	Saiz et al. Berkeley, CA	Polymer foams coated, compressed after infiltration, then calcined	HAp powder	Yes: 700–1,300 °C	–	100–200 μm	–	Porosity control: extent of compression, HAp loading
2006	Murugan et al. Singapore + USA	Bovine bone cleaned, calcined	Bovine bone	Yes: 500 °C	–	Retention of nano-sized pores	–	Porosity control: native porosity of bovine bone
2006	Xu et al. Gaithersburg, MD	Directly injectable $CaPO_4$ cement, self hardens, mannitol as porogen	Nanocrystalline HAp	No	2.2–4.2 MPa (flexural)	0–50% macroporous	65–82%	Porosity control: mannitol mass fraction in mixture
2004	Landi et al. Italy + Indonesia	Sponge impregnation, isotactic pressing, sintering of HAp in simulated body fluid	$CaO + H_3PO_4$	Yes: 1,250 °C for 1 h	23 ± 3.8 MPa	Closed 6% open 60%	66%	Porosity control: possibly by controlling HAp particle size. Not suggested by authors
2003	Charriere et al. EPFL, Switzerland	Thermoplastic negative porosity by Ink jet printing, slip casting process for HAp	DCPA + calcite	No: 90 °C for 1 day	12.5 ± 4.6 MPa	–	44%	Porosity control: negative printing

(continued)

Table 5.2 (continued)

Year	Location	Process	Apatite from:	Sintering	Compressive strength	Pore size	Porosity	Method of porosity control
2003	Almirall et al. Barcelona, Spain	α-TCP foamed with hydrogen peroxide at different conc., liq. ratios, poured in polytetrafluoroethylene molds	α-TCP + (10% and 20% H_2O_2)	No: 60 °C for 2 h	1.41 ± 0.27 MPa 2.69 ± 0.91 MPa	35.7% macro 29.7% micro 26.8% macro 33.8% micro	65.5% 60.7%	Porosity control: different concentration, α-TCP particle sizes
2003	Ramay et al. Seattle, WA	Slurries of HAp prepared: gel-casting + polymer sponge technique, sintered	HAp powder	Yes: 600 °C for 1 h 1,350 °C for 2 h	0.5–5 MPa	200–400 μm	70–77%	Porosity control: replicate of polymer sponge template
2003	Miao et al. Singapore	TTCP to $CaPO_4$ cement. Slurry cast on polymer foam, sintered	TTCP	Yes: 1,200 °C for 2 h	–	1 mm macro 5 μm micro	~70%	Porosity control: recoating time, polyurethane foam
2003	Uemura et al. China + Japan	Slurry of HAp with polyoxyethylene lauryl ether (cross-linked) and sintered	HAp powders	Yes: 1,200 °C for 3 h	2.25 MPa (0 week) 4.92 MPa (12 weeks) 11.2 MPa (24 weeks)	500 μm 200 μm interconnects	~77%	Porosity control: polymer interconnects cross-linking
2003	Ma et al. Singapore + USA	Electrophoretic deposition of HAp, sintering	HAp powders	Yes: 1,200 °C for 2 h	860 MPa	0.5 μm 130 μm	~20%	Porosity control: electrophoresis field
2002	Barralet et al. Birmingham, London, UK	$CaPO_4$ cement + sodium phosphate ice, evaporated	$CaCO_3$ + DCPD	1st step: 1,400 °C for 1 day	0.6 ± 0.27 MPa	2 μm	62 ± 9%	Porosity control: porogen shape

powder at 100–300 °C (30 MPa, 2 h) [325]. In another approach, bi-continuous water-filled microemulsions have been used as pre-organized systems for the fabrication of needle-like frameworks of crystalline HAp (2 °C, 3 weeks) [515, 516]. Besides, porous $CaPO_4$ might be prepared by a combination of gel casting and foam burn out methods [248, 250], as well as by hardening of the self-setting formulations [465, 466, 473, 474, 476, 486, 487, 545]. Lithography was used to print a polymeric material, followed by packing with HAp and sintering [525]. Hot pressing was applied as well [296, 297]. More to the point, a HAp suspension can be cast into a porous $CaCO_3$ skeleton, which is then dissolved, leaving a porous network [521]. 3D periodic macroporous frame of HAp has been fabricated via a template-assisted colloidal processing technique [526, 527]. In addition, porous HAp bioceramics might be prepared by using different starting HAp powders and sintering at various temperatures by a pressureless sintering [523]. Porous bioceramics with an improved strength might be fabricated from $CaPO_4$ fibers or whiskers. In general, fibrous porous materials are known to exhibit an improved strength due to fiber interlocking, crack deflection and/or pullout [561]. Namely, porous bioceramics with well-controlled open pores was processed by sintering of fibrous HAp particles [522]. In another approach, porosity was achieved by firing apatite-fiber compacts mixed with carbon beads and agar. By varying the compaction pressure, firing temperature and carbon/HAp ratio, the total porosity was controlled in the ranges from ~40% to ~85% [64]. Finally, a superporous (~85% porosity) HAp bioceramics was developed as well [541–543]. Additional information on the processing routes to produce porous ceramics might be found in literature [562].

Bioceramic microporosity (pore size <10 μm), which is defined by its capacity to be impregnated by biological fluids [563], results from the sintering process, while the pore dimensions mainly depend on the material composition, thermal cycle and sintering time. The microporosity provides both a greater surface area for protein adsorption and increased ionic solubility. For example, embedded osteocytes distributed throughout microporous rods might form a mechanosensory network, which would not be possible in scaffolds without microporosity [564, 565]. $CaPO_4$ bioceramics with nanodimensional (<100 nm) pores might be fabricated as well [183, 566–570]. It is important to stress, that differences in porogens usually influence the bioceramics' macroporosity, while differences in sintering temperatures and conditions affect the percentage of microporosity. Usually, the higher the sintering temperature, the lower both the microporosity content and the specific surface area of bioceramics. Namely, HAp bioceramics sintered at ~1,200 °C shows significantly less microporosity and a dramatic change in crystal sizes, if compared with that sintered at ~1,050 °C (Fig. 5.9) [571]. Furthermore, the average shape of pores was found to transform from strongly oblate to round at higher sintering temperatures [572]. The total porosity (macroporosity + microporosity) of $CaPO_4$ bioceramics was reported to be ~70% [573] or even ~85% [541–543] of the entire volume. In the case of coralline HAp or bovine-derived apatites, the porosity of the original biologic material (coral or bovine bone) is usually preserved during processing [574]. To finalize the production topic, creation of the desired porosity in $CaPO_4$ bioceramics is a rather complicated engineering task and the interested readers are referred to the additional publications on the subject [343, 446, 544, 575–583].

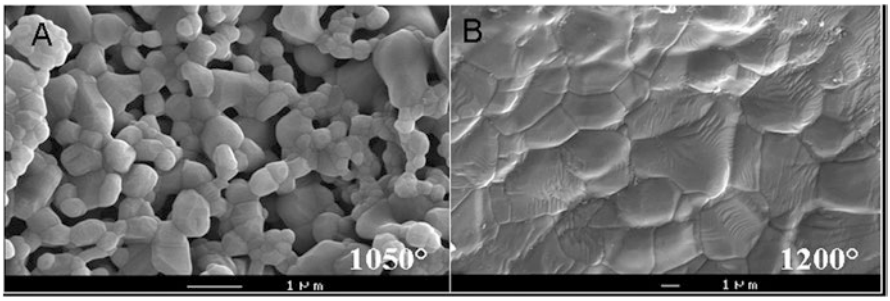

Fig. 5.9 SEM pictures of HAp bioceramics sintered at (**a**) 1,050 °C and (**b**) 1,200 °C. Note the presence of microporosity in (**a**) and not in (**b**) [571]

Regarding the biomedical importance of porosity, studies revealed that increasing of both the specific surface area and pore volume of bioceramics might greatly accelerate the in vivo process of apatite deposition and, therefore, enhance the bone-forming bioactivity. More importantly, a precise control over the porosity, pore dimensions and internal pore architecture of bioceramics on different length scales is essential for understanding of the structure-bioactivity relationship and the rational design of better bone-forming biomaterials [581, 584, 585]. Namely, in antibiotic charging experiments, a $CaPO_4$ bioceramics with nanodimensional (<100 nm) pores showed a much higher charging capacity (1621 μg/g) than that of commercially available $CaPO_4$ (100 μg/g), which did not contain nanodimensional porosity [577]. In other experiments, porous blocks of HAp were found to be viable carriers with sustained release profiles for drugs [586] and antibiotics over 12 days [587] and 12 weeks [588], respectively. Unfortunately, porosity significantly decreases the strength of implants [336, 344, 376]. Thus, porous $CaPO_4$ implants cannot be loaded and are used to fill only small bone defects. However, their strength increases gradually when bones ingrow into the porous network of $CaPO_4$ implants [119, 589–592]. For example, bending strengths of 40–60 MPa for porous HAp implants filled with 50–60% of cortical bone were reported [589], while in another study an ingrown bone increased strength of porous HAp bioceramics by a factor of 3 to 4 [591].

Unfortunately, the biomedical effects of bioceramics' porosity are not straightforward. For example, the in vivo response of $CaPO_4$ of different porosity was investigated and a hardly any effect of macropore dimensions (~150, ~260, ~510 and ~1,220 μm) was observed [593]. In another study, a greater differentiation of mesenchymal stem cells was observed when cultured on ~200 μm pore size HAp scaffolds when compared to those on ~500 μm pore size HAp [594]. The latter finding was attributed to the fact that a higher pore volume in ~500 μm macropore scaffolds might contribute to a lack of cell confluency leading to the cells proliferating before beginning differentiation. Besides, the authors hypothesized that bioceramics having a less than the optimal pore dimensions induced quiescence in differentiated osteoblasts due to reduced cell confluency [594]. In still another study, the use of BCP (HAp/TCP = 65/35 wt. %) scaffolds with cubic pores of ~500 μm resulted

in the highest bone formation compared with the scaffold with lower (~100 μm) or higher (~1,000 μm) pore sizes [595]. Furthermore, $CaPO_4$ bioceramics with greater strut porosity appeared to be more osteoinductive [596]. Already in 1979, Holmes suggested that the optimal pore range was 200–400 μm with the average human osteon size of ~223 μm [597]. In 1997, Tsurga and coworkers implied that the optimal pore size of bioceramics that supported ectopic bone formation was 300–400 μm [598]. Thus, there is no need to create $CaPO_4$ bioceramics with very big pores; however, the pores must be interconnected [448, 462, 463, 599]. Interconnectivity governs a depth of cells or tissue penetration into the porous bioceramics, as well as it allows development of blood vessels required for new bone nourishing and wastes removal [563, 600]. Nevertheless, the total porosity of implanted bioceramics appears to be important. For example, 60% porous β-TCP granules achieved a higher bone fusion rate than 75% porous β-TCP granules in lumbar posterolateral fusion [564].

5.5 Biomedical Applications

Since Levitt et al. described a method of preparing a FA bioceramics and suggested its possible use in medical applications in 1969 [601], $CaPO_4$ bioceramics have been widely tested for clinical applications. Namely, a great number of forms, compositions and trademarks (Table 5.3) currently are either in use or under a consideration in many areas of orthopedics and dentistry, with even more in development. In addition, various formulations containing demineralized bone matrix (commonly abbreviated as DBM) are produced for bone grafting. For example, bulk materials, available in dense and porous forms, are used for alveolar ridge augmentation, immediate tooth replacement and maxillofacial reconstruction [4]. Other examples comprise burr-hole buttons [602, 603], cosmetic (non-functional) eye replacements such as Bio-Eye® [604–612], increment of the hearing ossicles [613–615], spine fusion [616–619] and repair of bone defects [118, 620, 621]. In order to permit growth of new bone into defects, a suitable bioresorbable material should fill these defects. Otherwise, ingrowth of fibrous tissue might prevent bone formation within the defects.

In spite of the aforementioned serious mechanical limitations (see Sect. 5.4.1 "Mechanical Properties"), bioceramics of $CaPO_4$ is available in various physical forms: powders, particles, granules (or granulates), dense blocks, porous scaffolds, self-setting formulations, implant coatings and composite component of different origin (natural, biological or synthetic) often with the specific shapes, such as implants, prostheses or prosthetic devices. In addition, $CaPO_4$ are also applied as non-hardening injectable formulations [622–628] and pastes [628–632]. Generally, they consist of a mixture of $CaPO_4$ powders or granules and a "glue", which can be a highly viscous hydrogel. More to the point, custom-designed shapes like wedges for tibial opening osteotomy, cones for spine and knee and inserts for vertebral cage fusion are also available [573]. Various trademarks of the commercially available

Table 5.3 Registered commercial trademarks (current and past) of $CaPO_4$-based bioceramics and biomaterials

Calcium orthophosphate	Trade name and producer (when available)
CDHA	Calcibon (Biomet, IN, USA)
	Cementek (Teknimed, France)
	nanoXIM (Fluidinova, Portugal)
	OsteoGen (Impladent, NY, USA)
	Without trade name (Himed, NY, USA)
HAp	Actifuse (ApaTech, UK)
	Alveograf (Cooke-Waite Laboratories, USA)
	Apaceram (HOYA Corp., PENTAX New Ceramics Division, Japan)
	Apafill-G (Habana, Cuba)
	ApaPore (ApaTech, UK)
	Bio-Eye (Integrated Orbital Implants, CA, USA)
	BioGraft (IFGL BIO CERAMICS, India)
	Bioroc (Depuy Bioland, France)
	Boneceram (Sumitomo Osaka Cement, Japan)
	Bonefil (Pentax, Japan)
	BoneSource (Stryker Orthopaedics, NJ, USA)
	Bonetite (Pentax, Japan)
	Bongros-HA (Daewoong Pharmaceutical, Korea)
	CAFOS DT (Chemische Fabrik Budenheim, Germany)
	Calcitite (Zimmer Dental, CA, USA)
	CAMCERAM HA (CAM Implants, Netherlands)
	CAPTAL (Plasma Biotal, UK)
	Cerapatite (Ceraver, France)
	Durapatite (unknown producer)
	ENGIpore (JRI Orthopaedics, UK)
	G-Bone (Surgiwear, india)
	HA BIOCER (CHEMA – ELEKTROMET, Poland)
	HA^{nano} Surface (Promimic, Sweden)
	IngeniOs HA (Zimmer Dental, CA, USA)
	nanoXIM (Fluidinova, Portugal)
	Neobone (Covalent Materials, Japan)
	Osbone (Curasan, Germany)
	OSPROLIFE HA (Eurocoating, Italy)
	OssaBase-HA (Lasak, Czech Republic)
	Ostegraf (Ceramed, CO, USA)
	Ostim (Heraeus Kulzer, Germany)
	Periograf (Cooke-Waite Laboratories, USA)
	PermaOS (Mathys, Switzerland)
	PurAtite (PremierBiomaterials, Ireland)

(continued)

Table 5.3 (continued)

Calcium orthophosphate	Trade name and producer (when available)
	REGENOS (Kuraray, Japan)
	Synatite (SBM, France)
	Synthacer (KARL STORZ Recon, Germany)
	Without trade name (CaP Biomaterials, WI, USA)
	Without trade name (Ensail Beijing, China)
	Without trade name (Himed, NY, USA)
	Without trade name (MedicalGroup, France)
	Without trade name (SigmaGraft, CA, USA)
	Without trade name (Taihei Chemical Industrial, Japan)
	Without trade name (Xpand Biotechnology, Netherlands)
Mg-HAp	SINTlife (JRI Orthopaedics, UK)
HAp suspended in water	Skelifil (Osteotec, UK)
HAp embedded or suspended in a gel	NanoBone (Artoss, Germany)
	Nanogel (Teknimed, France)
	RADIESSE (Merz Aesthetics, Germany)
HAp/collagen, CDHA/collagen and/or carbonate apatite/collagen	AUGMATRIX (Wright Medical Technology, TN, USA)
	Bioimplant (Connectbiopharm, Russia)
	Bio-Oss Collagen (Geitslich, Switzerland)
	Boneject (Koken, Japan)
	Collagraft (Zimmer and Collagen Corporation, USA)
	CollapAn (Intermedapatite, Russia)
	COLLAPAT (Symatese, France)
	G-Graft (Surgiwear, india)
	HAPCOL (Polystom, Russia)
	Healos (DePuy Spine, USA)
	LitAr (LitAr, Russia)
	OsteoTape (Impladent, NY, USA)
	RegenOss (JRI Orthopaedics, UK)
HAp/sodium alginate	Bialgin (Biomed, Russia)
HAp/poly-L-Lactic Acid	Biosteon (Biocomposites, UK)
	SuperFIXSORB30 (Takiron, Japan)
HAp/polyethylene	HAPEX (Gyrus, TN, USA)
HAp/$CaSO_4$	BioWrist Bone Void Filler (Skeletal Kinetics, CA, USA)
	CERAMENT (BONESUPPORT, Sweden)
	Hapset (LifeCore, MN, USA)
	PerOssal (aap Implantate, Germany)
Coralline HAp	BoneMedik-S (Meta Biomed, Korea)
	Interpore (Interpore, CA, USA)
	ProOsteon (Interpore, CA, USA)
Algae-derived HAp	FRIOS Algipore (Dentsply Friadent, Germany)

(continued)

Table 5.3 (continued)

Calcium orthophosphate	Trade name and producer (when available)
Bovine bone apatite (unsintered)	Apatos (OsteoBiol, Italy)
	Bio-Oss (Geitslich, Switzerland)
	Bonefill (Bionnovation, SP, Brazil).
	CANCELLO-PURE (Wright Medical Technology, TN, USA)
	CopiOs Cancellous Particulate Xenograft (Zimmer, IN, USA)
	GenOs (OsteoBiol, Italy)
	InterOss (SigmaGraft, CA, USA)
	Laddec (Ost-Developpement, France)
	Lubboc (Ost-Developpement, France)
	MatrixCellect (Curasan, Germany)
	Oxbone (Bioland biomateriaux, France)
	Tutobone (Tutogen Medical, Germany)
	Tutofix (Tutogen Medical, Germany)
	Tutoplast (Tutogen Medical, Germany)
	Without trade name (MedicalGroup, France)
Bovine bone apatite (sintered)	4Bone XBM (MIS Implants, Israel)
	BonAP (unknown producer)
	Cerabone (aap Implantate, Germany and botiss, Germany)
	Endobon (Merck, Germany)
	GenoxInorgânico (Baumer, SP, Brazil)
	Navigraft (Zimmer Dental, USA)
	Osteograf (Ceramed, CO, USA)
	PepGen P-15 (Dentsply Friadent, Germany)
	Pyrost (Osteo AG, Germany)
	Sinbone (Purzer Pharmaceutical, Taiwan)
Hyman bone allograft	ALLOPURE (Wright Medical Technology, TN, USA)
	Allosorb (Curasan, Germany)
	CancellOss (Impladent, NY, USA)
	CurOss (Impladent, NY, USA)
	J Bone Block (Impladent, NY, USA)
	Maxgraft (botiss, Germany)
	NonDemin (Impladent, NY, USA)
	Osnatal (aap Implantate, Germany)
	OsteoDemin (Impladent, NY, USA)
	OsteoWrap (Curasan, Germany)
	PentOS OI (Citagenix, QC, Canada)
	RAPTOS (Citagenix, QC, Canada)
	TenFUSE (Wright Medical Technology, TN, USA)
Equine	BioGen (unknown producer)

(continued)

Table 5.3 (continued)

Calcium orthophosphate	Trade name and producer (when available)
α-TCP	ArrowBone (BrainBase Corporation, Japan)
	BioBase (Biovision, Germany)
	Tetrabone (unknown producer)
	Without trade name (Cam Bioceramics, Netherlands)
	Without trade name (Ensail Beijing, China)
	Without trade name (Himed, NY, USA)
	Without trade name (InnoTERE, Germany)
	Without trade name (PremierBiomaterials, Ireland)
	Without trade name (Taihei Chemical Industrial, Japan)
β-TCP	AdboneTCP (Medbone Medical Devices, Portugal)
	AFFINOS (Kuraray, Japan)
	Allogran-R (Biocomposites, UK)
	Antartik TCP (MedicalBiomat, France)
	Betabase (Biovision, Germany)
	BioGraft (IFGL BIO CERAMICS, India)
	Bioresorb (Sybron Implant Solutions, Germany)
	Biosorb (SBM, France)
	Bi-Ostetic (Berkeley Advanced Biomaterials, CA, USA)
	BoneSigma TCP (SigmaGraft, CA, USA)
	C 13-09 (Chemische Fabrik Budenheim, Germany)
	Calc-i-oss classic (Degradable Solutions, Switzerland)
	Calciresorb (Ceraver, France)
	CAMCERAM TCP (CAM Implants, Netherlands)
	CELLPLEX (Wright Medical Technology, TN, USA)
	Cerasorb (Curasan, Germany)
	Ceros (Mathys, Switzerland)
	ChronOS (Synthes, PA, USA)
	Cidemarec (KERAMAT, Spain)
	Conduit (DePuy Spine, USA)
	cyclOS (Mathys, Switzerland)
	GenerOs (Berkeley Advanced Biomaterials, CA, USA)
	HT BIOCER (CHEMA – ELEKTROMET, Poland)
	IngeniOs β-TCP (Zimmer Dental, CA, USA)
	ISIOS+ (Kasios, France)
	JAX (Smith and Nephew Orthopaedics, USA)
	Keramedic (KERAMAT, Spain)
	KeraOs (KERAMAT, Spain)
	microTCP (Conmed, USA)
	nanoXIM (Fluidinova, Portugal)
	Osferion (Olympus Terumo Biomaterials, Japan)
	OSPROLIFE β-TCP (Eurocoating, Italy)
	OsSatura TCP (Integra Orthobiologics, CA, USA)

(continued)

Table 5.3 (continued)

Calcium orthophosphate	Trade name and producer (when available)
	PORESORB-TCP (Lasak, Czech Republic)
	Repros (JRI Orthopaedics, UK)
	SigmaOs TCP (SigmaGraft, CA, USA)
	Sorbone (Meta Biomed, Korea)
	Syncera (Oscotec, Korea)
	SynthoGraft (Bicon, MA, USA)
	Synthos (unknown producer)
	Syntricer (KARL STORZ Recon, Germany)
	TCP (Kasios, France)
	TriCaFor (BioNova, Russia)
	Triha + (Teknimed, France)
	Vitoss (Orthovita, PA, USA)
	Without trade name (CaP Biomaterials, WI, USA)
	Without trade name (Ensail Beijing, China)
	Without trade name (Himed, NY, USA)
	Without trade name (Shanghai Bio-lu Biomaterials, China)
	Without trade name (SigmaGraft, CA, USA)
	Without trade name (Taihei Chemical Industrial, Japan)
	Without trade name (Xpand Biotechnology, Netherlands)
β-TCP/$CaSO_4$	Genex (Biocomposites, UK)
β-TCP/poly-lactic acid	Bilok (Biocomposites, UK)
	Duosorb (SBM, France)
	Matryx® Interference Screws (Conmed, USA)
βTCP/bone marrow aspirate	Induce (Skeletal Kinetics, CA, USA)
β-TCP/collagen	Integra Mozaik (Integra Orthobiologics, CA, USA)
β-TCP/rhPDGF-BB solution	AUGMENT Bone Graft (Wright Medical Group, TN, USA)
BCP (HAp + β-TCP)	4Bone BCH (MIS Implants, Israel)
	AdboneBCP (Medbone Medical Devices, Portugal)
	Antartik (MedicalBiomat, France)
	ARCA BONE (ARCA-MEDICA, Switzerland)
	Artosal (aap Implantate, Germany)
	BCP BiCalPhos (Medtronic, MN, USA)
	BioGraft (IFGL BIO CERAMICS, India)
	Biosel (Depuy Bioland, France)
	BonaGraft (Biotech One, Taiwan)
	BoneCeramic (Straumann, Switzerland)
	BoneMedik-DM (Meta Biomed, Korea)
	BoneSave (Stryker Orthopaedics, NJ, USA)
	BoneSigma BCP (SigmaGraft, CA, USA)
	BONITmatrix (DOT, Germany)

(continued)

Table 5.3 (continued)

Calcium orthophosphate	Trade name and producer (when available)
	Calcicoat (Zimmer, IN, USA)
	Calciresorb (Ceraver, France)
	Calc-i-oss crystal (Degradable Solutions, Switzerland)
	CellCeram (Scaffdex, Finland)
	Ceraform (Teknimed, France)
	Ceratite (NGK Spark Plug, Japan)
	Cross.Bone (Biotech Dental, France)
	CuriOs (Progentix Orthobiology BV, Netherlands)
	DM-Bone (Meta Biomed, Korea)
	Eclipse (Citagenix, QC, Canada)
	Eurocer (FH Orthopedics, France)
	GENESIS-BCP (DIO Corporation, Korea)
	GenPhos HA TCP (Baumer, Brazil)
	Graftys BCP (Graftys, France)
	Hatric (Arthrex, Naples, FL, USA)
	Indost (Polystom, Russia)
	Kainos (Signus, Germany)
	MasterGraft (Medtronic Sofamor Danek, TN, USA)
	Maxresorb (botiss, Germany)
	MBCP (Biomatlante, France)
	NT-BCP (OssGen, Korea)
	NT-Ceram (Meta Biomed, Korea)
	OdonCer (Teknimed, France)
	OpteMX (Exactech, FL, USA)
	OrthoCer HA TCP (Baumer, Brazil)
	OSPROLIFE HA-βTCP (Eurocoating, Italy)
	OsSatura BCP (Integra Orthobiologics, CA, USA)
	Ossceram nano (bredent medical, Germany)
	OsteoFlux (VIVOS-Dental, Switzerland)
	OSTEON (GENOSS, Korea)
	Osteosynt (Einco, Brazil)
	Ostilit (Stryker Orthopaedics, NJ, USA)
	ReproBone (Ceramisys, UK)
	SBS (Expanscience, France)
	Scaffdex (Scaffdex Oy, Finland)
	SigmaOs BCP (SigmaGraft, CA, USA)
	SinboneHT (Purzer Pharmaceutical, Taiwan)
	SkeliGraft (Osteotec, UK)
	Synergy (unknown producer)
	TCH (Kasios, France)
	Triosite (Zimmer, IN, USA)
	Tribone (Stryker, Europe)

(continued)

Table 5.3 (continued)

Calcium orthophosphate	Trade name and producer (when available)
	Without trade name (Cam Bioceramics, Netherlands)
	Without trade name (CaP Biomaterials, WI, USA)
	Without trade name (Himed, NY, USA)
	Without trade name (MedicalGroup, France)
	Without trade name (SigmaGraft, CA, USA)
	Without trade name (Xpand Biotechnology, Netherlands)
BCP (HAp + α-TCP)	Skelite (Millennium Biologix, ON, Canada)
BCP (HAp + β-TCP)/ collagen	Allograft (Zimmer, IN, USA)
	Collacone max (botiss, Germany)
	Collagraft (Zimmer, IN, USA)
	Cross.Bone Matrix (Biotech Dental, France)
	MasterGraft (Medtronic Sofamor Danek, TN, USA)
	MATRI BONE (Biom'Up, France)
	Without trade name (MedicalGroup, France)
BCP (HAp + β-TCP)/ hydrogel	Eclipse (Citagenix, QC, Canada)
BCP (HAp + β-TCP)/ polymer	In'Oss (Biomatlante, France)
	Hydros (Biomatlante, France)
	Osteotwin (Biomatlante, France)
BCP (HAp + TTCP)	OSPROLIFE HA-TTCP (Eurocoating, Italy)
BCP/fibrin	TricOS (Baxter BioScience, France)
BCP/silicon	FlexHA (Xomed, FL, USA)
FA	Without trade name (CaP Biomaterials, WI, USA)
FA + BCP (HAp + β-TCP)	FtAP (Polystom, Russia)
Carbonateapatite	Norian SRS (Norian, CA, USA)
DCPA	Without trade name (Himed, NY, USA)
DCPD	Without trade name (Himed, NY, USA)
DCPD/collagen	CopiOs Bone Void Filler (Zimmer, IN, USA)
DCPD + β-TCP/$CaSO_4$	PRO-DENSE (Wright Medical Group, TN, USA)
ACP	Without trade name (Himed, NY, USA)
OCP	OctoFor (BioNova, Russia)
	Without trade name (Himed, NY, USA)
OCP/fibrin	FibroFor (BioNova, Russia)
TTCP	Without trade name (Ensail Beijing, China)
	Without trade name (Himed, NY, USA)
	Without trade name (Taihei Chemical Industrial, Japan)
Undisclosed $CaPO_4$	Arex Bone (Osteotec, UK)

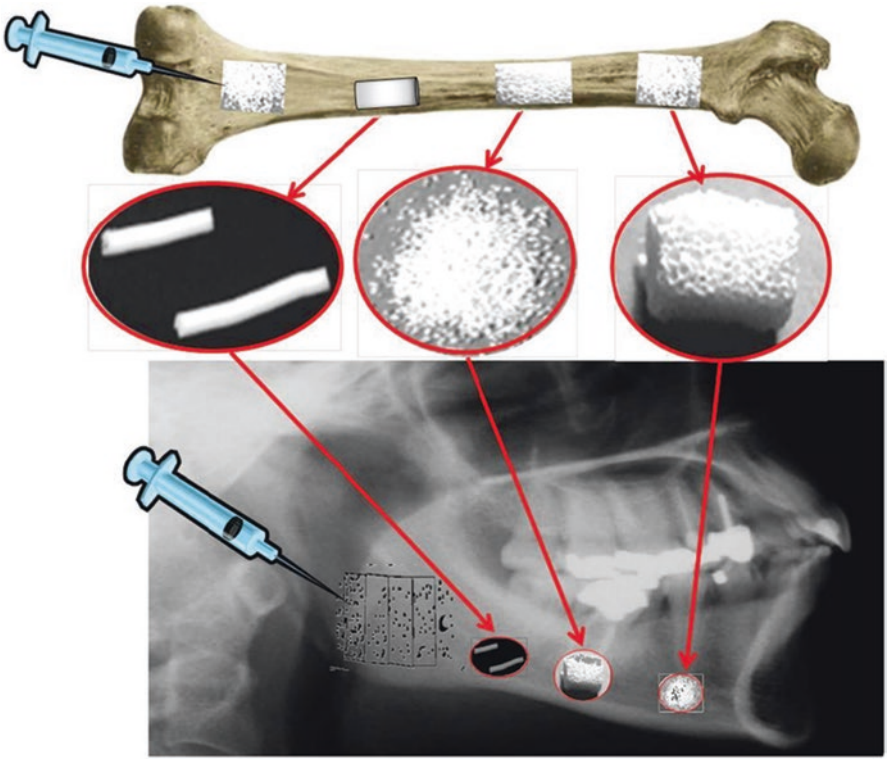

Fig. 5.10 Different types of biomedical applications of $CaPO_4$ bioceramics [633]

types of $CaPO_4$-based bioceramics and biomaterials have been summarized in Table 5.3, while their surgical applications are schematically shown in Fig. 5.10 [633]. A long list of both trademarks and producers clearly demonstrates that $CaPO_4$ bioceramics is easy to make and not very difficult to register for the biomedical applications. There is an ISO standard for $CaPO_4$-based bone substitutes [634].

One should note, that among the existing $CaPO_4$ (Table 5.1), only certain compounds are useful for biomedical applications, because those having the Ca/P ionic ratio less than 1 are not suitable for implantation due to their high solubility and acidity. Furthermore, due to its basicity, TTCP alone is not suitable either. However, to be applied in medicine, these "unsuitable" $CaPO_4$ might be successfully combined with either other types of $CaPO_4$ or other chemicals.

5.5.1 Self-Setting (Self-Hardening) Formulations

The need for bioceramics for minimal invasive surgery has induced a concept of self-setting (or self-hardening) formulations consisting of $CaPO_4$ only to be applied as injectable and/or mouldable bone substitutes [102, 103, 124, 487, 525, 635].

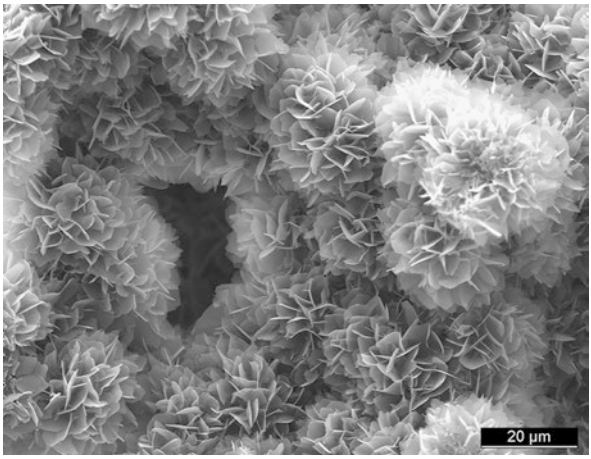

Fig. 5.11 A typical microstructure of a $CaPO_4$ cement after hardening. The mechanical stability is provided by the physical entanglement of crystals [639]

In addition, there are reinforced formulations, which, in a certain sense, might be defined as $CaPO_4$ concretes [102]. Furthermore, self-setting formulations able to produce porous $CaPO_4$ bioceramics are also available [465, 466, 473, 474, 476, 486, 487, 525, 545, 635–638].

All types of the self-setting $CaPO_4$ formulations belong to a low temperature bioceramics. They are divided into two major groups. The first one is a dry mixture of two different types of $CaPO_4$ (a basic one and an acidic one), in which, after being wetted, the setting reaction occurs according to an acid-base reaction. The second group contains only one $CaPO_4$, such as ACP with Ca/P molar ratio within 1.50–1.67 or α-TCP: both of them form CDHA upon contact with an aqueous solution [102, 124]. Chemically, setting (= hardening, curing) is due to the succession of dissolution and precipitation reactions. Mechanically, it results from crystal entanglement and intergrowth (Fig. 5.11) [639]. Sometimes, the self-set formulations are sintered to prepare high temperature $CaPO_4$ bioceramics [638]. Despite a large number of the initial compositions, all types of self-setting $CaPO_4$ formulations can form three products only: CDHA, DCPD and, rarely, DCPA [102, 103, 124, 487, 525, 635]. Special reviews on the subject are available [102, 103], where the interested readers are referred to get further details.

5.5.2 $CaPO_4$ Deposits (Coatings, Films and Layers)

For many years, the clinical application of $CaPO_4$-based bioceramics has been largely limited to non-load bearing parts of the skeleton due to their inferior mechanical properties. Therefore, materials with better mechanical properties appear to be necessary. For example, metallic implants are encountered in endoprostheses (total

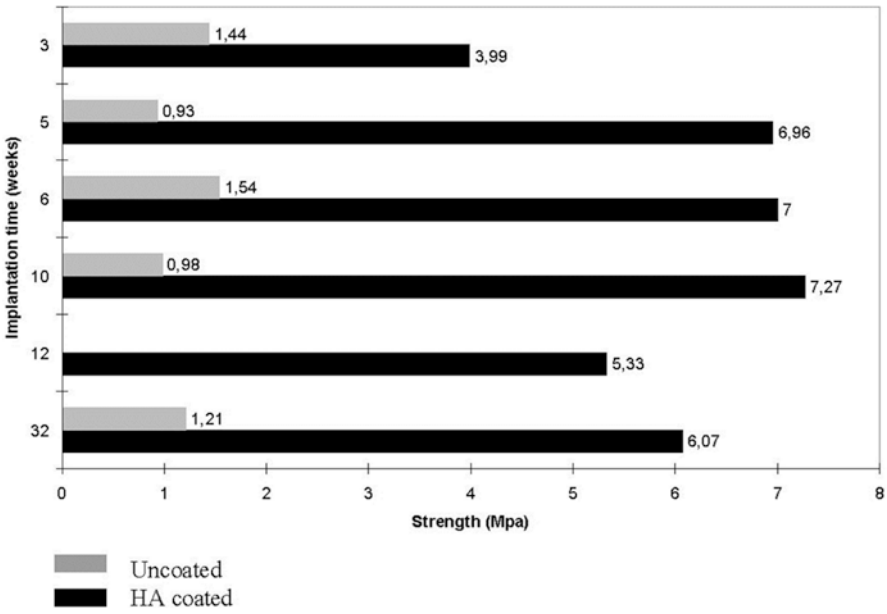

Fig. 5.12 Shows how a plasma-sprayed HAp coating on a porous titanium (*dark bars*) dependent on the implantation time will improve the interfacial bond strength compared to uncoated porous titanium (*light bars*) [50]

hip joint replacements) and artificial teeth sockets. As metals do not undergo bone bonding, i.e., do not form a mechanically stable link between the implant and bone tissue, ways have been sought to improve contacts at the interface. One major way is to coat metals with $CaPO_4$, which enables bonding ability between the metal and the bone [181, 193, 398, 640–642].

A number of factors influence the properties of $CaPO_4$ deposits (coatings, films and layers). They include thickness (this will influence coating adhesion and fixation – the agreed optimum now seems to be within 50–100 μm), crystallinity (this affects the dissolution and biological behavior), phase and chemical purity, porosity and adhesion. The coated implants combine the surface biocompatibility and bioactivity of $CaPO_4$ with the core strength of strong substrates (Fig. 5.12). Moreover, $CaPO_4$ deposits decrease a release of potentially hazardous chemicals from the core implant and shield the substrate surface from environmental attack. In the case of porous implants, the coated by $CaPO_4$ surface enhances bone ingrowth into the pores [336]. The clinical results for $CaPO_4$-deposited implants reveal that they have much longer life times after implantation than uncoated devices and they have been found to be particularly beneficial for younger patients. Further details on this topic are available in the special reviews [640–642].

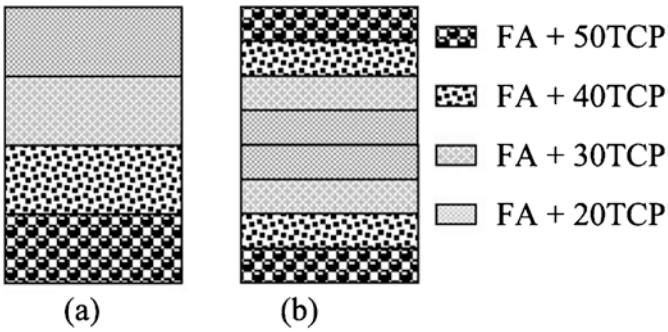

Fig. 5.13 A schematic diagram showing the arrangement of the FA/β-TCP biocomposite layers. (**a**) A non-symmetric functionally gradient material (FGM); (**b**) symmetric FGM [644]

5.5.3 Functionally Graded Bioceramics

In general, functionally gradient materials (FGMs) are defined as materials, having either compositional or structural gradient from their surface to the interior. The idea of FGMs allows one device to possess two different properties. One of the most important combinations for the biomedical field is that of a mechanical strength and biocompatibility. Namely, only surface properties govern a biocompatibility of the entire device. In contrast, the strongest material determines the mechanical strength of the entire device. Although, this subject belongs to the previous section on coatings, films and layers, in a certain sense, all types of implants covered by $CaPO_4$ might be also considered as a FGM.

Within the scope of this review, functionally graded bioceramics consisting of $CaPO_4$ is considered and discussed only. Such formulations have been developed [74, 509, 512, 579, 643–655]. For example, dense sintered bodies with gradual compositional changes from α-TCP to HAp were prepared by sintering a diamond-coated HAp compacts at 1,280 °C under a reduced pressure, followed by heating under the atmospheric conditions [643]. The content of α-TCP gradually decreased, while the content of HAp increased with increasing depth from the surface. This functionally gradient bioceramics consisting of HAp core and α-TCP surface showed a potential value as bone-substituting biomaterials [643]. Two types of functionally gradient FA/β-TCP biocomposites were prepared in another study [644]. As shown in Fig. 5.13, one of the graded biocomposites was in the shape of a disk and contained four different layers of about 1 mm thick. The other graded biocomposite was also in the shape of a disk but contained two sets of the four layers, each layer being 0.5 mm thick controlled by using a certain amount of the mixed powders. The final FA/β-TCP graded structures were formed at 100 MPa and sintered at 1,300 °C for 2 h [644]. The same approach was used in still another study, but HAp was used instead of FA and CDHA was used instead of β-TCP [655]. $CaPO_4$ coatings with graded crystallinity were prepared as well [650].

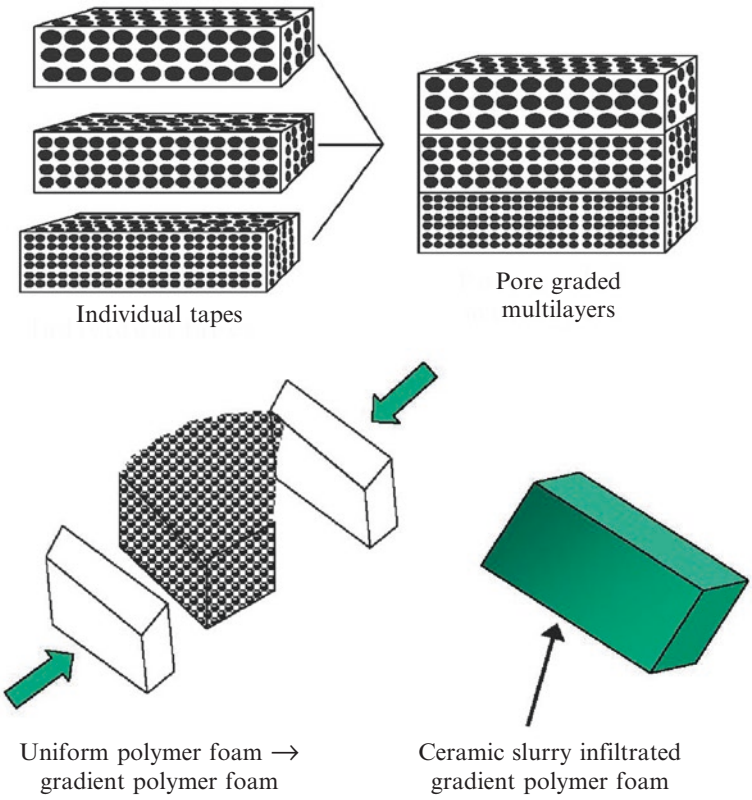

Fig. 5.14 Schematic illustrations of fabrication of pore-graded bioceramics: *top* – lamination of individual tapes, manufactured by tape casting; *bottom* – a compression molding process [443]

Besides, it is well known that a bone cross-section from cancellous to cortical bone is non-uniform in porosity and pore dimensions. Thus, in various attempts to mimic the porous structure of bones, $CaPO_4$ bioceramics with graded porosity have been fabricated [74, 443, 509, 512, 579, 643–648]. For example, graded porous $CaPO_4$ bioceramics can be produced by means of tape casting and lamination (Fig. 5.14, top). Other manufacturing techniques, such as a compression molding process (Fig. 5.14, bottom) followed by impregnation and firing, are known as well [443]. In the first method, a HAp slurry was mixed with a pore former. The mixed slurry was then cast into a tape. Using the same method, different tapes with different pore former sizes were prepared individually. The different tape layers were then laminated together. Firing was then done to remove the pore formers and sinter the HAp particle compacts, resulting in graded porous bioceramics [647]. This method was also used to prepare graded porous HAp with a dense part (core or layer) in order to improve the mechanical strength, as dense ceramics are much

stronger than porous ceramics. However, as in the pressure infiltration of mixed particles, this multiple tape casting also has the problem of poor connectivity of pores, although the pore size and the porosity are relatively easy to control. Furthermore, the lamination step also introduces additional discontinuity of the porosity on the interfaces between the stacked layers.

Since diverse biomedical applications require different configurations and shapes, the graded (or gradient) porous bioceramics can be grouped according to both the overall shape and the structural configuration [443]. The basic shapes include rectangular blocks and cylinders (or disks). For the cylindrical shape, there are configurations of dense core – porous layer, less porous core – more porous layer, dense layer – porous core and less porous layer – more porous core. For the rectangular shape, in the gradient direction i.e., the direction with varying porosity, pore size or composition, there are configurations of porous top – dense bottom (same as porous bottom – dense top), porous top – dense center – porous bottom, dense top – porous center – dense bottom, etc. Concerning biomedical applications, a dense core – porous layer structure is suitable for implants of a high mechanical strength and with bone ingrowth for stabilization, whereas a less porous layer – more porous core configuration can be used for drug delivery systems. Furthermore, a porous top – dense bottom structure can be shaped into implants of articulate surfaces for wear resistance and with porous ends for bone ingrowth fixation; while a dense top – porous center – dense bottom arrangement mimics the structure of head skull. Further details on bioceramics with graded porosity might be found in literature [443].

5.6 Biological Properties and In Vivo Behavior

The most important differences between bioactive bioceramics and all other implanted materials comprise inclusion in the metabolic processes of the organism, adaptation of either surface or the entire material to the biomedium, integration of a bioactive implant with bone tissues at the molecular level or the complete replacement of a resorbable bioceramics by healthy bone tissues. All of the enumerated processes are related to the effect of an organism on the implant. Nevertheless, another aspect of implantation is also important – the effect of the implant on the organism. For example, using of bone implants from corpses or animals, even after they have been treated in various ways, provokes a substantially negative immune reactions in the organism, which substantially limits the application of such implants. In this connection, it is useful to dwell on the biological properties of bioceramic implants, particularly those of $CaPO_4$, which in the course of time may be resorbed completely [656].

5.6.1 Interactions with Surrounding Tissues and the Host Responses

All interactions between implants and the surrounding tissues are dynamic processes. Water, dissolved ions, various biomolecules and cells surround the implant surface within initial few seconds after the implantation. It has been accepted that no foreign material placed inside a living body is completely compatible. The only substances that conform completely are those manufactured by the body itself (autogenous), while any other substance, which is recognized as foreign, initiates some types of reactions (a host-tissue response). The reactions occurring at the biomaterial/tissue interfaces lead to time-dependent changes in the surface characteristics of both the implanted biomaterials and the surrounding tissues [58, 657].

In order to develop new biomaterials, it is necessary to understand the in vivo host responses. Like any other species, biomaterials and bioceramics react chemically with their environment and, ideally, they should neither induce any changes nor provoke undesired reactions in the neighboring or distant tissues. In general, living organisms can treat artificial implants as biotoxic (or bioincompatible [53]), bioinert (or biostable [46]), biotolerant (or biocompatible [53]), bioactive and bioresorbable materials [1–3, 42, 43, 47, 50–53, 656–658]. Biotoxic (e.g., alloys containing cadmium, vanadium, lead and other toxic elements) materials release to the body substances in toxic concentrations and/or trigger the formation of antigens that may cause immune reactions ranging from simple allergies to inflammation to septic rejection with the associated severe health consequences. They cause atrophy, pathological change or rejection of living tissue near the material as a result of chemical, galvanic or other processes. Bioinert (this term should be used with care, since it is clear that any material introduced into the physiological environment will induce a response. However, for the purposes of biomedical implants, the term can be defined as a minimal level of response from the host tissue), such as zirconia, alumina, carbon and titanium, as well as biotolerant (e.g., polymethylmethacrylate, titanium and Co-Cr alloy) materials do not release any toxic constituents but also do not show positive interaction with living tissue. They evoke a physiological response to form a fibrous capsule, thus, isolating the material from the body. In such cases, thickness of the layer of fibrous tissue separating the material from other tissues of an organism can serve as a measure of bioinertness. Generally, both bioactivity and bioresorbability phenomena are fine examples of chemical reactivity and $CaPO_4$ (both non-substituted and ion-substituted ones) fall into these two categories of bioceramics [1–3, 42, 43, 47, 50–53, 656–658]. A bioactive material will dissolve slightly but promote formation of a surface layer of biological apatite before interfacing directly with the tissue at the atomic level, that result in formation of a direct chemical bonds to bones. Such implants provide a good stabilization for materials that are subject to mechanical loading. A bioresorbable material will dissolve over time (regardless of the mechanism leading to the material removal) and allow a

newly formed tissue to grow into any surface irregularities but may not necessarily interface directly with the material. Consequently, the functions of bioresorbable materials are to participate in dynamic processes of formation and re-absorption occurring in bone tissues; thus, bioresorbable materials are used as scaffolds or filling spacers allowing to the tissues their infiltration and substitution [181, 326, 659–661].

It is important to stress, that a distinction between the bioactive and bioresorbable bioceramics might be associated with structural factors only. Namely, bioceramics made from non-porous, dense and highly crystalline HAp behaves as a bioinert (but a bioactive) material and is retained in an organism for at least 5–7 years without noticeable changes (Fig. 5.2 bottom), while a highly porous bioceramics of the same composition can be resorbed approximately within a year. Furthermore, submicron-sized HAp powders are biodegraded even faster than the highly porous HAp scaffolds. Other examples of bioresorbable materials comprise porous bioceramic scaffolds made of biphasic, triphasic or multiphasic $CaPO_4$ formulations [79] or bone grafts (dense or porous) made of CDHA [121], TCP [74, 662, 663] and/or ACP [488, 664]. One must stress that at the beginning of 2000s the concepts of bioactive and bioresorbable materials have been converged and bioactive materials are made bioresorbable, while bioresorbable ones are made bioactive [665].

Although in certain in vivo experiments inflammatory reactions were observed after implantation or injection of $CaPO_4$ [666–675], the general conclusion on using $CaPO_4$ with Ca/P ionic ratio within 1.0–1.7 is that all types of implants (bioceramics of various porosities and structures, powders or granules) are not only nontoxic but also induce neither inflammatory nor foreign-body reactions [108, 676, 677]. The biological response to implanted $CaPO_4$ follows a similar cascade observed in fracture healing. This cascade includes a hematoma formation, inflammation, neovascularization, osteoclastic resorption and a new bone formation. An intermediate layer of fibrous tissue between the implants and bones has been never detected. Furthermore, $CaPO_4$ implants display the ability to directly bond to bones [1–3, 42, 43, 47, 50–53, 656–658]. For further details, the interested readers are referred to a good review on cellular perspectives of bioceramic scaffolds for bone tissue engineering [498].

One should note that the aforementioned rare cases of the inflammatory reactions to $CaPO_4$ bioceramics were often caused by “other” reasons. For example, a high rate of wound inflammation occurred when highly porous HAp was used. In that particular case, the inflammation was explained by sharp implant edges, which irritated surrounding soft tissues [667]. To avoid this, only rounded material should be used for implantation (Fig. 5.15) [678]. Another reason for inflammation produced by porous HAp could be due to micro movements of the implants, leading to simultaneous disruption of a large number of micro-vessels, which grow into the pores of the bioceramics. This would immediately produce an inflammatory reaction. Additionally, problems could arise in clinical tests connected with migration of granules used for alveolar ridge augmentation, because it might be difficult to achieve a mechanical stability of implants at the implantation sites [667]. Besides, presence of calcium pyrophosphate impurity might be the reason of inflammation [670]. Additional details on inflammatory cell responses to $CaPO_4$ might be found in a special review on this topic [671].

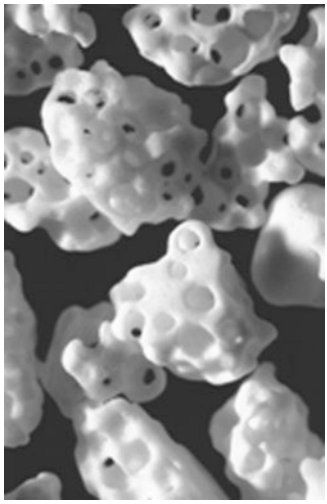

Fig. 5.15 Rounded β-TCP granules of 2.6–4.8 mm in size, providing no sharp edges for combination with bone cement [678]

5.6.2 Osteoinduction

Before recently, it was generally considered, that alone, any type of synthetic bioceramics possessed neither osteogenic (osteogenesis is the process of laying down new bone material by osteoblasts [679]) nor osteoinductive (is the property of the material to induce bone formation de novo or ectopically (i.e., in non-bone forming sites) [679]) properties and demonstrated a minimal immediate structural support. However, a number of reports have already shown the osteoinductive properties of certain types of $CaPO_4$ bioceramics [152, 571, 596, 680–699] and the amount of such publications rapidly increases. For example, bone formation was found to occur in dog muscle inside porous $CaPO_4$ with surface microporosity, while bone was not observed on the surface of dense bioceramics [684]. Furthermore, implantation of porous β-TCP bioceramics appeared to induce bone formation in soft tissues of dogs, while no bone formation was detected in any α-TCP implants [681]. More to the point, titanium implants coated by a microporous layer of OCP were found to induce ectopic bone formation in goat muscles, while a smooth layer of carbonated apatite on the same implants was not able to induce bone formation there [682, 683]. In another study, β-TCP powder, biphasic (HAp + β-TCP) powder and intact biphasic (HAp + β-TCP) rods were implanted into leg muscles of mice and dorsal muscles of rabbits [690]. One month and 3 months after implantation, samples were harvested for biological and histological analysis. New bone tissues were observed in ten of ten samples for β-TCP powder, three of ten samples biphasic powder and nine of ten samples for intact biphasic rods at third month in mice, but not in rabbits. The authors concluded that the chemical composition was the prerequisite in osteoinduction, while porosity contributed to more bone formation [690]. Therefore, researchers have already discovered the ways to prepare osteoinductive $CaPO_4$ bioceramics.

Unfortunately, the underlying mechanism(s) leading to bone induction by synthetic materials remains largely unknown. Nevertheless, besides the specific genetic factors [688] and chosen animals [690], the dissolution/precipitation behavior of $CaPO_4$ [700], their particle size [698], microporosity [686, 690, 701, 702], physicochemical properties [684, 686], composition [690], the specific surface area [702], nanostructure [689], as well as the surface topography and geometry [685, 703–707] have been pointed out as the relevant parameters. A positive effect of increased microporosity on the ectopic bone formation could be both direct and indirect. Firstly, an increased microporosity is directly related to the changes in surface topography, i.e. increases a surface roughness, which affects the cellular differentiation [707]. Secondly, an increased microporosity indirectly means a larger surface that is exposed to the body fluids leading to elevated dissolution/precipitation phenomena as compared to non-microporous surfaces. In addition, other hypotheses are also available. Namely, Reddi explained the apparent osteoinductive properties as an ability of particular bioceramics to concentrate bone growth factors, which are circulating in biological fluids, and those growth factors induce bone formation [703]. Other researchers proposed a similar hypothesis that the intrinsic osteoinduction by $CaPO_4$ bioceramics is a result of adsorption of osteoinductive substances on their surface [685]. Moreover, Ripamonti [704] and Kuboki et al. [705] independently postulated that the geometry of $CaPO_4$ bioceramics is a critical parameter in bone induction. Specifically, bone induction by $CaPO_4$ was never observed on flat bioceramic surfaces. All osteoinductive cases were observed on either porous structures or structures contained well-defined concavities. What's more, bone formation was never observed on the peripheries of porous implants and was always found inside the pores or concavities, aligning the surface [181]. Some researchers speculated that a low oxygen tension in the central region of implants might provoke a dedifferentiation of pericytes from blood micro-vessels into osteoblasts [708]. Finally but yet importantly, both nanostructured rough surfaces and a surface charge on implants were found to cause an asymmetrical division of the stem cells into osteoblasts, which is important for osteoinduction [701].

Nevertheless, to finalize this topic, it is worth citing a conclusion made by Boyan and Schwartz [709]: "Synthetic materials are presently used routinely as osteoconductive bone graft substitutes, but before purely synthetic materials can be used to treat bone defects in humans where an osteoinductive agent is required, a more complete appreciation of the biology of bone regeneration is needed. An understanding is needed of how synthetic materials modulate the migration, attachment, proliferation and differentiation of mesenchymal stem cells, how cells on the surface of a material affect other progenitor cells in the peri-implant tissue, how vascular progenitors can be recruited and a neovasculature maintained, and how remodeling of newly formed bone can be controlled" (p. 9).

5.6.3 *Biodegradation*

Shortly after implantation, a healing process is initiated by compositional changes of the surrounding bio-fluids and adsorption of biomolecules. Following this, various types of cells reach the $CaPO_4$ surface and the adsorbed layer dictates the ways the cells respond. Further, a biodegradation (which can be envisioned as an in vivo process by which an implanted material breaks down into either simpler components or components of the smaller dimensions) of the implanted $CaPO_4$ bioceramics begins. This process can occur by three possible ways: (1) physical: due to abrasion, fracture and/or disintegration, (2) chemical: due to physicochemical dissolution of the implanted phases of $CaPO_4$ with a possibility of phase transformations into other phases of $CaPO_4$, as well as their precipitation and (3) biological: due to cellular activity (so called, bioresorption). In biological systems, all these processes take place simultaneously and/or in competition with each other. Since the existing $CaPO_4$ are differentiated by Ca/P ratio, basicity/acidity and solubility (Table 5.1), in the first instance, their degradation kinetics and mechanisms depend on the chosen type of $CaPO_4$ [710, 711]. Since dissolution is a physical chemistry process, it is controlled by some factors, such as $CaPO_4$ solubility, surface area to volume ratio, local acidity, fluid convection and temperature. For HAp and FA, the dissolution mechanism in acids has been described by a sequence of four successive chemical equations, in which several other $CaPO_4$, such as TCP, DCPD/DCPA and MCPM/MCPA, appear as virtual intermediate phases [712, 713].

With a few exceptions, dissolution rates of $CaPO_4$ are inversely proportional to the Ca/P ratio (except of TTCP), phase purity and crystalline size, as well as it is directly related to both the porosity and the surface area. In addition, phase transformations might occur with DCPA, DCPD, OCP, α-TCP, β-TCP and ACP because they are unstable in aqueous environment under the physiological conditions [714]. Bioresorption is a biological process mediated by cells (mainly, osteoclasts and, in a lesser extent, macrophages) [715, 716]. It depends on the response of cells to their environment. Osteoclasts attach firmly to the implant and dissolve $CaPO_4$ by secreting an enzyme carbonic anhydrase or any other acid, leading to a local pH drop to ~4–5 [717]. Formation of multiple spine-like crystals at the exposed areas of β-TCP was discovered [718]. Furthermore, nanodimensional particles of $CaPO_4$ can also be phagocytosed by cells, i.e. they are incorporated into cytoplasm and thereafter dissolved by acid attack and/or enzymatic processes [719]. A study is available [720], in which a comparison was made between the solubility and osteoclastic resorbability of three types of $CaPO_4$ (DCPA, ACP and HAp) + β-calcium pyrophosphate (β-CPP) powders having the monodisperse particle size distributions. The authors discovered that with the exception of β-CPP, the difference in solubility among different calcium phosphates became neither mitigated nor reversed but augmented in the resorptive osteoclastic milieu. Namely, DCPA (the phase with the highest solubility) was resorbed more intensely than any other calcium phosphate,

whereas HAp (the phase with the lowest solubility) was resorbed the least. β-CPP became retained inside the cells for the longest period of time, indicating hindered digestion of only this particular type of calcium phosphate. Genesis of osteoclasts was found to be mildly hindered in the presence of HAp, ACP and DCPA, but not in the presence of β-CPP. HAp appeared to be the most viable compound with respect to the mitochondrial succinic dehydrogenase activity. The authors concluded that chemistry did have a direct effect on biology, while biology neither overrode nor reversed the chemical propensities of calcium phosphates with which it interacted, but rather augmented and took a direct advantage of them [720]. Similar conclusions on both the resorbability and dissolution behavior of OCP, β-TCP and HAp were made in another study [714]. In addition, in vivo biodegradation of MCPA was found to be faster than that of bovine HAp [721]. Thus, one can conclude that in vivo biodegradation kinetics of $CaPO_4$ seems to correlate well with their solubility. Nevertheless, one must keep in mind that this is a very complicated combination of various non-equilibrium processes, occurring simultaneously and/or in competition with each other [722].

Strictly speaking, the processes happen in vitro do not necessarily represent the ones occurring in vivo and vice versa; nevertheless, in vitro experiments are widely performed. Usually, an in vitro biodegradation of $CaPO_4$ bioceramics is simulated by suspending the material in a slightly acidic (pH ~4) buffer and monitoring the release of major ions with time [711, 723–726]. The acidic buffer, to some extent, mimics the acidic environment during osteoclastic activity. In one study, an in vivo behavior of porous β-TCP bioceramics prepared from rod-shaped particles and that prepared from non-rod-shaped particles in the rabbit femur was compared. Although the porosities of both types of β-TCP bioceramics were almost the same, a more active osteogenesis was preserved in the region where rod-shaped bioceramics was implanted [727]. Furthermore, the dimensions of both the particles [698] and the surface microstructure [693] were found to influence the osteoinductive potential of $CaPO_4$ bioceramics. These results implied that the microstructure affected the activity of bone cells and subsequent bone replacement.

The experimental results demonstrated that both the dissolution kinetics and in vivo biodegradation of biologically relevant $CaPO_4$ proceed in the following decreasing order: β-TCP > bovine bone apatite (unsintered) > bovine bone apatite (sintered) > coralline HAp > HAp. In the case of biphasic (HAp + TCP), triphasic and multiphasic $CaPO_4$ formulations, the biodegradation kinetics depends on the HAp/TCP ratio: the higher the ratio, the lower the degradation rate. Similarly, in vivo degradation rate of biphasic TCP (α-TCP + β-TCP) bioceramics appeared to be lower than that of α-TCP and higher than that of β-TCP bioceramics, respectively [93]. Furthermore, incorporation of doping ions can either increase (e.g., CO_3^{2-}, Mg^{2+} or Sr^{2+}) or decrease (e.g., F^-) the solubility (therefore, biodegradability) of CDHA and HAp. Contrarily to apatites, solubility of β-TCP is decreased by incorporation of either Mg^{2+} or Zn^{2+} ions [571]. Here, one should remind that ion-substituted $CaPO_4$ are not considered in this review; the interested readers are advised to read the original publications [17–41].

5.6.4 *Bioactivity*

Generally, bioactive materials interact with surrounding bone resulting in formation of a chemical bond to this tissue (bone bonding). The bioactivity phenomenon is determined by both chemical factors, such as crystal phases and molecular structures of a biomaterial, and physical factors, such as surface roughness and porosity. Currently, it is agreed that the newly formed bone bonds directly to biomaterials through a carbonated CDHA layer precipitating at the bone/biomaterial interface. Strange enough but a careful seeking in the literature resulted in just a few publications [571, 728–730], where the bioactivity mechanism of $CaPO_4$ was briefly described. For example, the chemical changes occurring after exposure of a synthetic HAp bioceramics to both in vivo (implantation in human) and in vitro (cell culture) conditions were studied. A small amount of HAp was phagocytozed but the major remaining part behaved as a secondary nucleator as evidenced by the appearance of a newly formed mineral [728]. In vivo, a cellular activity (e.g., of macrophages or osteoclasts) associated with an acidic environment were found to result in partial dissolution of $CaPO_4$, causing liberation of calcium and orthophosphate ions to the microenvironment. The liberated ions increased a local supersaturation degree of the surrounding biologic fluids, causing precipitation of nano-sized crystals of biological apatite with simultaneous incorporating of various ions presented in the fluids. Infrared spectroscopic analyses demonstrated that these nanodimensional crystals were intimately associated with bioorganic components (probably proteins), which might also have originated from the biologic fluids, such as serum [571].

Therefore, one should consider the bioactivity mechanism of other biomaterials, particularly of bioactive glasses – the concept introduced by Prof. Larry L. Hench [50, 51]. The bonding mechanism of bioactive glasses to living tissues involves a sequence of 11 successive reaction steps (Fig. 5.16), some of which comprise $CaPO_4$. The initial five steps occurred on the surface of bioactive glasses are "chemistry" only, while the remaining six steps belong to "biology" because the latter include colonization by osteoblasts, followed by proliferation and differentiation of the cells to form a new bone that had a mechanically strong bond to the implant surface. Therefore, in the case of bioactive glasses the border between "dead" and "alive" is postulated between stages 5 and 6. According to Hench, all bioactive materials "form a bone-like apatite layer on their surfaces in the living body and bond to bone through this apatite layer. The formation of bone-like apatite on artificial material is induced by functional groups, such as Si–OH (in the case of biological glasses), Ti–OH, Zr–OH, Nb–OH, Ta–OH, –COOH and $–H_2PO_4$ (in the case of other materials). These groups have specific structures revealing negatively charge and induce apatite formation via formations of an amorphous calcium compound, *e.g.*, calcium silicate, calcium titanate and ACP" [50, 51].

In addition, one should mention another set of 11 successive reaction steps for bonding mechanism of unspecified bioceramics, developed by Prof. Paul Ducheyne (Fig. 5.17) [58]. One can see that the Ducheyne's model is rather similar to that proposed by Hench; however, there are noticeable differences between them.

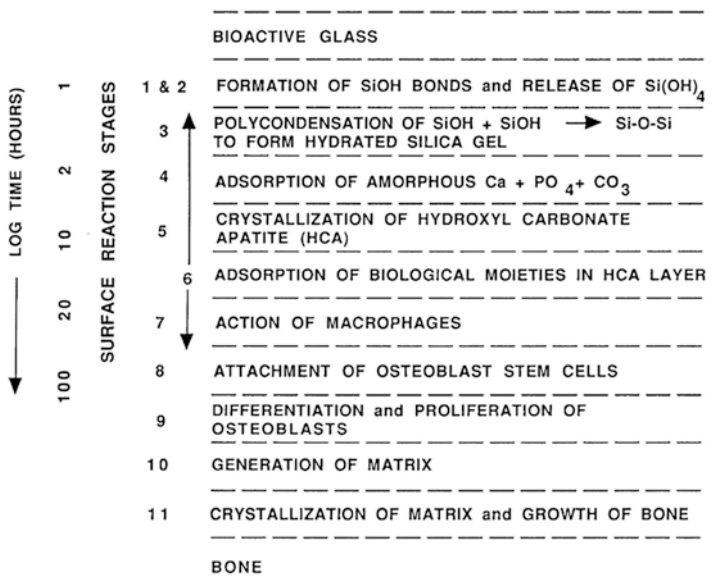

Fig. 5.16 A sequence of interfacial reactions involved in forming a bond between tissue and bioactive ceramics [50, 51]

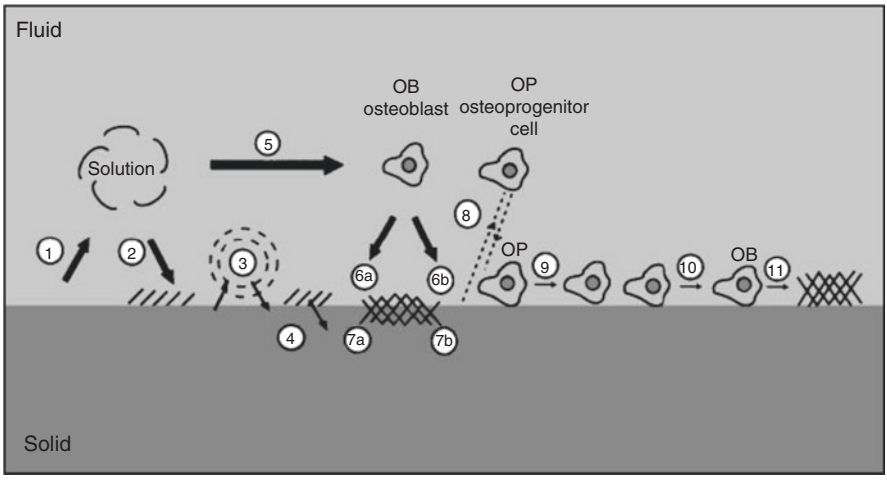

Fig. 5.17 A schematic diagram representing the events, which take place at the interface between bioceramics and the surrounding biological environment: (*1*) dissolution of bioceramics; (*2*) precipitation from solution onto bioceramics; (*3*) ion exchange and structural rearrangement at the bioceramic/tissue interface; (*4*) interdiffusion from the surface boundary layer into the bioceramics; (*5*) solution-mediated effects on cellular activity; (*6*) deposition of either the mineral phase (**a**) or the organic phase (**b**) without integration into the bioceramic surface; (*7*) deposition of either the mineral phase (**a**) or the organic phase (**b**) with integration into the bioceramics; (*8*) chemotaxis to the bioceramic surface; (*9*) cell attachment and proliferation; (*10*) cell differentiation; (*11*) extracellular matrix formation. All phenomena, collectively, lead to the gradual incorporation of a bioceramic implant into developing bone tissue [58]

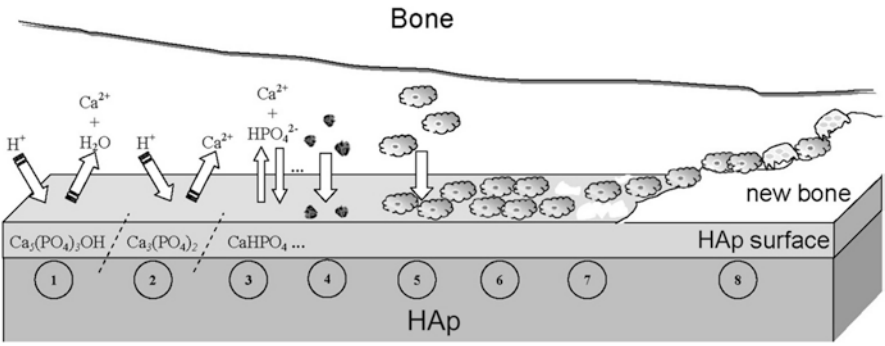

Fig. 5.18 A schematic diagram representing the phenomena that occur on HAp surface after implantation: (*1*) beginning of the implant procedure, where a solubilization of the HAp surface starts; (*2*) continuation of the solubilization of the HAp surface; (*3*) the equilibrium between the physiological solutions and the modified surface of HAp has been achieved (changes in the surface composition of HAp does not mean that a new phase of DCPA or DCPD forms on the surface); (*4*) adsorption of proteins and/or other bioorganic compounds; (*5*) cell adhesion; (*6*) cell proliferation; (*7*) beginning of a new bone formation; (*8*) new bone has been formed [730]

For example, Ducheyne mentions on ion exchange and structural rearrangement at the bioceramic/tissue interface (stage 3), as well as on interdiffusion from the surface boundary layer into bioceramics (stage 4) and deposition with integration into the bioceramics (stage 7), which are absent in the Hench's model. On the other hand, Hench describes six biological stages (stages 6–11), while Ducheyne describes only four ones (stages 8–11). Both models have been developed almost two decades ago and, to the best of my knowledge, remain unchanged since then. Presumably, both approaches have *pro et contra* of their own and, obviously, should be updated and/or revised. Furthermore, in literature there are at least two other descriptions of the biological and cellular events occurring at the bone/implant interface [731, 732]. Unfortunately, both of them comprise lesser number of stages. In 2010, one more hypothesis has been proposed (Fig. 5.18). For the first time, it describes reasonable surface transformations, happening with $CaPO_4$ bioceramics (in that case, HAp) shortly after the implantation [730]. However, one must stress that the schemes displayed in Figs. 5.16, 5.17, and 5.18 do not represent the real mechanisms but only descriptions of the observable events occurring at the $CaPO_4$ interface after implantation. Furthermore, many events occur simultaneously; therefore, none of the schemes should be considered in terms of the strict time sequences.

An important study on formation of $CaPO_4$ precipitates on various types of bioceramic surfaces in both simulated body fluid (SBF) and rabbit muscle sites was performed [733]. The bioceramics were sintered porous solids, including bioglass, glass-ceramics, α-TCP, β-TCP and HAp. An ability to induce $CaPO_4$ precipitation was compared among these types of bioceramics. The following conclusions were made: (1) OCP formation ubiquitously occurred on all types of bioceramic surfaces

both in vitro and in vivo, except on β-TCP. (2) Apatite formation did not occur on every type of bioceramic surface; it was less likely to occur on the surfaces of HAp and α-TCP. (3) Precipitation of $CaPO_4$ on the bioceramic surfaces was more difficult in vivo than in vitro. (4) Differences in $CaPO_4$ precipitation among the bioceramic surfaces were less noticeable in vitro than that in vivo. (5) β-TCP bioceramics showed a poor ability of $CaPO_4$ precipitation both in vitro and in vivo [733]. These findings clearly revealed that apatite formation in the physiological environments could not be confirmed as the common feature of bioceramics. Nevertheless, for want of anything better, currently the bioactivity mechanism of $CaPO_4$ bioceramics should be described by a reasonable combination of Figs. 5.16, 5.17, and 5.18, e.g., by updating the Ducheyne's and Hench's models by three initial stages taken from Fig. 5.18.

Interestingly that bioactivity of HAp bioceramics might be enhanced by a high-energy ion irradiation [734]. The effect was attributed to formation of a unique 3D macroporous apatite layer of decreased crystallinity and crystal size on the irradiated surfaces. Obviously, to get further insights into the bioactivity phenomenon, the atomic and molecular processes occurring at the bioceramic surface in aqueous solutions and their effects on the relevant reaction pathways of cells and tissues must be elucidated in more details.

5.6.5 Cellular Response

Fixation of any implants in the body is a complex dynamic process that remodels the interface between the implants and living tissues at all dimensional levels, from the molecular up to the cell and tissue morphology level, and at all time scales, from the first second up to several years after implantation. Immediately following the implantation, a space filled with biological fluids appears next to the implant surface. With time, cells are adsorbed at the implant surface that will give rise to their proliferation and differentiation towards bone cells, followed by revascularisation and eventual gap closing. Ideally, a strong bond is formed between the implants and surrounding tissues [53]. An interesting study on the interfacial interactions between calcined HAp and substrates has been performed [735], where the interested readers are referred for further details.

The aforementioned paragraph clearly demonstrates an importance of studies on cellular responses to $CaPO_4$ bioceramics. Therefore, such investigations have been performed extensively for several decades [671, 736–751]. For example, bioceramic discs made of seven different types of $CaPO_4$ (TTCP, HAp, carbonate apatite, β-TCP, α-TCP, OCP and DCPD) were incubated in osteoclastic cell cultures for 2 days. In all cases, similar cell morphologies and good cell viability were observed; hoverer, different levels of resorbability of various types of $CaPO_4$ were detected [739]. Similar results were found for fluoridated HAp coatings [741]. Experiments performed with human osteoblasts revealed that nanostructured bioceramics prepared from nano-sized HAp showed significant enhancement in mineralization compared

to microstructured HAp bioceramics [740]. In addition, the influence of lengths and surface areas of rod-shaped HAp on cellular response were studied. Again, similar cell morphologies and good cell viability were observed; however, it was concluded that high surface area could increase cell-particle interaction [744]. Nevertheless, another study with cellular response to rod-shaped HAp bioceramics, revealed that some types of crystals might trigger a severe inflammatory response [747]. In addition, $CaPO_4$-based sealers appeared to show less cytotoxicity and inflammatory mediators compared with other sealers [742]. More examples are available in literature.

Cellular biodegradation of $CaPO_4$ bioceramics is known to depend on its phases. For example, a higher solubility of β-TCP was shown to prevent L-929 fibroblast cell adhesion, thereby leading to damage and rupture of the cells [752]. A mouse ectopic model study indicated the maximal bone growth for the 80: 20 β-TCP: HAp biphasic formulations preloaded with human mesenchymal stem cells when compared to other $CaPO_4$ [753]. The effects of substrate microstructure and crystallinity have been corroborated with an in vivo rabbit femur model, where rod-like crystalline β-TCP was reported to enhance osteogenesis when compared to non-rod like crystalline β-TCP [727]. Additionally, using a dog mandibular defect model, a higher bone formation on a scaffold surface coated by nanodimensional HAp was observed when compared to that coated by a micro-dimensional HAp [754]. Furthermore, studies revealed a stronger stress signaling response by osteoblast precursor cells in 3D scaffolds when compared to 2D surfaces [755].

Mesenchymal stem cells are one of the most attractive cellular lines for application as bone grafts [756, 757]. Early investigations by Okumura et al. indicated an adhesion, proliferation and differentiation, which ultimately became new bone and integrated with porous HAp bioceramics [737]. Later, a sustained co-culture of endothelial cells and osteoblasts on HAp scaffolds for up to 6 weeks was demonstrated [758]. Furthermore, a release of factors by endothelial and osteoblast cells in co-culture supported proliferation and differentiation was suggested to ultimately result in microcapillary-like vessel formation and supported a neo-tissue growth within the scaffold [498]. More to the point, investigation of rat calvaria osteoblasts cultured on transparent HAp bioceramics, as well as the analysis of osteogenic-induced human bone marrow stromal cells at different time points of culturing indicated to a good cytocompatibility of HAp bioceramics and revealed favorable cell proliferation [434]. The positive results for other types of cells have been obtained in other studies [190, 433, 457–459, 759–761].

Interestingly that HAp scaffolds with marrow stromal cells in a perfused environment were reported to result in ~85% increase in mean core strength, a ~130% increase in failure energy and a ~355% increase in post-failure strength. The increase in mineral quantity and promotion of the uniform mineral distribution in that study was suggested to attribute to the perfusion effect [590]. Additionally, other investigators indicated to mechanical properties increasing for other $CaPO_4$ scaffolds after induced osteogenesis [589, 592].

To finalize this section, one should mention on the recent developments to influence the cellular response. First, to facilitate interactions with cells, the $CaPO_4$ surfaces could be functionalized [762–766]. Second, it appears that crystals of

biological apatite of calcified tissues exhibit different orientations depending on the tissue. Namely, in vertebrate bones and tooth enamel surfaces, the respective *a*, *b*-planes and *c*-planes of the apatite crystals are preferentially exposed. Therefore, ideally, this should be taken into account in artificial bone grafts. Recently, a novel process to fabricate dense HAp bioceramics with highly preferred orientation to the *a, b*-plane was developed. The results revealed that increasing the *a, b*-plane orientation degree shifted the surface charge from negative to positive and decreased the surface wettability with simultaneous decreasing of cell attachment efficiency [767–769]. The latter finding resulted in further developments on preparation of oriented $CaPO_4$ compounds [770–772].

5.7 Non-biomedical Applications of $CaPO_4$

Due to their strong adsorption ability, surface acidity or basicity and ion exchange abilities, some types of $CaPO_4$ possess a catalytic activity [15, 773–785]. As seen from the references, $CaPO_4$ are able to catalyze oxidation and reduction reactions, as well as formation of C–C bonds. Namely, the application in oxidation reactions mainly includes oxidation of alcohol and dehydrogenation of hydrocarbons, while the reduction reactions include hydrogenolysis and hydrogenation. The formation of C–C bonds mainly comprises Claisen-Schmidt and Knoevenagel condensation reactions, Michael addition reaction, as well as Friedel-Crafts, Heck, Diels-Alder and adol reactions [780].

In addition, due to the chemical similarity to the inorganic part of mammalian calcified tissues, $CaPO_4$ powders appear to be good solid carriers for chromatography of biological substances. Namely, such high-value biological materials, as recombinant proteins, therapeutic antibodies and nucleic acids are separated and purified [786–792]. Finally, some types of $CaPO_4$ are used as a component of various sensors [377, 378, 382, 383, 386, 793–796]. However, since these subjects are almost irrelevant to bioceramics, they are not detailed further.

5.8 $CaPO_4$ Bioceramics in Tissue Engineering

5.8.1 Tissue Engineering

Tissue/organ repair has been the ultimate goal of surgery from ancient times to nowadays [56, 57]. The repair has traditionally taken two major forms: tissue grafting followed by organ transplantation and alloplastic or synthetic material replacement. Both approaches, however, have limitations. Grafting requires second surgical sites with associated morbidity and is restricted by limited amounts of material, especially for organ replacement. Synthetic materials often integrate poorly with host tissue and fail over time due to wear and fatigue or adverse body response

[797]. In addition, all modern orthopedic implants lack three of the most critical abilities of living tissues: (i) self-repairing; (ii) maintaining of blood supply; (iii) self-modifying their structure and properties in response to external aspects such as a mechanical load [798]. Needless to mention, that bones not only possess all of these properties but, in addition, they are self-generating, hierarchical, multifunctional, nonlinear, composite and biodegradable; therefore, the ideal artificial bone grafts must possess similar properties [61].

The last decades have seen a surge in creative ideas and technologies developed to tackle the problem of repairing or replacing diseased and damaged tissues, leading to the emergence of a new field in healthcare technology now referred to as *tissue engineering*, which might be defined as "the creation of new tissue for the therapeutic reconstruction of the human body, by the deliberate and controlled stimulation of selected target cells through a systematic combination of molecular and mechanical signals" [799]. Briefly, this is an interdisciplinary field that exploits a combination of living cells, engineering materials and suitable biochemical factors in a variety of ways to improve, replace, restore, maintain or enhance living tissues and whole organs [800–802]. However, since two of three major components (namely, cells and biochemical factors) of the tissue engineering subject appear to be far beyond the scope of this review, the topic of tissue engineering is narrowed down to the engineering materials prepared from $CaPO_4$ bioceramics only.

Regeneration, rather than a repair, is the central goal of any tissue engineering strategy; therefore, it aims to create tissues and organs de novo [801]. This field of science started more than two decades ago [803, 804] and the famous publication by Langer and Vacanti [805] has greatly contributed to the promotion of tissue engineering research worldwide. The field of tissue engineering, particularly when applied to bone substitutes where tissues often function in a mechanically demanding environment [806–808], requires a collaboration of excellence in cell and molecular biology, biochemistry, material sciences, bioengineering and clinical research. For the success, it is necessary that researchers with expertise in one area have an appreciation of the knowledge and challenges of the other areas. However, since the technical, regulatory and commercial challenges might be substantial, the introduction of new products is likely to be slow [801].

Nowadays, tissue engineering is at full research potential due to the following key advantages: (i) the solutions it provides are long-term, much safer than other options and cost-effective as well; (ii) the need for a donor tissue is minimal, which eliminates the immuno-suppression problems; (iii) the presence of residual foreign material is eliminated as well [809, 810].

5.8.2 Scaffolds and Their Properties

It would be very convenient to both patients and physicians if devastated tissues or organs of patients can be regenerated by simple cell injections to the target sites but such cases are rare. The majority of large-sized tissues and organs with distinct 3D

form require a support for their formation from cells. The support is called scaffold, template and/or artificial extracellular matrix [127, 128, 561, 803, 806–814]. The major function of scaffolds is similar to that of the natural extracellular matrix that assists proliferation, differentiation and biosynthesis of cells. In addition, scaffolds placed at the regeneration sites will prevent disturbing cells from invasion into the sites of action [815, 816]. The role of scaffolds has been perfectly described by a Spanish classical guitarist Andrés Segovia (1893–1987): "When one puts up a building one makes an elaborate scaffold to get everything into its proper place. But when one takes the scaffold down, the building must stand by itself with no trace of the means by which it was erected. That is how a musician should work." However, for the future of tissue engineering, the term 'template' might become more suitable because, according to David F. Williams, the term scaffold "conveys an old fashioned meaning of an inert external structure that is temporarily used to assist in the construction or repair of inanimate objects such as buildings, taking no part in the characteristics of the finished product" ([817], p. 1129).

Therefore, the idea behind tissue engineering is to create or engineer autografts by either expanding autologous cells in vitro guided by a scaffold or implanting an acellular template in vivo and allowing the patient's cells to repair the tissue guided by the scaffold. The first phase is the in vitro formation of a tissue construct by placing the chosen cells and scaffolds in a metabolically and mechanically supportive environment with growth media (in a bioreactor), in which the cells proliferate and elaborate extracellular matrix. It is expected that cells infiltrate into the porous matrix and consequently proliferate and differentiate therein [818, 819]. In the second phase, the construct is implanted in the appropriate anatomic location, where remodeling in vivo is intended to recapitulate the normal functional architecture of an organ or a tissue [820, 821]. The key processes occurring during both in vitro and in vivo phases of the tissue formation and maturation are: (1) cell proliferation, sorting and differentiation, (2) extracellular matrix production and organization, (3) biodegradation of the scaffold, (4) remodeling and potentially growth of the tissue [822].

To achieve the goal of tissue reconstruction, the scaffolds (templates) must meet a number of the specific requirements [127, 128, 811, 812, 817]. For example, a reasonable surface roughness is necessary to facilitate cell seeding and fixation [707, 823–828]. A sufficient mechanical strength and stiffness are mandatory to oppose contraction forces and later for the remodeling of damaged tissues [829, 830]. A high porosity and an adequate pore dimensions (Tables 5.2 and 5.4) are very important to allow cell migration, vascularization, as well as a diffusion of nutrients [448]. A French architect Robert le Ricolais (1894–1977) stated: "The art of structure is where to put the holes". Therefore, to enable proper tissue ingrowth, vascularization and nutrient delivery, scaffolds should have a highly interconnected porous network, formed by a combination of macro- and micropores, in which more than ~60% of the pores should have a size ranging from ~150 to ~400 μm and at least ~20% should be smaller than ~20 μm [16, 448, 456, 457, 463, 557, 558, 563, 565, 571, 593–600, 797, 831–839]. In addition, scaffolds must be manufactured from the materials with controlled biodegradability and/or bioresorbability, such as $CaPO_4$, so that a new bone will eventually replace the scaffold [806, 833, 840].

Table 5.4 A hierarchical pore size distribution that an ideal scaffold should exhibit [949]

Pore sizes of a 3D scaffold	A biochemical effect or function
<1 μm	Interaction with proteins
	Responsible for bioactivity
1–20 μm	Type of cells attracted
	Cellular development
	Orientation and directionality of cellular ingrowth
100–1,000 μm	Cellular growth
	Bone ingrowth
	Predominant function in the mechanical strength
>1,000 μm	Implant functionality
	Implant shape
	Implant esthetics

Furthermore, the degradation by-products of scaffolds must be non-cytotoxic. More to the point, the resorption rate has to coincide as much as possible with the rate of bone formation (i.e., between a few months and about 2 years) [841]. This means that while cells are fabricating their own natural matrix structure around themselves, the scaffold is able to provide a structural integrity within the body and eventually it will break down leaving the newly formed tissue that will take over the mechanical load. However, one should bear in mind that the scaffold's architecture changes with the degradation process and the degradation by-products affect the biological response. Besides, scaffolds should be easily fabricated into a variety of shapes and sizes [842], be malleable to fit irregularly shaped defects, while the fabrication processes should be effortlessly scalable for mass production. In many cases, ease of processability, as well as easiness of conformation and injectability, such as self-setting $CaPO_4$ formulations possess (see Sect. 5.5.1 "Self-Setting (Self-Hardening) Formulations"), can determine the choice of a certain biomaterial. Finally, sterilization with no loss of properties is a crucial step in scaffold production at both a laboratory and an industrial level [806–808]. Thus, each scaffold (template) should fulfill many functions before, during and after implantation.

Many fabrication techniques are available to produce porous $CaPO_4$ scaffolds (Table 5.2) with varying architectural features (for details, see Sects. 5.3.3 "Forming and shaping" and 5.4.4 "Porosity"). In order to achieve the desired properties at the minimum expenses, the production process should be optimized [843]. The main goal is to develop a high potential synthetic bone substitute (so called "smart scaffold") which will not only promote osteoconduction but also osteopromotion, i.e. the ability to enhance of osteoinduction [844]. In the case of $CaPO_4$, a smart scaffold represents a biphasic (HAp/β-TCP ratio of 20/80) formulation with a total porosity of ~73%, constituted of macropores (>100 μm), mesopores (10–100 μm) and a high content (~40%) of micropores (<10 μm) with the crystal dimensions within <0.5–1 μm and the specific surface area ~6 m^2/g [845]. With the advent of $CaPO_4$ in tissue engineering, the search is on for the ultimate option consisting of a

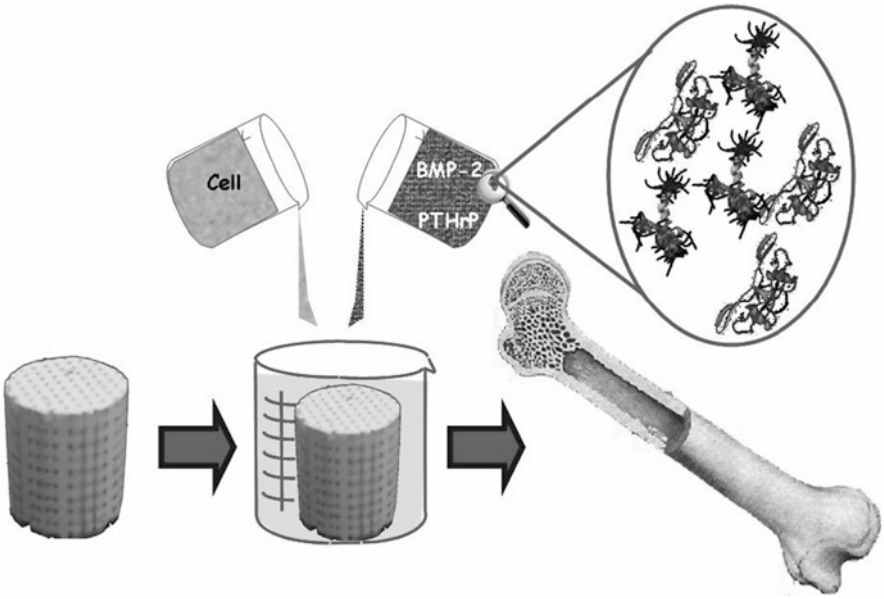

Fig. 5.19 A schematic view of a third generation biomaterial, in which porous $CaPO_4$ bioceramics acts as a scaffold or a template for cells, growth factors, etc. [46]

synthetic smart scaffold impregnated with cells and growth factors. Figure 5.19 schematically depicts a possible fabrication process of such item that, afterwards, will be implanted into a living organism to induce bone regeneration [46].

To finalize this topic, one should mention on fundamental unfeasibility to create so-called "ideal scaffold" for bone grafting. Since bones of human skeleton have very different dimensions, shapes and structures depending on their functions and locations, synthetic bone grafts of various sizes, shapes, porosity, mechanical strength, composition and resorbability appear to be necessary. Therefore, HAp bioceramics of 0–15% porosity is used as both ilium and intervertebral spacers, where a high strength is required, HAp bioceramics of 30–40% porosity is useful as spinous process spacer for laminoplasty, where both bone formation and middle strength are necessary, while HAp bioceramics of 40–60% porosity is useful for the calvarias plate, where a fast bone formation is needed (Fig. 5.20) [543]. Furthermore, defining the optimum parameters for artificial scaffolds is in fact an attempt to find a reasonable compromise between various conflicting functional requirements. Namely, an increased mechanical strength of bone substitutes requires solid and dense structures, while colonization of their surfaces by cells requires interconnected porosity. Additional details and arguments on this subject are well described elsewhere [846], in which the authors concluded: "there is enough evidence to postulate that ideal scaffold architecture does not exist" (p. 478).

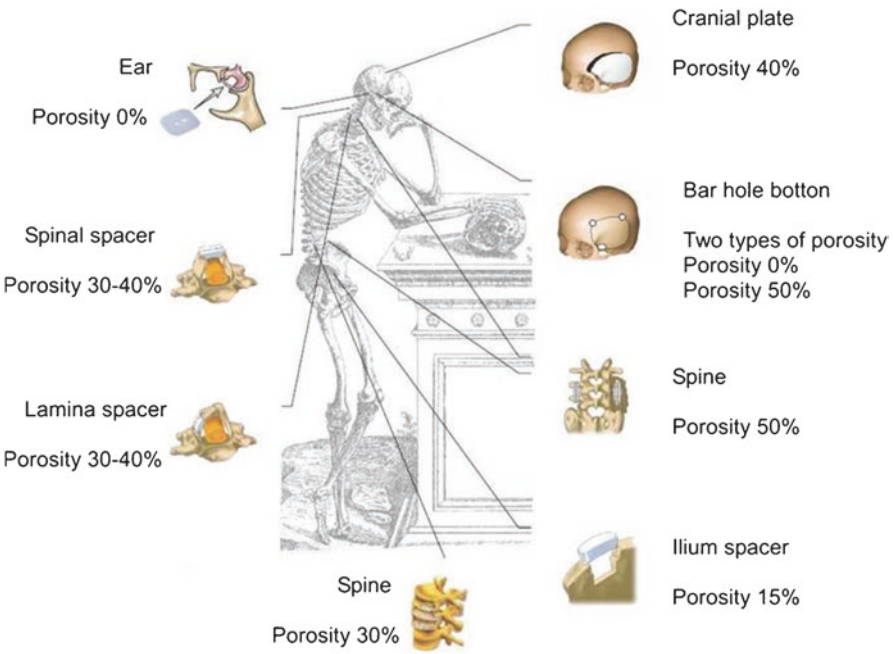

Fig. 5.20 A schematic drawing presenting the potential usage of HAp with various degrees of porosity [543]

5.8.3 Bioceramic Scaffolds from $CaPO_4$

Philosophically, the increase in life expectancy requires biological solutions to all biomedical problems, including orthopedic ones, which were previously managed with mechanical solutions. Therefore, since the end of 1990s, the biomaterials research focuses on tissue regeneration instead of tissue replacement [847]. The alternatives include use hierarchical bioactive scaffolds to engineer in vitro living cellular constructs for transplantation or use bioresorbable bioactive particulates or porous networks to activate in vivo the mechanisms of tissue regeneration [848, 849]. Thus, the aim of $CaPO_4$ is to prepare artificial porous bioceramic scaffolds able to provide the physical and chemical cues to guide cell seeding, differentiation and assembly into 3D tissues of a newly formed bone. Particle sizes, shape and surface roughness of the scaffolds are known to affect cellular adhesion, proliferation and phenotype [707, 823–828]. Additionally, the surface energy might play a role in attracting particular proteins to the bioceramic surface and, in turn, this will affect the cells affinity to the material. More to the point, cells are exceedingly sensitive to the chemical composition and their bone-forming functions can be dependent on grain morphology of the scaffolds. For example, osteoblast functions were found to increase on nanodimensional fibers if compared to nanodimensional spheres

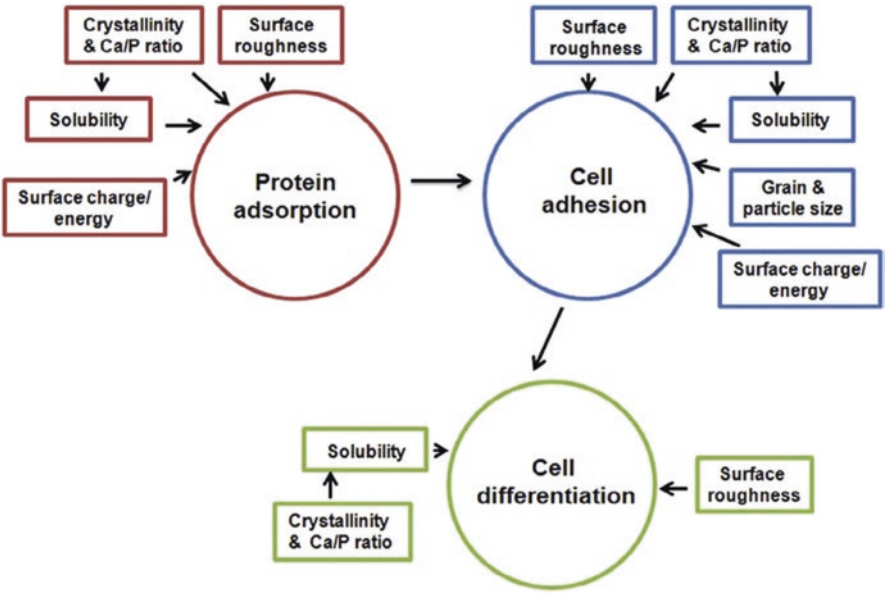

Fig. 5.21 A schematic drawing of the key scaffold properties affecting a cascade of biological processes occurring after $CaPO_4$ implantation [852]

because the former more closely approximated the shape of biological apatite in bones [850]. Besides, a significantly higher osteoblast proliferation on HAp bioceramics sintered at 1,200 °C as compared to that on HAp bioceramics sintered at 800 °C and 1,000 °C was reported [851]. Furthermore, since ions of calcium and orthophosphate are known to regulate bone metabolism, $CaPO_4$ appear to be among the few bone graft substitute materials, which can be considered as a drug. A schematic drawing of the key scaffold properties affecting a cascade of biological processes occurring after $CaPO_4$ implantation is shown in Fig. 5.21 [852].

Thus, to meet the tissue engineering requirements, much attention is devoted to further improvements of $CaPO_4$ bioceramics [853–855]. From the chemical point of view, the developments include synthesis of novel ion-substituted $CaPO_4$ [17–41]. From the material point of view, the major research topics include nanodimensional and nanocrystalline structures [856–859], amorphous compounds [860, 861], (bio) organic/$CaPO_4$ biocomposites and hybrid formulations [361, 862, 863], biphasic, triphasic and multiphasic formulations [79], as well as various types of structures, forms and shapes. The latter comprise fibers, whiskers and filaments [236, 864–877], macro-, micro- and nano-sized spheres, beads and granules [876–896], micro- and nano-sized tubes [897–901], porous 3D scaffolds made of ACP [488, 664, 902], TCP [68, 71, 141–143, 903–906], HAp [148, 462, 463, 505, 533, 534, 843, 907–911] and biphasic formulations [250, 495, 509, 559, 881, 893, 906, 912–917], structures with graded porosity [74, 443, 509, 512, 579, 643–648] and hierarchically

organized ones [918, 919]. Furthermore, an addition of defects through an intensive milling [920, 921] or their removal by a thermal treatment [922] can be used to modify a chemical reactivity of $CaPO_4$. Besides, more attention should be paid to a crystallographically aligned $CaPO_4$ bioceramics [767–772, 923].

In general, there are three principal therapeutic strategies for treating diseased or injured tissues in patients: (i) implantation of freshly isolated or cultured cells; (ii) implantation of tissues assembled in vitro from cells and scaffolds; (iii) in situ tissue regeneration. For cellular implantation, individual cells or small cellular aggregates from the patient or a donor are either injected into the damaged tissue directly or are combined with a degradable scaffold in vitro and then implanted. For tissue implantation, a complete 3D tissue is grown in vitro using patient or donor cells and a bioresorbable scaffold and then is implanted into the patients to replace diseased or damaged tissues. For in situ regeneration, a scaffold implanted directly into the injured tissue stimulates the body's own cells to promote local tissue repair [329, 800]. In any case, simply trapping cells at the particular point on a surface is not enough: the cells must be encouraged to differentiate, which is impossible without the presence of suitable biochemical factors [924]. All previously mentioned clearly indicates that, for the purposes of tissue engineering, $CaPO_4$ bioceramics plays an auxiliary role; namely, it acts as a suitable material to manufacture the appropriate 3D templates, substrates or scaffolds to be colonized by living cells before the successive implantation [844, 845, 925, 926]. The in vitro evaluation of potential $CaPO_4$ scaffolds for tissue engineering has been described elsewhere [927], while the data on the mechanical properties of $CaPO_4$ bioceramics for use in tissue engineering are also available [928–930]. The effect of a HAp-based biomaterial on gene expression in osteoblast-like cells was reported as well [931]. To conclude this part, the excellent biocompatibility of $CaPO_4$ bioceramics, its possible osteoinductivity [152, 571, 596, 680–699] and a high affinity for drugs [54–57, 932–934], proteins and cells [934, 935] make them very functional for the tissue engineering applications. The feasible production of scaffolds with tailored structures and properties opens up a spectacular future for $CaPO_4$ bioceramics [931–936].

5.8.4 A Clinical Experience

To date, there are just a few publications on clinical application of cell-seeded $CaPO_4$ bioceramics for bone tissue engineering of humans. Namely, Quarto et al. [937] were the first to report a treatment of large (4–7 cm) bone defects of the tibia, ulna and humerus in three patients from 16 to 41 years old, where the conventional surgical therapies had failed. The authors implanted a custom-made unresorbable porous HAp scaffolds seeded with in vitro expanded autologous bone marrow stromal cells. In all three patients, radiographs and computed tomographic scans revealed abundant callus formation along the implants and good integration at the interfaces with the host bones by the second month after surgery [937]. In the same year, Vacanti et al. [938] reported the case of a man who had a traumatic avulsion of

the distal phalanx of a thumb. The phalanx was replaced with a specially treated natural coral (porous HAp; 500-pore ProOsteon (see Table 5.3)) implant that was previously seeded with in vitro expanded autologous periosteal cells. The procedure resulted in the functional restoration of a stable and biomechanically sound thumb of normal length, without the pain and complications that are usually associated with harvesting a bone graft.

Morishita et al. [939] treated a defect resulting from surgery of benign bone tumors in three patients using HAp scaffolds seeded with in vitro expanded autologous bone marrow stromal cells after osteogenic differentiation of the cells. Two bone defects in a tibia and one defect in a femur were treated. Although ectopic implants in nude mice were mentioned to show the osteogenicity of the cells, details such as the percentage of the implants containing bone and at what quantities were not reported. Furthermore, cell-seeded $CaPO_4$ scaffolds were found to be superior to autograft, allograft or cell-seeded allograft in terms of bone formation at ectopic implantation sites [940]. Besides, it has been hypothesized that dental follicle cells combined with β-TCP bioceramics might become a novel therapeutic strategy to restore periodontal defects [941]. In still another study, the behavior of human periodontal ligament stem cells on a HAp-coated genipin-chitosan scaffold in vitro was studied followed by evaluation on bone repair in vivo [942]. The study demonstrated the potential of this formulation for bone regeneration.

To finalize this section, one must mention that $CaPO_4$ bioceramics is also used in veterinary orthopedics for favoring animal bone healing in areas, in which bony defects exist [943, 944].

5.9 Conclusions and Outlook

The available chronology of seeking for a suitable bioceramics for bone substitutes is as follows: since the 1950s, the first aim was to use bioinert bioceramics, which had no reaction with living tissues. They included inert and tolerant compounds, which were designed to withstand physiological stress without, however, stimulating any specific cellular responses. Later on, in the 1980s, the trend changed towards exactly the opposite: the idea was to implant bioceramics that reacted with the surrounding tissues by producing newly formed bone (a "responsive" bioceramics because it was able to elicit biological responses). These two stages have been referred to as the first and the second generations of bioceramics, respectively [945] and, currently, both of them have been extensively commercialized. Thus, the majority of the marketable products listed in Table 5.3 belong to the first and the second generations of bone substitute biomaterials. However, the progress keeps going and, in current century, scientists search for the third generation of bioceramics [329], which will be able to "instruct" the physiological environment toward desired biological responses (i.e., bioceramics will be able to regenerate bone tissues by stimulating specific responses at the molecular level) [44, 46]. Since each generation represents an evolution on the requirements and properties of the

biomaterials involved, one should stress that these three generations should not be interpreted as the chronological but the conceptual ones. This means that at present, research and development is still devoted to biomaterials and bioceramics that, according to their properties, could be considered to be of the first or the second generations, because the second generation of bioceramics with added porosity is one of the initial approaches in developing of the third generation of bioceramics [946]. Furthermore, there is another classification of the history of biomaterials introduced by Prof. James M. Anderson. According to Anderson, within 1950–1975 the researchers studied bioMATERIALS, within 1975–2000 they studied BIOMATERIALS and since 2000 the time for BIOmaterials has been coming [947]. Here, the capital letters emphasis the major direction of the research efforts in the complex subject of biomaterials. As bioceramics are biomaterials of the ceramic origin (see Sect. 5.2 "General Knowledge and Definitions"), the Anderson's historical classification appears to be applicable to the bioceramics field as well.

The history development of biomaterials informs that their widespread use experiences two major difficulties. The first is an incomplete understanding of the physical and chemical functioning of biomaterials and of the human response to these materials. Recent advances in material characterization and computer science, as well as in cell and molecular biology are expected to play a significant role in studies of biomaterials. A second difficulty is that many biomaterials do not perform as desirably as we would like. This is not surprising, since many materials used in medicine were not designed for medical purposes. It needs to be mentioned here that biomaterials are expected to perform in our body's internal environment, which is very aggressive. For example, solution pH of body fluids in various tissues varies in the range from 1 to 9. During daily activities, bones are subjected to a stress of ~4 MPa, whereas the tendons and ligaments experience peak stresses in the range of 40–80 MPa. The mean load on a hip joint is up to three times body weight (3,000 N) and peak load during jumping can be as high as ~10 times body weight. More importantly, these stresses are repetitive and fluctuating, depending on the activities, such as standing, sitting, jogging, stretching and climbing. All of these require careful designing of biomaterials in terms of composition, shape, physical and biocompatibility properties. Therefore, a significant challenge is the rational design of human biomaterials based on a systematic evaluation of desired biological, chemical and engineering requirements.

Nevertheless, the field of biomaterials is in the midst of a revolutionary change in which the life sciences are becoming equal in importance to materials science and engineering as the foundation of the field. Simultaneously, advances in engineering (for example nanotechnology) are greatly increasing the sophistication with which biomaterials are designed and have allowed fabrication of biomaterials with increasingly complex functions [948]. Specifically, during last ~40 years, $CaPO_4$ bioceramics has become an integral and vital segment of our modern health care delivery system. In the modern fields of the third generation bioceramics (Hench) or BIOceramics (Anderson), the full potential of $CaPO_4$ has only begun to be recognized. Namely, $CaPO_4$, which were intended as osteoconductive bioceramics in the past, stand for materials to fabricate osteoinductive implants nowadays [152, 571,

596, 680–699]. Some steps in this direction have been already made by fabricating scaffolds for bone tissue engineering through the design of controlled 3D-porous structures and increasing the biological activity through development of novel ion-substituted $CaPO_4$ bioceramics [573, 949]. The future of biosynthetic bone implants will point to better mimicking the autologous bone grafts. Therefore, the composition, structure and molecular surface chemistry of various types of $CaPO_4$ will be tailored to match the specific biological and metabolic requirements of tissues or disease states [950, 951]. This new generation of $CaPO_4$ bioceramics should enhance the quality of life of millions of people, as they grow older.

However, in spite of the great progress, there is still a great potential for major advances to be made in the field of $CaPO_4$ bioceramics. This includes requirements for [952]:

- Improvement of the mechanical performance of existing types of bioceramics.
- Enhanced bioactivity in terms of gene activation.
- Improvement in the performance of biomedical coatings in terms of their mechanical stability and ability to deliver biological agents.
- Development of smart biomaterials capable of combining sensing with bioactivity.
- Development of improved biomimetic composites.

Furthermore, still there are needs for a better understanding of the biological systems. For example, the bonding mechanism between the bone mineral and collagen remains unclear. It is also unclear whether a rapid repair that is elicited by the new generation of bioceramics is a result of the enhancement of mineralization per se or whether there is a more complex signaling process involving proteins in collagen. If we were able to understand the fundamentals of bone response to specific ions and the signals they activate, then we would be able to design better bioceramics for the future [952].

To finalize this review, it is completely obvious that the present status of research and development in the field of $CaPO_4$ bioceramics is still at the starting point for the solution of new problems at the confluence of materials science, biology and medicine, concerned with the restoration of damaged functions in the human organisms. A large increase in active elderly people has dramatically raised the need for load-bearing bone graft substitutes, for example, for bone reconstruction during revision arthroplasty or for the reinforcement of osteoporotic bones. Strategies applied in the last four decades towards this goal have failed. So new strategies, possibly based on self-assembling and/or nanofabrication, will have to be proposed and developed [953]. Furthermore, in future, it should be feasible to design a new generation of gene-activating $CaPO_4$ based scaffolds tailored for specific patients and disease states. Perhaps, sometime bioactive stimuli will be used to activate genes in a preventative treatment to maintain the health of aging tissues. Currently this concept seems impossible. However, we need to remember that only ~40 years ago the concept of a material that would not be rejected by living tissues also seemed impossible [665].

References

1. Ducheyne P, Healy K, Hutmacher DE, Grainger DW, Kirkpatrick CJ, editors. Comprehensive biomaterials, vol. 6. Amsterdam: Elsevier; 2011. 3672 pp
2. Ratner BD, Hoffman AS, Schoen FJ, Lemons JE, editors. Biomaterials science: an introduction to materials in medicine. 3rd ed. Oxford: Academic; 2013. 1573 pp
3. Dorozhkin SV. Calcium orthophosphate-based bioceramics and biocomposites. Weinheim: Wiley-VCH; 2016. 405 pp
4. Dorozhkin SV. Calcium orthophosphates ($CaPO_4$) and dentistry. Bioceram Dev Appl. 2016; 6:096. (28 pages)
5. http://www.prweb.com/releases/bone_grafts/standard_bone_allografts/prweb8953883.htm. Accessed in Dec 2016.
6. Dorozhkin SV. Calcium orthophosphates: applications in nature, biology, and medicine. Singapore: Pan Stanford; 2012. 850 pp
7. Balazsi C, Weber F, Kover Z, Horvath E, Nemeth C. Preparation of calcium-phosphate bioceramics from natural resources. J Eur Ceram Soc. 2007;27:1601–6.
8. Oktar FN. Microstructure and mechanical properties of sintered enamel hydroxyapatite. Ceram Int. 2007;33:1309–14.
9. Han F, Wu L. Preparing and characterizing natural hydroxyapatite ceramics. Ceram Int. 2010;220:281–5.
10. Gergely G, Wéber F, Lukács I, Illés L, Tóth AL, Horváth ZE, Mihály J, Balázsi C. Nano-hydroxyapatite preparation from biogenic raw materials. Cent Eur J Chem. 2010;8:375–81.
11. Mondal S, Mahata S, Kundu S, Mondal B. Processing of natural resourced hydroxyapatite ceramics from fish scale. Adv Appl Ceram. 2010;109:234–9.
12. Lim KT, Suh JD, Kim J, Choung PH, Chung JH. Calcium phosphate bioceramics fabricated from extracted human teeth for tooth tissue engineering. J Biomed Mater Res B Appl Biomater. 2011;99B:399–411.
13. Seo DS, Hwang KH, Yoon SY, Lee JK. Fabrication of hydroxyapatite bioceramics from the recycling of pig bone. J Ceram Proc Res. 2012;13:586–9.
14. Ho WF, Hsu HC, Hsu SK, Hung CW, Wu SC. Calcium phosphate bioceramics synthesized from eggshell powders through a solid state reaction. Ceram Int. 2013;39:6467–73.
15. Piccirillo C, Dunnill CW, Pullar RC, Tobaldi DM, Labrincha JA, Parkin IP, Pintado MM, Castro PML. Calcium phosphate-based materials of natural origin showing photocatalytic activity. J Mater Chem A. 2013;1:6452–61.
16. Salma-Ancane K, Stipniece L, Irbe Z. Effect of biogenic and synthetic starting materials on the structure of hydroxyapatite bioceramics. Ceram Int. 2016;42:9504–10.
17. Ergun C, Webster TJ, Bizios R, Doremus RH. Hydroxylapatite with substituted magnesium, zinc, cadmium, and yttrium. I Structure and microstructure. J Biomed Mater Res. 2002;59: 305–11.
18. Webster TJ, Ergun C, Doremus RH, Bizios R. Hydroxylapatite with substituted magnesium, zinc, cadmium, and yttrium. II. Mechanisms of osteoblast adhesion. J Biomed Mater Res. 2002;59:312–7.
19. Kim SR, Lee JH, Kim YT, Riu DH, Jung SJ, Lee YJ, Chung SC, Kim YH. Synthesis of Si, Mg substituted hydroxyapatites and their sintering behaviors. Biomaterials. 2003;24:1389–98.
20. Landi E, Celotti G, Logroscino G, Tampieri A. Carbonated hydroxyapatite as bone substitute. J Eur Ceram Soc. 2003;23:2931–7.
21. Vallet-Regí M, Arcos D. Silicon substituted hydroxyapatites. A method to upgrade calcium phosphate based implants. J Mater Chem. 2005;15:1509–16.
22. Gbureck U, Thull R, Barralet JE. Alkali ion substituted calcium phosphate cement formation from mechanically activated reactants. J Mater Sci Mater Med. 2005;16:423–7.
23. Gbureck U, Knappe O, Grover LM, Barralet JE. Antimicrobial potency of alkali ion substituted calcium phosphate cements. Biomaterials. 2005;26:6880–6.

24. Reid JW, Tuck L, Sayer M, Fargo K, Hendry JA. Synthesis and characterization of single-phase silicon substituted α-tricalcium phosphate. Biomaterials. 2006;27:2916–25.
25. Tas AC, Bhaduri SB, Jalota S. Preparation of Zn-doped β-tricalcium phosphate (β-$Ca_3(PO_4)_2$) bioceramics. Mater Sci Eng C. 2007;27:394–401.
26. Pietak AM, Reid JW, Stott MJ, Sayer M. Silicon substitution in the calcium phosphate bioceramics. Biomaterials. 2007;28:4023–32.
27. Landi E, Tampieri A, Celotti G, Sprio S, Sandri M, Logroscino G. Sr-substituted hydroxyapatites for osteoporotic bone replacement. Acta Biomater. 2007;3:961–9.
28. Kannan S, Ventura JMG, Ferreira JMF. Synthesis and thermal stability of potassium substituted hydroxyapatites and hydroxyapatite/β-tricalcium phosphate mixtures. Ceram Int. 2007; 33:1489–94.
29. Kannan S, Rebelo A, Lemos AF, Barba A, Ferreira JMF. Synthesis and mechanical behaviour of chlorapatite and chlorapatite/β-TCP composites. J Eur Ceram Soc. 2007;27:2287–94.
30. Kannan S, Goetz-Neunhoeffer F, Neubauer J, Ferreira JMF. Ionic substitutions in biphasic hydroxyapatite and β-tricalcium phosphate mixtures: structural analysis by Rietveld refinement. J Am Ceram Soc. 2008;91:1–12.
31. Meejoo S, Pon-On W, Charnchai S, Amornsakchai T. Substitution of iron in preparation of enhanced thermal property and bioactivity of hydroxyapatite. Adv Mater Res. 2008;55–57: 689–92.
32. Kannan S, Goetz-Neunhoeffer F, Neubauer J, Ferreira JMF. Synthesis and structure refinement of zinc-doped β-tricalcium phosphate powders. J Am Ceram Soc. 2009;92:1592–5.
33. Matsumoto N, Yoshida K, Hashimoto K, Toda Y. Thermal stability of β-tricalcium phosphate doped with monovalent metal ions. Mater Res Bull. 2009;44:1889–94.
34. Boanini E, Gazzano M, Bigi A. Ionic substitutions in calcium phosphates synthesized at low temperature. Acta Biomater. 2010;6:1882–94.
35. Habibovic P, Barralet JE. Bioinorganics and biomaterials: bone repair. Acta Biomater. 2011;7:3013–26.
36. Mellier C, Fayon F, Schnitzler V, Deniard P, Allix M, Quillard S, Massiot D, Bouler JM, Bujoli B, Janvier P. Characterization and properties of novel gallium-doped calcium phosphate ceramics. Inorg Chem. 2011;50:8252–60.
37. Ansar EB, Ajeesh M, Yokogawa Y, Wunderlich W, Varma H. Synthesis and characterization of iron oxide embedded hydroxyapatite bioceramics. J Am Ceram Soc. 2012;95:2695–9.
38. Zhang M, Wu C, Li H, Yuen J, Chang J, Xiao Y. Preparation, characterization and in vitro angiogenic capacity of cobalt substituted β-tricalcium phosphate ceramics. J Mater Chem. 2012;22:21686–94.
39. Shepherd JH, Shepherd DV, Best SM. Substituted hydroxyapatites for bone repair. J Mater Sci Mater Med. 2012;23:2335–47.
40. Ishikawa K. Carbonate apatite bone replacement. Key Eng Mater. 2014;587:17–20.
41. Šupová M. Substituted hydroxyapatites for biomedical applications: a review. Ceram Int. 2015;41:9203–31.
42. Williams DF. The Williams dictionary of biomaterials. Liverpool: Liverpool University Press; 1999. 368 pp
43. Williams DF. On the nature of biomaterials. Biomaterials. 2009;30:5897–909.
44. Bongio M, van den Beucken JJJP, Leeuwenburgh SCG, Jansen JA. Development of bone substitute materials: from 'biocompatible' to 'instructive'. J Mater Chem. 2010;20:8747–59.
45. Mann S, editor. Biomimetic materials chemistry. New York/Chichester: Wiley-VCH; 1996. 400 pp
46. Vallet-Regí M. Bioceramics: where do we come from and which are the future expectations. Key Eng Mater. 2008;377:1–18.
47. Jandt KD. Evolutions, revolutions and trends in biomaterials science – a perspective. Adv Eng Mater. 2007;9:1035–50.
48. Meyers MA, Chen PY, Lin AYM, Seki Y. Biological materials: structure and mechanical properties. Prog Mater Sci. 2008;53:1–206.

49. https://en.wikipedia.org/wiki/Ceramic. Accessed in Dec 2016.
50. Hench LL. Bioceramics. J Am Ceram Soc. 1998;81:1705–28.
51. Hench LL, Day DE, Höland W, Rheinberger VM. Glass and medicine. Int J Appl Glas Sci. 2010;1:104–17.
52. Pinchuk ND, Ivanchenko LA. Making calcium phosphate biomaterials. Powder Metall Metal Ceram. 2003;42:357–71.
53. Heimann RB. Materials science of crystalline bioceramics: a review of basic properties and applications. CMU J. 2002;1:23–46.
54. Tomoda K, Ariizumi H, Nakaji T, Makino K. Hydroxyapatite particles as drug carriers for proteins. Colloid Surf B. 2010;76:226–35.
55. Zamoume O, Thibault S, Regnié G, Mecherri MO, Fiallo M, Sharrock P. Macroporous calcium phosphate ceramic implants for sustained drug delivery. Mater Sci Eng C. 2011;31:1352–6.
56. Bose S, Tarafder S. Calcium phosphate ceramic systems in growth factor and drug delivery for bone tissue engineering: a review. Acta Biomater. 2012;8:1401–21.
57. Arcos D, Vallet-Regí M. Bioceramics for drug delivery. Acta Mater. 2013;61:890–911.
58. Ducheyne P, Qiu Q. Bioactive ceramics: the effect of surface reactivity on bone formation and bone cell function. Biomaterials. 1999;20:2287–303.
59. Dorozhkin SV. Calcium orthophosphates and human beings. A historical perspective from the 1770s until 1940. Biomaterials. 2012;2:53–70.
60. Dorozhkin SV. A detailed history of calcium orthophosphates from 1770-s till 1950. Mater Sci Eng C. 2013;33:3085–110.
61. Vallet-Regí M, González-Calbet JM. Calcium phosphates as substitution of bone tissues. Prog Solid State Chem. 2004;32:1–31.
62. Taş AC, Korkusuz F, Timuçin M, Akkaş N. An investigation of the chemical synthesis and high-temperature sintering behaviour of calcium hydroxyapatite (HA) and tricalcium phosphate (TCP) bioceramics. J Mater Sci Mater Med. 1997;8:91–6.
63. Layrolle P, Ito A, Tateishi T. Sol-gel synthesis of amorphous calcium phosphate and sintering into microporous hydroxyapatite bioceramics. J Am Ceram Soc. 1998;81:1421–8.
64. Engin NO, Tas AC. Manufacture of macroporous calcium hydroxyapatite bioceramics. J Eur Ceram Soc. 1999;19:2569–72.
65. Ahn ES, Gleason NJ, Nakahira A, Ying JY. Nanostructure processing of hydroxyapatite-based bioceramics. Nano Lett. 2001;1:149–53.
66. Khalil KA, Kim SW, Dharmaraj N, Kim KW, Kim HY. Novel mechanism to improve toughness of the hydroxyapatite bioceramics using high-frequency induction heat sintering. J Mater Process Technol. 2007;187–188:417–20.
67. Laasri S, Taha M, Laghzizil A, Hlil EK, Chevalier J. The affect of densification and dehydroxylation on the mechanical properties of stoichiometric hydroxyapatite bioceramics. Mater Res Bull. 2010;45:1433–7.
68. Kitamura M, Ohtsuki C, Ogata S, Kamitakahara M, Tanihara M. Microstructure and bioresorbable properties of α-TCP ceramic porous body fabricated by direct casting method. Mater Trans. 2004;45:983–8.
69. Kawagoe D, Ioku K, Fujimori H, Goto S. Transparent β-tricalcium phosphate ceramics prepared by spark plasma sintering. J Ceram Soc Jpn. 2004;112:462–3.
70. Wang CX, Zhou X, Wang M. Influence of sintering temperatures on hardness and Young's modulus of tricalcium phosphate bioceramic by nanoindentation technique. Mater Charact. 2004;52:301–7.
71. Ioku K, Kawachi G, Nakahara K, Ishida EH, Minagi H, Okuda T, Yonezawa I, Kurosawa H, Ikeda T. Porous granules of β-tricalcium phosphate composed of rod-shaped particles. Key Eng Mater. 2006;309–311:1059–62.
72. Kamitakahara M, Ohtsuki C, Miyazaki T. Review paper: behavior of ceramic biomaterials derived from tricalcium phosphate in physiological condition. J Biomater Appl. 2008;23:197–212.

73. Vorndran E, Klarner M, Klammert U, Grover LM, Patel S, Barralet JE, Gbureck U. 3D powder printing of β-tricalcium phosphate ceramics using different strategies. Adv Eng Mater. 2008;10:B67–71.
74. Descamps M, Duhoo T, Monchau F, Lu J, Hardouin P, Hornez JC, Leriche A. Manufacture of macroporous β-tricalcium phosphate bioceramics. J Eur Ceram Soc. 2008;28:149–57.
75. Liu Y, Kim JH, Young D, Kim S, Nishimoto SK, Yang Y. Novel template-casting technique for fabricating β-tricalcium phosphate scaffolds with high interconnectivity and mechanical strength and in vitro cell responses. J Biomed Mater Res A. 2010;92A:997–1006.
76. Carrodeguas RG, de Aza S. α-tricalcium phosphate: synthesis, properties and biomedical applications. Acta Biomater. 2011;7:3536–46.
77. Zhang Y, Kong D, Feng X. Fabrication and properties of porous β-tricalcium phosphate ceramics prepared using a double slip-casting method using slips with different viscosities. Ceram Int. 2012;38:2991–6.
78. Kim IY, Wen J, Ohtsuki C. Fabrication of α-tricalcium phosphate ceramics through two-step sintering. Key Eng Mater. 2015;631:78–82.
79. Dorozhkin SV. Multiphasic calcium orthophosphate ($CaPO_4$) bioceramics and their biomedical applications. Ceram Int. 2016;42:6529–54.
80. LeGeros RZ, Lin S, Rohanizadeh R, Mijares D, LeGeros JP. Biphasic calcium phosphate bioceramics: preparation, properties and applications. J Mater Sci Mater Med. 2003;14: 201–9.
81. Daculsi G, Laboux O, Malard O, Weiss P. Current state of the art of biphasic calcium phosphate bioceramics. J Mater Sci Mater Med. 2003;14:195–200.
82. Dorozhkina EI, Dorozhkin SV. Mechanism of the solid-state transformation of a calcium-deficient hydroxyapatite (CDHA) into biphasic calcium phosphate (BCP) at elevated temperatures. Chem Mater. 2002;14:4267–72.
83. Daculsi G. Biphasic calcium phosphate granules concept for injectable and mouldable bone substitute. Adv Sci Technol. 2006;49:9–13.
84. Lecomte A, Gautier H, Bouler JM, Gouyette A, Pegon Y, Daculsi G, Merle C. Biphasic calcium phosphate: a comparative study of interconnected porosity in two ceramics. J Biomed Mater Res B Appl Biomater. 2008;84B:1–6.
85. Daculsi G, Baroth S, LeGeros RZ. 20 years of biphasic calcium phosphate bioceramics development and applications. Ceram Eng Sci Proc. 2010;30:45–58.
86. Lukić M, Stojanović Z, Škapin SD, Maček-Kržmanc M, Mitrić M, Marković S, Uskoković D. Dense fine-grained biphasic calcium phosphate (BCP) bioceramics designed by two-step sintering. J Eur Ceram Soc. 2011;31:19–27.
87. Descamps M, Boilet L, Moreau G, Tricoteaux A, Lu J, Leriche A, Lardot V, Cambier F. Processing and properties of biphasic calcium phosphates bioceramics obtained by pressureless sintering and hot isostatic pressing. J Eur Ceram Soc. 2013;33:1263–70.
88. Chen Y, Wang J, Zhu XD, Tang ZR, Yang X, Tan YF, Fan YJ, Zhang XD. Enhanced effect of β-tricalcium phosphate phase on neovascularization of porous calcium phosphate ceramics: in vitro and in vivo evidence. Acta Biomater. 2015;11:435–48.
89. Li Y, Kong F, Weng W. Preparation and characterization of novel biphasic calcium phosphate powders (α-TCP/HA) derived from carbonated amorphous calcium phosphates. J Biomed Mater Res B Appl Biomater. 2009;89B:508–17.
90. Sureshbabu S, Komath M, Varma HK. In situ formation of hydroxyapatite – alpha tricalcium phosphate biphasic ceramics with higher strength and bioactivity. J Am Ceram Soc. 2012; 95:915–24.
91. Radovanović Ž, Jokić B, Veljović D, Dimitrijević S, Kojić V, Petrović R, Janaćković D. Antimicrobial activity and biocompatibility of Ag^+- and Cu^{2+}-doped biphasic hydroxyapatite/α-tricalcium phosphate obtained from hydrothermally synthesized Ag^+- and Cu^{2+}-doped hydroxyapatite. Appl Surf Sci. 2014;307:513–9.
92. Oishi M, Ohtsuki C, Kitamura M, Kamitakahara M, Ogata S, Miyazaki T, Tanihara M. Fabrication and chemical durability of porous bodies consisting of biphasic tricalcium phosphates. Phosphorus Res Bull. 2004;17:95–100.

93. Kamitakahara M, Ohtsuki C, Oishi M, Ogata S, Miyazaki T, Tanihara M. Preparation of porous biphasic tricalcium phosphate and its in vivo behavior. Key Eng Mater. 2005; 284–286:281–4.
94. Wang R, Weng W, Deng X, Cheng K, Liu X, Du P, Shen G, Han G. Dissolution behavior of submicron biphasic tricalcium phosphate powders. Key Eng Mater. 2006;309–311:223–6.
95. Li Y, Weng W, Tam KC. Novel highly biodegradable biphasic tricalcium phosphates composed of α-tricalcium phosphate and β-tricalcium phosphate. Acta Biomater. 2007;3:251–4.
96. Zou C, Cheng K, Weng W, Song C, Du P, Shen G, Han G. Characterization and dissolution–reprecipitation behavior of biphasic tricalcium phosphate powders. J Alloys Compd. 2011;509:6852–8.
97. Xie L, Yu H, Deng Y, Yang W, Liao L, Long Q. Preparation and in vitro degradation study of the porous dual alpha/beta-tricalcium phosphate bioceramics. Mater Res Innov. 2016;20: 530–7.
98. Albuquerque JSV, Nogueira REFQ, da Silva TDP, Lima DO, da Silva MHP. Porous triphasic calcium phosphate bioceramics. Key Eng Mater. 2004;254–256:1021–4.
99. Mendonça F, Lourom LHL, de Campos JB, da Silva MHP. Porous biphasic and triphasic bioceramics scaffolds produced by gelcasting. Key Eng Mater. 2008;361–363:27–30.
100. Vani R, Girija EK, Elayaraja K, Parthiban PS, Kesavamoorthy R, Narayana Kalkura S. Hydrothermal synthesis of porous triphasic hydroxyapatite/(α and β) tricalcium phosphate. J Mater Sci Mater Med. 2009;20(Suppl. 1):S43–8.
101. Ahn MK, Moon YW, Koh YH, Kim HE. Production of highly porous triphasic calcium phosphate scaffolds with excellent in vitro bioactivity using vacuum-assisted foaming of ceramic suspension (VFC) technique. Ceram Int. 2013;39:5879–85.
102. Dorozhkin SV. Self-setting calcium orthophosphate formulations. J Funct Biomater. 2013;4: 209–311.
103. Tamimi F, Sheikh Z, Barralet J. Dicalcium phosphate cements: brushite and monetite. Acta Biomater. 2012;8:474–87.
104. Drouet C, Largeot C, Raimbeaux G, Estournès C, Dechambre G, Combes C, Rey C. Bioceramics: spark plasma sintering (SPS) of calcium phosphates. Adv Sci Technol. 2006; 49:45–50.
105. Ishihara S, Matsumoto T, Onoki T, Sohmura T, Nakahira A. New concept bioceramics composed of octacalcium phosphate (OCP) and dicarboxylic acid-intercalated OCP via hydrothermal hot-pressing. Mater Sci Eng C. 2009;29:1885–8.
106. Barinov SM, Komlev VS. Osteoinductive ceramic materials for bone tissue restoration: octacalcium phosphate (review). Inorg Mater Appl Res. 2010;1:175–81.
107. Moseke C, Gbureck U. Tetracalcium phosphate: synthesis, properties and biomedical applications. Acta Biomater. 2010;6:3815–23.
108. Morimoto S, Anada T, Honda Y, Suzuki O. Comparative study on in vitro biocompatibility of synthetic octacalcium phosphate and calcium phosphate ceramics used clinically. Biomed Mater. 2012;7:045020.
109. Tamimi F, Nihouannen DL, Eimar H, Sheikh Z, Komarova S, Barralet J. The effect of autoclaving on the physical and biological properties of dicalcium phosphate dihydrate bioceramics: brushite vs. monetite. Acta Biomater. 2012;8:3161–9.
110. Suzuki O. Octacalcium phosphate (OCP)-based bone substitute materials. Jpn Dent Sci Rev. 2013;49:58–71.
111. Suzuki O, Anada T. Octacalcium phosphate: a potential scaffold material for controlling activity of bone-related cells in vitro. Mater Sci Forum. 2014;783–786:1366–71.
112. Komlev VS, Barinov SM, Bozo II, Deev RV, Eremin II, Fedotov AY, Gurin AN, Khromova NV, Kopnin PB, Kuvshinova EA, Mamonov VE, Rybko VA, Sergeeva NS, Teterina AY, Zorin VL. Bioceramics composed of octacalcium phosphate demonstrate enhanced biological behavior. ACS Appl Mater Interfaces. 2014;6:16610–20.
113. LeGeros RZ. Calcium phosphates in oral biology and medicine, Monographs in oral science, vol. 15. Basel: Karger; 1991. 201 pp

114. Narasaraju TSB, Phebe DE. Some physico-chemical aspects of hydroxylapatite. J Mater Sci. 1996;31:1–21.
115. Elliott JC. Structure and chemistry of the apatites and other calcium orthophosphates, Studies in inorganic chemistry, vol. 18. Amsterdam: Elsevier; 1994. 389 pp
116. Brown PW, Constantz B, editors. Hydroxyapatite and related materials. Boca Raton: CRC Press; 1994. 343 pp
117. Amjad Z, editor. Calcium phosphates in biological and industrial systems. Boston: Kluwer Academic Publishers; 1997. 529 pp
118. da Silva RV, Bertran CA, Kawachi EY, Camilli JA. Repair of cranial bone defects with calcium phosphate ceramic implant or autogenous bone graft. J Craniofac Surg. 2007;18: 281–6.
119. Okanoue Y, Ikeuchi M, Takemasa R, Tani T, Matsumoto T, Sakamoto M, Nakasu M. Comparison of in vivo bioactivity and compressive strength of a novel superporous hydroxyapatite with beta-tricalcium phosphates. Arch Orthop Trauma Surg. 2012;132:1603–10.
120. Draenert M, Draenert A, Draenert K. Osseointegration of hydroxyapatite and remodeling-resorption of tricalciumphosphate ceramics. Microsc Res Tech. 2013;76:370–80.
121. Okuda T, Ioku K, Yonezawa I, Minagi H, Gonda Y, Kawachi G, Kamitakahara M, Shibata Y, Murayama H, Kurosawa H, Ikeda T. The slow resorption with replacement by bone of a hydrothermally synthesized pure calcium-deficient hydroxyapatite. Biomaterials. 2008;29: 2719–28.
122. Daculsi G, Bouler JM, LeGeros RZ. Adaptive crystal formation in normal and pathological calcifications in synthetic calcium phosphate and related biomaterials. Int Rev Cytol. 1997;172:129–91.
123. Zhu XD, Zhang HJ, Fan HS, Li W, Zhang XD. Effect of phase composition and microstructure of calcium phosphate ceramic particles on protein adsorption. Acta Biomater. 2010;6:1536–41.
124. Bohner M. Calcium orthophosphates in medicine: from ceramics to calcium phosphate cements. Injury. 2000;31(Suppl. 4):D37–47.
125. Ahato I. Reverse engineering the ceramic art of algae. Science. 1999;286:1059–61.
126. Popişter F, Popescu D, Hurgoiu D. A new method for using reverse engineering in case of ceramic tiles. Qual Access Success. 2012;13(Suppl. 5):409–12.
127. Yang S, Leong KF, Du Z, Chua CK. The design of scaffolds for use in tissue engineering. Part II. Rapid prototyping techniques. Tissue Eng. 2002;8:1–11.
128. Yeong WY, Chua CK, Leong KF, Chandrasekaran M. Rapid prototyping in tissue engineering: challenges and potential. Trends Biotechnol. 2004;22:643–52.
129. Ortona A, D'Angelo C, Gianella S, Gaia D. Cellular ceramics produced by rapid prototyping and replication. Mater Lett. 2012;80:95–8.
130. Eufinger H, Wehniöller M, Machtens E, Heuser L, Harders A, Kruse D. Reconstruction of craniofacial bone defects with individual alloplastic implants based on CAD/CAM-manipulated CT-data. J Cranio-Maxillofac Surg. 1995;23:175–81.
131. Klein M, Glatzer C. Individual CAD/CAM fabricated glass-bioceramic implants in reconstructive surgery of the bony orbital floor. Plast Reconstr Surg. 2006;117:565–70.
132. Yin L, Song XF, Song YL, Huang T, Li J. An overview of in vitro abrasive finishing & CAD/CAM of bioceramics in restorative dentistry. Int J Mach Tools Manuf. 2006;46:1013–26.
133. Li J, Hsu Y, Luo E, Khadka A, Hu J. Computer-aided design and manufacturing and rapid prototyped nanoscale hydroxyapatite/polyamide (n-HA/PA) construction for condylar defect caused by mandibular angle ostectomy. Aesthet Plast Surg. 2011;35:636–40.
134. Ciocca L, Donati D, Fantini M, Landi E, Piattelli A, Iezzi G, Tampieri A, Spadari A, Romagnoli N, Scotti R. CAD-CAM-generated hydroxyapatite scaffold to replace the mandibular condyle in sheep: preliminary results. J Biomater Appl. 2013;28:207–18.
135. Yardimci MA, Guceri SI, Danforth SC. Process modeling for fused deposition of ceramics. Ceram Eng Sci Proc. 1996;17:78–82.
136. Bellini A, Shor L, Guceri SI. New developments in fused deposition modeling of ceramics. Rapid Prototyp J. 2005;11:214–20.

137. Tan KH, Chua CK, Leong KF, Cheah CM, Cheang P, Abu Bakar MS, Cha SW. Scaffold development using selective laser sintering of polyetheretherketone-hydroxyapatite biocomposite blends. Biomaterials. 2003;24:3115–23.
138. Wiria FE, Leong KF, Chua CK, Liu Y. Poly-ε-caprolactone/hydroxyapatite for tissue engineering scaffold fabrication via selective laser sintering. Acta Biomater. 2007;3:1–12.
139. Xiao K, Dalgarno KW, Wood DJ, Goodridge RD, Ohtsuki C. Indirect selective laser sintering of apatite-wollostonite glass-ceramic. Proc Inst Mech Eng H. 2008;222:1107–14.
140. Zhou WY, Lee SH, Wang M, Cheung WL, Ip WY. Selective laser sintering of porous tissue engineering scaffolds from poly(L-lactide)/carbonated hydroxyapatite nanocomposite microspheres. J Mater Sci Mater Med. 2008;19:2535–40.
141. Shuai CJ, Li PJ, Feng P, Lu HB, Peng SP, Liu JL. Analysis of transient temperature distribution during the selective laser sintering of β-tricalcium phosphate. Laser Eng. 2013;26: 71–80.
142. Shuai C, Zhuang J, Hu H, Peng S, Liu D, Liu J. In vitro bioactivity and degradability of β-tricalcium phosphate porous scaffold fabricated via selective laser sintering. Biotechnol Appl Biochem. 2013;60:266–73.
143. Shuai C, Zhuang J, Peng S, Wen X. Inhibition of phase transformation from β- to α-tricalcium phosphate with addition of poly (L-lactic acid) in selective laser sintering. Rapid Prototyp J. 2014;20:369–76.
144. Lusquiños F, Pou J, Boutinguiza M, Quintero F, Soto R, León B, Pérez-Amor M. Main characteristics of calcium phosphate coatings obtained by laser cladding. Appl Surf Sci. 2005;247:486–92.
145. Wang DG, Chen CZ, Ma J, Zhang G. In situ synthesis of hydroxyapatite coating by laser cladding. Colloid Surf B. 2008;66:155–62.
146. Comesaña R, Lusquiños F, del Val J, Malot T, López-Álvarez M, Riveiro A, Quintero F, Boutinguiza M, Aubry P, de Carlos A, Pou J. Calcium phosphate grafts produced by rapid prototyping based on laser cladding. J Eur Ceram Soc. 2011;31:29–41.
147. Lv X, Lin X, Hu J, Gao B, Huang W. Phase evolution in calcium phosphate coatings obtained by in situ laser cladding. Mater Sci Eng C. 2012;32:872–7.
148. Leukers B, Gülkan H, Irsen SH, Milz S, Tille C, Schieker M, Seitz H. Hydroxyapatite scaffolds for bone tissue engineering made by 3D printing. J Mater Sci Mater Med. 2005; 16:1121–4.
149. Gbureck U, Hölzel T, Klammert U, Würzler K, Müller FA, Barralet JE. Resorbable dicalcium phosphate bone substitutes prepared by 3D powder printing. Adv Funct Mater. 2007;17: 3940–5.
150. Gbureck U, Hölzel T, Doillon CJ, Müller FA, Barralet JE. Direct printing of bioceramic implants with spatially localized angiogenic factors. Adv Mater. 2007;19:795–800.
151. Khalyfa A, Vogt S, Weisser J, Grimm G, Rechtenbach A, Meyer W, Schnabelrauch M. Development of a new calcium phosphate powder-binder system for the 3D printing of patient specific implants. J Mater Sci Mater Med. 2007;18:909–16.
152. Habibovic P, Gbureck U, Doillon CJ, Bassett DC, van Blitterswijk CA, Barralet JE. Osteoconduction and osteoinduction of low-temperature 3D printed bioceramic implants. Biomaterials. 2008;29:944–53.
153. Fierz FC, Beckmann F, Huser M, Irsen SH, Leukers B, Witte F, Degistirici O, Andronache A, Thie M, Müller B. The morphology of anisotropic 3D-printed hydroxyapatite scaffolds. Biomaterials. 2008;29:3799–806.
154. Seitz H, Deisinger U, Leukers B, Detsch R, Ziegler G. Different calcium phosphate granules for 3-D printing of bone tissue engineering scaffolds. Adv Eng Mater. 2009;11:B41–6.
155. Suwanprateeb J, Sanngam R, Panyathanmaporn T. Influence of raw powder preparation routes on properties of hydroxyapatite fabricated by 3D printing technique. Mater Sci Eng C. 2010;30:610–7.
156. Butscher A, Bohner M, Roth C, Ernstberger A, Heuberger R, Doebelin N, von Rohr RP, Müller R. Printability of calcium phosphate powders for three-dimensional printing of tissue engineering scaffolds. Acta Biomater. 2012;8:373–85.

157. Butscher A, Bohner M, Doebelin N, Galea L, Loeffel O, Müller R. Moisture based three-dimensional printing of calcium phosphate structures for scaffold engineering. Acta Biomater. 2013;9:5369–78.
158. Butscher A, Bohner M, Doebelin N, Hofmann S, Müller R. New depowdering-friendly designs for three-dimensional printing of calcium phosphate bone substitutes. Acta Biomater. 2013;9:9149–58.
159. Tarafder S, Davies NM, Bandyopadhyay A, Bose S. 3D printed tricalcium phosphate bone tissue engineering scaffolds: effect of SrO and MgO doping on in vivo osteogenesis in a rat distal femoral defect model. Biomater Sci. 2013;1:1250–9.
160. Maazouz Y, Montufar EB, Guillem-Marti J, Fleps I, Öhman C, Persson C, Ginebra MP. Robocasting of biomimetic hydroxyapatite scaffolds using self-setting inks. J Mater Chem B. 2014;2:5378–86.
161. Akkineni AR, Luo Y, Schumacher M, Nies B, Lode A, Gelinsky M. 3D plotting of growth factor loaded calcium phosphate cement scaffolds. Acta Biomater. 2015;27:264–74.
162. Trombetta R, Inzana JA, Schwarz EM, Kates SL, Awad HA. 3D printing of calcium phosphate ceramics for bone tissue engineering and drug delivery. Ann Biomed Eng. 2016;45: 23–44. (Early view)
163. Porter NL, Pilliar RM, Grynpas MD. Fabrication of porous calcium polyphosphate implants by solid freeform fabrication: a study of processing parameters and in vitro degradation characteristics. J Biomed Mater Res. 2001;56:504–15.
164. Leong KF, Cheah CM, Chua CK. Solid freeform fabrication of three-dimensional scaffolds for engineering replacement tissues and organs. Biomaterials. 2003;24:2363–78.
165. Calvert JW, Brenner KA, Mooney MP, Kumta P, Weiss LE. Cellular fusion of hydroxyapatite layers: solid freeform fabrication of synthetic bone grafts. Riv Ital Chir Plast. 2004;36: 145–50.
166. Jongpaiboonkit L, Lin CY, Krebsbach PH, Hollister SJ, Halloran JW. Mechanical behavior of complex 3D calcium phosphate cement scaffolds fabricated by indirect solid freeform fabrication in vivo. Key Eng Mater. 2006;309–311:957–60.
167. Dellinger JG, Cesarano 3rd J, Jamison RD. Robotic deposition of model hydroxyapatite scaffolds with multiple architectures and multiscale porosity for bone tissue engineering. J Biomed Mater Res A. 2007;82A:383–94.
168. Shanjani Y, de Croos JNA, Pilliar RM, Kandel RA, Toyserkani E. Solid freeform fabrication and characterization of porous calcium polyphosphate structures for tissue engineering purposes. J Biomed Mater Res B Appl Biomater. 2010;93B:510–9.
169. Kim J, Lim D, Kim YH, Koh YH, Lee MH, Han I, Lee SJ, Yoo OS, Kim HS, Park JC. A comparative study of the physical and mechanical properties of porous hydroxyapatite scaffolds fabricated by solid freeform fabrication and polymer replication method. Int J Precis Eng Manuf. 2011;12:695–701.
170. Shanjani Y, Hu Y, Toyserkani E, Grynpas M, Kandel RA, Pilliar RM. Solid freeform fabrication of porous calcium polyphosphate structures for bone substitute applications: in vivo studies. J Biomed Mater Res B Appl Biomater. 2013;101B:972–80.
171. Kwon BJ, Kim J, Kim YH, Lee MH, Baek HS, Lee DH, Kim HL, Seo HJ, Lee MH, Kwon SY, Koo MA, Park JC. Biological advantages of porous hydroxyapatite scaffold made by solid freeform fabrication for bone tissue regeneration. Artif Organs. 2013;37:663–70.
172. Li X, Li D, Lu B, Wang C. Fabrication of bioceramic scaffolds with pre-designed internal architecture by gel casting and indirect stereolithography techniques. J Porous Mater. 2008;15:667–71.
173. Maeda C, Tasaki S, Kirihara S. Accurate fabrication of hydroxyapatite bone models with porous scaffold structures by using stereolithography. IOP Conf Ser Mater Sci Eng. 2011;18:072017.
174. Bian W, Li D, Lian Q, Li X, Zhang W, Wang K, Jin Z. Fabrication of a bio-inspired beta-tricalcium phosphate/collagen scaffold based on ceramic stereolithography and gel casting for osteochondral tissue engineering. Rapid Prototyp J. 2012;18:68–80.

175. Ronca A, Ambrosio L, Grijpma DW. Preparation of designed poly(D,L-lactide)/nanosized hydroxyapatite composite structures by stereolithography. Acta Biomater. 2013;9:5989–96.
176. Saber-Samandari S, Gross KA. The use of thermal printing to control the properties of calcium phosphate deposits. Biomaterials. 2010;31:6386–93.
177. de Meira CR, Gomes DT, Braga FJC, de Moraes Purquerio B, Fortulan CA. Direct manufacture of hydroxyapatite scaffolds using blue laser. Mater Sci Forum. 2015;805:128–33.
178. Narayan RJ, Jin C, Doraiswamy A, Mihailescu IN, Jelinek M, Ovsianikov A, Chichkov B, Chrisey DB. Laser processing of advanced bioceramics. Adv Eng Mater. 2005;7:1083–98.
179. Nather A, editor. Bone grafts and bone substitutes: basic science and clinical applications. Singapore: World Scientific; 2005. 592 pp
180. Bártolo P, Bidanda B, editors. Bio-materials and prototyping applications in medicine. New York: Springer; 2008. 216 pp
181. Kokubo T, editor. Bioceramics and their clinical applications. Abington: Woodhead Publishing; 2008. 784 pp
182. Narayan R, editor. Biomedical materials. New York: Springer; 2009. 566 pp
183. Raksujarit A, Pengpat K, Rujijanagul G, Tunkasiri T. Processing and properties of nanoporous hydroxyapatite ceramics. Mater Des. 2010;31:1658–60.
184. Park J. Bioceramics: properties, characterizations, and applications. New York: Springer; 2008. 364 pp
185. Rodríguez-Lorenzo LM, Vallet-Regí M, Ferreira JMF. Fabrication of hydroxyapatite bodies by uniaxial pressing from a precipitated powder. Biomaterials. 2001;22:583–8.
186. Miranda P, Pajares A, Saiz E, Tomsia AP, Guiberteau F. Mechanical behaviour under uniaxial compression of robocast calcium phosphate scaffolds. Eur Cells Mater. 2007;14(Suppl. 1):79.
187. Nazarpak MH, Solati-Hashjin M, Moztarzadeh F. Preparation of hydroxyapatite ceramics for biomedical applications. J Ceram Process Res. 2009;10:54–7.
188. Uematsu K, Takagi M, Honda T, Uchida N, Saito K. Transparent hydroxyapatite prepared by hot isostatic pressing of filter cake. J Am Ceram Soc. 1989;72:1476–8.
189. Itoh H, Wakisaka Y, Ohnuma Y, Kuboki Y. A new porous hydroxyapatite ceramic prepared by cold isostatic pressing and sintering synthesized flaky powder. Dent Mater. 1994;13:25–35.
190. Takikawa K, Akao M. Fabrication of transparent hydroxyapatite and application to bone marrow derived cell/hydroxyapatite interaction observation in-vivo. J Mater Sci Mater Med. 1996;7:439–45.
191. Gautier H, Merle C, Auget JL, Daculsi G. Isostatic compression, a new process for incorporating vancomycin into biphasic calcium phosphate: comparison with a classical method. Biomaterials. 2000;21:243–9.
192. Tadic D, Epple M. Mechanically stable implants of synthetic bone mineral by cold isostatic pressing. Biomaterials. 2003;24:4565–71.
193. Onoki T, Hashida T. New method for hydroxyapatite coating of titanium by the hydrothermal hot isostatic pressing technique. Surf Coat Technol. 2006;200:6801–7.
194. Ergun C. Enhanced phase stability in hydroxylapatite/zirconia composites with hot isostatic pressing. Ceram Int. 2011;37:935–42.
195. Ehsani N, Ruys AJ, Sorrell CC. Hot isostatic pressing (HIPing) of fecralloy-reinforced hydroxyapatite. J Biomim Biomater Tissue Eng. 2013;17:87–102.
196. Irsen SH, Leukers B, Höckling C, Tille C, Seitz H. Bioceramic granulates for use in 3D printing: process engineering aspects. Materwiss Werksttech. 2006;37:533–7.
197. Hsu YH, Turner IG, Miles AW. Fabrication and mechanical testing of porous calcium phosphate bioceramic granules. J Mater Sci Mater Med. 2007;18:1931–7.
198. Zyman ZZ, Glushko V, Dedukh N, Malyshkina S, Ashukina N. Porous calcium phosphate ceramic granules and their behaviour in differently loaded areas of skeleton. J Mater Sci Mater Med. 2008;19:2197–205.
199. Viana M, Désiré A, Chevalier E, Champion E, Chotard R, Chulia D. Interest of high shear wet granulation to produce drug loaded porous calcium phosphate pellets for bone filling. Key Eng Mater. 2009;396–398:535–8.

200. Chevalier E, Viana M, Cazalbou S, Chulia D. Comparison of low-shear and high-shear granulation processes: effect on implantable calcium phosphate granule properties. Drug Dev Ind Pharm. 2009;35:1255–63.
201. Lakevics V, Locs J, Loca D, Stepanova V, Berzina-Cimdina L, Pelss J. Bioceramic hydroxyapatite granules for purification of biotechnological products. Adv Mater Res. 2011;284–286: 1764–9.
202. Camargo NHA, Franczak PF, Gemelli E, da Costa BD, de Moraes AN. Characterization of three calcium phosphate microporous granulated bioceramics. Adv Mater Res. 2014;936:687–94.
203. Reikerås O, Johansson CB, Sundfeldt M. Bone ingrowths to press-fit and loose-fit implants: comparisons between titanium and hydroxyapatite. J Long-Term Eff Med Implants. 2006; 16:157–64.
204. Rao RR, Kannan TS. Dispersion and slip casting of hydroxyapatite. J Am Ceram Soc. 2001;84:1710–6.
205. Sakka Y, Takahashi K, Matsuda N, Suzuki TS. Effect of milling treatment on texture development of hydroxyapatite ceramics by slip casting in high magnetic field. Mater Trans. 2007;48:2861–6.
206. Zhang Y, Yokogawa Y, Feng X, Tao Y, Li Y. Preparation and properties of bimodal porous apatite ceramics through slip casting using different hydroxyapatite powders. Ceram Int. 2010;36:107–13.
207. Zhang Y, Kong D, Yokogawa Y, Feng X, Tao Y, Qiu T. Fabrication of porous hydroxyapatite ceramic scaffolds with high flexural strength through the double slip-casting method using fine powders. J Am Ceram Soc. 2012;95:147–52.
208. Hagio T, Yamauchi K, Kohama T, Matsuzaki T, Iwai K. Beta tricalcium phosphate ceramics with controlled crystal orientation fabricated by application of external magnetic field during the slip casting process. Mater Sci Eng C. 2013;33:2967–70.
209. Marçal RLSB, da Rocha DN, da Silva MHP. Slip casting used as a forming technique for hydroxyapatite processing. Key Eng Mater. 2017;720:219–22.
210. Sepulveda P, Ortega FS, Innocentini MDM, Pandolfelli VC. Properties of highly porous hydroxyapatite obtained by the gel casting of foams. J Am Ceram Soc. 2000;83:3021–4.
211. Padilla S, Vallet-Regí M, Ginebra MP, Gil FJ. Processing and mechanical properties of hydroxyapatite pieces obtained by the gel-casting method. J Eur Ceram Soc. 2005;25: 375–83.
212. Woesz A, Rumpler M, Stampfl J, Varga F, Fratzl-Zelman N, Roschger P, Klaushofer K, Fratzl P. Towards bone replacement materials from calcium phosphates via rapid prototyping and ceramic gel casting. Mater Sci Eng C. 2005;25:181–6.
213. Sánchez-Salcedo S, Werner J, Vallet-Regí M. Hierarchical pore structure of calcium phosphate scaffolds by a combination of gel-casting and multiple tape-casting methods. Acta Biomater. 2008;4:913–22.
214. Chen B, Zhang T, Zhang J, Lin Q, Jiang D. Microstructure and mechanical properties of hydroxyapatite obtained by gel-casting process. Ceram Int. 2008;34:359–64.
215. Marcassoli P, Cabrini M, Tirillò J, Bartuli C, Palmero P, Montanaro L. Mechanical characterization of hydroxiapatite micro/macro-porous ceramics obtained by means of innovative gel-casting process. Key Eng Mater. 2010;417–418:565–8.
216. Kim TW, Ryu SC, Kim BK, Yoon SY, Park HC. Porous hydroxyapatite scaffolds containing calcium phosphate glass-ceramics processed using a freeze/gel-casting technique. Met Mater Int. 2014;20:135–40.
217. Asif A, Nazir R, Riaz T, Ashraf N, Zahid S, Shahid R, Ur-Rehman A, Chaudhry AA, Ur Rehman I. Influence of processing parameters and solid concentration on microstructural properties of gel-casted porous hydroxyapatite. J Porous Mater. 2014;21:31–7.
218. Dash SR, Sarkar R, Bhattacharyya S. Gel casting of hydroxyapatite with naphthalene as pore former. Ceram Int. 2015;41:3775–90.
219. Fomin AS, Barinov SM, Ievlev VM, Smirnov VV, Mikhailov BP, Belonogov EK, Drozdova NA. Nanocrystalline hydroxyapatite ceramics produced by low-temperature sintering after high-pressure treatment. Dokl Chem. 2008;418:22–5.

220. Zhang J, Yin HM, Hsiao BS, Zhong GJ, Li ZM. Biodegradable poly(lactic acid)/hydroxyl apatite 3D porous scaffolds using high-pressure molding and salt leaching. J Mater Sci. 2014;49:1648–58.
221. Kankawa Y, Kaneko Y, Saitou K. Injection molding of highly-purified hydroxylapatite and TCP utilizing solid phase reaction method. J Ceram Soc Jpn. 1991;99:438–42.
222. Cihlář J, Trunec M. Injection moulded hydroxyapatite ceramics. Biomaterials. 1996;17: 1905–11.
223. Jewad R, Bentham C, Hancock B, Bonfield W, Best SM. Dispersant selection for aqueous medium pressure injection moulding of anhydrous dicalcium phosphate. J Eur Ceram Soc. 2008;28:547–53.
224. Kwon SH, Jun YK, Hong SH, Lee IS, Kim HE, Won YY. Calcium phosphate bioceramics with various porosities and dissolution rates. J Am Ceram Soc. 2002;85:3129–31.
225. Fooki ACBM, Aparecida AH, Fideles TB, Costa RC, Fook MVL. Porous hydroxyapatite scaffolds by polymer sponge method. Key Eng Mater. 2009;396–398:703–6.
226. Sopyan I, Kaur J. Preparation and characterization of porous hydroxyapatite through polymeric sponge method. Ceram Int. 2009;35:3161–8.
227. Bellucci D, Cannillo V, Sola A. Shell scaffolds: a new approach towards high strength bioceramic scaffolds for bone regeneration. Mater Lett. 2010;64:203–6.
228. Cunningham E, Dunne N, Walker G, Maggs C, Wilcox R, Buchanan F. Hydroxyapatite bone substitutes developed via replication of natural marine sponges. J Mater Sci Mater Med. 2010;21:2255–61.
229. Sung JH, Shin KH, Koh YH, Choi WY, Jin Y, Kim HE. Preparation of the reticulated hydroxyapatite ceramics using carbon-coated polymeric sponge with elongated pores as a novel template. Ceram Int. 2011;37:2591–6.
230. Mishima FD, Louro LHL, Moura FN, Gobbo LA, da Silva MHP. Hydroxyapatite scaffolds produced by hydrothermal deposition of monetite on polyurethane sponges substrates. Key Eng Mater. 2012;493–494:820–5.
231. Hannickel A, da Silva MHP. Novel bioceramic scaffolds for regenerative medicine. Bioceram Dev Appl. 2015;5:1000082.
232. Das S, Kumar S, Doloi B, Bhattacharyya B. Experimental studies of ultrasonic machining on hydroxyapatite bio-ceramics. Int J Adv Manuf Technol. 2016;86:829–39.
233. Velayudhan S, Ramesh P, Sunny MC, Varma HK. Extrusion of hydroxyapatite to clinically significant shapes. Mater Lett. 2000;46:142–6.
234. Yang HY, Thompson I, Yang SF, Chi XP, Evans JRG, Cook RJ. Dissolution characteristics of extrusion freeformed hydroxyapatite – tricalcium phosphate scaffolds. J Mater Sci Mater Med. 2008;19:3345–53.
235. Yang S, Yang H, Chi X, Evans JRG, Thompson I, Cook RJ, Robinson P. Rapid prototyping of ceramic lattices for hard tissue scaffolds. Mater Des. 2008;29:1802–9.
236. Yang HY, Chi XP, Yang S, Evans JRG. Mechanical strength of extrusion freeformed calcium phosphate filaments. J Mater Sci Mater Med. 2010;21:1503–10.
237. Cortez PP, Atayde LM, Silva MA, da Silva PA, Fernandes MH, Afonso A, Lopes MA, Maurício AC, Santos JD. Characterization and preliminary in vivo evaluation of a novel modified hydroxyapatite produced by extrusion and spheronization techniques. J Biomed Mater Res B Appl Biomater. 2011;99B:170–9.
238. Lim S, Chun S, Yang D, Kim S. Comparison study of porous calcium phosphate blocks prepared by piston and screw type extruders for bone scaffold. Tissue Eng Regen Med. 2012;9:51–5.
239. Blake DM, Tomovic S, Jyung RW. Extrusion of hydroxyapatite ossicular prosthesis. Ear Nose Throat J. 2013;92:490–4.
240. Muthutantri AI, Huang J, Edirisinghe MJ, Bretcanu O, Boccaccini AR. Dipping and electrospraying for the preparation of hydroxyapatite foams for bone tissue engineering. Biomed Mater. 2008;3:25009. (14 pages)
241. Roncari E, Galassi C, Pinasco P. Tape casting of porous hydroxyapatite ceramics. J Mater Sci Lett. 2000;19:33–5.

242. Tian T, Jiang D, Zhang J, Lin Q. Aqueous tape casting process for hydroxyapatite. J Eur Ceram Soc. 2007;27:2671–7.
243. Tanimoto Y, Shibata Y, Murakami A, Miyazaki T, Nishiyama N. Effect of varying HAP/TCP ratios in tape-cast biphasic calcium phosphate ceramics on responcce in vitro. J Hard Tissue Biol. 2009;18:71–6.
244. Tanimoto Y, Teshima M, Nishiyama N, Yamaguchi M, Hirayama S, Shibata Y, Miyazaki T. Tape-cast and sintered β-tricalcium phosphate laminates for biomedical applications: effect of milled Al_2O_3 fiber additives on microstructural and mechanical properties. J Biomed Mater Res B Appl Biomater. 2012;100B:2261–8.
245. Khamkasem C, Chaijaruwanich A. Effect of binder/plasticizer ratios in aqueous-based tape casting on mechanical properties of bovine hydroxyapatite tape. Ferroelectrics. 2013;455:129–35.
246. Suzuki S, Itoh K, Ohgaki M, Ohtani M, Ozawa M. Preparation of sintered filter for ion exchange by a doctor blade method with aqueous slurries of needlelike hydroxyapatite. Ceram Int. 1999;25:287–91.
247. Nishikawa H, Hatanaka R, Kusunoki M, Hayami T, Hontsu S. Preparation of freestanding hydroxyapatite membranes excellent biocompatibility and flexibility. Appl Phys Express. 2008;1:088001.
248. Padilla S, Roman J, Vallet-Regí M. Synthesis of porous hydroxyapatites by combination of gel casting and foams burn out methods. J Mater Sci Mater Med. 2002;13:1193–7.
249. Yang TY, Lee JM, Yoon SY, Park HC. Hydroxyapatite scaffolds processed using a TBA-based freeze-gel casting/polymer sponge technique. J Mater Sci Mater Med. 2010;21: 1495–502.
250. Baradararan S, Hamdi M, Metselaar IH. Biphasic calcium phosphate (BCP) macroporous scaffold with different ratios of HA/β-TCP by combination of gel casting and polymer sponge methods. Adv Appl Ceram. 2012;111:367–73.
251. Inoue K, Sassa K, Yokogawa Y, Sakka Y, Okido M, Asai S. Control of crystal orientation of hydroxyapatite by imposition of a high magnetic field. Mater Trans. 2003;44:1133–7.
252. Iwai K, Akiyama J, Tanase T, Asai S. Alignment of HAp crystal using a sample rotation in a static magnetic field. Mater Sci Forum. 2007;539–543(Part 1):716–9.
253. Iwai K, Akiyama J, Asai S. Structure control of hydroxyapatite using a magnetic field. Mater Sci Forum. 2007;561–565(Part 2):1565–8.
254. Sakka Y, Takahashi K, Suzuki TS, Ito S, Matsuda N. Texture development of hydroxyapatite ceramics by colloidal processing in a high magnetic field followed by sintering. Mater Sci Eng A. 2008;475:27–33.
255. Fleck NA. On the cold compaction of powders. J Mech Phys Solids. 1995;43:1409–31.
256. Kang J, Hadfield M. Parameter optimization by Taguchi methods for finishing advanced ceramic balls using a novel eccentric lapping machine. Proc Inst Mech Eng B. 2001;215: 69–78.
257. Kulkarni SS, Yong Y, Rys MJ, Lei S. Machining assessment of nano-crystalline hydroxyapatite bio-ceramic. J Manuf Process. 2013;15:666–72.
258. Kurella A, Dahotre NB. Surface modification for bioimplants: the role of laser surface engineering. J Biomater Appl. 2005;20:5–50.
259. Oktar FN, Genc Y, Goller G, Erkmen EZ, Ozyegin LS, Toykan D, Demirkiran H, Haybat H. Sintering of synthetic hydroxyapatite compacts. Key Eng Mater. 2004;264–268:2087–90.
260. Georgiou G, Knowles JC, Barralet JE. Dynamic shrinkage behavior of hydroxyapatite and glass-reinforced hydroxyapatites. J Mater Sci. 2004;39:2205–8.
261. Fellah BH, Layrolle P. Sol-gel synthesis and characterization of macroporous calcium phosphate bioceramics containing microporosity. Acta Biomater. 2009;5:735–42.
262. Dudek A, Kolan C. Assessments of shrinkage degree in bioceramic sinters HA+ZrO_2. Diffus Defect Data B Solid State Phenom. 2010;165:25–30.
263. Ben Ayed F, Bouaziz J, Bouzouita K. Pressureless sintering of fluorapatite under oxygen atmosphere. J Eur Ceram Soc. 2000;20:1069–76.

264. He Z, Ma J, Wang C. Constitutive modeling of the densification and the grain growth of hydroxyapatite ceramics. Biomaterials. 2005;26:1613–21.
265. Rahaman MN. Sintering of ceramics. Boca Raton: CRC Press; 2007. 388 pp
266. Monroe EA, Votava W, Bass DB, McMullen J. New calcium phosphate ceramic material for bone and tooth implants. J Dent Res. 1971;50:860–1.
267. Landi E, Tampieri A, Celotti G, Sprio S. Densification behaviour and mechanisms of synthetic hydroxyapatites. J Eur Ceram Soc. 2000;20:2377–87.
268. Chen S, Wang W, Kono H, Sassa K, Asai S. Abnormal grain growth of hydroxyapatite ceramic sintered in a high magnetic field. J Cryst Growth. 2010;312:323–6.
269. Ruys AJ, Wei M, Sorrell CC, Dickson MR, Brandwood A, Milthorpe BK. Sintering effect on the strength of hydroxyapatite. Biomaterials. 1995;16:409–15.
270. van Landuyt P, Li F, Keustermans JP, Streydio JM, Delannay F, Munting E. The influence of high sintering temperatures on the mechanical properties of hydroxylapatite. J Mater Sci Mater Med. 1995;6:8–13.
271. Pramanik S, Agarwal AK, Rai KN, Garg A. Development of high strength hydroxyapatite by solid-state-sintering process. Ceram Int. 2007;33:419–26.
272. Haberko K, Bućko MM, Brzezińska-Miecznik J, Haberko M, Mozgawa W, Panz T, Pyda A, Zarebski J. Natural hydroxyapatite – its behaviour during heat treatment. J Eur Ceram Soc. 2006;26:537–42.
273. Haberko K, Bućko MM, Mozgawa W, Pyda A, Brzezińska-Miecznik J, Carpentier J. Behaviour of bone origin hydroxyapatite at elevated temperatures and in O_2 and CO_2 atmospheres. Ceram Int. 2009;35:2537–40.
274. Janus AM, Faryna M, Haberko K, Rakowska A, Panz T. Chemical and microstructural characterization of natural hydroxyapatite derived from pig bones. Microchim Acta. 2008;161:349–53.
275. Bahrololoom ME, Javidi M, Javadpour S, Ma J. Characterisation of natural hydroxyapatite extracted from bovine cortical bone ash. J Ceram Process Res. 2009;10:129–38.
276. Mostafa NY. Characterization, thermal stability and sintering of hydroxyapatite powders prepared by different routes. Mater Chem Phys. 2005;94:333–41.
277. Suchanek W, Yashima M, Kakihana M, Yoshimura M. Hydroxyapatite ceramics with selected sintering additives. Biomaterials. 1997;18:923–33.
278. Kalita SJ, Bose S, Bandyopadhyay A, Hosick HL. Oxide based sintering additives for HAp ceramics. Ceram Trans. 2003;147:63–72.
279. Kalita SJ, Bose S, Hosick HL, Bandyopadhyay A. $CaO–P_2O_5–Na_2O$-based sintering additives for hydroxyapatite (HAp) ceramics. Biomaterials. 2004;25:2331–9.
280. Safronova TV, Putlyaev VI, Shekhirev MA, Tretyakov YD, Kuznetsov AV, Belyakov AV. Densification additives for hydroxyapatite ceramics. J Eur Ceram Soc. 2009;29:1925–32.
281. Muralithran G, Ramesh S. Effects of sintering temperature on the properties of hydroxyapatite. Ceram Int. 2000;26:221–30.
282. Eskandari A, Aminzare M, Hassani H, Barounian H, Hesaraki S, Sadrnezhaad SK. Densification behavior and mechanical properties of biomimetic apatite nanocrystals. Curr Nanosci. 2011;7:776–80.
283. Ramesh S, Tolouei R, Tan CY, Aw KL, Yeo WH, Sopyan I, Teng WD. Sintering of hydroxyapatite ceramic produced by wet chemical method. Adv Mater Res. 2011;264–265:1856–61.
284. Ou SF, Chiou SY, Ou KL. Phase transformation on hydroxyapatite decomposition. Ceram Int. 2013;39:3809–16.
285. Bernache-Assollant D, Ababou A, Champion E, Heughebaert M. Sintering of calcium phosphate hydroxyapatite $Ca_{10}(PO_4)_6(OH)_2$ I. Calcination and particle growth. J Eur Ceram Soc. 2003;23:229–41.
286. Ramesh S, Tan CY, Bhaduri SB, Teng WD, Sopyan I. Densification behaviour of nanocrystalline hydroxyapatite bioceramics. J Mater Process Technol. 2008;206:221–30.
287. Wang J, Shaw LL. Grain-size dependence of the hardness of submicrometer and nanometer hydroxyapatite. J Am Ceram Soc. 2010;93:601–4.

288. Kobayashi S, Kawai W, Wakayama S. The effect of pressure during sintering on the strength and the fracture toughness of hydroxyapatite ceramics. J Mater Sci Mater Med. 2006;17: 1089–93.
289. Chen IW, Wang XH. Sintering dense nanocrystalline ceramics without final-stage grain growth. Nature. 2000;404:168–70.
290. Mazaheri M, Haghighatzadeh M, Zahedi AM, Sadrnezhaad SK. Effect of a novel sintering process on mechanical properties of hydroxyapatite ceramics. J Alloys Compd. 2009;471: 180–4.
291. Lin K, Chen L, Chang J. Fabrication of dense hydroxyapatite nanobioceramics with enhanced mechanical properties via two-step sintering process. Int J Appl Ceram Technol. 2012;9: 479–85.
292. Panyata S, Eitssayeam S, Rujijanagul G, Tunkasiri T, Pengpat K. Property development of hydroxyapatite ceramics by two-step sintering. Adv Mater Res. 2012;506:190–3.
293. Esnaashary M, Fathi M, Ahmadian M. The effect of the two-step sintering process on consolidation of fluoridated hydroxyapatite and its mechanical properties and bioactivity. Int J Appl Ceram Technol. 2014;11:47–56.
294. Feng P, Niu M, Gao C, Peng S, Shuai C. A novel two-step sintering for nano-hydroxyapatite scaffolds for bone tissue engineering. Sci Report. 2014;4:5599.
295. Halouani R, Bernache-Assolant D, Champion E, Ababou A. Microstructure and related mechanical properties of hot pressed hydroxyapatite ceramics. J Mater Sci Mater Med. 1994;5:563–8.
296. Kasuga T, Ota Y, Tsuji K, Abe Y. Preparation of high-strength calcium phosphate ceramics with low modulus of elasticity containing β-$Ca(PO_3)_2$ fibers. J Am Ceram Soc. 1996;79: 1821–4.
297. Suchanek WL, Yoshimura M. Preparation of fibrous, porous hydroxyapatite ceramics from hydroxyapatite whiskers. J Am Ceram Soc. 1998;81:765–7.
298. Kim Y, Kim SR, Song H, Yoon H. Preparation of porous hydroxyapatite/TCP composite block using a hydrothermal hot pressing method. Mater Sci Forum. 2005;486–487:117–20.
299. Li JG, Hashida T. In situ formation of hydroxyapatite-whisker ceramics by hydrothermal hot-pressing method. J Am Ceram Soc. 2006;89:3544–6.
300. Li JG, Hashida T. Preparation of hydroxyapatite ceramics by hydrothermal hot-pressing method at 300 °C. J Mater Sci. 2007;42:5013–9.
301. Petrakova NV, Lysenkov AS, Ashmarin AA, Egorov AA, Fedotov AY, Shvorneva LI, Komlev VS, Barinov SM. Effect of hot pressing temperature on the microstructure and strength of hydroxyapatite ceramic. Inorg Mater Appl Res. 2013;4:362–7.
302. Nakahira A, Murakami T, Onoki T, Hashida T, Hosoi K. Fabrication of porous hydroxyapatite using hydrothermal hot pressing and post-sintering. J Am Ceram Soc. 2005;88:1334–6.
303. Auger MA, Savoini B, Muñoz A, Leguey T, Monge MA, Pareja R, Victoria J. Mechanical characteristics of porous hydroxyapatite/oxide composites produced by post-sintering hot isostatic pressing. Ceram Int. 2009;35:2373–80.
304. Silva CC, Graça MPF, Sombra ASB, Valente MA. Structural and electrical study of calcium phosphate obtained by a microwave radiation assisted procedure. Phys Rev B Condens Matter. 2009;404:1503–8.
305. Chanda A, Dasgupta S, Bose S, Bandyopadhyay A. Microwave sintering of calcium phosphate ceramics. Mater Sci Eng C. 2009;29:1144–9.
306. Veljović D, Zalite I, Palcevskis E, Smiciklas I, Petrović R, Janaćković D. Microwave sintering of fine grained HAP and HAP/TCP bioceramics. Ceram Int. 2010;36:595–603.
307. Kalita SJ, Verma S. Nanocrystalline hydroxyapatite bioceramic using microwave radiation: synthesis and characterization. Mater Sci Eng C. 2010;30:295–303.
308. Veljović D, Palcevskis E, Dindune A, Putić S, Balać I, Petrović R, Janaćković D. Microwave sintering improves the mechanical properties of biphasic calcium phosphates from hydroxyapatite microspheres produced from hydrothermal processing. J Mater Sci. 2010;45: 3175–83.

309. Wu Q, Zhang X, Wu B, Huang W. Effects of microwave sintering on the properties of porous hydroxyapatite scaffolds. Ceram Int. 2013;39:2389–95.
310. Tarafder S, Balla VK, Davies NM, Bandyopadhyay A, Bose S. Microwave-sintered 3D printed tricalcium phosphate scaffolds for bone tissue engineering. J Tissue Eng Regen Med. 2013;7:631–41.
311. Thuault A, Savary E, Hornez JC, Moreau G, Descamps M, Marinel S, Leriche A. Improvement of the hydroxyapatite mechanical properties by direct microwave sintering in single mode cavity. J Eur Ceram Soc. 2014;34:1865–71.
312. Tovstonoh H, Sych O, Skorokhod V. Effect of microwave sintering temperature on structure and properties of bioceramics based on biogenic hydroxyapatite. Funct Mater. 2014;21: 487–91.
313. Tarafder S, Dernell WS, Bandyopadhyay A, Bose S. SrO- and MgO-doped microwave sintered 3D printed tricalcium phosphate scaffolds: mechanical properties and in vivo osteogenesis in a rabbit model. J Biomed Mater Res B Appl Biomater. 2015;103B:679–90.
314. Nakamura T, Fukuhara T, Izui H. Mechanical properties of hydroxyapatites sintered by spark plasma sintering. Ceram Trans. 2006;194:265–72.
315. Zhang F, Lin K, Chang J, Lu J, Ning C. Spark plasma sintering of macroporous calcium phosphate scaffolds from nanocrystalline powders. J Eur Ceram Soc. 2008;28:539–45.
316. Grossin D, Rollin-Martinet S, Estournès C, Rossignol F, Champion E, Combes C, Rey C, Geoffroy C, Drouet C. Biomimetic apatite sintered at very low temperature by spark plasma sintering: physico-chemistry and microstructure aspects. Acta Biomater. 2010;6:577–85.
317. Chesnaud A, Bogicevic C, Karolak F, Estournès C, Dezanneau G. Preparation of transparent oxyapatite ceramics by combined use of freeze-drying and spark-plasma sintering. Chem Commun. 2007;15:1550–2.
318. Eriksson M, Liu Y, Hu J, Gao L, Nygren M, Shen Z. Transparent hydroxyapatite ceramics with nanograin structure prepared by high pressure spark plasma sintering at the minimized sintering temperature. J Eur Ceram Soc. 2011;31:1533–40.
319. Liu Y, Shen Z. Dehydroxylation of hydroxyapatite in dense bulk ceramics sintered by spark plasma sintering. J Eur Ceram Soc. 2012;32:2691–6.
320. Yoshida H, Kim BN, Son HW, Han YH, Kim S. Superplastic deformation of transparent hydroxyapatite. Scr Mater. 2013;69:155–8.
321. Kim BN, Prajatelistia E, Han YH, Son HW, Sakka Y, Kim S. Transparent hydroxyapatite ceramics consolidated by spark plasma sintering. Scr Mater. 2013;69:366–9.
322. Yun J, Son H, Prajatelistia E, Han YH, Kim S, Kim BN. Characterisation of transparent hydroxyapatite nanoceramics prepared by spark plasma sintering. Adv Appl Ceram. 2014; 113:67–72.
323. Li Z, Khor KA. Transparent hydroxyapatite obtained through spark plasma sintering: optical and mechanical properties. Key Eng Mater. 2015;631:51–6.
324. Yanagisawa K, Kim JH, Sakata C, Onda A, Sasabe E, Yamamoto T, Matamoros-Veloza Z, Rendón-Angeles JC. Hydrothermal sintering under mild temperature conditions: preparation of calcium-deficient hydroxyapatite compacts. Z Naturforsch B. 2010;65:1038–44.
325. Hosoi K, Hashida T, Takahashi H, Yamasaki N, Korenaga T. New processing technique for hydroxyapatite ceramics by the hydrothermal hot-pressing method. J Am Ceram Soc. 1996;79:2771–4.
326. Gross KA, Berndt CC. Biomedical application of apatites. In: Hughes JM, Kohn M, Rakovan J, editors. Phosphates: geochemical, geobiological and materials importance, Series: Reviews in Mineralogy and Geochemistry, vol. 48. Washington, DC: Mineralogical Society of America; 2002. p. 631–72.
327. Champion E. Sintering of calcium phosphate bioceramics. Acta Biomater. 2013;9:5855–75.
328. Evans JRG. Seventy ways to make ceramics. J Eur Ceram Soc. 2008;28:1421–32.
329. Hench LL, Polak JM. Third-generation biomedical materials. Science. 2002;295:1014–7.
330. Black J. Biological performance of materials: fundamentals of biocompatibility. 4th ed. Boca Raton: CRC Press; 2005. 520 pp

331. Carter CB, Norton MG. Ceramic materials: science and engineering. 2nd ed. New York: Springer; 2013. 766 pp
332. Benaqqa C, Chevalier J, Saädaoui M, Fantozzi G. Slow crack growth behaviour of hydroxyapatite ceramics. Biomaterials. 2005;26:6106–12.
333. Pecqueux F, Tancret F, Payraudeau N, Bouler JM. Influence of microporosity and macroporosity on the mechanical properties of biphasic calcium phosphate bioceramics: modelling and experiment. J Eur Ceram Soc. 2010;30:819–29.
334. Ramesh S, Tan CY, Sopyan I, Hamdi M, Teng WD. Consolidation of nanocrystalline hydroxyapatite powder. Sci Technol Adv Mater. 2007;8:124–30.
335. Wagoner Johnson AJ, Herschler BA. A review of the mechanical behavior of CaP and CaP/polymer composites for applications in bone replacement and repair. Acta Biomater. 2011;7:16–30.
336. Suchanek WL, Yoshimura M. Processing and properties of hydroxyapatite-based biomaterials for use as hard tissue replacement implants. J Mater Res. 1998;13:94–117.
337. Fan X, Case ED, Ren F, Shu Y, Baumann MJ. Part I: porosity dependence of the Weibull modulus for hydroxyapatite and other brittle materials. J Mech Behav Biomed Mater. 2012;8:21–36.
338. Fan X, Case ED, Gheorghita I, Baumann MJ. Weibull modulus and fracture strength of highly porous hydroxyapatite. J Mech Behav Biomed Mater. 2013;20:283–95.
339. Cordell J, Vogl M, Johnson A. The influence of micropore size on the mechanical properties of bulk hydroxyapatite and hydroxyapatite scaffolds. J Mech Behav Biomed Mater. 2009;2:560–70.
340. Suzuki S, Sakamura M, Ichiyanagi M, Ozawa M. Internal friction of hydroxyapatite and fluorapatite. Ceram Int. 2004;30:625–7.
341. Suzuki S, Takahiro K, Ozawa M. Internal friction and dynamic modulus of polycrystalline ceramics prepared from stoichiometric and Ca-deficient hydroxyapatites. Mater Sci Eng B. 1998;55:68–70.
342. Bouler JM, Trecant M, Delecrin J, Royer J, Passuti N, Daculsi G. Macroporous biphasic calcium phosphate ceramics: influence of five synthesis parameters on compressive strength. J Biomed Mater Res. 1996;32:603–9.
343. Tancret F, Bouler JM, Chamousset J, Minois LM. Modelling the mechanical properties of microporous and macroporous biphasic calcium phosphate bioceramics. J Eur Ceram Soc. 2006;26:3647–56.
344. le Huec JC, Schaeverbeke T, Clement D, Faber J, le Rebeller A. Influence of porosity on the mechanical resistance of hydroxyapatite ceramics under compressive stress. Biomaterials. 1995;16:113–8.
345. Hsu YH, Turner IG, Miles AW. Mechanical properties of three different compositions of calcium phosphate bioceramic following immersion in Ringer's solution and distilled water. J Mater Sci Mater Med. 2009;20:2367–74.
346. Torgalkar AM. Resonance frequency technique to determine elastic modulus of hydroxyapatite. J Biomed Mater Res. 1979;13:907–20.
347. Gilmore RS, Katz JL. Elastic properties of apatites. J Mater Sci. 1982;17:1131–41.
348. Fan X, Case ED, Ren F, Shu Y, Baumann MJ. Part II: fracture strength and elastic modulus as a function of porosity for hydroxyapatite and other brittle materials. J Mech Behav Biomed Mater. 2012;8:99–110.
349. de Aza PN, de Aza AH, de Aza S. Crystalline bioceramic materials. Bol Soc Esp Ceram V. 2005;44:135–45.
350. Fritsch A, Dormieux L, Hellmich C, Sanahuja J. Mechanical behavior of hydroxyapatite biomaterials: an experimentally validated micromechanical model for elasticity and strength. J Biomed Mater Res A. 2009;88A:149–61.
351. Ching WY, Rulis P, Misra A. Ab initio elastic properties and tensile strength of crystalline hydroxyapatite. Acta Biomater. 2009;5:3067–75.
352. Fritsch A, Hellmich C, Dormieux L. The role of disc-type crystal shape for micromechanical predictions of elasticity and strength of hydroxyapatite biomaterials. Philos Trans R Soc Lond A. 2010;368:1913–35.

353. Menéndez-Proupin E, Cervantes-Rodríguez S, Osorio-Pulgar R, Franco-Cisterna M, Camacho-Montes H, Fuentes ME. Computer simulation of elastic constants of hydroxyapatite and fluorapatite. J Mech Behav Biomed Mater. 2011;4:1011–120.
354. Sun JP, Song Y, Wen GW, Wang Y, Yang R. Softening of hydroxyapatite by vacancies: a first principles investigation. Mater Sci Eng C. 2013;33:1109–15.
355. Sha MC, Li Z, Bradt RC. Single-crystal elastic constants of fluorapatite, $Ca_5F(PO_4)_3$. J Appl Phys. 1994;75:7784–7.
356. Wakai F, Kodama Y, Sakaguchi S, Nonami T. Superplasticity of hot isostatically pressed hydroxyapatite. J Am Ceram Soc. 1990;73:457–60.
357. Tago K, Itatani K, Suzuki TS, Sakka Y, Koda S. Densification and superplasticity of hydroxyapatite ceramics. J Ceram Soc Jpn. 2005;113:669–73.
358. Burger EL, Patel V. Calcium phosphates as bone graft extenders. Orthopedics. 2007;30: 939–42.
359. Rodriguez-Lorenzo LM, Vallet-Regí M, Ferreira JMF, Ginebra MP, Aparicio C, Planell J. A hydroxyapatite ceramic bodies with tailored mechanical properties for different applications. J Biomed Mater Res. 2002;60:159–66.
360. Song J, Liu Y, Zhang Y, Jiao L. Mechanical properties of hydroxyapatite ceramics sintered from powders with different morphologies. Mater Sci Eng A. 2011;528:5421–7.
361. Dorozhkin SV. Calcium orthophosphate-containing biocomposites and hybrid biomaterials for biomedical applications. J Funct Biomater. 2015;6:708–832.
362. Bouslama N, Ben Ayed F, Bouaziz J. Sintering and mechanical properties of tricalcium phosphate – fluorapatite composites. Ceram Int. 2009;35:1909–17.
363. Suchanek W, Yashima M, Kakihana M, Yoshimura M. Processing and mechanical properties of hydroxyapatite reinforced with hydroxyapatite whiskers. Biomaterials. 1996;17:1715–23.
364. Suchanek W, Yashima M, Kakihana M, Yoshimura M. Hydroxyapatite/hydroxyapatite-whisker composites without sintering additives: mechanical properties and microstructural evolution. J Am Ceram Soc. 1997;80:2805–13.
365. Simsek D, Ciftcioglu R, Guden M, Ciftcioglu M, Harsa S. Mechanical properties of hydroxyapatite composites reinforced with hydroxyapatite whiskers. Key Eng Mater. 2004;264–268: 1985–8.
366. Bose S, Banerjee A, Dasgupta S, Bandyopadhyay A. Synthesis, processing, mechanical, and biological property characterization of hydroxyapatite whisker-reinforced hydroxyapatite composites. J Am Ceram Soc. 2009;92:323–30.
367. Lie-Feng L, Xiao-Yi H, Cai YX, Weng J. Reinforcing of porous hydroxyapatite ceramics with hydroxyapatite fibres for enhanced bone tissue engineering. J Biomim Biomater Tissue Eng. 2011;1314:67–73.
368. Shiota T, Shibata M, Yasuda K, Matsuo Y. Influence of β-tricalcium phosphate dispersion on mechanical properties of hydroxyapatite ceramics. J Ceram Soc Jpn. 2009;116:1002–5.
369. Shuai C, Feng P, Nie Y, Hu H, Liu J, Peng S. Nano-hydroxyapatite improves the properties of β-tricalcium phosphate bone scaffolds. Int J Appl Ceram Technol. 2013;10:1003–13.
370. Dorozhkin SV, Ajaal T. Toughening of porous bioceramic scaffolds by bioresorbable polymeric coatings. Proc Inst Mech Eng H. 2009;223:459–70.
371. Dorozhkin SV, Ajaal T. Strengthening of dense bioceramic samples using bioresorbable polymers – a statistical approach. J Biomim Biomater Tissue Eng. 2009;4:27–39.
372. Dressler M, Dombrowski F, Simon U, Börnstein J, Hodoroaba VD, Feigl M, Grunow S, Gildenhaar R, Neumann M. Influence of gelatin coatings on compressive strength of porous hydroxyapatite ceramics. J Eur Ceram Soc. 2011;31:523–9.
373. Martinez-Vazquez FJ, Perera FH, Miranda P, Pajares A, Guiberteau F. Improving the compressive strength of bioceramic robocast scaffolds by polymer infiltration. Acta Biomater. 2010;6:4361–8.
374. Fedotov AY, Bakunova NV, Komlev VS, Barinov SM. High-porous calcium phosphate bioceramics reinforced by chitosan infiltration. Dokl Chem. 2011;439:233–6.
375. Martínez-Vázquez FJ, Pajares A, Guiberteau F, Miranda P. Effect of polymer infiltration on the flexural behavior of β-tricalcium phosphate robocast scaffolds. Materials. 2014;7: 4001–18.

376. He LH, Standard OC, Huang TT, Latella BA, Swain MV. Mechanical behaviour of porous hydroxyapatite. Acta Biomater. 2008;4:577–86.
377. Yamashita K, Owada H, Umegaki T, Kanazawa T, Futagamu T. Ionic conduction in apatite solid solutions. Solid State Ionics. 1988;28–30:660–3.
378. Nagai M, Nishino T. Surface conduction of porous hydroxyapatite ceramics at elevated temperatures. Solid State Ionics. 1988;28–30:1456–61.
379. Valdes JJP, Rodriguez AV, Carrio JG. Dielectric properties and structure of hydroxyapatite ceramics sintered by different conditions. J Mater Res. 1995;10:2174–7.
380. Fanovich MA, Castro MS, Lopez JMP. Analysis of the microstructural evolution in hydroxyapatite ceramics by electrical characterisation. Ceram Int. 1999;25:517–22.
381. Bensaoud A, Bouhaouss A, Ferhat M. Electrical properties in compressed poorly crystalline apatite. J Solid State Electrochem. 2001;5:362–5.
382. Mahabole MP, Aiyer RC, Ramakrishna CV, Sreedhar B, Khairnar RS. Synthesis, characterization and gas sensing property of hydroxyapatite ceramic. Bull Mater Sci. 2005;28: 535–45.
383. Tanaka Y, Takata S, Shimoe K, Nakamura M, Nagai A, Toyama T, Yamashita K. Conduction properties of non-stoichiometric hydroxyapatite whiskers for biomedical use. J Ceram Soc Jpn. 2008;116:815–21.
384. Tanaka Y, Nakamura M, Nagai A, Toyama T, Yamashita K. Ionic conduction mechanism in Ca-deficient hydroxyapatite whiskers. Mater Sci Eng B. 2009;161:115–9.
385. Wang W, Itoh S, Yamamoto N, Okawa A, Nagai A, Yamashita K. Electrical polarization of β-tricalcium phosphate ceramics. J Am Ceram Soc. 2010;93:2175–7.
386. Mahabole MP, Mene RU, Khairnar RS. Gas sensing and dielectric studies on cobalt doped hydroxyapatite thick films. Adv Mater Lett. 2013;4:46–52.
387. Horiuchi N, Nakaguki S, Wada N, Nozaki K, Nakamura M, Nagai A, Katayama K, Yamashita K. Polarization-induced surface charges in hydroxyapatite ceramics. J Appl Phys. 2014;116: 014902.
388. Tofail SAM, Gandhi AA, Gregor M, Bauer J. Electrical properties of hydroxyapatite. Pure Appl Chem. 2015;87:221–9.
389. Kaygili O, Keser S, Ates T, Kirbag S, Yakuphanoglu F. Dielectric properties of calcium phosphate ceramics. Medziagotyra. 2016;22:65–9.
390. Suresh MB, Biswas P, Mahender V, Johnson R. Comparative evaluation of electrical conductivity of hydroxyapatite ceramics densified through ramp and hold, spark plasma and post sinter hot isostatic pressing routes. Mater Sci Eng C. 2017;70:364–70.
391. Gandhi AA, Wojtas M, Lang SB, Kholkin AL, Tofail SAM. Piezoelectricity in poled hydroxyapatite ceramics. J Am Ceram Soc. 2014;97:2867–72.
392. Bystrov VS. Piezoelectricity in the ordered monoclinic hydroxyapatite. Ferroelectrics. 2015;475:148–53.
393. Nakamura S, Takeda H, Yamashita K. Proton transport polarization and depolarization of hydroxyapatite ceramics. J Appl Phys. 2001;89:5386–92.
394. Gittings JP, Bowen CR, Turner IG, Baxter FR, Chaudhuri JB. Polarisation behaviour of calcium phosphate based ceramics. Mater Sci Forum. 2008;587–588:91–5.
395. Itoh S, Nakamura S, Kobayashi T, Shinomiya K, Yamashita K, Itoh S. Effect of electrical polarization of hydroxyapatite ceramics on new bone formation. Calcif Tissue Int. 2006;78: 133–42.
396. Iwasaki T, Tanaka Y, Nakamura M, Nagai A, Hashimoto K, Toda Y, Katayama K, Yamashita K. Rate of bonelike apatite formation accelerated on polarized porous hydroxyapatite. J Am Ceram Soc. 2008;91:3943–9.
397. Itoh S, Nakamura S, Kobayashi T, Shinomiya K, Yamashita K. Enhanced bone ingrowth into hydroxyapatite with interconnected pores by electrical polarization. Biomaterials. 2006;27: 5572–9.
398. Kobayashi T, Itoh S, Nakamura S, Nakamura M, Shinomiya K, Yamashita K. Enhanced bone bonding of hydroxyapatite-coated titanium implants by electrical polarization. J Biomed Mater Res A. 2007;82A:145–51.

399. Bodhak S, Bose S, Bandyopadhyay A. Role of surface charge and wettability on early stage mineralization and bone cell-materials interactions of polarized hydroxyapatite. Acta Biomater. 2009;5:2178–88.
400. Sagawa H, Itoh S, Wang W, Yamashita K. Enhanced bone bonding of the hydroxyapatite/β--tricalcium phosphate composite by electrical polarization in rabbit long bone. Artif Organs. 2010;34:491–7.
401. Ohba S, Wang W, Itoh S, Nagai A, Yamashita K. Enhanced effects of new bone formation by an electrically polarized hydroxyapatite microgranule/platelet-rich plasma composite gel. Key Eng Mater. 2013;529–530:82–7.
402. Yamashita K, Oikawa N, Umegaki T. Acceleration and deceleration of bone-like crystal growth on ceramic hydroxyapatite by electric poling. Chem Mater. 1996;8:2697–700.
403. Teng NC, Nakamura S, Takagi Y, Yamashita Y, Ohgaki M, Yamashita K. A new approach to enhancement of bone formation by electrically polarized hydroxyapatite. J Dent Res. 2001; 80:1925–9.
404. Kobayashi T, Nakamura S, Yamashita K. Enhanced osteobonding by negative surface charges of electrically polarized hydroxyapatite. J Biomed Mater Res. 2001;57:477–84.
405. Park YJ, Hwang KS, Song JE, Ong JL, Rawls HR. Growth of calcium phosphate on poling treated ferroelectric $BaTiO_3$ ceramics. Biomaterials. 2002;23:3859–64.
406. Hwang KS, Song JE, Jo JW, Yang HS, Park YJ, Ong JL, Rawls HR. Effect of poling conditions on growth of calcium phosphate crystal in ferroelectric $BaTiO_3$ ceramics. J Mater Sci Mater Med. 2002;13:133–8.
407. Yamashita K. Enhanced bioactivity of electrically poled hydroxyapatita ceramics and coatings. Mater Sci Forum. 2003;426–432:3237–42.
408. Nakamura S, Kobayashi T, Yamashita K. Highly orientated calcification in newly formed bones on negatively charged hydroxyapatite electrets. Key Eng Mater. 2005;284–286:897–900.
409. Kato R, Nakamura S, Katayama K, Yamashita K. Electrical polarization of plasma-spray-hydroxyapatite coatings for improvement of osteoconduction of implants. J Biomed Mater Res A. 2005;74A:652–8.
410. Nakamura S, Kobayashi T, Nakamura M, Itoh S, Yamashita K. Electrostatic surface charge acceleration of bone ingrowth of porous hydroxyapatite/β-tricalcium phosphate ceramics. J Biomed Mater Res A. 2010;92A:267–75.
411. Tarafder S, Bodhak S, Bandyopadhyay A, Bose S. Effect of electrical polarization and composition of biphasic calcium phosphates on early stage osteoblast interactions. J Biomed Mater Res B Appl Biomater. 2011;97B:306–14.
412. Ohba S, Wang W, Itoh S, Takagi Y, Nagai A, Yamashita K. Acceleration of new bone formation by an electrically polarized hydroxyapatite microgranule/platelet-rich plasma composite. Acta Biomater. 2012;8:2778–87.
413. Tarafder S, Banerjee S, Bandyopadhyay A, Bose S. Electrically polarized biphasic calcium phosphates: adsorption and release of bovine serum albumin. Langmuir. 2010;26:16625–9.
414. Itoh S, Nakamura S, Nakamura M, Shinomiya K, Yamashita K. Enhanced bone regeneration by electrical polarization of hydroxyapatite. Artif Organs. 2006;30:863–9.
415. Nakamura M, Nagai A, Ohashi N, Tanaka Y, Sekilima Y, Nakamura S. Regulation of osteoblast-like cell behaviors on hydroxyapatite by electrical polarization. Key Eng Mater. 2008;361–363:1055–8.
416. Nakamura M, Nagai A, Tanaka Y, Sekilima Y, Yamashita K. Polarized hydroxyapatite promotes spread and motility of osteoblastic cells. J Biomed Mater Res A. 2010;92A:783–90.
417. Nakamura M, Nagai A, Yamashita K. Surface electric fields of apatite electret promote osteoblastic responses. Key Eng Mater. 2013;529–530:357–60.
418. Nakamura S, Kobayashi T, Yamashita K. Extended bioactivity in the proximity of hydroxyapatite ceramic surfaces induced by polarization charges. J Biomed Mater Res. 2002;61: 593–9.
419. Wang W, Itoh S, Tanaka Y, Nagai A, Yamashita K. Comparison of enhancement of bone ingrowth into hydroxyapatite ceramics with highly and poorly interconnected pores by electrical polarization. Acta Biomater. 2009;5:3132–40.

420. Cartmell SH, Thurstan S, Gittings JP, Griffiths S, Bowen CR, Turner IG. Polarization of porous hydroxyapatite scaffolds: influence on osteoblast cell proliferation and extracellular matrix production. J Biomed Mater Res A. 2014;102A:1047–52.
421. Nakamura M, Kobayashi A, Nozaki K, Horiuchi N, Nagai A, Yamashita K. Improvement of osteoblast adhesion through polarization of plasma-sprayed hydroxyapatite coatings on metal. J Med Biol Eng. 2014;34:44–8.
422. Nagai A, Tanaka K, Tanaka Y, Nakamura M, Hashimoto K, Yamashita K. Electric polarization and mechanism of B-type carbonated apatite ceramics. J Biomed Mater Res A. 2011;99A:116–24.
423. Nakamura M, Niwa K, Nakamura S, Sekijima Y, Yamashita K. Interaction of a blood coagulation factor on electrically polarized hydroxyapatite surfaces. J Biomed Mater Res B Appl Biomater. 2007;82B:29–36.
424. Nagai M, Shibuya Y, Nishino T, Saeki T, Owada H, Yamashita K, Umegaki T. Electrical conductivity of calcium phosphate ceramics with various Ca/P ratios. J Mater Sci. 1991;26:2949–53.
425. Laghzizil A, Elherch N, Bouhaouss A, Lorente G, Coradin T, Livage J. Electrical behavior of hydroxyapatites $M_{10}(PO_4)_6(OH)_2$ (M = Ca, Pb, Ba). Mater Res Bull. 2001;36:953–62.
426. Louati B, Guidara K, Gargouri M. Dielectric and ac ionic conductivity investigations in the monetite. J Alloys Compd. 2009;472:347–51.
427. Gittings JP, Bowen CR, Dent AC, Turner IG, Baxter FR, Chaudhuri JB. Electrical characterization of hydroxyapatite-based bioceramics. Acta Biomater. 2009;5:743–54.
428. Tofail SAM, Baldisserri C, Haverty D, McMonagle JB, Erhart J. Pyroelectric surface charge in hydroxyapatite ceramics. J Appl Phys. 2009;106:106104.
429. Ioku K. Tailored bioceramics of calcium phosphates for regenerative medicine. J Ceram Soc Jpn. 2010;118:775–83.
430. Fang Y, Agrawal DK, Roy DM, Roy R. Fabrication of transparent hydroxyapatite ceramics by ambient-pressure sintering. Mater Lett. 1995;23:147–51.
431. Varma H, Vijayan SP, Babu SS. Transparent hydroxyapatite ceramics through gel-casting and low-temperature sintering. J Am Ceram Soc. 2002;85:493–5.
432. Watanabe Y, Ikoma T, Monkawa A, Suetsugu Y, Yamada H, Tanaka J, Moriyoshi Y. Fabrication of transparent hydroxyapatite sintered body with high crystal orientation by pulse electric current sintering. J Am Ceram Soc. 2005;88:243–5.
433. Kotobuki N, Ioku K, Kawagoe D, Fujimori H, Goto S, Ohgushi H. Observation of osteogenic differentiation cascade of living mesenchymal stem cells on transparent hydroxyapatite ceramics. Biomaterials. 2005;26:779–85.
434. John A, Varma HK, Vijayan S, Bernhardt A, Lode A, Vogel A, Burmeister B, Hanke T, Domaschke H, Gelinsky M. In vitro investigations of bone remodeling on a transparent hydroxyapatite ceramic. Biomed Mater. 2009;4:015007. (9 pages)
435. Wang J, Shaw LL. Transparent nanocrystalline hydroxyapatite by pressure-assisted sintering. Scr Mater. 2010;63:593–6.
436. Tan N, Kou Z, Ding Y, Leng Y, Liu C, He D. Novel substantial reductions in sintering temperatures for preparation of transparent hydroxyapatite bioceramics under ultrahigh pressure. Scr Mater. 2011;65:819–22.
437. Boilet L, Descamps M, Rguiti E, Tricoteaux A, Lu J, Petit F, Lardot V, Cambier F, Leriche A. Processing and properties of transparent hydroxyapatite and β tricalcium phosphate obtained by HIP process. Ceram Int. 2013;39:283–8.
438. Han YH, Kim BN, Yoshida H, Yun J, Son HW, Lee J, Kim S. Spark plasma sintered superplastic deformed transparent ultrafine hydroxyapatite nanoceramics. Adv Appl Ceram. 2016;115:174–84.
439. Kobune M, Mineshige A, Fujii S, Iida H. Preparation of translucent hydroxyapatite ceramics by HIP and their physical properties. J Ceram Soc Jpn. 1997;105:210–3.
440. Barralet JE, Fleming GJP, Campion C, Harris JJ, Wright AJ. Formation of translucent hydroxyapatite ceramics by sintering in carbon dioxide atmospheres. J Mater Sci. 2003; 38:3979–93.

441. Chaudhry AA, Yan H, Gong K, Inam F, Viola G, Reece MJ, Goodall JBM, Ur Rehman I, McNeil-Watson FK, Corbett JCW, Knowles JC, Darr JA. High-strength nanograined and translucent hydroxyapatite monoliths via continuous hydrothermal synthesis and optimized spark plasma sintering. Acta Biomater. 2011;7:791–9.
442. Tancred DC, McCormack BA, Carr AJ. A synthetic bone implant macroscopically identical to cancellous bone. Biomaterials. 1998;19:2303–11.
443. Miao X, Sun D. Graded/gradient porous biomaterials. Materials. 2010;3:26–47.
444. Schliephake H, Neukam FW, Klosa D. Influence of pore dimensions on bone ingrowth into porous hydroxylapatite blocks used as bone graft substitutes. A histometric study. Int J Oral Maxillofac Surg. 1991;20:53–8.
445. Otsuki B, Takemoto M, Fujibayashi S, Neo M, Kokubo T, Nakamura T. Pore throat size and connectivity determine bone and tissue ingrowth into porous implants: three-dimensional micro-CT based structural analyses of porous bioactive titanium implants. Biomaterials. 2006;27:5892–900.
446. Hing KA, Best SM, Bonfield W. Characterization of porous hydroxyapatite. J Mater Sci Mater Med. 1999;10:135–45.
447. Lu JX, Flautre B, Anselme K, Hardouin P, Gallur A, Descamps M, Thierry B. Role of interconnections in porous bioceramics on bone recolonization in vitro and in vivo. J Mater Sci Mater Med. 1999;10:111–20.
448. Karageorgiou V, Kaplan D. Porosity of 3D biomaterial scaffolds and osteogenesis. Biomaterials. 2005;26:5474–91.
449. Jones AC, Arns CH, Sheppard AP, Hutmacher DW, Milthorpe BK, Knackstedt MA. Assessment of bone ingrowth into porous biomaterials using MICRO-CT. Biomaterials. 2007;28:2491–504.
450. Tamai N, Myoui A, Kudawara I, Ueda T, Yoshikawa H. Novel fully interconnected porous hydroxyapatite ceramic in surgical treatment of benign bone tumor. J Orthop Sci. 2010;15:560–8.
451. Sakane M, Tsukanishi T, Funayama T, Kobayashi M, Ochiai N. Unidirectional porous β-tricalcium phosphate bone substitute: examination of balance between new bone formation and absorption. Key Eng Mater. 2012;493–494:132–4.
452. Panzavolta S, Torricelli P, Amadori S, Parrilli A, Rubini K, Della Bella E, Fini M, Bigi A. 3D interconnected porous biomimetic scaffolds: in vitro cell response. J Biomed Mater Res A. 2013;101A:3560–70.
453. Jin L, Feng ZQ, Wang T, Ren Z, Ma S, Wu J, Sun D. A novel fluffy hydroxylapatite fiber scaffold with deep interconnected pores designed for three-dimensional cell culture. J Mater Chem B. 2014;2:129–36.
454. Flautre B, Descamps M, Delecourt C, Blary MC, Hardouin P. Porous HA ceramic for bone replacement: role of the pores and interconnections – experimental study in the rabbits. J Mater Sci Mater Med. 2001;12:679–82.
455. Tamai N, Myoui A, Tomita T, Nakase T, Tanaka J, Ochi T, Yoshikawa H. Novel hydroxyapatite ceramics with an interconnective porous structure exhibit superior osteoconduction in vivo. J Biomed Mater Res. 2002;59:110–7.
456. Mastrogiacomo M, Scaglione S, Martinetti R, Dolcini L, Beltrame F, Cancedda R, Quarto R. Role of scaffold internal structure on in vivo bone formation in macroporous calcium phosphate bioceramics. Biomaterials. 2006;27:3230–7.
457. Okamoto M, Dohi Y, Ohgushi H, Shimaoka H, Ikeuchi M, Matsushima A, Yonemasu K, Hosoi H. Influence of the porosity of hydroxyapatite ceramics on in vitro and in vivo bone formation by cultured rat bone marrow stromal cells. J Mater Sci Mater Med. 2006;17:327–36.
458. Zhang L, Hanagata N, Maeda M, Minowa T, Ikoma T, Fan H, Zhang X. Porous hydroxyapatite and biphasic calcium phosphate ceramics promote ectopic osteoblast differentiation from mesenchymal stem cells. Sci Technol Adv Mater. 2009;10:025003. (9 pages)
459. Li X, Liu H, Niu X, Fan Y, Feng Q, Cui FZ, Watari F. Osteogenic differentiation of human adipose-derived stem cells induced by osteoinductive calcium phosphate ceramics. J Biomed Mater Res B Appl Biomater. 2011;97B:10–9.

460. Hong MH, Kim SM, Han MH, Kim YH, Lee YK, Oh DS. Evaluation of microstructure effect of the porous spherical β-tricalcium phosphate granules on cellular responses. Ceram Int. 2014;40:6095–102.
461. de Godoy RF, Hutchens S, Campion C, Blunn G. Silicate-substituted calcium phosphate with enhanced strut porosity stimulates osteogenic differentiation of human mesenchymal stem cells. J Mater Sci Mater Med. 2015;26:54. (12 pages)
462. Omae H, Mochizuki Y, Yokoya S, Adachi N, Ochi M. Effects of interconnecting porous structure of hydroxyapatite ceramics on interface between grafted tendon and ceramics. J Biomed Mater Res A. 2006;79A:329–37.
463. Yoshikawa H, Tamai N, Murase T, Myoui A. Interconnected porous hydroxyapatite ceramics for bone tissue engineering. J R Soc Interface. 2009;6:S341–8.
464. Ribeiro GBM, Trommer RM, dos Santos LA, Bergmann CP. Novel method to produce β-TCP scaffolds. Mater Lett. 2011;65:275–7.
465. Silva TSN, Primo BT, Silva Jr AN, Machado DC, Viezzer C, Santos LA. Use of calcium phosphate cement scaffolds for bone tissue engineering: in vitro study. Acta Cir Bras. 2011;26:7–11.
466. de Moraes MacHado JL, Giehl IC, Nardi NB, dos Santos LA. Evaluation of scaffolds based on α-tricalcium phosphate cements for tissue engineering applications. IEEE Trans Biomed Eng. 2011;58:1814–9.
467. Li SH, de Wijn JR, Layrolle P, de Groot K. Novel method to manufacture porous hydroxyapatite by dual-phase mixing. J Am Ceram Soc. 2003;86:65–72.
468. de Oliveira JF, de Aguiar PF, Rossi AM, Soares GDA. Effect of process parameters on the characteristics of porous calcium phosphate ceramics for bone tissue scaffolds. Artif Organs. 2003;27:406–11.
469. Swain SK, Bhattacharyya S. Preparation of high strength macroporous hydroxyapatite scaffold. Mater Sci Eng C. 2013;33:67–71.
470. Maeda H, Kasuga T, Nogami M, Kagami H, Hata K, Ueda M. Preparation of bonelike apatite composite sponge. Key Eng Mater. 2004;254–256:497–500.
471. le Ray AM, Gautier H, Bouler JM, Weiss P, Merle C. A new technological procedure using sucrose as porogen compound to manufacture porous biphasic calcium phosphate ceramics of appropriate micro- and macrostructure. Ceram Int. 2010;36:93–101.
472. Li SH, de Wijn JR, Layrolle P, de Groot K. Synthesis of macroporous hydroxyapatite scaffolds for bone tissue engineering. J Biomed Mater Res. 2002;61:109–20.
473. Hesaraki S, Sharifi D. Investigation of an effervescent additive as porogenic agent for bone cement macroporosity. Biomed Mater Eng. 2007;17:29–38.
474. Hesaraki S, Moztarzadeh F, Sharifi D. Formation of interconnected macropores in apatitic calcium phosphate bone cement with the use of an effervescent additive. J Biomed Mater Res A. 2007;83A:80–7.
475. Pal K, Pal S. Development of porous hydroxyapatite scaffolds. Mater Manuf Process. 2006;21:325–8.
476. Tas AC. Preparation of porous apatite granules from calcium phosphate cement. J Mater Sci Mater Med. 2008;19:2231–9.
477. Yao X, Tan S, Jiang D. Improving the properties of porous hydroxyapatite ceramics by fabricating methods. J Mater Sci. 2005;40:4939–42.
478. Song HY, Youn MH, Kim YH, Min YK, Yang HM, Lee BT. Fabrication of porous β-TCP bone graft substitutes using PMMA powder and their biocompatibility study. Korean J Mater Res. 2007;17:318–22.
479. Youn MH, Paul RK, Song HY, Lee BT. Fabrication of porous structure of BCP sintered bodies using microwave assisted synthesized HAp nano powder. Mater Sci Forum. 2007; 534–536:49–52.
480. Almirall A, Larrecq G, Delgado JA, Martínez S, Ginebra MP, Planell JA. Fabrication of low temperature hydroxyapatite foams. Key Eng Mater. 2004;254–256:1001–4.

481. Almirall A, Larrecq G, Delgado JA, Martínez S, Planell JA, Ginebra MP. Fabrication of low temperature macroporous hydroxyapatite scaffolds by foaming and hydrolysis of an α-TCP paste. Biomaterials. 2004;25:3671–80.
482. Huang X, Miao X. Novel porous hydroxyapatite prepared by combining H_2O_2 foaming with PU sponge and modified with PLGA and bioactive glass. J Biomater Appl. 2007;21: 351–74.
483. Strnadova M, Protivinsky J, Strnad J, Vejsicka Z. Preparation of porous synthetic nanostructured HA scaffold. Key Eng Mater. 2008;361–363:211–4.
484. Li B, Chen X, Guo B, Wang X, Fan H, Zhang X. Fabrication and cellular biocompatibility of porous carbonated biphasic calcium phosphate ceramics with a nanostructure. Acta Biomater. 2009;5:134–43.
485. Cheng Z, Zhao K, Wu ZP. Structure control of hydroxyapatite ceramics via an electric field assisted freeze casting method. Ceram Int. 2015;41:8599–604.
486. Takagi S, Chow LC. Formation of macropores in calcium phosphate cement implants. J Biomed Mater Res. 2001;12:135–9.
487. Walsh D, Tanaka J. Preparation of a bone-like apatite foam cement. J Mater Sci Mater Med. 2001;12:339–44.
488. Tadic D, Beckmann F, Schwarz K, Epple M. A novel method to produce hydroxylapatite objects with interconnecting porosity that avoids sintering. Biomaterials. 2004;25:3335–40.
489. Komlev VS, Barinov SM. Porous hydroxyapatite ceramics of bi-modal pore size distribution. J Mater Sci Mater Med. 2002;13:295–9.
490. Sepulveda P, Binner JG, Rogero SO, Higa OZ, Bressiani JC. Production of porous hydroxyapatite by the gel-casting of foams and cytotoxic evaluation. J Biomed Mater Res. 2000;50:27–34.
491. Hsu YH, Turner IG, Miles AW. Mechanical characterization of dense calcium phosphate bioceramics with interconnected porosity. J Mater Sci Mater Med. 2007;18:2319–29.
492. Zhang HG, Zhu Q. Preparation of porous hydroxyapatite with interconnected pore architecture. J Mater Sci Mater Med. 2007;18:1825–9.
493. Chevalier E, Chulia D, Pouget C, Viana M. Fabrication of porous substrates: a review of processes using pore forming agents in the biomaterial field. J Pharm Sci. 2008;97: 1135–54.
494. Tang YJ, Tang YF, Lv CT, Zhou ZH. Preparation of uniform porous hydroxyapatite biomaterials by a new method. Appl Surf Sci. 2008;254:5359–62.
495. Abdulqader ST, Rahman IA, Ismail H, Ponnuraj Kannan T, Mahmood Z. A simple pathway in preparation of controlled porosity of biphasic calcium phosphate scaffold for dentin regeneration. Ceram Int. 2013;39:2375–81.
496. Stares SL, Fredel MC, Greil P, Travitzky N. Paper-derived hydroxyapatite. Ceram Int. 2013;39:7179–83.
497. Wen FH, Wang F, Gai Y, Wang MT, Lai QH. Preparation of mesoporous hydroxylapatite ceramics using polystyrene microspheres as template. Appl Mech Mater. 2013;389:194–8.
498. Guda T, Appleford M, Oh S, Ong JL. A cellular perspective to bioceramic scaffolds for bone tissue engineering: the state of the art. Curr Top Med Chem. 2008;8:290–9.
499. Habraken WJEM, Wolke JGC, Jansen JA. Ceramic composites as matrices and scaffolds for drug delivery in tissue engineering. Adv Drug Deliv Rev. 2007;59:234–48.
500. Tian J, Tian J. Preparation of porous hydroxyapatite. J Mater Sci. 2001;36:3061–6.
501. Swain SK, Bhattacharyya S, Sarkar D. Preparation of porous scaffold from hydroxyapatite powders. Mater Sci Eng C. 2011;31:1240–4.
502. Zhao K, Tang YF, Qin YS, Luo DF. Polymer template fabrication of porous hydroxyapatite scaffolds with interconnected spherical pores. J Eur Ceram Soc. 2011;31:225–9.
503. Sung JH, Shin KH, Moon YW, Koh YH, Choi WY, Kim HE. Production of porous calcium phosphate (CaP) ceramics with highly elongated pores using carbon-coated polymeric templates. Ceram Int. 2012;38:93–7.

504. Oha DS, Kim YH, Ganbat D, Han MH, Lim P, Back JH, Lee FY, Tawfeek H. Bone marrow absorption and retention properties of engineered scaffolds with micro-channels and nano-pores for tissue engineering: a proof of concept. Ceram Int. 2013;39:8401–10.
505. Deville S, Saiz E, Tomsia AP. Freeze casting of hydroxyapatite scaffolds for bone tissue engineering. Biomaterials. 2006;27:5480–9.
506. Lee EJ, Koh YH, Yoon BH, Kim HE, Kim HW. Highly porous hydroxyapatite bioceramics with interconnected pore channels using camphene-based freeze casting. Mater Lett. 2007;61:2270–3.
507. Fu Q, Rahaman MN, Dogan F, Bal BS. Freeze casting of porous hydroxyapatite scaffolds. I. Processing and general microstructure. J Biomed Mater Res B Appl Biomater. 2008; 86B:125–35.
508. Impens S, Schelstraete R, Luyten J, Mullens S, Thijs I, van Humbeeck J, Schrooten J. Production and characterisation of porous calcium phosphate structures with controllable hydroxyapatite/β-tricalcium phosphate ratios. Adv Appl Ceram. 2009;108:494–500.
509. Macchetta A, Turner IG, Bowen CR. Fabrication of HA/TCP scaffolds with a graded and porous structure using a camphene-based freeze-casting method. Acta Biomater. 2009;5: 1319–27.
510. Potoczek M, Zima A, Paszkiewicz Z, Ślósarczyk A. Manufacturing of highly porous calcium phosphate bioceramics via gel-casting using agarose. Ceram Int. 2009;35:2249–54.
511. Zuo KH, Zeng YP, Jiang D. Effect of polyvinyl alcohol additive on the pore structure and morphology of the freeze-cast hydroxyapatite ceramics. Mater Sci Eng C. 2010;30:283–7.
512. Soon YM, Shin KH, Koh YH, Lee JH, Choi WY, Kim HE. Fabrication and compressive strength of porous hydroxyapatite scaffolds with a functionally graded core/shell structure. J Eur Ceram Soc. 2011;31:13–8.
513. Hesaraki S. Freeze-casted nanostructured apatite scaffold obtained from low temperature biomineralization of reactive calcium phosphates. Key Eng Mater. 2014;587:21–6.
514. Ng S, Guo J, Ma J, Loo SCJ. Synthesis of high surface area mesostructured calcium phosphate particles. Acta Biomater. 2010;6:3772–81.
515. Walsh D, Hopwood JD, Mann S. Crystal tectonics: construction of reticulated calcium phosphate frameworks in bicontinuous reverse microemulsions. Science. 1994;264:1576–8.
516. Walsh D, Mann S. Chemical synthesis of microskeletal calcium phosphate in bicontinuous microemulsions. Chem Mater. 1996;8:1944–53.
517. Zhao K, Tang YF, Qin YS, Wei JQ. Porous hydroxyapatite ceramics by ice templating: freezing characteristics and mechanical properties. Ceram Int. 2011;37:635–9.
518. Zhou K, Zhang Y, Zhang D, Zhang X, Li Z, Liu G, Button TW. Porous hydroxyapatite ceramics fabricated by an ice-templating method. Scr Mater. 2011;64:426–9.
519. Flauder S, Gbureck U, Muller FA. TCP scaffolds with an interconnected and aligned porosity fabricated via ice-templating. Key Eng Mater. 2013;529–530:129–32.
520. Zhang Y, Zhou K, Bao Y, Zhang D. Effects of rheological properties on ice-templated porous hydroxyapatite ceramics. Mater Sci Eng C. 2013;33:340–6.
521. White E, Shors EC. Biomaterial aspects of Interpore-200 porous hydroxyapatite. Dent Clin N Am. 1986;30:49–67.
522. Aizawa M, Howell SF, Itatani K, Yokogawa Y, Nishizawa K, Toriyama M, Kameyama T. Fabrication of porous ceramics with well-controlled open pores by sintering of fibrous hydroxyapatite particles. J Ceram Soc Jpn. 2000;108:249–53.
523. Nakahira A, Tamai M, Sakamoto K, Yamaguchi S. Sintering and microstructure of porous hydroxyapatite. J Ceram Soc Jpn. 2000;108:99–104.
524. Rodriguez-Lorenzo LM, Vallet-Regí M, Ferreira JMF. Fabrication of porous hydroxyapatite bodies by a new direct consolidation method: starch consolidation. J Biomed Mater Res. 2002;60:232–40.
525. Charriere E, Lemaitre J, Zysset P. Hydroxyapatite cement scaffolds with controlled macroporosity: fabrication protocol and mechanical properties. Biomaterials. 2003;24:809–17.
526. Eichenseer C, Will J, Rampf M, Wend S, Greil P. Biomorphous porous hydroxyapatite-ceramics from rattan (*Calamus Rotang*). J Mater Sci Mater Med. 2010;21:131–7.

527. Zhou L, Wang D, Huang W, Yao A, Kamitakahara M, Ioku K. Preparation and characterization of periodic porous frame of hydroxyapatite. J Ceram Soc Jpn. 2009;117:521–4.
528. Kawata M, Uchida H, Itatani K, Okada I, Koda S, Aizawa M. Development of porous ceramics with well-controlled porosities and pore sizes from apatite fibers and their evaluations. J Mater Sci Mater Med. 2004;15:817–23.
529. Koh YH, Kim HW, Kim HE, Halloran JW. Fabrication of macrochannelled-hydroxyapatite bioceramic by a coextrusion process. J Am Ceram Soc. 2002;85:2578–80.
530. Kitamura M, Ohtsuki C, Ogata SI, Kamitakahara M, Tanihara M, Miyazaki T. Mesoporous calcium phosphate via post-treatment of α-TCP. J Am Ceram Soc. 2005;88:822–6.
531. Walsh D, Boanini E, Tanaka J, Mann S. Synthesis of tri-calcium phosphate sponges by interfacial deposition and thermal transformation of self-supporting calcium phosphate films. J Mater Chem. 2005;15:1043–8.
532. Gonzalez-McQuire R, Green D, Walsh D, Hall S, Chane-Ching JY, Oreffo ROC, Mann S. Fabrication of hydroxyapatite sponges by dextran sulphate/amino acid templating. Biomaterials. 2005;26:6652–6.
533. Xu S, Li D, Lu B, Tang Y, Wang C, Wang Z. Fabrication of a calcium phosphate scaffold with a three dimensional channel network and its application to perfusion culture of stem cells. Rapid Prototyp J. 2007;13:99–106.
534. Saiz E, Gremillard L, Menendez G, Miranda P, Gryn K, Tomsia AP. Preparation of porous hydroxyapatite scaffolds. Mater Sci Eng C. 2007;27:546–50.
535. Kamitakahara M, Ohtsuki C, Kawachi G, Wang D, Ioku K. Preparation of hydroxyapatite porous ceramics with different porous structures using a hydrothermal treatment with different aqueous solutions. J Ceram Soc Jpn. 2008;116:6–9.
536. Peña J, Román J, Cabañas MV, Vallet-Regí M. An alternative technique to shape scaffolds with hierarchical porosity at physiological temperature. Acta Biomater. 2010;6:1288–96.
537. Nakamura S, Nakahira A. Synthesis and evaluation of porous hydroxyapatite prepared by hydrothermal treatment and subsequent sintering method. J Ceram Soc Jpn. 2008;116:42–5.
538. Zhang J, Fujiwara M, Xu Q, Zhu Y, Iwasa M, Jiang D. Synthesis of mesoporous calcium phosphate using hybrid templates. Microporous Mesoporous Mater. 2008;111:411–6.
539. Song HY, Islam S, Lee BT. A novel method to fabricate unidirectional porous hydroxyapatite body using ethanol bubbles in a viscous slurry. J Am Ceram Soc. 2008;91:3125–7.
540. Kawachi G, Misumi H, Fujimori H, Goto S, Ohtsuki C, Kamitakahara M, Ioku K. Fabrication of porous blocks of calcium phosphate through hydrothermal processing under glycine coexistence. J Ceram Soc Jpn. 2010;118:559–63.
541. Sakamoto M, Nakasu M, Matsumoto T, Okihana H. Development of superporous hydroxyapatites and their examination with a culture of primary rat osteoblasts. J Biomed Mater Res A. 2007;82A:238–42.
542. Sakamoto M. Development and evaluation of superporous hydroxyapatite ceramics with triple pore structure as bone tissue scaffold. J Ceram Soc Jpn. 2010;118:753–7.
543. Sakamoto M, Matsumoto T. Development and evaluation of superporous ceramics bone tissue scaffold materials with triple pore structure (a) hydroxyapatite, (b) beta-tricalcium phosphate. In: Tal H, editor. Bone regeneration. Rijeka: InTech Europe; 2012. p. 301–20.
544. Deisinger U. Generating porous ceramic scaffolds: processing and properties. Key Eng Mater. 2010;441:155–79.
545. Ishikawa K, Tsuru K, Pham TK, Maruta M, Matsuya S. Fully-interconnected pore forming calcium phosphate cement. Key Eng Mater. 2012;493–494:832–5.
546. Yoon HJ, Kim UC, Kim JH, Koh YH, Choi WY, Kim HE. Fabrication and characterization of highly porous calcium phosphate (CaP) ceramics by freezing foamed aqueous CaP suspensions. J Ceram Soc Jpn. 2011;119:573–6.
547. Ahn MK, Shin KH, Moon YW, Koh YH, Choi WY, Kim HE. Highly porous biphasic calcium phosphate (BCP) ceramics with large interconnected pores by freezing vigorously foamed BCP suspensions under reduced pressure. J Am Ceram Soc. 2011;94:4154–6.
548. Ji L, Jell G, Dong Y, Jones JR, Stevens MM. Template synthesis of ordered macroporous hydroxyapatite bioceramics. Chem Commun. 2011;47:9048–50.

549. Wang XY, Han YC, Li SP. Preparation and characterization of calcium phosphate crystals by precursor thermolysis method. Key Eng Mater. 2012;493–494:191–4.
550. Schlosser M, Kleebe HJ. Vapor transport sintering of porous calcium phosphate ceramics. J Am Ceram Soc. 2012;95:1581–7.
551. Tanaka T, Yoshioka T, Ikoma T, Kuwayama T, Higaki T, Tanaka M. Fabrication of three different types of porous carbonate-substituted apatite ceramics for artificial bone. Key Eng Mater. 2013;529–530:143–6.
552. Zheng W, Liu G, Yan C, Xiao Y, Miao XG. Strong and bioactive tri-calcium phosphate scaffolds with tube-like macropores. J Biomim Biomater Tissue Eng. 2014;19:65–75.
553. Tsuru K, Nikaido T, Munar ML, Maruta M, Matsuya S, Nakamura S, Ishikawa K. Synthesis of carbonate apatite foam using β-TCP foams as precursors. Key Eng Mater. 2014;587: 52–5.
554. Chen ZC, Zhang XL, Zhou K, Cai H, Liu CQ. Novel fabrication of hierarchically porous hydroxyapatite scaffolds with refined porosity and suitable strength. Adv Appl Ceram. 2015;114:183–7.
555. Swain SK, Bhattacharyya S, Sarkar D. Fabrication of porous hydroxyapatite scaffold via polyethylene glycol-polyvinyl alcohol hydrogel state. Mater Res Bull. 2015;64:257–61.
556. Charbonnier B, Laurent C, Marchat D. Porous hydroxyapatite bioceramics produced by impregnation of 3D-printed wax mold: slurry feature optimization. J Eur Ceram Soc. 2016;36:4269–79.
557. Roy DM, Linnehan SK. Hydroxyapatite formed from coral skeletal carbonate by hydrothermal exchange. Nature. 1974;247:220–2.
558. Zhang X, Vecchio KS. Conversion of natural marine skeletons as scaffolds for bone tissue engineering. Front Mater Sci. 2013;7:103–17.
559. Yang Y, Yao Q, Pu X, Hou Z, Zhang Q. Biphasic calcium phosphate macroporous scaffolds derived from oyster shells for bone tissue engineering. Chem Eng J. 2011;173:837–45.
560. Thanh TNX, Maruta M, Tsuru K, Matsuya S, Ishikawa K. Three – dimensional porous carbonate apatite with sufficient mechanical strength as a bone substitute material. Adv Mater Res. 2014;891–892:1559–64.
561. Moroni L, de Wijn JR, van Blitterswijk CA. Integrating novel technologies to fabricate smart scaffolds. J Biomater Sci Polym Ed. 2008;19:543–72.
562. Studart AR, Gonzenbach UT, Tervoort E, Gauckler LJ. Processing routes to macroporous ceramics: a review. J Am Ceram Soc. 2006;89:1771–89.
563. Hing K, Annaz B, Saeed S, Revell P, Buckland T. Microporosity enhances bioactivity of synthetic bone graft substitutes. J Mater Sci Mater Med. 2005;16:467–75.
564. Wang Z, Sakakibara T, Sudo A, Kasai Y. Porosity of β-tricalcium phosphate affects the results of lumbar posterolateral fusion. J Spinal Disord Tech. 2013;26:E40–5.
565. Lan Levengood SK, Polak SJ, Wheeler MB, Maki AJ, Clark SG, Jamison RD, Wagoner Johnson AJ. Multiscale osteointegration as a new paradigm for the design of calcium phosphate scaffolds for bone regeneration. Biomaterials. 2010;31:3552–63.
566. Ruksudjarit A, Pengpat K, Rujijanagul G, Tunkasiri T. The fabrication of nanoporous hydroxyapatite ceramics. Adv Mater Res. 2008;47–50:797–800.
567. Murugan R, Ramakrishna S, Rao KP. Nanoporous hydroxy-carbonate apatite scaffold made of natural bone. Mater Lett. 2006;60:2844–7.
568. Li Y, Tjandra W, Tam KC. Synthesis and characterization of nanoporous hydroxyapatite using cationic surfactants as templates. Mater Res Bull. 2008;43:2318–26.
569. El Asri S, Laghzizil A, Saoiabi A, Alaoui A, El Abassi K, M'hamdi R, Coradin T. A novel process for the fabrication of nanoporous apatites from Moroccan phosphate rock. Colloid Surf A. 2009;350:73–8.
570. Ramli RA, Adnan R, Bakar MA, Masudi SM. Synthesis and characterisation of pure nanoporous hydroxyapatite. J Phys Sci. 2011;22:25–37.
571. LeGeros RZ. Calcium phosphate-based osteoinductive materials. Chem Rev. 2008;108: 4742–53.

572. Prokopiev O, Sevostianov I. Dependence of the mechanical properties of sintered hydroxyapatite on the sintering temperature. Mater Sci Eng A. 2006;431:218–27.
573. Daculsi G, Jegoux F, Layrolle P. The micro macroporous biphasic calcium phosphate concept for bone reconstruction and tissue engineering. In: Basu B, Katti DS, Kumar A, editors. Advanced biomaterials: fundamentals, processing and applications. Hoboken: American Ceramic Society, Wiley; 2009. 768 pp.
574. Shipman P, Foster G, Schoeninger M. Burnt bones and teeth: an experimental study of color, morphology, crystal structure and shrinkage. J Archaeol Sci. 1984;11:307–25.
575. Rice RW. Porosity of ceramics. New York: Marcel Dekker; 1998. 560 pp
576. Wang H, Zhai L, Li Y, Shi T. Preparation of irregular mesoporous hydroxyapatite. Mater Res Bull. 2008;43:1607–14.
577. Fan J, Lei J, Yu C, Tu B, Zhao D. Hard-templating synthesis of a novel rod-like nanoporous calcium phosphate bioceramics and their capacity as antibiotic carriers. Mater Chem Phys. 2007;103:489–93.
578. Sopyan I, Mel M, Ramesh S, Khalid KA. Porous hydroxyapatite for artificial bone applications. Sci Technol Adv Mater. 2007;8:116–23.
579. Hsu YH, Turner IG, Miles AW. Fabrication of porous bioceramics with porosity gradients similar to the bimodal structure of cortical and cancellous bone. J Mater Sci Mater Med. 2007;18:2251–6.
580. Abdurrahim T, Sopyan I. Recent progress on the development of porous bioactive calcium phosphate for biomedical applications. Recent Pat Biomed Eng. 2008;1:213–29.
581. Munch E, Franco J, Deville S, Hunger P, Saiz E, Tomsia AP. Porous ceramic scaffolds with complex architectures. JOM. 2008;60:54–9.
582. Ohji T, Fukushima M. Macro-porous ceramics: processing and properties. Int Mater Rev. 2012;57:115–31.
583. Naqshbandi AR, Sopyan I, Gunawan. Development of porous calcium phosphate bioceramics for bone implant applications: a review. Rec Pat Mater Sci. 2013;6:238–52.
584. Yan X, Yu C, Zhou X, Tang J, Zhao D. Highly ordered mesoporous bioactive glasses with superior in vitro bone-forming bioactivities. Angew Chem Int Ed Engl. 2004;43: 5980–4.
585. Izquierdo-Barba I, Ruiz-González L, Doadrio JC, González-Calbet JM, Vallet-Regí M. Tissue regeneration: a new property of mesoporous materials. Solid State Sci. 2005;7:983–9.
586. Cosijns A, Vervaet C, Luyten J, Mullens S, Siepmann F, van Hoorebeke L, Masschaele B, Cnudde V, Remon JP. Porous hydroxyapatite tablets as carriers for low-dosed drugs. Eur J Pharm Biopharm. 2007;67:498–506.
587. Uchida A, Shinto Y, Araki N, Ono K. Slow release of anticancer drugs from porous calcium hydroxyapatite ceramic. J Orthop Res. 1992;10:440–5.
588. Shinto Y, Uchida A, Korkusuz F, Araki N, Ono K. Calcium hydroxyapatite ceramic used as a delivery system for antibiotics. J Bone Joint Surg (Br). 1992;74:600–4.
589. Martin RB, Chapman MW, Sharkey NA, Zissimos SL, Bay B, Shors EC. Bone ingrowth and mechanical properties of coralline hydroxyapatite 1 yr after implantation. Biomaterials. 1993;14:341–8.
590. Kazakia GJ, Nauman EA, Ebenstein DM, Halloran BP, Keaveny TM. Effects of in vitro bone formation on the mechanical properties of a trabeculated hydroxyapatite bone substitute. J Biomed Mater Res A. 2006;77A:688–99.
591. Hing KA, Best SM, Tanner KE, Bonfield W, Revell PA. Mediation of bone ingrowth in porous hydroxyapatite bone graft substitutes. J Biomed Mater Res A. 2004;68A:187–200.
592. Vuola J, Taurio R, Goransson H, Asko-Seljavaara S. Compressive strength of calcium carbonate and hydroxyapatite implants after bone marrow induced osteogenesis. Biomaterials. 1998;19:223–7.
593. von Doernberg MC, von Rechenberg B, Bohner M, Grünenfelder S, van Lenthe GH, Müller R, Gasser B, Mathys R, Baroud G, Auer J. In vivo behavior of calcium phosphate scaffolds with four different pore sizes. Biomaterials. 2006;27:5186–98.

594. Mygind T, Stiehler M, Baatrup A, Li H, Zou X, Flyvbjerg A, Kassem M, Bunger C. Mesenchymal stem cell ingrowth and differentiation on coralline hydroxyapatite scaffolds. Biomaterials. 2007;28:1036–47.
595. Mankani MH, Afghani S, Franco J, Launey M, Marshall S, Marshall GW, Nissenson R, Lee J, Tomsia AP, Saiz E. Lamellar spacing in cuboid hydroxyapatite scaffolds regulates bone formation by human bone marrow stromal cells. Tissue Eng A. 2011;17:1615–23.
596. Chan O, Coathup MJ, Nesbitt A, Ho CY, Hing KA, Buckland T, Campion C, Blunn GW. The effects of microporosity on osteoinduction of calcium phosphate bone graft substitute biomaterials. Acta Biomater. 2012;8:2788–94.
597. Holmes RE. Bone regeneration within a coralline hydroxyapatite implant. Plast Reconstr Surg. 1979;63:626–33.
598. Tsuruga E, Takita H, Wakisaka Y, Kuboki Y. Pore size of porous hydoxyapatite as the cell-substratum controls BMP-induced osteogenesis. J Biochem. 1997;121:317–24.
599. LeGeros RZ, LeGeros JP. Calcium phosphate bioceramics: past, present, future. Key Eng Mater. 2003;240–242:3–10.
600. Woodard JR, Hilldore AJ, Lan SK, Park CJ, Morgan AW, Eurell JAC, Clark SG, Wheeler MB, Jamison RD, Wagoner JAJ. The mechanical properties and osteoconductivity of hydroxyapatite bone scaffolds with multi-scale porosity. Biomaterials. 2007;28:45–54.
601. Levitt GE, Crayton PH, Monroe EA, Condrate RA. Forming methods for apatite prosthesis. J Biomed Mater Res. 1969;3:683–5.
602. Easwer HV, Rajeev A, Varma HK, Vijayan S, Bhattacharya RN. Cosmetic and radiological outcome following the use of synthetic hydroxyapatite porous-dense bilayer burr-hole buttons. Acta Neurochir. 2007;149:481–5.
603. Kashimura H, Ogasawara K, Kubo Y, Yoshida K, Sugawara A, Ogawa A. A newly designed hydroxyapatite ceramic burr-hole button. Vasc Health Risk Manag. 2010;6:105–8.
604. Jordan DR, Gilberg S, Bawazeer A. Coralline hydroxyapatite orbital implant (Bio-Eye): experience with 158 patients. Ophthal Plast Reconstr Surg. 2004;20:69–74.
605. Liao HF, Xiao W, Chen QJ. Ophthalmic applications of hydroxyapatite and its polymer composites. J Clin Rehabil Tissue Eng Res. 2008;12:8905–8.
606. Yoon JS, Lew H, Kim SJ, Lee SY. Exposure rate of hydroxyapatite orbital implants. A 15-year experience of 802 cases. Ophthalmology. 2008;115:566–72.
607. Chai GR, Chen M. Clinical effect of hydroxyapatite orbital implantation. Int J Ophthalmol. 2010;10:999–1000.
608. Tabatabaee Z, Mazloumi M, Rajabi TM, Khalilzadeh O, Kassaee A, Moghimi S, Eftekhar H, Goldberg RA. Comparison of the exposure rate of wrapped hydroxyapatite (Bio-Eye) versus unwrapped porous polyethylene (Medpor) orbital implants in enucleated patients. Ophthal Plast Reconstr Surg. 2011;27:114–8.
609. Ma XZ, Bi HS, Zhang X. Effect of hydroxyapatite orbital implant for plastic surgery of eye in 52 cases. Int Eye Sci. 2012;12:988–90.
610. Wang L. Simple fixation of hydroxyapatite artificial eye mount of auto sclera. Int Eye Sci. 2012;12:1394–5.
611. Kundu B, Sanyal D, Basu D. Physiological and elastic properties of highly porous hydroxyapatite potential for integrated eye implants: effects of SIRC and L-929 cell lines. Ceram Int. 2013;39:2651–64.
612. Baino F, Vitale-Brovarone C. Bioceramics in ophthalmology. Acta Biomater. 2014;10: 3372–97.
613. Wehrs RE. Hearing results with incus and incus stapes prostheses of hydroxylapatite. Laryngoscope. 1991;101:555–6.
614. Smith J, Gardner E, Dornhoffer JL. Hearing results with a hydroxylapatite/titanium bell partial ossicular replacement prosthesis. Laryngoscope. 2002;112:1796–9.
615. Doi T, Hosoda Y, Kaneko T, Munemoto Y, Kaneko A, Komeda M, Furukawa M, Kuriyama H, Kitajiri M, Tomoda K, Yamashita T. Hearing results for ossicular reconstruction using a cartilage-connecting hydroxyapatite prosthesis with a spearhead. Otol Neurotol. 2007;28: 1041–4.

616. Thalgott JS, Fritts K, Giuffre JM, Timlin M. Anterior interbody fusion of the cervical spine with coralline hydroxyapatite. Spine. 1999;24:1295–9.
617. Mashoof AA, Siddiqui SA, Otero M, Tucci JJ. Supplementation of autogenous bone graft with coralline hydroxyapatite in posterior spine fusion for idiopathic adolescent scoliosis. Orthopedics. 2002;25:1073–6.
618. Minamide A, Yoshida M, Kawakami M, Yamasaki S, Kojima H, Hashizume H, Boden SD. The use of cultured bone marrow cells in type I collagen gel and porous hydroxyapatite for posterolateral lumbar spine fusion. Spine. 2005;30:1134–8.
619. Liu WY, Mo JW, Gao H, Liu HL, Wang MY, He CL, Tang W, Ye YJ. Nano-hydroxyapatite artificial bone serves as a spacer for fusion with the cervical spine after bone grafting. Chin J Tissue Eng Res. 2012;16:5327–30.
620. Silva RV, Camilli JA, Bertran CA, Moreira NH. The use of hydroxyapatite and autogenous cancellous bone grafts to repair bone defects in rats. Int J Oral Maxillofac Surg. 2005; 34:178–84.
621. Damron TA. Use of 3D β-tricalcium phosphate (Vitoss®) scaffolds in repairing bone defects. Nanomedicine. 2007;2:763–75.
622. Busso M, Karlsberg PL. Cheek augmentation and rejuvenation using injectable calcium hydroxylapatite (Radiesse®). Cosmet Dermatol. 2006;19:583–8.
623. Bass LS, Smith S, Busso M, McClaren M. Calcium hydroxylapatite (Radiesse) for treatment of nasolabial folds: long-term safety and efficacy results. Aesthet Surg J. 2010;30:235–8.
624. Low KL, Tan SH, Zein SHS, Roether JA, Mouriño V, Boccaccini AR. Calcium phosphate-based composites as injectable bone substitute materials. J Biomed Mater Res B Appl Biomater. 2010;94B:273–86.
625. Daculsi G, Uzel AP, Weiss P, Goyenvalle E, Aguado E. Developments in injectable multiphasic biomaterials. The performance of microporous biphasic calcium phosphate granules and hydrogels. J Mater Sci Mater Med. 2010;21:855–61.
626. Suzuki K, Anada T, Honda Y, Kishimoto KN, Miyatake N, Hosaka M, Imaizumi H, Itoi E, Suzuki O. Cortical bone tissue response of injectable octacalcium phosphate-hyaluronic acid complexes. Key Eng Mater. 2013;529–530:296–9.
627. Pastorino D, Canal C, Ginebra MP. Drug delivery from injectable calcium phosphate foams by tailoring the macroporosity-drug interaction. Acta Biomater. 2015;12:250–9.
628. Miramond T, Aguado E, Goyenvalle E, Borget P, Baroth S, Daculsi G. In vivo comparative study of two injectable/moldable calcium phosphate bioceramics. Key Eng Mater. 2013; 529–530:291–5.
629. Bohner M, Baroud G. Injectability of calcium phosphate pastes. Biomaterials. 2005;26: 1553–63.
630. Laschke MW, Witt K, Pohlemann T, Menger MD. Injectable nanocrystalline hydroxyapatite paste for bone substitution: in vivo analysis of biocompatibility and vascularization. J Biomed Mater Res B Appl Biomater. 2007;82B:494–505.
631. Lopez-Heredia MA, Barnewitz D, Genzel A, Stiller M, Peters F, Huebner WD, Stang B, Kuhr A, Knabe C. In vivo osteogenesis assessment of a tricalcium phosphate paste and a tricalcium phosphate foam bone grafting materials. Key Eng Mater. 2015;631:426–9.
632. Torres PMC, Gouveia S, Olhero S, Kaushal A, Ferreira JMF. Injectability of calcium phosphate pastes: effects of particle size and state of aggregation of β-tricalcium phosphate powders. Acta Biomater. 2015;21:204–16.
633. Salinas AJ, Esbrit P, Vallet-Regí M. A tissue engineering approach based on the use of bioceramics for bone repair. Biomater Sci. 2013;1:40–51.
634. ISO 13175-3:2012 Implants for surgery – calcium phosphates – oart 3: hydroxyapatite and beta-tricalcium phosphate bone substitutes. https://www.iso.org/obp/ui/#iso:std:iso:13175:-3:ed-1:v1:en.
635. Chow LC. Next generation calcium phosphate-based biomaterials. Dent Mater J. 2009; 28:1–10.
636. Victor SP, Kumar TSS. Processing and properties of injectable porous apatitic cements. J Ceram Soc Jpn. 2008;116:105–7.

637. Hesaraki S, Nemati R, Nosoudi N. Preparation and characterisation of porous calcium phosphate bone cement as antibiotic carrier. Adv Appl Ceram. 2009;108:231–40.
638. Stulajterova R, Medvecky L, Giretova M, Sopcak T. Structural and phase characterization of bioceramics prepared from tetracalcium phosphate–monetite cement and in vitro osteoblast response. J Mater Sci Mater Med. 2015;26:1–9.
639. Bohner M. Resorbable biomaterials as bone graft substitutes. Mater Today. 2010;13:24–30.
640. Paital SR, Dahotre NB. Calcium phosphate coatings for bio-implant applications: materials, performance factors, and methodologies. Mater Sci Eng R. 2009;66:1–70.
641. León B, Jansen JA, editors. Thin calcium phosphate coatings for medical implants. New York: Springer; 2009. 326 pp
642. Dorozhkin SV. Calcium orthophosphate deposits: preparation, properties and biomedical applications. Mater Sci Eng C. 2015;55:272–326.
643. Kon M, Ishikawa K, Miyamoto Y, Asaoka K. Development of calcium phosphate based functional gradient bioceramics. Biomaterials. 1995;16:709–14.
644. Wong LH, Tio B, Miao X. Functionally graded tricalcium phosphate/fluoroapatite composites. Mater Sci Eng C. 2002;20:111–5.
645. Tampieri A, Celotti G, Sprio S, Delcogliano A, Franzese S. Porosity-graded hydroxyapatite ceramics to replace natural bone. Biomaterials. 2001;22:1365–70.
646. Lu WW, Zhao F, Luk KDK, Yin YJ, Cheung KMC, Cheng GX, Yao KD, Leong JCY. Controllable porosity hydroxyapatite ceramics as spine cage: fabrication and properties evaluation. J Mater Sci Mater Med. 2003;14:1039–46.
647. Werner J, Linner-Krcmar B, Friess W, Greil P. Mechanical properties and in vitro cell compatibility of hydroxyapatite ceramics with graded pore structure. Biomaterials. 2002;23: 4285–94.
648. Rodriguez-Lorenzo LM, Ferreira JMF. Development of porous ceramic bodies for applications in tissue engineering and drug delivery systems. Mater Res Bull. 2004;39:83–91.
649. Watanabe T, Fukuhara T, Izui H, Fukase Y, Okano M. Properties of HAp/β-TCP functionally graded material by spark plasma sintering. Trans Jpn Soc Mech Eng A. 2009;75:612–8.
650. Bai X, Sandukas S, Appleford MR, Ong JL, Rabiei A. Deposition and investigation of functionally graded calcium phosphate coatings on titanium. Acta Biomater. 2009;5:3563–72.
651. Roy M, Balla VK, Bandyopadhyay A, Bose S. Compositionally graded hydroxyapatite/ tricalcium phosphate coating on Ti by laser and induction plasma. Acta Biomater. 2011;7: 866–73.
652. Tamura A, Asaoka T, Furukawa K, Ushida T, Tateishi T. Application of α-TCP/HAp functionally graded porous beads for bone regenerative scaffold. Adv Sci Technol. 2013;86:63–9.
653. Gasik M, Keski-Honkola A, Bilotsky Y, Friman M. Development and optimisation of hydroxyapatite-β-TCP functionally gradated biomaterial. J Mech Behav Biomed Mater. 2014;30:266–73.
654. Zhou C, Deng C, Chen X, Zhao X, Chen Y, Fan Y, Zhang X. Mechanical and biological properties of the micro-/nano-grain functionally graded hydroxyapatite bioceramics for bone tissue engineering. J Mech Behav Biomed Mater. 2015;48:1–11.
655. Marković S, Lukić MJ, Škapin SD, Stojanović B, Uskoković D. Designing, fabrication and characterization of nanostructured functionally graded HAp/BCP ceramics. Ceram Int. 2015;41:2654–67.
656. Dubok VA. Bioceramics – yesterday, today, tomorrow. Powder Metall Met Ceram. 2000; 39:381–94.
657. Heness G, Ben-Nissan B. Innovative bioceramics. Mater Forum. 2004;27:104–14.
658. Ohtsuki C, Kamitakahara M, Miyazaki T. Bioactive ceramic-based materials with designed reactivity for bone tissue regeneration. J R Soc Interface. 2009;6:S349–60.
659. Greenspan DC. Bioactive ceramic implant materials. Curr Opin Solid State Mater Sci. 1999;4:389–93.
660. Blokhuis TJ, Termaat MF, den Boer FC, Patka P, Bakker FC, Haarman HJTM. Properties of calcium phosphate ceramics in relation to their in vivo behavior. J Trauma. 2000;48: 179–89.

661. Kim HM. Bioactive ceramics: challenges and perspectives. J Ceram Soc Jpn. 2001;109: S49–57.
662. Seeley Z, Bandyopadhyay A, Bose S. Tricalcium phosphate based resorbable ceramics: influence of NaF and CaO addition. Mater Sci Eng C. 2008;28:11–7.
663. Descamps M, Richart O, Hardouin P, Hornez JC, Leriche A. Synthesis of macroporous β-tricalcium phosphate with controlled porous architectural. Ceram Int. 2008;34:1131–7.
664. Cushnie EK, Khan YM, Laurencin CT. Amorphous hydroxyapatite-sintered polymeric scaffolds for bone tissue regeneration: physical characterization studies. J Biomed Mater Res A. 2008;84A:54–62.
665. Hench LL, Thompson I. Twenty-first century challenges for biomaterials. J R Soc Interface. 2010;7:S379–91.
666. Nagase M, Baker DG, Schumacher HR. Prolonged inflammatory reactions induced by artificial ceramics in the rat pouch model. J Rheumatol. 1988;15:1334–8.
667. Rooney T, Berman S, Indersano AT. Evaluation of porous block hydroxylapatite for augmentation of alveolar ridges. J Oral Maxillofac Surg. 1988;46:15–8.
668. Prudhommeaux F, Schiltz C, Lioté F, Hina A, Champy R, Bucki B, Ortiz-Bravo E, Meunier A, Rey C, Bardin T. Variation in the inflammatory properties of basic calcium phosphate crystals according to crystal type. Arthritis Rheum. 1996;39:1319–26.
669. Ghanaati S, Barbeck M, Orth C, Willershausen I, Thimm BW, Hoffmann C, Rasic A, Sader RA, Unger RE, Peters F, Kirkpatrick CJ. Influence of β-tricalcium phosphate granule size and morphology on tissue reaction in vivo. Acta Biomater. 2010;6:4476–87.
670. Lin K, Yuan W, Wang L, Lu J, Chen L, Wang Z, Chang J. Evaluation of host inflammatory responses of β-tricalcium phosphate bioceramics caused by calcium pyrophosphate impurity using a subcutaneous model. J Biomed Mater Res B Appl Biomater. 2011;99B: 350–8.
671. Velard F, Braux J, Amedee J, Laquerriere P. Inflammatory cell response to calcium phosphate biomaterial particles: an overview. Acta Biomater. 2013;9:4956–63.
672. Rydén L, Molnar D, Esposito M, Johansson A, Suska F, Palmquist A, Thomsen P. Early inflammatory response in soft tissues induced by thin calcium phosphates. J Biomed Mater Res A. 2013;101A:2712–7.
673. Chatterjea A, van der Stok J, Danoux CB, Yuan H, Habibovic P, van Blitterswijk CA, Weinans H, de Boer J. Inflammatory response and bone healing capacity of two porous calcium phosphate ceramics in a critical size cortical bone defects. J Biomed Mater Res A. 2014; 102A:1399–407.
674. Friesenbichler J, Maurer-Ertl W, Sadoghi P, Pirker-Fruehauf U, Bodo K, Leithner A. Adverse reactions of artificial bone graft substitutes: lessons learned from using tricalcium phosphate geneX®. Clin Orthop Relat Res. 2014;472:976–82.
675. Chang TY, Pan SC, Huang YH, Hsueh YY. Blindness after calcium hydroxylapatite injection at nose. J Plast Reconstr Aesthet Surg. 2014;67:1755–7.
676. Jacovella PF, Peiretti CB, Cunille D, Salzamendi M, Schechtel SA. Long-lasting results with hydroxylapatite (Radiesse) facial filler. Plast Reconstr Surg. 2006;118:15S–21S.
677. Ghanaati S, Barbeck M, Detsch R, Deisinger U, Hilbig U, Rausch V, Sader R, Unger RE, Ziegler G, Kirkpatrick CJ. The chemical composition of synthetic bone substitutes influences tissue reactions in vivo: histological and histomorphometrical analysis of the cellular inflammatory response to hydroxyapatite, beta-tricalcium phosphate and biphasic calcium phosphate ceramics. Biomed Mater. 2012;7:015005.
678. Draenert K, Draenert M, Erler M, Draenert A, Draenert Y. How bone forms in large cancellous defects: critical analysis based on experimental work and literature. Injury. 2011;42(Suppl. 2):S47–55.
679. Albrektsson T, Johansson C. Osteoinduction, osteoconduction and osseointegration. Eur Spine J. 2001;10:S96–S101.
680. Yuan H, Kurashina K, de Bruijn DJ, Li Y, de Groot K, Zhang X. A preliminary study of osteoinduction of two kinds of calcium phosphate bioceramics. Biomaterials. 1999;20: 1799–806.

681. Yuan HP, de Bruijn JD, Li YB, Feng JQ, Yang ZJ, de Groot K, Zhang XD. Bone formation induced by calcium phosphate ceramics in soft tissue of dogs: a comparative study between porous α-TCP and β-TCP. J Mater Sci Mater Med. 2001;12:7–13.
682. Barrere F, van der Valk CM, Dalmeijer RA, Meijer G, van Blitterswijk CA, de Groot K, Layrolle P. Osteogenecity of octacalcium phosphate coatings applied on porous titanium. J Biomed Mater Res A. 2003;66A:779–88.
683. Habibovic P, van der Valk CM, van Blitterswijk CA, de Groot K, Meijer G. Influence of octacalcium phosphate coating on osteoinductive properties of biomaterials. J Mater Sci Mater Med. 2004;15:373–80.
684. Ripamonti U, Richter PW, Nilen RW, Renton L. The induction of bone formation by smart biphasic hydroxyapatite tricalcium phosphate biomimetic matrices in the non human primate *Papio ursinus*. J Cell Mol Med. 2008;12:2609–21.
685. Cheng L, Ye F, Yang R, Lu X, Shi Y, Li L, Fan H, Bu H. Osteoinduction of hydroxyapatite/β--tricalcium phosphate bioceramics in mice with a fractured fibula. Acta Biomater. 2010; 6:1569–74.
686. Yuan H, Fernandes H, Habibovic P, de Boer J, Barradas AMC, de Ruiter A, Walsh WR, van Blitterswijk CA, de Bruijn JD. Osteoinductive ceramics as a synthetic alternative to autologous bone grafting. Proc Natl Acad Sci U S A. 2010;107:13614–9.
687. Yao JF, Li XY, Wang AJ, Liang R, Bao CY, Chen ZQ. Osteoinductive calcium phosphate ceramics for in vivo construction of tissue engineered bone in adipose tissue. J Clin Rehabil Tissue Eng Res. 2011;15:2109–12.
688. Barradas AM, Yuan H, van der Stok J, le Quang B, Fernandes H, Chaterjea A, Hogenes MC, Shultz K, Donahue LR, van Blitterswijk C, de Boer J. The influence of genetic factors on the osteoinductive potential of calcium phosphate ceramics in mice. Biomaterials. 2012;33: 5696–705.
689. Li B, Liao X, Zheng L, Zhu X, Wang Z, Fan H, Zhang X. Effect of nanostructure on osteoinduction of porous biphasic calcium phosphate ceramics. Acta Biomater. 2012;8:3794–804.
690. Cheng L, Shi Y, Ye F, Bu H. Osteoinduction of calcium phosphate biomaterials in small animals. Mater Sci Eng C. 2013;33:1254–60.
691. Song G, Habibovic P, Bao C, Hu J, van Blitterswijk CA, Yuan H, Chen W, Xu HHK. The homing of bone marrow MSCs to non-osseous sites for ectopic bone formation induced by osteoinductive calcium phosphate. Biomaterials. 2013;34:2167–76.
692. He P, Sahoo S, Ng KS, Chen K, Toh SL, Goh JCH. Enhanced osteoinductivity and osteoconductivity through hydroxyapatite coating of silk-based tissue-engineered ligament scaffold. J Biomed Mater Res A. 2013;101A:555–66.
693. Davison NL, Gamblin AL, Layrolle P, Yuan H, de Bruijn JD, Barrère-de Groot F. Liposomal clodronate inhibition of osteoclastogenesis and osteoinduction by submicrostructured beta-tricalcium phosphate. Biomaterials. 2014;35:5088–97.
694. Huang Y, He J, Gan L, Liu X, Wu Y, Wu F, Gu ZW. Osteoconductivity and osteoinductivity of porous hydroxyapatite coatings deposited by liquid precursor plasma spraying: in vivo biological response study. Biomed Mater. 2014;9:065007.
695. Lü X, Wang J, Li B, Zhang Z, Zhao L. Gene expression profile study on osteoinductive effect of natural hydroxyapatite. J Biomed Mater Res A. 2014;102A:2833–41.
696. Wang J, Chen Y, Zhu X, Yuan T, Tan Y, Fan Y, Zhang X. Effect of phase composition on protein adsorption and osteoinduction of porous calcium phosphate ceramics in mice. J Biomed Mater Res A. 2014;102A:4234–43.
697. Hongmin L, Wei Z, Xingrong Y, Jing W, Wenxin G, Jihong C, Xin X, Fulin C. Osteoinductive nanohydroxyapatite bone substitute prepared via in situ hydrothermal transformation of cuttlefish bone. J Biomed Mater Res B Appl Biomater. 2015;103B:816–24.
698. Wang L, Barbieri D, Zhou H, de Bruijn JD, Bao C, Yuan H. Effect of particle size on osteoinductive potential of microstructured biphasic calcium phosphate ceramic. J Biomed Mater Res A. 2015;103A:1919–29.
699. Cheng L, Wang T, Zhu J, Cai P. Osteoinduction of calcium phosphate ceramics in four kinds of animals for 1 year: dog, rabbit, rat, and mouse. Transplant Proc. 2016;48:1309–14.

700. Habibovic P, Li J, van der Valk CM, Meijer G, Layrolle P, van Blitterswijk CA, de Groot K. Biological performance of uncoated and octacalcium phosphate-coated Ti6Al4V. Biomaterials. 2005;26:23–36.
701. Habibovic P, Yuan H, van der Valk CM, Meijer G, van Blitterswijk CA, de Groot K. 3D microenvironment as essential element for osteoinduction by biomaterials. Biomaterials. 2005;26:3565–75.
702. Habibovic P, Sees TM, van den Doel MA, van Blitterswijk CA, de Groot K. Osteoinduction by biomaterials – physicochemical and structural influences. J Biomed Mater Res A. 2006;77A:747–62.
703. Reddi AH. Morphogenesis and tissue engineering of bone and cartilage: inductive signals, stem cells and biomimetic biomaterials. Tissue Eng. 2000;6:351–9.
704. Ripamonti U. The morphogenesis of bone in replicas of porous hydroxyapatite obtained by conversion of calcium carbonate exoskeletons of coral. J Bone Joint Surg A. 1991;73: 692–703.
705. Kuboki Y, Takita H, Kobayashi D. BMP-induced osteogenesis on the surface of hydroxyapatite with geometrically feasible and nonfeasible structures: topology of osteogenesis. J Biomed Mater Res. 1998;39:190–9.
706. Zhang J, Luo X, Barbieri D, Barradas AMC, de Bruijn JD, van Blitterswijk CA, Yuan H. The size of surface microstructures as an osteogenic factor in calcium phosphate ceramics. Acta Biomater. 2014;10:3254–63.
707. Zhang J, Barbieri D, Ten Hoopen H, de Bruijn JD, van Blitterswijk CA, Yuan H. Microporous calcium phosphate ceramics driving osteogenesis through surface architecture. J Biomed Mater Res A. 2015;103A:1188–99.
708. Diaz-Flores L, Gutierrez R, Lopez-Alonso A, Gonzalez R, Varela H. Pericytes as a supplementary source of osteoblasts in periosteal osteogenesis. Clin Orthop Relat Res. 1992; 275:280–6.
709. Boyan BD, Schwartz Z. Are calcium phosphate ceramics 'smart' biomaterials? Nat Rev Rheumatol. 2011;7:8–9.
710. Lu J, Descamps M, Dejou J, Koubi G, Hardouin P, Lemaitre J, Proust JP. The biodegradation mechanism of calcium phosphate biomaterials in bone. J Biomed Mater Res Appl Biomater. 2002;63:408–12.
711. Wang H, Lee JK, Moursi A, Lannutti JJ. Ca/P ratio effects on the degradation of hydroxyapatite in vitro. J Biomed Mater Res A. 2003;67A:599–608.
712. Dorozhkin SV. Inorganic chemistry of the dissolution phenomenon, the dissolution mechanism of calcium apatites at the atomic (ionic) level. Comment Inorg Chem. 1999;20: 285–99.
713. Dorozhkin SV. Dissolution mechanism of calcium apatites in acids: a review of literature. World J Methodol. 2012;2:1–17.
714. Sakai S, Anada T, Tsuchiya K, Yamazaki H, Margolis HC, Suzuki O. Comparative study on the resorbability and dissolution behavior of octacalcium phosphate, β-tricalcium phosphate, and hydroxyapatite under physiological conditions. Dent Mater J. 2016;35:216–24.
715. Wenisch S, Stahl JP, Horas U, Heiss C, Kilian O, Trinkaus K, Hild A, Schnettler R. In vivo mechanisms of hydroxyapatite ceramic degradation by osteoclasts: fine structural microscopy. J Biomed Mater Res A. 2003;67A:713–8.
716. Riihonen R, Nielsen S, Väänänen HK, Laitala-Leinonen T, Kwon TH. Degradation of hydroxyapatite in vivo and in vitro requires osteoclastic sodium-bicarbonate co-transporter NBCn1. Matrix Biol. 2010;29:287–94.
717. Teitelbaum SL. Bone resorption by osteoclasts. Science. 2000;289:1504–8.
718. Matsunaga A, Takami M, Irié T, Mishima K, Inagaki K, Kamijo R. Microscopic study on resorption of β-tricalcium phosphate materials by osteoclasts. Cytotechnology. 2015;67: 727–32.
719. Narducci P, Nicolin V. Differentiation of activated monocytes into osteoclast-like cells on a hydroxyapatite substrate: an in vitro study. Ann Anat. 2009;191:349–55.

720. Wu VM, Uskoković V. Is there a relationship between solubility and resorbability of different calcium phosphate phases in vitro? Biochim Biophys Acta. 1860;2016:2157–68.
721. Tamimi F, Torres J, Bassett D, Barralet J, Cabarcos EL. Resorption of monetite granules in alveolar bone defects in human patients. Biomaterials. 2010;31:2762–9.
722. Sheikh Z, Abdallah MN, Hanafi AA, Misbahuddin S, Rashid H, Glogauer M. Mechanisms of in vivo degradation and resorption of calcium phosphate based biomaterials. Materials. 2015;8:7913–25.
723. Raynaud S, Champion E, Lafon JP, Bernache-Assollant D. Calcium phosphate apatites with variable Ca/P atomic ratio. III. Mechanical properties and degradation in solution of hot pressed ceramics. Biomaterials. 2002;23:1081–9.
724. Barrère F, van der Valk CM, Dalmeijer RAJ, van Blitterswijk CA, de Groot K, Layrolle P. In vitro and in vivo degradation of biomimetic octacalcium phosphate and carbonate apatite coatings on titanium implants. J Biomed Mater Res A. 2003;64A:378–87.
725. Souto RM, Laz MM, Reis RL. Degradation characteristics of hydroxyapatite coatings on orthopaedic TiAlV in simulated physiological media investigated by electrochemical impedance spectroscopy. Biomaterials. 2003;24:4213–21.
726. Dellinger JG, Wojtowicz AM, Jamison RD. Effects of degradation and porosity on the load bearing properties of model hydroxyapatite bone scaffolds. J Biomed Mater Res A. 2006; 77A:563–71.
727. Okuda T, Ioku K, Yonezawa I, Minagi H, Kawachi G, Gonda Y, Murayama H, Shibata Y, Minami S, Kamihara S, Kurosawa H, Ikeda T. The effect of the microstructure of β-tricalcium phosphate on the metabolism of subsequently formed bone tissue. Biomaterials. 2007; 28:2612–21.
728. Orly I, Gregoire M, Menanteau J, Heughebaert M, Kerebel B. Chemical changes in hydroxyapatite biomaterial under in vivo and in vitro biological conditions. Calcif Tissue Int. 1989;45:20–6.
729. Sun L, Berndt CC, Gross KA, Kucuk A. Review: material fundamentals and clinical performance of plasma sprayed hydroxyapatite coatings. J Biomed Mater Res Appl Biomater. 2001;58:570–92.
730. Bertazzo S, Zambuzzi WF, Campos DDP, Ogeda TL, Ferreira CV, Bertran CA. Hydroxyapatite surface solubility and effect on cell adhesion. Colloid Surf B. 2010;78:177–84.
731. Schwartz Z, Boyan BD. Underlying mechanisms at the bone-biomaterial interface. J Cell Biochem. 1994;56:340–7.
732. Puleo DA, Nanci A. Understanding and controlling the bone-implant interface. Biomaterials. 1999;20:2311–21.
733. Xin R, Leng Y, Chen J, Zhang Q. A comparative study of calcium phosphate formation on bioceramics in vitro and in vivo. Biomaterials. 2005;26:6477–86.
734. Girija EK, Parthiban SP, Suganthi RV, Elayaraja K, Joshy MIA, Vani R, Kularia P, Asokan K, Kanjilal D, Yokogawa Y, Kalkura SN. High energy irradiation – a tool for enhancing the bioactivity of hydroxyapatite. J Ceram Soc Jpn. 2008;116:320–4.
735. Okada M, Furukawa K, Serizawa T, Yanagisawa Y, Tanaka H, Kawai T, Furuzono T. Interfacial interactions between calcined hydroxyapatite nanocrystals and substrates. Langmuir. 2009;25:6300–6.
736. Callis PD, Donaldson K, McCord JF. Early cellular responses to calcium phosphate ceramics. Clin Mater. 1988;3:183–90.
737. Okumura M, Ohgushi H, Tamai S. Bonding osteogenesis in coralline hydroxyapatite combined with bone marrow cells. Biomaterials. 1990;12:28–37.
738. Holtgrave EA, Donath K. Response of odontoblast-like cells to hydroxyapatite ceramic granules. Biomaterials. 1995;16:155–9.
739. Doi Y, Iwanaga H, Shibutani T, Moriwaki Y, Iwayama Y. Osteoclastic responses to various calcium phosphates in cell cultures. J Biomed Mater Res. 1999;47:424–33.
740. Guo X, Gough JE, Xiao P, Liu J, Shen Z. Fabrication of nanostructured hydroxyapatite and analysis of human osteoblastic cellular response. J Biomed Mater Res A. 2007;82A: 1022–32.

741. Wang Y, Zhang S, Zeng X, Ma LL, Weng W, Yan W, Qian M. Osteoblastic cell response on fluoridated hydroxyapatite coatings. Acta Biomater. 2007;3:191–7.
742. Bae WJ, Chang SW, Lee SI, Kum KY, Bae KS, Kim EC. Human periodontal ligament cell response to a newly developed calcium phosphate-based root canal sealer. J Endod. 2010;36:1658–63.
743. Li J, Song Y, Zhang S, Zhao C, Zhang F, Zhang X, Cao L, Fan Q, Tang T. In vitro responses of human bone marrow stromal cells to a fluoridated hydroxyapatite coated biodegradable Mg-Zn alloy. Biomaterials. 2010;31:5782–8.
744. Zhao X, Heng BC, Xiong S, Guo J, Tan TT-Y, Boey FYC, Ng KW, Loo JSC. In vitro assessment of cellular responses to rod-shaped hydroxyapatite nanoparticles of varying lengths and surface areas. Nanotoxicology. 2011;5:182–94.
745. Detsch R, Schaefer S, Deisinger U, Ziegler G, Seitz H, Leukers B. In vitro-osteoclastic activity studies on surfaces of 3D printed calcium phosphate scaffolds. J Biomater Appl. 2011;26:359–80.
746. Kanayama K, Sriarj W, Shimokawa H, Ohya K, Doi Y, Shibutani T. Osteoclast and osteoblast activities on carbonate apatite plates in cell cultures. J Biomater Appl. 2011;26:435–49.
747. Liu X, Zhao M, Lu J, Ma J, Wei J, Wei S. Cell responses to two kinds of nanohydroxyapatite with different sizes and crystallinities. Int J Nanomedicine. 2012;7:1239–50.
748. Marchi J, Ribeiro C, de Almeida Bressiant AH, Marquesd MM. Cell response of calcium phosphate based ceramics, a bone substitute material. Mater Res. 2013;16:703–12.
749. Perez RA, Kim TH, Kim M, Jang JH, Ginebra MP, Kim HW. Calcium phosphate cements loaded with basic fibroblast growth factor: delivery and in vitro cell response. J Biomed Mater Res A. 2013;101A:923–31.
750. Yin P, Feng FF, Lei T, Zhong XH, Jian XC. Osteoblastic cell response on biphasic fluorhydroxyapatite/strontium-substituted hydroxyapatite coatings. J Biomed Mater Res A. 2014; 102A:621–7.
751. Lobo SE, Glickman R, da Silva WN, Arinzeh TL, Kerkis I. Response of stem cells from different origins to biphasic calcium phosphate bioceramics. Cell Tissue Res. 2015;361: 477–95.
752. Suzuki T, Ohashi R, Yokogawa Y, Nishizawa K, Nagata F, Kawamoto Y, Kameyama T, Toriyama M. Initial anchoring and proliferation of fibroblast L-929 cells on unstable surface of calcium phosphate ceramics. J Biosci Bioeng. 1999;87:320–7.
753. Arinzeh TL, Tran T, McAlary J, Daculsi G. A comparative study of biphasic calcium phosphate ceramics for human mesenchymal stem-cell-induced bone formation. Biomaterials. 2005;26:3631–8.
754. Oh S, Oh N, Appleford M, Ong JL. Bioceramics for tissue engineering applications – a review. Am J Biochem Biotechnol. 2006;2:49–56.
755. Appleford M, Oh S, Cole JA, Carnes DL, Lee M, Bumgardner JD, Haggard WO, Ong JL. Effects of trabecular calcium phosphate scaffolds on stress signaling in osteoblast precursor cells. Biomaterials. 2007;28:2747–53.
756. Gamie Z, Tran GT, Vyzas G, Korres N, Heliotis M, Mantalaris A, Tsiridis E. Stem cells combined with bone graft substitutes in skeletal tissue engineering. Expert Opin Biol Ther. 2012;12:713–29.
757. Manfrini M, di Bona C, Canella A, Lucarelli E, Pellati A, d'Agostino A, Barbanti-Bròdano G, Tognon M. Mesenchymal stem cells from patients to assay bone graft substitutes. J Cell Physiol. 2013;228:1229–37.
758. Unger RE, Sartoris A, Peters K, Motta A, Migliaresi C, Kunkel M, Bulnheim U, Rychly J, Kirkpatrick CJ. Tissue-like self-assembly in cocultures of endothelial cells and osteoblasts and the formation of microcapillary like structures on three-dimensional porous biomaterials. Biomaterials. 2007;28:3965–76.
759. Nazir NM, Dasmawati M, Azman SM, Omar NS, Othman R. Biocompatibility of in house β-tricalcium phosphate ceramics with normal human osteoblast cell. J Eng Sci Technol. 2012;7:169–76.

760. Tan F, O'Neill F, Naciri M, Dowling D, Al-Rubeai M. Cellular and transcriptomic analysis of human mesenchymal stem cell response to plasma-activated hydroxyapatite coating. Acta Biomater. 2012;8:1627–38.
761. Li B, Liao X, Zheng L, He H, Wang H, Fan H, Zhang X. Preparation and cellular response of porous A-type carbonated hydroxyapatite nanoceramics. Mater Sci Eng C. 2012;32:929–36.
762. Teixeira S, Fernandes MH, Ferraz MP, Monteiro FJ. Proliferation and mineralization of bone marrow cells cultured on macroporous hydroxyapatite scaffolds functionalized with collagen type I for bone tissue regeneration. J Biomed Mater Res A. 2010;95A:1–8.
763. Yan-Zhong Z, Yan-Yan H, Jun Z, Shai-Hong Z, Zhi-You L, Ke-Chao Z. Characteristics of functionalized nano-hydroxyapatite and internalization by human epithelial cell. Nanoscale Res Lett. 2011;6:600. (8 pages)
764. Borcard F, Staedler D, Comas H, Juillerat FK, Sturzenegger PN, Heuberger R, Gonzenbach UT, Juillerat-Jeanneret L, Gerber-Lemaire S. Chemical functionalization of bioceramics to enhance endothelial cells adhesion for tissue engineering. J Med Chem. 2012;27:7988–97.
765. Treccani L, Klein TY, Meder F, Pardun K, Rezwan K. Functionalized ceramics for biomedical, biotechnological and environmental applications. Acta Biomater. 2013;9:7115–50.
766. Russo L, Taraballi F, Lupo C, Poveda A, Jiménez-Barbero J, Sandri M, Tampieri A, Nicotra F, Cipolla L. Carbonate hydroxyapatite functionalization: a comparative study towards (bio) molecules fixation. Interface Focus. 2014;4:20130040.
767. Zhuang Z, Yoshimura H, Aizawa M. Synthesis and ultrastructure of plate-like apatite single crystals as a model for tooth enamel. Mater Sci Eng C. 2013;33:2534–40.
768. Zhuang Z, Fujimi TJ, Nakamura M, Konishi T, Yoshimura H, Aizawa M. Development of *a, b*-plane-oriented hydroxyapatite ceramics as models for living bones and their cell adhesion behavior. Acta Biomater. 2013;9:6732–40.
769. Aizawa M, Matsuura T, Zhuang Z. Syntheses of single-crystal apatite particles with preferred orientation to the *a*- and *c*-axes as models of hard tissue and their applications. Biol Pharm Bull. 2013;36:1654–61.
770. Lin K, Wu C, Chang J. Advances in synthesis of calcium phosphate crystals with controlled size and shape. Acta Biomater. 2014;10:4071–102.
771. Chen W, Long T, Guo YJ, Zhu ZA, Guo YP. Hydrothermal synthesis of hydroxyapatite coatings with oriented nanorod arrays. RSC Adv. 2014;4:185–91.
772. Guan JJ, Tian B, Tang S, Ke QF, Zhang CQ, Zhu ZA, Guo YP. Hydroxyapatite coatings with oriented nanoplate arrays: synthesis, formation mechanism and cytocompatibility. J Mater Chem B. 2015;3:1655–66.
773. Freidlin LK, Sharf VZ. Two paths for the dehydration of 1,4-butandiol to divinyl with a tricalcium phosphate catalyst. Bull Acad Sci USSR Div Chem Sci. 1960;9:1577–9.
774. Bett JAS, Christner LG, Hall WK. Studies of the hydrogen held by solids. XII. Hydroxyapatite catalysts. J Am Chem Soc. 1967;89:5535–41.
775. Monma H. Catalytic behavior of calcium phosphates for decompositions of 2-propanol and ethanol. J Catal. 1982;75:200–3.
776. Tsuchida T, Yoshioka T, Sakuma S, Takeguchi T, Ueda W. Synthesis of biogasoline from ethanol over hydroxyapatite catalyst. Ind Eng Chem Res. 2008;47:1443–52.
777. Tsuchida T, Kubo J, Yoshioka T, Sakuma S, Takeguchi T, Ueda W. Reaction of ethanol over hydroxyapatite affected by Ca/P ratio of catalyst. J Catal. 2008;259:183–9.
778. Xu J, White T, Li P, He C, Han YF. Hydroxyapatite foam as a catalyst for formaldehyde combustion at room temperature. J Am Chem Soc. 2010;132:13172–3.
779. Hatano M, Moriyama K, Maki T, Ishihara K. Which is the actual catalyst: chiral phosphoric acid or chiral calcium phosphate? Angew Chem Int Ed Engl. 2010;49:3823–6.
780. Zhang D, Zhao H, Zhao X, Liu Y, Chen H, Li X. Application of hydroxyapatite as catalyst and catalyst carrier. Prog Chem. 2011;23:687–94.
781. Gruselle M, Kanger T, Thouvenot R, Flambard A, Kriis K, Mikli V, Traksmaa R, Maaten B, Tõnsuaadu K. Calcium hydroxyapatites as efficient catalysts for the Michael C-C bond formation. ACS Catal. 2011;1:1729–33.

782. Stošić D, Bennici S, Sirotin S, Calais C, Couturier JL, Dubois JL, Travert A, Auroux A. Glycerol dehydration over calcium phosphate catalysts: effect of acidic-basic features on catalytic performance. Appl Catal A. 2012;447–448:124–34.
783. Ghantani VC, Lomate ST, Dongare MK, Umbarkar SB. Catalytic dehydration of lactic acid to acrylic acid using calcium hydroxyapatite catalysts. Green Chem. 2013;15:1211–7.
784. Chen G, Shan R, Shi J, Liu C, Yan B. Biodiesel production from palm oil using active and stable K doped hydroxyapatite catalysts. Energy Convers Manag. 2015;98:463–9.
785. Gruselle M. Apatites: a new family of catalysts in organic synthesis. J Organomet Chem. 2015;793:93–101.
786. Urist MR, Huo YK, Brownell AG, Hohl WM, Buyske J, Lietze A, Tempst P, Hunkapiller M, de Lange RJ. Purification of bovine bone morphogenetic protein by hydroxyapatite chromatography. Proc Natl Acad Sci U S A. 1984;81:371–5.
787. Kawasaki T. Hydroxyapatite as a liquid chromatographic packing. J Chromatogr. 1991;544: 147–84.
788. Kuiper M, Sanches RM, Walford JA, Slater NKH. Purification of a functional gene therapy vector derived from moloney murine leukaemia virus using membrane filtration and ceramic hydroxyapatite chromatography. Biotechnol Bioeng. 2002;80:445–53.
789. Jungbauer A, Hahn R, Deinhofer K, Luo P. Performance and characterization of a nanophased porous hydroxyapatite for protein chromatography. Biotechnol Bioeng. 2004;87:364–75.
790. Wensel DL, Kelley BD, Coffman JL. High-throughput screening of chromatographic separations: III. Monoclonal antibodies on ceramic hydroxyapatite. Biotechnol Bioeng. 2008;100: 839–54.
791. Hilbrig F, Freitag R. Isolation and purification of recombinant proteins, antibodies and plasmid DNA with hydroxyapatite chromatography. Biotechnol J. 2012;7:90–102.
792. Cummings LJ, Frost RG, Snyder MA. Monoclonal antibody purification by ceramic hydroxyapatite chromatography. Methods Mol Biol. 2014;1131:241–51.
793. Nagai M, Nishino T, Saeki T. A new type of CO_2 gas sensor comprising porous hydroxyapatite ceramics. Sensors Actuators. 1988;15:145–51.
794. Petrucelli GC, Kawachi EY, Kubota LT, Bertran CA. Hydroxyapatite-based electrode: a new sensor for phosphate. Anal Commun. 1996;33:227–9.
795. Tagaya M, Ikoma T, Hanagata N, Chakarov D, Kasemo B, Tanaka J. Reusable hydroxyapatite nanocrystal sensors for protein adsorption. Sci Technol Adv Mater. 2010;11:045002.
796. Khairnar RS, Mene RU, Munde SG, Mahabole MP. Nano-hydroxyapatite thick film gas sensors. AIP Conf Proc. 2011;1415:189–92.
797. Hollister SJ. Porous scaffold design for tissue engineering. Nat Mater. 2005;4:518–24.
798. Jones JR, Hench LL. Regeneration of trabecular bone using porous ceramics. Curr Opin Solid State Mater Sci. 2003;7:301–7.
799. Williams DF. On the mechanisms of biocompatibility. Biomaterials. 2008;29:2941–53.
800. Griffith LG, Naughton G. Tissue engineering – current challenges and expanding opportunities. Science. 2002;295:1009–14.
801. Goldberg VM, Caplan AI. Orthopedic tissue engineering basic science and practice. New York: Marcel Dekker; 2004. 338 pp
802. van Blitterswijk CA, Thomsen P, Hubbell J, Cancedda R, de Bruijn JD, Lindahl A, Sohier J, Williams DF, editors. Tissue engineering. Burlington: Academic; 2008. 760 pp
803. Ikada Y. Challenges in tissue engineering. J R Soc Interface. 2006;3:589–601.
804. Cima LG, Langer R. Engineering human tissue. Chem Eng Prog. 1993;89:46–54.
805. Langer R, Vacanti JP. Tissue engineering. Science. 1993;260:920–6.
806. El-Ghannam A. Bone reconstruction: from bioceramics to tissue engineering. Expert Rev Med Dev. 2005;2:87–101.
807. Kneser U, Schaefer DJ, Polykandriotis E, Horch RE. Tissue engineering of bone: the reconstructive surgeon's point of view. J Cell Mol Med. 2006;10:7–19.
808. Scott TG, Blackburn G, Ashley M, Bayer IS, Ghosh A, Biris AS, Biswas A. Advances in bionanomaterials for bone tissue engineering. J Nanosci Nanotechnol. 2013;13:1–22.

809. Lutolf MP, Hubbell JA. Synthetic biomaterials as instructive extracellular microenvironments for morphogenesis in tissue engineering. Nat Biotechnol. 2005;23:47–55.
810. Ma PX. Biomimetic materials for tissue engineering. Adv Drug Deliv Rev. 2008;60: 184–98.
811. Yang S, Leong KF, Du Z, Chua CK. The design of scaffolds for use in tissue engineering. Part I. Traditional factors. Tissue Eng. 2001;7:679–89.
812. Hutmacher DW. Scaffolds in tissue engineering bone and cartilage. Biomaterials. 2000;21: 2529–43.
813. Ma PX. Scaffolds for tissue fabrication. Mater Today. 2004;7:30–40.
814. Yasuhiko T. Biomaterial technology for tissue engineering applications. J R Soc Interface. 2009;6:S311–24.
815. Ma PX, Elisseeff J, editors. Scaffolding in tissue engineering. Boca Raton: CRC Press; 2006. 638 pp
816. Schieker M, Seitz H, Drosse I, Seitz S, Mutschler W. Biomaterials as scaffold for bone tissue engineering. Eur J Trauma. 2006;32:114–24.
817. Williams DF. The biomaterials conundrum in tissue engineering. Tissue Eng A. 2014;20: 1129–31.
818. Freed LE, Guilak F, Guo XE, Gray ML, Tranquillo R, Holmes JW, Radisic M, Sefton MV, Kaplan D, Vunjak-Novakovic G. Advanced tools for tissue engineering: scaffolds, bioreactors, and signaling. Tissue Eng. 2006;12:3285–305.
819. Gandaglia A, Bagno A, Naso F, Spina M, Gerosa G. Cells, scaffolds and bioreactors for tissue-engineered heart valves: a journey from basic concepts to contemporary developmental innovations. Eur J Cardiothorac Surg. 2011;39:523–31.
820. Hui JHP, Buhary KS, Chowdhary A. Implantation of orthobiologic, biodegradable scaffolds in osteochondral repair. Orthop Clin N Am. 2012;43:255–61.
821. Vanderleyden E, Mullens S, Luyten J, Dubruel P. Implantable (bio)polymer coated titanium scaffolds: a review. Curr Pharm Des. 2012;18:2576–90.
822. Service RF. Tissue engineers build new bone. Science. 2000;289:1498–500.
823. Deligianni DD, Katsala ND, Koutsoukos PG, Missirlis YF. Effect of surface roughness of hydroxyapatite on human bone marrow cell adhesion, proliferation, differentiation and detachment strength. Biomaterials. 2001;22:87–96.
824. Fini M, Giardino R, Borsari V, Torricelli P, Rimondini L, Giavaresi G, Aldini NN. In vitro behaviour of osteoblasts cultured on orthopaedic biomaterials with different surface roughness, uncoated and fluorohydroxyapatite-coated, relative to the in vivo osteointegration rate. Int J Artif Organs. 2003;26:520–8.
825. Sato M, Webster TJ. Designing orthopedic implant surfaces: harmonization of nanotopographical and chemical aspects. Nanomedicine. 2006;1:351–4.
826. Li X, van Blitterswijk CA, Feng Q, Cui F, Watari F. The effect of calcium phosphate microstructure on bone-related cells in vitro. Biomaterials. 2008;29:3306–16.
827. Kumar G, Waters MS, Farooque TM, Young MF, Simon CG. Freeform fabricated scaffolds with roughened struts that enhance both stem cell proliferation and differentiation by controlling cell shape. Biomaterials. 2012;33:4022–30.
828. Holthaus MG, Treccani L, Rezwan K. Osteoblast viability on hydroxyapatite with well-adjusted submicron and micron surface roughness as monitored by the proliferation reagent WST2-1. J Biomater Appl. 2013;27:791–800.
829. Zhou Y, Chen F, Ho ST, Woodruff MA, Lim TM, Hutmacher DW. Combined marrow stromal cell-sheet techniques and high-strength biodegradable composite scaffolds for engineered functional bone grafts. Biomaterials. 2007;28:814–24.
830. Vitale-Brovarone C, Baino F, Verné E. High strength bioactive glass-ceramic scaffolds for bone regeneration. J Mater Sci Mater Med. 2009;20:643–53.
831. Ebaretonbofa E, Evans JR. High porosity hydroxyapatite foam scaffolds for bone substitute. J Porous Mater. 2002;9:257–63.
832. Specchia N, Pagnotta A, Cappella M, Tampieri A, Greco F. Effect of hydroxyapatite porosity on growth and differentiation of human osteoblast-like cells. J Mater Sci. 2002;37:577–84.

833. Hing KA. Bioceramic bone graft substitutes: influence of porosity and chemistry. Int J Appl Ceram Technol. 2005;2:184–99.
834. Malmström J, Adolfsson E, Arvidsson A, Thomsen P. Bone response inside free-form fabricated macroporous hydroxyapatite scaffolds with and without an open microporosity. Clin Implant Dent Relat Res. 2007;9:79–88.
835. Peng Q, Jiang F, Huang P, Zhou S, Weng J, Bao C, Zhang C, Yu H. A novel porous bioceramics scaffold by accumulating hydroxyapatite spherules for large bone tissue engineering in vivo. I. Preparation and characterization of scaffold. J Biomed Mater Res A. 2010;93A: 920–9.
836. Lew KS, Othman R, Ishikawa K, Yeoh FY. Macroporous bioceramics: a remarkable material for bone regeneration. J Biomater Appl. 2012;27:345–58.
837. Ren LM, Todo M, Arahira T, Yoshikawa H, Myoui A. A comparative biomechanical study of bone ingrowth in two porous hydroxyapatite bioceramics. Appl Surf Sci. 2012;262:81–8.
838. Guda T, Walker JA, Singleton B, Hernandez J, Oh DS, Appleford MR, Ong JL, Wenke JC. Hydroxyapatite scaffold pore architecture effects in large bone defects in vivo. J Biomater Appl. 2014;28:1016–27.
839. Shao R, Quan R, Zhang L, Wei X, Yang D, Xie S. Porous hydroxyapatite bioceramics in bone tissue engineering: current uses and perspectives. J Ceram Soc Jpn. 2015;123:17–20.
840. Stevens MM. Biomaterials for bone tissue engineering. Mater Today. 2008;11:18–25.
841. Artzi Z, Weinreb M, Givol N, Rohrer MD, Nemcovsky CE, Prasad HS, Tal H. Biomaterial resorbability and healing site morphology of inorganic bovine bone and beta tricalcium phosphate in the canine: a 24-month longitudinal histologic study and morphometric analysis. Int J Oral Maxillofac Implants. 2004;19:357–68.
842. Burg KJL, Porter S, Kellam JF. Biomaterial developments for bone tissue engineering. Biomaterials. 2000;21:2347–59.
843. Ajaal TT, Smith RW. Employing the Taguchi method in optimizing the scaffold production process for artificial bone grafts. J Mater Process Technol. 2009;209:1521–32.
844. Daculsi G. Smart scaffolds: the future of bioceramic. J Mater Sci Mater Med. 2015;26:154.
845. Daculsi G, Miramond T, Borget P, Baroth S. Smart calcium phosphate bioceramic scaffold for bone tissue engineering. Key Eng Mater. 2013;529–530:19–23.
846. Bohner M, Loosli Y, Baroud G, Lacroix D. Commentary: deciphering the link between architecture and biological response of a bone graft substitute. Acta Biomater. 2011;7:478–84.
847. Peppas NA, Langer R. New challenges in biomaterials. Science. 1994;263:1715–20.
848. Hench LL. Biomaterials: a forecast for the future. Biomaterials. 1998;19:1419–23.
849. Barrère F, Mahmood TA, de Groot K, van Blitterswijk CA. Advanced biomaterials for skeletal tissue regeneration: instructive and smart functions. Mater Sci Eng R. 2008;59:38–71.
850. Liu H, Webster TJ. Nanomedicine for implants: a review of studies and necessary experimental tools. Biomaterials. 2007;28:354–69.
851. Wang C, Duan Y, Markovic B, Barbara J, Howlett CR, Zhang X, Zreiqat H. Proliferation and bone-related gene expression of osteoblasts grown on hydroxyapatite ceramics sintered at different temperature. Biomaterials. 2004;25:2949–56.
852. Samavedi S, Whittington AR, Goldstein AS. Calcium phosphate ceramics in bone tissue engineering: a review of properties and their influence on cell behavior. Acta Biomater. 2013;9:8037–45.
853. Matsumoto T, Okazaki M, Nakahira A, Sasaki J, Egusa H, Sohmura T. Modification of apatite materials for bone tissue engineering and drug delivery carriers. Curr Med Chem. 2007;14:2726–33.
854. Chai YC, Carlier A, Bolander J, Roberts SJ, Geris L, Schrooten J, van Oosterwyck H, Luyten FP. Current views on calcium phosphate osteogenicity and the translation into effective bone regeneration strategies. Acta Biomater. 2012;8:3876–87.
855. Denry I, Kuhn LT. Design and characterization of calcium phosphate ceramic scaffolds for bone tissue engineering. Dent Mater. 2016;32:43–53.
856. Traykova T, Aparicio C, Ginebra MP, Planell JA. Bioceramics as nanomaterials. Nanomedicine. 2006;1:91–106.

857. Kalita SJ, Bhardwaj A, Bhatt HA. Nanocrystalline calcium phosphate ceramics in biomedical engineering. Mater Sci Eng C. 2007;27:441–9.
858. Dorozhkin SV. Nanodimensional and nanocrystalline calcium orthophosphates. Int J Chem Mater Sci. 2013;1:105–74.
859. Šupová M. Isolation and preparation of nanoscale bioapatites from natural sources: a review. J Nanosci Nanotechnol. 2014;14:546–63.
860. Zhao J, Liu Y, Sun WB, Zhang H. Amorphous calcium phosphate and its application in dentistry. Chem Cent J. 2011;5:40. (7 pages)
861. Dorozhkin SV. Amorphous calcium orthophosphates: nature, chemistry and biomedical applications. Int J Mater Chem. 2012;2:19–46.
862. Liu B, Lun DX. Current application of β-tricalcium phosphate composites in orthopaedics. Orthop Surg. 2012;4:139–44.
863. Venkatesan J, Kim SK. Nano-hydroxyapatite composite biomaterials for bone tissue engineering – a review. J Biomed Nanotechnol. 2014;10:3124–40.
864. Wu Y, Hench LL, Du J, Choy KL, Guo J. Preparation of hydroxyapatite fibers by electrospinning technique. J Am Ceram Soc. 2004;87:1988–91.
865. Ramanan SR, Venkatesh R. A study of hydroxyapatite fibers prepared via sol-gel route. Mater Lett. 2004;58:3320–3.
866. Aizawa M, Porter AE, Best SM, Bonfield W. Ultrastructural observation of single-crystal apatite fibres. Biomaterials. 2005;26:3427–33.
867. Park YM, Ryu SC, Yoon SY, Stevens R, Park HC. Preparation of whisker-shaped hydroxyapatite/β-tricalcium phosphate composite. Mater Chem Phys. 2008;109:440–7.
868. Aizawa M, Ueno H, Itatani K, Okada I. Syntheses of calcium-deficient apatite fibres by a homogeneous precipitation method and their characterizations. J Eur Ceram Soc. 2006; 26:501–7.
869. Seo DS, Lee JK. Synthesis of hydroxyapatite whiskers through dissolution-reprecipitation process using EDTA. J Cryst Growth. 2008;310:2162–7.
870. Tas AC. Formation of calcium phosphate whiskers in hydrogen peroxide (H_2O_2) solutions at 90°C. J Am Ceram Soc. 2007;90:2358–62.
871. Neira IS, Guitián F, Taniguchi T, Watanabe T, Yoshimura M. Hydrothermal synthesis of hydroxyapatite whiskers with sharp faceted hexagonal morphology. J Mater Sci. 2008;43: 2171–8.
872. Yang HY, Yang SF, Chi XP, Evans JRG, Thompson I, Cook RJ, Robinson P. Sintering behaviour of calcium phosphate filaments for use as hard tissue scaffolds. J Eur Ceram Soc. 2008;28:159–67.
873. Junginger M, Kübel C, Schacher FH, Müller AHE, Taubert A. Crystal structure and chemical composition of biomimetic calcium phosphate nanofibers. RSC Adv. 2013;3:11301–8.
874. Cui YS, Yan TT, Wu XP, Chen QH. Preparation and characterization of hydroxyapatite whiskers. Appl Mech Mater. 2013;389:21–4.
875. Lee JH, Kim YJ. Hydroxyapatite nanofibers fabricated through electrospinning and sol-gel process. Ceram Int. 2014;40:3361–9.
876. Zhang H, Zhu Q. Synthesis of nanospherical and ultralong fibrous hydroxyapatite and reinforcement of biodegradable chitosan/hydroxyapatite composite. Mod Phys Lett B. 2009; 23:3967–76.
877. Wijesinghe WPSL, Mantilaka MMMGPG, Premalal EVA, Herath HMTU, Mahalingam S, Edirisinghe M, Rajapakse RPVJ, Rajapakse RMG. Facile synthesis of both needle-like and spherical hydroxyapatite nanoparticles: effect of synthetic temperature and calcination on morphology, crystallite size and crystallinity. Mater Sci Eng C. 2014;42:83–90.
878. Ribeiro CC, Barrias CC, Barbosa MA. Preparation and characterisation of calcium-phosphate porous microspheres with a uniform size for biomedical applications. J Mater Sci Mater Med. 2006;17:455–63.
879. Kimura I, Honma T, Riman RE. Preparation of hydroxyapatite microspheres by interfacial reaction in a multiple emulsion. J Ceram Soc Jpn. 2007;115:888–93.

880. Zhou WY, Wang M, Cheung WL, Guo BC, Jia DM. Synthesis of carbonated hydroxyapatite nanospheres through nanoemulsion. J Mater Sci Mater Med. 2008;19:103–10.
881. Lim JH, Park JH, Park EK, Kim HJ, Park IK, Shin HY, Shin HI. Fully interconnected globular porous biphasic calcium phosphate ceramic scaffold facilitates osteogenic repair. Key Eng Mater. 2008;361–363:119–22.
882. Kawai T, Sekikawa H, Unuma H. Preparation of hollow hydroxyapatite microspheres utilizing poly(divinylbenzene) as a template. J Ceram Soc Jpn. 2009;117:340–3.
883. Descamps M, Hornez JC, Leriche A. Manufacture of hydroxyapatite beads for medical applications. J Eur Ceram Soc. 2009;29:369–75.
884. Cho JS, Jung DS, Han JM, Kang YC. Spherical shape hydroxyapatite powders prepared by flame spray pyrolysis. J Ceram Process Res. 2008;9:348–52.
885. Yao A, Ai F, Liu X, Wang D, Huang W, Xu W. Preparation of hollow hydroxyapatite microspheres by the conversion of borate glass at near room temperature. Mater Res Bull. 2010;45:25–8.
886. Cho JS, Ko YN, Koo HY, Kang YC. Synthesis of nano-sized biphasic calcium phosphate ceramics with spherical shape by flame spray pyrolysis. J Mater Sci Mater Med. 2010;21:1143–9.
887. Ye F, Guo H, Zhang H, He X. Polymeric micelle-templated synthesis of hydroxyapatite hollow nanoparticles for a drug delivery system. Acta Biomater. 2010;6:2212–8.
888. He W, Tao J, Pan H, Xu R, Tang R. A size-controlled synthesis of hollow apatite nanospheres at water-oil interfaces. Chem Lett. 2010;39:674–5.
889. Itatani K, Tsugawa T, Umeda T, Musha Y, Davies IJ, Koda S. Preparation of submicrometer-sized porous spherical hydroxyapatite agglomerates by ultrasonic spray pyrolysis technique. J Ceram Soc Jpn. 2010;118:462–6.
890. Xiao W, Fu H, Rahaman MN, Liu Y, Bal BS. Hollow hydroxyapatite microspheres: a novel bioactive and osteoconductive carrier for controlled release of bone morphogenetic protein-2 in bone regeneration. Acta Biomater. 2013;9:8374–83.
891. Bohner M, Tadier S, van Garderen N, de Gasparo A, Döbelin N, Baroud G. Synthesis of spherical calcium phosphate particles for dental and orthopedic applications. Biomaterials. 2013;3:e25103.
892. Rahaman MN, Fu H, Xiao W, Liu Y. Bioactive ceramic implants composed of hollow hydroxyapatite microspheres for bone regeneration. Ceram Eng Sci Proc. 2014;34:67–76.
893. Ito N, Kamitakahara M, Ioku K. Preparation and evaluation of spherical porous granules of octacalcium phosphate/hydroxyapatite as drug carriers in bone cancer treatment. Mater Lett. 2014;120:94–6.
894. Li Z, Wen T, Su Y, Wei X, He C, Wang D. Hollow hydroxyapatite spheres fabrication with three-dimensional hydrogel template. Cryst Eng Commun. 2014;16:4202–9.
895. Feng J, Chong M, Chan J, Zhang ZY, Teoh SH, Thian ES. Fabrication, characterization and in-vitro evaluation of apatite-based microbeads for bone implant science. Ceram Trans. 2014;247:179–90.
896. Kovach I, Kosmella S, Prietzel C, Bagdahn C, Koetz J. Nano-porous calcium phosphate balls. Colloid Surf B. 2015;132:246–52.
897. Kamitakahara M, Murakami S, Takahashi H, Watanabe N, Ioku K. Formation of hydroxyapatite microtubes assisted with anatase under hydrothermal conditions. Chem Lett. 2010;39:854–5.
898. Chandanshive B, Dyondi D, Ajgaonkar VR, Banerjee R, Khushalani D. Biocompatible calcium phosphate based tubes. J Mater Chem. 2010;20:6923–8.
899. Kamitakahara M, Takahashi H, Ioku K. Tubular hydroxyapatite formation through a hydrothermal process from α-tricalcium phosphate with anatase. J Mater Sci. 2012;47:4194–9.
900. Ustundag CB, Kaya F, Kamitakahara M, Kaya C, Ioku K. Production of tubular porous hydroxyapatite using electrophoretic deposition. J Ceram Soc Jpn. 2012;120:569–73.
901. Li C, Ge X, Li G, Lu H, Ding R. In situ hydrothermal crystallization of hexagonal hydroxyapatite tubes from yttrium ion-doped hydroxyapatite by the Kirkendall effect. Mater Sci Eng C. 2014;45:191–5.

902. Nonoyama T, Kinoshita T, Higuchi M, Nagata K, Tanaka M, Kamada M, Sato K, Kato K. Arrangement techniques of proteins and cells using amorphous calcium phosphate nanofiber scaffolds. Appl Surf Sci. 2012;262:8–12.
903. Sohier J, Daculsi G, Sourice S, de Groot K, Layrolle P. Porous beta tricalcium phosphate scaffolds used as a BMP-2 delivery system for bone tissue engineering. J Biomed Mater Res A. 2010;92A:1105–14.
904. Stähli C, Bohner M, Bashoor-Zadeh M, Doebelin N, Baroud G. Aqueous impregnation of porous β-tricalcium phosphate scaffolds. Acta Biomater. 2010;6:2760–72.
905. Lin K, Chen L, Qu H, Lu J, Chang J. Improvement of mechanical properties of macroporous β-tricalcium phosphate bioceramic scaffolds with uniform and interconnected pore structures. Ceram Int. 2011;37:2397–403.
906. Wójtowicz J, Leszczyńska J, Chróścicka A, Ślósarczyk A, Paszkiewicz Z, Zima A, Rozniatowski K, Jeleń P, Lewandowska-Szumieł M. Comparative in vitro study of calcium phosphate ceramics for their potency as scaffolds for tissue engineering. Biomed Mater Eng. 2014;24:1609–23.
907. Simon JL, Michna S, Lewis JA, Rekow ED, Thompson VP, Smay JE, Yampolsky A, Parsons JR, Ricci JL. In vivo bone response to 3D periodic hydroxyapatite scaffolds assembled by direct ink writing. J Biomed Mater Res A. 2007;83A:747–58.
908. Yoshikawa H, Myoui A. Bone tissue engineering with porous hydroxyapatite ceramics. J Artif Organs. 2005;8:131–6.
909. Min SH, Jin HH, Park HY, Park IM, Park HC, Yoon SY. Preparation of porous hydroxyapatite scaffolds for bone tissue engineering. Mater Sci Forum. 2006;510–511:754–7.
910. Deville S, Saiz E, Nalla RK, Tomsia AP. Strong biomimetic hydroxyapatite scaffolds. Adv Sci Technol. 2006;49:148–52.
911. Buckley CT, O'Kelly KU. Fabrication and characterization of a porous multidomain hydroxyapatite scaffold for bone tissue engineering investigations. J Biomed Mater Res B Appl Biomater. 2010;93B:459–67.
912. Ramay HRR, Zhang M. Biphasic calcium phosphate nanocomposite porous scaffolds for load-bearing bone tissue engineering. Biomaterials. 2004;25:5171–80.
913. Chen G, Li W, Zhao B, Sun K. A novel biphasic bone scaffold: β-calcium phosphate and amorphous calcium polyphosphate. J Am Ceram Soc. 2009;92:945–8.
914. Guo D, Xu K, Han Y. The in situ synthesis of biphasic calcium phosphate scaffolds with controllable compositions, structures, and adjustable properties. J Biomed Mater Res A. 2009;88A:43–52.
915. Sarin P, Lee SJ, Apostolov ZD, Kriven WM. Porous biphasic calcium phosphate scaffolds from cuttlefish bone. J Am Ceram Soc. 2011;94:2362–70.
916. Kim DH, Kim KL, Chun HH, Kim TW, Park HC, Yoon SY. In vitro biodegradable and mechanical performance of biphasic calcium phosphate porous scaffolds with unidirectional macro-pore structure. Ceram Int. 2014;40:8293–300.
917. Marques CF, Perera FH, Marote A, Ferreira S, Vieira SI, Olhero S, Miranda P, Ferreira JMF. Biphasic calcium phosphate scaffolds fabricated by direct write assembly: mechanical, anti-microbial and osteoblastic properties. J Eur Ceram Soc. 2017;37:359–68.
918. Furuichi K, Oaki Y, Ichimiya H, Komotori J, Imai H. Preparation of hierarchically organized calcium phosphate-organic polymer composites by calcification of hydrogel. Sci Technol Adv Mater. 2006;7:219–25.
919. Wei J, Jia J, Wu F, Wei S, Zhou H, Zhang H, Shin JW, Liu C. Hierarchically microporous/macroporous scaffold of magnesium-calcium phosphate for bone tissue regeneration. Biomaterials. 2010;31:1260–9.
920. Gbureck U, Grolms O, Barralet JE, Grover LM, Thull R. Mechanical activation and cement formation of β-tricalcium phosphate. Biomaterials. 2003;24:4123–31.
921. Gbureck U, Barralet JE, Hofmann M, Thull R. Mechanical activation of tetracalcium phosphate. J Am Ceram Soc. 2004;87:311–3.

922. Bohner M, Luginbühl R, Reber C, Doebelin N, Baroud G, Conforto E. A physical approach to modify the hydraulic reactivity of α-tricalcium phosphate powder. Acta Biomater. 2009;5:3524–35.
923. Hagio T, Tanase T, Akiyama J, Iwai K, Asai S. Formation and biological affinity evaluation of crystallographically aligned hydroxyapatite. J Ceram Soc Jpn. 2008;116:79–82.
924. Blawas AS, Reichert WM. Protein patterning. Biomaterials. 1998;19:595–609.
925. Kasai T, Sato K, Kanematsu Y, Shikimori M, Kanematsu N, Doi Y. Bone tissue engineering using porous carbonate apatite and bone marrow cells. J Craniofac Surg. 2010;21:473–8.
926. Wang L, Fan H, Zhang ZY, Lou AJ, Pei GX, Jiang S, Mu TW, Qin JJ, Chen SY, Jin D. Osteogenesis and angiogenesis of tissue-engineered bone constructed by prevascularized β-tricalcium phosphate scaffold and mesenchymal stem cells. Biomaterials. 2010;31: 9452–61.
927. Sánchez-Salcedo S, Izquierdo-Barba I, Arcos D, Vallet-Regí M. In vitro evaluation of potential calcium phosphate scaffolds for tissue engineering. Tissue Eng. 2006;12:279–90.
928. Meganck JA, Baumann MJ, Case ED, McCabe LR, Allar JN. Biaxial flexure testing of calcium phosphate bioceramics for use in tissue engineering. J Biomed Mater Res A. 2005; 72A:115–26.
929. Case ED, Smith IO, Baumann MJ. Microcracking and porosity in calcium phosphates and the implications for bone tissue engineering. Mater Sci Eng A. 2005;390:246–54.
930. Tripathi G, Basu B. A porous hydroxyapatite scaffold for bone tissue engineering: physicomechanical and biological evaluations. Ceram Int. 2012;38:341–9.
931. Sibilla P, Sereni A, Aguiari G, Banzi M, Manzati E, Mischiati C, Trombelli L, del Senno L. Effects of a hydroxyapatite-based biomaterial on gene expression in osteoblast-like cells. J Dent Res. 2006;85:354–8.
932. Verron E, Bouler JM. Calcium phosphate ceramics as bone drug-combined devices. Key Eng Mater. 2010;441:181–201.
933. Zhou TH, Su M, Shang BC, Ma T, Xu GL, Li HL, Chen QH, Sun W, Xu YQ. Nanohydroxyapatite/β-tricalcium phosphate ceramics scaffolds loaded with cationic liposomal ceftazidime: preparation, release characteristics in vitro and inhibition to *Staphylococcus aureus* biofilms. Drug Dev Ind Pharm. 2012;38:1298–304.
934. Kolmas J, Krukowski S, Laskus A, Jurkitewicz M. Synthetic hydroxyapatite in pharmaceutical applications. Ceram Int. 2016;42:2472–87.
935. Rapoport A, Borovikova D, Kokina A, Patmalnieks A, Polyak N, Pavlovska I, Mezinskis G, Dekhtyar Y. Immobilisation of yeast cells on the surface of hydroxyapatite ceramics. Process Biochem. 2011;46:665–70.
936. Mastrogiacomo M, Muraglia A, Komlev V, Peyrin F, Rustichelli F, Crovace A, Cancedda R. Tissue engineering of bone: search for a better scaffold. Orthod Craniofac Res. 2005;8:277–84.
937. Quarto R, Mastrogiacomo M, Cancedda R, Kutepov SM, Mukhachev V, Lavroukov A, Kon E, Marcacci M. Repair of large bone defects with the use of autologous bone marrow stromal cells. N Engl J Med. 2001;344:385–6.
938. Vacanti CA, Bonassar LJ, Vacanti MP, Shufflebarger J. Replacement of an avulsed phalanx with tissue-engineered bone. N Engl J Med. 2001;344:1511–4.
939. Morishita T, Honoki K, Ohgushi H, Kotobuki N, Matsushima A, Takakura Y. Tissue engineering approach to the treatment of bone tumors: three cases of cultured bone grafts derived from patients' mesenchymal stem cells. Artif Organs. 2006;30:115–8.
940. Eniwumide JO, Yuan H, Cartmell SH, Meijer GJ, de Bruijn JD. Ectopic bone formation in bone marrow stem cell seeded calcium phosphate scaffolds as compared to autograft and (cell seeded) allograft. Eur Cell Mater. 2007;14:30–9.
941. Zuolin J, Hong Q, Jiali T. Dental follicle cells combined with beta-tricalcium phosphate ceramic: a novel available therapeutic strategy to restore periodontal defects. Med Hypotheses. 2010;75:669–70.

942. Ge S, Zhao N, Wang L, Yu M, Liu H, Song A, Huang J, Wang G, Yang P. Bone repair by periodontal ligament stem cell-seeded nanohydroxyapatite-chitosan scaffold. Int J Nanomedicine. 2012;7:5405–14.
943. Franch J, Díaz-Bertrana C, Lafuente P, Fontecha P, Durall I. Beta-tricalcium phosphate as a synthetic cancellous bone graft in veterinary orthopaedics: a retrospective study of 13 clinical cases. Vet Comp Orthop Traumatol. 2006;19:196–204.
944. Vertenten G, Gasthuys F, Cornelissen M, Schacht E, Vlaminck L. Enhancing bone healing and regeneration: present and future perspectives in veterinary orthopaedics. Vet Comp Orthop Traumatol. 2010;23:153–62.
945. Hench LL, Wilson J. Surface-active biomaterials. Science. 1984;226:630–6.
946. Navarro M, Michiardi A, Castano O, Planell JA. Biomaterials in orthopaedics. J R Soc Interface. 2008;5:1137–58.
947. Anderson JM. The future of biomedical materials. J Mater Sci Mater Med. 2006;17:1025–8.
948. Huebsch N, Mooney DJ. Inspiration and application in the evolution of biomaterials. Nature. 2009;462:426–32.
949. Sanchez-Sálcedo S, Arcos D, Vallet-Regí M. Upgrading calcium phosphate scaffolds for tissue engineering applications. Key Eng Mater. 2008;377:19–42.
950. Chevalier J, Gremillard L. Ceramics for medical applications: a picture for the next 20 years. J Eur Ceram Soc. 2009;29:1245–55.
951. Salgado PC, Sathler PC, Castro HC, Alves GG, de Oliveira AM, de Oliveira RC, Maia MDC, Rodrigues CR, Coelh PG, Fuly A, Cabral LM, Granjeiro JM. Bone remodeling, biomaterials and technological applications: revisiting basic concepts. J Biomater Nanobiotechnol. 2011;2:318–28.
952. Vallet-Regí M. Evolution of bioceramics within the field of biomaterials. C R Chim. 2010;13:174–85.
953. Hartgerink JD, Beniash E, Stupp SI. Self-assembly and mineralization of peptide-amphiphile nanofibers. Science. 2001;294:1684–8.

Chapter 6
Nanostructured Calcium Phosphates for Drug, Gene, DNA and Protein Delivery and as Anticancer Chemotherapeutic Devices

Andy H. Choi, Innocent J. Macha, Sibel Akyol, Sophie Cazalbou, and Besim Ben-Nissan

Abstract During the past two decades, a number of materials and devices have been utilised in drug delivery applications. A range of biomaterials with different morphologies and pore sizes are currently utilised. For any given biomaterial or bioceramic, having an adequate control of the chemical composition as well as the critical pore sizes is important in terms of controlling the effectiveness when used to deliver drugs locally. In comparison to all currently known and used biomaterials, given the fact that it possesses chemical similarity to human bone, and most importantly its dissolution characteristics which allow for bone regeneration and growth, calcium phosphate holds a special consideration. Moreover, due to their interconnected pore structure, marine materials such as shells and coral exoskeletons show

A.H. Choi • B. Ben-Nissan (✉)
Advanced Tissue Regeneration & Drug Delivery Group, School of Life Sciences, University of Technology Sydney, P.O. Box 123, Broadway, NSW 2007, Australia
e-mail: Besim.Ben-Nissan@uts.edu.au

I.J. Macha
Department of Mechanical and Industrial Engineering, University of Dar es Salaam, P.O Box 35131, Dar es Salaam, Tanzania

Advanced Tissue Regeneration & Drug Delivery Group, School of Life Sciences, University of Technology Sydney, P.O. Box 123, Broadway, NSW 2007, Australia

S. Akyol
Advanced Tissue Regeneration & Drug Delivery Group, School of Life Sciences, University of Technology Sydney, P.O. Box 123, Broadway, NSW 2007, Australia

Department of Physiology, Cerrahpasa Medical Faculty, University of Istanbul, Cerrahpasa, Istanbul 34099, Turkey

S. Cazalbou
Laboratoire CIRIMAT – UMR 5085 UPS-INPT-CNRS, 35 chemin des maraichers, 31062 Toulouse cedex 09, France

Advanced Tissue Regeneration & Drug Delivery Group, School of Life Sciences, University of Technology Sydney, P.O. Box 123, Broadway, NSW 2007, Australia

G. Kaur (ed.), *Clinical Applications of Biomaterials*,
DOI 10.1007/978-3-319-56059-5_6

potential for applications in drug delivery due to their easy conversion to calcium phosphates with controllable dissolution rates. This chapter covers a range of current methods used specifically for natural materials that can be converted to calcium phosphates and mixed with polymeric materials as thin film or nanostructured drug, genes, protein and range of delivery and as anticancer chemotherapeutic devices.

Keywords Hydroxyapatite • Foraminifera • Marine material • Coral skeleton • Liposomes • Surface modifications • Biomimetics

6.1 Introduction

A material containing delicate structures and sizes that fall within the range of 1–100 nm is referred to as a nanostructured material. As a result of this size, an extensive development of nanotechnology has taken place during the past decade in the fields of materials science and engineering. The microstructure and properties of nanostructured materials depend in an extreme manner on their chemistry, structure and the method of their synthesis and their processing route. Consequently, it is extremely important to select the most appropriate technique when preparing nanomaterials and composites with desired properties and property combinations.

The synthesis techniques most commonly used for the production of advanced ceramics include pressing, as well as wet chemical processing techniques such as co-precipitation and sol-gel, all of which have been used to produce nanoparticles, nanocoatings and nanostructured solid blocks and shapes.

In modern ceramics technology, pressing is accomplished by placing the powder into a die and applying pressure to achieve compaction. Hot pressing (HP) and hot isostatic pressing are the most common methods used to produce bioceramics. Hot isostatic pressing can induce the higher densities and small grain structures required by bioceramics, whereby heat and pressure are applied simultaneously and the pressure is applied from all directions via a pressurised gas such as helium or argon. In contrast, flat plates or blocks and non-uniform components are relatively easily produced using hot pressing.

Sol-gel processing is unique in that it can be used to produce different forms, such as powders, platelets, coatings, fibres and monoliths of the same composition, merely by varying the chemistry, viscosity and other factors of a given solution. The advantages of the sol-gel technique are numerous including it is applied at the nanoscale and it results in a stoichiometric, homogeneous and pure product, owing to the mixing on the molecular scale. Furthermore, high purity can be maintained as grinding can be avoided. It also allows for a reduction in the firing temperatures as a result of the small particle sizes with high surface areas. Currently, the materials most commonly used for clinical applications are those selected from a handful of well-characterised and available biocompatible ceramics, metals, polymers and their combinations as composites or hybrids.

These unique production techniques, together with the advancements in new enabling technologies such as microscale, nanoscale, bioinspired fabrication (biomimetics) and surface modification methods, have the potential to drive at an unprecedented rate the design and development of new nanomaterials that are useful in medical applications. The current focus is on the production of new nanoceramics that are relevant to a broad range of applications, including implantable surface-modified medical devices for better hard- and soft-tissue attachment, increased bioactivity for tissue regeneration and engineering, cancer treatment, drug and gene delivery, treatment of bacterial and viral infections, delivery of oxygen to damaged tissues and materials for minimally invasive surgery. A more futuristic view, which could in fact become reality within two decades, includes nanorobotics, nanobiosensors, bioreactors and micro- and nanodevices for a wide range of biomedical applications. Combination of nanodevices and the use of immunotherapies to treat a range of diseases will be the next decade's challenges.

During the early 1970s, bioceramics were employed as implants to perform singular, biologically inert roles. The limitations of these synthetic materials as tissue substitutes were highlighted with the increasing realisation that the cells and tissues of the body perform many other vital regulatory and metabolic roles.

The demands of bioceramics have since changed, from maintaining an essentially physical function without eliciting a host response to providing a more positive interaction with the host. This has been accompanied by increasing demands on medical devices that they not only improve the quality of life but also extend its duration. Most importantly, nanobioceramics – at least potentially – can be used as body-interactive materials, helping the body to heal or promoting the regeneration of tissues, thus restoring physiological functions.

The main factors in the clinical success of any biomaterial are its biocompatibility and biofunctionality, both of which are related directly to tissue/implant interface interactions. This approach is currently being explored in the development of a new generation of nanobioceramics with a widened range of medical applications. The improvement of interface bonding by nanoscale coatings, based on biomimetics, has been of worldwide interest during the past decade, and today several companies are in early commercialisation stages of new-generation, nanoscale-modified implants for orthopaedic, ocular and maxillofacial surgery, as well as for hard- and soft-tissue engineering.

Biomimetic processing is based on the notion that biological systems store and process information at the molecular level, and the extension of this concept to the processing of nanocomposites for biomedical devices and tissue engineering, such as scaffolds for bone regeneration, has been brought out during the past decade [1]. Several research groups have reported the synthesis of novel bone nanocomposites of hydroxyapatite (HAp) and collagen, gelatin or chondroitin sulphate, through a self-assembly mechanism. These self-assembled experimental bone nanocomposites have been reported to exhibit similarities to natural bone in not only their structure but also their physiological properties [2].

The term nanocomposite can be defined as a heterogeneous combination of two or more materials, in which at least one of those materials should be on a nanometre scale. By using the composite approach, it is possible to manipulate the mechanical

properties such as strength and modulus of the composites closer to those of natural bone, with the help of secondary substitution phases. For example, HAp-polymer composites have been shown to have an elastic modulus close to that of the bone.

The fabrication of a nanocomposite can be achieved by physically mixing or introducing a new component into an existing nanosized material, which allows for property modifications of the nanostructured materials and may even offer new material functions. For example, some biopolymers and biomolecules, such as poly(lactic acid) (PLA), poly(lactic-co-glycolic acid) (PLGA), polyamide, collagen, silk fibrin, chitosan and alginate, have been reported to mix into nano-hydroxyapatite (nano-HAp) systems. Another form of nanocomposite which has been developed for biomedical applications is the gel system. For this, nanostructured materials can be entrapped in to a gel (a three-dimensional (3-D) network immersed in a fluid), such that the properties of the nanomaterials can be improved and tailored to suit the specific needs of certain biomedical devices. A nanogel, which is a nanosized, flexible hydrophilic polymer gel [3], is an example of a gel that can be used in drug delivery carriers. These nanogels can bind and encapsulate spontaneously (through ionic interactions) any type of negatively charged oligonucleotide drug. A key advantage of nanogels is that they allow for a high "payload" of macromolecules (up to 50 weight percent), a value which normally cannot be approached with conventional nanodrug carriers [4].

6.2 Drug Delivery Systems

The field in the development of suitable biomaterials for drug delivery systems has been the focus of ongoing research since the 1940s when the first drug delivery system was developed to raise the drug concentration in blood plasma. Still the full replacement of living long bone tissue techniques and materials that are completely satisfactory are not available in clinical practice. In addition, it is well known that the composition, anatomical structure and final function of culture-derived tissue do not accurately simulate the human archetype.

To do this properly requires a support framework (scaffold) with features of an extracellular matrix, proteins to control development and potentiated cell types that reassemble into tissues. As of now scaffold-based tissue engineering is providing many useful structural environments where tissues can be reconstituted in their natural form and with normal functions.

However, there are two outstanding issues that need to be addressed if tissues are to be regenerated fully in the laboratory. The first is to recreate a blood system within the developing tissue and provide adequate nutrition; this involves structures with interconnected right size porosity. The second is to simulate the delivery schedule of developmental proteins to cells for proliferation and differentiation into whole tissues.

So far, clinical trials implementing these factors, in the regeneration of tissues, have not led to the anticipated results. The problem lies in the failure to recreate an interwoven cellular and molecular ecosystem made up of blood vessels, neurons,

cells and regenerative biochemicals. This is a major necessity for proper tissue development. This has led to a shift in approach towards fabricating materials and structures containing bioactive ions and proteins, which are dispersed in controlled ways in scaffolds, to encourage endogenous repair, remodelling and regeneration.

Tissue-promoting proteins used in experimental and clinical regenerative therapies are expensive to produce. The production of proteins using recombinant technology is imperfect, and that made it difficult to make genuine native proteins with their entire set of evolved functions. Thus, there are good scientific reasons for developing relatively straightforward, low cost alternatives that include structures with appropriate proteins and other.

Marine invertebrates are one potential, unexamined source of structures that can be converted to calcium phosphates and select proteins with potential utility in strategies for regenerative medicine, in the laboratory and possibly for the patient. They can further be incorporated with a range of drugs that can be utilised as local drug delivery systems. Other marine origin materials such as nacres and sponges also provide an abundant new source of inorganic scaffolding material for drug delivery and tissue engineering applications. Research and development in this area has primarily focused on the applications of soft- and hard-tissue repair. However, the application of using marine shells as a carrier for drugs just recently entered to the clinical field.

6.2.1 Properties of Drug Delivery Systems

While technological advancement has produced innovative and refined new drug delivery systems, the fundamental basis that defines what a drug delivery system remains unchanged. It is a system that is capable of releasing a preloaded bioactive element (pharmaceutical drugs or metallic ions) to a targeted site at a specific rate and, most importantly, at a therapeutically efficient and relevant concentration.

The main aim of this type of system compared with conventional drug intake is to take into account the low rate of intraosseous diffusion which makes the conventional treatments administered intravenously or orally often long and ineffective. These new delivery systems facilitate the local specific area delivery, dosage and duration control and hence appropriate drug delivery while causing minimal side effects and no harm to the patient. The therapeutic advantages of these systems can be attributed to many underlining factors: predictability of release rate and minimised drug concentration, thereby reducing any adverse systemic effect.

Prolonged duration of drug therapy providing the need for frequent re-dosing and thus improving patient care and compliance has been problematic in many global applications of drugs such as the treatment protocol of malaria. Many factors are considered in the development of drug delivery systems in accordance to the desired application. This includes the agent to be carried, the administration route, the material used, the degradation rate, the loading efficiency, the physical and chemical properties of the material, the practicality for large-scale production and

toxicity, amongst other parameters. Targetability and local delivery mechanisms and methods have been major issues in immunotherapy and the treatment of cancer and related clinical conditions.

6.3 Calcium Phosphate

In the search for a suitable biomaterial to replace and mimic the bone, an ideal choice would be synthetic calcium phosphate as they can replicate the composition and structure of a bone mineral referred to as natural hydroxyapatite. HAp with a chemical formula of $Ca_{10}(PO_4)_6(OH)_2$ is accepted widely as a biocompatible material chemically resembling the same chemical components of the teeth and bone [5–7]. It is well regarded as fully biocompatible and immunologically well accepted.

Most published information concerning HAp is classified under calcium phosphate to which HAp belongs. As a result, the chemical properties of HAp will be considered from the perspective that it is calcium phosphate even though it will have reactivities and properties dissimilar from those of other phosphates within the physiological environment. Despite the fact of having a similar chemistry as well as composition to that of human bone, the mechanical properties of calcium phosphates are far from being in close proximity to those of human bone as a result of their inorganic nature and brittleness. For these reasons, this restricts their use in load-bearing applications without further modifications.

It has a very welcoming structure and a high reactivity which makes it possible to favour the ionic substitutions with the surrounding fluids.

Calcium phosphates are categorised by particular solubilities, for example, when bonded to surrounding tissues along with their capacity to degrade and be replaced by proceeding bone growth. The surface ions of calcium phosphate (or HAp) can be exchanged with those of the aqueous solution when it comes into contact with bodily fluid. On the other hand, various ions and molecules such as proteins and collagen can be adsorbed onto the surface [7].

The solubilities of various calcium phosphate compounds can be represented as follows [8, 9]:

$$HAp > \beta - tricalcium\ phosphate > \alpha - tricalcium\ phosphate > tetracalcium\ phosphate > dibasic\ calcium\ phosphate > amorphous\ calcium\ phosphate$$

HAp with interconnecting pores ranging from 100 to 500 μm in diameter is commonly used as bone graft materials. The chemistry and structure of calcium phosphate govern its dissolution rates, this in turn influences their in situ strength and long-term stability [9–11].

Early studies on synthetic apatites and related calcium phosphates were made to achieve a better understanding into the composition, properties and structure of biological apatites and, in particular, human enamel apatites. In spite of this, investigations

on synthetic apatites had been centred on their preparation and application in dentistry and medicine as well as their application as scaffolds for teeth and bone regeneration in the past 30 years. Synthetic calcium phosphate biomaterials commercially available at the moment are classified on the basis of composition which include α-tri-calcium phosphate and β-tri-calcium phosphate with a chemical formula of $Ca_3(PO_4)_2$, HAp and biphasic calcium phosphate which is a mixture of β-tri-calcium phosphate and HAp with a variable ratio of HAp/β-tri-calcium phosphate [8, 11]. Other commercially available HAp biomaterials have been synthesised from biological materials such as hydrothermally converted coral or derived from marina algae, bovine bone and processed human bone [7–11].

In general, it has been accepted that natural and synthetic calcium phosphate bioceramics are not (unless modified) or possess the ability to form bone when implanted in non-osseous sites but are osteoconductive or have the ability to support bone formation and tissue ingrowth. Orthopaedic and dental medical applications of calcium phosphate bioceramics include repair of bone defects, repair of periodontal defects, alveolar ridge augmentation, ear implants, eye implants, maxillofacial reconstruction, spine fusion, bone space fillers, bone cement additives, composites and implant coatings.

6.4 Delivery of Gene, Protein, and Drugs Using Calcium Phosphate

The primary aim for drug delivery is to target drugs or bioactive metallic ions to specific sites within the human body and to release the pharmaceuticals in a controllable fashion. However, for many current delivery systems, release is sudden rather than steady state, and control of the release rates is difficult. Some type of release is also particularly undesirable and problematic when the guest molecule such as an antitumour drug that is cytotoxic might potentially harm healthy cells and tissues before being delivered to the affected sites [12].

In the case of ceramics such as calcium phosphate, the phase composition and the critical pore and grain size and interconnectivity may be varied from a few nanometres up to microns in order to control the ease of delivery and dispersion of a material to the targeted area. A variety of calcium phosphate nanoceramic-based drug delivery systems are currently undergoing clinical evaluation. In addition to reducing toxicity to non-diseased or healthy cells, these systems have the potential to increase drug efficiency, which translates to significant cost savings for the expensive drug treatment that currently are being engineered.

The main concern for any drug carriers is the appropriate circulation time within the body. The surface modification of nanoparticles with a range of biocompatible non-ionic surfactant or polymeric macromolecules has proved to be the most successful for maintaining nanoparticle presence in the blood for prolonged periods [13].

As mentioned previously, calcium phosphates are characterised by particular solubilities and their ability to degrade and be replaced by advancing bone growth. Consequently, they also widen the effective means of administration for successful treatment of bone diseases [14]. Nanodrug delivery systems embedded within a matrix or not also have the exceptional attribute of being capable of delivering and controlling dissolution with high precision due to their high surface areas. It is not surprising that the number of research papers covering drug, gene and mineral delivery of nanoparticles, nanocoatings and composites published during the last decade is very high and increasing [15–38].

6.4.1 Gene Delivery

In the field of tissue engineering, the role of gene therapy in aiding wound healing and treating various diseases or defects has become increasingly important. The use of calcium phosphate nanoparticles in gene delivery has emerged as a popular and necessary delivery vehicle for obtaining controlled gene delivery [15, 16]. The main challenge for any successful small interfering ribonucleic acid (siRNA)-based therapies is the research and development of an efficient in vivo delivery vehicle. Li et al. [15] suggested the efficient delivery via intravenous administration of siRNA to a xenograft tumour model using a calcium phosphate nanoparticle with an average diameter of about 60–80 nm coated with liposome. They observed that untargeted nanoparticles had a very low silencing effect, while a three- to fourfold in vitro silencing effect was observed with the lipid-coated calcium phosphate nanoparticle. They hypothesised that after entering the cells, the lipid-coated calcium phosphate nanoparticle would dissemble at low pH in the endosome, which would cause endosome swelling and bursting to release the entrapped siRNA. Later, Pittella et al. [16] examined the possibility of utilising smart polymer/calcium phosphate/siRNA hybrid nanoparticles approximately 100 nm in size for siRNA-based cancer treatment. According to the authors, the nanoparticle showed high gene silencing efficiency in cultured pancreatic cancer cells without associated cytotoxicity. Intravenously injected nanoparticles incorporating vascular endothelium growth factor siRNA led to significant reduction in tumour growth.

Currently, calcium phosphate is one of the most attractive non-viral vectors being investigated for the in vitro delivery of plasmid DNA (pDNA) into cultured cells due to factors such as ease of handling, biodegradability, biocompatibility and known adsorption capacity for pDNA. On the other hand, when compared to viral approaches, traditional calcium phosphate synthesis methods often lead to lower and less consistent transfection efficiency [17–19]. Olton et al. [17] claimed that more consistent levels of gene expression could be achieved by optimising both the stoichiometry (Ca/P ratio) of the calcium phosphate particles in addition to the mode in which the precursor solutions are mixed. The optimised forms of these calcium phosphate particles were approximately 25–50 nm in size (when complexed with pDNA), and maximum transfection efficiencies in both HeLa and MC3T3-E1 cell lines were obtained when a Ca/P ratio between 100 and 300 was used.

In an effort to improve the transfection efficiency and to stabilise the particle size and inhibit further growth of the particle, Liu et al. [18] coated calcium phosphate nanoparticles with protamine sulphate, and based on atomic force microscopy, the protamine sulphate-coated calcium phosphate nanoparticles were observed to be much smaller than classical calcium phosphate particles, and in vitro studies showed that the smaller nanoparticles enhanced the transfection efficiency by promoting the endocytic delivery of DNA into cells.

Furthermore, growth factors such as transforming growth factor beta-1 (TGF-β1), in general, have been used to enhance the tissue-forming efficiency and to accomplish the goal of tissue regeneration. TGF-β1, which possesses multifunctional capacities that regulate many aspects of cellular activity, including cell proliferation, differentiation and extracellular matrix metabolism, in a time- and concentration-dependent manner, was selected by Cao et al. [20] to stimulate cartilage tissue formation. A three-dimensional nanocomposite gene delivery system based on collagen/chitosan scaffolds, in which plasmid TGF-β1/calcium phosphate nanoparticles mixed with fibronectin, was used to transfect mesenchymal stem cells (MSCs). They noticed the MSCs transfected with nanocomposite system showed remarkably high levels of the growth factor over long periods. Observations made based on an immunohistochemistry analysis revealed greater amounts of collagen II was produced by the nanocomposite-transfected MSCs than MSCs transfected by the Lipofectamine 2000 method. The authors hypothesised that transfection with the nanocomposite gene delivery system could successfully induce MSC chondrogenic differentiation in vitro without dexamethasone.

For any practical application of a nanoscale medical delivery system, it is essential that no dissolved biomolecules are accompanying the delivery system and as well to know precisely the dose of the applied biomolecules. An efficient delivery system based on biodegradable multi-shell calcium phosphate-oligonucleotide nanoparticles as carriers for the immunoactive toll-like receptor ligands CpG and polyinosinic-polycytidylic acid for the activation of dendritic cells combined with the viral antigen haemagglutinin was attempted by Sokolova et al. [21]. They discovered that the purified calcium phosphate nanoparticles (without dissolved biomolecules) are capable of inducing adaptive immunity by activation of dendritic cells. Immunostimulatory effects of purified calcium phosphate nanoparticles on dendritic cells were demonstrated by increased expression of co-stimulatory molecules and MHC II and by cytokine secretion. Furthermore, dendritic cells treated with purified functionalised calcium phosphate nanoparticles induced an antigen-specific T-cell response in vitro [21].

6.4.2 Protein Delivery

Nanocarriers such as those based on calcium phosphate provide improvement in effectiveness during the delivery of therapeutic proteins for cancer therapy compared to naked protein drugs [22, 23]. The loading of proteins (bovine serum albumin and lysozyme) into calcium phosphate nanoparticles approximately 50 nm in

size was attempted by Han et al. [22] through an inverse micelle technique and the protein loading efficiency and release profiles at different pH conditions investigated. X-ray photoelectron spectroscopy revealed that the proteins were not adsorbed onto the surface of the nanoparticles suggesting the proteins were entrapped within the particle matrix. Release studies showed that protein release was more rapid at lower pH conditions than at physiological pH.

Paul and Sharma [23] also examined the option of using calcium phosphate-based nanoparticles as oral delivery carriers for their model protein drug insulin. The majority of the nanoparticles were less than 100 nm in size and were shown to be non-cytotoxic. They discovered lauric acid-conjugated calcium phosphate nanoparticles were highly compatible with insulin, and it is possible to use the nanoparticle system to deliver insulin in a sustained manner in the physiological pH of the intestine with no degradation or conformational changes of entrapped insulin.

6.4.3 Drug Delivery

Due to their favourable properties in cancer chemotherapy, a variety of nanoceramic drug delivery systems such as those that are based on calcium phosphate are currently investigated. It has been postulated that besides factors such as particle size and roughness, the surface morphology of the particles also plays an important consideration when it comes to drug loading and release capacity as well as obtaining the highest cell viability and reducing negative cell responses [24].

The effects of four morphologically different calcium phosphate particles (flaky, elongated orthogonal, brick shaped and spherical) on sustained drug release profiles were carried out by Uskoković et al. [24]. The spherical nanosized particles were observed to be the most effective in both drug loading and release. Moreover, the spherical nanoparticles also possess the highest cell viability, the largest gene expression upregulation of three different osteogenic markers and the least disrupted cell cytoskeleton and cell morphologies. Kester et al. [25] hypothesised using a 20–30 nm diameter, pH-responsive, non-agglomerating and non-toxic calcium phosphate nanoparticle matrix to encapsulate hydrophobic antineoplastic chemotherapeutics. The nanoparticles were found to be capable of encapsulating both fluorophores and chemotherapeutics and are colloidally stable in physiological solution for an extended time at 37 °C.

Bastakoti and co-workers [26] suggested that sub-100 nm colloidal nanoparticles loaded with fluorescent dyes and anticancer drugs, along with a controlled mineralisation technology, could lead to the successful development of robust, biocompatible hybrid nanocarriers for the simultaneous delivery of drugs and imaging agents.

Various factors relating to the materials of the drug delivery vehicle such as immune reaction of the host against the system and poor control over the release of drugs influence the success of the delivery system in cancer treatment [27]. A range of anticancer drugs have been examined including docetaxel, doxorubicin

hydrochloride, methotrexate and 5-fluorouracil [27–32]. Zhao et al. [28] investigated the drug loading and release behaviour of lipid-coated calcium phosphate hybrid nanoparticles synthesised through self-assembly loaded with the anticancer drug docetaxel. The average diameter of the hybrid nanoparticles was approximately 72 nm. They reported that the nanoparticles showed excellent biocompatibility and high drug loading capacity. In another study, the in vitro drug release and cell inhibition effect of calcium phosphate hybrid nanoparticles were attempted by Liang et al. [29]. Heparin/$CaCO_3$/calcium phosphate nanoparticles with a size of less than 50 nm were prepared through co-precipitation technique and loaded with the anticancer drug doxorubicin hydrochloride. From in vitro cellular cytotoxicity study, the unloaded hybrid nanoparticles possessed good biocompatibility, whereas the drug-loaded nanoparticles exhibited a strong cell inhibition effect. An efficient drug delivery system consisted of an amphiphilic gelatin-iron oxide core, and calcium phosphate shells were also attempted [30].

Highly water-soluble magnetic mesoporous amorphous calcium phosphate nanoparticles with a diameter of 41 nm were prepared by Rout et al. [31]. Platinum pharmacophore cis-diaquadiamine platinum (II), folic acid and rhodamine isothiocyanate were conjugated on these nanoparticles and its antitumour potential investigated against human cervical carcinoma cells by MTT assay. They discovered the nanoparticles can effectively target cancer cells and optimally deliver cisplatin resulting in cell death following the induction of apoptosis.

The therapeutic efficacy of a porous silica-calcium phosphate nanocomposites was also investigated as a new delivery system for the anticancer drug 5-fluorouracil [27]. Based on the results of their in vitro studies, they noticed that the nanocomposites were very cytotoxic for 4T1 mammary tumour cells. Release kinetics studies showed the nanocomposites containing 5-fluorouracil provided a burst release of the anticancer drug in the first 24 h followed by a sustained release of a therapeutic dose of the drug for up to 32 days. The in vivo subcutaneous implantation in an immunocompetent murine model of breast cancer also suggested that the nanocomposites containing 5-fluorouracil can cease the growth of 4T1 tumour. Calcium phosphate nanoparticle containing an anticancer drug methotrexate was synthesised and characterised by Mukesh et al. [32]. The average size of the nanoparticles was approximately 262 nm, and they have an entrapment efficiency of 58%. In vitro release study revealed slow release of methotrexate at physiological pH, while greater than 90% release was observed within 3–4 h at endosomal pH.

Using a biomimetic approach, Chen et al. [33] attempted to engineer mesoporous silica nanoparticles with calcium phosphate-hyaluronic acid hybrid shell to be used as a pH-responsive targeted drug delivery vehicle. They noticed that the addition of another layer of hyaluronic acid on the calcium phosphate surfaces not only stabilises the nanocomposites but also confers target ability towards CD44-overexpressed cancer cells. Furthermore, the nanomaterials were found to possess the ability to control the release of loaded anticancer drugs in acidic subcellular environments after receptor-mediated endocytosis.

Chiu et al. [34] hypothesised that small calcium phosphate core-protein shell nanoparticles synthesised via biomimetic approach might be effective vehicles for delivery of adjuvanted antigen to dendritic cells. They utilised cell surface display to identify disulphide-constrained calcium phosphate binding peptides that, when inserted within the active site loop of *E. coli*thioredoxin 1 (TrxA), readily and reproducibly drive the production of nanoparticles which were 50–70 nm in hydrodynamic diameter and consisted of an approximately 25 nm amorphous calcium phosphate core stabilised by the protein shell. When compared to a commercial aluminium phosphate adjuvant, they observed the small core-shell assemblies led to a threefold increase in mice anti-TrxA titres 3 weeks postinjection.

In addition to delivering anticancer chemotherapeutics, calcium phosphate nanoparticle-based systems were also investigated for the potential delivery of common drugs such as aspirin, insulin and vitamins [35–38]. To address the problem of stomach irrigation caused by aspirin, the use of a composite microsphere delivery vehicle composed of porous nano-HAp particles and poly(styrene-divinylbenzene) was explored [35]. The aspirin-loaded microspheres were observed to exhibit excellent buoyancy with relatively short instantaneous floating time and a long sustained floating time in simulated gastric juice. The microspheres also offered good sustained release of aspirin of up to 8 h. Ignjatović et al. [36] examined the effects of the local delivery of cholecalciferol (vitamin D_3) using nanoparticulate carriers composed of HAp and PLGA. Two types of multifunctional nanoparticulate HAp-based powders were prepared and tested: HAp nanoparticles as direct cholecalciferol delivery agents and HAp nanoparticles coated with cholecalciferol-loaded PLGA for sustained delivery. They observed the fast delivery was achieved by desorption of the drug from the HAp particle surface, while the slow delivery was conditioned by the rather slow degradation of PLGA in physiological conditions.

The methazolamide-loaded calcium phosphate nanoparticles with a mean diameter of approximately 256 nm were prepared by Chen et al. [37]. From the in vitro release studies, they observed diffusion-controlled release of methazolamide from the nanoparticles over a period of 4 h, while in vivo studies showed the intraocular pressure-lowering effect of the nanoparticle eye drops which lasted for 18 h. Ramachandran et al. [38] examined the possibility of PEGylated calcium phosphate nanoparticles with an average particle size of 48 nm as oral carriers for insulin. The non-cytotoxic nature of the PEGylated calcium phosphate nanoparticles has been established through the MTT assay. The release profiles revealed negligible release in gastric pH after the nanoparticles were coated with a pH-sensitive polymer, while a sustained release of insulin at intestinal pH for over 8 h was recorded. They also discovered that the insulin-loading process in the PEG-conjugated calcium phosphate nanoparticles did not affect the conformation and stability of insulin.

6.5 Surface Modifications and Liposomes for Drug Delivery Applications

The appropriate dissolution rates and their control within the human body are the main concern for drug carriers containing nanoparticles and nanothin films [23]. As previously stated, the use of calcium phosphate as a delivery system also broadens its effectiveness as a result of their capacity to locally deliver additional metallic ions such as Mg and Sr as well as its main constituents calcium and phosphate, other active ions and biogenic materials such as bone morphogenetic proteins and stem cells if required to be used in the successful treatment of the bone or related diseases.

Through the use of a wide range of biological, chemical and/or physical surface modification approaches, the surfaces of nanostructured materials such as nanocoatings can essentially be altered and functionalised to assist us in targeted slow drug delivery. Furthermore, surface modification can also be used to achieve enhancements in stability as well as controlling the long-range solubility of thin films and nanocoatings within an aqueous media.

In the quest for the surface modifications of nanostructured materials, techniques such as macro-, micro- and nanocoatings have emerged as the leading strategies resulting in better functionalisation of the surfaces of materials and for better osseointegration in the long term.

The biological modification of surfaces of nanocoatings is at times essential for the functionality of the devices. Biospecific molecules can be incorporated into the nanocoatings or thin films by using physical or chemical methods, thus presenting biospecific sites for the further immobilisation of ligands specific to these molecules. The immobilisations of specific ligands such as antibody antigen and receptor ligand can be carried out using biologically specific reactions [14]. Current research work in these areas is very promising.

It is well known that different biomedical applications require different functions and properties of materials. As a result, techniques available to modify nanostructured materials or thin films can vary in order to meet the demands of various biomedical systems. In spite of the advantages offered by nanocoatings and nanoparticle containing composite thin films, such as their small surface pore sizes and loading efficiency, a number of issues such as control of the appropriate drug release rates restricted their use clinical applications.

The targeting ability and efficacy of any drug delivery system are sometimes hindered by the rapid dissolution of the carrier system within the human body. A good example is their side effects in chemotherapy drug delivery for the cancer patients. The long circulation time within the blood is the primary concern for drug carriers of both local and systemic delivery. For this reason, a number of investigations have been carried out to examine ways in which “long-circulating-time” carriers can be designed and engineered.

Amongst these, the surface modification of thin films and nanocoatings with a variety of polymeric macromolecules or non-ionic surfactant has been demonstrated to be the most effective for maintaining the presence of drug delivery particles in the blood for prolonged periods [39].

Considered as one of the most clinically recognised thin film nanoscale systems, liposomes consist of a single layer or multiple concentric lipid bilayers that encapsulate an aqueous compartment and are currently utilised in the delivery of antifungal drugs, vaccines and genes [19, 40–45]. The exceptional clinical profile of liposome coatings in comparison to other delivery systems is based on their reduced toxicity, biodegradability and capacity for size and surface manipulations [46]. An improvement in the biocompatibility of liposomes as well as an increase in nanoparticle hydrophilicity and stability in plasma can be achieved through the encapsulation of nanomaterials such as calcium phosphate within liposomes.

The use of surface modification is used in gene therapy in an effort to obtain controlled delivery of small interfering RNA (siRNA) and plasmid DNA (pDNA) particularly in an acidic pH environment [15–19]. The use of cationic liposomes as transfection vectors has become an ideal choice and most widely employed in the transfer of pDNA due to their weak immunogenicity and low toxicity [17]. A study by Zhou et al. [19] has suggested that coating calcium phosphate with liposomes could provide consistently efficient and satisfactory delivery of pDNA. Using mammalian cell culture, their findings showed the application of a lipid coating resulted in a tenfold increase in the transfection of pDNA compared to uncoated calcium phosphate.

In a previous study, multilayered liposomes with the incorporation of nano-HAp and other metallic ions such as strontium, magnesium and zinc showed an excellent encapsulation that can help to control drug delivery rates in medical applications such as chemotherapy drug delivery for oncology patients [46]. This observed ease of coating and release delay ability is one of the strong reasons calcium phosphate-based nanoparticle containing thin films and liposome coatings are ideal candidates for drug delivery and bone regeneration systems [46, 47]. In addition, combinatory therapy modalities can be accomplished by utilising the ability of liposome coatings to carry hydrophobic and hydrophilic moieties as well as their capacity to incorporate therapeutic and diagnostic agents into a single liposome delivery system [46].

Huang et al. [43] have suggested that the nucleation process for new bone formation could be improved by the presence of negatively charged liposome coatings. In their experiments carried out in miniature swine, artificial bony defects on one side were implanted with liposome-coated tri-calcium phosphate, while defects on the other side served as controls. They reported that at 3 weeks post-implantation, dense connective tissues surrounded the implant material, and new bone formation was visible after 6 weeks.

Using a different strategy, Wang et al. explored the possibility of producing collagen-calcium phosphate scaffolds with the incorporation of liposome thin films for the controlled release of bioactive molecules in bone regeneration and repair [44]. They suggested that bisphosphonate-functionalised liposome encapsulation could be isolated within mineral-containing scaffolds can be better drug delivery system that

localise their drug cargo to the directed area. The liposome encapsulation used consisted of cholesterol, distearoylphosphodioline, distearoyl phosphoethanolamine-poly(ethylene glycol). Based on their observations, the encapsulation of bisphosphonate within liposomes displayed a strong affinity to the scaffolds, and the drugs entrapped within the bisphosphonate liposomes showed a slower release rate from the scaffolds as compared to drugs that were un-encapsulated or encapsulated in polyethylene glycol (PEG) liposomes.

A study by Xu et al. [40] explored the possibility of synthesising a multifunctional thin film drug carrier with sustained drug release capability provided by the inner core liposome and osteoconductivity for bone cells supported by the HAp outer layer. The liposomes were produced from 1,2-dimyristoyl-sn-glycero-3-phosphate (DMPA) and 1,2-dimyristoyl-sn-glycero-3-phosphocholine (DMPC) which is then loaded with the lipophilic drug indomethacin. The release profile of indomethacin was measured at two different pH levels (4 and 7.4). As expected by coating the liposome with HAp, they reported a reduction in release rate of indomethacin in comparison to uncoated liposomes. They also reported that without these coatings, the rate of drug release occurred more rapidly at pH 7.4 rather than at pH 4.

It has been reported that the management of possible post-operative infections from bone grafts and prostheses as well as the treatment of bone diseases such as bone metastases will benefit greatly if there is a delivery system which has a high affinity towards bone tissues, thereby maximising its therapeutic effect on bone-related diseases [40, 43]. Using this approach, Anada et al. [41] attempted to develop a calcium phosphate-binding liposome coating for a bone-targeting drug delivery system by synthesising an amphipathic molecule bearing a bisphosphonate head group to recognise and bind to HAp. Liposomes loaded with the drug doxorubicin adsorbed onto the surfaces of HAp were observed to significantly reduce the number of viable human osteosarcoma MG63 cells. Based on these observations, they suggested that the system can be excellent coated carriers for anticancer drugs as they specifically target bone tissue [40].

6.6 Calcium Phosphate Derived from Marine Materials

Marine organisms are created and organised in such a way that the material itself possesses a wide range of characteristic and properties that might warrant their possible application within the biomedical arena. In addition, the pledge to exploit natural marine resources in a sustainable manner generates a highly interesting stage for the development of novel biomaterials along with both environmental and economic benefits. As a result, a growing number of compounds of different types are being isolated from aquatic organisms and converted into products for health applications including tissue engineering and controlled drug delivery devices.

Abundant sources of marine materials and structures are presently available that can be used to perform functions different to their originally proposed or intended application. A simple strategy is to use a predesigned and preformed structure such

as unique marine structures and modify it in a specific manner to suit its new intended purpose [48]. Furthermore, we can learn from nature and attempt to duplicate the essential components and reinvent in a laboratory. In addition, we strive to learn more from nature the principle of minimising energy usage during the synthesis process, the importance of structural organisation and the execution of transformative self-assembly and non-equilibrium chemistry.

These materials, as well as its designs, have played an influential role in the introduction of one of the easiest resolutions to crucial problems in regenerative medicine and in providing frameworks and highly accessible avenues of osteopromotive analogues, nanofibres, micro- and macrospheres and mineralizing proteins. This is demonstrated by the biological efficiency of marine structures such as shells, corals and sponge skeletons to accommodate self-sustaining musculoskeletal tissues and to promote bone formation through the use of nacre seashells and sponging extracts [49].

It has been discovered that molecules essential for regulating and guiding bone morphogenesis and in particular the actions accompanying mineral metabolism and deposition also exist in the earliest marine organisms. This is based on the fact that they symbolise the first molecular components recognised for calcification, morphogenesis and wound healing. It has emerged that bone morphogenetic protein, the main cluster of bone growth factors for human bone morphogenesis, is secreted by endodermal cells into the developing skeleton. Furthermore, organic and inorganic components of marine skeletons possess an ideal environment for the proliferation of added mesenchymal stem cell populations and promoting bone formation that is clinically acceptable.

The marine environment is distinctively rich in highly functional architectural structures with interconnected open pores. The chemical compositions and relatively high mechanical strength of these structures make them ideal to be used for human implantation either in its original form or convert to materials more suitable for biomedical applications.

Areas such as new pharmaceutical drug delivery systems with enhanced properties and a more efficient design, hard and soft tissue engineering and the discovery of a new generation of organic molecules have been the major emphases in the field of marine-based structures during the last two decades. More and more investigations on proteins and biopolymers produced by marine organisms have been carried out to examine its applications in the biomedical arena. At the moment, a growing number of compounds and materials are being identified from marine organisms such as calcium carbonates and proteins and applied to medical applications [49].

In tissue engineering applications, converted coralline apatites and coral skeletons are perfect examples [50]. They have demonstrated substantial clinical success as templates for tissue reconstruction. This has encouraged researchers to explore other skeletons with improved mechanical and/or biological properties. These unique three-dimensional marine structures are able to support the growth as well as an enhancement in differentiation of stem cell progenitors into bone cells. This is different to standard carbonate frameworks which do not induce stem cell differentiation.

6.6.1 Biomimetic Approach

In nature, biomaterials possess desirable properties such as complexity and sophistication, and we are gradually discovering ways to imitate nature to create similar levels of sophistication even though it is to a limited extent. Current 3D printing methods are good examples; however, we are only able to recreate microscopic structures with some level of biomimetic detail. For the replication of bioinorganic structures, this has been particularly true. The utilisation of biological microstructures as templates for the recreation of inorganic structures with identical features has emerged as a versatile approach. Through this technique, ordered silica microstructures have been produced using bacterial filaments and nanotubes produced from tobacco mosaic virus [51].

The main purpose in biomimetics is to synthetically duplicate the structures of selected inorganic biomatrices [51], and they play a clear part in the production of replacements for calcified tissues. This can be accomplished using techniques in biomineral-inspired materials chemistry. The idea is to make skeletons from molecules into macroscopic structures by utilising the consecutive developmental pathway of systems that nature employs. The space of construction is defined by the foundations which are laid. Constant delivery of all the necessary building materials is provided and maintained throughout construction. In nature, the process begins with supramolecular pre-organisation, interfacial recognition and vectorial regulation lending to multilevel processing [48]. The continual multiplication of these assemblies accumulates into the emergence of morphology and macroscale biomimetic forms. In the fabrication of the simplest skeletons, researchers have realised the great benefits of using emulsion droplets to create porous hollow shells, foams and bead templates in conjunction with using biocontinuous microemulsions to produce microskeletal networks [52].

Investigators have also examined another approach that uses the controlled mineralisation of adapted organic matrices from natural skeletons [51] and has generated clinically relevant end results. These bio-imitation approaches and strategies are being examined with cellular and extracellular matrix inputs such as mineralisations of reverse microemulsions [53] and bi-liquid foams and bio-continuous microemulsions [54, 55] and template-mediated biomineralisation of organic biomatrices [56]. Biomimetic microspheres synthesised within self-organising microemulsions were routinely employed as highly functional constructs for the localised delivery of growth factors and genes to primary human cells. These unique particles were also capable of producing osteoid and neocartilage [57].

6.6.2 Synthetic Implants, Devices and Prosthetics

A century ago, artificial or man-made implants and devices were produced from all sorts of materials such as gold and wood, and the development of these devices has reached a point where they could be used to replace different components of

the human body. These materials are capable of being in contact with bodily fluids and tissues for prolonged periods of time while demonstrating little or if any adverse reactions.

During the last two decades, acknowledging the importance of tissue-implant interactions on the nanoscale has led to the extensive development and application of nanotechnology in science and engineering. This is also based on the consideration that functional nanostructured materials are capable of being modified and incorporated into a range of biomedical devices. In addition, most biological systems such as viruses, protein complex and membrane exhibit natural nanostructures. The synthesis method and the processing routes will govern the microstructure and properties of these new-generation nanostructured materials. Therefore, it is vital that the most appropriate technique is selected for the fabrication of materials with preferred design and property combinations.

Techniques such as solid-state, liquid-state and gaseous ionic-state processing methods are frequently used for the synthesis of inorganic materials such as advanced ceramics. Additionally, wet chemical processing techniques such as sol-gel and co-precipitation have also been employed to obtain nanocoatings, nanoparticles and nanostructured solid shapes and blocks. In modern ceramic technology, pressing is achieved by placing the powder into a dye and compacting it through the exertion of pressure. For the production of bioceramics, the most commonly used methods are hot pressing and hot isostatic pressing. Compared to hot pressing, higher-density and smaller grain structure, essential for obtaining good mechanical properties, can be achieved through the use of hot isostatic pressure, whereby heat and pressure are applied simultaneously with the pressure being applied from all directions via a pressurised gas such as argon or helium. It is relatively easy to produce flat plates or blocks and non-uniform components using hot pressing or hot isostatic pressing.

Sol-gel processing is unique in that it can be utilised to synthesise various forms of the same composition such as coatings, fibres, powders, platelets and monoliths simply by changing factors such as chemistry and viscosity of a given solution [9]. The sol-gel technique possesses a number of advantages, for instance, it is of the nanoscale, and it results in a stoichiometric, homogeneous and pure product as mixing takes place on the molecular scale. It also has the ability to produce uniform fine-grained structures and can be easily applied to complex shapes with a range of coating techniques.

Appropriate surface finish is required for most biomaterials intended to be utilised within the physiological environment to permit the attachment of soft or hard tissue without any adverse reaction. Furthermore, biomaterials with a similar chemical composition to the bone are needed for hard-tissue attachment. For the majority of the animals, the microstructure of the bone is composed of interconnected pores micro- and nanoscopic in size. The hard tissues contain calcium and phosphate ions and their combined form as calcium phosphate compounds with a variety of other ionic species from the surrounding fluids. With our currently available production techniques, it is of great difficulty or in some cases almost impossible to copy and produce synthetically these complicated designs as a consequence

of the limitations in resolution. However, in the near future, this could be achieved through the use of the new-generation three-dimensional printing techniques.

Nature, on the other hand, has provided a solution to obtaining these intricately fine porous structures. As a product to their natural need, some marine structures contain excellent interconnected pores and architectures that can meet and answer the problems discussed previously. These marine structures have very fine interconnected pores from nanometre to a few hundred microns in range as well as excellent mechanical properties. More importantly, most of them are composed of or contain inorganic materials such as calcium phosphates and calcium carbonate with a range of metallic ions containing magnesium, strontium and silicon which assist in improving the properties of hard tissues after implantation. Although small, the organic matter within the marine skeletons contains a variety of materials, for example, proteins with very promising possible medical applications [58–60].

Mankind is facing the creation of new biomimetic material synthesis systems using living cells, and producing tailor-made biomaterials to our specifications and requirements accurately in a beaker or test tube can be considered to be one of the most fascinating bio-inspired approaches ever known [58]. This can be accomplished by careful adjustment in the growing environment. The convenient starting points are single- and multicelled organisms such as Foraminifera, Diatoms and coccolithophores as they are the most basic and elementary organisms to grow and support in artificial culture and provide enough utility for providing this approach as practically beneficial [49].

Of great interest for the advancement of new strategies in nanotechnology and molecular assembly are diatoms as they offer modes of construction at these scales that can potentially benefit the research and development of new-generation drug delivery devices as a result of their microscopic size and internal pore network structure [59]. Discovered throughout marine and freshwater environments, diatoms are photosynthetic secondary endosymbionts and are believed to be responsible for approximately one-fifth of the primary productivity on the planet. The genome sequence of the marine centric diatom *Thalassiosira pseudonana* was recently reported, revealing a wealth of information about diatom biology.

Diatoms have also been labelled as “natural-born” lithographers [61] and inspired the fabrication of nanostructured templates for nano-imprint processes where large structural areas with nanometre precision are required. Sussman et al. [61] exploited the mechanisms of patterning by diatoms for applications in patterning microchips, while Belegratis et al. [62] investigated the technical capabilities of the precise 3D laser lithography based on two-photon polymerisation of organic materials. This approach enabled the fabrication of arbitrary artificial diatom-inspired micro- and nanostructures and the design of an inverse structure. Therefore, only one replication step is required to obtain a template for nano-imprint processes.

There is also a vision to grow materials with living cells integrated during synthesis and construction in the field of biomimetic photonic materials. This represents an attractive proposition, and through this approach, the directed evolution may be conceivable with specific organisms that reproduce rapidly so that many thousands of generations are produced in short experimental time frames. At the

moment, protocols are well established for the mass production of new proteins using site random mutagenesis combined with high-throughput screening [63].

6.7 Marine Structures in Drug Delivery Applications

Various materials such as polymers, ceramics, polysaccharides and alginate have shown potential advantages as drug delivery systems [64]. In spite of this, marine materials such as coral exoskeletons and marine shells show better potential due to their easy conversion to calcium phosphates, intricate interconnected pores and their controllable dissolution rates. Furthermore, the uniform porosity of the exoskeletons offers a more constant drug loading and therefore providing a more predictable drug release rate of which both are vital factors that directly influence the effectiveness of the drug delivery system.

6.7.1 Coral Exoskeletons

The marine environment, with its enormous wealth of biological and chemical diversity [65, 66], represents an abundant and untapped source of useful natural structures awaiting discovery. While marine-derived chitosan, alginate and polysaccharides have shown potential advantages as drug delivery systems, coral exoskeletons can also be applied as an alternative material suitable for this task. For over 30 years, coral exoskeletons have been extensively studied and used as bone grafts where other marine structures have led to the development of pharmaceutics and their application in medicine [67–72].

Calcium carbonate (in the form of aragonite or calcite) can be found in many of the currently known marine organisms [73–75]. Each coral species possesses its unique architecture, namely, porosity, pore size and pore interconnectivity, microstructural composition and mechanical properties [76] that compliment key defining parameters of a drug delivery system. The pore size and interconnectivity of the coral pores are a critical factor in the rate of coral as a bone graft and slow drug delivery material. This interconnected porous network in coral exoskeletons can allow drugs to infiltrate to the centrum of the material [77]. Moreover, the uniform porosity of the exoskeletons provides a more constant drug loading and therefore providing a more predictable drug release rate of which both are crucial factors that directly impact the effectiveness of the drug delivery system.

Biological structures often exhibit intricate morphologies that justify the efforts for biomimetic approach. Biomineralising organisms are natural manufacturers with which mankind only can try to compete possibly with limited success. There are a number of marine structures in addition to coral that has a unique structure. One class of marine structure belonging to the Foraminifera shell family has shown to be suitable for drug delivery applications.

Foraminifera are abundant as fossils for the last 540 million years and are found in all marine environments, but different species exists depending on the surrounding habitat. Foraminifera are single-celled organisms with shells consisting of multilayer inner chambers commonly divided and added during its growth.

6.7.2 Coral Sources and Purity

The beginning of the coral life cycle starts with the polyps which absorb the calcium ions and carbonic acid present in the seawater to produce the calcium carbonate in the form of aragonite crystals representing 97–99% of the coral exoskeleton [78]. The remaining composition is made up of various elements and is dependent on the environment but mainly consists of trace elements of magnesium (0.05–0.2%), strontium, fluorine and phosphorous in the phosphate form (0.02–0.03%) [79, 80]. These elements that are composed in the coral exoskeleton structure are known to play a critical role in the bone mineralisation process and in the activation of key enzymes associated with bone remodelling cells.

Through extensive investigations, strontium has shown to contribute to the mineralisation process by stimulating osteoblasts while inhibiting osteoclasts [81]. Likewise, the presence of fluorine (coral possesses about 1.25–2.5 times more fluorine than found in human bone) helps bone formation through similar stimulatory effect on osteoblast proliferation [78]. Magnesium is also beneficial in bone remodelling as it has been shown to increase the mechanical properties of newly formed bone [82]. Evidently, most of the elements in the bone can be found in corals but they differ in their distribution. The source of the coral and the cleanliness of the environment influence the purity. Current synthetic coral production techniques under clean, controlled conditions by farming methods are possibly one of the most important ways of solving purity problem and the environmental concerns.

The issues of purity as well as a consistent supply source are two significant limitations concerning the development of marine biopharmaceutics. As previously mentioned coral and marine shells both natural and synthetic forms are widely abundant and available commercially and thereby making it an attractive source of material for research and clinical applications.

Before any marine material can be used as a carrier material, it must first undergo a rigorous process to control its quality from collection to manufacturing and to its final application. With increased sensitivity with modern screening techniques, studies can be performed to ensure that, within the limits of detection, no foreign entities or organic materials are left and that the material is of the highest quality. These studies can include optical, radiographic, chromatographic, spectrophotometric and biocompatibility analyses [80, 83].

Unless specifically protein and organic matter required, prior to sterilisation of calcium carbonate material, any residual organic constituents are removed by immersing in a solution of sodium hypochlorite for at least 1 h then drying at about 100 °C followed by and not limited to ultrasound treatment [50].

6.7.3 Conversion to Calcium Phosphate

It has been reported that marine-derived calcium carbonate exoskeletons possess fast degradation rate that may not be suitable for long-term drug therapy. However it should be noted that this trait might potentially be useful for drug delivery applications that require fast-acting and short-term therapy. In order to avoid this limitation, a number of authors have shown the process of converting the calcium carbonate exoskeleton of coral to the more stable structure of calcium phosphates and its derivatives [50, 84, 85]. One of these processes is commonly referred to as the hydrothermal exchange conversion strategy that was developed by Roy and Linnehan in 1974 [86]. In simple terms, this process exchanges the carbonate component of the coral for phosphate to produce calcium phosphates and its derivatives using high temperatures between 200 and 260 °C for 24–48 h following the reaction as shown below:

$$10CaCO_3 + 6(NH_4)_2HPO_4 + 2H_2O \Rightarrow Ca_{10}(PO_4)_6(OH)_2 + 6(NH_4)_2CO_3 + 4H_2CO_3$$

The calcium to phosphate molar ratio can be adjusted accordingly to yield different forms of calcium phosphates. In certain circumstances of drug delivery applications, tri-calcium phosphates (TCP) presents the more ideal composition compared with other calcium phosphates. Tri-calcium phosphate has been extensively studied for use as bone grafts [87–90] and for drug delivery systems [91–94] owing to appropriate dissolution rate [95–97]. The hydrothermal conversion from calcium carbonate exoskeletons to TCP would require a ratio between calcium and phosphorus of 1.5. The time variant is an important factor as a conversion period of less than 24 h would yield carbonated TCP, while a conversion period of 48 h would complete the transformation [77]. Obviously this also depends on the size of the material converted.

Chemical compositional analysis of marine structures can be examined by various techniques including mass spectroscopy. Elemental quantification by inductively coupled plasma mass spectroscopy (ICP) exhibits that the majority of the calcium, magnesium and strontium ions are preserved during this conversion process. A key benefit in employing the use of hydrothermal exchange is the preservation of the structural integrity of the original material. The chemical composition has changed, but the structure remains intact.

6.7.4 Delivery of Drugs

6.7.4.1 Bone Stimulatory Drug: Controlled Release of Simvastatin

Bone repair and formation is a complex process that would require stimulatory compounds in the form of pharmaceutics, growth factors, proteins, etc. to assist in the regeneration process. In the case of osteoporosis where there is an imbalance in bone remodelling process, the use of stimulants is even more crucial.

The last few decades have witness the development of various bone stimulatory drugs like bisphosphonates and its derivatives and more recently simvastatin. In previous studies, simvastatin was successfully loaded with the Foraminifera-derived β-tri-calcium phosphate (SV/β-TCP) with a 75% loading efficiency. To control the release of simvastatin and control its release rate, an apatite coating was made around the β-TCP material (Ap/SV/β-TCP) [98]. This reduced the release of simvastatin from 44% down to 22% which gave an approximately 50% reduction in the release. This will allow a more prolong release of the drug into the local area, thereby increasing the therapeutic efficacy of the system. This system was tested in an osteoporotic mice model where significant cortical and cancellous bone formation was observed in the localised area [99]. Furthermore, Ap/SV/β-TCP produced significantly stronger bones compared with the experimental groups. This is thought to be the effect of slower local release of simvastatin which again reinforces the potential benefits of using this drug delivery system. However if the treatment is aimed for systemic applications such as osteoporosis, new strategies are needed to be developed.

To assess the difference between local and systemic delivery in a separate study, Ap/SV/β-TCP system was compared with direct injection of equal amount of simvastatin. The results over the 6-week experimental period showed that direct injection ignited severe localised muscle inflammation, whereas the Ap/SV/β-TCP showed no sign of any adverse effects [100]. This is again attributed to the slower controlled release of simvastatin within the range of therapeutic efficacy compared with direct injection of the drug. Depending on the application and the duration of the therapy required, the unique structures of these foraminifera can be adapted and modified to achieve the desired therapeutic effect.

6.7.4.2 Antibiotic: Gentamicin Against Methicillin-Resistant *Staphylococcus aureus* (MRSA)

Despite the advancements in hygiene management related to surgical protocols, bacterial infections are still prevalent in modern surgeries. In second- or third-world operating theatres, the cases for infections are even higher. In orthopaedic surgery, *Staphylococcus aureus* (*S. aureus*) are the most common strain in the cause of infections. These infections generally go unnoticed till it is too late as the bacteria progressively proliferate and spread in the body.

With bacteria evolving into superbugs and becoming ever more resistant to antibiotics, the use and application of antibiotics are even more crucial especially in the hospitals. In the past PMMA loaded with antibiotics has been used widely in orthopaedic surgeries as the treatment of choice. However, PMMA is not biodegradable and as such would require another surgery to remove it after its intended function. This would again risk the patient the chance of repeated surgery and possible further infection.

What is agreed upon scientists is the need for effective treatment and prevention systems against *S. aureus* and its kind ideally by a biodegradable carrier. With this aim in mind, foramina-derived β-tri-calcium phosphate was loaded with gentamicin-sulphate

antibiotic (GS-TCP) and evaluated to treat and/or prevent the occurrence of clinical strain methicillin resistant *Staphylococcus aureus* (MRSA) in vitro [101]. The study showed that a single GS-TCP was capable of releasing antibiotics to prevent the growth of MRSA during its exponential growth phase. Furthermore, a time-delayed study where GS-TCP was introduced to the MRSA at various times (5, 10, 15, 30, 60 and 1,440 mins) showed the negative presence of the MRSA, thereby signifying the potential antibacterial efficacy of the GS-TCP.

6.7.4.3 Zinc: Surface Modification of β-Tri-Calcium Phosphate

The previous two studies showed the potential of using Foraminifera and marine structure-derived β-tri-calcium phosphate or hydroxyapatite as carriers for drugs, and it should be noted that calcium phosphates can be synthetically modified to alter the chemical composition of the thereby changing its biological properties. As stated earlier trace elements, such as strontium and magnesium, that are involved in bone formation have been extensively studied and evaluUpdatedated by incorporation into biomaterials for their ability to stimulate bone formation [81, 82].

Zinc, another trace element that is required in cell regulation, has also shown bone stimulatory effects, and studies have linked zinc deficiency in osteoporotic patients [102, 103]. Zinc can promote bone growth [104], bone resorption and inhibit inflammatory reaction [105], along with antimicrobial resistance [106] which can impart multifunctionality in a drug delivery system. However, like all pharmaceutics, precautions must be taken as high concentration of zinc can exhibit adverse side effects. By incorporating key ions into the lattice structure of the material, the system can achieve further biological activities and allowing the unfilled porous network to be incorporated with other compounds as a dual drug delivery system.

6.8 Concluding Remarks

Multifunctional materials utilising surface modifications, encapsulation or coating of therapeutic and nutritional products will increase. Targeted immunotherapies, cancer treatment and slow drug delivery will make use of nanopowders, nanocoatings and nanocomposite devices. In drug delivery systems, there are numerous possibilities that contribute to suitable approaches to a range of major medical applications. The nanoparticle approach and hence the increased surface area usually improve solubility, targeting tissues, cells and cellular receptors.

In nature, structures possess desirable properties, and gradually we are discovering new ways of reproducing nature to create similar levels of sophistication even though only to a limited extent. One versatile approach is to use biological microstructures as templates for the reproduction of inorganic structures with identical features. They have a distinct consequence to the production of replacements

for calcified tissues. This is achieved by using techniques in biomineral-inspired materials chemistry. The concept is to utilise the consecutive developmental pathway of systems that nature employs to make skeletons from molecules into micro- and macroscopic structures.

Marine structures have been widely explored during the past decade from the imitation of efficient designs of nature or biomimetics to soft- and hard-tissue engineering as well as from slow or controlled drug delivery to biosensors and bioreactor applications. The new approaches include the use of natural organic and inorganic skeletons, micro- and nanoscale slow drug delivery devices, new medical treatment protocols inspired by unique designs and devices incorporating stem cells, proteins and peptides.

The development and application of using marine exoskeletons as a precursor material to produce calcium phosphate carriers for drugs have shown to be potentially advantageous. The oceans are still filled with a vast diversity of prospective and innovative structures that are awaiting scientists to explore for tissue engineering applications and learn from their natural synthesis and growth methods. Biomimetics and the hydrothermal conversion method allow us to utilise a wide range of marine-based materials that possess unique structures suitable as carriers for drugs amongst other biomedical applications. In today's competitive economic climate, development of drug delivery systems is presented with increase challenges. However, it is not difficult to imagine the use of marine structures as therapeutic materials with synthetic modification in the treatment of current and future bone-related ailments.

References

1. Chang MC, Ko CC, Douglas WH. Conformational change of hydroxyapatite/gelatin nanocomposite by glutaraldehyde. Biomaterials. 2003;24:3087–94.
2. Zhang W, Liao SS, Cui FZ. Hierarchical self-assembly of nano-fibrils in mineralized collagen. Chem Mater. 2003;15:3221–6.
3. Vinogradov SV, Bronich TK, Kabanov AV. Nanosized cationic hydrogels for drug delivery: preparation, properties and interactions with cells. Adv Drug Deliv Rev. 2002;54:135–47.
4. Vinogradov SV, Batrakova EV, Kabanov AV. Nanogels for oligonucleotide delivery to the brain. Bioconjug Chem. 2004;15:50–60.
5. de Groot KR, Geesink R, Klein CPAT, Serekian P. Plasma sprayed coatings of hydroxylapatite. J Biomed Mater Res. 1987;21:1375–81.
6. Hench LL. Bioceramics: from concept to clinic. J Am Ceram Soc. 1991;74:1487–510.
7. Choi AH, Ben-Nissan B, Matinlinna JP, Conway RC. Current perspectives: calcium phosphate nanocoatings and nanocomposite coatings in dentistry. J Dent Res. 2013;92:853–9.
8. LeGeros RZ. Biodegradation and bioresorption of calcium phosphate ceramics. Clin Mater. 1993;14:65–88.
9. Ben-Nissan B, Choi AH. Sol-gel production of bioactive nanocoatings for medical applications: part I: an introduction. Nanomedicine. 2006;1:311–9.
10. Choi AH, Ben-Nissan B. Sol-gel production of bioactive nanocoatings for medical applications: part II: current research and development. Nanomedicine. 2007;2:51–61.
11. LeGeros RZ. Properties of osteoconductive biomaterials: calcium phosphates. Clin Orthop Relat Res. 2002;395:81–98.

12. Giri S, Trewyn BG, Lin VS. Mesoporous silica nanomaterial-based biotechnological and biomedical delivery systems. Nanomedicine. 2007;2:99–111.
13. Wu C, Chang J, Zhai W, Ni S. A novel bioactive porous bredigite ($Ca_7MgSi_4O_{16}$) scaffold with biomimetic apatite layer for bone tissue engineering. J Mater Sci Mater Med. 2007;18:857–64.
14. Victor SP, Sharma CP. Calcium phosphates as drug delivery systems. J Biomater Tissue Eng. 2012;2:269–79.
15. Li J, Chen YC, Tseng YC, Mozumdar S, Huang L. Biodegradable calcium phosphate nanoparticle with lipid coating for systemic siRNA delivery. J Control Release. 2010;142:416–21.
16. Pittella F, Miyata K, Maeda Y, Suma T, Watanabe S, Chen Q, Christie RJ, Osada K, Nishiyama N, Kataoka K. Pancreatic cancer therapy by systemic administration of VEGF siRNA contained in calcium phosphate/charge-conversional polymer hybrid nanoparticles. J Control Release. 2012;161:868–74.
17. Olton D, Li J, Wilson ME, Rogers T, Close J, Huang L, Kumta PN, Sfeir C. Nanostructured calcium phosphates (NanoCaPs) for non-viral gene delivery: influence of the synthesis parameters on transfection efficiency. Biomaterials. 2007;28:1267–79.
18. Liu Y, Wang T, He F, Liu Q, Zhang D, Xiang S, Su S, Zhang J. An efficient calcium phosphate nanoparticle-based nonviral vector for gene delivery. Int J Nanomedicine. 2011;6:721–7.
19. Zhou C, Yu B, Yang X, Huo T, Lee LJ, Barth RF, Lee RJ. Lipid-coated nano-calcium-phosphate (LNCP) for gene delivery. Int J Pharm. 2010;392:201–8.
20. Cao X, Deng W, Wei Y, Yang Y, Su W, Wei Y, Xu X, Yu J. Incorporating pTGF-β1/calcium phosphate nanoparticles with fibronectin into 3-dimensional collagen/chitosan scaffolds: efficient, sustained gene delivery to stem cells for chondrogenic differentiation. Eur Cell Mater. 2012;23:81–93.
21. Sokolova V, Knuschke T, Buer J, Westendorf AM, Epple M. Quantitative determination of the composition of multi-shell calcium phosphate-oligonucleotide nanoparticles and their application for the activation of dendritic cells. Acta Biomater. 2011;7:4029–36.
22. Han JY, Tan TTY, Loo JSC. Utilizing inverse micelles to synthesize calcium phosphate nanoparticles as nano-carriers. J Nanopart Res. 2011;13:3441–54.
23. Paul W, Sharma CP. Fatty acid conjugated calcium phosphate nanoparticles for protein delivery. Int J Appl Ceram Technol. 2010;7:129–38.
24. Uskoković V, Batarni SS, Schweicher J, King A, Desai TA. Effect of calcium phosphate particle shape and size on their antibacterial and osteogenic activity in the delivery of antibiotics in vitro. ACS Appl Mater Interfaces. 2013;5:2422–31.
25. Kester M, Heakal Y, Fox T, Sharma A, Robertson GP, Morgan TT, Altinoğlu EI, Tabaković A, Parette MR, Rouse SM, Ruiz-Velasco V, Adair JH. Calcium phosphate nanocomposite particles for in vitro imaging and encapsulated chemotherapeutic drug delivery to cancer cells. Nano Lett. 2008;8:4116–21.
26. Bastakoti BP, Hsu YC, Liao SH, Wu KC, Inoue M, Yusa S, Nakashima K, Yamauchi Y. Inorganic-organic hybrid nanoparticles with biocompatible calcium phosphate thin shells for fluorescence enhancement. Chem Asian J. 2013;8:1301–5.
27. El-Ghannam A, Ricci K, Malkawi A, Jahed K, Vedantham K, Wyan H, Allen LD, Dréau D. A ceramic-based anticancer drug delivery system to treat breast cancer. J Mater Sci Mater Med. 2010;21:2701–10.
28. Zhao XY, Zhu YJ, Chen F, Lu BQ, Qi C, Zhao J, Wu J. Calcium phosphate hybrid nanoparticles: self-assembly formation, characterization, and application as an anticancer drug nanocarrier. Chem Asian J. 2013;8:1306–12.
29. Liang P, Zhao D, Wang CQ, Zong JY, Zhuo RX, Cheng SX. Facile preparation of heparin/$CaCO_3$/CaP hybrid nano-carriers with controllable size for anticancer drug delivery. Colloids Surf B: Biointerfaces. 2013;102:783–8.
30. Li WM, Chen SY, Liu DM. In situ doxorubicin-CaP shell formation on amphiphilic gelatin-iron oxide core as a multifunctional drug delivery system with improved cytocompatibility, pH-responsive drug release and MR imaging. Acta Biomater. 2013;9:5360–8.
31. Rout SR, Behera B, Maiti TK, Mohapatra S. Multifunctional magnetic calcium phosphate nanoparticles for targeted platin delivery. Dalton Trans. 2012;41:10777–83.

32. Mukesh U, Kulkarni V, Tushar R, Murthy RS. Methotrexate loaded self stabilized calcium phosphate nanoparticles: a novel inorganic carrier for intracellular drug delivery. J Biomed Nanotechnol. 2009;5:99–105.
33. Chen Z, Li Z, Lin Y, Yin M, Ren J, Qu X. Biomineralization inspired surface engineering of nanocarriers for pH-responsive, targeted drug delivery. Biomaterials. 2013;34:1364–71.
34. Chiu D, Zhou W, Kitayaporn S, Schwartz DT, Murali-Krishna K, Kavanagh TJ, Baneyx F. Biomineralization and size control of stable calcium phosphate core-protein shell nanoparticles: potential for vaccine applications. Bioconjug Chem. 2012;23:610–7.
35. Li S, Wang K, Chang KC, Zong M, Wang J, Cao YG, Bai YH, Wei TM, Zhang ZR. Preparation and evaluation of nano-hydroxyapatite/poly(styrene-divinylbenzene) porous microsphere for aspirin carrier. Sci China Chem. 2012;55:1134–9.
36. Ignjatović N, Uskoković V, Ajduković Z, Uskoković D. Multifunctional hydroxyapatite and poly(D, L-lactide-co-glycolide) nanoparticles for the local delivery of cholecalciferol. Mater Sci Eng C. 2013;33:943–50.
37. Chen R, Qian Y, Li R, Zhang Q, Liu D, Wang M, Xu Q. Methazolamide calcium phosphate nanoparticles in an ocular delivery system. Yakugaku Zasshi. 2010;130:419–24.
38. Ramachandran R, Paul W, Sharma CP. Synthesis and characterization of PEGylated calcium phosphate nanoparticles for oral insulin delivery. J Biomed Mater Res B Appl Biomater. 2009;88:41–8.
39. Xu T, Zhang N, Nichols HL, Shi D, Wen X. Modification of nanostructured materials for biomedical applications. Mater Sci Eng C. 2007;27:579–94.
40. Xu Q, Tanaka Y, Czernuszka JT. Encapsulation and release of a hydrophobic drug from hydroxyapatite coated liposomes. Biomaterials. 2007;28:2687–94.
41. Anada T, Takeda Y, Honda Y, Sakurai K, Suzuki O. Synthesis of calcium phosphate-binding liposome for drug delivery. Bioorg Med Chem Lett. 2009;19:4148–50.
42. Zhu CT, Xu YQ, Shi J, Li J, Ding J. Liposome combined porous β-TCP scaffold: preparation, characterization, and anti-biofilm activity. Drug Deliv. 2010;17:391–8.
43. Huang JS, Liu KM, Chen CC, Ho KY, Wu YM, Wang CC, Cheng YM, Ko WL, Liu CS, Ho YP, Wang YP, Hong K. Liposomes-coated hydroxyapatite and tricalcium phosphate implanted in the mandibular bony defect of miniature swine. Kaohsiung J Med Sci. 1997;13:213–28.
44. Wang G, Babadağli ME, Uludağ H. Bisphosphonate-derivatized liposomes to control drug release from collagen/hydroxyapatite scaffolds. Mol Pharm. 2011;8:1025–34.
45. Al-Jamal WT, Kostarelos K. Liposome-nanoparticle hybrids for multimodal diagnostic and therapeutic applications. Nanomedicine. 2007;2:85–98.
46. Ben-Nissan B, Macha I, Cazalbou S, Choi AH. Calcium phosphate nanocoatings and nanocomposites, part 2: thin films for slow drug delivery and osteomyelitis. Nanomedicine. 2016;11:531–44.
47. Choi AH, Ben-Nissan B, Conway RC, Macha I. Advances in calcium phosphate nanocoatings and nanocomposites. In: Ben-Nissan B, editor. Advances in calcium phosphate biomaterials, Springer series in biomaterials science and engineering (SSBSE). Berlin: Springer; 2014. p. 485–509.
48. Ben-Nissan B, Green DW. Marine materials in drug delivery and tissue engineering: from natural role models, to bone regeneration and repair and slow delivery of therapeutic drugs, proteins and genes. In: Kim S-K, editor. Marine biomaterials. Boca Raton: Taylor and Francis/CSR Books; 2013. p. 575–602.
49. Green DW, Li G, Milthrope B, Ben-Nissan B. Adult stem cell coatings using biomaterials for regenerative medicine. Mater Today. 2012;15:61–8.
50. Ben-Nissan B. Natural bioceramic: from coral to bone and beyond. Curr Opin Solid State Mater Sci. 2003;7:283–8.
51. Mann S. Mineralization in biological systems. Struct Bond. 1983;54:125.
52. Gonzalez-McQuire R, Green D, Walsh D, Hall S, Chane-Ching JY, Oreffo RO, Mann S. Fabrication of hydroxyapatite sponges by dextran sulfate/amino acid templating. Biomaterials. 2005;26:6652–6.
53. Green D, Walsh D, Yang X, Mann S, Oreffo ROC. Stimulation of human bone marrow stromal cells using growth factor-encapsulated calcium carbonate porous microspheres. J Mater Chem. 2004;14:2206–12.

54. Walsh D, Mann S. Feigning nature's sculptures. Chem Br. 1996;32:31–4.
55. Walsh D, Boanini E, Tanaka J, Mann S. Synthesis of tri-calcium phosphate sponges by interfacial deposition and thermal transformation of self-supporting inorganic films. J Mater Chem. 2005;15:1043–8.
56. Hall SR, Swinerd VM, Newby FN, Collins AM, Mann S. Fabrication of porous titania (brookite) microparticles with complex morphology by sol-gel replication of pollen grains. Chem Mater. 2006;18:598–600.
57. Green DW. Bio-inspired ceramic structures: from invertebrate marine skeletons to biomimetic crystal engineering. J Aust Ceram Soc. 2004;40:1–7.
58. Parker AR, Martini N. Structural color in animals-simple to complex optics. Opt Laser Technol. 2006;38:315–22.
59. Ben-Nissan B, Green DW. Marine structures as templates for biomaterials. In: Ben-Nissan B, editor. Advances in calcium phosphate biomaterials, springer series in biomaterials science and engineering (SSBSE). Berlin: Springer; 2014. p. 391–414.
60. Choi AH, Cazalbou S, Ben-Nissan B. Biomimetics and marine materials in drug delivery and tissue engineering. In: Antoniac IV, editor. Handbook of bioceramics and Biocomposites. Berlin: Springer; 2015. p. 1–24.
61. Mock T, Samanta MP, Iverson V, Berthiaume C, Robison M, Holtermann K, Durkin C, Bondurant SS, Richmond K, Rodesch M, Kallas T, Huttlin EL, Cerrina F, Sussman MR, Armbrust EV. Whole-genome expression profiling of the marine diatom Thalassiosira pseudonana identifies genes involved in silicon bioprocesses. Proc Natl Acad Sci U S A. 2008;105:1579–84.
62. Belegratis MR, Schmidt V, Nees D, Stadlober B, Hartmann P. Diatom-inspired templates for 3D replication: natural diatoms versus laser written artificial diatoms. Bioinspir Biomi. 2014;9:016004.
63. Kim ES. Directed evolution: a historical exploration into an evolutionary experimental system of nanobiotechnology, 1965–2006. Minerva. 2008;46:463–84.
64. Bose S, Tarafder S. Calcium phosphate ceramic systems in growth factor and drug delivery for bone tissue engineering: a review. Acta Biomater. 2012;8:1401–21.
65. Fuhrman J, McCallum K, Davis A. Phylogenetic diversity of subsurface marine microbial communities from the Atlantic and Pacific oceans. Appl Environ Microbiol. 1995;61:4517.
66. Rossbach M, Kniewald G. Concepts of marine specimen banking. Chemosphere. 1997;34:1997–2010.
67. Leupold J, Barfield W, An Y, Hartsock L. A comparison of ProOsteon, DBX, and collagraft in a rabbit model. J Biomed Mater Res B Appl Biomater. 2006;79:292–7.
68. Luesch H, Harrigan G, Goetz G, Horgen F. The cyanobacterial origin of potent anticancer agents originally isolated from sea hares. Curr Med Chem. 2002;9:1791–806.
69. Pettit GR, Xu JP, Hogan F, Williams MD, Doubek DL, Schmidt JM, Cerny RL, Boyd MR. Isolation and structure of the human cancer cell growth inhibitory cyclodepsipeptide dolastatin 16. J Nat Prod. 1997;60:752–4.
70. Simmons TL, Coates RC, Clark BR, Engene N, Gonzalez D, Esquenazi E, Dorrestein PC, Gerwick WH. Biosynthetic origin of natural products isolated from marine microorganism-invertebrate assemblages. Proc Natl Acad Sci U S A. 2008;105:4587–94.
71. Simmons T, Andrianasolo E, McPhail K, Flatt P, Gerwick W. Marine natural products as anticancer drugs. Mol Cancer Ther. 2005;4:333–42.
72. Sithranga Boopathy N, Kathiresan K. Anticancer drugs from marine flora: an overview. J Oncol. 2010;2010:214186.
73. Stanley G. The evolution of modern corals and their early history. Earth Sci Rev. 2003;60:195–225.
74. Sethmann I, Worheide G. Structure and composition of calcareous sponge spicules: a review and comparison to structurally related biominerals. Micron. 2008;39:209–28.
75. Wilt F, Kilian C, Livingston B. Development of calcareous skeletal elements in invertebrates. Differentiation. 2003;71:237–50.
76. Laine J, Labady M, Albornoz A, Yunes S. Porosities and pore sizes in coralline calcium carbonate. Mater Charact. 2008;59:1522–5.

77. Chou J, Valenzuela S, Bishop D, Ben-Nissan B, Milthorpe B. Strontium- and magnesium-enriched biomimetic β-TCP macrospheres with potential for bone tissue morphogenesis. J Tissue Eng Regen Med. 2012;8:771–8.
78. Demers C, Hamdy C, Corsi K, Chellat F, Tabrizian M, Yahia L. Natural coral exoskeleton as a bone graft substitute: a review. Biomed Mater Eng. 2002;12:15–35.
79. Baudet-Pommel M, Collangettes-Peyrat D, Couvet-Lejczyk V. Autotransplantation: clinical results, radiography, orthodontics, criteria for success. Acta Odontol. 1988;163:463–72.
80. Patat J, Guillemin G. Natural coral used as a replacement biomaterial in bone grafts. Ann Chir Plast Esthet. 1989;34:221–5.
81. Bonnelye E, Chabadel A, Saltel F, Jurdic P. Dual effect of strontium ranelate: stimulation of osteoblast differentiation and inhibition of osteoclast formation and resorption in vitro. Bone. 2008;42:129–38.
82. LeGeros R. Apatites in biological systems. Prog Cryst Growth Charact. 1981;41:1–45.
83. Papacharalambous S, Anastasoff K. Natural coral skeleton used as onlay graft for contour augmentation of the face. A preliminary report. Int J Oral Maxillofac Surg. 1993;22:260–4.
84. Chou J, Ben-Nissan B, Choi A, Wuhrer R, Green D. Conversion of coral sand to calcium phosphate for biomedical application. J Aust Ceram Soc. 2007;43:44–8.
85. Ben-Nissan B, Milev A, Vago R. Morphology of sol-gel derived nano-coated coralline hydroxyapatite. Biomaterials. 2004;25:4971–5.
86. Roy D, Linnehan S. Hydroxyapatite formed from coral skeletal carbonate by hydrothermal exchange. Nature. 1974;247:220–2.
87. Damron T, Lisle J, Craig T, Wade M, Silbert W, Cohen H. Ultraporous β-tricalcium phosphate alone or combined with bone marrow aspirate for benign cavitary lesions: comparison in a prospective randomized clinical trial. J Bone Joint Surg Am. 2013;95:158–66.
88. Guyton G, Miller S. Stem cells in bone grafting: trinity allograft with stem cells and collagen/β-tricalcium phosphate with concentrated bone marrow aspirate. Foot Ankle Clin. 2010;15:611–9.
89. Barber F, Dockery W. Long-term absorption of β-tricalcium phosphate poly-L-lactic acid interference screws. Arthroscopy. 2008;24:441–7.
90. Somanathan R, Simunek A. Evaluation of the success of β-tricalcium phosphate and deproteinized bovine bone in maxillary sinus augmentation using histomorphometry: a review. Acta Med. 2006;49:87–9.
91. Florczyk SJ, Leung M, Jana S, Li Z, Bhattarai N, Huang JI, Hopper RA, Zhang M. Enhanced bone tissue formation by alginate gel-assisted cell seeding in porous ceramic scaffolds and sustained release of growth factor. J Biomed Mater Res A. 2012;100:3408–15.
92. Zhou J, Fang T, Wang Y, Dong J. The controlled release of vancomycin in gelatin/β-TCP composite scaffolds. J Biomed Mater Res A. 2012;100:2295–301.
93. La W, Kwon S, Lee T, Yang H, Park J, Kim B. The effect of the delivery carrier on the quality of bone formed via bone morphogenetic protein-2. Artif Organs. 2012;36:642–7.
94. Suarez-Gonzalez D, Lee J, Lan Levengood S, Vanderby RJ, Murphy W. Mineral coatings modulate β-TCP stability and enable growth factor binding and release. Acta Biomater. 2012;8:1117–24.
95. Paschalis E, Wikiel K, Nancollas G. Dual constant composition kinetics characterization of apatitic surfaces. J Biomed Mater Res. 1994;28:1411–8.
96. Tang R, Hass M, Wu W, Gulde S, Nancollas G. Constant composition dissolution of mixed phases. II. Selective dissolution of calcium phosphates. J Colloid Interface Sci. 2003;260:379–84.
97. LeGeros R, Lin S, Rohanizadeh R, Mijares D, LeGeros J. Biphasic calcium phosphate bioceramics: preparation, properties and applications. J Mater Sci Mater Med. 2003;14:201–9.
98. Chou J, Ito T, Bishop D, Otsuka M, Ben-Nissan B, Milthorpe B. Controlled release of simvastatin from biomimetic β-TCP drug delivery system. PLoS One. 2013;8:e54676.
99. Chou J, Ito T, Otsuka M, Ben-Nissan B, Milthorpe B. The effectiveness of the controlled release of simvastatin from β-TCP macrosphere in the treatment of OVX mice. J Tissue Eng Regen Med. 2016;10:E195–203.

100. Chou J, Ito T, Otsuka M, Ben-Nissan B, Milthorpe B. Simvastatin-loaded β-TCP drug delivery system induces bone formation and prevents rhabdomyolysis in OVX mice. Adv Healthc Mater. 2013;2:678–81.
101. Chou J, Ben-Nissan B, Green D, Valenzuela S, Kohan L. Targeting and dissolution characteristics of bone forming and antibacterial drugs by harnessing the structure of micro-spherical shells from coral beach sand. Adv Eng Mater. 2010;13:93–9.
102. Kawamura H, Ito A, Miyakawa S, Layrolle P, Ojima K, Ichinose N, Tateishi T. Stimulatory effect of zinc-releasing calcium phosphate implant on bone formation in rabbit femora. J Biomed Mater Res. 2000;50:184–90.
103. Relea P, Revilla M, Ripoll E, Arribas I, Villa LF, Rico H. Zinc, biochemical markers of nutrition, and type I osteoporosis. Age Ageing. 1995;24:303–7.
104. Yamaguchi M, Oishi H, Suketa Y. Stimulatory effect of zinc on bone formation in tissue culture. Biochem Pharmacol. 1987;36:4007–12.
105. Moonga B, Dempster D. Zinc is a potent inhibitor of osteoclastic bone resorption in vitro. J Bone Miner Res. 1995;10:453–7.
106. Hernández-Sierra JF1, Ruiz F, Pena DC, Martínez-Gutiérrez F, Martínez AE, Guillén Ade J, Tapia-Pérez H, Castañón GM. The antimicrobial sensitivity of Streptococcus mutans to nanoparticles of silver, zinc oxide, and gold. Nanomedicine. 2008;4:237–40.

Chapter 7
Synthesis and Functionalization of Mesoporous Bioactive Glasses for Drug Delivery

F. Branda

Abstract Recently Mesoporous bioactive glasses were synthesized for which outstanding applications in the biomedical field are expected. It is nowadays recognized, in fact, that microporous and mesoporous inorganic and hybrid organic-inorganic bioactive matrices and scaffolds can be produced with controlled rates of resorption and controlled surface chemistries. The type and concentration of released inorganic and organic species and their release sequence can be tuned; this is a vital requirement in stimulating cell proliferation and enhancing subsequent cell differentiation. The ability to bond to living tissues and the high pore volume allow to exploit mesoporous bioactive materials also simply for local drug delivery allowing to overcome the limitations of systemic delivery: therapeutic concentrations at the site of infection, but for short periods of time, forcing repeated dosing for longer periods.

The chapter is organized in four sections. The first one deals with synthesis and mechanism of formation of mesoporous bioactive glasses. The second one analyses the bioactive behavior. The third one is devoted to understand the specificity of bioactive response induced by the mesoporous structure. The fourth one deals with drug delivery from mesoporous bioactive glasses. In a first subparagraph the advantages of using bioactive glasses for local derivery and the construction of tissue engineering scaffolds are analysed. In the second one the complexity of therapeutics delivery from mesoporous bioactive glasses is analysed.

Keywords Mesoporous particles • Bioactivity • Scaffolds • Tissue engineering • Drug delivery

F. Branda (✉)
Dipartimento di Ingegneria Chimica, dei Materiali e della Produzione Industriale (Department of Chemical, Materials and Production Engineering) – DICMaPI, University of Naples "Federico II", P.le Tecchio, Naples, Italy
e-mail: branda@unina.it

G. Kaur (ed.), *Clinical Applications of Biomaterials*,
DOI 10.1007/978-3-319-56059-5_7

7.1 Introduction

Bioactive glasses and bioactive fixation were discovered by Hench at the beginning of 1970s. Bioactive fixation is defined as the "interfacial bonding of an implant to tissue by means of formation of a biologically active hydroxyapatite layer on the implant surface" [29]. These materials arose great expectations in the revolutionary period for medical care beginning just about 50 years ago. For centuries the problem of diseased or damaged body tissues had had little solution but the removal of the offending part. About 50 years ago transplantation or implantation became possible, but also implants made from biomaterials became available. These last had significant advantages over the first ones with regard to availability, reproducibility, and reliability. However they suffered problems of interfacial stability with host tissues and, obviously, lacked, with respect to living tissues, the ability to self-repair and to modify structure and properties in response to environmental factors such as mechanical load or blood flow.

The chapter is organized in four sections. The first one deals with synthesis and mechanism of formation of mesoporous bioactive glasses. The second one analyses the bioactive behavior. The third one is devoted to understand the specificity of bioactive response induced by the mesoporous structure. The fourth one deals with drug delivery from mesoporous bioactive glasses. In a first subparagraph the advantages of using bioactive glasses for local derivery and the construction of tissue engineering scaffolds are analysed. In the second one the complexity of therapeutics delivery from mesoporous bioactive glasses is analysed.

In order to improve orthopedic prostheses, lifetime special care was devoted to get better interfaces. Great attention was devoted to morphological fixation, exploiting large interface areas or fenestrations, or biological fixation, based on bone ingrowth, as alternative to cement fixation. Because of the ability to assure, after 3–6 months, a strength equal to or greater than the bone, bioactive bond to bone appeared to be a panacea for the interfacial stability problem. However at the end of the last century, it was recognized [29] that this is not true. The mismatch in mechanical properties at the bonded interface and the inability of the bioactive bonded interface to remodel in response to applied load have a detrimental effect on long-term interface stability [29]. Hench recognized [29] the need "to shift the emphasis of biomaterials research toward assisting or enhancing the body's own reparative capacity," that is, the need of a biomaterial that may enhance the regeneration of natural tissues, some kind of "regenerative allograft." He also very lucidly predicted that bioactive materials would keep on playing an outstanding role [29]. It is nowadays recognized that microporous and mesoporous inorganic and hybrid organic–inorganic bioactive matrices and scaffolds can be produced with controlled rates of resorption and controlled surface chemistries. The type and concentration of released inorganic and organic species and their release sequence can be tuned; this is a vital requirement in stimulating cell proliferation and enhancing subsequent cell differentiation [30, 34, 90]. The ability to bond to living tissues and the high pore

volume allow to exploit mesoporous bioactive materials also simply for local drug delivery allowing to overcome the limitations of systemic delivery: therapeutic concentrations at the site of infection but, for short periods of time, forcing repeated dosing for longer periods.

The chapter is organized in four sections. The first one deals with synthesis and mechanism of formation of mesoporous bioactive glasses. The second one analyzes the bioactive behavior. The third one is devoted to understand the specificity of bioactive response induced by the mesoporous structure. The fourth one deals with drug delivery from mesoporous bioactive glasses. In a first subparagraph, the advantages of using bioactive glasses for local delivery and the construction of tissue engineering scaffolds are analyzed. In the second one, the complexity of therapeutic delivery from mesoporous bioactive glasses is analyzed.

7.2 Mesoporous Bioactive Glasses (MBG)

According to the IUPAC definition [15], porous materials are divided into three classes: microporous (<2 nm), mesoporous (2–50 nm), and macroporous (>50 nm). Because of their high specific surface areas, porous solids were intensively studied [93] in the past for applications as adsorbents, catalysts, and catalyst support and, successively, in the field of sensors, drug delivery, and optical devices. A very great research activity was addressed [15] to zeolites that join good catalytic activity to the microporous structure. The relatively small pore openings however limited the range of their applicability. Porous glasses and gels do possess [15] larger pores, in the mesoporous dominion; however they show disordered pore system with broad pore size distributions. Intercalation of layered materials (double hydroxides, phosphates, and clays) gave also mesoporous solids with very broad mesopore size distributions.

MCM41 (Mobil Composition of Matter 41), discovered in 1992, was the first mesoporous solid possessing a regularly ordered pore arrangement and a very narrow pore size distribution [17, 48]. It can be produced in a wide range of experimental conditions exploiting interactions between silica and cationic surfactants. The strong adsorption of surfactant on the surface of silica particles had been, in earlier works, already exploited to control the flocculation of colloidal silica [39]. Moreover Iler in his book [40] reports on a patent of 1971 of V. Chiola et al. [14] assigned to Sylvania Electric Products Inc. in which “low bulk density silica” was described to be produced during hydrolysis and polycondensation of tetraethylorthosilicate (TEOS) in the presence of cationic surfactants. No other characterization than bulk density was reported in the patent. However, taking into account that when a surfactant is added to a soluble silicate MCM-41 is the more likely condensation product [17], the low density material of Chiola may be considered a forerunner of MCM-41 and also of surfactant template materials of different compositions [17, 35, 36].

7.2.1 Synthesis of Mesoporous Glasses

The production of mesoporous glasses exploits the templating action of surfactant molecules during the glass sol–gel synthesis. Generally speaking the sol–gel process is [3, 6] a synthesis route consisting in the preparation of a sol and successive gelation. Very popular precursors of the sol–gel synthesis of silicates are the metal-organic compounds like tetraethylorthosilicate (or tetraethoxysilane) $Si(OC_2H_5)_4$, shortly indicated with the acronym TEOS. A silicatic framework may be obtained through hydrolysis:

$$\equiv Si-OR + H_2O \leftrightarrow \equiv Si-OH + ROH$$

and polycondensation reactions:

$$\equiv Si-OR + HO-Si \equiv \leftrightarrow \equiv Si-O-Si \equiv + Si-OH$$

$$\equiv Si-OH + HO-Si \equiv \leftrightarrow \equiv Si-O-Si \equiv + H_2O$$

Polycondensation turns monomers into oligomers and, finally, inorganic polymers in the form of gels. The gels may then be converted to xerogels, glasses, and films. When the hydrolysis and polycondensation of alkoxysilicates occurs in basic (ammonia) alcoholic solutions (Stöber method), monodisperse particles from less than 0.05 to 2 μm may be easily obtained [3, 6, 94].

MCM 41 is the most popular product of the series M41S that may be obtained from solutions of tetraethylorthosilicate (TEOS), water, and cetyltrimethylammonium (CTMA) cation at 100 °C.

If the surfactant/silica molar ratio increased from 0.5 to 2, the siliceous products obtained were identified [102] and could be classified into four separate groups: MCM-41 (hexagonal), MCM-48 (cubic), thermally unstable M41S, and, a molecular species, the organic octamer $[(CTMA)SiO_{2.5}]_8$. One of the thermally unstable structures was identified as a lamellar phase. In Figs. 7.1 and 7.2, the structures of MCM41 (hexagonal) and MCM48 (cubic) are represented.

A liquid crystal templating mechanism was initially proposed. In Fig. 7.3 the schematic drawing of the liquid crystal templating mechanism initially proposed for MCM41 is shown. Hexagonal arrays of cylindrical micelles form (possibly mediated by the presence of silicate ions) with the polar groups of surfactant to the outside. In mechanism A silicate species then occupy the spaces between the cylinders. Alternatively (mechanism B) the silicate species generated in the reaction mixture influence the ordering of surfactant micelles. The final calcination step burns off the original organic material leaving hollow cylinders of inorganic material. The formation of hexagonal, cubic, or lamellar M41S structures by varying the silica concentration at constant surfactant concentration was considered [102] as a support for pathway B.

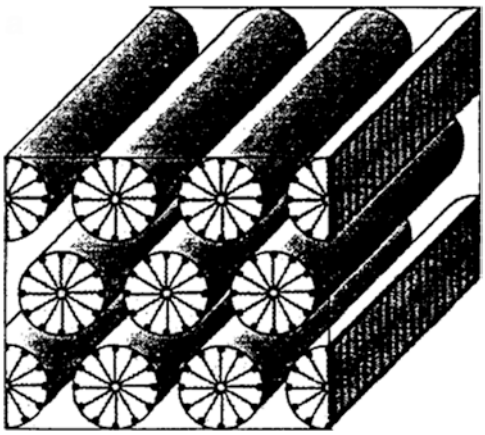

Fig. 7.1 Structure of MCM-41 (*hexagonal*) [92]

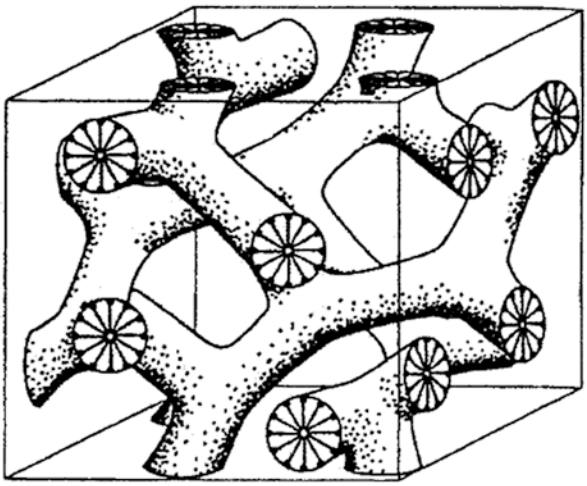

Fig. 7.2 Structure of MCM-48 (cubic) [92]

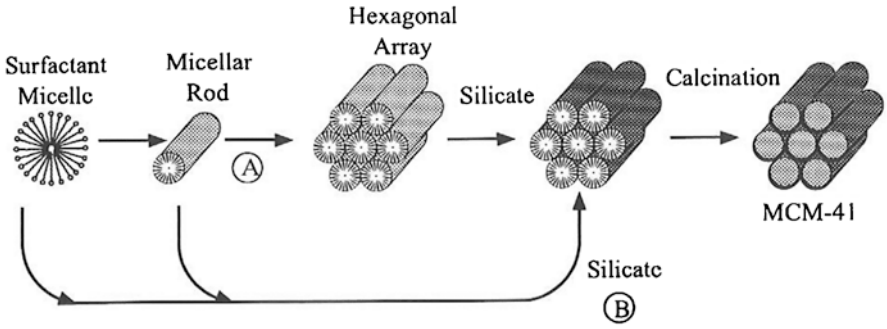

Fig. 7.3 Possible mechanistic pathways for the formation of MCM41: (**a**) Liquid crystal phase initiated; (**b**) silicate anions initiated [102]

However, M41S materials are limited to a pore diameter of approximately 80 Å, and, furthermore, they have significant external surface areas. These characteristics limit [48] their use in size-selective separations of large biomolecules such as proteins and enzymes.

Zhao et al. [117, 118] extended the family of highly ordered mesoporous silicates by synthesizing Santa Barbara Amorphous (SBA)-type materials. These have pore size ranging between 20 and 300 Å and use nonionic block copolymers as structure-directing agents in highly acidic media. SBA-15 raised particular interest [48]. It was synthesized using tri-block copolymer poly(ethylene oxide)–poly(propylene oxide)–poly(ethylene oxide), which is commercially available as pluronics P123 (EO20PO70EO20). SBA-15 possesses large BET surface area (>700 m^2/g), large pore diameter, and large pore wall thickness. The large wall thickness results in higher hydrothermal stability than M41S materials [117]. SBA-15 was synthesized as thin films [97], spheres [37, 54–57, 65, 96, 114, 120], fibers [8, 56, 57], and membranes [119]. It was also synthesized [48] as monodisperse, micrometer-sized (4–10 μm) spherical particles with large pore diameter (28–127 Å).

In the particle synthesis, parameters such as stirring rate, temperature, ionic strength, pH, and reactant composition so as the use of cosurfactants and swelling agents can influence the morphology of SBA-15 particles [48, 114]. In a typical synthesis [48], TEOS was added drop by drop to the surfactant solution; the mixture was vigorously stirred at 35 °C, stored at 75 °C, and finally aged in the range 80–125 °C. The surfactant solution was obtained by dissolving initially P123 into (1.5 M) HCl and successively adding the desired amount of aqueous solution of an ionic cosurfactant (cetyltrimethyl ammonium bromide (CTAB)) and a swelling agent (TMB, 1,3,5-trimethylbenzene). The addition of the swelling agent allowed [48] to obtain greater pore diameter and pore volume without change of surface area but gave pore size distribution more skewed and wider and could change the particle morphology from the spherical one. The presence of CTAB and TMB was important [48] to obtain spherical particles; however the yield of them decreased as the CTAB concentration was increased. This should be correlated to the role played by the ionic cosurfactant CTAB at level of the interaction between the surfactant and positively charged silica. The aging temperature also has influence [48]; its increase makes the pore size to grow and the microporosity to decrease.

New spherical silica nanoparticles with radial wrinkle structure (wrinkled silica nanoparticles (WSNs)) were recently synthesized [71, 81, 84, 116]. Their radial wrinkle structure which widens radially outward is expected to enhance the accessibility of functional materials inside their pores. They are obtained from oil-in-water macroemulsions within which droplets that are constituted of bicontinuous microemulsion are dispersed [71].

Recently a simple evaporation-induced self-assembly (EISA) process was proposed [7, 64, 78, 79] that enables a rapid production of patterned porous or nanocomposites materials in the form of films, fibers, and powders. It is based on the rapid evaporation of solutions of surfactants and pre-hydrolyzed alkoxysilanes. In a

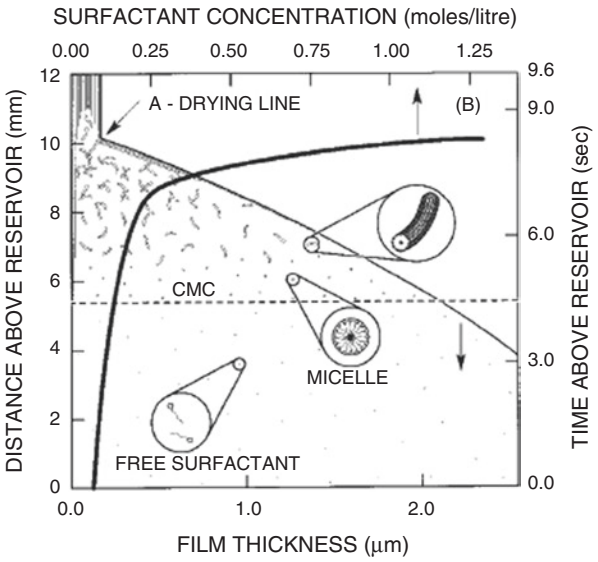

Fig. 7.4 Steady-state film cross section, showing changes in film thickness and composition (reported on the *horizontal axes*) as a function of distance above the sol reservoir surface and the corresponding time required for the substrate to move that distance (reported on the vertical axes) [64]

typical synthesis, films may be deposited on a substrate by dipcoating. Figure 7.4 shows the changes of both film thickness and concentration profiles [7, 64] as a function of distance above reservoir and time elapsed. It shows that, after a short time and at a short distance from the sol reservoir (about 8 s and 10 mm for the experiment reported in the figure), the film profile becomes steady, in correspondence of a thickness of about 0.2 μm. The initially homogeneous colloidal solution of silica and surfactant in ethanol/water solvent with a surfactant concentration less than the critical micelle concentration (cmc) is subjected to alcohol evaporation during drawing from the sol reservoir. The concentration of all species increases, but their ratio, in particular the surfactant/silica one, remains constant. So as schematically shown in Fig. 7.4, the progressively increasing surfactant concentration drives, above cmc, self-assembly of silica–surfactant micelles and their further organization into liquid crystalline mesophases. The silica–surfactant mesostructures present at solid–liquid and liquid–vapor interfaces at c<cmc serve to nucleate and orient mesophase development with respect to the substrate. Changes of initial alcohol/water/surfactant mole ratios reflect in different final mesostructures: hexagonal, cubic, and lamellar.

In a similar way (Brinker 1999), in the aerosol-assisted self-assembly, evaporation-induced self-assembly of liquid droplets allows to produce nanostructured particles with well-defined pore sizes and pore connectivities.

Mesoporous silica is bioactive. Recently bioactive glasses of more complex composition in the systems $CaO\text{-}SiO_2\text{-}P_2O_5$ and $SrO\text{-}SiO_2$ were successfully synthesized as highly ordered mesoporous ones by exploiting the surfactant templating route [34, 41, 107–109, 113]. They were obtained by adding calcium or strontium nitrate salts and, in the case of the ternary glass, triethyl phosphate to the surfactant/TEOS synthesis batch. In a typical synthesis the surfactant, TEOS, $Ca(NO_3)_2.4H_2O$, triethyl phosphate, and a solution 0.5 M HCl were dissolved, in due amounts, in ethanol and stirred at room temperature for 1 day. The resulting sol was introduced into a petri dish for an evaporation-induced self-assembly process, and then the dry gel was calcined at 700 °C for 5 h to obtain mesoporous bioactive glass powders. TEM micrograph reported in Fig. 7.5 shows that these mesoporous bioactive glass powders possess highly ordered one-dimensional channel structure with a pore size of 5 nm.

The mechanism of formation of mesoporous particles has been discussed in the literature with reference to silica particles. It is reported in the next paragraph.

7.2.2 Mechanism of Formation of Mesoporous Silica

Sometimes the mesoporous silica particles are in the nanometer size and do appear to contain hundreds of empty channels (mesopores) arranged in a 2D network of honeycomb-like porous structure so as can be seen in Figs. 7.1 and 7.5.

Recently more complex structures were reported ([60, 75, 82, 95, 96], Rankin 2004). In Fig. 7.6 the direct image of the internal structure of a mesoporous silica particle embedded in epoxy resin and sectioned using an electron beam is shown [75].

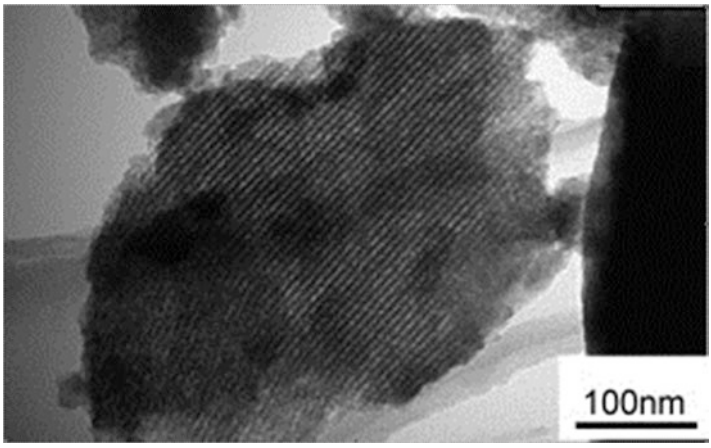

Fig. 7.5 TEM image of $CaO\text{-}SiO_2\text{-}P_2O_5$ mesoporous bioactive glass (Si/Ca/P ¼ 80/15/5) [107]

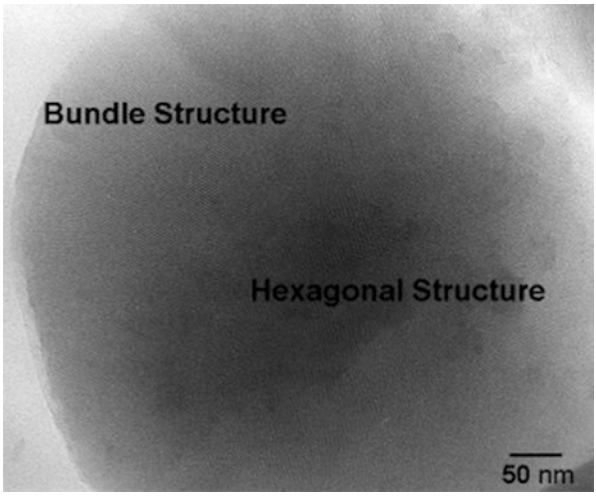

Fig. 7.6 Transmission electron micrograph (*TEM*) image of a sample embedded in an epoxy resin. The embedded sample was cut by an electron beam [75]

A structure consisting of bundled mesopores can be clearly seen near the surface of the hemisphere. Meanwhile, a hexagonal structure is observed at the center of the hemisphere, similar to the one shown in Figs. 7.1 and 7.5. The bundles of mesopores appear [75] to be aligned in three directions from the center to the surface of the particle. Meanwhile, radially aligned mesopores are observed on all surfaces of the growing particle. The mesopore alignment was followed during the course of the particle growth: it changed from three initial distinct directions to omnidirectional.

The development of uniform mesopores was first explained by a liquid crystal templating mechanism [58] and then by a cooperative templating mechanism [21, 35, 36]. Recently [75] a more complex mechanism was proposed to explain the formation of particles like the one shown in Fig. 7.6 that were obtained from tetramethylorthosilicate (TMOS) under basic conditions from methanol/water solutions, using hexadecyltrimethylammonium chloride (C16-TMACl) as the surfactant.

The mechanism of Nakamura [75] is represented in Fig. 7.7. The surfactant molecules are drawn as individual molecules rather than as micelles; this should be true as long as surfactant concentrations are less than the critical micelle concentration. Initially, hydrolyzed TMOS monomers condense to form oligomeric silica precursors through the reactions reminded in Sect. 7.2.1. However, when silica precursors attain a certain size by oligomerization, they are forced to precipitate as an organic–inorganic composite. In fact silica precursors contain a fair amount of silanols that dissociate to $Si\text{-}O^-$ and protons. In consequence, they are negatively charged. By contrast, surfactant heads have a positive charge. Therefore, silica precursors and surfactants can contact each other throughout the reaction. Upon certain size, the oligomeric silica structures, with surfactant molecules attached, assemble into small mesoporous silica particles with hexagonal regularity (of the type represented in Figs. 7.1 and 7.5), which then emerge from solution as primary particles. Any residual silica precursors then react preferentially with the surface silanols on the existing particles, eventually preventing the generation of new particles. It is not possible, however, that the particles grow by

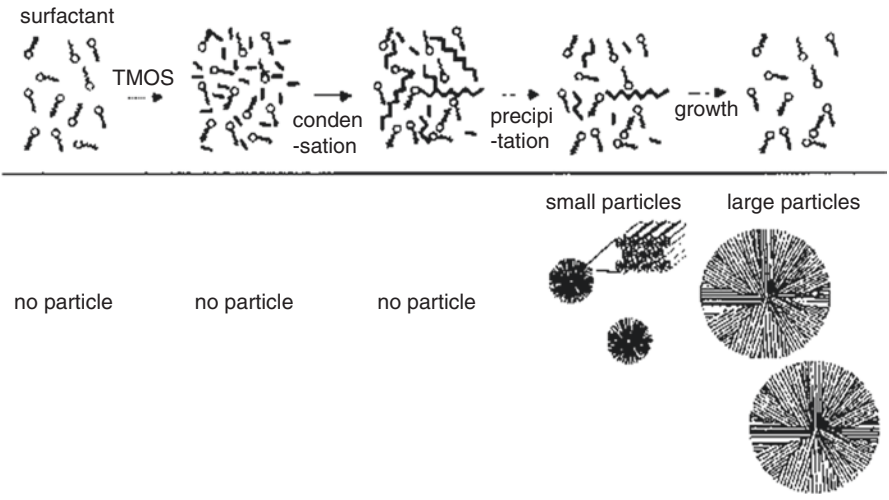

Fig. 7.7 Proposed mechanism for the formation of monodispersed mesoporous silica spheres. Progress of TMOS condensation is described above. Precipitation of particles is shown below. *Short lines* represent TMOS. *Zigzag lines* represent oligomeric TMOS [75]

the co-aggregation of smaller particles of the type represented in Figs. 7.1 and 7.5 (so as in the Stöber method). In this case the external "bundle structure" shown in Fig. 7.6 with mesopores aligned radially from the center to the surface of the particles and pointing in all directions could not be formed.

The mechanism proposed suggest that [75] the size of the particles could be enlarged by the addition of further TMOS. To confirm this, equimolar amounts of TMOS were added every hour for 4 h after the completion of the initial reaction (=1 h later). Figure 7.8 shows SEM images [75] of the particles that were obtained after two and four additions of TMOS to the initial reaction mixture. The diameters of the particles clearly increased upon the addition of TMOS while retaining their monodispersed characteristics (standard deviation are reported in parentheses). This result supports the notion that the additional TMOS would react preferentially with the surface silanol groups on the already formed particles rather than generating new particles and suggests a simple method to make the particles to grow. It was also shown [75] a method (hypothesized on the basis of the mechanism) to create monodispersed core/shell mesoporous silica spheres.

7.2.3 Mechanism of Formation of Mesoporous Silica When Using Two Immiscible Solvents (Wrinkled Particles)

Wrinkled particles may be obtained when two immiscible solvents are used. In a typical synthesis, 0.5 g (1.3 mmol) of cetylpyridinium bromide and 0.3 g (5.0 mmol) of urea were dissolved in 15 mL of water. Subsequently, 15 mL of cyclohexane and

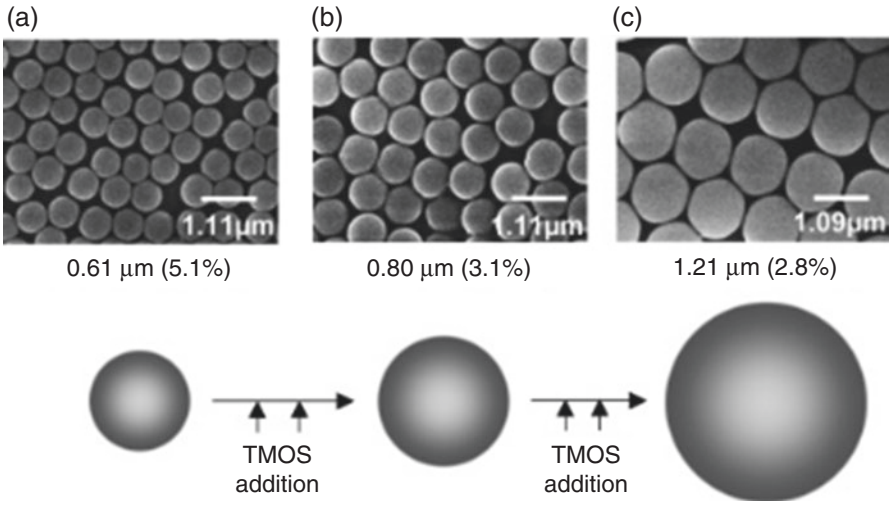

Fig. 7.8 SEM images of expanded particles obtained by the different TMOS addition times, (**a**) 0, (**b**) 2, and (**c**) 4, and schematic illustration of the particle growth. Standard deviations are in parentheses [75]

0.46 mL (6 mmol) of isopropanol is added to the solution. A two-phase system is obtained consisting of an upper microemulsion and a lower aqueous phase. Fast mechanical stirring gives an oil-in-water macroemulsion in which droplets, consisting of bicontinuous microemulsion, are dispersed [71]. With vigorous stirring, 1.25 g (6 mmol) of TEOS is added dropwise to the mixed solution. After vigorous stirring for 30 min at room temperature, the reaction mixture is heated up to 70 °C, and this state is maintained for 16 h.

The mechanism is represented in Fig. 7.9.

All reactions occur in the droplets that are, by themselves, bicontinuous microemulsions. TEOS dissolved in the oil layer comes into contact with the water at the emulsion interface where hydrolysis and condensation reactions occur. Ionized silicate monomers and oligomers have negative charges and bind to headgroups of cationic surfactants by the Coulomb interaction. As the condensation reaction proceeds, the amount of partially condensed silica tetrahedra (Q^3 = silica tetrahedra with three bridging oxygens and one non-bridging oxygen negatively charged) decreases and that of fully condensed (Q^4 = silica tetrahedra with four bridging oxygens) increases. As Q^4 silicates cannot be ionized, the total negative charge density of silicates decreases. In order to maintain charge balance, the number of silicate attached to a headgroup of surfactant with multidentate binding increases, and, consequently, the headgroup area of the surfactant increases. Accordingly, the curvature of the water−oil interface surrounded by surfactants increases to the positive direction. The interface can form closed structure such of spherical or cylindrical shapes. The aggregation of these surfactant–silicate particles leads to the formation of a repetitive mesophase. Finally, through water layers that are connected with ridges, newly formed mesophases are deposited on nanoparticle seeds, and the overall structure of nanoparticle assumes the wrinkle shape.

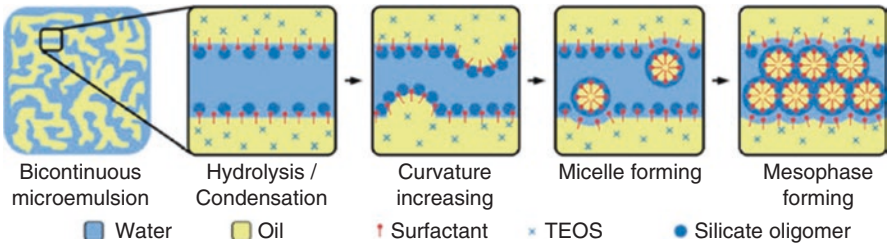

Fig. 7.9 Schematic illustration of the mesophase-forming mechanism from the microemulsion interface [71]

7.3 Bioactive Glasses

The first bioactive material was a glass obtained by quenching a melt of SiO_2 (45wt%), CaO (24.5wt%), Na_2O (24.5wt%), and P_2O_5 (6wt%), denoted bioglass 45S5. Successively [29, 33, 49, 53, 61, 83, 104] other compositions in the system SiO_2/CaO/P_2O_5 and in the quaternary system SiO_2/CaO/MgO/P_2O_5 at low P_2O_5 content were discovered to be bioactive. In Fig. 7.10 the compositional range of bioactive compositions in the ternary system SiO_2-CaO-P_2O_5 is reported. Figure 7.10 shows also that when produced through sol–gel method, the glasses were more bioactive, and the compositional range of bioactivity was extended till pure gel silica [29].

Figure 7.11 shows how good the interface between the bioactive glass and bone may be. It shows the SEM micrograph of the interface between the glass S46P0 and bone after 8 weeks in rabbit tibia [2]. SEM/EDX analysis shows that a continuous change of composition occurs at the interface from the glass to the bone one.

Bioactivity is the result of a complex process occurring at the surface of the glass [29]. The interaction [28, 30, 50, 51] is, at the beginning, due to the reactions between the glass and the blood plasma, which is an aqueous solution buffered at slightly basic pH = 7.2–7.4. The first five steps are:

1. First, the rapid exchange reaction of alkaline or alkaline earth ions with H^+ from solution:

$$\equiv SiO_2^- Ca^{2+} + 2H^+ \leftrightarrow 2SiOH + Ca^{2+}$$

It is well known in fact [86] that alkali or alkaline hearth silicate glasses in acidic or weakly alkaline (pH < 10) conditions are subjected to leaching of the less tightly bonded modifier cations (alkali or alkaline hearth ones) present in their composition

2. Loss of soluble silica in the form of $Si(OH)_4$ to the solution as the effect of hydrolysis reaction:

$$\equiv Si-O-Si\equiv + H_2O \leftrightarrow 2\equiv Si-OH$$

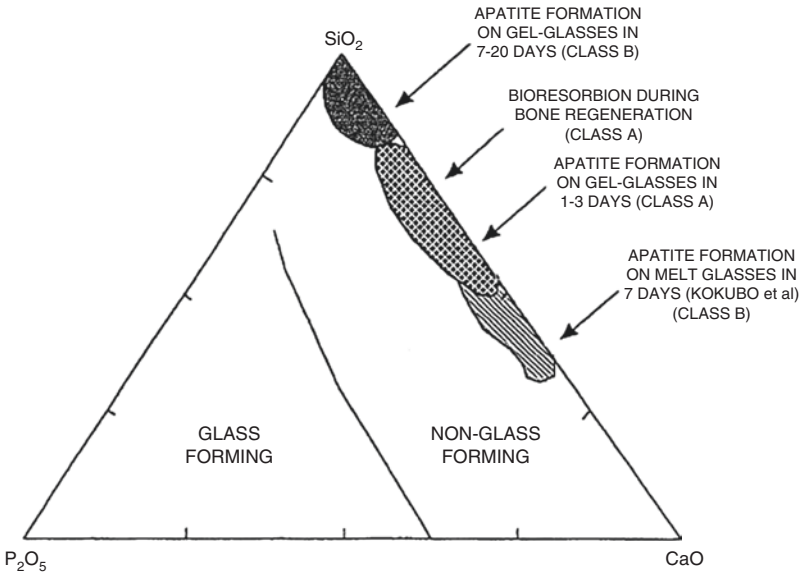

Fig. 7.10 Compositional range of bioactive gel glasses in the system $SiO_2/CaO/P_2O_5$ [29]

This may become possible as the result of pH increase in the reaction layer due to the occurrence of step 1

3. Condensation and repolymerization to form a gel SiO_2-rich layer on the surface depleted in the alkaline and alkaline earth cations:

$$\equiv Si-OH+HO-Si \equiv \leftrightarrow Si-O-Si+H_2O$$

In fact while some silica may be lost as the result of reactions described in step 2, some silanols groups may recondense giving a "gel" network, looser than the original one

4. Migration of Ca^{2+} ions to the surface through the gel SiO_2-rich layer and formation of an amorphous $CaO–P_2O_5$-rich film by precipitation from the supersaturated solution

$$\equiv Si-OH+HPO_4^{2-} \leftrightarrow \equiv Si-O-PO_3^{2-}+H_2O$$

5. Crystallization of the amorphous $CaO–P_2O_5$ film by incorporation of OH^- and/or CO_3^{2-} anions from solution to form a mixed hydroxyl carbonate apatite layer

The described steps give well account of the SEM/EDX results of Fig. 7.11 showing progressive changes of SiO_2, P_2O_5, and CaO concentrations at the bioactive glass/bone interface: a hydroxyl carbonate apatite (HCA) layer forms well anchored in the gel silica layer that forms trough degradation of glass surface. The behavior

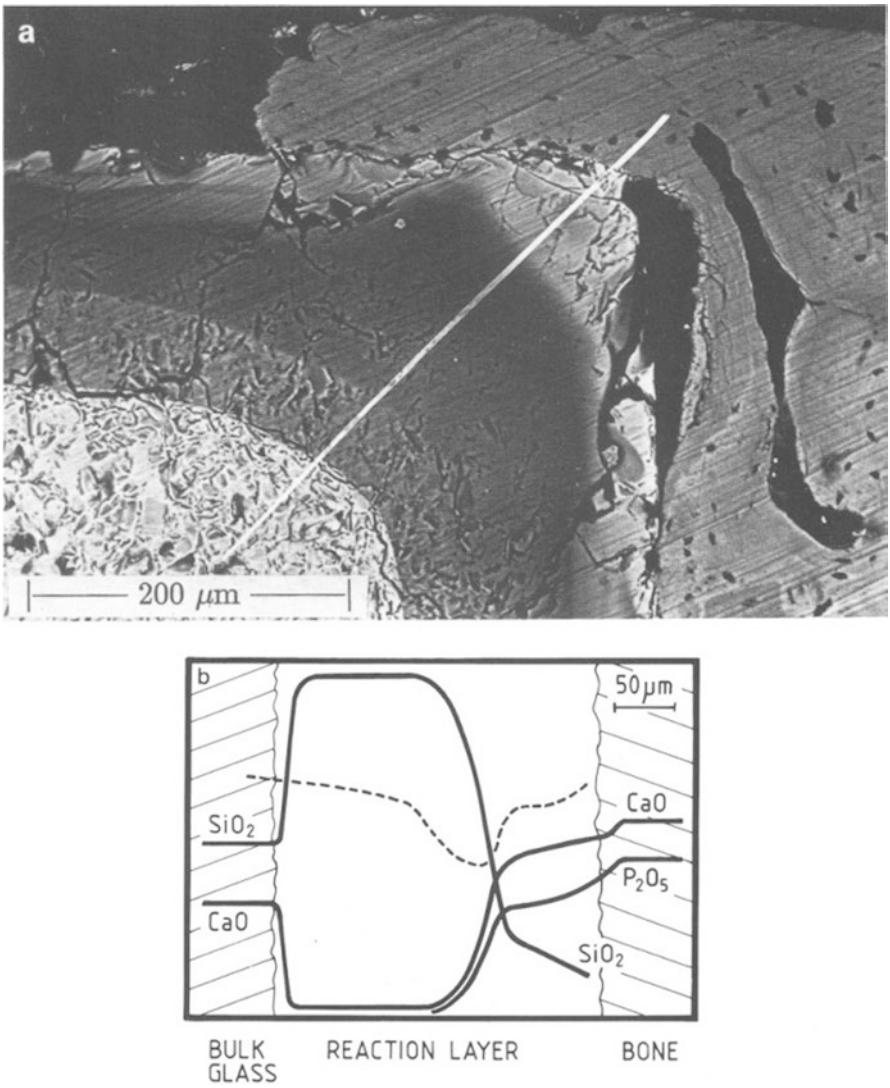

Fig. 7.11 Interface between the glass S46P0 and bone after 8 weeks in rabbit tibia [2]

strongly depends on the acidic character of silanol groups. When the glass composition is changed by addition of other components influencing the silanol acidity (like oxides of formula M_2O_3 where M = La, Y, In, Ga, Al), the ability to form a calcium phosphate layer is modified [4]. It is believed that the formed hydroxyl carbonate apatite is compositionally and structurally similar to the one present in the bone; this makes it biologically active and allows the following (6–11) steps to occur [29]:

6. Adsorption of biological moieties in HCA layer
7. Action of macrophages
8. Attachment of stem cells
9. Differentiation of stem cells
10. Generation of matrix
11. Crystallization of matrix

The formation of HCA layer is considered to be essential for the development of bioactivity. This allows to study bioactivity and to select bioactive compositions through an "in vitro" methodology allowing to remarkably reduce the number of animals used and the duration of animal experiments [52]. In fact in 1980, Hench et al. [80] had showed that an SiO_2-rich layer and calcium phosphate film form on the surface of bioglass when implanted in the body environment, which allows bonding to the living bone, and that the in vivo formation of the calcium phosphate film can be reproduced in a buffer solution consisting of Tris hydroxymethylaminomethane and hydrochloric acid (Tris buffer solution) at pH 7.4. In the early 1990s, Kokubo et al. proposed [52] to assess bioactivity by exposing the material to a protein-free acellular simulated body fluid (SBF) having pH and ionic composition very close to the blood plasma one and verifying the formation of HCA. The composition of SBF was successively revised and slightly corrected [52]. Good correlations were found between the in vitro and in vivo tests, and the "SBF method" was standardized as the solution for in vitro evaluation of apatite-forming ability of implant materials by the International Organization for Standardization (ISO 23317:2014). Many bioactive materials have been discovered [18, 83, 101]. They are distinguished in two classes [29]. Many exhibit only osteoconductivity [42], defined as the characteristic of bone growth and bonding along a surface (bioactive materials of class B). An example is constituted by synthetic hydroxyapatite. Class A bioactive materials are, instead, both osteoconductive than osteoproductive (also said osteoinductive). Osteoproduction is linked to enhanced mitosis and differentiation of osteoblast stem cells stimulated by slow resorption of the Class A bioactive particles [29]. Ionic products release from the glass play, therefore, a fundamental role. Some bioactive glasses are able to bond also to soft tissues [29]. The bioactivity of different materials may be compared [29] on the basis of the index of bioactivity $I_B = 100/t_{0.500}$, where $t_{0.500}$ is the time for 50% of the interface to be bonded to the bone.

7.4 Bioactivity of Mesoporous Glasses

Mesoporous silica produced through hydrolysis and polycondensation of alkoxysilanes is bioactive. Recently several more complex mesoporous bioactive glasses were produced [25, 34, 41, 43, 63, 90, 107–109, 113, 115].

Mesoporous glasses, also called template glasses, express accelerated bioactive response compared with conventional or sol–gel glasses of analogous composition [41, 90]. For example in the case of the mesoporous glass, S58 m (58% SiO_2–37%

$CaO – 5\%P_2O_5$) formation of calcium hydroxyapatite (HCA) occurs in 8 h, whereas in the correspondent sol–gel glass, its formation requires 3 days [41]. Moreover a greater amount of calcium phosphate is observed to form and crystallization of the initially amorphous phosphate layer occurs through formation of octacalcium phosphate (OCP) that successively transforms into the HCA crystalline phase, whereas HCA directly forms in the case of conventional and sol–gel glasses. These differences can be explained [41, 90] considering the higher values of specific surface area and pore volume of template glasses as well as the higher concentration of silanol (Si–OH) groups on the template glasses surface. The bioactivity mechanism, in fact, is similar to the one proposed in paragraph 7.3, except for some differences strictly linked to the compositional and structural differences reminded above. In fact, with reference to the mechanism reported in paragraph 7.3, we may expect and/or observe [41, 90] that:

(a) The exchange of Ca^{2+} in glass with H^+ in the solution (step 1 of the bioactivity mechanism) is quicker and produces a higher incorporation of H^+ ions and a higher density of silanols (Si–OH) groups.
(b) A highly protonated silica gel forms after the condensation of silanol groups (steps 1–3 of the mechanism), leading to an acid local pH (possibly pH = 6.7) on the glass surface.
(c) The precipitation of amorphous calcium phosphate (ACP) layer (step 4) is higher.
(d) The crystallization of ACP by incorporation of Ca^{2+} and HPO_4^{2-} leads to octacalcium phosphate (OCP) formation instead of carboxylate hydroxyapatite (HCA).
(e) OCP converts, later, into HCA through dehydration and hydrolysis reaction.

It is worth remembering that OCP is considered to be a precursor of carboxylate hydroxyapatite in the process of the tooth enamel, dentine, and bone formation in the living organisms. The formation, at first, of OCP instead of HCA (that directly forms in the case of the glasses obtained through melt quenching or sol–gel in the absence of surfactant) would occur [41, 90] because of the acidic character the surface of mesoporous bioactive glasses do possess when precipitation and crystallization of phosphate layer occurs. It is known in fact that OCP forms in acidic conditions. Therefore the process of formation of HCA in mesoporous bioactive glass (MBG) more closely resembles the one occurring in nature.

7.5 Drug Delivery from Mesoporous Bioactive Glasses

Because of their ability to bond to living tissues, bioactive glasses allow to exploit the approach of “local delivery” and overcome the problems connected also with systemic deliverable vectors [1, 34, 72]. In systemic delivery biomolecules can be inactivated by enzymes or chemical reactions in the blood, and so a relatively high concentration of drug is needed to provide sufficient dose at the desired location. These problems may be partly overcome with the use of vectors; some therapeutics may, however, be lost in other body compartments than the one they are

addressed to. Considerable research effort is therefore addressed [34, 90] to the topic of using bioactive glasses for the encapsulation, delivery, and controlled release of bioactive molecules and therapeutic drugs. Moreover, so as predicted by Hench [29], there is today a very great interest and research activity addressed to the use of bioactive glasses to produce scaffolds for tissue engineering [11, 13, 22, 23, 27, 44, 85]. Key properties like drug-delivery ability, biocompatibility, biodegradability, osteoconductivity, as well as osteogenic and angiogenic potential make them [34] excellent candidates for bone tissue scaffolds [76]. However a number of other strict requirements may be successfully satisfied by bioactive glasses so as described in the first subparagraph. The second paragraph is instead strictly related to the therapeutics release.

7.5.1 Bioactive Glasses for Local Drug Delivery and Tissue Engineering

Osteoporosis, fracture healing, defects filling, and spinal lesion reparation affect millions of people with a very big social cost [24]. The expectations from tissue engineering are great, particularly to overcome the problem of the shortage of living tissues and organs available for transplantation. Tissue engineering needs a scaffold that is a porous structure that must guide new tissue formation by supplying a matrix with interconnected porosity and tailored surface chemistry for cell growth and proliferation and the transport of nutrients and metabolic waste [24]. The scaffold should mimic the morphology, structure, and function of the bone in order to optimize integration with surrounding tissues. To do all this, the ideal scaffold should [24, 38]:

- Possess high three-dimensional interconnected porosity for cell growth, flow transport of nutrients, and metabolic waste and angiogenesis
- Be biocompatible and bioresorbable with a controllable degradation and resorption rate to match cell/tissue growth in vitro and/or in vivo
- Possess suitable surface chemistry for cell attachment, proliferation, and differentiation
- Possess mechanical properties (e.g., stiffness, strength, and fracture resistance) to match those of the tissues at the site of implantation

Concerning the first requirement, interconnected pores with a mean diameter (or width) of 100 μm or greater and open porosity of >50% are considered to be the minimum requirements to permit tissue ingrowth and function in porous scaffolds [23, 47]. It may be satisfied through one of the several well-established bioactive glass scaffold fabrication methods [23]:

- Sol–gel processing
- Thermal bonding of particles or fibers
- Polymer foam replication

- Solid freeform fabrication
- Freeze casting of suspensions

It is expected that by properly selecting composition and fabrication method, also the other above reminded requirements may be fulfilled.

When comparing the strength and elastic modulus of natural and synthetic materials (typically with a dense microstructure containing no porosity) [23, 105], it appears that the mechanical response of the bone is not matched by the biodegradable polymers, ceramics, or alloys currently used in orthopedic applications. Recently it was shown that, by optimizing the composition, processing and sintering conditions, bioactive glass scaffolds can be created with predesigned pore architectures and with strength comparable to human trabecular and cortical bones [22, 23, 62]. Moreover the compressive strengths of bioactive glass scaffolds strongly depend on composition and fabrication method [23]. In particular porous bioactive glass scaffolds can be fabricated with compressive strengths comparable to the values reported for human trabecular and cortical bones [23]. Toughening of bioactive glass scaffolds can be obtained through polymer coating. Biodegradable polymers, such as poly(D,L-lactic acid), PDLLA, poly(3-hydroxybutyrate), P(3HB), alginate, and PCL, have been used to coat bioactive glass scaffolds [5, 12, 23, 73]. The main energy dissipation mechanism was believed [23] to be polymeric fibril extension and crack bridging, so as in the bone which is a composite of hydroxyapatite and collagen.

The second requirement (biocompatibility and bioresorbability) may also be fulfilled if we take into account that, so as predicted by the bioactivity mechanisms reminded in Sects. 7.3 and 7.4, surface reactions leading to the bond formation of bioactive materials and living tissues start with a partial dissolution of the material surface. As a consequence bioactive materials may become bioresorbable when the sizes are reduced. It has been well demonstrated with bioglass particles. If small enough particles of a bioactive ceramic are used, the surface degradation may finally produce the total degradation of the particles [90]. Wilson and Noletti [90] found that particles of 100 μm in diameter of bioglass were resorbed or phagocytosed by macrophages in vivo, while larger particles were bioactive stimulating the bone growth. Schepers and Ducheyne [91] and Salinas and Vallet-Regı [87] indicated that particles under 300 μm in size were fully resorbed in vivo. Moreover a peculiar characteristic of the glasses is the lack of stoichiometric ratios of the chemical components: glass structures may be easily enriched with other components, in contents that may be largely changed and optimized with respect to the property required. Therefore the structure and chemistry of glasses can be tailored over a wide range, by changing either composition or thermal or environmental processing history, making possible to design glass scaffolds with variable degradation rates to match that of bone ingrowth and remodeling [23].

The requirement about surface chemistry for cell attachment, proliferation, and differentiation is treated in more detail in the paragraph 7.5.2.

7.5.2 *Release of Therapeutics from Mesoporous Bioactive Glasses*

It is recognized, from a long time, that a biologically relevant release of ionic products occurs from the surface of bioactive glasses. They may induce angiogenesis in addition to influencing gene expression and promoting osteoblastic differentiation. In addition therapeutic drugs or biologically active molecules may be easily introduced. Owing to their high pore volume, mesoporous bioactive glasses offer, in this respect, additional exceptional opportunities. In the following these three topics will be better addressed. The first two subparagraphs refer generally to bioactive glasses. The third one shows the additional great opportunities linked to the mesoporous structure.

7.5.2.1 Ionic Dissolution Products from Bioactive Glasses

Recently, the ionic dissolution products from bioglass (e.g., Si, Ca, P) and from other silicate-based glasses were shown to stimulate expression of several genes of osteoblastic cells and angiogenesis in vitro and in vivo, while possible antibacterial and inflammatory effects of bioactive glasses have also been investigated [31, 34].

A schematic overview of biological responses to ionic dissolution products of bioactive glasses is given in Fig. 7.12. Table 7.1 gives a summary of biological

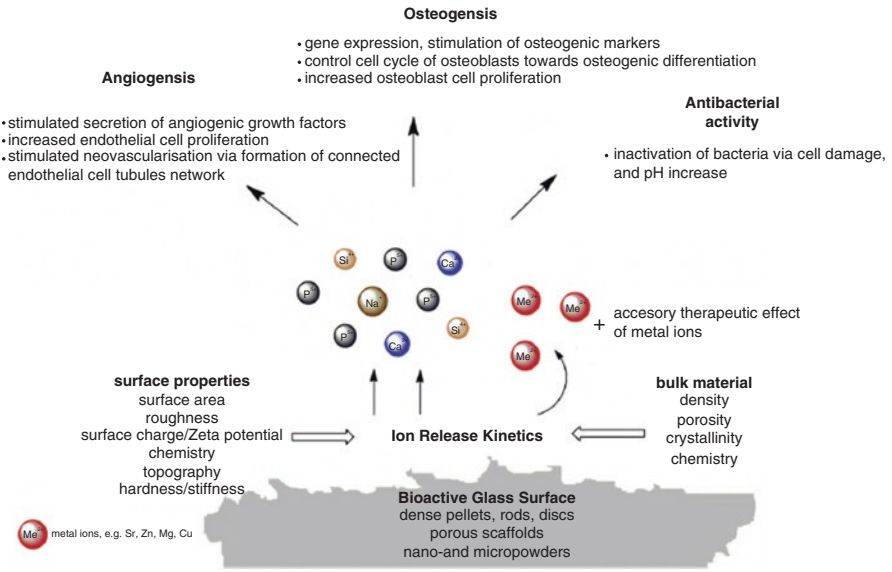

Fig. 7.12 Overview of biological responses to ionic dissolution products of bioactive glasses [31]

Table 7.1 Effect of selected metallic ions on human bone metabolism and angiogenesis: summary of literature studies [31]

	Biological response in vivo/in vitro	Reference
Si	Essential for metabolic processes, formation, and calcification of bone tissue	[9, 10]
	Dietary intake of Si increases bone mineral density (BMD)	[45]
	Aqueous Si induces hydroxyapatite (HAp) precipitation	[16]
	$Si(OH)_4$ stimulates collagen I formation and osteoblastic differentiation	[87]
Ca	Favors osteoblast proliferation, differentiation, and extracellular matrix (ECM) mineralization	[66]
	Activates Ca-sensing receptors in osteoblast cells and increases expression of growth factors, e.g., IGF-I or IGF-II	[69, 100]
P	Stimulates expression of matrix gla protein (MGP) a key regulator in bone formation	[46]
Zn	Shows anti-inflammatory effect and stimulates bone formation in vitro by activation protein synthesis in osteoblasts	[111]
	Increases ATPase activity and regulates transcription of osteoblastic differentiation genes, e.g., collagen I, ALP, osteopontin, and osteocalcin	[59]
Mg	Stimulates new bone formation	[121]
	Increases bone cell adhesion and stability (probably due to interactions with integrins)	[121, 112]
Sr	Shows beneficial effects on bone cells and bone formation in vivo	[69, 67]
	Promising agent for treating osteoporosis	[70]
Cu	Significant amounts of cellular Cu are found in human endothelial cells when undergoing angiogenesis	[20]
	Promotes synergetic stimulating effects on angiogenesis when associated with angiogenic growth factor FGF-2	[26]
	Stimulates proliferation of human endothelial cells	[32]
	Induces differentiation of mesenchymal cells toward the osteogenic lineage	[88]
B	Stimulates RNA synthesis in fibroblast cells	[77, 19]
	Dietary boron stimulates bone formation	[99]

responses to single inorganic species. Some ionic species (Ca, Si, P...) are usually present because bioactive glasses are often calcium phosphosilicate; the presence of other species (like Zn and Mg ions) may be assured by adding their oxides to the batch. Glasses, in fact, have not stoichiometric composition; this last may be widely and continuously changed like the composition of a solution.

Unfortunately the exact mechanism of interaction between the ionic dissolution products of such inorganic materials and human cells is not yet fully understood. Of course the favorable effects are expressed in correspondence of specific extracellular matrix compositions. These topics are nowadays actively investigated [31]. The release rates are a function of the glass surface and bulk properties so as indicated in Fig. 7.12. Producing glasses with tailored ion release kinetics and controlled biological response in the relevant physiological environment is expected to be successfully performed in the near future.

7.5.2.2 Therapeutic Drug or Biologically Active Molecule Release from Bioactive Glasses

An effective drug-delivery system should assure a controlled release of carried drug molecules in active form. Small molecule therapeutic drugs may cause, in fact, unwanted adverse events and systemic toxicity so as described and studied by pharmacokinetics (PK), determining the fate of substances administered to a living organism, and pharmacodynamics (PD), studying how the drug affects the organism. A therapeutic index is defined:

$$TI = LD_{50} / ED_{50}$$

where LD_{50} is the dose lethal in 50% of subjects and ED_{50} is the dose efficacious in 50% of subjects. Other adverse factors in systemic delivery are low aqueous solubility due to drug hydrophobicity, rapid clearance and extensive metabolism of the drugs in vivo, and nonspecific tissue accumulation. All these problems may be solved with the use of drug-delivery platforms. A very great interest is nowadays addressed to the bioactive glasses, especially the mesoporous ones, for the possibility they offer to have local delivery. The synthesis of them through sol–gel chemistry appears particularly valuable because it can be performed at room temperature. Therefore proteins, drugs, or other bioactive molecules can be incorporated by adding them directly to the synthesis batch since room temperature processing preserves their functionality. Another approach is soaking bioactive glass samples (eventually produced through melt quenching) in a solution of the desired loading molecule, which can be entrapped inside pores with or without chemical bonding . It's worth reminding, in fact, that molecules can be physically adsorbed on the pore or external glass surfaces; alternatively chemical bonding can be accomplished by the interaction of hydroxyl and amino groups of the molecules with the Si–OH groups and P-OH groups present on the bioactive glass surface.

Sol–gel bioactive glasses were successfully charged with antibiotics added to the initial alkoxide solution [34]. This is an important topic: antibiotics may avoid the consequences associated with the application of bone-filling materials, orthopedic implants, or bone replacements, inflammatory response or infections, e.g., osteomyelitis. A good example of the other approach is reported for melt-derived borate glass powders of composition $6Na_2O–8K_2O–8MgO–22CaO–54B_2O_3–2P_2O_5$ mol%. They were added [34] to a phosphate-buffered solution (PBS) with 80 mg/g vancomycin. The mixture was placed into rubber molds without compression and dried for 24 h, forming pellets which were ready to use. In vivo results showed that these borate glass delivery systems were effective in the treatment of chronic osteomyelitis in rabbits.

Bone morphogenetic proteins (BMPs), especially recombinant human BMP (rhBMP), are the main growth factors playing an important role in bone regeneration and in tissue engineering. Their addition should enhance [34] the bone regeneration capability of scaffolds leading to successful healing of critical bone defects. These proteins may be added to bioactive glasses in the above described manners. An example was documented by Tolli (2016) [98]. Different amounts of reindeer

bone extract (till 40 mg) were added to carboxymethyl cellulose (CMC) to form a gel that was combined with granules of bioactive glass S53P4 (composition of 53% SiO_2, 23% Na_2O, 20% CaO, and 4% P_2O_5 in wt%) at a ratio of 40:60wt%, shaped into rods with diameter of 5 mm and lyophilized. Bone proteins were expected to adhere to the surface of the bioactive glass granules and released upon bioactive glass dissolution. A beneficial effect of these composite implants in filling rabbit tibia defects was documented [98].

7.5.2.3 Drug Release from Mesoporous Bioactive Glasses

Enhanced in vitro and in vivo drug-delivery properties of mesoporous bioactive glasses (MBG) with respect to the non-mesoporous ones were well proved [34, 107–109]. This can be correlated, first of all, with the greater pore volume of MBG. A correlation, sometimes of direct proportionality, between the efficiency of drug loading and the pore volume of the material was found [34].

Drug molecules can be easily incorporated within the mesopores using the immersion technique. The drug release pattern is influenced by the pore diameter. It's worth remembering in fact that there are four different states of molecules hosted in MBG [34, 110]:

1. Molecules lying at the window of the mesopore
2. Molecules entrapped inside the mesopore without bonding
3. Molecules entrapped in the mesopore with bonding
4. Molecules adsorbed on the external MBG surface

As a consequence three drug release behaviors may be detected [34, 110]:

(a) An initial fast release rate due to molecules in the state described at points 1 and 4
(b) A reduced rate when molecules in the state 2 are released
(c) A final release stage, with an even more reduced rate, involving molecules in the state 3

A marked influence of the pore diameter is observed on the transition from regime b to c. In fact when reducing the pore diameter, the pore-specific surface (ratio of surface to volume of the pore) increases; the result is that the proportion of molecules entrapped in the mesopore with bonding (type 3) increases with respect to the nonbonded ones (type 2) with the consequent effects on the duration and relative relevance of stages b and c.

Taking into account that the bonding within the mesopores is accomplished due to the interaction of the hydroxyl and amino groups of the biomolecules with the Si–OH groups and P-OH groups in MBG, the effects of pH may be predicted. In fact the changes with pH of the silanol groups protonation and deprotonation equilibrium ($Si\text{-}O\text{-}H \Leftrightarrow Si\text{-}O^- + H^+$) make the interaction with biomolecules to change.

Recently on-demand release processes (also termed "switch on/off") were proposed which, in principle, allow tailored release profiles with excellent spatial, temporal, and dosage control [74, 103]. On-demand drug delivery is becoming feasible

through the design of stimuli-responsive systems that recognize their microenvironment and react in a dynamic way, mimicking the responsiveness of living organisms.

The literature relative to nanodelivery systems that carry therapeutic molecules attached through covalent linkers ("conjugated") was recently thoroughly and smartly reviewed [106]. It was recognized that there are numerous mechanisms of drug release via linker cleavage [74, 106]: ester, amide, or hydrazone hydrolysis, disulfide exchange, hypoxia activation, Mannich base, self-immolation, photochemistry, thermolysis, and azo reduction. The conditions that control drug release by triggering linker cleavage involve [74, 106] pathophysiological features and subcellular properties specific to diseased cells. Triggering mechanisms [74, 106] include tumor hypoxia (low oxygen levels due to increased metabolic rates in tumor cells), low intracellular pH (endosomes and lysosomes where targeted nanomaterials are taken up), lowered extracellular pH for tumor cells, tumor-specific enzymes (matrix metalloproteinase, prostate-specific membrane antigen) overexpressed on the cell membrane, and upregulation of glutathione.

Extracorporeal physical stimuli can be also applied. Sustained drug release can also be achieved by thermo-, magnetic-, light- or ultrasound-sensitive nanoparticulate systems.

The stimuli-responsive approach takes advantage of the existence of a great number of commercially available organoalkoxysilane molecules that allow easy surface functionalization of silica and silicates. The most popular one is aminopropyltrietoxysilane (APTS): $(C_2H_5O)_3Si(CH_2)_3NH_2$. The hydrolysis of the three ethoxy groups to silanol (Si-O-H) allows this molecule to graft to silica surfaces through condensation with silanols therein present. The non-hydrolyzable group linked through Si-C bond (in the case of APTS, the aminopropyl one) remains therefore exposed on the silica surface. This is a simple functionalizing process that allows to have at the surface of silica a great number of reactive groups. Examples of alternative commercially available organoalkoxysilane molecules are:

- Vinyltriethoxysilane: $CH_2=CHSi(C_2H_5O)_3$
- 3-(Trimethoxysilyl)propyl methacrylate: $H_2C=C(CH_3)CO_2(CH_2)_3Si(OCH_3)_3$
- 3-Glycidoxypropyltrimethoxysilane: $CH_2(O)CHCH_2O(CH_2)_3Si(OCH_3)_3$

As an example, a smart application of these concepts exploits [89] the low melting temperature of a nucleic acid duplex and the ability of superparamagnetic nanocrystals covalently linked to a nucleic acid strand to capture external electromagnetic energy: the energy released under an alternating magnetic field allows to break the hydrogen bonding pattern with its complementary strand. To do this, oligonucleotide-modified mesoporous silica, encapsulating magnetite superparamagnetic nanoparticles, was capped with magnetic nanocrystals functionalized with the complementary strand. The chosen DNA duplex had a melting temperature of 47 °C, which corresponds to the upper limit of therapeutic magnetic hyperthermia. Magnetite nanoparticles, produced through the Massart method and surface functionalized with APTS, were incorporated into mesoporous silica matrices by simply adding them to the synthesis reaction batch of silica. These magnetic silica particles were surface aminated through reaction with APTS. The oligonucleotide was anchored to

the aminated surfaces with the aid of a sulfo-SMCC linker (sulfosuccinimidyl-4-[N-aleimidomethyl]cyclohexane-1-carboxylate); 4-(N-maleimidomethyl)cyclohexane-1-carboxylic acid-3-sulfo-N-hydroxysuccinimide ester). The magnetic component of the whole system allowed reaching hyperthermic temperatures (42–47 °C) under an alternating magnetic field. Progressive double-stranded DNA melting, as a result of temperature increase, gave rise to uncapping and the subsequent release of a mesopore filling model drug, fluorescein. This example is a smart application in which magnetic and thermal stimuli-responsive materials are coupled to have a remote-controlled release of drug from mesoporous materials.

Other examples are reported in the literature [74, 89, 106].

7.6 Conclusions

Recently mesoporous bioactive glasses were synthesized for which outstanding applications in the biomedical field are expected.

The coupling of bioactivity to mesoporous structure allows local drug-delivery applications. The structure and chemistry of glasses can be tailored over a wide range, by changing either composition or thermal or environmental processing history, making possible to design glass scaffolds that match the requirements of porosity, bioresorbability, mechanical properties, and surface chemistry for cell attachment, proliferation, and differentiation.

The delivery of therapeutics is complex and offers unique perspectives. Bioactive glasses degrade by releasing ionic species of different types able to activate relevant biological responses that span from the stimulation of expression of several genes to angiogenesis and antibacterial effects. Some ionic species (Ca, Si, P...) are usually present because bioactive glasses are often calcium phosphosilicate; the presence of other species (like Zn and Mg ions) may be assured by adding their oxides to the batch. Glasses, in fact, have not stoichiometric composition; this last may be widely and continuously changed like the composition of a solution. Antibiotics and proteins may be easily added to bioactive glasses through soaking techniques. When using the sol–gel synthesis, they can be directly added to the synthesis reaction batch, thanks to the low synthesis temperatures at which their functionalities are preserved.

Enhanced in vitro and in vivo drug-delivery properties are recorded in the case of bioactive glasses possessing mesoporous structure, thanks to their high pore volume and possibility of modulating pore size. High pore volumes assure high payloads. The release kinetics are sensitive to the pore size. Finally mesoporous glasses may be easily surface functionalized. This makes possible to design “switch on/off’” release platforms.

References

1. Allen TM, Cullis PR. Drug delivery systems: entering the mainstream. Science. 2004; 303(5665):1818–22.
2. Andersson OH, Karlsson KH, Kangasniemi K. Calcium phosphate formation at the surface of bioactive glass in vivo. J Non Cryst Solids. 1990;119:290–6.
3. Branda F. The Sol-Gel route to nanocomposites. In: Boreddy SR, editor. Advances in nanocomposites – synthesis, characterization and industrial applications. Reddy, INTECH open access publisher; 2011. Available online: (http://www.intechopen.com/articles/show/title/the-sol-gel-route-to-nanocomposites).
4. Branda F, Arcobello-Varlese F, Costantini A, Luciani G. Effect of the substitution of M_2O_3 (M=La,Y,In,Ga,Al) for CaO on the bioactivity of 2.5CaO _ $2SiO_2$ glass. Biomaterials. 2002; 23:711–6.
5. Bretcanu O, Misra S, Roy I, Renghini C, Fiori F, Boccaccini AR, Salih V. In vitro biocompatibility of 45S5 bioglass-derived glass–ceramic scaffolds coated with poly(3-hydroxybutyrate). J Tissue Eng Regen Med. 2009;3:139–48.
6. Brinker CJ, Sherer W. Sol-gel science: the physics and chemistry of Sol-gel processing. San Diego: Academic Press; 1990.
7. Brinker JC, Lu Y, Sellinger A, Fan H. Evaporation-induced self-assembly: nanostructures made easy. Adv. Mater. 1999;11(7):579–85.
8. Bruinsma PJ, Kim AY, Liu J, Baskaran S. Chem Mater. 1997;9:2507.
9. Carlisle EM. Silicon: a possible factor in bone calcification. Science. 1970;167(3916):279–80.
10. Carlisle E. Silicon: a requirement in bone formation independent of vitamin D1. Calcif Tissue Int. 1981;33(1):27–34.
11. Chatzistavrou X, Tsigkou O, Amin HD, Paraskevopoulos KM, Salih V, Boccaccini AR. Sol–gel based fabrication and characterization of new bioactive glass–ceramic composites for dental applications. J Eur Ceram Soc. 2012;32:3051.
12. Chen QZ, Boccaccini AR. Poly(D,L-lactic acid) coated 45S5 bioglass®-based scaffolds: processing and characterization. J Biomed Mater Res A. 2006;77A:445–57.
13. Chen Q, Roether JA, Boccaccini AR. Chapter 6: Tissue engineering scaffolds from bioactive glass and composite materials. In: Ashammakhi N, Reis R, Chiellini F, editors. Topics in tissue engineering, vol. 4. 2008. http://www.oulu.fi/spareparts/ebook_topics_in_t_e_vol4/
14. Chiola V, Ritsko JE, Vanderpool CD, US Patent 3556725, 1971.
15. Ciesla U, Schüth F. Ordered mesoporous materials – review. Microporous Mesoporous Mater. 1999;27:131–49.
16. Damen JJM, Ten Cate JM. Silica-induced precipitation of calcium phosphate in the presence of inhibitors of hydroxyapatite formation. J Dent Res. 1992;71(3):453–7.
17. Di Renzo F, Cambon H, Dudartre R. A 28 years old synthesis of micelle templated mesoporous silica. Microporous Mater. 1997;10:283–6.
18. Duchène P. Stimulation of biological function with bioactive glass. MRS Bull. 1998;23(11): 43–9.
19. Dzondo-Gadet M, Mayap-Nzietchueng R, Hess K, Nabet P, Belleville F, Dousset B. Action of boron at the molecular level. Biol Trace Elem Res. 2002;85(1):23–33.
20. Finney L, Vogt S, Fukai T, Glesne D. Copper and angiogenesis: unraveling a relationship key to cancer progression. Clin Exp Pharmacol Physiol. 2009;36(1):88–94.
21. Firouzi A, Kumar D, Bull LM, Besier T, Sieger P, Huo Q, Walker SA, Zasadzinki JA, Glinka C, Nicol J, Margolese D, Stucky GD, Chmelka BF. Science. 1995;267:1138.
22. Fu Q, Saiz E, Tomsia AP. Bioinspired strong and highly porous glass scaffolds. Adv Funct Mater. 2011;21:1058–63.
23. Fu Q, Saiz E, Rahaman MN, Tomsia AP. Bioactive glass scaffolds for bone tissue engineering: state of the art and future perspectives. Mater Sci Eng C. 2011;31:1245–56.
24. Fu Q, Saiz E, Tomsia AP. Direct ink writing of highly porous and strong glass scaffolds for load-bearing bone defects repair and re generation. Acta Biomater. 2011;7:3547–54.

25. Garcıa A, Cicuéndez M, Izquierdo-Barba I, Arcos D, Vallet-Régı M. Essential role of calcium phosphate heterogeneities in 2D-hexagonal and 3D-cubic SiO_2-CaO-P_2O_5 mesoporous bioactive glasses. Chem Mater. 2009;21:5474–84.
26. Gérard C, Bordeleau L-J, Barralet J, Doillon CJ. The stimulation of angiogenesis and collagen deposition by copper. Biomaterials. 2010;31(5):824–31.
27. Gerhardt LC, Boccaccini AR. Bioactive glass and glass-ceramic scaffolds for bone tissue engineering. Materials. 2010;3:3867–910.
28. Hench LL. Bioceramics: from concept to clinic. J Am Ceram Soc. 1991;74(7):1487–510.
29. Hench LL. Biomaterials: a forecast for the future. Biomaterials. 1998;19:1419–23.
30. Hench LL, Splint RJ, Allen WC, Greenlee TK. Bonding mechanism at the interface of ceramic prosthetic materials. J Biomed Mater Res Symp. 1971;2(Part 1):117–41.
31. Hoppe A, Güldal NS, Boccaccini AR. A review of the biological response to ionic dissolution products from bioactive glasses and glass-ceramics. Biomaterials. 2011;32:2757–74.
32. Hu GF. Copper stimulates proliferation of human endothelial cells under culture. J Cell Biochem. 1998;69(3):326–35.
33. Hulbert SF, Young FA, Mathews RS, Klawitter JJ, Talbert CD, Stelling FH. Potential of ceramic materials as permanently implantable skeletal prosthesis. J Biomed Mater Res. 1970;4:433–56.
34. Hum J, Boccaccini AR. Bioactive glasses as carriers for bioactive molecules and therapeutic drugs: a review. J Mater Sci Mater Med. 2012;23:2317–33.
35. Huo Q, Margolese DI, Clesia U, Feng P, Gier TE, Sieger P, Leon R, Petroff PM, Schüth F, Stucky GD. Generalized synthesis of periodic surfactant/inorganic composite materials. Nature. 1994a;368:317–21.
36. Huo Q, Margolese DI, Ciesra U, Feng P, Gier TE, Sieger P, Firouzi A, Chmelka BF, Schuth F, Stucky GD. Organization of organic molecules with inorganic molecular species into nanocomposite biphase arrays. Chem Mater. 1994b;6:1176–91.
37. Huo Q, Feng J, Schüth F, Stucky GD. Preparation of hard mesoporous silica spheres. Chem Mater. 1997;9:14–7.
38. Hutmacher DW. Scaffolds in tissue engineering bone and cartilage. Biomaterials. 2000; 21:2529–43.
39. Iler RK, US Patent 2663650, 1953.
40. Iler RK. The chemistry of silica. New York: Wiley; 1971. p. 562.
41. Izquierdo-Barba I, Arcos D, Sakamoto Y, Terasaki O, Lopez-Noriega A, Vallet-Régı M. High-performance mesoporous bioceramics mimicking bone mineralization. Chem Mater. 2008; 20:3191–8.
42. Jarcho M, Bolen CH, Thomas MB, Bobick J, Kayand JF, Doremus RH. Hydroxylapatite synthesis and characterization in dense polycrystalline form. J Mater Sci. 1976;11:2027.
43. Jones JR. Review of bioactive glass: from Hench to hybrids. Acta Biomater. 2013;9:4457–86.
44. Jones JR, Ehrenfried LM, Hench LL. Optimising bioactive glass scaffolds for bone tissue engineering. Biomaterials. 2006;27:964–73.
45. Jugdaohsingh R, Tucker KL, Qiao N, Cupples LA, Kiel DP, Powell JJ. Dietary silicon intake is positively associated with bone mineral density in men and premenopausal women of the Framingham offspring cohort. J Bone Miner Res. 2004;19(2):297–307.
46. Julien M, Khoshniat S, Lacreusette A, Gatius M, Bozec A, Wagner EF, Wittrant Y, Masson M, Weiss P, Beck L, Magne D, Guicheux J. Phosphate-dependent regulation of MGP in osteoblasts: role of ERK1/2 and Fra-1. J Bone Miner Res. 2009;24(11):1856–68.
47. Karageorgiou V, Kaplan D. Porosity of 3D biomaterial scaffolds and osteogenesis. Biomaterials. 2005;26:5474–91.
48. Katiyar A, Yadav S, Smirniotis PG, Pinto NG. Synthesis of ordered large pore SBA-15 spherical particles for adsorption of biomolecules. J Chromatogr A. 2006;1122:13–20.
49. Klein C, Patka P, der Hollander W. Macroporous calcium phosphate bioceramics in dog femora: a histological study of interface and biodegradation. Biomaterials. 1989;10:59–62.
50. Kokubo T. Surface chemistry of bioactive glass-ceramics. J Non Cryst Solids. 1990;120: 138–51.

51. Kokubo T. Novel bioactive materials derived from glasses, proceedings of the XVI international congress on glass, Madrid, vol. 1. Bol Soc Esp Ceram Vid. 1992;31-C(1):119–37.
52. Kokubo T, Takadama H. How useful is SBF in predicting in vivo bone bioactivity? Biomaterials. 2006;27:2907–15.
53. Kokubo T, Ito S, Shigematsu M, Sakka S, Yamamuro T. Mechanical properties of a new type of apatite-containing glass-ceramic for prosthetic application. J Mater Sci. 1985;20:2001–4.
54. Kosuge K, Singh PS. Rapid synthesis of Al-containing mesoporous silica hard spheres of 30-50 μm diameter. Chem Mater. 2001;13:2476–82.
55. Kosuge K, Murakami T, Kikukawa N, Takemori M. Direct synthesis of porous pure and thiol-functional silica spheres through the $S^+X^-I^+$ assembly pathway. Chem Mater. 2003;15:3184–9.
56. Kosuge K, Kikukawa N, Takemori M. One-step preparation of porous silica spheres from sodium silicate using triblock copolymer templating. Chem Mater. 2004;16:4181–6.
57. Kosuge K, Sato T, Kikukawa N, Takemori M. Morphological control of rod- and fiberlike SBA-15 type mesoporous silica using water-soluble sodium silicate. Chem Mater. 2004;16:899–905.
58. Kresge CT, Leonowicz ME, Roth WJ, Vartuli JC, Beck JS. Ordered mesoporous molecular sieves synthesized by a liquid-crystal template mechanism. Nature. 1992;359:710–2.
59. Kwun I-S, Cho Y-E, Lomeda R-AR, Shin H-I, Choi J-Y, Kang Y-H, Beattie JH. Zinc deficiency suppresses matrix mineralization and retards osteogenesis transiently with catch-up possibly through Runx 2 modulation. Bone. 2010;46(3):732–41.
60. Lebedev OI, Van Tendeloo G, Collart O, Cool P, Vansant EF. Structure and microstructure of nanoscale mesoporous silica sphere. Solid State Sci. 2004;6:489–98.
61. LeGeros RZ. Biologically relevant calcium phosphates: preparation and characterization. In: Myers H, editor. Calcium phosphates in oral biology and medicine, monographs in oral sciences. Basel: Karger; 1991.
62. Liu X, Rahaman MN, Fu QA. Oriented bioactive glass (13-93) scaffolds with controllable pore size by unidirectional freezing of camphene-based suspensions: microstructure and mechanical response. Acta Biomater. 2011;7:406–16.
63. Lopez-Noriega A, Arcos D, Izquierdo-Barba I, Sakamoto Y, Terasaki O, Vallet-Régı M. Ordered mesoporous bioactive glasses for bone tissue regeneration. Chem Mater. 2006;18:3137–44.
64. Lu Y, Ganguli R, Celeste A, Drewien CA, Anderson MT, Brinker CJ, Gong W, Guo Y, Soyez H, Dunn B, Huang MH, Zink JI. Continuous formation of supported cubic and hexagonal mesoporous films by sol–gel dip-coating. Nature. 1997;389:364–8.
65. Ma Y, Qi L, Ma J, Wu Y, Liu O, Cheng H. Large-pore mesoporous silica spheres: synthesis and application in HPLC. Colloids Surf A. 2003;229:1–8.
66. Maeno S, Niki Y, Matsumoto H, Morioka H, Yatabe T, Funayama A, Toyama Y, Taguchi T, Tanaka J. The effect of calcium ion concentration on osteoblast viability, proliferation and differentiation in monolayer and 3D culture. Biomaterials. 2005;26(23):4847–55.
67. Marie PJ. Strontium ranelate: a physiological approach for optimizing bone formation and resorption. Bone. 2006;38(2, Suppl. 1):10–4.
68. Marie PJ. The calcium-sensing receptor in bone cells: a potential therapeutic target in osteoporosis. Bone. 2010;46(3):571–6.
69. Marie PJ, Ammann P, Boivin G, Rey C. Mechanisms of action and therapeutic potential of strontium in bone. Calcif Tissue Int. 2001;69(3):121–9.
70. Meunier PJ, Slosman DO, Delmas PD, Sebert JL, Brandi ML, Albanese C, Lorenc R, Pors-Nielsen S, De Vernejoul MC, Roces A, Reginster JY. Strontium ranelate: dose-dependent effects in established postmenopausal vertebral osteoporosis: a 2-year randomized placebo controlled trial. J Clin Endocrinol Metab. 2002;87(5):2060–6.
71. Moon DS, Lee JK. Tunable synthesis of hierarchical mesoporous silica nanoparticles with radial wrinkle structure. Langmuir. 2012;28:12341–7.
72. Mourino V, Boccaccini AR. Bone tissue engineering therapeutics: controlled drug delivery in three-dimensional scaffolds. J Roy Soc. 2010;7(43):209–27.

73. Mourino V, Newby P, Boccaccini AR. Preparation and characterization of gallium releasing 3-D alginate coated 45S5 bioglass based scaffolds for bone tissue engineering. Adv Eng Mater. 2010;12:B283–91.
74. Mura S, Nicolas J, Couvreur P. Stimuli-responsive nanocarriers for drug delivery. Nat Mater. 2013;12:991–1003. www.nature.com/naturematerials
75. Nakamura T, Mizutani M, Nozaki H, Suzuki N, Yano K. Formation mechanism for monodispersed mesoporous silica spheres and its application to the synthesis of Core/Shell particles. J Phys Chem C. 2007;111:1093–100.
76. Newby CP, Boccaccini AR. Bioactive glass and glass ceramic scaffolds for bone tissue engineering. In: Bioactive glasses – materials properties and applications, a volume in Woodhead publishing series in biomaterials. 2011. p. 107–28.
77. Nielsen FH. Is boron nutritionally relevant? Nutr Rev. 2008;66(4):183–91.
78. Ogawa M. Formation of novel oriented transparent films of layered silica-surfactant nanocomposites. J Am Chem SOC. 1994;116:7941–2.
79. Ogawa M. A simple sol-gel route for the preparation of silica-surfactant mesostructured. Mater Chem Commun. 1996: 1149–50.
80. Ogino M, Ohuchi F, Hench LL. Compositional dependence of the formation of calcium phosphate films on bioglass. J Biomed Mater Res. 1980;14:55–64.
81. Pan W, Ye J, Ning G, Lin Y, Wang J. A novel synthesis of micrometer silica hollow sphere. Mater Res Bull. 2009;44:280–3.
82. Pauwels B, Van Tendeloo G, Thoelen C, Van Rhijn W, Jacobs PA. Structure determination of spherical MCM-41 particles. Adv Mater. 2001;13(17):1317–20.
83. Peltola T, Jokinen M, Rahiala H, Levanen E, Rosenholm JB, Kangasniemi I, Yli-Urpo A. Calcium phosphate formation on porous sol-gel-derived SiO_2 and $CaO\text{-}P_2O_5\text{-}SiO_2$ substrates in vitro. J Biomed Mater Res. 1999;44:12–21.
84. Polshettiwar V, Cha D, Zhang X, Basset JM. High-surface-area silica nanospheres (KCC-1) with a fibrous morphology. Angew Chem Int Ed. 2010;49:9652–6.
85. Rahaman MN, Day DE, Bal BS, Fu Q, Jung SB, Bonewald LF, Tomsia AP. Bioactive glass in tissue engineering. Acta Biomater. 2011;7:2355–73.
86. Rawson H. Inorganic glass-forming system. London: Academic Press; 1967.
87. Reffitt DM, Ogston N, Jugdaohsingh R, Cheung HFJ, Evans BAJ, Thompson RPH, Powell JJ, Hampson GN. Orthosilicic acid stimulates collagen type 1 synthesis and osteoblastic differentiation in human osteoblast-like cells in vitro. Bone. 2003;32(2):127–35.
88. Rodríguez JP, Ríos S, González M. Modulation of the proliferation and differentiation of human mesenchymal stem cells by copper. J Cell Biochem. 2002;85(1):92–100.
89. Ruiz-Hernández E, Baeza A, Vallet-Regí M. Smart drug delivery through DNA/magnetic nanoparticle gates. ACS Nano. 2011;5:1259–66.
90. Salinas AJ, Vallet-Regı M. Bioactive ceramics: from bone grafts to tissue engineering. RSC Adv. 2013;3:11116–31.
91. Schepers EJG, Ducheyne P. Bioactive glass particles of narrow size range for the treatment of oral bone defects: a 1–24 month experiment with several materials and particle sizes and size ranges. J Oral Rehabil. 1997;24:171–81.
92. Schumacher K, Ravikovitch PI, Du Chesne A, Neimark AV, Unger KK. Characterization of MCM-48 materials. Langmuir. 2000;16:4648–54.
93. Sing KSW, Everett DH, Haul RHV, Moscou L, Pierotti RA, Rouquerol J, Siemieniewsk T. Reporting physisorption data for gas/solid systems with special reference to the determination of surface area and porosity. Pure Appl Chem. 1985;57(4):603–19.
94. Stöber W, Fink A, Bohn E. Controlled growth of monodisperse silica spheres in the micron size range. J Colloid Interface Sci. 1968;26:62–9.
95. Tan B, Rankin SE. Interfacial alignment mechanism of forming spherical silica with radially oriented nanopores. J Phys Chem B. 2004;108:20122–9.
96. Tendeloo GV, Lebedev OI, Collart O, Cool P, Vansant EF. Structure of nanoscale mesoporous silica spheres? J Phys Condens Matter. 2003;15:S3037–46. Online at: stacks.iop.org/JPhysCM/15/S3037

97. Tolbert SH, Schaffer TE, Feng J, Hansma PK, Stucky GD. A new phase of oriented mesoporous silicate thin films. Chem Mater. 1997;9:1962–7.
98. Tolli H, Kujala S, Levonen K, Jamsa T, Jalovaara P. Bioglass as a carrier for reindeer bone protein extract in the healing of rat femur defect. J Mater Sci Mater Med. 2010;21(5): 1677–84.
99. Uysal T, Ustdal A, Sonmez MF, Ozturk F. Stimulation of bone formation by dietary boron in an orthopedically expanded suture in rabbits. Angle Orthod. 2009;79(5):984–90.
100. Valerio P, Pereira MM, Goes AM, Leite MF. Effects of extracellular calcium concentration on the glutamate release by bioactive glass (BG60S) preincubated osteoblasts. Biomed Mater. 2009;4:045011.
101. Vallet-Regı M, Ragel CV, Salinas AJ. Glasses with medical applications. Eur J Inorg Chem. 2003;6:1029–42.
102. Vartuli JC, Schmitt KD, Kresge CT, Roth WJ, Leonowicz ME, McCullen SB, Hellring SD, Beck JS, Schlenker JL, Olson DH, Sheppard EW. Development of a formation mechanism for M41S materials. Stud Surf Sci Catal. 1994;84:53–60. http://dx.doi.org/10.1016/S0167-2991(08)64096-3
103. Vivero-Escoto JL, Slowing II, Trewyn BG, Lin VSY. Mesoporous silica nanoparticles for intracellular controlled drug delivery. Small. 2010;6(18):1952–67.
104. Vogel W, Holand W, Nauman K, Gumel J. Development of machineable bioactive glass ceramics for medical uses. J Non Cryst Solids. 1986;80:34–41.
105. Wegst UGK, Ashby MF. The mechanical efficiency of natural materials. Philos Mag. 2004;84(21):2167–81. http://dx.doi.org/10.1080/14786430410001680935
106. Wong PT, Choi SK. Mechanisms of drug release in nanotherapeutic delivery systems. Chem Rev. 2015;115:3388–432. doi:10.1021/cr5004634.
107. Wu C, Ramaswamy Y, Zhu Y, Zheng R, Appleyard R, Howard A, Zreiqat H. The effect of mesoporous bioactive glass on the physiochemical, biological and drug-release properties of poly(DL-lactide-co-glycolide) films. Biomaterials. 2009;30(12):2199–208.
108. Wu C, Zhang Y, Zhou Y, Fan W, Xiao Y. A comparative study of mesoporous-glass/silk and non-mesoporous-glass/silk scaffolds: physiochemistry and in vivo osteogenesis. Acta Biomater. 2011;7(5):2229–36.
109. Wu C, Fan W, Gelinsky M, Xiao Y, Simon P, Schulze R, Doert T, Luo Y, Cuniberti G. Bioactive SrO–SiO_2 glass with well-ordered mesopores: characterization, physiochemistry and biological properties. Acta Biomater. 2011;7(4):1797–806.
110. Xia W, Chang J. Well-ordered mesoporous bioactive glasses (MBG): a promising bioactive drug delivery system. J Control Release. 2006;110(3):522–30.
111. Yamaguchi M. Role of zinc in bone formation and bone resorption. J Trace Elem Exp Med. 1998;11(2e3):119–35.
112. Yamasaki Y, Yoshida Y, Okazaki M, Shimazu A, Uchida T, Kubo T, Akagawa Y, Hamada Y, Takahashi J, Matsuura N. Synthesis of functionally graded $MgCO_3$ apatite accelerating osteoblast adhesion. J Biomed Mater Res. 2002;62(1):99–105.
113. Yan X, Yu C, Zhou X, Tang J, Zhao D. Highly ordered mesoporous bioactive glasses with superior in vitro bone-forming bioactivities. Angew Chem Int Ed. 2004;43:5980–4.
114. Yu C, Fan J, Tian B, Zhao D. Morphology development of mesoporous materials: a colloidal phase separation mechanism. Chem Mater. 2004;16:889–98.
115. Yun H, Kim S, Hyeon Y. Highly ordered mesoporous bioactive glasses with Im3m symmetry. Mater Lett. 2007;61:4569–72.
116. Zhang H, Li Z, Xu P, Wu R, Jiao Z. A facile two step synthesis of novel chrysanthemum-like mesoporous silica nanoparticles for controlled pyrene release. Chem Commun. 2010;46: 6783–5.
117. Zhao D, Feng J, Huo Q, Melosh N, Fredrickson GH, Chmelka BF, Stucky GD. Triblock copolymer syntheses of mesoporous silica with periodic 50 to 300 angstrom pores. Science. 1998;279:548–52.

118. Zhao D, Huo Q, Feng J, Chmelka BF, Stucky GD. Nonionic triblock and star Diblock copolymer and oligomeric surfactant syntheses of highly ordered, hydrothermally stable mesoporous silica structures. J Am Chem Soc. 1998;120:6024–36.
119. Zhao D, Yang P, Chmelka BF, Stucky GD. Multiphase assembly of mesoporous-macroporous membranes. Chem Mater. 1999;11:1174–8.
120. Zhao D, Sun J, Li Q, Stucky GD. Morphological control of highly ordered mesoporous silica SBA-15. Chem Mater. 2000;12:275–9.
121. Zreiqat H, Howlett CR, Zannettino A, Evans P, Schulze-Tanzil G, Knabe C, Shakibaei M. Mechanisms of magnesium-stimulated adhesion of osteoblastic cells to commonly used orthopaedic implants. J Biomed Mater Res. 2002;62(2):175–84.

Chapter 8
Bioactive Glass/Polymer Composites for Drug Delivery

Telma Zambanini, Roger Borges, and Juliana Marchi

Abstract Drugs are compounds that interfere on the signaling pathway of cells and organs in a living organism, and depending on its concentration in the bloodstream or in the target tissue, a drug may play a role as a toxic or therapeutic compound. Keeping the drug within therapeutic concentrations (also as known as therapeutic window) is challenging, because the therapeutic compound may be metabolized or biotransformed along its course in the human body. Therefore, new technologies have been developed in order to deliver drugs direct into the target tissue and to release the therapeutic compound over a controlled manner. In this chapter, we review the main properties of bioactive glasses and polymers and how composites made of such materials can be used for drug delivery. In addition, it is reported how the physical-chemical aspects of polymeric matrixes and bioactive glasses play an important role on the design of new carrier systems. At the final of this chapter, practical examples are covered, and a special section of clinical applications is discussed.

Keywords Biomaterials • Biocompatibility • Bioactive Glasses • Polymeric Scaffolds • Toxicity • Pharmacology • Pharmacokinetics • Controlled Release • Sustained Release

8.1 Drug Delivery Concepts and Its Relationship with Materials Selection

Along the development of pharmaceutical science, there were established the two most important variables of drug efficacy: pharmacokinetic and pharmacodynamics [10, 24]. The first is the study of kinetics of drugs in the bloodstream, also taking into account the analysis of some variables, such as drug absorption, distribution, metabolism, and excretion. The second, it is the evaluation of drug effect per se, providing the correlation between the dose taken and the time in which the desired

T. Zambanini • R. Borges • J. Marchi (✉)
Center of Natural Science and Humanities, Federal University of ABC,
Santo André, São Paulo, Brazil
e-mail: jujumarchi@gmail.com

G. Kaur (ed.), *Clinical Applications of Biomaterials*,
DOI 10.1007/978-3-319-56059-5_8

effect happens. Both concepts are the basis of drug delivery, once the intended benefit of this approach is to improve the kinetics of drug release in the human body and to bring a better outcome. Then, what is drug delivery?

Drug delivery is a general term used to refer to technologies that involve the release of drugs and bioactive molecules (e.g., growth factors, proteins, lipids, genes, etc.) [40]. Usually, it involves a material that carriers the drug into the desired tissue and leaves the therapeutic agent in this specific site. This material is commonly referred as carrier or the matrix of the system. More often than not, the conception of drug delivery has been strongly bonded to the notion of controlled release. Controlled release, in turn, refers to the delivery and release of a therapeutic agent under a time-dependent manner. This sustained release is required because it affects the dose that should be taken by a patient and the rate in which the drug is absorbed by an organism [32, 34].

Trying to find a material that best fit as a carrier in drug delivery systems is quite challenging. There are some factors to be taken into account, such as the degradation rate, how the drug could be loaded in the matrix, and the interaction between the carrier and the host tissue. All these factors together will influence on the drug release and its consequent concentration in the target tissue. The concentration of therapeutic agent is an important deal in drug delivery systems, once it can be either toxic or medicinal. In order to overcome this issue, the pharmaceutic science uses the concept of therapeutic window.

Therapeutic window are the limits between the minimum toxic concentration (MTC) and the minimum effective concentration (MEC). MTC works as an upper limit, because it is the minimum concentration enough to trigger a toxic response in a living organism. On the other hand, MEC works as a lower limit, because the minimum concentration is enough to bring the desired effect. Therefore, the drug concentration must be always within the therapeutic windows in order to maintain the drug effect without any toxic response (Fig. 8.1) [20].

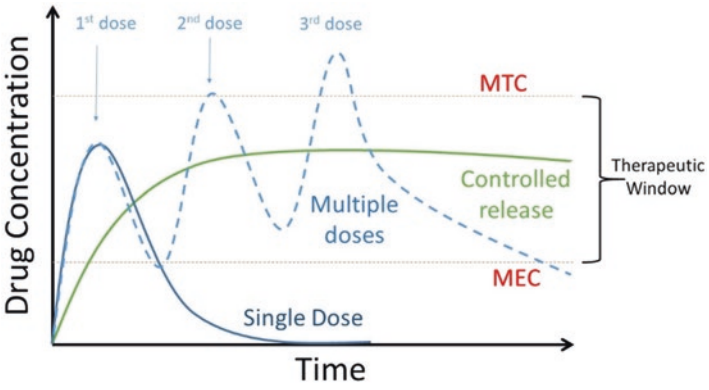

Fig. 8.1 Drug concentration in the plasma after a single dose (*blue solid line*), after multiple doses (*dotted line*), and zero-order controlled release (*green solid line*). The range between the minimum toxic concentration (MTC) and the minimum effective concentration (MEC) is defined as therapeutic window, i.e., the range in which a drug dose is effective without any toxic effect

Once we already know the concept of therapeutic window, we need to understand how to keep the drug concentration within this limit, so that we will be able to choose a material for drug delivery system. As shown in Fig. 8.1, a drug may be administrated through several doses over the time or through a controlled release system. Pills and injections usually follow the several doses model, which the doses are taken over and over again in order to maintain the drug concentration within the therapeutic windows. Additionally, the drug concentration peaks after the administration and falls down with the time because the organism metabolizes the therapeutic agent. It is not the most effective model, because the doses have to be administrated over a specific interval of time, and it is sometimes a responsibility of the patient, who may not be a disciplined person. Divergently, the controlled release model, which is used in drug delivery technology, is based on a burst release that enables the drug concentration to be within the therapeutic window, and then the drug is slowly released over the time, preventing the drug to be above the MTC or under the MEC. Therefore, the challenge is to choose a material that enables the drug to be controlled delivery.

There are several mechanisms in which a drug may be release by a material; here we will focus on the most used ones. These mechanisms can be classified into two main classes: non-responsive and responsive. Non-responsive mechanisms are those that do not need an external stimulus to deliver a drug, i.e., the therapeutic agent is released due to the matrix swelling or degradation. Below are listed non-responsive mechanisms [44]:

- Diffusion mechanism: it is based on the interaction between water (from the body fluid) and matrix where the drug is loaded. There are two kinds of matrices that follow this mechanism: monolithic and reservoir matrices. If the drug is uniformly dispersed in the matrix, and is able to diffuse through the pores as the matrix is degraded, then this carrier is considered as a monolithic matrix. Otherwise, the matrix is classified as reservoir, that is, the matrix has a coating on its surface, and the drug is dispersed through this coating layer. Then, in reservoir matrices the superficial layer controls the release kinetics. Both systems are usually characterized by a burst release followed by a zero-order kinetics
- Controlled osmosis: it is when the difference of drug concentration between the matrix and the surrounding fluid causes an osmotic pressure that works as the driven force to diffuse the drug outward the matrix. This mechanism often follows a zero-order kinetics
- Ionic exchange: it is associated with ionic drugs that replace ions in the living tissue over a gradient concentration
- Erosion mechanism: it is based on the erosion of the matrix. It can be separated into two stages: First, the matrix is superficially degraded, allowing therapeutic agents to be released under a zero-order kinetics. Later, the bulk is degraded, and the whole matrix is dissolved with the time, also enhancing the drug release. Usually, if the first stage is controlled, sensitive drugs can be mostly delivered in the target tissue and avoid their earlier degradation

In relation to sensitive mechanisms of drug delivery, they are defined as those mechanisms that need an external stimulus to allow the therapeutic agent release. Usually, these mechanisms are more sophisticated and engineered and allow a better

specificity and controlled release. They are also classified according to the external stimulus used to deliver the therapeutic agent: pH sensitive, thermoresponsive, magnetic field sensitive, ultrasound sensitive, and light sensitive, among others. These mechanisms are more common in polymers that have their chemical bonds sensitive to any of these physical or chemical responses and have their structure changed because of this bond rearrangement. However, ceramic materials can also be decorated with molecules that are sensitive to these responses, also allowing the obtainment of sensitive ceramics. Along this chapter we will cover some of these examples, as long as each case is very particular.

8.2 Materials in Drug Delivery Systems

In this section it will cover the characteristics of ceramic and polymeric biomaterials, properties of composites made of bioactive glass and polymers that are promisors for drug delivery, and the influence of the physical-chemical properties on the design of carrier systems.

8.2.1 Ceramics for Biomedical Applications

Bioceramics have been applied as bone grafting for bone regeneration applications for a long time. Although the class of ceramic biomaterials involves bioinert, bioactive, and resorbable ceramics, only the bioactive ceramics (e.g., hydroxyapatite, bioactive glass, glass ceramics) and the resorbable ceramics (e.g., tricalcium phosphate and biocompatible glasses) are suitable for bone regeneration applications as scaffolds, because they allow the adherence and proliferation of cells from the host tissue [2].

Bioactive glasses are noncrystalline ceramics and are usually classified as bioactive ceramics due to their ability to nucleate a hydroxyapatite layer onto their surface when in continuous immersion in human plasma. Commonly, these materials are silicate glasses usually containing sodium, calcium, and/or phosphor oxides as main components of the glass matrix. However, other oxides may be incorporated in the glass composition in order to improve physical, chemical, or biological properties. In addition, there are glasses in which are phosphate- or borate based, and also exhibit bioactivity (ability to grow hydroxyapatite onto the surface in plasmatic solution), and sometimes have also low chemical durability, being possible to classify them as resorbable bioceramics. Therefore, it is simpler to use the term "biocompatible glasses" as an alternative way to talk about glasses that exhibit biocompatibility but are not necessarily bioactive [6].

The first glasses were developed by L.L. Hench in 1969 and were based on the SiO2-Na2O-CaO-P2O5 system. The first in vivo tests using rabbits showed these glasses were able to chemically bond to the bone, showing the potential use of such materials in biomedical applications. Since then, bioactive glasses were introduced to other applications, such as periodontal reconstructions and development of 3D scaffolds.

Furthermore, new synthesis routes were developed as an alternative to the melting-cooling approach. Among these routes, the sol-gel synthesis had a huge emphasis, because it made possible to obtain particulate glasses at lower temperatures (around 400–700 °C) than melt-derived glasses. With the advent of sol-gel synthesis, it developed the synthesis of mesoporous bioactive glasses (MBG), which was obtained similarly to the production of SBA-based silica. Moreover, from bone regeneration to dental treatments, different products containing biocompatible glasses have been developed and are yet available for clinical usage.

Regarding bone regeneration applications, there is no doubt about the effectiveness of bioactive and resorbable ceramics, but even the newest bioceramic is unable to avoid the occurrence of pathological effects after its implantation. These pathological effects may be related to the presence of microorganisms, such as bacteria. In this sense drugs have been used together with bioceramics in order to deliver antibiotics or anti-inflammatory drugs into the host tissue and then to avoid these pathological reactions. In other words, the appeal of overcoming undesired effects led to the development of drug delivery systems made of bioceramics. Over time, bioceramics were also allied to growth factors, genes, proteins, and other biomolecules in order to promote osteoconduction and/or angiogenesis and then to improve the regeneration potential of such materials [2]. Ever since, many studies have been conducted in order to obtain biocompatible glasses with suitable drug delivery properties, as we shall cover along the next sections.

8.2.2 Polymers for Biomedical Applications

Different polymers can be used for drug delivery, nonbiodegradable and biodegradable polymers. Nonbiodegradable polymers are not considered optimal for biological applications in tissue engineering and drug delivery, because in some cases a second surgery is necessary to remove these implants. Biodegradable polymers for biological applications need to degrade into products as normal metabolites of the body or elements that can be eliminated from body without significant metabolic changes [27]. Example of nonbiodegradable polymer used for drug delivery is polymethylmethacrylate. Polymethylmethacrylate is an acrylic cement and is the most widely cement used to fix metallic implants [30] but has also been used for drug delivery.

Biodegradable polymers can be classified into synthetic and natural. Natural polymers present some advantages, such as bioactivity, proteolytic degradation, natural remodeling, and capacity to induce tissue ingrowth. However natural polymers have also some obstacles, such as purification, different degradation rates, and disease transmission. Differently, synthetic polymers are easier to be tailored, and it is possible to control their molecular weight and physical characteristics, despite they are biologically inert [12, 18]. Examples of biodegradable natural polymers are proteins – such as collagen and gelatin – and carbohydrates such as chitin, chitosan, hyaluronic acid, and silk fibroin. Examples of biodegradable synthetic polymers are aliphatic

polyesters, such as polylacticacid, polyglycolic acid, poly-(D/L-lactic-co-glycolic) acid, and poly-Ɛ-caprolactone.

In regard to natural biodegradable polymers for biological applications, they have resorption rates that can be controlled by modifications on degradation kinetics. These polymers are degraded in the organism through hydrolytic or enzymatic mechanisms. In relation to polymers degraded by hydrolytic process, when water molecules react with ester bound, they break the polymeric chain and decrease the molecular weight, which can compromise the mechanical properties of the material. In polymers degraded by enzymatic process, degradation occurs on surface and does not affect the bulk material, maintaining the mechanical properties [35].

Enzymatic degradation is often found along the degradation of collagen and gelatin. Collagen is abundant in human body as component of extracellular matrix, and then it is commonly used in bioactive glass/polymer composites. Similarly, gelatin is a cheap material and has received more attention as biomedical material. Both of them are only degraded by proteolysis, by collagenase and gelatinase, respectively, and their degradation rates can be controlled by chemical crosslink of molecules, because crosslink makes collagen/gelatin less accessible for enzymes (collagenase and gelatinase) degradation [13].

Some parameters are important in dissolution kinetic, such as molecular weight, crystallinity, morphology, and hydrophilicity. For example, chitin is a polysaccharide founded in outer shell of crustaceans and insect exoskeletons, insoluble in common solvents, and chitosan is a semicrystalline polymer derivated of chitin, soluble in aqueous media. Chitosan degradation rate can be controlled by degree of acetylation and crystallinity [27]. Another example is hyaluronic acid, which is a protein founded in human body with proteolytic degradation by hyaluronidases [13]. Degradation rate of hyaluronic acid can be controlled by changing the extent of esterification [27]. Silk fibroin can also be cited as example, because it can be degradable and presents a range of mechanical and functional properties. Its crystallinity can be controllable, and it can be processed under ambient conditions, what makes it interesting for drug delivery, avoiding degradation of labile pharmaceuticals [18].

With respect to synthetic biodegradable polymers, hydrolysis is the degradation mechanism of these polymers, and their degradation properties can be tailored by changing molecular weight and tactility [13].

The ideal resorption should occur simultaneously with the healing of a tissue: implants should maintain properties and function until total healing of natural tissue. Controlling resorption rates is important since each tissue has a healing rate varying from days until months [12]. For natural polymers, control of modifications and kinetics is more difficult, because their chains, sometimes, are not uniform and their properties may change between different samples [35].

Others polymers can also be used in biological applications, such as polycarbonate, poly(ethylene oxide), poly(ethylene glycol), polyurethanes, and poly(sebacic anhydride) [13, 18, 27].

8.2.3 *Bioactive Glass/Polymer Composites*

Different classes of materials have their own advantages and disadvantages. For example, polymers may have a variety of forms, compositions, and physical characteristics, but they are too flexible and weak for some applications; bioactive glasses and others ceramic materials present good biocompatibility, compression resistance, and corrosion resistance, but they have problems as brittleness, low fracture strength, and high density [30]. In this sense, composites made of polymers and ceramics have joined the advantages of each class of materials, also overcoming their disadvantages.

Polymers used in bioactive glass/polymer composites can improve the mechanical and physical properties of bioactive glasses and can also modify drug release profiles [13]. On the other side, bioactive glass particles dispersed into polymers enhance their mechanical performance and improve bioactivity of material [12].

Particularly, bioactive glasses/polymer composite materials represent a new class of materials. This combination keeps the properties of both materials: bioactivity and mechanical strength of bioactive glasses and flexibility and shape formability of polymers. Another advantage of ceramic/polymer composites is the possibility of polymerization in vivo, and then these materials can be tailored to be injectable, expanding their prospects of use [35].

Association between polymers and bioactive glass may occur by different morphologies, such as by dispersion of bioactive glass particles into a polymeric matrix or polymeric fibers, by coating of a polymer on the surface of a bioactive glass scaffold and by coating of a bioactive glass particles on the surface of a polymeric scaffold. Each system displays particular mechanical characteristics and properties and can be used for specific applications (Fig. 8.2).

Moreover, distinct interactions occur with different sizes and forms of particles and different polymer compositions. In this section we will focus on how the particle size and shape of glasses and different polymers alter the morphology and chemical interactions of a composite.

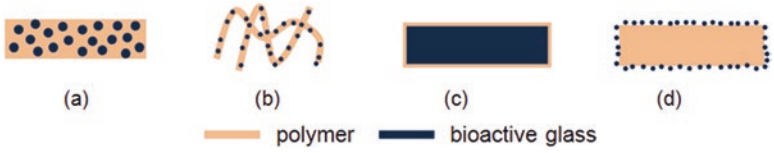

Fig. 8.2 Schematic diagrams of: (**a**) bioactive glass particles in a polymeric matrix; (**b**) bioactive glass particles in polymeric fibers; (**c**) coating of a bioactive glass scaffold with polymer; and (**d**) coating of a polymeric scaffold with bioactive glasses particles

8.2.4 Physical-Chemical and Biological Properties of Bioactive Glasses and Polymers

Particle size and morphology of bioactive glass play an interesting role in ceramic/polymer composites when these particles are dispersed into a polymeric matrix. It is expected that the ceramic material exhibits suitable adherence in the polymeric matrix, so that the interaction between them is optimized, and a suitable adherence is the key in composite materials for improvement of properties. For example, considering mechanical properties, bioactive glass (BG)/polymer composites hold the mechanical strength of glasses because the work done in the matrix (polymer) is transferred to the glass particles if BG-polymer interface is well joined, and then the energy due to the work done is trapped in the chemical bonds of the glass. The chemical bonds of the glasses only will break if the energy related to the done work is higher than the energy associated with the glass bonds. Otherwise, the glasses will keep absorbing the work done without leading to any fracture. Note that this mechanism of mechanical behavior only happens because it is supposed that the glass and the polymer establish a suitable adherence on their surface.

Controlling the particle size (i.e., the specific surface area) to be dispersed in the polymeric matrix may be an interesting strategy to increase the adherence between polymer and ceramic. The higher the specific surface area, the more intense are the interactions between the matrix and the particles, because there is a higher area to interact with the matrix, which enables more intermolecular interactions. For example, bioactive glass nanoparticles have larger specific surface area than micrometric bioactive glasses, which means that nanometric glasses are more reactive than micrometric ones. When nanobioactive glasses are dispersed into polymeric matrices, these nanoparticles increase mechanical strength and stiffness, as long as more surface interactions are available [5].

Besides changes in mechanical properties, nanobioactive glasses can also provide enhanced angiogenic response. Several studies have already shown that bioactive glasses are able to induce angiogenic response. It happens because the glass dissolves in the body fluid and ions from the glass are lixiviated to the host tissue. These ions, in turn, interact with cells surrounding the glass and lead to angiogenic response after a cascade of biochemical reactions. When glasses are in the nanoscale, they exhibit a higher surface area available to interact with the body fluid. Consequently, there is a quicker dissolution in the host tissue, and more ions can interact with the surrounding cells. Therefore, the amount of nanoparticles in the matrix plays an important role as cell response inductor. Vargas et al. [37] prepared composite made of collagen type I films with bioactive glass nanoparticles. They investigated in vivo angiogenic response of these films with different concentrations of bioactive glass nanoparticles using the quail chorioallantoic membrane as alternative to mammalian model of angiogenesis. Pure collagen films had the same result in native quail chorioallantoic membrane (without implanted material). On the other hand, films with 10 wt% of bioactive glass nanoparticles showed an increase of 41% on number of blood vessels after 24 h postimplantation, but, in

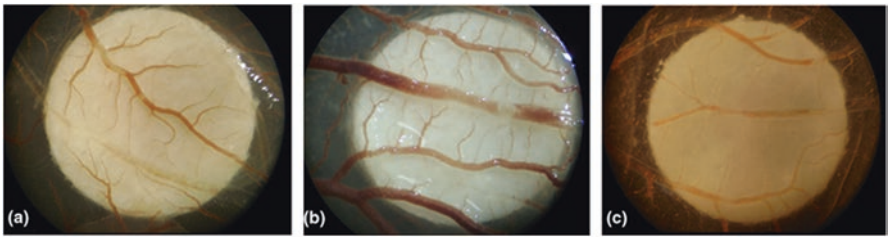

Fig. 8.3 Stereomicroscopic views of chorioallantoic membrane tissue response at 24 h postimplantation. (**a**) Collagen film, (**b**) collagen film with 10 wt% of bioactive glass nanoparticles, and (**c**) collagen film with 20 wt% of bioactive glass nanoparticles (From: Vargas et al. [37])

contrast, films with 20 wt% of bioactive glass nanoparticles had an antiangiogenic effect, with a decrease of 49% on number of blood vessels after 24 h; both are compared with pure collagen films (Fig. 8.3).

The authors associated the unexpected response of films containing 20 wt% bioactive glass nanoparticles with an intense inflammatory response, which resulted in higher ionic concentration and drastic pH change. This example shows the importance of controlling the amount of nanoparticles in the polymer matrix.

Biocompatibility and bioactivity may also be modulated by the size and surface area of BG particles. There are several examples in the literature showing the effect of nanobioactive glasses in polymeric matrices, and most of them establish a relationship between change in the morphology of the matrix and composite bioactivity. As example, Misra et al. [25] prepared a composite films of poly(3-hydroxybutyrate)/bioactive glass nanoparticles. The presence of nanoparticles changed the surface morphology of the matrix due to their exposure on the surface, increasing roughness. This fact results in higher cell attachment, contributing to biocompatibility of the composite films. Boccaccini et al. [5] suggest that the addition of nanoparticles creates a nanostructured topography on surface of the film, inducing higher protein absorption compared with polymeric films/microparticle composites, which presents a different topography (Fig. 8.4).

Mesoporous bioactive glass (MBG) may also influence on the bioactivity. MBG has larger specific surface area improving bioactivity properties, and with porous between 2 and 50 nm, this material can release drugs or other molecules [3, 15]. According to Izquierdo-Barba and Vallet-Regí [15], mesoporous bioactive glasses exhibit bioactivity after 4 h soaking in a simulated body fluid, whereas melting and sol-gel bioactive glasses need 7 and 3 days, respectively. This fact may be explained as an effect of the larger specific surface area associated with the morphology of the mesostructure and the surface area within the mesopores (Fig. 8.5).

Improving the bioactivity may be either worthwhile or disadvantageous. According to Hum and Boccaccini [14], the formation of apatite layer can inhibit the release of drugs; after an initial burst, the drug release rate decreases, while the hydroxyapatite layer is formed, achieving a sustained release. This release rate depends on the drug, the interaction between bioactive glass, and the drug and bioactive glass composition and synthesis.

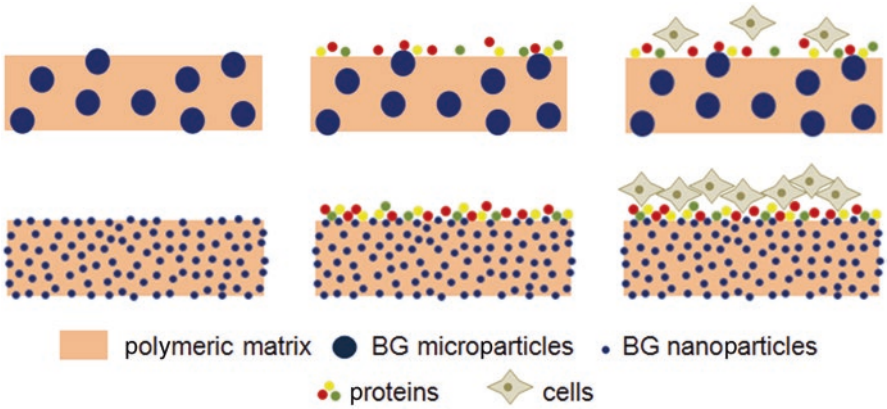

Fig. 8.4 Schematic diagrams of dispersion of BG particles into polymeric matrix adsorption of proteins on surface and cell attachment with nanometric particles (*bottom*) and micrometric particles (*top*)

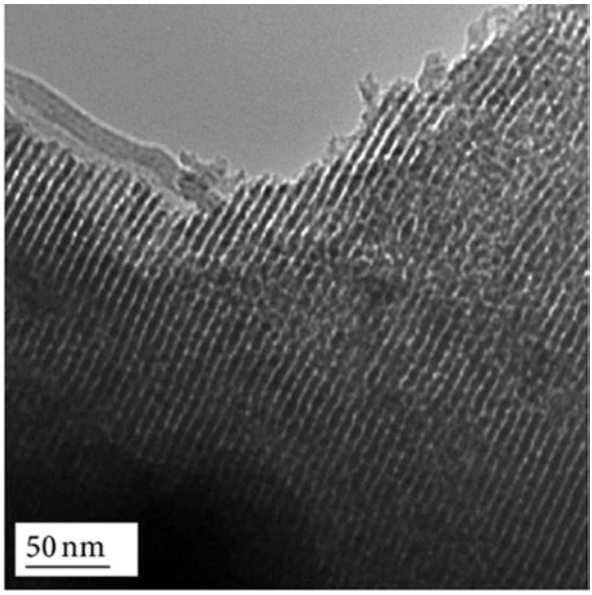

Fig. 8.5 Transmission electron microscopy image of mesoporous bioactive class/carbon composite (From: Zhu et al. [48])

Wu et al. [41] supported this fact in their work. They developed a system of protein (bovine serum albumin) release from bioactive mesoporous glass microspheres. The drug load was done by soaking of the microspheres in a solution of 100 mg of bovine serum albumin dissolved in 50 mL of simulated body fluids, at 37 °C for various periods (0, 1, 3 and 7 days). The authors observed that the loading efficiency and release kinetics can be controlled changing the density of the apatite layer on surface of microspheres: loading capacity of protein in microspheres increased with the time of soaking in simulated body fluids, and release rate

decreased with an increased apatite layer deposition. The capacity of bovine serum albumin loading increased with more apatite particles deposited because initially the protein trapped inner microspheres porous and binds with hydroxyl groups on surface, but with the apatite layer deposition, the protein also binds with chemical groups of apatite (OH^-, PO_4^{3-} and CO_3^{2-}) increasing the loading capacity.

Similar results were found by Arcos et al. [1], but using SBF solution instead of a serum bovine one. The authors synthesized bioactive glass/polymethylmethacrylate composites adding gentamicin sulfate in the polymer matrix. The composite showed a drug release modulated by the hydroxyapatite nucleated on its surface when immersed in an SBF solution. The system was soaked in simulated body fluid for 14 days, and high-dose release (80%) occurred in the first 48 h. Oppositely, the composite showed slower drug release after this time with 90% of released drug after 14 days until the end of experiment. The authors suggest the drug release process is not only a single process of diffusion, but also the changes produced in simulated body fluid, such as increase in the concentration of Ca^{2+} ions and pH, influence the release rate as these changes occur along the process (Fig. 8.6).

Increasing in loading capacity and decreasing in release rate can occur with all kinds of molecules which can bind with groups present in the bioactive glass surface and apatite particles. Therefore, the amount of deposited apatite can change the release rate of drugs and can be used to control this rate according to desired kinetics. Other researches also highlighted this fact as the work of Ladrón de Guevara-Fernández et al. [19] that developed a system to deliver ibuprofen, an anti-inflammatory drug.

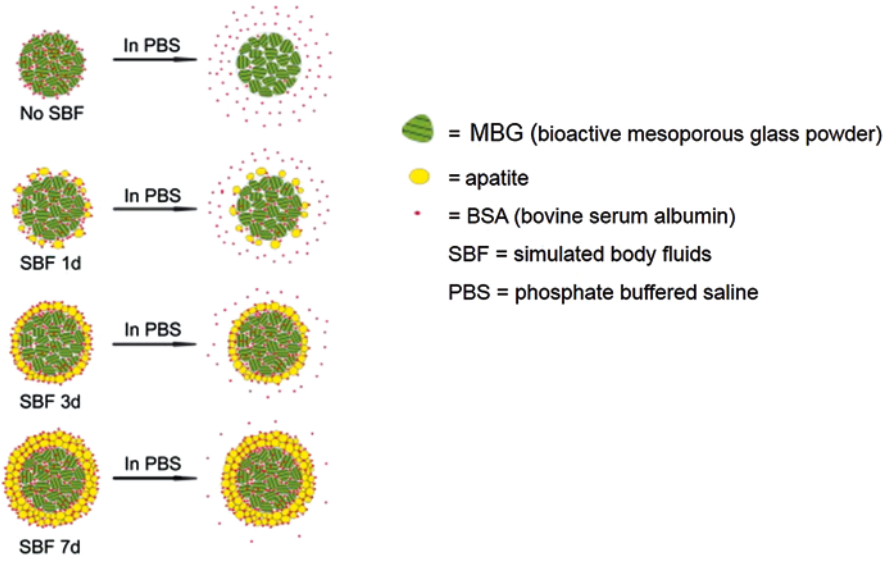

Fig. 8.6 Schematic illustrations of BSA loading and release in four MBG microspheres. The *left* column is BSA loading, and the *right* column is BSA release. With the increase of soaking time in SBF, more and more apatite particles deposited on the surface of MBG microspheres, which enhanced BSA loading efficiency and decreased BSA release kinetics (From: Wu et al. [41])

8.3 Bioactive Glass/Polymer for Drug Delivery

Bioactive glasses/polymer composites can be used as carrier to deliver drugs, ions, and bioactive molecules as peptides, hormones, and growth factors. These systems can be used to control pharmacokinetics and biodistribution of molecules, acting as reservoirs and maintaining sustained release. Local delivery avoids inactivation by enzymes in the blood and excretion by renal filtration increasing the drug effectiveness. In case of proteins and growth factors, sustained release avoids immediate diffusion and removal by drainage [14]. Local release of drugs has also other advantages as possibility to deliver drugs with short half-life with minimal loss in therapeutic activity, improving delivery of drug of low bioavailability, diminishing drug pharmacokinetics variability between patients [18], and avoiding problems with repeated administration and under- or overdosage [27]. Moreover, the use of bioactive glass/polymer composites to release therapeutic agents is an interesting alternative to locally maintain high concentrations of drugs and avoid collateral effects from systemic applications, such as happens with pills and arterial injections [11].

In these systems, the drug may be loaded either in the glass or in the polymeric matrix. The drug loading in polymers can be achieved by incorporation of drugs in a polymer matrix [27]. When the drug is loaded in the glass particles, it can be done through two approaches (Fig. 8.7):

- The drug can be incorporated during the synthesis of material. In this case, melting process is not indicated because of the high temperatures involved, so that sol-gel techniques enable to add drugs and other molecules because this process occurs at room temperature [14].
- The drug can also be entrapped inside porous or by hydrogen bonds between groups present on bioactive glass surface, as Si-OH and P-OH and groups present on drugs (hydroxyl and amino) [14].

An example of drug loading by hydrogen bonds between groups present on bioactive glass surface and groups present on drugs was observed in the work of El-Kady and Farag [9], where bioactive glass nanoparticles were used as carrier for sustained 5-fluorouracil release. 5-fluorouracil is an anticancer drug with a short biological half-life (8–20 min) and toxic side effects due to a nonspecificity action

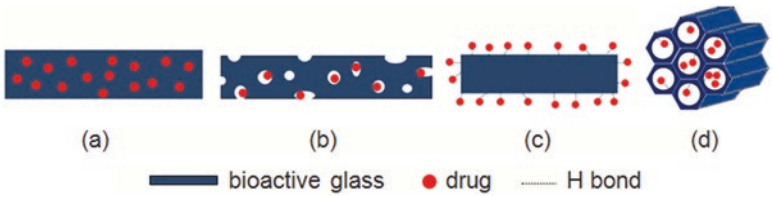

Fig. 8.7 Schematic diagrams of: (**a**) drug incorporated during sol-gel syntheses of bioactive glass; (**b**) drug entrapped inside porous of bioactive glass; (**c**) drug bonded by H bond on surface of bioactive glass; and (**d**) drug bonded by H bond on inner surface of mesoporous bioactive glass

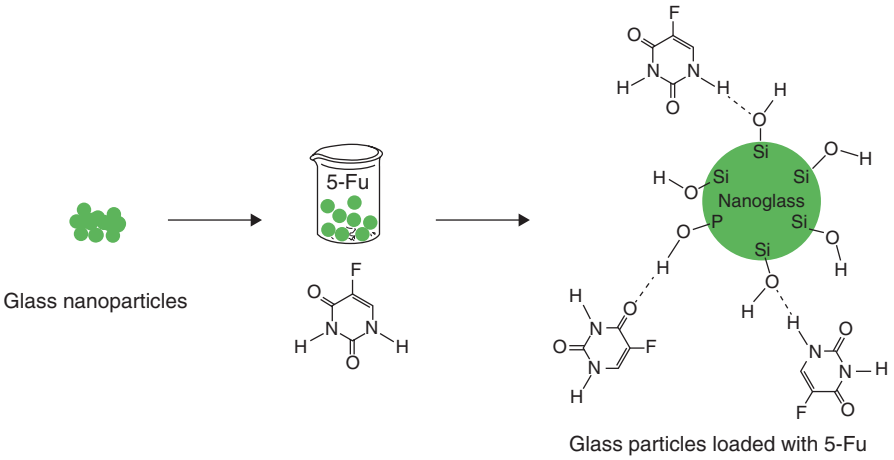

Fig. 8.8 Nanoparticles surveying as a delivery system for 5-fluorouracil (5-FU) (From: El-Kady and Farag [9])

(its action occurs in tumoral and normal cells).The drug was adsorbed in surface of nanoparticles by soaking (Fig. 8.8), and the release profile showed an initial faster release (28% at the first day) followed by a slower release (around 45% after 32 days). The analysis described by the authors suggest that the 5-fluorouracil release is influenced by the bioactive glass dissolution, glass particle diameter and changes of the surface area.

The bond strength between the OH groups and the drug may influence on the drug release, but other factors might also influence on the release profile, such as drug solubility in aqueous media. Rámila et al. [31] described the release kinetics of two drugs from bioactive glass/polymethylmethacrylate samples. The drugs used were ibuprofen and gentamicin. The first is practically insoluble in aqueous media, while the second is freely soluble. Their release profiles were different, gentamicin showed high release in the first day, and a total release after 150 h. Differently, initial release rate of ibuprofen was much slower in the first day and after 600 h did not reach total release [31].

Another example of drug bonded on the surface of bioactive glass is observed in Zhao et al. [46] work, which studied tetracycline release behavior from mesoporous bioactive glass (MBG). They loaded tetracycline into the mesoporous and reported that the CaO content in MBG is in direct proportion with amount of drug loaded, which is also related with drug release rate. In other words, drug release kinetics are strongly dependent of MBG composition. They proposed two mechanisms for adsorption of the drug molecules in mesoporous: physical and chemical, showing an initial release associated with drug physically adsorbed when materials were immersed in simulated body fluid (SBF) (Fig. 8.9).

Surfaces of bioactive glass can be functionalized for improving drug loading and release. Vallet-Regí et al. [36], through studying mesoporous bioactive glass (MBG), stated that functionalization with organic groups provides increased drug-surface interactions and enables links between surface and drug through ionic bonds or ester

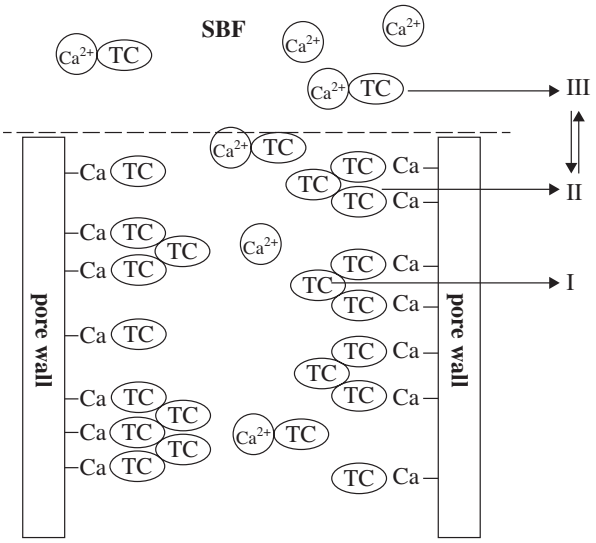

Fig. 8.9 Proposed scheme for adsorption of tetracycline in MBG and during release process: (*I*) physically adsorbed; (*II*) chemically adsorbed with calcium on the pore wall; and (*III*) chemically adsorbed with calcium ions in SBF solution (From: Zhao et al. [46])

groups bonds, which can effectively improve drug release rates. Figure 8.10 exemplifies functionalized pore wall of MBG.

Besides the way in which drugs are loaded in the composites, the structure of the whole systems may also alter the drug release. For example, polymer coating on bioactive glass scaffold can change the drug release profile and change mechanical properties of scaffolds, and at the same time it can maintain its bioactive characteristics.

Belluci et al. [4] prepared gelatin-coated bioactive glass-derived scaffold to mimic the morphology of bone. They investigate the influence of the coating on porosity and bioactivity of the materials in vitro, and results showed coating maintains porous open and interconnected and preserves the bioactivity, forming a hydroxyapatite layer in few days (Fig. 8.11).

In order to the potential of gelatin coating as drug delivery, Gentile et al. [11] studied ceramic scaffolds of bioactive glass and hydroxyapatite coated with uniform polymeric layer (gelatin) incorporating indomethacin-loaded polyesterurethane nanoparticles. Authors refer the use of polyesterurethane nanoparticles as nanocarrier to improve control of release of drug, resulting in sustained drug release of 65–70% within first week in physiological solution. Authors also described the incorporation of nanoparticles on coating increased compressive modulus. In addition, Yao et al. [43] studied uncoated and coated (polycaprolactone and chitosan) bioactive glass scaffolds in which were loaded with vancomycin hydrochloride. The release profiles were studied using a phosphate-buffered saline (PBS) solution. The authors observed a sharp release of drug in 8 h for both scaffolds, but the drug was release completely in 24 h for the uncoated scaffold. In contrast, the coated scaffold exhibited a sustained release for 11 days.

Sometimes, the presence of a second polymer in the composite can modify the release kinetics. Ladrón de Guevara-Fernández et al. [19] prepared samples composed by bioactive glass, poly-L-lactic acid, and polymethylmethacrylate to

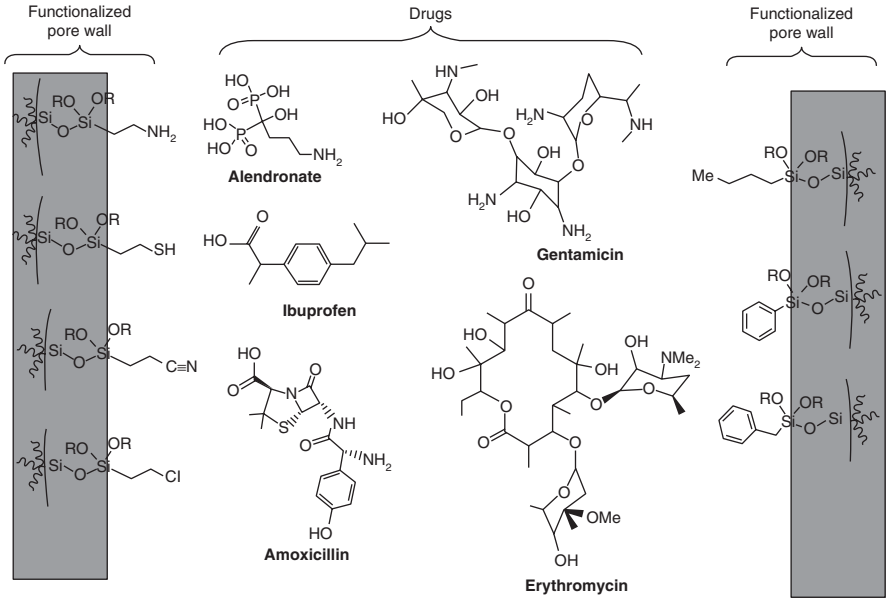

Fig. 8.10 Pore-wall functionalization in silica mesoporous materials and structures of several drugs used in these systems (From: Vallet-Regí et al. [36])

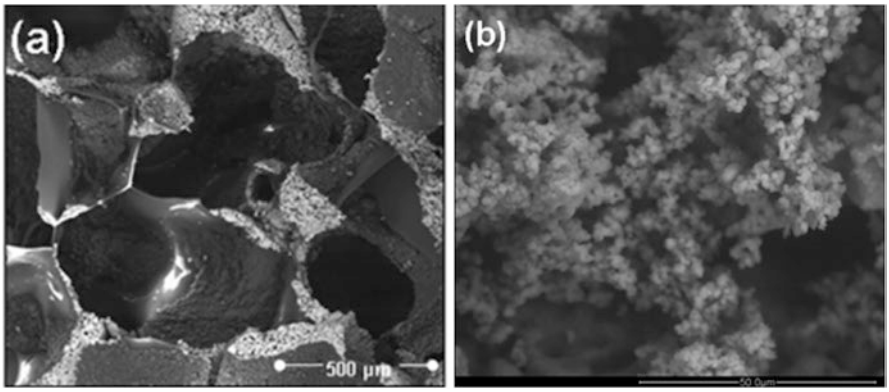

Fig. 8.11 (**a**) Micrograph of the shell scaffold surface before soaking in simulated body fluid and (**b**) micrograph of the hydroxyapatite formed on the shell scaffold surface after 3 days in simulated body fluid (From: Belluci et al. [4])

release ibuprofen, an anti-inflammatory drug used in bone diseases. The release rate of ibuprofen is related to its crystallinity: when the drug is in amorphous state, the release is slower. The absence of poly-L-lactic acid in this system leads a decrease of release rate of drug, because it induces an amorphous state of ibuprofen. The authors reported that the release rate of ibuprofen can also be related with kinetics of apatite-like layer formation.

8.4 Clinical Applications of Bioactive Glass/Polymer for Drug Delivery

Different drugs can be locally released using bioactive glass/polymer composites. Different drugs have been used in drug delivery systems, such as anti-inflammatory, osteogenic, anticancer, and antibiotics. In this section, we will cover some applications of these drugs loaded in glass/polymer matrixes.

8.4.1 Antibiotics

The main group of drugs used in local release is antibiotics, because the use of biomaterials as bone filling, bone substitute, or orthopedic implants may result in undesirable consequences like infections.

Glass/polymer scaffolds are better than using glass and polymers in separated, because it is possible to join the osteogenic response of glasses and the drug release by the composite. In addition, it is possible to locally release high doses of drugs, increasing the specificity of the treatment. Regarding bone infections like osteomyelitis, this ability is needed because it allows the delivery of high doses of antibiotics to avascular areas by diffusion, where the systemic application cannot reach [7]. A wide array of research is found that proposed different bioactive glass/polymer scaffolds to release antibiotics.

Jia et al. [17] developed teicoplanin-loaded borate/chitosan composite mixing chitosan citric acid and glucose solution with bioactive glass powder and teicoplanin. They produced pellets with this material and determined the drug release profile in phosphate buffer solution (PBS). Around 45–47% of drug was release in first day followed by a slowly stable release up to 25–37 days. The author associated the sustained drug release with the chitosan structure, which shows free amine and polycationic groups that form complexation reactions; when immersed in PBS, due to the presence of citric acid in the composite. Additionally, the deposition of PO_4^{3-} (from PBS) on the glass surface lead to an improvement in crosslinking reaction and an increase in viscosity of chitosan, maintaining drug molecules entrapped within the structure. These facts reduce the initial release of drug and result in slowly sustained release rate for more time.

In another work, Ding et al. [7] purposed a local delivery of vancomycin using injectable cement composed of chitosan-bonded borate bioactive glass particles. Injectable systems present some advantages compared with traditional surgery: they are less invasive and less aggressive for health, cause less pain, and require shorter time to patient recover. They are also more precise at filling defects, which result in less space for bacterial growth. The authors suggested such drug delivery systems may be more effective than intravenous application of the antibiotic in treatment of infections. This system presents a fast initial release with a decrease rate with time.

For huge bone losses in which tissue self-regeneration is impossible, metallic implants still are the main option. However, metallic implants have the risk of microbial infection. Coatings made of bioactive glass/polymer composites containing antibiotic deposited on the surface of metallic implants are able to improve long-term fixation and to avoid postsurgical infection. Moreover, the use of bioactive glass in these coatings can improve the potential for bone regeneration. Patel et al. [29] developed coatings for metallic bone implants using chitosan/bioactive glass nanoparticles containing ampicillin, which was deposited on the surface of metallic implants by eletrophoretic deposition. The coatings were uniform and exhibited thickness between few to 10 μm varying according to adjustments of deposition parameters (Fig. 8.12). In vitro studies showed the coating led to a controlled drug release up to 10–11 weeks, which means that using such coating may be an interesting alternative to uncoated implants.

In another work, Ordikhani and Simchi [28] purposed the use of bioactive glass/chitosan coatings loaded with vancomycin. They fabricated the coating by a single-step electrophoretic deposition technique, resulting in a uniform layer with a thickness of 55 μm. Vancomycin is an antibiotic usually used for treating implant infections. The release kinetics in vitro showed an initial burst in the first hour (40% of drug delivered) followed by a slower release over 4 weeks, being a potential system for long-term drug eluting.

Many other systems have been developed to release antibiotics, among them some works are listed in the Table 8.1.

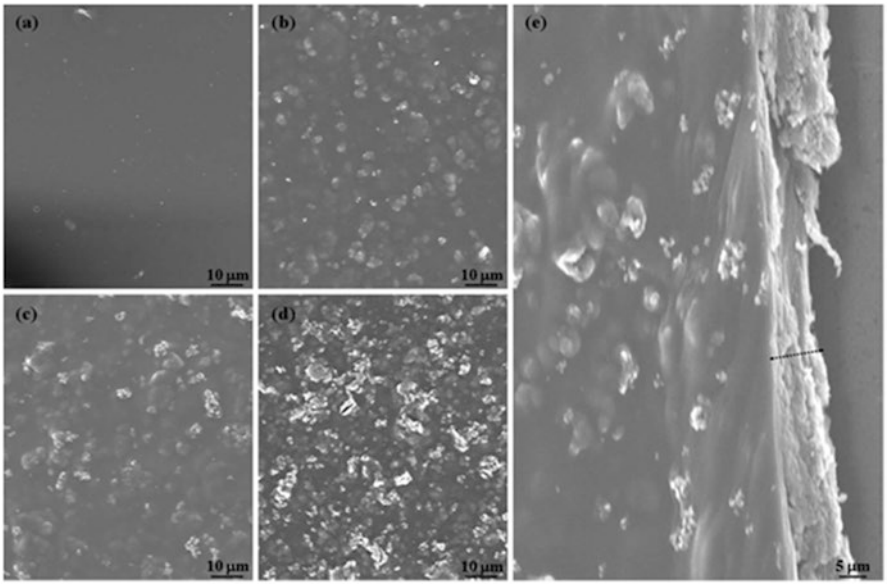

Fig. 8.12 Scanning electronic microscopy of coating layers: (**a**) chitosan, (**b–d**) chitosan and different amounts of bioactive glass nanoparticles, and (**e**) coating layer was scratched off from the Ti substrate to reveal a coating layer with a level of thickness (*indicated an arrow*) (From: Patel et al. [29])

Table 8.1 The effect of bioactive glass/polymers scaffolds loaded with antibiotics

Drug delivery systems	Effect	Citations
Macroporous poly(L-lactic acid) + gentamicin (broad-spectrum antibiotic drug) coated with mesoporous bioactive glass	Improved hydrophilicity and cell adhesion/growth on the surface of the scaffold	Zhu et al. [47]
Highly porous scaffold of bioactive glass coated with poly(3-hydroxybutyrate-co-3-hydroxyvalerate) encapsulating vancomycin (broad-spectrum antimicrobial drug)	Protection against Gram-positive bacterial infections	Li et al. [21]
Polyvinyl alcohol scaffold with dispersed bioactive glass nanoparticles loaded with ciprofloxacin (an fluroquinolone derivative antibiotic)	The glass particles improved the mechanical properties of PVA scaffolds, and allowed a sustainable release	Mabrouk et al. [23]
Membranes coated with bioactive glass nanoparticles containing tetracycline hydrochloride (a broad-spectrum antibiotic that inhibits protein synthesis)	Release of tetracycline inhibited *S. aureus* growth, and membranes have potential to prevent wound infections	Rivadeneira et al. [33]
Scaffolds of chitosan matrix containing bioactive glass plus gentamicin	Scaffolds is bioactive, and drug rate release was tailored by content of chitosan	Wers et al. [39]

8.4.2 Anti-inflammatory

Inflammatory responses are frequent after surgical or implantations. Local release of anti-inflammatory drugs can be an alternative to minimize this problem. Anti-inflammatory response is important to tissue regenerate because it helps to eliminate foreign pathogens, but if this response is severe, it will be counterproductive, resulting in damage to the tissue.

In the aforementioned work of Ladrón de Guevara-Fernández et al. [19], a system with bioactive glass, poly-L-lactic acid, and polymethylmethacrylate for release of ibuprofen was developed. The authors affirmed that the system without poly-L-lactic acid, which presents slow and continuous drug release, is indicated to form inner parts of implants for longer release, while system with poly-L-lactic acid, which presents fast drug delivery, is suitable to be used for acute inflammatory response.

Zhang et al. [45] produced mesoporous bioactive glasses/silk fibroin scaffolds with dispersion of bioactive glass particles in a silk fibroin matrix and used a freeze-drying method to obtain porous scaffold and loaded these scaffolds with aspirin, a nonsteroidal anti-inflammatory drug that improves osteogenesis and inhibited osteoclastogenesis. Drug loading was loading using a vacuum pump for decompression, aspirin solution was infused in low pressure, then the pressure come back to normal; after 1 h of immersion at normal pressure, samples were freeze dried. Composite scaffolds improved drug loading and releasing in vitro in comparison with silk scaffolds, because the presence of bioactive glass modifies silk fibroin. The loading was around 80% at bioactive glass/silk composite scaffold and 60% at pure silk scaffold. Releasing at the first 12 h was 69% and 45% for bioactive glass/silk composite and pure silk scaffolds, respectively.

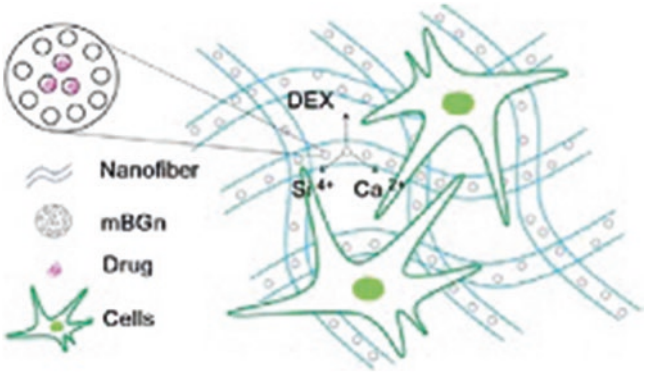

Fig. 8.13 Schematic diagram showing the therapeutic fiber scaffolds incorporating nanospheres of mesoporous bioactive glass with dexamethasone (DEX-loaded mBGn), where the drug-releasing effect and bioactivity of mBGn can be synergized to regulate osteogenic responses (From: El-Fiqi et al. [8])

8.4.3 Bone Regeneration and Osteoporosis

When there is significant bone loss, osteogenic drugs can improve the regenerative potential of bioactive glass/polymer systems. El-Fiqi et al. [8] designed an electrospun fibrous scaffold of polycaprolactone-gelatin and used nanospheres of mesoporous bioactive glass as drug loading/delivery (Fig. 8.13). They loaded the nanospheres with dexamethasone, an osteogenic drug that improves the therapeutic potential of such system. These nanospheres were incorporated into fibers at 2.5, 5, and 10 wt% by electrospinning technique. The nanosphere-added fibers scaffold presented improved mechanical tensile strength, elasticity, and hydrophilicity when compared to pure polymer fibers scaffold. The release kinetic of the drug from fibers was highly sustainable, being almost linear on a period of 28 days (test period). On the other hand, in fibers not containing glasses, the release was very quick, demonstrating the potential to sustained and long-term release only promoted by fibrous composite scaffold. In vitro tests, using stem cells derived from periodontal ligament and in vivo tests, in rat calvarium defect model showed that dexamethasone delivery led to higher differentiation of stem cells from osteogenic lineage and increased the bone density in comparison to fibers without drugs.

In addition, the bone regeneration potential of bioactive glasses can be allied to drugs to regenerate osteoporotic bones. Osteoporosis is a disease common in the elderly, characterized by loss in bone density and risk of bone fractures. Moreover, osteoporotic fractures might compromise the quality of life due to pain and lack of locomotion. As reported by Mondal et al. [26], oral use of bisphosphonates has been used as osteoporosis treatment. Bisphosphonates act on osteoclastic activity, inhibiting bone resorption. Local delivery of these drugs can improve the treatment, and delivery system with bioactive glass can stimulate bone regeneration.

Mondal et al. [26] prepared poly(lactide-co-caprolactone) microspheric scaffold. Bioactive glass powder and alendronate sodium (a bisphosphonate drug) were dispersed into polymeric matrices. Loaded microspheres can be directly delivered into the bone defect as an injectable system, with ability of both bioactive glass to improve bone regeneration and drug to inhibit bone resorption. Furthermore, in vivo studies in rat tibia model resulted in expressive new bone formation, proving the effectiveness of this system.

8.4.4 Cancer Treatment

Another problem that results in loss in bone mass is bone cancer. A usual treatment for bone cancer is chemotherapy, with the use of one or more drugs systemically administrated in order to eliminate cancer cells. Chemotherapy has a negative issue: side effects affect the entire body and compromise quality of life of patients. Local drug delivery for treatment of bone cancer could potentiate drug action against cancer cells and reduce or eliminate side effects. The association with bioactive glasses could also stimulate the regeneration of lost tissue.

Jayalekshmi and Sharma [16] developed a system composed by gold nanoparticles incorporated with bioactive glass encapsulated in a chitosan-gelatin matrix. The samples were loaded with doxorubicin by immersion in drug-/phosphate-buffered saline solution. Doxorubicin is a chemotherapeutic drug with toxic side effects, and local delivery is an option to use this drug in chemotherapy. Incorporation of gold nanoparticles in bioactive glass controlled the drug delivery characteristics, and the system can be used to avoid multiresistant of cancer cells. The authors observed higher release rates of doxorubicin at pH = 5 and a controlled release for 8 days in phosphate-buffered saline. At pH 5 breaking of the bonds occurs between drug and bioactive glass/polymer composite, and the drug is released, but the links are unaffected under normal body conditions, which can be observed on fluorescence spectra of the composite with and without gold nanoparticles at pH 7.4 and at 5. This condition makes the system a good target to the intracellular environment of cancer cells (Fig. 8.14).

Wang et al. [38] developed a system able to deliver drugs, monitor drug release, and stimulate bone regeneration. They used a layer-by-layer strategy to prepare core-shell structures with upconversion nanoparticles coated with mesoporous SiO_2/Ca layer. The use of upconversion nanoparticles is important because they are capable of visible/near-infrared light emission when excited with near-infrared light. Red emission is improved by addition of calcium ions, and imaging of deep tissue became possible with increase of fluorescence penetration (Fig. 8.15). Zinc phthalocyanine (a photodynamic anticancer drug) was loaded into the structure, then it was possible to monitor and to trigger the drug release in vivo and the relationship between fluorescence intensity and loading concentration of drug can be established.

Taken all these examples together, it is noted that bioactive glass/polymer systems are promisor candidates for cancer treatment.

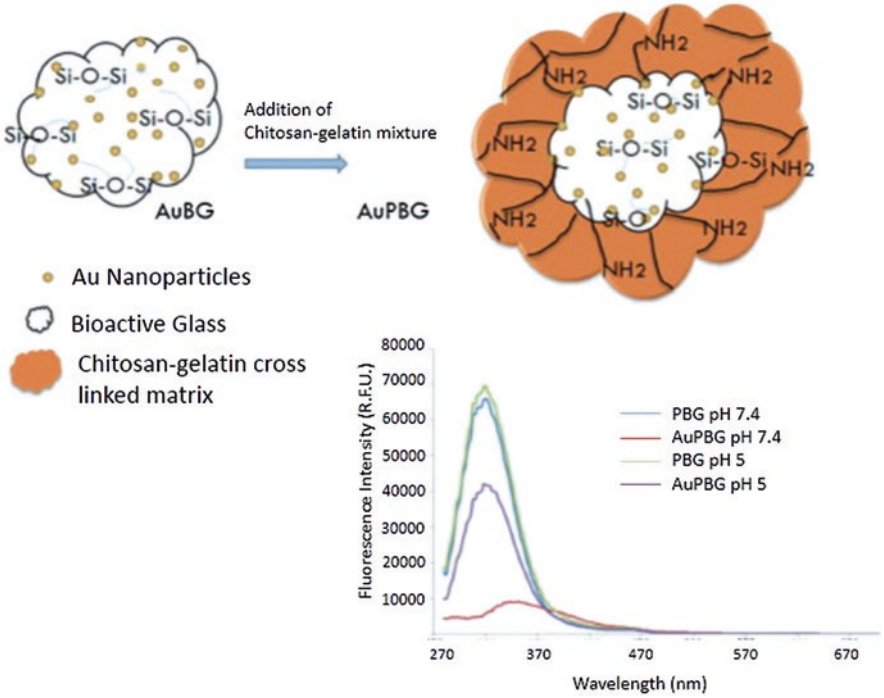

Fig. 8.14 The scheme of the reaction and the fluorescence spectra of the composite with and without gold nanoparticles at pH 7.4 and at 5 (From: Jayalekshmi and Sharma [16])

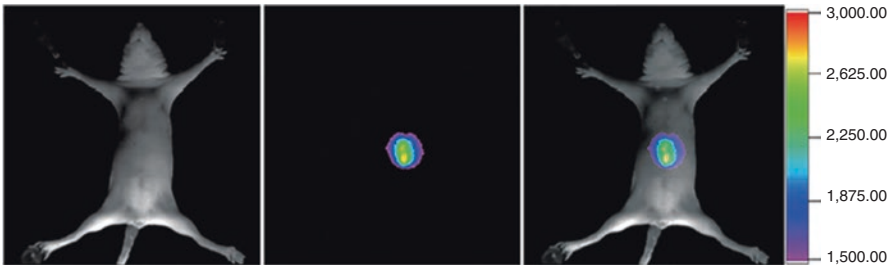

Fig. 8.15 In vivo upconversion luminescence imaging of athymic nude mice with intravenous injections of upconversion nanoparticles coated with mesoporous SiO_2/Ca layer (From: Wang et al. [38])

8.4.5 Multifunctional Drug Delivery Systems

Besides coatings, other more complexes have been developed, such as systems for delivering multiple drugs. Ma et al. [22] synthesized porous bioactive glass with macro- and mesoporous silica SBA-15 containing magnetic particles (magnetic SBA-15). Ibuprofen (an anti-inflammatory drug) was loaded in magnetic SBA-15 by immersion in a solution of hexane/ibuprofen, then, after loading, the composites was coated with poly(lactic-co-glycolic acid). Metformin HCl (drug for treatment of diabetes) was subsequently loaded in bioactive glasses. The release profiles of both drugs were observed in vitro. Release rates of metformin HCl showed an initial burst of molecules adsorbed on surface and a sustained release up to 36 h. Release rates of ibuprofen were found to vary with different amounts of poly(lactic-co-glycolic acid) as a surface layer. Depending how thick is the layer, ibuprofen would be released from 24 up to 180 h. In overall, the dual release system showed to be effective, because it was possible to modulate the delivery of both drugs in separate ways. The authors did not analyze this characteristic, but they cited the potential for hyperthermia of magnetic particles due to their conductibility with an external magnetic fielding.

In some cases drugs are released simultaneously, but some studies try to develop dual-drug delivery system with independent drug release. Xia et al. [42] prepared mesoporous bioactive glass/polypeptide (poly(c-benzyl-L-glutamate)-poly(ethylene glycol)) graft copolymer nanomicelle composites to deliver gentamicin and naproxen. They developed a pH-controlled delivery, with release of gentamicin from bioactive glass and release of naproxen from polypeptide nanomicelles. At an initial pH of 1.2, gentamicin was totally released after 2 h, and only 17% of naproxen was released at this meanwhile. When the pH reached 10, 55% of naproxen was released after 2 days, and 72% after 10 days. On the contrary, at an initial pH of 10.0, 65% of naproxen and only 26% of gentamicin were released after 24 h, and changing pH to 1.2, release of gentamicin was totally within 1 h (Fig. 8.16).

The different release rates of drugs were adjusted by simulated physiological pHs. In acid medium, Si-OH groups dissociate and relase H^+ species, which, in turn, weaken gentamincin-glass interactions, leading to the relase of gentamicin from the pores of mesoporous biaoctive glasses. In basic medium, carboxyl groups of naproxen are ionized, and the migration of drug molecules from the inner to outer of nanomicelles is facilitated, leading to the release of naproxen. Therefore, the authors obtained a dual pH drug delivery system triggered by the pH of the surrounding environment [42].

8.5 Concluding Remarks

Composites made of bioactive glass and polymers have been successfully developed, and their efficacy has been demonstrated by either in vivo or in vitro tests. However, there is a lack of studies using humans, which would be addressed to the fact that these

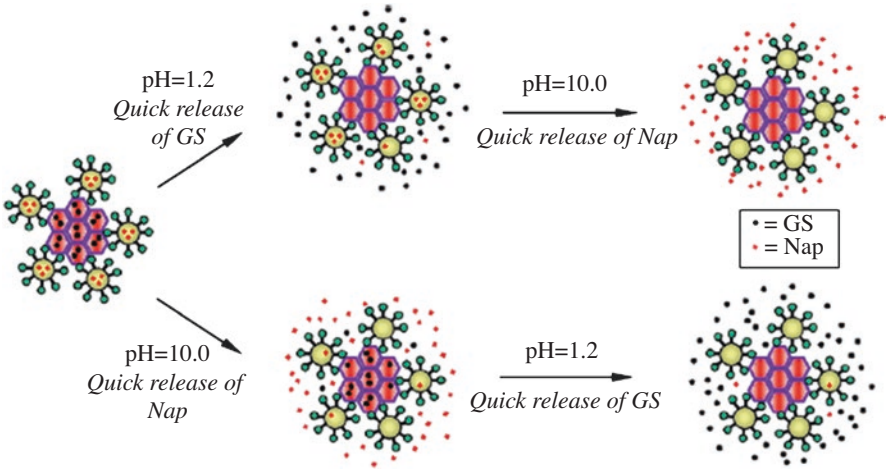

Fig. 8.16 Schematic illustration of the dual-drug delivery system, which demonstrated a pH-responsive drug release behavior (From: Xia et al. [42])

materials have been developed in the last 10 years. In addition, the development of new systems may step toward new stimuli-responsive composites due to their ability to deliver drugs on the desired site with much more specificity than other systems.

References

1. Arcos D, Rage CV, Vallet-Regi M. Bioactivity in glass/PMMA composites used as drug delivery system. Biomaterials. 2001;22:701–8.
2. Arcos D, Vallet-Regi M. Bioceramics for drug delivery. Acta Biomater. 2013;61(3):890–911.
3. Baino F, Fiorilli S, Vitale-Brovarone C. Bioactive glass-based materials with hierarchical porosity for medical applications: review of recent advances. Acta Biomater. 2016;42:18–32.
4. Bellucci D, Sola A, Gentile P, Ciardelli G, Cannillo V. Biomimetic coating on bioactive glass-derived scaffolds mimicking bone tissue. J Biomed Mater Res Part A. 2012;100A:3259–66.
5. Boccaccini AR, Erol M, Stark WJ, Mohn D, Hong Z, Mano JF. Polymer/bioactive glass nanocomposites for biomedical applications: a review. Compos Sci Technol. 2010;70:1764–76.
6. Borges R, Kai KC, Marchi J. Biocompatible glasses for controlled release technology. Marchi J Biocompatible glasses: from bone regeneration to cancer treatment. Advanced Structural Materials 53 (2016) Heidelberg, Springer
7. Ding H, Zhao C-J, Cui X, Gu Y-F, Jia W-T, Rahaman MN, Wang Y, Huang W-H, Zhang C-QA. Novel injectable borate bioactive glass cement as an antibiotic delivery vehicle for treating osteomyelitis. PLoS One. 2014;9(1):e85472. Available in: www.plosone.org
8. El-Fiqi A, Kim J-H, Kim H-W. Osteoinductive fibrous scaffolds of biopolymer/mesoporous bioactive glass nanocarriers with excellent bioactivity and long-term delivery of osteogenic drug. ACS Appl Mater Interfaces. 2015;7:1140–52.
9. El-Kady AM, Farag MM. Bioactive glass nanoparticles as a new delivery system for sustained 5-fluorouracil release: characterization and evaluation of drug release mechanism. J Nanomater. 2015;2015:839207, 11p.
10. Gabrielsson J, Green AR. Quantitative pharmacology or pharmacokinetic pharmacodynamic integration should be a vital component in integrative pharmacology. J Pharmacol Exp Ther. 2009;331:767–74. doi:10.1124/jpet.109.157172.

11. Gentile P, Bellucci D, Sola A, Mattu C, Cannillo V, Ciardelli G. Composite scaffolds for controlled drug release: role of the polyurethane nanoparticles on the physical properties and cell behavior. J Mech Behav Biomed Mater. 2015;44:53–60.
12. Gomes ME, Reis RL. Biodegradable polymers and composites in biomedical applications: from catgut to tissue engineering. Part 1 available systems and their properties. Int Mater Rev. 2004;49(5):261–73.
13. Habraken WJEM, Wolke JGC, Jansen JA. Ceramic composites as matrices and scaffolds for drug delivery in tissue engineering. Adv Drug Deliv Rev. 2007;59:234–48.
14. Hum J, Boccaccini AR. Bioactive glasses as carriers for bioactive molecules and therapeutic drugs: a review. J Mater Sci Mater Med. 2012;23:2317–33.
15. Izquierdo-Barba I, Vallet-Regí M. Mesoporous bioactive glasses: relevance of their porous structure compared to that of classical bioglasses. Biomed Glasses. 2015;1:140–50.
16. Jayalekshmi AC, Sharma CP. Gold nanoparticle incorporated polymer/bioactive glass composite for controlled drug delivery application. Colloids Surf B Biointerfaces. 2015;126:280–7.
17. Jia W-T, Xin Zhang X, Zhang C-Q, Liu X, Huang W-H, Rahaman MN, Day DE. Elution characteristics of teicoplanin-loaded biodegradable borate glass/chitosan composite. Int J Pharm. 2010;387:184–6.
18. Khan W, Challa VGS, Langer R, Domb AJ Biodegradable polymers for focal delivery system. Domb AJ, Khan W Focal controlled drug delivery. Springer New York (2014): 3–32.
19. Ladrón de Guevara-Fernández S, Ragel CV, Vallet-Reg M. Bioactive glass-polymer materials for controlled release of ibuprofen. Biomaterials. 2003;24:4037–43.
20. Lee JH, Yeo Y. Controlled drug release from pharmaceutical nanocarriers. Chem Eng Sci. 2015;125:75–84. doi:10.1016/j.ces.2014.08.046.
21. Li W, Nooeaid P, Roether JA, Schubert DW, Boccaccini AR. Preparation and characterization of vancomycin releasing PHBV coated45S5 Bioglass®-based glass–ceramic scaffolds for bone tissue engineering. J Eur Ceram Soc. 2014;34:505–14.
22. Ma J, Lin H, Li X, Bian C, Xiang D, Han X, Wu X, Qu F. Hierarchical porous bioactive glasses/PLGA-magnetic SBA-15 for dual-drug release. Mater Sci Eng. 2014;39:21–8.
23. Mabrouk M, Mostafa AA, Oudadesse H, Mahmoud AA, El-Gohary MI. Effect of ciprofloxacin incorporation in PVA and PVA bioactive glass composite scaffolds. Ceram Int. 2014;40(3):4833–45.
24. Mager DE. Quantitative structure–pharmacokinetic/pharmacodynamic relationships. Adv Drug Deliv Rev. 2006;58:1326–56. doi:10.1016/j.addr.2006.08.002.
25. Misra SK, Ansari T, Mohn D, Valappil SP, Brunner TJ, Stark WJ, Roy I, Knowles JC, Sibbons PD, Jones EV, Boccaccini AR, Salih V. Effect of nanoparticulate bioactive glass particles on bioactivity and cytocompatibility of poly(3-hydroxybutyrate) composites. J R Soc Interface. 2010;7:453–65.
26. Mondal T, Sunny MC, Khastgir D, Varma HK, Ramesh P. Poly (L-lactide-co-Єcaprolactone) microspheres laden with bioactive glass-ceramic and alendronate sodium as bone regenerative scaffolds. Mater Sci Eng C. 2012;32:697–706.
27. Nair LS, Laurencin CT. Polymers as biomaterials for tissue engineering and controlled drug delivery. Adv Biochem Eng Biotechnol. 2006;102:47–90.
28. Ordikhani F, Simchi A. Long-term antibiotic delivery by chitosan-based composite coatings with bone regenerative potential. Appl Surf Sci. 2014;317:56–66.
29. Patel KD, El-Fiqi A, Lee H-Y, Singh RK, Kim D-A, Lee H-H, Kim H-W. Chitosan–nanobioactive glass electrophoretic coatings with bone regenerative and drug delivering potential. J Mater Chem. 2012;22:24945–56.
30. Ramakrishna S, Mayer J, Wintermantel E, Leong KW. Biomedical applications of polymer-composite materials: a review. Compos Sci Technol. 2001;61:1189–224.
31. Rámila A, Del Real RP, Marcos R, Horcajada P, Vallet-Regí M. Drug release and in vitro assays of bioactive polymer/glass mixtures. J Sol-Gel Sci Technol. 2003;26:1195–8.
32. Reddy LH, Bazile D. Drug delivery design for intravenous route with integrated physicochemistry, pharmacokinetics and pharmacodynamics: illustration with the case of taxane therapeutics. Adv Drug Deliv Rev. 2014;71:34–57. doi:10.1016/j.addr.2013.10.007.

33. Rivadeneira J, Luz GM, Audisio MC, Mano JF, Gorustovich AA. Novel antibacterial bioactive glass nanocomposite functionalized with tetracycline hydrochloride. Biomed Glasses. 2015;1:128–35.
34. Tiwari G, et al. Drug delivery systems: an updated review. Int J Pharm Invest. 2012;2:2–11. doi:10.4103/2230-973X.96920.
35. Valliant EM, Jones JR. Softening bioactive glass for bone regeneration: sol–gel hybrid materials. Soft Matter. 2011;7:5083–95.
36. Vallet-Regí M, Balas F, Arcos D. Mesoporous materials for drug delivery. Angew Chem Int Ed. 2007;46:7548–58.
37. Vargas GE, Durand LAH, Cadena V, Romero M, Mesones RV, Mackovic M, Spallek S, Spiecker E, Boccaccini A, Gorustovich AA. Effect of nano-sized bioactive glass particles on the angiogenic properties of collagen based composites. J Mater Sci Mater Med. 2013;24:1261–9.
38. Wang F, Zhai D, Wu C. Multifunctional mesoporous bioactive glass/upconversion nanoparticle nanocomposites with strong red emission to monitor drug delivery and stimulate osteogenic differentiation of stem cells. Nano Res. 2016;9(4):1193–208.
39. Wers EH, Oudadesse H, Lefeuvre B, Merdrignac-Conanec O, Barroug A. Evaluation of the kinetic and relaxation time of gentamicin sulfate released from hybrid biomaterial Bioglass-chitosan scaffold. Appl Surf Sci. 2015;353:200–8.
40. Wilson CG. The need for drugs and drug delivery systems. In: Siepmann J, et al., editors. Fundamentals and applications of controlled release drug delivery, Advances in delivery science and technology; 2012. p. 3–18. doi:10.1007/978-1-4614-0881-9_9.
41. Wu C, Zhang Y, Ke X, Xie Y, Zhu H, Crawford R, Xiao Y. Bioactive mesopore-glass microspheres with controllable protein-delivery properties by biomimetic surface modification. J Biomed Mater Res A. 2010;95(2):476–85.
42. Xia W, Chang J, Lin J, Zhu J. The pH-controlled dual-drug release from mesoporous bioactive glass/polypeptide graft copolymer nanomicelle composites. Eur J Pharm Biopharm. 2008;69:546–52.
43. Yao Q, Nooeaid P, Roether JA, Dong Y, Zhang Q, Boccaccini AR. Bioglass®-based scaffolds incorporating polycaprolactone and chitosan coatings for controlled vancomycin delivery. Ceram Int. 2013;39(7):7517–22. doi:10.1016/j.ceramint.2013.03.002.
44. Yun YH, Lee BK, Park K. Controlled drug delivery: historical perspective for the next generation. J Control Release. 2015;219:2–7. doi:10.1016/j.jconrel.2015.10.005.
45. Zhang X, Zhang J, Shi BJ. Mesoporous bioglass/silk fibroin scaffolds as a drug delivery system: fabrication, drug loading and release in vitro and repair Calvarial defects in vivo. J Wuhan Univ Technol Mater Sci Ed. 2014;29(2):401–6.
46. Zhao L, Yan X, Zhou X, Zhou L, Wang H, Tang J, Yu C. Mesoporous bioactive glasses for controlled drug release. Microporous Mesoporous Mater. 2008;109:210–5.
47. Zhu M, Zhang L, He Q, Zhao J, Limin G, Shi J. Mesoporous bioactive glass-coated poly(L-lactic acid) scaffolds: a sustained antibiotic drug release system for bone repairing. J Mater Chem. 2011;21:1064–72.
48. Zhu M, Zhang J, Zhou Y, Liu Y, He X, Tao C, Zhu Y. Preparation and characterization of magnetic mesoporous bioactive glass/carbon composite scaffolds. J Chem. 2013; Article ID 893479, 11 p, 2013. doi:10.1155/2013/893479

Chapter 9
Restorative Dental Glass-Ceramics: Current Status and Trends

Maziar Montazerian and Edgar Dutra Zanotto

Abstract Most restorative dental materials are inert and biocompatible and are used in the restoration and reconstruction of teeth. Among them, glass-ceramics (GCs) are of great importance because they are easy to process and have outstanding esthetics, translucency, low thermal conductivity, high strength, chemical durability, biocompatibility, wear resistance, and hardness similar to that of natural teeth. However, research and development are still underway to further improve their mechanical properties and esthetics to enable them to compete with their current contenders (e.g., zirconia and hybrids) for posterior restorations. Throughout this chapter, we summarize the processing, properties, and applications of restorative dental glass-ceramics. Current commercial dental glass-ceramics are explained, and also selected papers that address promising types of dental glass-ceramics are reviewed. Finally, we include trends on relevant open issues and research possibilities.

Keywords Glass-ceramic • Dental • Mechanical properties • Biomedical

9.1 Introduction

The dental materials market is composed of several segments, including implants, cores, restorative materials, impression materials, dental cements, and bonding agents [1]. Most restorative dental materials are inert and biocompatible and are used in the restoration and reconstruction of teeth [1]. Among these materials, restorative dental glass-ceramics are of great importance because they are easy to process via advanced technology like CAD/CAM and have outstanding esthetics, translucency, low thermal conductivity, high strength, chemical durability, biocompatibility, wear resistance, and hardness similar to that of natural teeth [2–14].

M. Montazerian (✉) • E.D. Zanotto
Department of Materials Engineering (DEMa), Center for Research, Technology and Education in Vitreous Materials (CeRTEV), Federal University of São Carlos (UFSCar), São Carlos, SP, 13, .565-905, Brazil
e-mail: maziar_montaz@yahoo.com

G. Kaur (ed.), *Clinical Applications of Biomaterials*,
DOI 10.1007/978-3-319-56059-5_9

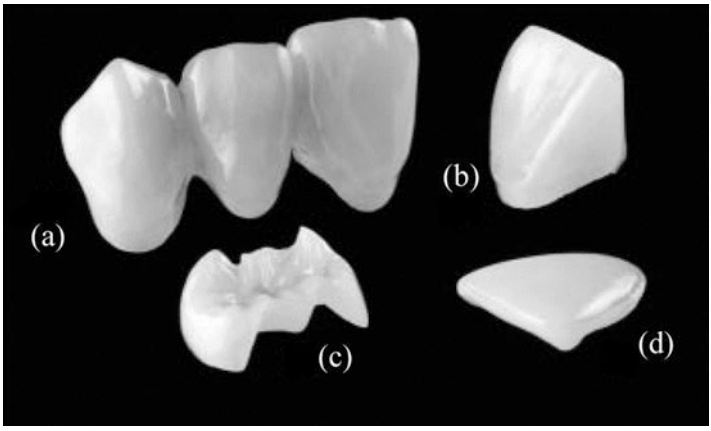

Fig. 9.1 Examples of restorative dental glass-ceramics: (**a**) three-unit bridge, (**b**) crown, (**c**) onlay, (**d**) veneer [14]

Glass-ceramics were discovered by D. R. Stookey at Corning Glass Works, USA, in 1953. They are polycrystalline materials produced by controlled heat treatment of certain glasses that contain one or more crystal phases embedded in a residual glass matrix [14]. The distinct chemical/physical properties of these phases and glass matrix have led to various unusual combinations of properties and applications in the domestic, space, defense, health, electronics, architecture, chemical, energy, and waste management fields. For instance, restorative dental glass-ceramics can mimic the tooth properties and are used as inlays, onlays, full crowns, partial crowns, bridges, and veneers [14]. Figure 9.1 shows a selection of these applications.

The basic stages of the synthesis of glass-ceramics, which involve melting, forming, and controlled heat treatment, are explained in many textbooks and review papers [11–14]. These stages for a controlled double-stage heat treatment are illustrated schematically in Fig. 9.2.

In general, dental technicians prepare dental glass-ceramics using the following four popular methods [13, 14]: lost-wax casting, heat-pressing, CAD/CAM (computer-aided design and computer-aided manufacturing), and pressureless sintering.

In *lost-wax* casting, a model of the restoration which is prepared by a dentist is shaped on the cast using a particular type of wax. The model is invested in special refractory materials. During firing stage, wax burnout takes place at 900 °C, and the ceramic mold is partially sintered. The material for fabrication of a glass-ceramic is supplied as a glassy ingot, which is located in a furnace specially designed for casting. The glass ingot becomes liquid during heating, and following a short time hold at 1300–1500 °C, the melt is forced into a mold by centrifugal force. The glass casting is retrieved, excess glass is polished off, and after the final controlled heat treatment and coloring processes, the glass-ceramic restoration is ready for clinical use [13, 14]. In the *heat-pressing* method, the dental technician uses as-prepared

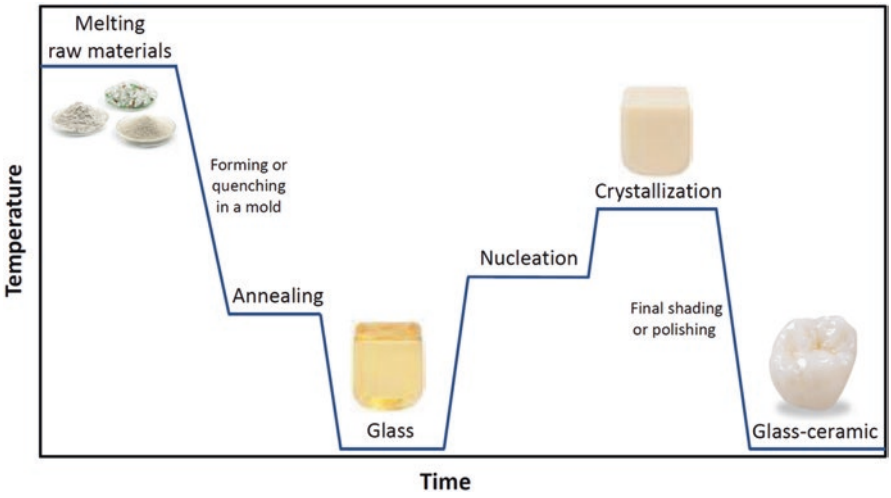

Fig. 9.2 Main stages in synthesis of glass-ceramics via controlled double-stage heat treatment

glass-ceramic ingot to produce the final restoration. First, a mold is produced via the previously described lost-wax procedure. The mold and glass-ceramic ingot are placed in a furnace specially designed for this processing method. Once the glass-ceramic ingot has become a very viscous liquid of approximately 10^{11} Pa.s, it is forced by an Al_2O_3 plunger (via application of a relatively low force of 200–300 N) into the hollow portion of the mold at approximately 1000–1200 °C. After the cylinder has adequately cooled, the investment material is removed from the glass-ceramic restoration by blasting it with silica sand, aluminum oxide, glass beads, or silicon carbide grit [13, 14]. In the third method, machinable restorative glass-ceramics are fabricated using a *CAD/CAM* system. Typically, CAD/CAM dental restorations are machined from solid blocks of partially crystallized glass-ceramics (containing a machinable crystal phase) that are subjected to further heat treatment to fully develop the glass-ceramic and achieve adequate properties and color that closely match the basic shade of the restored tooth [13, 14]. In the fourth method, known as *pressureless sintering*, a thin layer of glass-ceramic is veneered over restorative materials such as zirconia, metals, or glass-ceramics. Veneering is performed to adjust the final shade of the restoration. In general, a slurry containing glass-ceramic fine powders plus coloring agents is brushed over the surface. The artifact is held in a furnace at an appropriate temperature for the required time to sinter and crystallize the glass-ceramic and fuse it to the restoration [13, 14].

Glass-ceramics always contain a residual glassy phase and one or more embedded crystal phases. The crystal content varies between 0.5% and 99.5% but most frequently lies between 30% and 70%, and the remaining content is the residual glass phase. The types of crystals, crystal volume fraction, distribution in the matrix, and physicochemical properties of both the crystals and the residual glass control

the properties of glass-ceramics (including dental GCs), such as translucency, strength, fracture toughness, machinability, and chemical durability [13, 14]. These properties should meet the minimum requirements of the ISO 6872 standards [15]. Therefore, a dental glass-ceramic must have notably good chemical, mechanical, and optical properties comparable to those of natural teeth [15]. For example, the chemical durability must be higher than that of natural teeth. The mechanical properties of dental glass-ceramics such as fracture strength (σ), fracture toughness (K_{IC}), and wear resistance are highly important for avoiding material damage and breakage. In terms of optical properties, these materials must exhibit translucency, color, opalescence, and fluorescence similar to those of natural teeth [15].

An analysis of glass-ceramic research and commercialization suggests that glass-ceramics for biomedical applications are of great importance [3]. For example, our comprehensive review on the history and trends of commercial bioactive and inert glass-ceramics revealed that persistent competition exists among dozens of companies and academia to develop new bioactive dental glass-ceramics (BDGCs) or restorative dental glass-ceramics (RDGCs) [13]. Therefore, throughout this chapter, we summarize the properties and applications of commercial restorative dental glass-ceramic in Sect. 2. Recent researches and survival rates of commercial dental glass-ceramics are also reviewed. In this context, in Sect. 3, we report on selected valuable papers that have addressed promising types of dental glass-ceramics. Finally, we include future trends, open issues, and guidance from a materials engineering perspective in Sect. 4.

9.2 Commercial Dental Glass-Ceramics

Various types of restorative dental glass-ceramics have already reached the market. These materials and their typical characteristics are listed in Table 9.1. Additionally, the main mechanical properties, commercial names, and recommended applications for these materials are summarized in Table 9.2. More details on these products have been reported in our recent review paper [13] and Höland and Beall's book [14].

Hereafter, we review current status and recent developments regarding to the commercial restorative dental glass-ceramics (Tables 9.1 and 9.2).

9.2.1 Mica-Based Glass-Ceramics

Mica-based glass-ceramics such as Dicor® are old materials which are still used by dentists and technicians who know and trust them. However, a high risk of fracture is observed, and a relatively low mechanical strength and difficult processing conditions are the main drawbacks of mica-based glass-ceramics, which restrict their application and popularity [13, 14]. Therefore, numerous attempts in the 1990s and early 2000s were made to overcome the weakness of this material. Prof. Denry's

Table 9.1 Typical dental glass-ceramics and their representative compositions and main characteristics [13, 14]

Commercial dental	Typical glass composition (wt.%)												Fabrication procedures	Typical crystalline phase(s)
Glass-ceramics	SiO_2	Al_2O_3	MgO	CaO	Li_2O	Na_2O	K_2O	ZnO	ZrO_2	P_2O_5	CeO_2	Others		
Mica-based GCs	56–64	0–2	15–20	–	–	–	12–18	–	0–5	–	0.05	(4–9)F	Lost-wax casting and CAD/CAM	Mica ($KMg_3AlSi_3O_{10}F_2$)
Leucite-based GCs	59–63	19–23.5	–	0.5–3	–	3.5–6.5	10–14	–	–	–	0–1	(0–1) B_2O_3 (0–1.5) BaO (0–0.5) TiO_2	Heat-pressing and CAD/CAM	Leucite ($KAlSi_2O_6$)
Lithium disilicate GCs	57–80	0–5	0–5	–	11–19	–	0–13	0–8	0–8	0–11	–	–	Heat-pressing and CAD/CAM	Lithium disilicate (Li_2O-$2SiO_2$)
Apatite-based GCs	60–65	8–12	–	0–1	–	6–9	6–8	2–3	–	0–1	–	(0–1)F	Pressureless sintering	Fluorapatite ($Ca_5(PO_4)_3F$)
Lithium zirconium silicate GCs	42–59	3–5	–	–	7–15	2–3	4–5	–	15–28	4–15	–	–	Heat-pressing	Lithium phosphate (Li_3PO_4) and Zirconia (ZrO_2)

Table 9.2 Typical/approximate mechanical properties and recommended applications for dental glass-ceramics [14, 13]

Dental glass-ceramics	Bending strength (MPa)	Fracture toughness ($MPa.m^{1/2}$)	Young's modulus (GPa)	Vickers hardness (HV)	Thermal expansion coefficient ($\times 10^{-6}\ K^{-1}$)	Recommended applications	Typical commercial products (COMPANY NAME)
Mica-based GCs	150	1.4–1.5	70	3.5	7.2	Veneers/inlays/onlays/crowns	Dicor/Dicor MGC (DENTSPLY)
Leucite-based GCs	160	1.3	65	6.2	15–18.25	Veneers/inlays/onlays/crowns	Paradigm (3M), Lumineers (DEN-MAT), Ceramco/Cergo Kiss (DENTSPLY), IPS Empress (IVOCLAR), IPS InLine (IVOCLAR), EX-3 Press (NORITAKE), Optec OPC (PENTRON), Vitablocs (VITA)
Lithium disilicate GCs	350–450	2.3–2.8	70	6–6.5	10.5–11.5	Crown/bridge	Cameo (AIDITE), Celtra Duo (DENTSPLY), Obsidian (GLIDEWELL), IPS Empress II/Press/CAD (IVOCLAR), 3G (PENTRON), UpSil Press/CAD (UPCERA), Suprinity (VITA)
Apatite-based GCs	90	–	–	5.4	9.5	Veneered over restorative materials	IPS d.SIGN (IVOCLAR), IPS Eris (IVOCLAR), IPS e.max Ceram (IVOCLAR), IPS e.max ZirPress (IVOCLAR), Vitapm (VITA)
Lithium zirconium silicate GCs	160–260	1.1–1.9	55–59	5.3–6.3	9.4–9.7	Placed on ZrO_2 post and abutment	IPS Empress Cosmo (IVOCLAR)

group at Ohio State University pioneered modifications of the composition of Dicor® and improved its properties. The Denry group replaced potassium with lithium and developed tainiolite, a lithium-containing tetrasilicic fluormica ($KLiMg_2Si_4O_{10}F_2$) with improved thermal and mechanical properties [16]. By changing the glass composition, a new glass-ceramic was developed based on the crystallization of mica ($KNaMg_2Si_4O_{10}F_2$) and K-fluorrichterite ($KNaCaMg_5Si_8O_{22}F_2$) crystals, which were tougher (Sect. 9.3.1) [17–19]. Uno et al. [20] and Qin et al. [21] substituted K^+ or Na^+ with Ba^{2+} or Ca^{2+} as the interlayer ions of mica crystals, which resulted in the formation of high-strength mica glass-ceramics [20, 21]. Oriented mica glass-ceramics fabricated by hot-pressing or extrusion processes had higher strength and toughness than the conventional castable mica glass-ceramics that contained randomly oriented mica crystals with a house-of-cards structure [22–26]. In addition, these materials could be reinforced with ZrO_2 crystallized from the bulk glass [27–31]. It has been reported that a calcium mica-based nanocomposite containing nano-size (20–50 nm) tetragonal-ZrO_2 particles exhibits notably a high flexural strength (500 MPa) and fracture toughness (3.2 $MPa.m^{½}$) [27]. The excellent mechanical performance is related to crack deflection by mica plates and ZrO_2 particles [27]. According to Serbena et al. [32], the main toughening mechanisms in glass-ceramics (without the chance of phase transformation toughening) are caused by crack bowing and trapping (for low crystallized volume fractions), as well as by the greater elastic modulus and fracture toughness of the crystal precipitates. All of these modifications improved the properties of mica-based glass-ceramics, but they still could not compete with alternative materials such as lithium disilicate GC to survive in this competitive market.

9.2.2 Leucite-Based Glass-Ceramics

Leucite glass-ceramics are used as veneers, inlays, onlays, and anterior and posterior crowns, but their strength is insufficient for fixed posterior bridges. For bridges, this type of GC is veneered onto a flexible, tough metallic framework [14]. However, the risk of the glass-ceramic pulling away from the metal surface still exists. Therefore, sintering should be carefully performed within a temperature range of 550–900 °C, and shrinkage must be controlled to prevent tearing [33, 34]. Michel et al. [35] attempted to minimize this risk by developing nano-coatings on leucite-fluorapatite glass-ceramic particles prior to sintering. The coating influences the rheology of the slurry and the properties of the veneer. The following two substances were chosen for the coatings: (a) a combination of inorganic chemicals ($ZnCl_2$, $AlCl_3$, or BCl_3) and polyethylene glycol (PEG) and (b) an exclusive polymer. Both groups of materials positively improved the sintering properties of the glass-ceramics and suppressed extensive tearing [35]. A nano-sized leucite glass-ceramic was further developed by Theocharopoulos et al. [36], who sintered nano-sized commercial glass particles (Ceramco® and IPS Empress®) prepared by high-energy milling to trigger surface crystallization of leucite crystals at the

nanoscale. As a result, these new glass-ceramics showed an increased leucite crystal number at the nanoscale (median crystal sizes of ~0.05 μm^2). These new glass-ceramics had a higher mean bending strength than the competing commercial materials. The mean bending strengths were, e.g., 255 ± 35 MPa for the nano-leucite glass-ceramic, 76 ± 7 MPa for Ceramco® (restorative porcelain), and 166 ± 31 MPa for IPS Empress® (Leucite GC) [36]. More recently, Aurélio et al. [37] observed an increased bending strength and decreased surface roughness for a leucite-based glass-ceramic sintered at a higher sintering temperature after machining. The crystalline structure was not modified. However, increased sintering time and firing below T_g significantly reduced the fracture strength [37]. Leucite-based glass-ceramics are also well suited for the CAD/CAM process developed by Ivoclar Vivadent AG. This glass-ceramic consists of a total of four to eight main and intermediate layers [38].

In 2000–2011, novel low-wear/high-strength leucite-based glass-ceramics were developed at Queen Mary University by Dr. Cattell's team to prevent fracture and wear of dental ceramic restorations. Dr. Cattell began his research to overcome problems related to the brittle fracture of porcelain restorations and their poor survival rates and intended to develop leucite-based glass-ceramics by heat extrusion. This novel method led to a homogenous distribution of fine crystals and increased reliability (Weibull modulus, $m = 9.4$, and $\sigma = 159$ MPa) compared with commercial materials ($m = 6.1$ and $\sigma = 120$ MPa, Empress®) [39]. Additionally, controlling the leucite crystal size to 0.15 ± 0.09 μm^2 was the key to enhancing the properties of Dr. Cattell's glass-ceramic [40, 41]. The Cattell team also focused on the fundamental aspects of nucleation and crystal growth of leucite glass-ceramics and powder processing to control surface crystallization and produce first fine and later nanoscale leucite glass-ceramics [42]. These studies were critical to reduce the size of the leucite crystals and had enormous benefits in terms of reduced enamel wear, improved esthetics, and increased strength. Leucite glass-ceramics were subsequently produced with significantly higher flexural strength ($\sigma > 250$ MPa), reliability ($m = 12$), and lower enamel wear [43, 44]. This material could be processed using heat extrusion, CAD-CAM, and 3D printing and was later commercialized by Den-Mat Holdings as an esthetic restorative material with the name of Lumineers® (Table 9.2).

9.2.3 Lithium Disilicate Glass-Ceramics

Lithium disilicate (LS2) glass-ceramics are the third generation of dental glass-ceramic, which were introduced for single- and multiple-unit frameworks. These materials are available as a heat-pressable ingot and a partially crystallized machinable block and are successfully used to produce a crown or bridge framework with mechanical properties that were almost three times higher than those of the leucite-based glass-ceramic. Currently, lithium disilicate glass-ceramic is the most popular restorative glass-ceramic in the field of dental materials, and numerous researches

are underway to further improve their properties [13, 14]. Chung et al. [45] have reported that repeated heat-pressing can produce a statistically significant increase in the flexural strength of lithium disilicate glass-ceramic (IPS Empress® II). An interesting study by Lien et al. [46] revealed that intermediate heat treatments in temperature ranges below 590 °C, between 590 and 780 °C, and above 780 °C can influence the final microstructure and properties of the lithium disilicate glass-ceramic (IPS e.max® CAD). The finely knitted mesh of Li_2O-SiO_2 predominated below 590 °C; spherical-like phases of Li_2O-SiO_2, Li_2O-$2SiO_2$, and Li_3PO_4 emerged between 590 and 780 °C; and irregularly oblate crystals of Li_2O-$2SiO_2$ arose above 780 °C. At each of those three evolutionary stages, the glass-ceramic formed through controlled crystallization often yielded a microstructure that possessed interesting and sometimes peculiar combinations of properties. Additionally, the growth of Li_2O-$2SiO_2$ crystals within the IPS e.max® CAD blocks was independent of the overall heating time but dependent on a minimum temperature threshold (780 °C). Groups of samples heated above the minimum temperature threshold (780 °C) up to 840 °C exhibited enhanced flexural strength, fracture toughness, and elastic modulus compared with those of groups that were intentionally not heated above 780 °C [46].

Recent research by Al Mansour et al. [47] showed that spark plasma sintering (SPS) can be used to refine the microstructure of lithium disilicate glass-ceramics (IPS e.max® CAD). Densification by SPS results in textured and fine nanocrystalline microstructures. This group believes that SPS generated glass-ceramic might have unique properties and could be useful in the production of CAD/CAM materials for dentistry [47].

Although P_2O_5 and ZnO initiate microphase separation, which induces the crystallization pathways and kinetics, it appears that ZrO_2 has a more beneficial effect on the crystallization and strengthening of lithium disilicate glass-ceramics [48, 49]. New commercial lithium disilicate glass-ceramics for CAD/CAM are advertised as tougher and more reliable due to the presence of at least 10 wt% ZrO_2 dissolved in the residual glass. These glass-ceramics (Table 9.2) are Celtra Duo® (Dentsply), IPS e.max CAD® (Ivoclar), and Suprinity® (Vita). Zirconia influences the crystallization by hampering crystal growth. With increasing ZrO_2 content, the crystals become smaller. By increasing the crystallization temperature, the crystal growth decreases, as expected. The translucency of the glass-ceramic can be adjusted by adding ZrO_2. A highly translucent glass-ceramic with a contrast ratio of ~0.4 and high three-point bending strength (700–800 MPa) was developed [48].

The current dental glass-ceramics still show a lower load-bearing capacity than polycrystalline ceramics (e.g., Al_2O_3 and ZrO_2); therefore long-span restorative and high-stress areas (e.g., three-unit bridges, implant abutments, etc.) are restricted to ZrO_2, Al_2O_3, or metals. A brand new strategy for strengthening these materials was pursued by Belli et al. [50] to form reinforcing sites by microstructural design of LS2 GC. Such approach demonstrated a potential for application with lithium disilicate (LS2) glass-ceramics, which contain needlelike $Li_2Si_2O_5$ crystals that deflect propagating cracks. By a special process of heat-pressing of the glass melt through specifically oriented injection channels, crystals were aligned in patterns that led to

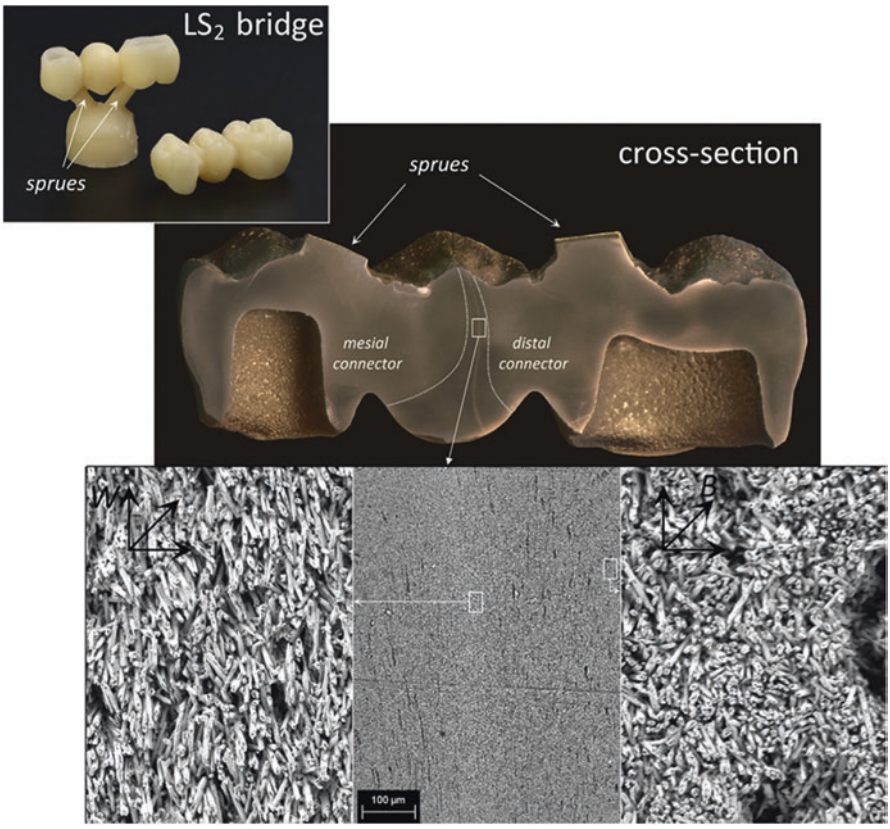

Fig. 9.3 Cross section of a LS2 dental bridge showing the crystal alignment pattern. Different crystal orientations can be distinguished on the gold-sputtered cross section from the different "shadows" on the surface. An S-shaped bundle of parallel crystals formed orthogonal to the long axis of the bridge to the *left* of the distal connector, *right* at the midspan. Around it, in the area defined by the *dotted lines*, crystals follow a distinct orientation due to the convex geometry of the artificial tooth pontic. Mixed orientation patterns formed above the distal connector, leading to negative crack deflection angles and wavy fracture surfaces [50]

high mechanical anisotropy (Fig. 9.3) [50]. A strong anisotropic fracture behavior was obtained with the LS2 glass-ceramic through local crystal alignment, leading to fracture energies higher than for the isotropic 3Y-TZP ceramic (Fig. 9.4) [50].

9.2.4 Apatite-Based Glass-Ceramics

To further improve the translucency and shade match and to adjust the wear behavior to that of the natural tooth, lithium disilicate, leucite glass-ceramics, and sintered ZrO_2 are veneered with an appropriate apatite-containing glass-ceramic using a

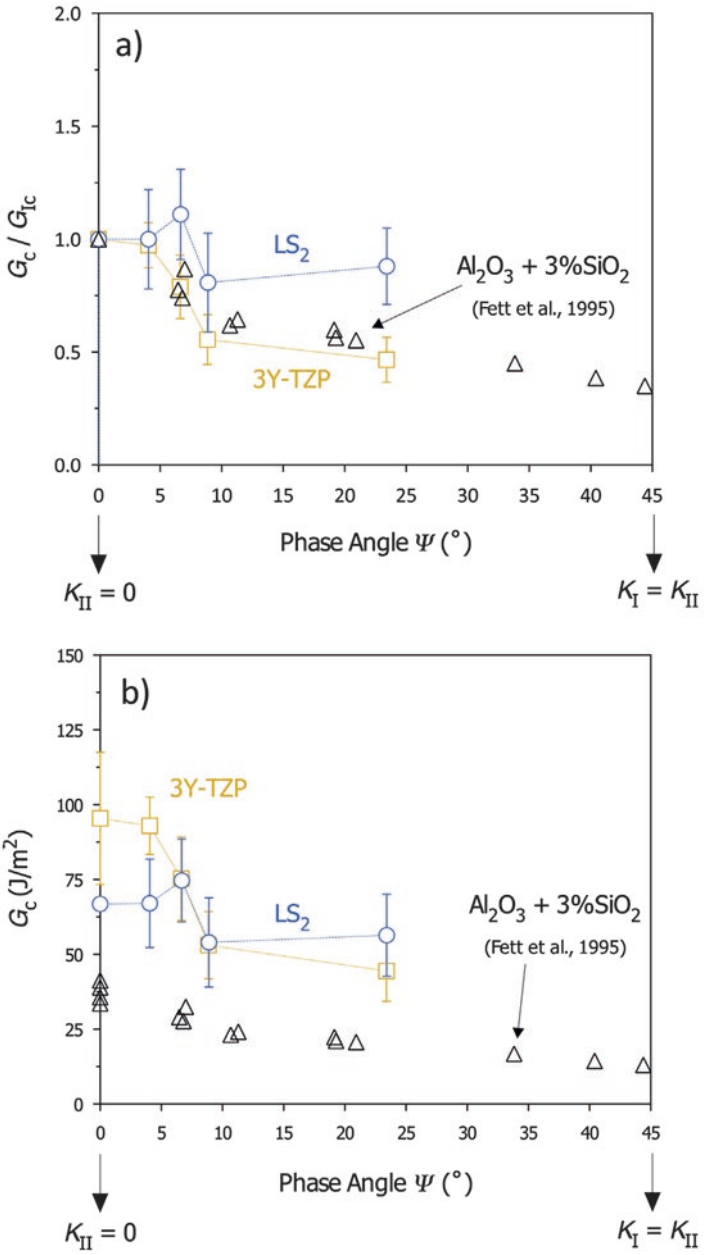

Fig. 9.4 Plots of the fracture energy G versus the phase angle ψ. In (**a**) G was normalized by the mode-I fracture toughness G_{IC} to illustrate the increase or decrease in energy to fracture. In (**b**) the total energy consumed in the fracture was plotted and showed that for notches submitted to higher phase angles, the energy to fracture of the LS2 glass-ceramic became comparable and even surpassed that of the 3Y-TZP ceramic [50]

pressureless sintering process. These glass-ceramics are offered in powdered form for the slurry layering technique and is available in all classical tooth shades [13, 14]. The properties, applications, and typical compositions of these glass-ceramics are summarized in Tables 9.1 and 9.2. Through the development of apatite-based glass-ceramics, researchers reached a stage at which it became possible to produce restorations that contain building blocks in the form of needlelike apatite, similar to those of natural teeth. The needlelike apatite crystals positively influence the esthetic properties and various mechanical parameters of the material. The base glass also contains fluorine, which induces the formation of fluorapatite ($Ca_5(PO_4)_3F$) and enhances the chemical properties of the material (Table 9.1). Therefore, this glass-ceramic is available (Table 9.2) as a sintered glass-ceramic to replace dentin, reproduce the incisal area, and create specific optical effects (e.g., opalescence over a metallic substrate) [13, 14].

9.2.5 Lithium Zirconium Silicate Glass-Ceramic

After the development of the ZrO_2 root canal post and implant abutment, a restorative material was required that can be placed on ZrO_2. To fulfill this need, a lithium zirconium silicate glass-ceramic was developed by Schweiger et al. [51] to adjust the coefficient of linear thermal expansion to that of ZrO_2 and achieve a certain degree of opacity. This glass-ceramic is layered on the ZrO_2 post via heat-pressing and is available in the market (Table 9.2). The improved mechanical properties of the glass-ceramic containing 20 wt% ZrO_2 make this material appropriate for use in the posterior region because the esthetics and the opacity of the glass-ceramic play a less important role in this region of the mouth. Finally, the coefficients of linear thermal expansion for glass-ceramics are somewhat lower than that of the ZrO_2 post. As a result of this adjustment, a crack-free bond between the glass-ceramic and the ZrO_2 abutment is achieved [14, 51].

9.2.6 Survival Rates of Dental Glass-Ceramics

A recent comprehensive review and meta-analysis revealed that survival rates for ceramic inlays, onlays, and overlays including glass-ceramics were between 92% and 95% at 5 years (n = 5811 restorations) and were 91% at 10 years (n = 2154 restorations). Failures were related to fractures/chipping (4%), followed by endodontic complications (3%), secondary caries (1%), debonding (1%), and severe marginal staining (0%). Odds ratios (95% confidence intervals) were 0.19 (0.04–0.96) and 0.54 (0.17–1.69) for pulp vitality and type of tooth involved (premolars vs. molars), respectively. Ceramic inlays, onlays, and overlays showed high survival rates at 5 years and 10 years, and fractures were the most frequent cause of failure [52]. Furthermore, Fradeani et al. [53] reported on the survival rate of leucite

glass-ceramic crowns. Crowns were studied over periods ranging from 4 to 11 years. The probability of survival of 125 crowns was 95.2% at 11 years (98.9% in the anterior segment and 84.4% in the posterior segment). Only six crowns had to be replaced. Most of the 119 successful crowns were rated as excellent. According to Kaplan-Meier method, the cumulative survival rate of lithium disilicate crowns is 94.8% after 9 years [54], but only 71.4% of three-unit bridges survive after 10 years [55]. Therefore, crowns made of a lithium disilicate framework can be safely used in the anterior and posterior regions [54], but bridges present a higher risk of fracture than metal-porcelain prostheses or other more recently developed ceramic materials, such as zirconia and alumina [55, 56]. Among the machinable dental glass-ceramics, LS2 has shown significant superior clinical survival rates. This has been shown from a recent database retrospective cohort study performed by Belli et al. [57]. They connected clinical reality and structural investigations on reasons to fracture. They investigated the clinical lifetime of nearly 35,000 all-ceramic restorations placed over 3.5 years (Fig. 9.5), from which 491 fractures were reported. The study also pointed to a trend of clinicians replacing the use of leucite-based glass-ceramics toward the LS2 glass-ceramics for inlays, onlays, crowns, and ZrO_2-supported bridges. They concluded that LS2 glass-ceramics increasingly gain acceptability and use within clinical indications [57].

9.3 Miscellaneous Dental Glass-Ceramics

As described previously, dental glass-ceramics are attractive materials for dental restoration. However, compared with those of metals and ceramics, the low mechanical strength and fracture toughness of these materials restrict their application for long-term high load-bearing posterior restorations. Therefore, continuous attempts have been made to develop new glass-ceramics with improved mechanical properties and good clinical performance. Some of these glass-ceramics are fluorrichterite, fluorcanasite, diopside, and apatite-mullite glass-ceramics.

9.3.1 Fluorrichterite Glass-Ceramics

The main characteristics of fluorrichterite glass-ceramics are their high fracture toughness ($K_{IC} > 3$ MPa.m^{½}), optical translucency, and high resistance to thermal shock [14]. High-performance laboratory tableware and domestic kitchenware are manufactured from these glass-ceramics [14]. In 1999, Denry and Holloway [17] began to develop fluorrichterite glass-ceramic for use in dentistry and first investigated the role of MgO content in a glass composition of $67.5SiO_2$–$2Al_2O_3$–12MgO–$9CaF_2$–$4Na_2O$–$3.5K_2O$–$1Li_2O$–1BaO (wt%). The hypothesis was that increasing the amount of magnesium might promote the crystallization of double-chain silicate (amphibole) crystals. The high fracture toughness of amphibole-based

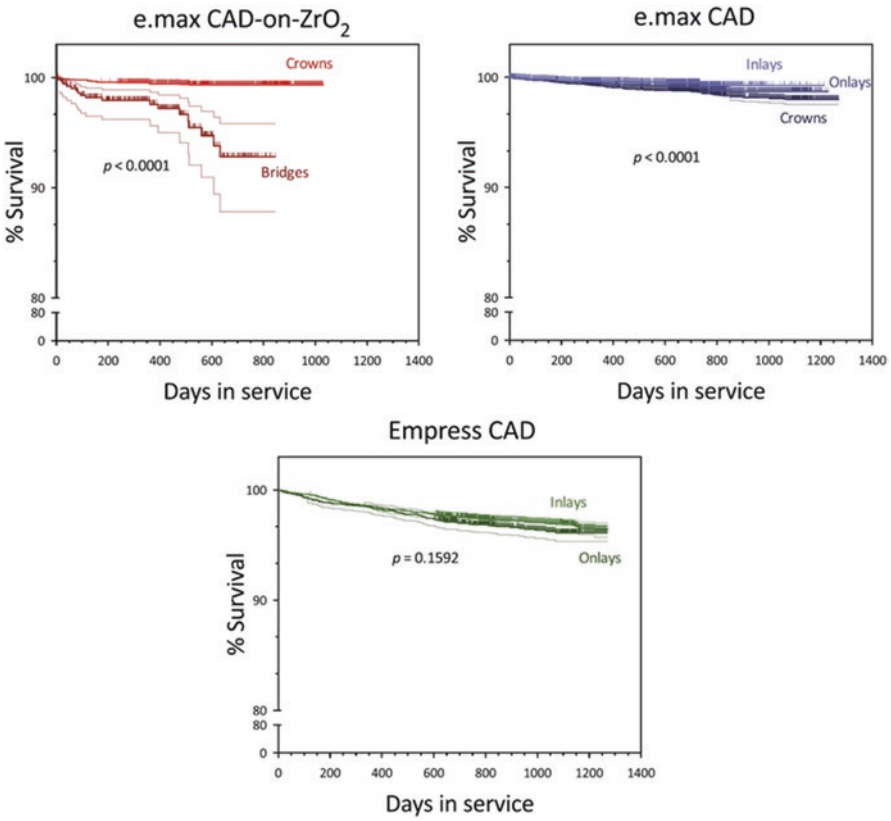

Fig. 9.5 Kaplan-Meier survival curves comparing the restoration type for the same restorative system. IPS e.max CAD and IPS Empress CAD are lithium disilicate and leucite-based glass-ceramics, respectively [57]

glass-ceramics is due to the random orientation of the interlocked crystals, which gives rise to crack deflection [14]. Denry and Holloway also found that in a glass containing 18 wt% MgO, both mica and fluorrichterite are crystallized. In this material, the microstructure consists of interlocked acicular crystals of fluorrichterite (5–10 μm) and mica, and this structure promoted crack deflection and arrest [17]. Furthermore, this same research group increased the sodium amounts in a base glass composition of $57.7SiO_2$–$23.9MgO$–$6CaF_2$–$0Na_2O$–$8.5K_2O$–$3Li_2O$–$1BaO$ (wt%). Increasing sodium content led to a decrease in all transformation temperatures, including the onset of melting. A decrease in the viscosity of the glass-ceramics was observed for the glass-ceramic composed of fluorrichterite and mica and was retained after heat treatment at 1000 °C for 4 h [18]. The glass-ceramic containing 1.9 wt% sodium had the highest mean fracture toughness of 2.26 ± 0.15 MPa.m^{½}, which was not significantly different from that of the control material (OPC®, Pentron) [19]. The microstructure of this glass-ceramic exhibited

prismatic fluorrichterite and interlocked sheetlike mica crystals, which deflect propagating cracks. Crystallization of fluorrichterite might account for the significant increase in fracture toughness compared with that of mica-based glass-ceramics (as an example) [19]. In Fig. 9.6, crack deflection is observed at each interaction between the crack front and the fluorrichterite crystals [19].

The effect of crystallization heat treatment on the microstructure and biaxial strength of fluorrichterite glass-ceramics was also reported by the same authors [58], who observed twofold variation in the biaxial flexural strength of fluorrichterite glass-ceramics depending on the temperature and duration of the crystallization heat treatment. This result was believed to be due to the formation of a low-expansion surface layer composed of roedderite ($K_2Mg_5Si_{12}O_{30}$). The expansion mismatch promoted the development of surface compressive stresses and efficiently increased the flexural strength of the glass-ceramic. Higher heat treatment temperatures or longer durations likely led to an increase in thickness of this layer, thereby reducing the intensity of the surface compressive stresses and causing a decrease in strength. In addition, these conditions caused a coarsening of the microstructure

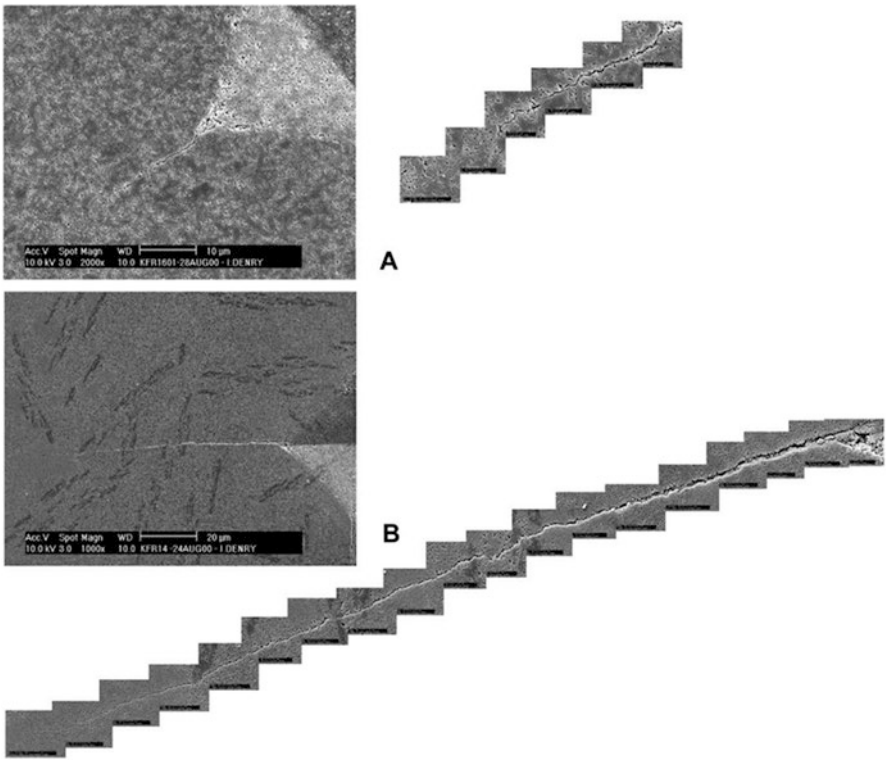

Fig. 9.6 Scanning electron micrographs of Vickers indentation-induced cracks in the fluorrichterite glass-ceramic containing (**a**) 1.9 wt% sodium and (**b**) the glass-ceramic containing 3.8 wt% sodium [19]

that could also weaken the glass-ceramic by reducing the number of possible crack-crystal interactions [58]. The significance and long-term goal of Denry and Holloway's work was to develop a dental glass-ceramic processed at low temperature, e.g., with heat-pressing, that retained the fluorrichterite microstructure and excellent mechanical properties. Later on, other scientists also attempted to crystallize different chain silicate minerals, such as diopside or wollastonite, in the vicinity of mica crystals to benefit from their toughening ability [59–61]. Almuhamadi et al. [62] and Sinthuprasirt et al. [63] also prepared diopside and leucite-diopside glass-ceramics, respectively, to produce novel strong and thermally compatible veneers for zirconia restoration to overcome chipping and failure issues. The improvements were significant, but it appears that these materials have not yet been considered for clinical applications.

9.3.2 Fluorcanasite Glass-Ceramics

Fluorcanasite ($Ca_5Na_4K_2Si_{12}O_{30}F_4$) is another double-chain silicate mineral which its crystallization in glasses with an acicular interlocked microstructure (Fig. 9.7) gives rise to strength and fracture toughness of the resulting glass-ceramics [14].

A number of initial studies were performed by Anusavice's and Noort's team at Florida and Sheffield Universities, respectively, to evaluate potential application of fluorcanasite glass-ceramics in restorative dentistry. In the period 1997–2003, van Noort et al. [65] demonstrated that fluorcanasite glass-ceramics derived from the base glass composition of $60SiO_2$–$10Na_2O$–$5K_2O$–$15CaO$–$10CaF_2$ (wt%) show promising properties and can be fabricated using conventional routes [64–66]. At the same time, Anusavice and Zhang [67] reported that the chemical durability of fluorcanasite glass-ceramics is not adequate for dental applications and they

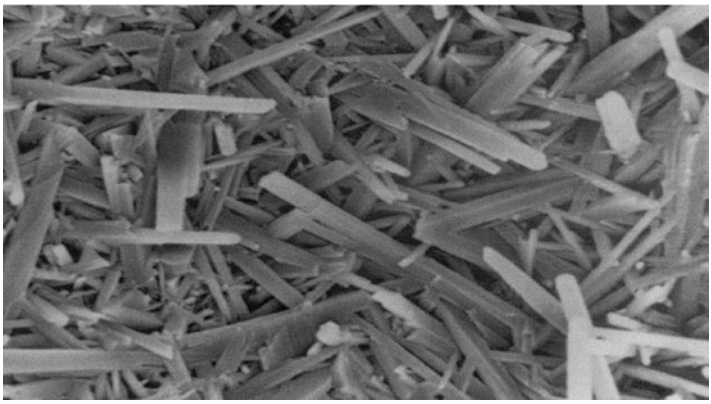

Fig. 9.7 SEM micrograph of a fracture surface of the canasite glass-ceramic (×2500 magnification) [64]

were not able to improve either chemical durability or mechanical strength via the addition of Al_2O_3 up to 15 wt%. It was observed that increased Al_2O_3 content significantly affected the crystal size, crystal shape, aspect ratio, and crystal aggregation characteristics of the fluorcanasite glass-ceramics [67, 68]. In an attempt to control the solubility of this glass-ceramic, systematic additions of SiO_2 and $AlPO_4$ were tested by Bubb et al. [69]. The solubility was reduced from 2359 to 624 μg/cm^2 (according to ISO 6872). An initial increase was observed in biaxial flexural strength, i.e., 123–222 MPa with small additions, but larger additions reduced the strength to 147 MPa. These findings were attributed to an increased volume fraction of residual glassy matrix [69]. Stockes et al. [70] attempted to further reduce the chemical solubility of these glass-ceramics by investigating the mixed alkali effect due to variation in the K and Na contents. They found that by changing the alkali ratio of the base glass composition (the above composition) from K/(K+Na) = 0.33 to 0.47, it was possible to significantly reduce the chemical solubility of the glass-ceramic. This glass-ceramic exhibited a minimum chemical solubility of 650 μg/cm^2 at a composition of K/Na = 7/8. This solubility is acceptable for dental core ceramics, which should have a solubility of less than 2000 μg/cm^2, but it is not suitable for direct contact with the mouth environment, which requires a solubility of less than 100 μg/cm^2 [15, 70]. Finally, Pollington and van Noort [71] managed to adjust the chemical solubility and mechanical properties of the glass-ceramic with ZrO_2 addition, and their optimum composition approximately contained $61SiO_2$–$6Na_2O$–$8K_2O$–$11CaO$–$12CaF_2$–$2ZrO_2$ (wt%). The appropriate melting schedule for this composition was found to be 1 h of holding and stirring at 1350 °C. The heat treatment schedule of 2 h nucleation and 2 h crystallization produced the greatest amount of the fluorcanasite phase. The glass-ceramic had an acceptable chemical solubility (722 ± 177 μg/cm^2) and high biaxial flexural strength (250 ± 26 MPa), fracture toughness (4.2 ± 0.3 MPa.m^{½}), and hardness (5.2 ± 0.2 GPa) and had the potential for use as a core material for veneered resin-bonded ceramic restorations. Furthermore, this fluorcanasite glass-ceramic was found to be machinable using standard CAD/CAM technology and demonstrated a high degree of translucency [71]. It has also been proved that this glass-ceramic forms a sufficient and durable bond when bonded with a composite resin, without the need for acid etching with HF solution [72]. More recently, Eilaghi et al. [73] have shown that fluorcanasite glass-ceramic can be pressureless sintered at 1000 °C to an appropriate relative density of 91.3 ± 0.1% and desirable mechanical properties (σ = 137 ± 7 MPa and K_{IC} = 2.6 ± 0.1 MPa.m^{½}) [73].

9.3.3 Apatite-Mullite Glass-Ceramics

In the mid-1990s, Hill et al. [74] introduced apatite-mullite glass-ceramics as potential dental or bioactive glass-ceramics. The optimum glass composition was $33.33SiO_2$–$11.11P_2O_5$–$22.22Al_2O_3$–$22.22CaO$–$11.11CaF_2$ in mol%. This glass-ceramic, which was heat treated at approximately 900 °C, consisted of elongated

fluorapatite ($Ca_{10}(PO_4)_6F_2$) and mullite ($3Al_2O_3.2SiO_2$) crystals. Crystallization occurred by an internal nucleation mechanism that involved prior amorphous phase separation. A fracture toughness value greater than 3 MPa.m^{½} was reported [74, 75]. Later, Gorman and Hill [76, 77] attempted to develop a dental restoration material using a similar glass-ceramic via the heat-pressing technique by reducing the Al_2O_3 content and envisioning that this reduction could adjust the viscosity for heat-pressing [76, 77]. The conclusion of these researchers was that glasses with various Al_2O_3 contents are easily formed and crystallized to fluorapatite. Mullite and anorthite were formed as a second crystal phase. However, crystallization during heat-pressing resulted in a loss of control of the process but was not considered detrimental if the future growth of these crystals could be controlled [76]. A fracture toughness of 2.7 ± 0.4 MPa.m^{½} was reported for the glass-ceramic containing $32.6SiO_2$–$10.9P_2O_5$–$20.3Al_2O_3$–$32.6CaO$–$3.6CaF_2$ (mol%) that was heat treated for 8 h at 1150 °C. The highest flexural strength of 194 ± 75 MPa was obtained by heat-pressing the same glass for 1 h at 1150 °C. Increasing the holding time increased the crystal size and the extent of microcracking in this glass-ceramic, thus lowering the flexural strength. Microcracks appeared to increase the fracture toughness of the glass-ceramics, probably by a crack termination mechanism [77]. However, the relatively high solubility of apatite-mullite glass-ceramics was always the main issue [78]. Consequently, Fathi et al. [79] evaluated the effect of varying the CaF_2 content on the chemical solubility. They increased the CaF_2 in the initial glass from 4 to 20 mol%. All compositions easily formed glasses and, upon heat treatment, crystallized to form apatite and apatite-mullite. Increasing the CaF_2 content led to an increase in bending strength but also increased the solubility. The chemical solubility (150–380 μg/cm^2) was still higher than that of the control glass-ceramic (IPS Empress® II, 78 μg/cm^2) but was acceptable for a dental core ceramic [79, 80]. A maximum bending strength of 157 ± 15 MPa was reported for a sample containing 20 mol% CaF_2 [80]. These same researchers also added TiO_2 and ZrO_2 to control the mechanical properties and solubility [81, 82], and their studies demonstrated that up to 1 mol% of ZrO_2 and TiO_2 were effective for controlling the solubility and mechanical properties of these apatite-mullite glass-ceramics [81]. The lowest chemical solubility and highest bending strength were 204 ± 29 μg/cm^2 and 174 ± 38 MPa, respectively [81]. However, increasing the TiO_2 concentration to greater than 2.5 wt% led to a significant increase in solubility and reduced bending strength [82]. Mollazadeh et al. [83] showed that 3 wt% TiO_2 and BaO addition increased the bending strength and fracture toughness of apatite-mullite glass-ceramics. However, 3 wt% ZrO_2 and an extra amount of SiO_2 had no significant effect [83]. The mechanical properties of the resulting glass-ceramics after temperature changes (5–60 °C) in aqueous media remained nearly unchanged for the samples containing TiO_2 and ZrO_2, whereas a high reduction was observed with the addition of BaO and extra amounts of SiO_2. Furthermore, after immersion in hot water, the concentration of Ca^{2+} and F^- ions released from samples with BaO or with excess amounts of SiO_2 was higher than those of TiO_2- and ZrO_2-containing glass-ceramics [84]. It is apparent that these apatite-mullite glass-ceramics are promising restorative materials, but their high chemical solubility still restricts their application for use in the mouth environment. Therefore, these materials must be first considered for core buildup.

9.4 Conclusions and Trends

Restorative dental materials are moving from metal alloy-containing to all-ceramic restorations, and this chapter demonstrates that glass-ceramics work well as all-ceramic restorations. The following ten topics warrant further research [13]:

1. Research and development are underway to further improve the fracture toughness and esthetics of dental glass-ceramics to enable them to compete with their current contenders (e.g., zirconia and hybrids) for posterior restorations. We agree with Höland et al. [85] that comprehensive knowledge of toughening mechanisms is a necessary step to open new directions for development of tough glass-ceramics. Therefore, future research activities should be focused on gaining a better understanding of the mechanisms of toughening, such as transformation toughening, bridging, microcracking, and pulling out, that can be stimulated by controlled crystallization of different crystals with a variety of morphologies and microstructures. Additionally, various coloring agents and pigments should be deeply and thoroughly tested to adjust the shades and esthetics of glass-ceramics. On the other hand, the morphology of crystals from the nano- to microscale, which can be controlled by precise adjustment of the chemical composition and crystallization process, might strongly influence their optical properties, but the published information on these topics is scarce.
2. New methods (e.g., meta-analyses) can be used to expand the range of glass-ceramic composition. For instance, it was recently demonstrated that new nano-glass-ceramics with a notably high ZrO_2 content can be synthesized using sol-gel methods [86, 87]. The technology required to achieve this goal could rely on chemistry-based and applied nanotechnology.
3. New or improved sintering/crystallization processes, such as microwave heating [88], laser crystallization [89, 90], spark plasma sintering [47, 91], biomimetic assemblage of crystals [92], textured crystallization, and electron beam crystallization, should be further developed.
4. Chemical strengthening of RDGCs by ion exchange, as tested by Kawai et al. [93] and Fischer et al. [94–96], is a promising route and should be further pursued.
5. Glass-ionomer composites are widely used in restorative dentistry. We believe that glass-ceramic powders, including bioactive formulations, can also be used as inorganic fillers in these composite restoratives. In at least two research studies, Liu et al. [97] and Mollazadeh et al. [98] used porous mica-fluorapatite and fluorapatite-mullite glass-ceramic fillers to reinforce dental resin-based composites.
6. New coating technologies and the properties of coatings on dental implants should be improved. For example, degradation over time, which leads to detachment of coating, is a noticeable drawback.
7. The development of restorative glass-ceramics or composites which in contact with bone and surrounding tissues show a cement-like behavior and facilitate biological surface responses for marginal attachment is another challenging field of research.

8. Glass-ceramic matrix composites have been rarely investigated for restorative dentistry and demand additional attention.
9. Dental tissue engineering for construction of tooth organs is a brand new and highly interesting direction. A clear and distinct shift is occurring in regenerative medicine from use of synthetic materials or tissue grafts to a more explicit approach that applies scaffolds for hosting cells and/or biological molecules to create functional replacement tissues in diseased or damaged dental sites.
10. Finally, (expensive, time-consuming) clinical tests should be encouraged to evaluate dental glass-ceramics in real application cases.

All of these ideas and several others not reported in this work can only be achieved by increasing interactions among materials engineers and scientists, chemists, dentists, and biologists.

Acknowledgments The authors are grateful to the São Paulo Research Foundation (FAPESP, # 2013/07793-6) for financial support of this work and for the postdoctoral fellowship granted to Maziar Montazerian (# 2015/13314-9).

References

1. Sakaguchi RL, Powers JM. Craig's restorative dental materials. 13th ed. Netherland: Elsevier; 2011.
2. Zanotto ED. A bright future for glass-ceramics. Am Ceram Soc Bull. 2010;89(8):19–27.
3. Montazerian M, Singh SP, Zanotto ED. An analysis of glass-ceramic research and commercialization. Am Ceram Soc Bull. 2015;94(4):30–5.
4. Höland W. Biocompatible and bioactive glass-ceramics – state of the art and new directions. J Non-Cryst Solids. 1997;219:192–7.
5. Höland W, Rheinberger V, Apel E, van't Hoen C, Höland M, Dommann A, Obrecht M, Mauth C, Graf-Hausner U. Clinical applications of glass-ceramics in dentistry. J Mater Sci Mater Med. 2006;17(11):1037–42.
6. Höland W, Rheinberger V. Dental glass-ceramics. In: Kokubo T, editor. Bioceramics and their clinical applications. Cambridge: Woodhead Publishing Limited; 2008. p. 548–68.
7. Höland W, Rheinberger V. Bioengineering of glass-ceramics and ceramics for dental restoration. In: Garcia A, Durand C, editors. Bioengineering: principles, methodologies and applications. Hauppauge: Nova Science Publishers; 2010. p. 169–78.
8. Pollington S. Novel glass-ceramics for dental restorations. J Contemp Dent Pract. 2011;12(1):60–7.
9. Johnson A, Sinthuprasirt P, Fathi H, Pollington S. Current glass-ceramic systems used in dentistry. In: Nandyala SH, Santos JD, editors. Current trends on glass and ceramic materials. Sharjah: Bentham Science Publishers Ltd.; 2013. p. 49–72.
10. Saint-Jean SJ. Dental glasses and glass-ceramics. In: Shen JZ, editor. Advanced ceramics for dentistry. Netherland: Elsevier; 2014. p. 255–77.
11. Montazerian M, Zanotto ED. History and trends of bioactive glass-ceramics. J Biomed Mater Res A. 2016;104(5):1231–49.
12. Montazerian M, Zanotto ED. Bioactive glass-ceramics: processing, properties and applications. In: Boccaccini AR, Brauer DS, Hupa L, editors. Bioactive glasses: fundamentals, technology and applications. London: Royal Society of Chemistry; 2016. p. 27–33.
13. Montazerian M, Zanotto ED. Bioactive and inert dental glass-ceramics. J Biomed Mater Res A. n.d. doi: 10.1002/jbm.a.35923, 2017;105(2):619–39.

14. Höland W, Beall G. Glass-ceramic technology. 2nd ed. Westerville: The American Ceramic Society & Wiley; 2012.
15. ISO 6872. Dentistry – ceramic materials. 2015.
16. Denry IL, Lejus AM, Théry J, Masse M. Preparation and characterization of a new lithium-containing glass-ceramic. Mater Res Bull. 1999;34(10–11):1615–27.
17. Denry IL, Holloway JA. Effect of magnesium content on the microstructure and crystalline phases of fluoramphibole glass-ceramics. J Biomed Mater Res. 2000;53(4):289–96.
18. Denry IL, Holloway JA. Effect of sodium content on the crystallization behavior of fluoramphibole glass-ceramics. J Biomed Mater Res. 2002;63(1):48–52.
19. Denry IL, Holloway AJ. Elastic constants, Vickers hardness, and fracture toughness of fluorrichterite-based glass-ceramics. Dent Mater. 2004;20(3):213–9.
20. Uno T, Kasuga T, Nakajima K. High-strength mica-containing glass-ceramics. J Am Ceram Soc. 1991;74(12):3139–41.
21. Qin F, Zheng S, Luo Z, Li Y, Guo L, Zhao Y, Fu Q. Evaluation of machinability and flexural strength of a novel dental machinable glass-ceramic. J Dent. 2009;37(10):776–80.
22. Cheng K, Wan J, Liang K. Hot-pressed mica glass-ceramics with high strength and toughness. J Am Ceram Soc. 1999;82(6):1633–4.
23. Cheng K, Wan J, Liang K. Enhanced mechanical properties of orientated mica glass-ceramics. Mater Lett. 1999;39(6):350–3.
24. Habelitz S, Carl G, Rüssel C. Processing, microstructure and mechanical properties of extruded mica glass-ceramics. Mater Sci Eng A. 2001;307(1–2):1–14.
25. Denry IL, Baranta G, Holloway JA, Gupta PK. Effect of processing variables on texture development in a mica-based glass-ceramic. J Biomed Mater Res B. 2003;64(2):70–7.
26. Denry IL, Holloway JA. Effect of heat pressing on the mechanical properties of a mica-based glass-ceramic. J Biomed Mater Res B. 2004;70(1):37–42.
27. Uno T, Kasuga T, Nakayama S, Ikushima AJ. Microstructure of mica-based nanocomposite glass-ceramics. J Am Ceram Soc. 1993;76(2):539–41.
28. Bürke H, Durschang B, Meinhardt J, Müller G. Nucleation and crystal growth kinetics in ZrO_2-strengthened mica-glass-ceramics for dental application. Glass Sci Technol Glastechnische Ber. 2000;73(1):270–7.
29. Li H, You D, Zhou C, Ran J. Study on machinable glass-ceramic containing fluorophlogopite for dental CAD/CAM system. J Mater Sci Mater Med. 2006;17(11):1133–7.
30. Montazerian M, Alizadeh P, Eftekhari Yekta B. Pressureless sintering and mechanical properties of mica glass-ceramic/Y-PSZ composite. J Eur Ceram Soc. 2008;28(14):2687–92.
31. Montazerian M, Alizadeh P, Eftekhari Yekta B. Processing and properties of a mica-apatite glass-ceramic reinforced with Y-PSZ particles. J Eur Ceram Soc. 2008;28(14):2693–9.
32. Serbena FC, Mathias I, Foerster CE, Zanotto ED. Crystallization toughening of a model glass-ceramic. Acta Mater. 2015;86:216–28.
33. Höland W, Rheinberger V, Wegner S, Frank M. Needle-like apatite-leucite glass-ceramic as a base material for the veneering of metal restorations in dentistry. J Mater Sci Mater Med. 2000;11(1):11–7.
34. Szabó I, Nagy B, Völksch G, Höland W. Structure, chemical durability and microhardness of glass-ceramics containing apatite and leucite crystals. J Non-Cryst Solids. 2000;272(2–3):191–9.
35. Michel K, Pantano CG, Ritzberger C, Rheinberger V, Höland W. Coatings on glass-ceramic granules for dental restorative biomaterials. Int J Appl Glas Sci. 2011;2(1):30–8.
36. Theocharopoulos A, Chen X, Wilson RM, Hill RG, Cattell MJ. Crystallization of high-strength nano-scale leucite glass-ceramics. Dent Mater. 2013;29(11):1149–57.
37. Aurélio IL, Fraga S, Dorneles LS, Bottino MA, May LG. Extended glaze firing improves flexural strength of a glass ceramic. Dent Mater. 2015;31(12):e316–24.
38. Ritzberger C, Apel E, Höland W, Peschke A, Rheinberger VM. Properties and clinical application of three types of dental glass-ceramics and ceramics for CAD-CAM technologies. Dent Mater. 2010;3(6):3700–13.

39. Cattell MJ, Chadwick TC, Knowles JC, Clarke RL, Lynch E. Flexural strength optimization of a leucite reinforced glass ceramic. Dent Mater. 2001;17(1):21–33.
40. Cattell MJ, Chadwick TC, Knowles JC, Clarke RL, Samarawickrama DYD. The nucleation and crystallization of fine grained leucite glass-ceramics for dental applications. Dent Mater. 2006;22(10):925–33.
41. Cattell MJ, Chadwick TC, Knowles JC, Clarke RL. Development and testing of glaze materials for application to the fit surface of dental ceramic restorations. Dent Mater. 2009;25(4): 431–41.
42. Chen XI, Chadwick TC, Wilson RM, Hill R, Cattell MJ. Crystallization of high strength-fine-sized leucite glass-ceramics. J Dent Res. 2010;89:1510–6.
43. Chen XI, Chadwick TC, Wilson RM, Hill R, Cattell MJ. Crystallization and flexural strength optimization of fine-grained leucite glass-ceramics for dentistry. Dent Mater. 2011;27(11): 1153–61.
44. Theocharopoulos A, Chen X, Hill R, Cattell MJ. Reduced wear of enamel with novel fine and nano-scale leucite glass-ceramics. J Dent. 2013;41(6):561–8.
45. Chung K-H, Liao J-H, Duh J-G, Chan DC-N. The effects of repeated heat-pressing on properties of pressable glass-ceramic. J Oral Rehabil. 2009;36(2):132–41.
46. Lien W, Roberts HW, Platt JA, Vandewalle KS, Hill TJ, Chu TG. Microstructural evolution and physical behavior of a lithium disilicate glass-ceramic. Dent Mater. 2015;31(8):928–40.
47. Al Mansour F, Karpukhina N, Grasso S, Wilson RM, Reece MJ, Cattell MJ. The effect of spark plasma sintering on lithium disilicate glass-ceramics. Dent Mater. 2015;31(10):e226–35.
48. Apel E, van't Hoen C, Rheinberger V, Höland W. Influence of ZrO_2 on the crystallization and properties of lithium disilicate glass-ceramics derived from a multi-component system. J Eur Ceram Soc. 2007;27(2–3):1571–7.
49. Khalkhali Z, Eftekhari Yekta B, Marghussian VK. Mechanical and chemical properties of Zr and P-doped lithium disilicate glass ceramics in dental restorations. Int J Appl Ceram Technol. 2012;9(3):497–506.
50. Belli R, Wendler M, Zorzin JI, da Silva LH, Petschelt A, Lohbauer U. Fracture toughness mode mixity at the connectors of monolithic 3Y-TZP and LS2 dental bridge constructs. J Eur Ceram Soc. 2015;35(13):3701–371.
51. Schweiger M, Frank M, Clausbruch CV, Höland W, Rheinberger V. Microstructure and properties of a composite system for dental applications composed of glass-ceramics in the SiO_2–Li_2O–ZrO_2–P_2O_5 system and ZrO_2-ceramic (TZP). J Mater Sci. 1999;34(18):4563–72.
52. Morimoto S, Rebello de Sampaio FBW, Braga MM, Sesma N, Özcan M. Survival rate of resin and ceramic inlays, onlays, and overlays: a systematic review and meta-analysis. J Dent Res. 2016;95(5):985–94.
53. Fradeani M, Redemagni M. An 11-year clinical evaluation of leucite-reinforced glass-ceramic crowns: a retrospective study. Quintessence Int. 2002;33(7):503–10.
54. Gehrt M, Wolfart S, Rafai N, Reich S, Edelhoff D. Clinical results of lithium-disilicate crowns after up to 9 years of service. Clin Oral Investig. 2013;17(1):275–84.
55. Solá-Ruiz MF, Lagos-Flores E, Román-Rodriguez JL, Highsmith JR, Fons-Font A, Granell-Ruiz M. Survival rates of a lithium disilicate-based core ceramic for three-unit esthetic fixed partial dentures: a 10-year prospective study. Int J Prosthodont. 2013;26(2):175–80.
56. Makarouna M, Ullmann K, Lazarek K, Boening KW. Six-year clinical performance of lithium disilicate fixed partial dentures. Int J Prosthodont. 2011;24(3):204–6.
57. Belli R, Petschelt A, Hofner B, Hajtó J, Scherrer SS, Lohbauer U. Fracture rates and lifetime estimation of CAD/CAM all-ceramic restorations. J Dent Res. 2016;95(1):67–73.
58. Denry IL, Holloway JA. Effect of crystallization heat treatment on the microstructure and biaxial strength of fluorrichterite glass-ceramics. J Biomed Mater Res B Appl Biomater. 2007;80(2):454–9.
59. Tulyaganov DU, Agathopoulos S, Fernandes HR, Ventura JM, Ferreira JMF. Preparation and crystallization of glasses in the system tetrasilicic mica-fluorapatite-diopside. J Eur Ceram Soc. 2004;24(13):3521–8.

60. Alizadeh P, Eftekhari Yekta B, Javadi T. Sintering behavior and mechanical properties of the mica-diopside machinable glass-ceramics. J Eur Ceram Soc. 2008;28(8):1569–73.
61. Faeghi-Nia A, Marghussian VK, Taheri-Nassaj E, Pascual MJ, Durán A. Pressureless sintering of apatite/wollastonite-phlogopite glass-ceramics. J Am Ceram Soc. 2009;92(7):1514–8.
62. Almuhamadi J, Karpukhina N, Cattell M. Diopside glass-ceramics for dental and biomedical applications. Adv Sci Technol. 2014;96:15–20.
63. Sinthuprasirt P, van Noort R, Moorehead R, Pollington S. Evaluation of a novel multiple phase veneering ceramic. Dent Mater. 2015;31(4):443–52.
64. Johnson A, Shareef MY, van Noort R, Walsh JM. Effect of furnace type and ceramming heat treatment conditions on the biaxial flexural strength of a canasite glass-ceramic. Dent Mater. 2000;16(4):280–4.
65. van Noort R, Shareef MY, Johnson A, James PF. Properties of a canasite-based castable glass-ceramic. J Dent Res. 1997;76(21):61–61.
66. Johnson A, Van Noort R, Hatton PV, Walsh JM. The effect of investment material and ceramming regime on the surface roughness of two castable glass-ceramic material. Dent Mater. 2003;19(3):218–25.
67. Anusavice KJ, Zhang N-Z. Chemical durability of dicor and fluorocanasite-based glass-ceramics. J Dent Res. 1998;77(7):1553–9.
68. Zhang N-Z, Anusavice KJ. Effect of alumina on the strength, fracture toughness, and crystal structure of fluorcanasite glass-ceramics. J Am Ceram Soc. 1999;82(9):2509–13.
69. Bubb NL, Wood DJ, Streit P. Reduction of the solubility of fluorcanasite based glass ceramics by additions of SiO_2 and $AlPO_4$. Glass Technol. 2004;45(2):91–3.
70. Stokes CW, Van Noort R, Hand R. Investigation of the chemical solubility of mixed-alkali fluorcanasite forming glasses. J Non-Cryst Solids. 2006;352(2):142–9.
71. Pollington S, van Noort R. Manufacture, characterisation and properties of novel fluorcanasite glass-ceramics. J Dent. 2012;40(11):1006–17.
72. Pollingtona S, Fabianelli A, van Noort R. Microtensile bond strength of a resin cement to a novel fluorcanasite following different surface treatments. Dent Mater. 2010;26(9):864–72.
73. Eilaghi M, Montazerian M, Eftekhari Yekta B. Effect of partial substitution of K_2O for Na_2O on sintering, crystallization and mechanical properties of $SiO_2{-}CaO{-}K_2O{-}Na_2O{-}CaF_2$ glass-ceramics. Trans Indian Ceram Soc. 2016;75(1):1–6.
74. Hill RG, Wood DJ. Apatite-mullite glass ceramics. J Mater Sci Mater Med. 1995;6(6):311–8.
75. Clifford A, Hill RG. Apatite-mullite glass-ceramics. J Non-Cryst Solids. 1996;196:346–52.
76. Gorman CM, Hill RG. Heat-pressed ionomer glass-ceramics part I: an investigation of flow and microstructure. Dent Mater. 2003;19(4):320–6.
77. Gorman CM, Hill RG. Heat-pressed ionomer glass-ceramics. Part II. Mechanical property evaluation. Dent Mater. 2004;20(3):252–61.
78. Hill RG. Bioactive glass-ceramics. In: Ducheyne P, editor. Comprehensive biomaterials, Volume 1: metallic, ceramic and polymeric biomaterials; 2011. p. 181–6.
79. Fathi H, Johnson A, van Noort R, Ward JM, Brook IM. The effect of calcium fluoride (CaF_2) on the chemical solubility of an apatite-mullite glass-ceramic material. Dent Mater. 2005;21(6):551–6.
80. Fathi H, Johnson A, van Noort R, Ward JM. The influence of calcium fluoride (CaF_2) on biaxial flexural strength of apatite-mullite glass-ceramic materials. Dent Mater. 2005;21(9):846–51.
81. Fathi HM, Miller C, Stokes C, Johnson A. The effect of ZrO_2 and TiO_2 on solubility and strength of apatite-mullite glass-ceramics for dental applications. J Mater Sci Mater Med. 2014;25(3):583–94.
82. Fathi HM, Johnson A. The effect of TiO_2 concentration on properties of apatite-mullite glass-ceramics for dental use. Dent Mater. 2016;32(2):311–22.
83. Mollazadeh S, Eftekhari Yekta B, Javadpour J, Yusefi A, Jafarzadeh TS. The role of TiO_2, ZrO_2, BaO and SiO_2 on the mechanical properties and crystallization behavior of fluorapatite-mullite glass-ceramics. J Non-Cryst Solids. 2013;361(1):70–7.

84. Mollazadeh S, Ajalli S, Kashi TSJ, Eftekhari Yekta B, Javadpour J, Jafari S, Youssefi A, Fazel A. The effect of aqueous media on the mechanical properties of fluorapatite-mullite glass-ceramics. Dent Mater. 2015;31(11):1370–6.
85. Höland W, Rheinberger V, Apel E, Ritzberger C, Rothbrust F, Kappert H, Krumeich F, Nesper R. Future perspectives of biomaterials for dental restoration. J Eur Ceram Soc. 2009;29(7): 1291–7.
86. Persson C, Unosson E, Ajaxon I, Engstrand J, Engqvist H, Xia W. Nano grain sized zirconia-silica glass ceramics for dental applications. J Eur Ceram Soc. 2012;32(16):4105–10.
87. Montazerian M, Schneider JF, Eftekhari Yekta B, Marghussian VK, Rodrigues AM, Zanotto ED. Sol-gel synthesis, structure, sintering and properties of bioactive and inert nano apatite-zirconia glass-ceramics. Ceram Int. 2015;41(9):11024–45.
88. Mahmoud M, Folz D, Suchicital C, Clark D, Fathi Z. Variable frequency microwave (VFM) processing: a new tool to crystallize lithium disilicate glass. Ceram Eng Sci Proc. 2006;27(6): 143–53.
89. Liu J, Zhang B, Yan C, Shi Y. The effect of processing parameters on characteristics of selective laser sintering dental glass-ceramic powder. Rapid Prototyp J. 2010;16(2):138–45.
90. Cam P, Neuenschwander B, Schwaller P, Köhli B, Lüscher B, Senn F, Kounga A, Appert C. A novel laser-based method for controlled crystallization in dental prosthesis materials, progress in biomedical optics and imaging – proceedings of SPIE 9306. 2015. Article number 930607.
91. Fu L, Wu C, Grandfield K, Unosson E, Chang J, Engqvist H, Xia W. Transparent single crystalline ZrO_2-SiO_2 glass nanoceramic sintered by SPS. J Eur Ceram Soc. 2016;36(14): 3487–94.
92. Fu Q, Beall G, Smith C. Nature-inspired design of strong, tough glass-ceramics, MRS Bulletin, accepted. 2017.
93. Kawai K, Inoue M, Tsuchitani Y. Effect of ion-exchange treatment on mechanical properties of new dental ceramics. Am J Dent. 2003;16(5):347–50.
94. Fischer H, Marx R. Suppression of subcritical crack growth in a leucite-reinforced dental glass by ion exchange. J Biomed Mater Res A. 2003;66(4):885–9.
95. Fischer H, Brehme M, Telle R, Marx R. Effect of ion exchange of glazed dental glass ceramics on strength parameters. J Biomed Mater Res A. 2005;72(2):175–9.
96. Fischer H, De Souza RA, Wätjen AM, Richter S, Edelhoff D, Mayer J, Martin M, Telle R. Chemical strengthening of a dental lithium disilicate glass-ceramic material. J Biomed Mater Res Part A. 2008;87(3):582–7.
97. Liu Y, Tan Y, Lei T, Xiang Q, Han Y, Huang B. Effect of porous glass–ceramic fillers on mechanical properties of light-cured dental resin composites. Dent Mater. 2009;25(6): 709–15.
98. Mollazadeh S, Javadpour J, Eftekhari Yekta B, Jafarzadeh TS, Youssefi A. Synthesis and characterisation of dental composite materials reinforced with fluoroapatite-mullite glass-ceramic particles. Adv Appl Ceram. 2013;112(5):294–300.

Chapter 10
Bioactive Glass-Based Composites for Cranioplasty Implants

Arnab Mahato and Biswanath Kundu

Abstract Craniectomy is a very frequently used procedure in modern neurosurgical practice required secondary to a traumatic skull bone fracture, tumour extraction or severe infection. The craniofacial region is a complex zone, comprising bone, cartilage, soft tissue, nerves and blood vessels. The bones provide the support and protection for other elements, and hence their reconstruction is of a great importance to restore normal functionalities. The aim of this chapter is to summarise the advancement in the field of bioactive glass composites for the use as a craniofacial implant and their studies in surgical challenges. Our discussion broadly covers innovations in material development part and fine-tuning of the composites with structural and functional improvisations to draw the attention of scientists and researchers by summarising recent advancement of craniofacial implants based on composites of bioactive glass and their studies in craniofacial surgical challenges along with their aftermath. With the vast versatility of bioactive glass composite materials, current innovations in implant material development together with structural and functional modifications are waiting to be explored more and more. First, we have discussed the history and evolution of cranioplasty and its requirements in craniofacial surgery including origin, shape and size of the defect and mechanical properties of cranial bone. Subsequently, different craniofacial implant materials starting from bioactive glass, its composite with polymers, ceramics and other materials have been discussed. Finally, the future aspects have been briefly outlined.

Keywords Cranioplasty • Allografts • Autogenous bone graft • Synthetic materials • Bioactive glass • Bone defect • Mechanical properties • Polymers • Fabrication of composites • Ceramics • Hydroxyapatite • Fibres

A. Mahato • B. Kundu (✉)
Bioceramics and Coating Division, CSIR-Central Glass and Ceramic Research Institute (CSIR-CGCRI), Kolkata 700032, India
e-mail: biswa_kundu@rediffmail.com; biswa.kundun@gmail.com

G. Kaur (ed.), *Clinical Applications of Biomaterials*,
DOI 10.1007/978-3-319-56059-5_10

10.1 Introduction

Craniectomy is a very frequently used procedure in modern neurosurgical practice required secondary to a traumatic skull bone fracture, tumour extraction or severe infection. Conditions like intercranial haemorrhage, congenital malformations, progressively deforming skeletal diseases and the absence of intact cranial vault in children also can compromise the normal function and architectonics of craniofacial bones, which may require craniotomy followed by cranioplasty [1].

Craniectomy: A neurosurgical procedure in which a cranial bone flap is removed.
Craniotomy: When a cranial bone flap is removed temporarily to access the underlying brain.
Cranioplasty: A surgical procedure which restores the contour of cranial bone and corrects the bone defect.

The craniofacial region is a complex zone, comprising bone, cartilage, soft tissue, nerves and blood vessels. The bones provide the support and protection for other elements, and hence their reconstruction is of a great importance to restore normal functionalities [2]. But after craniectomy, syndrome of trephined, subdural effusion, seizures, etc., can be seen; diminishing these symptoms is one of the objectives of cranioplasty [3, 4]. Cranioplasty has been shown to improve electroencephalographic abnormalities, cerebral blood flow abnormalities and other neurological abnormalities [5, 6].

History of reconstruction of large skull bone defects dates back to antiquity. Till then autogenous bone grafts remained the gold standard, which were generally harvested from the calvarium, iliac crest, tibia or fibula [7], though the use of metal plates in 2000 BC was found where the material used was contingent upon the socioeconomic rank of the patient [8]. With time and extended research, the disadvantages of different grafts were pointed out, and accordingly the use of grafts became more interesting topic of research. Problems like infection of the bone graft, donor-site morbidity, handling of bone graft and wastage of time reduced the usage of autogenous grafts. According to the source of the graft material, craniofacial implants are being called xenografts, allografts, autogenous bone graft and synthetic materials.

Xenografts: Grafts from different species transplanted into humans.
Allografts: Use of cartilage tissue in cranioplasty.
Autogenous bone graft: Implant taken from same species, from a different site.
Synthetic materials: Implant made synthetically in laboratories.

Along with the advantages and disadvantages of the said implants, an ideal craniofacial implant is yet to come. Depending on the research of craniofacial implants and subsequent case studies, the ideal material used for cranioplasty would be radiolucent, resistant to infections, not conductive of heat or cold, resistant to biochemical processes, malleable to fit defects and complete closure of the defect site [9]. The requirements and expectations from a synthetic graft material are quite high. An ideal graft material should be strong, lightweight, easily shaped, osteoinductive or osteoconductive and enable osteointegration. The best substitute should have the mechanical properties close to the surrounding bone. It was found that depending upon the species and age, a wide range of anisotropic elastic moduli of craniofacial bone can be obtained. The average elastic moduli of cranial bone, both foetal and matured, tested in a three-point bend set-up are 7.467 ± 5.39 GPa (0.5 m/s), 10.777 ± 9.38 GPa (1.0 m/s) and 15.547 ± 10.29 GPa (2.5 m/s), whereas the average porosity of cranial bones was 13.087 ± 4.23%, and the average percent bone volume (BV/TV) was 70.847 ± 10.13% [10].

A number of synthetic biomaterials are available for craniofacial bone substitute, such as titanium, polymethyl methacrylate (PMMA), polyethylene (PE), polyetheretherketone (PEEK), hydroxyapatite (HAp) or combinations/ composites of these materials. The principal aim of the current clinical biomaterial research is to address the limitations of now-available materials. Bioactive glasses (BGs) are a group of non-metallic ceramic biomaterials with osteoconductive, osteoinductive and bacteriostatic properties, which was first introduced in the field by Prof. L. L. Hench and his team. Apart from the unique advantageous features of bioactive glass ceramics, their heterogeneous macrostructure restricts their versatility and mechanical strength [11]. Evolution of research in this field evolved the area, and the limitations are now taken care of by going interdisciplinary and making composites with other materials for particular purposes. The components of the composite are chosen very wisely and calculatedly to overcome certain limitations. Composites have an interesting aspect of high adaptiveness and tuneable properties by varying the component ratio which is helpful to fabricate patient-specific implants [12–14].

The aim of this chapter is to summarise the advancement in the field of bioactive glass composites for the use as a craniofacial implant and their studies in surgical challenges. Our discussion broadly covers innovations in material development part and fine-tuning of the composites with structural and functional improvisations to draw the attention of scientists and researchers by summarising recent advancement of craniofacial implants based on composites of bioactive glass and their studies in craniofacial surgical challenges along with their aftermath. With the vast versatility of bioactive glass composite materials, current innovations in implant material development together with structural and functional modifications are waiting to be explored more and more.

10.2 History and Evolution of Cranioplasty

The first ever report regarding craniofacial reconstruction was written in 1505, though evidence of cranioplasty dates back to 7000 BC [9]. Ancient civilisations like the Incans, the Britons, the Asiatics, the North Africans and the Polynesians

practised cranioplasty quite experimentally using mostly metals. Socioeconomic rank of the patient decided the type of material to be used. The first documented description of cranioplasty explains the technique used in the sixteenth century written by Fallopius. He proposed that bone could be replaced in cranial fractures if the dura stays intact. Another textbook from 1505 guides the physicians to treat the wounds with the help of xenograft obtained from a goat or a dog. Another well-known and successful cranioplasty published by Van Meekeren in 1668 illustrates a treatment of a Russian man after a word injury using canine xenograft, and the outcome was good [15–17]. Bone grafts from dog, ape, goose, rabbit, calf and eagle have been implanted into humans after boiling. Xenografts were diminished by the high rate of infections and the better outcome of the autografts. In 1821, Walther first successfully transplanted autologous bone graft where the removed bone flap has been attached again on the site. This procedure avoids host-tissue rejection, but the main disadvantage is related to donor-site morbidity [17–19]. In 1889, Seydel used pieces of tibia to cover a parietal defect as a plastic reconstruction. Many other bone harvest sites were experimented such as the ilium, ribs, sternum, scapula, fascia, etc.; however the need of two operative fields creates hesitation. The use of the cranium became more popular comparing other donor sites by the Miiller-Konig procedure [20]. These types of grafts can be preserved by cryopreservation or by placing in an abdominal pocket. The common disadvantage related to autologous bone grafts is bone flap resorption causing structural breakdown. In addition to it, Matsuno et al. showed that autologous bone grafts have very high rates of infection compared to other synthetic materials [21].

As we know that cranioplasty was started by using synthetic materials like metals which resurged in the early 1900s. Metals were experimented excessively till then as they are strong but malleable. Aluminium was the first metal used in cranioplasty but was prone to infect and irritate surrounding tissues. Although people with high status used gold, it is unfavourable for general use because of its high cost and softness. In the twentieth century, silver was tested along with gold before and during World War I but later made obsolete by other advanced materials. After World War I, different alloys were investigated and proved as a potential candidate for reconstruction of cranial defects. These included a wide range of metals like platinum, lead, aluminium, tantalum, cobalt, chromium, steel and their different alloys. During World War II, tantalum was largely used due to its bioinert, malleable and noncorrosive nature [22]. Based on the advances in research and case studies, more disadvantages came to notice, and alloying was readily accepted at that time due to their tuneable properties. Alloys are known to bend their properties according to the requirement by changing the metal proportions. This feature made them irresistible for a range of different types of cranial defects. Titanium was introduced in the late 1965 and found that it is better than other metals in biocompatibility and mechanical strength [23–25].

Celluloid, a synthetic plastic, was first used as an implant in the late nineteenth century; however it was not completely biocompatible. In the mid-twentieth century, more suitable alternatives of thermoplastic resins were introduced. Methyl methacrylate was discovered in 1939 and introduced in cranioplasty in 1940. It is a polymerised ester of acrylic acid with a compatible mechanical strength. However,

the difficulty in the preparation of the implant was a major limitation as it was brittle in nature as well [26]. Despite these drawbacks, PMMA was used widely in that span of time as a cranial bone graft. Polyethylene was developed in 1936 but used in this field in 1948 in case of smaller cranial defects. The low mechanical strength barred its use for reconstruction of large-size defects [17, 27]. Development of porous polyethylene made it more suitable to use as a bone graft by allowing soft-tissue ingrowth [28, 29]. In the beginning of the twenty-first century, modern era of cranioplasty has been initiated in search of patient-specific implant. In this era, with the specific requirement of the patients, like size, shape, bioactivity, biocompatibility, implantation period, etc., properties of the grafts have been chosen. In order to get grafts with such tuneable properties, horizon of this field increased tremendously, and different new types of implants have been introduced. Also different modifications of old implant materials like calcium phosphates, especially hydroxyapatite, and bioactive glasses came to the picture [30]. New polymer materials like PEEK were introduced to cranial reconstruction [31, 32]. Plates and screws of verity of new synthetic resorbable polymers with innovative design were introduced to clinical practice. Research related to bone-forming cell activity at the defect site has been prioritised using a combination of bone particles and growth factors. Also composites of different materials like calcium phosphates, bioactive glasses with a range of different elements, polymers and metals have been experimented extensively to reconstruct cranial defects.

The use of bioactive glass composites in craniofacial application is still limited, but the possibility is enormous as bioactive glass has all the required eligibility as a craniofacial implant. By making composites, possibility will increase further as the properties can be tailored.

10.3 Requirements of Craniofacial Surgery

Depending upon the factors like size, shape and position of the defect, implantation time, mechanical properties of the surrounding bone and age of the patient, the requirements of cranioplastic implants differ. With the aim of making patient-specific implant, the factors are taken in consideration for the better future of craniofacial reconstruction. The desired properties of the implant can be achieved by making different composites, to use in unique surroundings of the respective patient.

10.3.1 Origin, Shape and Size of the Defect

According to the origin, cranial bone defects may be of congenital or acquired. Congenital defects mostly come from craniosynostosis, whereas the acquired cranial bone defects mainly occur as a result from head injury or surgical action upon an intracranial lesion, cranial bone tumour, bone resorption or osteomyelitis. Tendency

Table 10.1 Classification based on the size of a cranial bone defect [33–35]

	Defect	Size of the defect
Adult	Very small	Less than 4 cm^2
	Small	4–25 cm^2
	Medium	25–200 cm^2
	Large	Larger than 200 cm^2
Children	Small	Less than 4 cm^2
	Medium	4–16 cm^2
	Large	Larger than 16 cm^2

of traumatic aetiology is higher in children and young people, mostly male. There are two types of bone tumour, primary and secondary, which can cause skull defect. Primary bone tumours like namely, fibrosarcomas, osteosarcomas, chondrosarcomas, osteomas, etc., and secondary bone tumours like dermoids, epidermoids and Ewing sarcomas may affect cranial bones by means of pressure, or they may force the bone out of its normal position, even sometimes destroying the bone.

However, the cranial bone defect size is not very significant for surgical purposes, but it is an important parameter for engineering the implant. The materials required and their properties are vastly dependent on the shape and size of the defect. Recently Uygur et al. proposed a classification from small-sized (smaller than 25 cm^2), medium-sized (between 25 and 200 cm^2) and large-sized (larger than 200 cm^2) defect [33]. However, a standard classification of cranial bone defect size is not available yet (Table 10.1).

10.3.2 Mechanical Properties of Cranial Bone

The mechanical properties of skull bones have been extensively characterised, and it was found that cranial bone is comprised of a three-sandwich-type layered structure: external layers are made of compact, high-density cortical bone, whereas the central layer consists of a low-density, irregularly porous bone structure [10, 36–39]. Studies showed that foetal and adult cranial bones are vastly different in properties. Foetal cranial bone is thin and non-homogeneous which displays a highly directional fibre orientation [40]. With the maturity of the cranium, the bones structurally differentiate into a three-layered composite structure. With the structural development, the mechanical properties of the skull bones change diversely. The large variation of the mechanical properties can be attributed to the morphological differences between the subjects.

It was found that depending upon the species and age, a wide range of anisotropic elastic moduli of craniofacial bone have been obtained. The average elastic moduli of cranial bone, both foetal and matured, tested in a three-point bend set-up were found to be 7.467 ± 5.39 GPa (with 0.5 m/s crosshead speed), 10.777 ± 9.38 GPa (1.0 m/s) and 15.547 ± 10.29 GPa (2.5 m/s), whereas the average porosity of cranial

bones was 13.087 ± 4.23% with bone volume/total volume (BV/TV) was 70.847 ± 10.13%. A correlation between percent BV and elastic modulus ($r^2 = 0.1963$; $p = 0.0004$) and maximum bending stress ($r^2 = 0.2708$; $p < 0.0001$) was found [10]. These results reported play very important role in the processing of patient-specific implant. The maximum force to failure, elastic modulus and maximum bending stress are very significant to make a suitable implant. Porosity and bone thickness are two other important variants, which also control the role of the bone graft.

10.4 Requirements for Craniofacial Implant Material

The requirements and expectations of an optimal graft material vary from patient to patient. Complexity of the required properties is increasing day by day. Optimal biomaterial should have better mechanical strength, lightweight, easily shaped, osteoinductive or osteoconductive and a structure which enables osteointegration. Density, surface area and porosity are some other properties, which also play significant part to make an implant appropriate for application. Depending upon the requirement, it can be biodegradable or biostable, and it may be bioinert or bioactive. The suitable structural design would support ingrowth of bone so that the implant could be integrated with the surrounding bone. Hence an implant with porous structure ranging 50–400 μm is beneficial for osteointegration [41]. Porous structure works as a scaffold for osteoblast cells, which later forms bony ingrowth.

10.5 Bioactive Glass as a Craniofacial Implant

The maxillofacial area is a unique challenge for many decades to the surgeons because of its versatile properties (mechanical strength, thickness, bone structure) and infection sensitivity. Especially paranasal sinuses, upper respiratory tract and oral cavity are among the most sensitive areas, which need special attention. Since the first use of bioactive glass, it has attracted the attention of respective surgeons due to their osteoconductive as well as antimicrobial properties [42–47]. During the initial times, it was found to be very successful in dental applications with promising results. Bioactive glass has been used frequently in the treatment of intrabony defects and in dental extraction sites as filler before dental implant placement [48, 49]. Also the anti-gingivitis and antiplaque effects of bioactive glass (NovaMin®) have been studied with evident proof of gingival bleeding reduction and oral plaque formation [50]. The success in the dental field leads to the use of bioactive glass implant in other areas related to cranioplasty. Bioactive glass S53P4 was used in frontal sinus elimination and frontal bone reconstruction, nasal septum defect repair, orbital wall and nasal septum reconstruction and canal wall down mastoidectomy [51–53]. Middle ear implant made by bioactive glass for ossicular chain reconstruction also showed very good success rate even after 8 years [54].

However, bioactive glasses are very brittle and thus have limitations in shaping and flexibility for specific clinical requirements. These properties thus prevent the use of BG in load-bearing applications. Limitations led to the development of composite materials using bioactive glass to make use of its benefits up to full extent. Composite material is by definition a material composed of at least two different biomaterials. Over the last two decades, composites of bioactive glass have been used in different aspects and fields according to the properties of the composite materials. The arsenal of the application of bioactive glass has been increased enormously as the mechanical, biological and physiological properties of the composite materials can be tailored by changing the concentrations of base components.

10.5.1 Bioactive Glass Composite with Polymer

These composite materials consist of two phases, e.g. continuous phase, called the "matrix", and dispersed phase, which can be fillers or fibres. The concept of making composites by using polymer and ceramic material was introduced by Bonfield et al. [55]. Composite structures are believed to add functionality to the biomedical composites, such as bioactivity, sustained release of drug moiety and typical biodegradation profile. In this way, composites of bioactive glass and polymers can be applied according to the demands of patients. There are several methods and types of composite materials, like particle composite or fibre composite or composite coatings. Though some methods are still in basic research level, some methods have been established, and with time, new methods are being introduced. Major manufacturing methods include melt extrusion, self-reinforcing and solvent casting.

Melt extrusion process is mostly used for making products with continuous cross sections such as rods, pipes, sheets, fibres, etc. Mixing of polymer and bioactive glass can also be done via this process, which can be used in other manufacturing processes. The extruder consists of a heated barrel with feeding hopper into which the raw materials are fed. The raw materials then come into contact with the rotating screw, which is responsible for the stirring and homogenising of the polymer. Heating elements are placed over the barrel. The polymer gradually melts, as it is conveyed forward in the barrel. At the end of barrel is the heated die that has an orifice with the specific profile needed for the extrudate. The melted polymer paste is then forced to run through an orifice with specific profile and after that cooled to get the final shape.

Another important and significant method to manufacture composites is solvent casting/particulate leaching (SCPL), in which the matrix polymer is dissolved in a volatile solvent to form a stable solution. Thus, the solubility of polymer in bioactive glass solution is the most important criteria for solvent casting technique. However, bioactive glass can be added up to a certain limit, above which it may make the composite more brittle than the requirement [56]. Viscosity is another factor to be considered important during this process. After getting clear solution, reinforcements can be added into the solution. The final solution is then cast to the mould to get the necessary structure. Solvent casting can also be used to form

porous structures by using selective porogens, which is soluble in the particular solvent. Depending upon the required pore size and interconnectivity, porogens can be varied with temperature.

Other methods like direct foaming/freeze drying, salt leaching, thermally induced phase separation, solid-liquid phase separation, rapid prototyping/solid freeform and slurry-dip in coating of scaffold are also used to manufacture composites, but they are still not accepted by the larger community of surgeons (Table 10.2).

Bioactive glass-polymers are relatively new in the class of bioactive materials for the treatment of maxillofacial defects, but during a very short span of time, BG-polymer composites proved their utility in the restoration of cranial vault. Due to the combination of BG's mechanical and biological properties and polymers' great flexibility, implants are applicable into various types of cranial defects with a very successful outcome. Initial applications of BG-polymer composites were mostly in dental application, but nowadays the use of this type of implant materials is increasing rapidly in different aspects of craniofacial reconstruction like orbital floor fractures, frontal bone defects, calvarial bone defects, etc.

In 2005, Niemela et al. reported advantageous effects of BG-poly-L/DL-lactide 70/30 composites with improved mechanical, biological and physiological properties; however they also confirmed that the increase in bioactive glass concentration may increase the brittleness along with decreased bioactivity [61]. After the first composite material, many variations with different components were tried, and after a thorough research subsequently, poly(methyl methacrylate) [PMMA] was found most compatible with bioactive glass particles for craniofacial application. Since then PMMA is one of the most widely researched alloplastic components in composite materials for craniofacial surgery. Low thermal conductivity and a density closer to bone make PMMA more acceptable by soft tissues. In 2006, Tuusa et al. fabricated

Table 10.2 Advantages and disadvantages of different composite manufacturing methods [57–60]

Method	Advantages	Disadvantages
Melt extrusion	Useful of making continuous shaped composites Control over shape and size For making solid materials	Porous structure can't be done Use of temperature may hamper polymer Shear forces
Solvent casting/particulate leaching	Simple method Control over porous structure	Residual solvent Interconnectivity of pores Solubility of porogen materials
Thermally induced phase separation	High porosity Interconnected porous structure Uniform porosity	Processing duration
Solid-liquid phase separation	Control over porous structure, pore size and interconnectivity	Solvent residue
Rapid prototyping or solid freeform	Patient-specific implant Complex structure Control over pore size, distribution of pores	Limited polymer compatibility Expensive

an implant composed of fibre-reinforced composite (FRC) with bisphenol A-glycidyl methacrylate (BisGMA)-PMMA polymer matrix and a bioactive glass coating on the surface [62]. Though the results did not reveal a better bone formation than the controls, the procedure certainly made an impact and attracted researchers and surgeons to use composite materials in the arsenal of cranial reconstruction. Kessler et al. reported a successful production of filler material also made of BisGMA-PMMA matrix embedded with bioactive glass material with better outcomes [63]. In 2007, Ballo et al. experimented with a composition, which included BisGMA-TEGMA [tri(ethylene glycol) methacrylate], E-glass, PMMA and bioactive glass. Firstly, the E-glass fibre bundles were impregnated by BisGMA-TEGMA resin, followed by PMMA reinforcement. Three different types of specimens were fabricated: (a) unthreaded FRC with BG coating, (b) threaded FRC and (c) FRC coated with BG. They surprisingly found that the implant can withstand static load almost up to human maximal bite forces without fracture. Implant also showed better push-out force from dental plaster than a similar titanium implant [64]. Simultaneously, researchers found that BG-polymer composite implants can stimulate growth factor due to the effect of BG and nano-BG can adsorb proteins which ultimately favours bony ingrowth [65, 66]. Hautamaki et al. also found noticeable increase in osteoblast response of the specimens made of PMMA and bioactive glass in different ratios [67]. These findings supported and encouraged the application of BG-polymer composites in the areas never tried before. Another composite was made by impregnating E-glass FRC with MMA (methyl methacrylate)/BDDMA (butane-diol-di-methacrylate) copolymer system followed by BG granule coating and used as calvarial bone implant in rabbits. The implant seemed to promote bone healing process faster than the controls without any unwanted side effects [68]. Porous structure of the composite is found to mimic surrounding bone, while BG particles can enable new hard-tissue formation by osteoblasts on their surface. With the aim of mimicking Mother Nature, the use of natural polymer in composite implant materials was introduced. Peter et al. reported a novel composite implant fabricated by blending nano-bioactive glass with chitosan-gelatin biopolymer as a potential candidate for alveolar bone regeneration. Protein adsorption studies showed a significant increase of protein adsorption compared to control chitosan-gelatin scaffolds. Addition of bioactive glass nanoparticles also increased the cell attachment on the surface of the implant [69]. In 2010, four patients with pre-existing large calvarial (three patients) and midface (one patient) defects were operated by Dr. M. Peltola and his group by using implant containing BG and PMMA. After detecting the defects, implants were custom-made using powder-liquid PMMA bone cement matrix covered with 0.5–0.8 mm BG (BonAlive™) particles from both sides. The ratio of PMMA/BG was varied depending upon the requirements of the defects of concerning patient. Follow-up results proved a firm adhesion between the implant and skull, which may prevent long-term complications. Bone healing and new bone formation were seen between the implant and surrounding bone [70]. Another group reported successful periodontal tissue regeneration using biocompatible alginate/nano-bioactive glass composite material made by freeze drying method. The implants with pore size 100–300 μm showed good protein adsorption, cell attachment and cell proliferation [71]. BisGMA-

TEGDMA (triethylene glycol dimethacrylate) and BG composite material were used by Aitsalo et al. as an implant for 15 numbers of patients with defects as a consequence of craniotomies performed due to traumatic reasons. The implant material was composed of BisGMA-TEGDMA resin matrix reinforced by E-glass, and in between the layers, bioactive glass was used as a filler material [72]. The results were promising to the scientists which was also without infections or skin problems. In another study, Aitsalo et al. treated 12 patients (six male and six female) with skull bone defects after a tumour was surgically removed with pBisGMA-pTEGDMA (bisphenol A-glycidyl methacrylate/triethylene glycol dimethacrylate)/BG composite materials. The implants were composed of two FRC layers, supporting framework and porous layers. The porous layers containing bioactive glass were connected to each other by inter-connective elements. The standard size of the BG particles used was 500–800 μm. The resin matrix materials were made of pBisGMA-pTEGDMA coupled with silanised E-glass. The mechanical strength of the implants was found to be very good in comparison to the similar type of implants used before. The bone-mimicking porous structure combined with BG particles enables new bone formation [73]. In 2012, Posti et al. operated a 33-year-old woman with severe traumatic brain injury in head-on collision with a custom-made FRC-BG implant fabricated in Turku Clinical Biomaterials Centre, Turku, Finland. The implant was fabricated by hand laminating two layers of dimethacrylate resin matrix keeping the bioactive glass particles (S53P4) in between them. Though some initial side effects were observed like swelling, but after more than 2 years of study, it was found that the mechanical integrity of the composite implant was not affected by the in vivo period. Formation of fibrous tissue with blood vessels, osteoblasts and collagen fibres was reported along with small clusters of more mature hard tissue [74]. At the same time, chitosan-bioactive glass composites were tried by Mota et al. with the aim of supporting periodontal regeneration. The composite was made by solvent casting method and used as bone regeneration membrane [GTR (guided tissue regeneration) membrane]. The implant showed adequate extensibility in wet conditions [75]. Recently Kulkova et al. reported a successful fabrication of a novel implant using FRC, E-glass fibres and bioactive glass (S53P4) granules. The composite was made by combining BisGMA-TEGDMA matrix and BG granules by the effect of excimer laser surface etching. The implant showed excellent fatigue resistance and the mechanical properties matching to bone [76]. However almost all the studies were done by using only S53P4 bioactive glass, which encouraged the researchers to use other bioactive glass composites in craniofacial reconstruction.

10.5.2 Bioactive Glass Composite with Ceramic

Ceramic composites are made with the aim of combining significant properties of the components, which were not achievable with the components alone. Another advantage of these composite materials is that the properties can be tailored according to the requirements using the same components, only by varying the combining

ratio. Sometimes composite can be made to cover up some disadvantages of bioactive glass, like high rate of ion leaching and brittleness, or to add special functionalities like increase of the bone formation rate or control over porosity. Though there are several methods for composite fabrication like melt quenching, milling and liquid phase sintering, sol-gel method is considered to be the most accepted one.

Generally melt quenching technique is followed by milling. Melt quenching method is famous for synthesising bioactive glass where glass frits can be made. In this method, raw materials are mixed thoroughly in solid form or in a solvent. The solvent is then dried to get powder of the mixture, which was then melted at required temperature followed by quenching in distilled water. After getting the frits, they were milled to get particles of bioactive glass, which was then mixed with other ceramic substances via ball milling. As melt quenching is the mostly used procedure for bioactive glass making, this process is more acceptable than the others. Control over porosity is another advantageous aspect of this technique.

The sol-gel method is a transition of inorganic/polymeric precursors in liquid phase into a solid inorganic material allowing the fabrication of new glasses and ceramics. The best part of this method is that the microstructure and properties of the material can be tailored with precision [77]. The method is so versatile that wide range of composition can be used and the composition can be varied in accordance with the requirement. Purity of the glass from this technique is found to be higher than other processes with a rare chance of getting unwanted products. In addition, the use of low temperature makes it preferable than melt quenching method.

In between the ceramic materials, hydroxyapatite (HAp) has long been used in dentistry owing to its ability to attach chemically to bone as it contains the minerals almost identical to bones. From the last decade with the tendency to tune the dissolution kinetics of calcium phosphate, a combination with bioactive glasses has been considered. Another disadvantage of HAp is its very low resorption rate, which increases the risk of infection [78]. The use of bioactive glass-ceramic composite materials increased in the modern era of craniofacial reconstruction. The first relevant work was reported by Duarte et al., where a combination of hydroxyapatite and P_2O_5-base bioactive glass (P_2O_5 65%-CaO 15%-CaF_2 10%-Na_2O 10%) commercially named Bonelike® was applied as a bone graft in maxillofacial surgery to reconstruct a defected area after cyst excision. Sufficient new bone formation was observed in the defect area with resorption of the Bonelike® granules [79]. After the successful outcome of Bonelike® implants, it was studied extensively in different areas. Sousa et al. applied Bonelike® implants in maxillary cystic bone defects in 11 patients, aged between 24 and 53 years. After 48 weeks of implantation, the outcome was encouraging with high rate of bone formation. The patients were recovering from their bone lesions without any side effects or infections [80]. Pavan Kumar et al. tried Bonelike® implants in human intrabony periodontal angular defects, which showed promising bone filling and no adverse effects [81]. There are several other clinical trials that have been done using Bonelike®, which proved it as an effective composite material for craniofacial defect restoration [82–84]. Chatzistavrou et al. tried a different route and synthesised a sol-gel-based composite material made by combining a new glass ceramic (GC) (SiO_2 60%-P_2O_5 3%-Al_2O_3

14%-CaO 6%-Na_2O 7%-K_2O 10%) system with 58S bioactive glass (GC 30 wt%-BG 70 wt%). They used the implant as sealing material to fix dental restorations with successful outcome of periodontal tissue attachment, providing complete sealing of the marginal gap [85]. In 2011, Pratibha et al. tried BG-HAp (BG: $SiO_2$17%-CaO 53%-P_2O_5 30%) composite implant for periodontal defects with successful results [86]. More detailed clinical data was reported by Bhide et al. where a BG-HAp composite (50-50) was applied with autogenous cortical bone particulate in treatment of periodontal bone defects. The implant showed encouraging results of remarkable gain in probing attachment and depth reduction at 3 and 6 months [87]. A different approach was taken by Al-noaman, who made a composite of fluoro-apatite and bioactive glass (MgF_2 glass) with the aim of making a coating material for titanium dental implant [88, 89]. After that, no notable clinical research can be found in this area using bioactive glass-ceramic composites.

10.5.3 Bioactive Glass Composite with Other Materials

There are other materials also, which were used to make composites with bioactive glass which cannot be categorised. In 2001, maxillary sinus floor augmentation was done by using a composite of bioactive glass (45S5) and autogenous bone. The implant was used on 12 patients and observed that the implant successfully yielded sufficient volume of mineralised tissue with almost 3–5 mm of bone formation [90]. In another approach, enamel matrix protein derivative (EMD) was used with bioactive glass (45S5) to fabricate a bone graft for the treatment of intrabony periodontal defects in humans [91]. Turunen et al. compared the effect of adding bioactive glass in the treatment of maxillary sinus floor augmentation by making two compositions, one was autologous bone without BG and another was with BG (S53P4). The results showed that by incorporating BG, the need of autologous bone was decreased [92]. Another comparative study was done by Sculean et al. for the treatment of human intrabony defects following regenerative periodontal therapy. Among 30 patients, in each of the patient, one intrabony defect was randomly treated with either EMD + BG (test) (45S5) or with EMD alone (control), and the outcome confirmed almost similar results of two compositions with no additional improvement of clinical results in case of BG-incorporated implants [49, 93]. Demir et al. added bioactive glass with platelet-rich plasma (PRP) to evaluate the effect of BG on the clinical healing of intrabony defects. However the reports showed no advantageous effect of using bioactive glass [94]. Another work on bioactive glass-PRP composite was done by Carvalho et al. for the treatment of intrabony defects of dogs with no noticeable or advantageous differences [95]. A composite of bioactive glass and autogenous cortical bone (ACB) was also studied by Sumer et al. for the treatment of intra-osseous periodontal defects with the outcome of significant improvement of clinical and radiographic parameters. Bone heights were found to be increased in the patients treated with ACB-BG graft [96]. Recently Sandor et al. synthesised a

combination of bioactive glass (45S5) and adipose-derived stem cells to observe the effectiveness of bioactive glass in cranio-maxillofacial hard-tissue defects. The results came were sufficiently good even after 4 years of study [97].

10.6 Future Aspects

The field of bioactive glass composite for craniofacial reconstruction has been nurtured a lot in the last two decades, but there are still a lot of vacant spaces to fill up the store. A vast number of composites were tried with success, sometimes without success, but all the data made us more accurate in planning for the upcoming fabrication of composite materials. With the introduction of 3D scaffold designing in tissue engineering, a new door has opened; patient-specific implant got a new definition because of this technology. In the coming years, more emphasis will be given to make 3D implants based on bioactive glass or bioactive glass composites as bioactive glass can be used as to fabricate 3D scaffold. New ideas of adding stem cells and/or growth factors will get the attention of the researchers. The bioactive glass-based composites have been used in vitro using a wide range of cell types, and it's high time to use those data to apply the composites in clinical trials in vivo. The long-term understanding of in vivo in this field is still limited, specially related to the kinetics of degradation and ion release. The use of nano-scale composites will need to be investigated too. The results of these investigations will give a better insight of the synergistic effect of bioactive glass composites leading to more control over the strategies. The ongoing research efforts ensure that development of bioactive glass composite materials will remain a major area of application in the future.

Acknowledgements The authors gratefully acknowledge the support by the Director, CSIR-Central Glass and Ceramic Research Institute, Kolkata, India, and Council of Scientific and Industrial Research [through CSIR 12th 5 year plan programme (BIOCERAM)] for financial support.

References

1. Piitulainen JM, Kauko T, Aitasalo KMJ, Vuorinen V, Vallittu PK, Posti JP. Outcomes of cranioplasty with synthetic materials and autologous bone grafts. World Neurosurg. 2015;83:708–14.
2. Petrovic V, Zivkovic P, Petrovic D, Stefanovic V. Craniofacial bone tissue engineering. Oral Surg Oral Med Oral Pathol Oral Radiol. 2012;114:1–9.
3. Honeybul S, Ho KM. Long-term complications of decompressive craniectomy for head injury. J Neurotrauma. 2011;28:929–35.
4. Joseph V, Reilly P. Syndrome of the trephined: case report. J Neurosurg. 2009;111:650–2.
5. Coelho F, Oliveira AM, Paiva WS, Freire FR, Calado VT, Amorim RL, Neville IS, de Andrade AF, Bor-Seng-Shu E, Anghinah R. Comprehensive cognitive and cerebral hemodynamic evaluation after cranioplasty. Neuropsychiatr Dis Treat. 2014;10:695.
6. Honeybul S, Janzen C, Kruger K, Ho KM. The impact of cranioplasty on neurological function. Br J Neurosurg. 2013;27:636–41.

7. De Bonis P, Frassanito P, Mangiola A, Nucci CG, Anile C, Pompucci A. Cranial repair: how complicated is filling a "hole"? J Neurotrauma. 2012;29:1071–6.
8. Shah AM, Jung H, Skirboll S. Materials used in cranioplasty: a history and analysis. Neurosurg Focus. 2014;36:E19.
9. Aydin S, Kucukyuruk B, Abuzayed B, Aydin S, Sanus GZ. Cranioplasty: review of materials and techniques. J Neurosci Rural Pract. 2011;2:162–7.
10. Motherway JA, Verschueren P, Van der Perre G, Vander Sloten J, Gilchrist MD. The mechanical properties of cranial bone: the effect of loading rate and cranial sampling position. J Biomech. 2009;42:2129–35.
11. Tyagi S. Glasses and glass ceramics as biomaterials. Patiala: Thapar University; 2007.
12. Hench LL. Bioceramics: from concept to clinic. J Am Ceram Soc. 1991;74:1487–510.
13. Hench LL. Biomaterials: a forecast for the future. Biomaterials. 1998;19:1419–23.
14. Hench LL, Polak JM. Third-generation biomedical materials. Science. 2002;295:1014–7.
15. Courville CB. Cranioplasty in prehistoric times. Bull Los Angel Neurol Soc. 1959;24:1–8.
16. Kennedy KAR. Primitive surgery: skills before science. Spencer L. Rogers. Am Anthropol. 1987;89:217–8.
17. Sanan A, Haines SJ. Repairing holes in the head: a history of cranioplasty. Neurosurgery. 1997;40:588–603.
18. Bowers CA, Riva-Cambrin J, Hertzler DA, Walker ML. Risk factors and rates of bone flap resorption in pediatric patients after decompressive craniectomy for traumatic brain injury: clinical article. J Neurosurg Pediatr. 2013;11:526–32.
19. Stieglitz LH, Fung C, Murek M, Fichtner J, Raabe A, Beck J. What happens to the bone flap? Long-term outcome after reimplantation of cryoconserved bone flaps in a consecutive series of 92 patients. Acta Neurochir. 2015;157:275–80.
20. Durand J-L, Renier D, Marchac D. The history of cranioplasty. Ann Chir Plast Esthet. 1997;42:75–83.
21. Matsuno A, Tanaka H, Iwamuro H, Takanashi S, Miyawaki S, Nakashima M, Nakaguchi H, Nagashima T. Analyses of the factors influencing bone graft infection after delayed cranioplasty. Acta Neurochir. 2006;148:535–40.
22. Flanigan P, Kshettry VR, Benzel EC. World War II, tantalum, and the evolution of modern cranioplasty technique. Neurosurg Focus. 2014;36:E22.
23. Blake GB, MacFarlane MR, Hinton JW. Titanium in reconstructive surgery of the skull and face. Br J Plast Surg. 1990;43:528–35.
24. Goldstein JA, Paliga JT, Bartlett SP. Cranioplasty: indications and advances. Curr Opin Otolaryngol Head Neck Surg. 2013;21:400–9.
25. Hill CS, Luoma AMV, Wilson SR, Kitchen N. Titanium cranioplasty and the prediction of complications. Br J Neurosurg. 2012;26:832–7.
26. Marchac D, Greensmith A. Long-term experience with methylmethacrylate cranioplasty in craniofacial surgery. J Plast Reconstr Aesthet Surg. 2008;61:744–52.
27. Alexander Jr E, Dillard PH. The use of pure polyethylene plate for cranioplasty. J Neurosurg. 1950;7:492–8.
28. Klawitter JJ, Bagwell JG, Weinstein AM, Sauer BW, Pruitt JR. An evaluation of bone growth into porous high density polyethylene. J Biomed Mater Res. 1976;10:311–23.
29. Wang J-C, Wei L, Xu J, Liu J-F, Gui L. Clinical outcome of cranioplasty with high-density porous polyethylene. J Craniofac Surg. 2012;23:1404–6.
30. Hurel SJ, Thompson CJ, Watson MJ, Harris MM, Baylis PH, Kendall-Taylor P. The short synacthen and insulin stress tests in the assessment of the hypothalamic–pituitary–adrenal axis. Clin Endocrinol. 1996;44:141–6.
31. Chacón-Moya E, Gallegos-Hernández JF, Piña-Cabrales S, Cohn-Zurita F, Goné-Fernández A. Cranial vault reconstruction using computer-designed polyetheretherketone (PEEK) implant: case report. Cir Cir. 2009;77:437–40.
32. Lethaus B, Safi Y, ter Laak-Poort M, Kloss-Brandstätter A, Banki F, Robbenmenke C, Steinseifer U, Kessler P. Cranioplasty with customized titanium and PEEK implants in a mechanical stress model. J Neurotrauma. 2012;29:1077–83.

33. Uygur S, Eryilmaz T, Cukurluoglu O, Ozmen S, Yavuzer R. Management of cranial bone defects: a reconstructive algorithm according to defect size. J Craniofac Surg. 2013;24: 1606–9.
34. DeLuca L, Raszewski R, Tresser N, Guyuron B. The fate of preserved autogenous bone graft. Plast Reconstr Surg. 1997;99:1324–8.
35. Rogers GF, Greene AK. Autogenous bone graft: basic science and clinical implications. J Craniofac Surg. 2012;23:323–7.
36. Hardy WN, Foster CD, Mason MJ, Yang KH, King AI, Tashman S. Investigation of head injury mechanisms using neutral density technology and high-speed biplanar X-ray. Stapp Car Crash J. 2001;45:337–68.
37. Miller K, Chinzei K. Constitutive modelling of brain tissue: experiment and theory. J Biomech. 1997;30:1115–21.
38. Prange MT, Margulies SS. Regional, directional, and age-dependent properties of the brain undergoing large deformation. J Biomech Eng. 2002;124:244–52.
39. Gefen A, Margulies SS. Are in vivo and in situ brain tissues mechanically similar? J Biomech. 2004;37:1339–52.
40. McPherson GK, Kriewall TJ. The elastic modulus of fetal cranial bone: a first step towards an understanding of the biomechanics of fetal head molding. J Biomech. 1980;13:9–16.
41. Bobyn JD, Pilliar RM, Cameron HU, Weatherly GC. The optimum pore size for the fixation of porous-surfaced metal implants by the ingrowth of bone. Clin Orthop Relat Res. 1980;150: 263–70.
42. Hench LL, Andersson O. Bioactive glasses. Adv Ser Ceram. 1993;1:41–62.
43. Stoor P, Grênman R. Bioactive glass and turbinate flaps in the repair of nasal septal perforations. Ann Otol Rhinol Laryngol. 2004;113:655–61.
44. Zhang D, Munukka E, Leppäranta O, Hupa L, Ylänen HO, Salonen JI, Eerola E, Viljanen MK, Hupa M. Comparison of antibacterial effect of three bioactive glasses. Key Eng Mater. 2006;309–311:345–8. Trans Tech Publication
45. Zhang D, Munukka E, Hupa L, Ylänen HO, Viljanen MK, Hupa M. Factors controlling antibacterial properties of bioactive glasses. Key Eng Mater. 2007;330-332:173–6. Trans Tech Publication
46. Munukka E, Leppäranta O, Korkeamäki M, Vaahtio M, Peltola T, Zhang D, Hupa L, Ylänen H, Salonen JI, Viljanen MK. Bactericidal effects of bioactive glasses on clinically important aerobic bacteria. J Mater Sci Mater Med. 2008;19:27–32.
47. Leppäranta O, Vaahtio M, Peltola T, Zhang D, Hupa L, Hupa M, Ylänen H, Salonen JI, Viljanen MK, Eerola E. Antibacterial effect of bioactive glasses on clinically important anaerobic bacteria in vitro. J Mater Sci Mater Med. 2008;19:547–51.
48. Mengel R, Schreiber D, Flores-de-Jacoby L. Bioabsorbable membrane and bioactive glass in the treatment of intrabony defects in patients with generalized aggressive periodontitis: results of a 5-year clinical and radiological study. J Periodontol. 2006;77:1781–7.
49. Sculean A, Pietruska M, Schwarz F, Willershausen B, Arweiler NB, Auschill TM. Healing of human intrabony defects following regenerative periodontal therapy with an enamel matrix protein derivative alone or combined with a bioactive glass. J Clin Periodontol. 2005;32: 111–7.
50. Tai BJ, Bian Z, Jiang H, Greenspan DC, Zhong J, Clark AE, Du MQ. Anti-gingivitis effect of a dentifrice containing bioactive glass (NovaMin®) particulate. J Clin Periodontol. 2006;33:86–91.
51. Peltola M, Aitasalo K, Suonpää J, Varpula M, Yli-Urpo A. Bioactive glass S53P4 in frontal sinus obliteration: a long-term clinical experience. Head Neck. 2006;28:834–41.
52. Aitasalo K, Kinnunen I, Palmgren J, Varpula M. Repair of orbital floor fractures with bioactive glass implants. J Oral Maxillofac Surg. 2001;59:1390–5.
53. Della Santina CC, Lee SC. Ceravital reconstruction of canal wall down mastoidectomy: long-term results. Arch Otolaryngol Head Neck Surg. 2006;132:617–23.
54. Reck R, Störkel S, Meyer A. Bioactive glass-ceramics in middle ear surgery an 8-year review. Ann N Y Acad Sci. 1988;523:100–6.

55. Bonfield W, Grynpas MD, Tully AE, Bowman J, Abram J. Hydroxyapatite reinforced polyethylene-a mechanically compatible implant material for bone replacement. Biomaterials. 1981;2:185–6.
56. Cannillo V, Chiellini F, Fabbri P, Sola A. Production of Bioglass® 45S5–Polycaprolactone composite scaffolds via salt-leaching. Compos Struct. 2010;92:1823–32.
57. Ahmed I, Cronin PS, Abou Neel EA, Parsons AJ, Knowles JC, Rudd CD. Retention of mechanical properties and cytocompatibility of a phosphate-based glass fiber/polylactic acid composite. J Biomed Mater Res B Appl Biomater. 2009;89:18–27.
58. Bonfield W. Design of bioactive ceramic-polymer composites. Adv Ser Ceram. 1993;1: 299–304.
59. Peltola SM, Melchels FPW, Grijpma DW, Kellomäki M. A review of rapid prototyping techniques for tissue engineering purposes. Ann Med. 2008;40:268–80.
60. Puppi D, Chiellini F, Piras AM, Chiellini E. Polymeric materials for bone and cartilage repair. Prog Polym Sci. 2010;35:403–40.
61. Niemelä T, Niiranen H, Kellomäki M, Törmälä P. Self-reinforced composites of bioabsorbable polymer and bioactive glass with different bioactive glass contents. Part I: initial mechanical properties and bioactivity. Acta Biomater. 2005;1:235–42.
62. Tuusa SMR, Peltola MJ, Tirri T, Lassila LVJ, Vallittu PK. Frontal bone defect repair with experimental glass-fiber-reinforced composite with bioactive glass granule coating. J Biomed Mater Res B Appl Biomater. 2007;82:149–55.
63. Kessler S, Lee S. Use of bioactive glass in dental filling material, Google Patents. 2006.
64. Ballo AM, Lassila LV, Vallittu PK, Närhi TO. Load bearing capacity of bone anchored fiber-reinforced composite device. J Mater Sci Mater Med. 2007;18:2025–31.
65. Ehrlich H, Janussen D, Simon P, Bazhenov VV, Shapkin NP, Erler C, Mertig M, Born R, Heinemann S, Hanke T. Nanostructural organization of naturally occurring composites-part II: silica-chitin-based biocomposites. J Nanomater. 2008;2008:54.
66. Misra SK, Mohn D, Brunner TJ, Stark WJ, Philip SE, Roy I, Salih V, Knowles JC, Boccaccini AR. Comparison of nanoscale and microscale bioactive glass on the properties of P (3HB)/ Bioglass® composites. Biomaterials. 2008;29:1750–61.
67. Hautamäki M, Meretoja VV, Mattila RH, Aho AJ, Vallittu PK. Osteoblast response to polymethyl methacrylate bioactive glass composite. J Mater Sci Mater Med. 2010;21:1685–92.
68. Tuusa SMR, Peltola MJ, Tirri T, Puska MA, Röyttä M, Aho H, Sandholm J, Lassila LV, Vallittu PK. Reconstruction of critical size calvarial bone defects in rabbits with glass–fiber-reinforced composite with bioactive glass granule coating. J Biomed Mater Res B Appl Biomater. 2008; 84:510–9.
69. Peter M, Binulal NS, Nair SV, Selvamurugan N, Tamura H, Jayakumar R. Novel biodegradable chitosan–gelatin/nano-bioactive glass ceramic composite scaffolds for alveolar bone tissue engineering. Chem Eng J. 2010;158:353–61.
70. Peltola MJ, Vallittu PK, Vuorinen V, Aho AAJ, Puntala A, Aitasalo KMJ. Novel composite implant in craniofacial bone reconstruction. Eur Arch Otorhinolaryngol. 2012;269:623–8.
71. Srinivasan S, Jayasree R, Chennazhi KP, Nair SV, Jayakumar R. Biocompatible alginate/nano bioactive glass ceramic composite scaffolds for periodontal tissue regeneration. Carbohydr Polym. 2012;87:274–83.
72. Aitasalo K, Rekola J, Piitulainen J, Vallittu PK. Craniofacial bone reconstruction with a novel bioactive composite implant. J Neurol Surg Part B: Skull Base. 2012;73:A099.
73. Aitasalo KMJ, Piitulainen JM, Rekola J, Vallittu PK. Craniofacial bone reconstruction with bioactive fiber-reinforced composite implant. Head Neck. 2014;36:722–8.
74. Posti JP, Piitulainen JM, Hupa L, Fagerlund S, Frantzén J, Aitasalo KMJ, Vuorinen V, Serlo W, Syrjänen S, Vallittu PK. A glass fiber-reinforced composite–bioactive glass cranioplasty implant: a case study of an early development stage implant removed due to a late infection. J Mech Behav Biomed Mater. 2015;55:191–200.
75. Mota J, Yu N, Caridade SG, Luz GM, Gomes ME, Reis RL, Jansen JA, Walboomers XF, Mano JF. Chitosan/bioactive glass nanoparticle composite membranes for periodontal regeneration. Acta Biomater. 2012;8:4173–80.

76. Kulkova J, Moritz N, Huhtinen H, Mattila R, Donati I, Marsich E, Paoletti S, Vallittu PK. Bioactive glass surface for fiber reinforced composite implants via surface etching by excimer laser. Med Eng Phys. 2016;38:664–70.
77. Scherer GW, Brinker CJ. Sol-gel science: the physics and chemistry of sol-gel processing. USA: Academic Press; 1990.
78. Szpalski C, Barr J, Wetterau M, Saadeh PB, Warren SM. Cranial bone defects: current and future strategies. Neurosurg Focus. 2010;29:E8.
79. Duarte F, Santos JD, Afonso A. Medical applications of bonelike® in maxillofacial surgery. Mater Sci Forum. 2004;455:370–3.
80. Sousa RC, Lobato JV, Maurício AC, Hussain NS, Botelho CM, Lopes MA, Santos JD. A clinical report of bone regeneration in maxillofacial surgery using Bonelike® synthetic bone graft. J Biomater Appl. 2007;22:373–85.
81. Pavan Kumar G, Jaya Kumar A, Krishnanjaneya Reddy P, Nandyala SH, Lopes MA, Santos JD. Application of glass reinforced hydroxyapatite composite in the treatment of human intrabony periodontal angular defects–two case reports. Solid State Phenom. 2010;161: 93–101.
82. Lobato JV, Sooraj Hussain N, Sousa RC, Mauricio AC, S.J. D. Bone regeneration in maxillofacial surgery using novel Bonelike® synthetic bone graft – radiological and histological analysis. J Biomater Appl. 2008;22:373–85.
83. Lobato JV, Hussain NS, Lopes MA, Lobato JM, Mauricio AC, Afonso A, Ali N, Santos JD. Clinical applications of titanium dental implants coated with glass-reinforced hydroxyapatite composite (bonelike). Int J Nanomanufacturing. 2008;2:135–48.
84. Kumar PG, Kumar JA, Anumala N, Reddy KP, Avula H, Hussain SN. Volumetric analysis of intrabony defects in aggressive periodontitis patients following use of a novel composite alloplast: a pilot study. Quintessence Int. 2011;42:375–84.
85. Chatzistavrou X, Esteve D, Hatzistavrou E, Kontonasaki E, Paraskevopoulos KM, Boccaccini A. Sol–gel based fabrication of novel glass-ceramics and composites for dental applications. Mater Sci Eng C. 2010;30:730–9.
86. Pratibha PK, Bhide A, Bhat GS. Comparison of bioactive glass-hydroxyapatite alone and in combination with autogenous bone particulate in the management of periodontal defects, international conference on biology, environment and chemistry, IACSIT, Singapore. 2011.
87. Bhide A, Pratibha PK, Bhat GS. Evaluation of autogenous cortical bone particulate with bioactive glass-synthetic hydroxyapatite in treatment of periodontal bone defects. Int J Biosci Biochem Bioinforma. 2012;2:36.
88. Al-Noaman A, Karpukhina N, Rawlinson SCF, Hill RG. Effect of FA on bioactivity of bioactive glass coating for titanium dental implant. Part I: composite powder. J Non-Cryst Solids. 2013;364:92–8.
89. Al-Noaman A, Karpukhina N, Rawlinson SCF, Hill RG. Effect of FA addition on bioactivity of bioactive glass coating for titanium dental implant: part II—composite coating. J Non-Cryst Solids. 2013;364:99–106.
90. Cordioli G, Mazzocco C, Schepers E, Brugnolo E, Majzoub Z. Maxillary sinus floor augmentation using bioactive glass granules and autogenous bone with simultaneous implant placement. Clin Oral Implants Res. 2001;12:270–8.
91. Sculean A, Barbé G, Chiantella GC, Arweiler NB, Berakdar M, Brecx M. Clinical evaluation of an enamel matrix protein derivative combined with a bioactive glass for the treatment of intrabony periodontal defects in humans. J Periodontol. 2002;73:401–8.
92. Turunen T, Peltola J, Yli-Urpo A, Happonen RP. Bioactive glass granules as a bone adjunctive material in maxillary sinus floor augmentation. Clin Oral Implants Res. 2004;15:135–41.
93. Sculean A, Pietruska M, Arweiler NB, Auschill TM, Nemcovsky C. Four-year results of a prospective-controlled clinical study evaluating healing of intra-bony defects following treatment with an enamel matrix protein derivative alone or combined with a bioactive glass. J Clin Periodontol. 2007;34:507–13.
94. Demir B, Şengün D, Berberoğlu A. Clinical evaluation of platelet-rich plasma and bioactive glass in the treatment of intra-bony defects. J Clin Periodontol. 2007;34:709–15.

95. Carvalho MD, Suaid FF, Santamaria MP, Casati MZ, Nociti Jr FH, Sallum AW, Sallum EA. Platelet-rich plasma plus bioactive glass in the treatment of intra-bony defects: a study in dogs. J Appl Oral Sci. 2011;19:82–9.
96. Sumer M, Keles GC, Cetinkaya BO, Balli U, Pamuk F, Uckan S. Autogenous cortical bone and bioactive glass grafting for treatment of intraosseous periodontal defects. Eur J Dent. 2013;7:6–14.
97. Sándor GK, Numminen J, Wolff J, Thesleff T, Miettinen A, Tuovinen VJ, Mannerstrom B, Patrikoski M, Seppanen R, Miettinen S. Adipose stem cells used to reconstruct 13 cases with cranio-maxillofacial hard-tissue defects. Stem Cells Transl Med. 2014;3:530–40.

Chapter 11
Antibacterial Properties of Bioactive Glasses

Muhammad Akram and Rafaqat Hussain

Abstract Nanosized bioactive glasses, ion and natural organic substances and blended/doped bioactive glasses have been gaining growing attention due to their superior osteoconductivity and antibacterial characteristics in contrast to conventional (micron-sized) bioactive glass materials. The combination of bioactive glass nanoparticles with various ions like silver (Ag^{+}), copper (Cu^{2+}), cerium (Ce^{2+}), zinc (Zn^{2+}) and various organic naturally occurring substances can be used in various orthopaedic, soft tissue and dental applications, including tissue engineering and regenerative medicine to treat various bacterial infections that may have been caused by bacterial species like *Escherichia coli, Saprospira grandis, Streptococcus faecalis, Streptococcus aureus* and *Pseudomonas aeruginosa*. This chapter presents the available methods for the preparation of these materials, their application, type of bioactive glasses, factors that play a vital role in enhancing their antibacterial properties against various bacterial traits and a brief detail of techniques applied to carry out antibacterial studies of nanosized bioactive glasses.

Keywords Bioactive glass • Silicate glass • Phosphate glass • Borate glass • Processing techniques • Classification of bioactive glass • Types of bioactive glass • Metal doped bioactive glass • Antibacterial properties of bioactive glass • Silver • Copper • Cerium • Zinc • Surface area • Morphology • Simulate body fluid

11.1 Introduction

A material which has the potential to show an appropriate biological response and can establish a bond between the living body tissue and itself is considered as a bioactive material. Whereas bioactive glass-based materials are defined as those materials which have the capability to show a biological response after implanting in the living body and show bond formation with the body tissues. They are a

M. Akram
Department of Chemistry, Government Degree College, Raiwind, Pakistan

R. Hussain (✉)
Department of Physics, COMSATS Institute of Information Technology, Islamabad, Pakistan
e-mail: rafaqathussain@comsats.edu.pk

G. Kaur (ed.), *Clinical Applications of Biomaterials*,
DOI 10.1007/978-3-319-56059-5_11

combination of silicate-based materials with calcium and phosphate constituents [1]. Bioactive glasses (BGs) were invented over 50 years ago and have been in medical use since the 1980s in orthopaedics, otology and dentistry. Initially, these materials were synthesized as bioactive materials to eradicate bone defects; however, now their biomedical use covers an array of tissue engineering and therapeutic applications as well. Current research confirms that their applications are vastly increasing and are still far from being fully exploited. Classical applications of BGs include dental implants, bone filling materials and soft tissue regeneration. However, the fascinating question to be answered in the next few years is: how can antibacterial properties of BGs can be enhanced and how can they be more useful for wider medical applications?

BGs are bioactive synthetic materials, which are osteoconductive and angiogenic in nature and are biocompatible with natural tissues [2–5]. In general, BG can be defined as a material that can be applied to induce a specific biological activity [6, 7]. In a more concise sagacity, a BG structure can be stated as a bioactive material that may perform specific biological surface reactions upon implantation in the living body [8]. This structure further leads to show formation of hydroxyapatite (HAp), which has close resemblance with natural bone mineral and has the ability to make a bond with the live tissue [9]. Initially, glass ceramic materials were bioinert in nature; later they were modified and are now implanted as bioactive materials [10].

Hench and co-workers in 1969 reported that bone can be chemically bonded with certain glassy structures [1, 11]. They reported that glassy materials have the ability to show specific response on the interface and also show bond formation between the biological tissue and the glass material. This glass material can be used to reconstruct the damaged bones or diseased parts of bone. Their ability to integrate with natural hard and soft tissues was first explored in 1971 by L. Hench [1, 8]. Microbial infections are usually caused by Gram-positive organisms such as *Staphylococcus aureus*, *S. epidermidis* and *streptococci* or Gram-negative organisms such as *Escherichia coli*, *Pseudomonas aeruginosa* and *Enterobacter* [4]. Antibacterial, angiogenic and osteoconductive properties can be incorporated into BGs, which will enable them to simultaneously treat bone defects and bone infections [3–5, 8, 12–16]. BGs with antibacterial properties are the modern materials that can be prepared according to the specific clinical application and properties [16]. A brief detail of various processing techniques is given below.

11.2 Processing Techniques

Various methods such as conventional, flame synthesis, melt-quench, sol-gel and microwave processing can be used to manufacture BG powders; however, here we shall try to highlight the methods used to synthesize BG having high antibacterial character. While preparing these materials, the following precautions must be considered to avoid any inappropriateness which may affect the quality and phase purity of BGs powder.

1. Avoid contamination of glass structures because it may affect their reactivity.
2. Analytical grade chemicals must be used to prepare high purity products.
3. Highly pure silica (Flint glass) must be added to prepare high-quality structures.
4. According to Anderson, addition of calcium phosphate may be beneficial to furnish more crystalline glass materials [17, 18].

Synthesis of BG through conventional technique suffers from the following drawbacks:

1. A high purity is required for BG which is difficult to attain through conventional methods due to factors like high temperature, high alkali contents and low silica quantities used. In addition, due to their high reactivity, these glassy structures may capture various cations of types M^{3+}, M^{4+} and M^{5+} which can affect their tissue binding ability [19, 20].
2. The contaminants involved in BG powders can adversely affect their bioactivity.
3. The multistep processing in the costly platinum crucibles, laborious optimization of process parameters, involvement of costly equipments and quality assurance make conventional methods a difficult choice [21].
4. Lack of compositional control during conventional process due to high temperature and high viscosity of SiO_2 make conventional methods unpopular.

The details of various methods commonly used to synthesize BG powders are given below.

11.2.1 Melt-Quench Method

The first BG powder introduced in 1969 was synthesized by melting the mixture of 46.1 mol% SiO_2, 24.4 mol% Na_2O, 26.9 mol% CaO and 2.6 mol% P_2O_5. Melt quench is the traditional technique commonly employed to synthesize BG [22]. The temperature during this synthesis is kept relatively high (600–700 °C). The composition of BG powder can be decided according to the application and required properties of the product. An extensive research work is in process for more than 40 years, but only two compositions have been approved by the US food and drug administration (FDA) for clinical use, and these include 45S5 and S53P4 which involve a combination of four oxides (SiO_2, CaO, Na_2O and P_2O_5) [18, 23]. Both of these compositions are synthesized through melt-quench method. Although this technique is simple and can be handled easily however the major drawback of this technique is the poor porosity of the product due to the use of high temperature [24]. This poor porosity can result in low healing rate, and defects may occur in the tissue integration during in vivo testing. In addition, due to the high temperature, some volatile components like P_2O_3 can escape out [20].

11.2.2 Sol-Gel Method

Sol-gel path is a relatively low-temperature synthesis route for BG production, and it is therefore a more favourable method over the conventional processing technique. The use of low temperature further reduces its cost and has now become one of the most widely used synthesis protocol for the production of BG [21, 25]. Various steps like mixing of alkoxides in the solution to prepare inorganic matrix, hydrolysis, gelation and low-temperature calcination are involved in the synthesis of sol-gel-derived BG powder [26]. Low-temperature (600–700 °C) handling is the major advantage of this sol-gel process which not only helps in synthesizing BG powder, but in addition microscopic structure of BG can be modified by controlling the concentration of the reacting species, water to alkoxides ratio, catalyst and temperature of the reaction [27]. Easy BG synthesis, synthesis of homogeneous materials, broad range production of BG powder with controlled particle size, porous structure with increased surface area, morphology and effective and easy synthesis of thin films and coatings are the potential benefits of sol-gel method [21, 27, 28]. This technique also ensures the production of porous BG structures with increased surface area, which are very beneficial for different clinical applications [21, 29]. Composite glassy structures like disubstituted (CaO and SiO_2), trisubstituted (SiO_2–CaO–P_2O_5, SiO_2–CaO–Na_2O, P_2O_5–CaO–Na_2O) or even poly-substituted (SiO_2–CaO–P_2O_5–Ag_2O) can easily be synthesized through this method [30]. Similarly, other glassy materials like SiO_2–CaO–P_2O_5, SiO_2–P_2O_5–Al_2O_3–CaO–Na_2O–K_2O can also be manufactured through this technique [22]. Despite of many advantages, the preparation of crack free nanosized BG is the difficult task, and perhaps it is the major disadvantage of the sol-gel method. Furthermore, calcination at high temperature to remove organic reactants from the material is an important requirement of the route, and it is also considered as the disadvantage of this technique. Effective treatment of long bone infections is one of the major challenges for the orthopaedic surgeons [31–33].

11.2.3 Flame Synthesis Method

This is also a well-known route to synthesize BG powders [34]. Initially, the precursors are prepared and mixed slowly to furnish uniform mixture; this mixture is then fed into the oxygen/methane flame with the help of a capillary tube. Here the purpose of oxygen is to disperse the liquid. The major advantage of this method is its speciality to prepare the complex glass structures containing five elements. Except this, homogeneous and amorphous mixtures of BG can be produced through this method. High temperature of the flame helps in preparing the nanosized BG powders [35].

11.2.4 Microwave-Assisted Preparation of BG

Nowadays, microwave radiation-assisted with ultrasonic radiation-based synthesis is rapidly gaining attention of researchers as not only it can reduce the reaction time but it can also modify the reaction environment to produce nanosized BG powders [36, 37]. Microwave-based approach to synthesize BG is the cost-effective and efficient way to produce the materials. Typically, the precursor solution is treated with ultrasonic radiation for set time followed by the microwave irradiation of the mixture to furnish amorphous powder. This powder can be washed, dried and heat treated at 700 °C to obtain BG powder [38].

11.3 Mechanism of Action of BG

Initially, when placed in aqueous medium, the Na^+ ions dissolve rapidly from the surface of the glass through ion exchange method with H^+ ions, resulting in the change in the structure and composition of BG [39, 40]. This reaction accumulates surface layer with net negative charge. Dissolution of Na^+ ions breaks the silica network and furnishes the $Si(OH)_4$ groups [40]. These groups then repolymerize into silica-rich surface layer. This step is followed by the formation of amorphous Ca phosphate layer on the glass surface. This then develops bonding with the biological parts (blood proteins, growth factors and collagens).

BGs are the attractive materials due to their ability to develop a bond with the host tissue which is directly linked with the atomic structure of BGs. After implantation, BG gradually dissolves in the body, and ions are released during this process, which promotes growth of carbonated HAp on its surface [41]. In brief, in an aqueous environment, different ions like sodium ($Na^{+)}$, calcium (Ca^{2+}) and silica $(SiO_2)^{2-}$ are released from the surface of BG to facilitate the in vivo formation of HAp layer and thus permit the BG to repair the damaged bones. It has been shown that these soluble/dissolved ions kindle the process of osteogenesis through promotion, migration, proliferation or differentiation of osteoblast cells [42]. These surface reactions play a vital role in determining the level of bioactivity of these implanted materials and further help in knowing the level of their antibacterial influence against different microorganisms [42].

The dissolution process is enhanced due to the low connectivity of SiO_2 network and as a result of the presence of network modifiers like Na^+ and Ca^{2+} that can lead to the formation of non-bridging silicon-oxygen bonds [43]. Initially, Na^+ and Ca^{2+} ions replace H^+ from the biological fluid, and thus Si-OH bonds are formed. In addition, bioactivity of BG is also dependent upon their dissolution rate [44]. In this regard, morphology of BG may play a vital role to enhance their bioactivity [44]. BGs having high surface area may show better dissolution rate due to the enhancement in the contact area between the BG and the physiological fluid [45].

Currently, emphasis is being diverted to introduce such strategies to synthesize BGs, which can furnish nanosized high surface area porous products possessing strong activity against *E. coli*, *P. aeruginosa*, *S. Aureus* and *S. Epidermidis*.

11.4 Classification of Bioactive Glass Materials

In 1994, a classification was proposed for the BG materials, according to which BG materials can be subdivided in to two groups [46].

Class 1: Osteoproductive Materials
This class of BG includes materials which are both osteoproductive and osteoconductive in nature. BG materials in this class show bioactivity when it elicits both an intracellular and an extracellular response at its interface. 45S5 BGs are the best examples of this class.

Class 2: Osteoconductive Materials
This class of BG materials include materials that simply have the potential to provide a biocompatible interface along which bone shows growth. Osteoconductive bioactivity may crop up when a material demonstrates only an extracellular response at its interface. 45S5.6Sr is the best example of this class of materials [47].

11.5 Type of Bioactive Glass and Their Properties

11.5.1 Silicate Bioactive Glass

Silicate-based BG was first fabricated by Hench and co-workers in 1969 [23]. This class of BG represents a group of surface reactive materials that are able to bond to bone in physiological environment [8, 48]. This is the major class of BG structures, which have wide use in biomedical field. In silicate-based BG system, Na, Ca and P elements are mixed in different relative proportions to prepare the silicate network. The classical 45S5 BG composition (45 % SiO_2, 24.5 % Na_2O, 24.5 % CaO and 6 % P_2O_5) has been widely studied for biomedical applications [48]. Various features like low SiO_2 contents and high Na_2O and CaO contents are responsible for high bioactivity of 45S5 [4]. BG like 45S5 has many clinical applications especially for the treatments of periodontal diseases, bone filler as well as in middle ear surgery.

11.5.2 Phosphate Glass

This class of glasses are also important and include P_2O_5 glass-forming network in its composition. Besides this CaO and Na_2O can also be mixed in phosphate BG composition as modifiers. Phosphate BG structures have resemblance with natural

bone due to the trace amount of different ions in the organic mineral phase of bone. These glassy materials can be clinically applied as resorbable materials by controlling their solubility as well as their composition [4]. Phosphate BG materials are resorbable in nature, and their dissolution rate can be controlled according to their oxide composition [49].

11.5.3 Borate Bioactive Glass

Recent studies have shown that there are certain glass compositions of borate glass that have wonderful applications and are bioactive in nature [50]. Borate BGs are bioactive in nature, they have lower chemical durability and degrade rapidly and finally are converted to HAp-like structure. Borate BG materials have the capacity to support in vitro cell proliferation and differentiation as well as in vivo tissue infiltration for the treatment of bone infections [51]. Degradation rate of borate BG structures can be controlled by manipulating its composition. For instance, the degradation rate of borate BG can be varied over a wide range by partially replacing SiO_2 in silicate 45S5 or 13–93 glass (6 wt% Na_2O 12 wt% K_2O 5 wt% MgO 20 wt% CaO 4 wt% P_2O_5 53 wt% SiO_2) with B_2O_3 or fully replacing the SiO_2 with B_2O_3. This control of degradation rate of borate BG structures makes them useful for regeneration of bones. Furthermore, compositional flexibility of borate BG may serve as a source to incorporate many ions such as Zn^{2+}, Cu^{2+}, F^{1-}, Mn^{2+}, Sr^{2+} and B^{3+} in trace amounts to enhance the bone growth process [4]. Borate BG powders are more reactive than the silicate 45S5 BG and thus have higher bioactivity [52].

11.6 Modern Bioactive Glasses and Their Properties

11.6.1 Zinc-Substituted Bioactive Glasses

Zn is important for the normal growth of human body and bone, and it possesses good antibacterial properties [53–56]. Zn is involved in the calcification of bones and is the essential cofactor for many enzymes; it is also responsible for DNA (deoxyribonucleic acid) replication and acts as a stimulant for protein synthesis [57, 58]. The presence of Zn in BG enhances the chemical durability of the glass in the aqueous media as well as increases the mechanical durability of the glass [59]. In many studies, Zn-containing BG has also been fabricated using sol-gel, melt-quench and microwave-assisted methods [60]. Most of the studies confirmed that high surface area has important role in deciding the bioactivity of the glass structures [60, 61]. Additionally, the presence of Zn in the human hard tissues helps in

maintaining the pH of physiological solution and thus helps in the normal growth of the bone cells in a favourable environment [56, 59]. Although, the presence of Zn enhances the bioactivity of the cells and will also help in running many body systems. At high concentration, it may be fatal for the human body so its content in BGs must be carefully controlled [56].

11.6.2 Cerium-Substituted Bioactive Glasses

Current literature study has revealed that bacterial infections have become a serious threat to the use of implants as they sometimes show failure due to various infections. Although, BGs show some antibacterial properties, however antibacterial activity of BGs can be enhanced due to the incorporation of metal ions like cerium in the BGs [62].

Ce is the member of rare earth elements and has various uses in industry as a catalyst, fuel, additive and colouring component in glass manufacturing process [63]. Although, Ce has been known for various said applications however its use as a good antibacterial agent has not been fully explored [64]. However, in some investigations, its use as an efficient antibacterial agent has been reported [65, 66]. Antibacterial action of Ce is due to its ability to dissociate bacterial cell membrane from cytoplasmic membrane [67].

11.6.3 Copper-Substituted Bioactive Glasses

Cu is well known for its antibacterial properties [68–71]. It is widely accepted that at low concentrations it shows beneficial effects, whereas at high concentrations it inhibits the growth and thus becomes toxic and a major cause to kill the microorganisms [70]. It is well documented that small amount is sufficient against the microbes. In addition, Cu has significant influence against antimicrobial agents like *E. coli*, methicillin-resistant *S. aureus* and *Clostridium difficile* (*C. difficile*) [72, 73]. Cu binds itself with the protein functional groups first then interacts with microbial membrane [74]. This action causes structural changes due to its interaction with the microbial nucleic acid. This action is then followed by the production of hydroperoxide free radicals and inactivation of enzymes [75]. Although, Cu is well known for its antibacterial effects, however its incorporation into BG is only reported in few studies [76]. Similarly, alloys of Cu such as bronze, brass, Cu-Zn-Ni and Cu-Ni can also be doped in the BG materials to enhance their antibacterial activity [16, 77]. Cu has strong antimicrobial activity, at the same time it has the capability to play a vital role in the development of bone formation and its healing process.

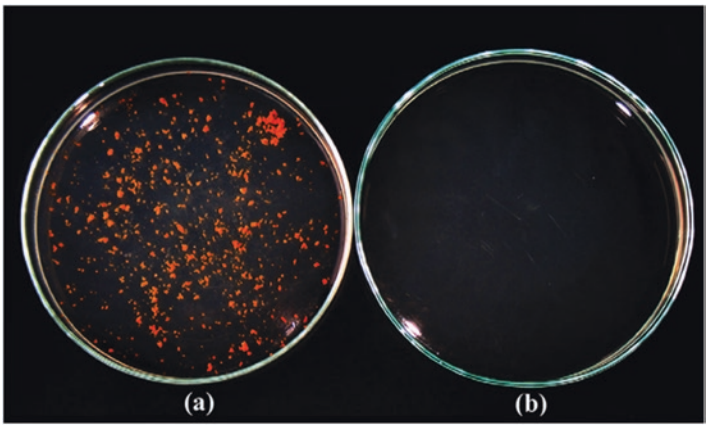

Fig. 11.1 Representative image of bactericidal action of (**a**) BG and (**b**) Ag-BG on *E. Coli* in the culture medium containing 20 mg/ml of bioglass material after 72 h exposure [87]

11.6.4 Silver-Substituted Bioactive Glasses

Ag has been widely used for its antibacterial properties [78]. BGs containing Ag have been synthesized by many researchers due to their powerful antibacterial properties [79–81]. Owing to such behaviour, Ag has been in use as substituent in many of the biomaterials to impart antibacterial properties [82, 83]. Ag-doped BG can also be applied as coating on medical sutures [84–86]. These coating may impart antibacterial properties in the materials and at the same time have the ability to enhance biocompatibility of the medical sutures. Ag has the potential to induce antibacterial properties in the biomaterials has been confirmed from the studies where materials having no Ag contents showed no antibacterial action [87] (Fig. 11.1). Culture plates (Fig. 11.1) revealed that antibacterial action of Ag-substituted BG is better than the pure BG.

The antibacterial action of Ag-substituted biomaterials could be the result of the following interactions [88–90]:

(a) Interaction with bacterial DNA and RNA (ribonucleic acid)
(b) Interference with electron transport
(c) Interaction with components of the cell
(d) Interaction with bacterial nucleophilic amino acid residues in proteins

Finally, these interactions help to denature the protein resulting in the death of cells. Ag-substituted BGs have shown good biological properties [75]. Therefore, the inclusion of Ag in BG powders is of great interest as it can increase the bioactivity and antimicrobial action. A study confirmed that inclusion of Ag contents in the BG coating can reduce the growth of *E. coli* bacteria. Antibacterial effect can be controlled by varying the concentrations of Ag in the material [91]. Another study demonstrated that sol-gel-synthesized Ag-doped BG (76% SiO_2, 19% CaO, 2% P_2O_5 and 3% Ag_2O) is very effective against *Pseudomonas aeruginosa* and

Staphylococcus aureus pathogens and not toxic to human osteoblast cells [92]. Another study has also shown that Ag-doped BG is better candidate in contrast to Ag-free BGs to kill microorganism (Enterococcus faecalis) [93].

11.6.5 Strontium-Substituted Bioactive Glasses

Sr is an important element that has good impact on the bone cells and can be substituted in BG to replace Ca^{2+}. Sr-doped BG gives better osteoblast stimulation and bone bonding. Similarly, Sr-substituted BGs can be used for the treatment of osteoporosis and in addition can be used to promote osteoblast proliferation [94]. Sr-substituted BGs have also been recognized for their wide-spread application for vertebral compression fractures [95].

The use of invasive devices increases the risk of microbial infections and Gram-positive bacteria such as Streptococcus, Staphylococcus and Bacillus microbes which are the sole reason for implant-related infections [96, 97]. To overcome such microbial infections, Sr-substituted BGs can be better substitutes for dental and orthopaedic biomaterials [98, 99]. Sr-doped BGs also have the capability to inhibit microbial infections by inhibiting the bacterial growth and their reproduction by impeding permeability of cell wall synthesis, reproduction of cell wall synthesis, cell metabolism and permeability of cytoplasmic membrane. In some of the studies, Sr^{2+} has been introduced for the treatment of osteoporosis, but detailed mode of antimicrobial action is yet not clear. Despite this fact, its use in the presence of F^{1-} to treat bacterial infections has been suggested [100]. D.S. Bruer and co-workers have synthesized Sr-doped BG (SiO_2–CaO–CaF_2–MgO) to study the effect of its substitution on the antimicrobial activity. Study was conducted against two Gram-positive microorganism (*S. aureus* and S. Faecalis), which confirmed that growth of *S. aureus* and *S. faecalis* was inhibited by Sr-doped BGs [95].

11.7 Applications of Bioactive Glass

BGs have wide spread applications in orthopaedic field due to their interesting properties mentioned in Table 11.1.

11.8 Common Methods Adopted to Conduct Antibacterial Study

Various techniques mentioned below are usually applied to carry out antibacterial studies using synthesized BG.

1. Spread plate method
2. Viable cell count method

Table 11.1 Mode of action and applications of bioactive glasses

No	Effect	Mechanism of action	Application	Reference
1	Antibacterial and antifungal	Act as antibacterial agent by releasing antibacterial ions like Ag^{+}, Cu^{2+}, Ce^{2+}, etc. Interfere with bacterial DNA and RNA replication and kill the bacterial cells	Wound healing	[86, 101]
		Antimicrobial activities are proceeded through Ce action with outer membrane of bacterial cells from cytoplasmic membrane	Orthopaedic surgery	[65, 67]
2	Rapid nerve cells healing	Release of ions like Ca^{2+} and Zn^{2+} enhances growth of nerve cell healing	Nerve regeneration	[102]
3	Generation of new cells	Orientation of glass fibres directs the growth process of the tissues	Muscle cell regeneration	[4]
4	Angiogenic	Release of Cu^{2+}-like ions (dissolution products) helps in promoting blood micro vessel formation	Skin regeneration	[2]
5	To repair the tooth roots and to provide a stable ridge for dentures	Medical devices with monolithic shape were inserted into fresh tooth extraction sites to get the true results	Dentistry	[103]

3. Bacterial counting method
4. Plate counting method
5. Qualitative diffusion disk method

11.9 Factors Controlling the Antibacterial Properties of Bioactive Glass

An ideal BG should include elements in its composition that have good antibacterial properties to prevent post-operative infection. In order to get a complete understanding of the antibacterial actions of BG, it will be helpful to consider the following factors.

11.9.1 Influence of Bioactive Glass Composition

To combat bacterial infections, it is of paramount importance to understand those factors which have profound effect on the inhibition of bacterial infections. Different studies have revealed that the composition and morphology of BG play an important

role in the antibacterial character of BG [3, 104–106]. Normally, pure BG materials show no activity towards killing of microbes or bacteria. Moreover, pure BGs have very few applications towards fighting post-operative infections, which may develop due to the lack of proper interaction between the hard tissues of the body and implanted biomaterial [107, 108]. The increasing use of implant materials to deal with various soft and hard tissue disorders and fractures is associated with a major risk of bacterial infections and ultimately failure of implant [109, 110]. However, drugs or implant materials having antibacterial properties can be the better choice to deal with the post-operative infections. Various BGs have been used to deal with oral, orthopaedic implant and wound dressing infections [111–117]. The rise of post-operative infection cases is also attributed to multidrug-resistant pathogens like methicillin-resistant *Staphylococcus aureus* (MRSA). These pathogens make the treatment of various infections very problematic with common antibiotics. In order to deal with such problems and make BGs more effective towards these infections and to kill the pathogens, composition of BGs can be changed to contain trace amount of elements like Ag, Zn. Cu, Ce, etc. These modified BGs will have potent activity against different microorganisms to combat microbial infections [118, 119]. Similarly, in an investigation designed by Yi-Fan Goh and co-workers, it was reported that the presence of Ce in BG is directly linked to the antibacterial activity of the resultant BG [63]. Ce-doped BGs having low concentration of Ce have less activity towards killing of bacteria, whereas Ce-doped BGs having high Ce contents (10 mol %) showed promising action towards the killing of bacteria [63]. Di-Zhang and co-workers in their work explored the antibacterial activity of six BGs, which confirmed that composition has pronounced affect on the pH which further influences the antibacterial behaviour of BGs (Fig. 11.2) [106].

According to another report, chemical composition of BGs and conditions for its dissolution in the surrounding atmosphere also have profound effect on their

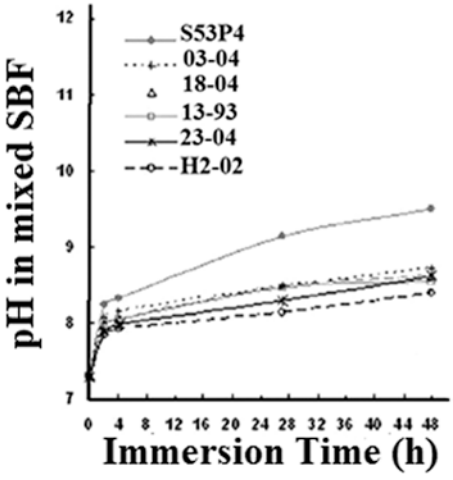

Fig. 11.2 Showing the effect of concentration on the pH [106]

antibacterial activity [12]. Manukka and co-workers have reported that BGs with high CaO contents (42.3 wt%) had better antibacterial action in contrast to BGs with low CaO contents (31.27 wt%) [120]. Similarly, BG having high concentration of SiO_2 could be more effective against bacterial attacks [28].

11.9.2 Influence of Bioactive Glass Morphology

Morphology of the BG materials is another important parameter which plays a major role in explaining the antibacterial properties of BG. BG having uniform spherical shape of particles and size in the nanometre range (<50 nm) may perform better against bacterial infections. An investigation conducted by M. Prabhu and co-workers confirmed that *Azadirachta indica* (Neem)-substituted BG showed the formation of spherical amorphous particles having particle size in the nanometre range (<50 nm). Furthermore, this study confirmed that amorphous particles with spherical shape have better activity against bacterial infections in comparison to the needle-like particles [16, 121]. It can be inferred that the needle-like particles have less exposed area and thus show little activity towards pathogens. M. Saqaei and co-workers synthesized BG-forsterite (58S-Mg_2SiO_4) using sol-gel method using 10, 20 and 30 % wt forsterite concentration and further employed to study their activity against various bacterial species (*E. coli* and *S. aureus*) [16]. Results proved that nanosized particles having uniform spherical shape have good antibacterial action. Their study also confirmed that the soaking time in SBF plays an important role in both dissolution of ions in the SBF solution and modifying the morphology of particles (Fig. 11.3).

Results further showed that BG 20F [58S BG (SiO_2 57.72 wt%, CaO 35.09 wt% and $P_2O_5$7.1 wt%) with 20 wt% $Mg_2(SiO_4)$] and BG30F possessed good antibacterial activity against *E. coli* and *S. aureus*. In addition, concentration of forsterite is also

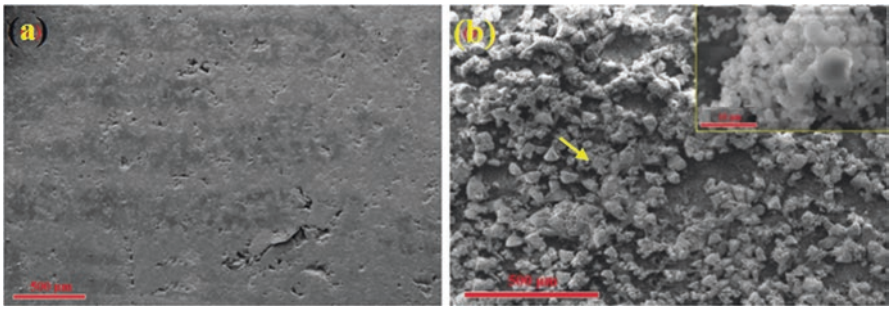

Fig. 11.3 SEM image of BG20F (20 % wt forsterite) (**a**) before soaking in SBF solution and (**b**) after 28 days of soaking in SBF solution [16]

important as at low concentration they showed no antibacterial activity; however, when concentration and immersion time was increased, both samples showed a good morphological change, and thus good antibacterial action was observed.

11.9.3 Influence of Bioactive Glass Dissolution Behaviour

Dissolution behaviour of BG in SBF can also have considerable effect of the antibacterial properties of BG. For instance, S53P4 (Na_2O 23%, CaO 20%, P_2O_4 4% and SiO_2 53%) BG has strong antibacterial action, which is usually attributed to their high dissolution rate and presence of high contents of silicon in the supernatant [112, 122]. Dissolution rate of BG directly affects the microbial infections that may occur on implanting the implant materials in the living body [87]. Balamaurugan A. and co-workers reported the effect of Ag-doped BG (SiO_2–CaO–P_2O_5–Ag_2O) on the antibacterial and biological properties. Results confirmed that the dissolution of Ag-doped BG has the better potential to kill *E. coli* as compared to pure BG [87].

11.9.4 Influence of pH

Besides composition and morphological characteristics, pH control in BG study is another important factor which must be carefully monitored and should be controlled as high pH value kills the microbes and in this way activity of BGs against bacteria is enhanced [122]. Release of cations like Na^+, Ca^{2+}, Mg^{2+}, etc. predominantly results in the raise of the pH of the medium [122]. Di Zhang and co-workers arranged a study to find the effect of pH on antibacterial activity of three BGs [S53P4 (Na_2O 23 wt%, CaO 23 wt%, P_2O_4 4 wt% and SiO_2 53 wt%), 13–93 (6 wt% Na_2O 12 wt% K_2O 5 wt% MgO 20 wt% CaO 4 wt% P_2O_5 53 wt% SiO_2) and 18–04 (15 wt% Na_2O, 4.5 wt% MgO, 20 wt% CaO, 2 wt% B_2O_3, 4 wt% P_2O_5 54.5 wt% SiO_2)]; they reported that the antimicrobial effect of BG is mostly dependent upon the increase of pH of the medium [122]. These three BGs were placed in the SBF solution, and the effect of release of ions on the pH was recorded. All the three samples showed rapid increase in the pH within the first 2 h. Furthermore, antibacterial study confirmed a good co-relation with increased pH profile. BG S53P4 showed antibacterial activity due to having high pH in contrast to other two BGs 13–93 and 18–04 [123].

In another investigation, Yi-Fan Goh and co-workers have reported in their work that increased pH level is beneficial to enhance their antibacterial properties [63]. In their study viable count method was used to carry out the antibacterial study of Ce-doped BGs. Antibacterial studies showed that increased pH level is an important factor to enhance antibacterial activity of BGs. Similarly, Stoor and co-workers reported that fine powder of S53P4 has good antimicrobial effect due to increased

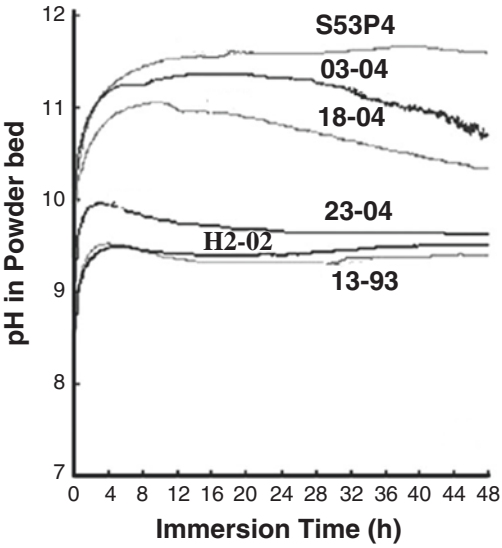

Fig. 11.4 pH of SBF solution as function of immersion time in powder bed [106]

pH and increased Na^+ concentration in the suspension [10]. The pH value of the solution increases strikingly after mixing it with BG, and this condition is unfavourable for the bacterial growth [15]. In addition, release of various ions (Na^+, Ca^{2+}or P^{3+}) increases the osmotic pressure of the environment, and this is detrimental for the growth of different bacterial species [23, 124]. An increase in pH value for six BGs is shown in Fig. 11.4. Although a similar trend has been indicated in this graph for six BG varieties, however a variation in the pH values can be observed depending upon the composition of BGs [106]. Figure 11.4 shows that pH value markedly increases within first 8 h.

Studies have confirmed that high pH level is responsible for the antibacterial activity of BGs which reduces the viability of bacterial suspension [125]. V. Mortazavi and co-workers in their research task also showed that the pH increase is an important parameter which controls antibacterial activities of BGs [28]. Figure 11.5 is demonstrating that the pH variations of broth containing BG 58S (SiO_2 57.72 wt%, CaO 35.09 wt% and P_2O_5 7.1 wt%) have higher pH (9) than 62S (SiO_2 62.17 wt%, CaO 28.47 wt% and P_2O_5 9.25 wt%) and 72S ($SiO_2$72.88 wt%, CaO 17.49 wt% and P_2O_5 9.56 wt%). The basicity of solution results from the silica concentration in the solution. Solution pH is affected by several chemical acid-base equilibrium steps, which include de-protonation and re-protonation of silica ions like $(SiO_4)^{4-}$, $(HSiO_4)^{3-}$ and $(H_2SiO_4)^{2-}$ [93, 126].

BGs containing high contents of CaO shows higher rate of CaO dissolution which on reacting with water boost up the pH of the medium in contrast to sample containing higher ratio of SiO_2 whose dissolution decreases the pH of solution, thus showing reduced antibacterial action [93].

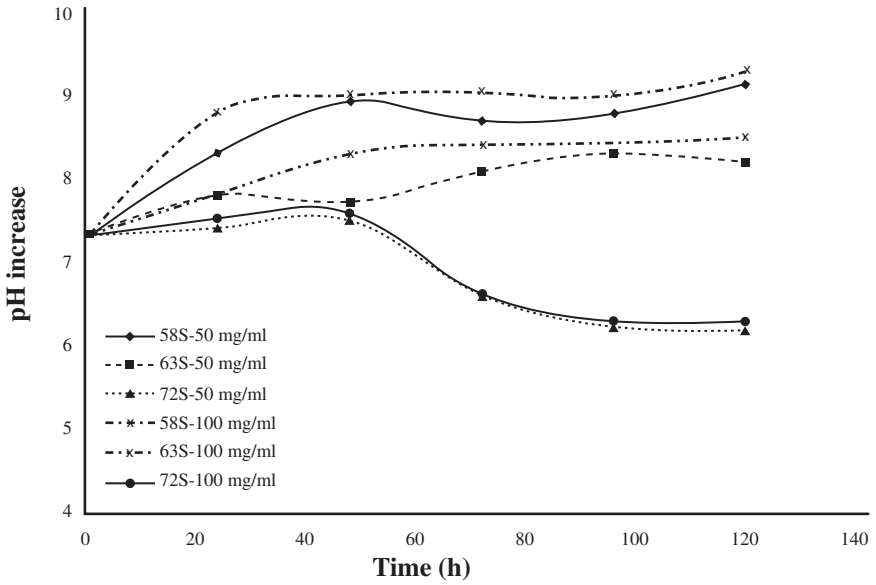

Fig. 11.5 Showing pH changes of broth containing BGs [28]

11.9.5 Influence of Particle Size and Surface Area

A decrease in the particle size of BG can have significant effect on the antibacterial efficiency of the material because reduction in size increases the active surface area and subsequently enhances the release of ions [113, 114, 127]. Seuss and co-workers reported that nanosized chitosan 45S5 BG has significant antibacterial action as compared to micron-sized particles [128]. There exists a strong assumption that high surface area and BG having size in nanometre range release more alkali metals and therefore show good antimicrobial activity [93]. Nanostructured BG materials have gained huge attention recently and are the best choice due to their superior osteoconductive properties in contrast to micron-sized BG [121]. A study has shown that by increasing the surface area antibacterial behaviour of BG can be upgraded [16].

11.9.6 Influence of Natural Organic Substance

Addition of increased amount of elements especially Ag^{1+} contents in BG may be fatal. Furthermore, some studies have confirmed that higher Ag^{1+} contents leads to the formation of incipient crystallisation of quartz and thus effect the biocompatibility of BG [129]. To overcome these issues, some natural organic components such

as *Azadirachta indica* (Neem) may be incorporated in the BG. *Azadirachta indica* has very good antibacterial ability against wide range of bacterial agents. It also has excellent anti-inflammatory, antimicrobial and antiviral properties [130]. Owing to the potent antibacterial properties of both *Azadirachta indica* and Ag^{1+} have been doped together in BG to enhance its antibacterial properties [121]. Silica- and phosphate-based BG ($58SiO_2$-$33CaO$-$9P_2O_5$) has been doped with *Azadirachta indica* using traditional sol-gel method. Results have confirmed that the *Azadirachta indica* leaf powder-substituted BG has remarkable biocompatibility and activity against certain pathogens like *S. Aureus and E. coli* in contrast to Ag-doped BGs [121]. This result hence confirmed that the natural resources may also be better alternative to enhance the antibacterial properties of BG. In another investigation uniform thickness 40–50 nm, nanocoatings of Cu-doped BGs were fabricated on egg shell membrane. The prepared BGs showed better in vivo angiogenesis rate and better antibacterial activity [131].

Natural extracellular matrix (ECM) isolated from the porcine bladder can also be a good source to produce BG having antibacterial properties [132]. Wang Y-Y and co-worker fabricated a novel BG by incorporating sol-gel-derived Ag-substituted BG in natural ECM hydrogel [132]. This Ag-BG/ECM was used to evade the bacterial infections caused by *Streptococcus mutans* (*S. mutans*) and *Lactobacillus casei* (*L. casei*). ECM hydrogels have already been extracted and employed in many regenerative medicine applications, and the results have shown that ECM hydrogels can promote in tissue healing [133–135]. Similarly, in another research study, it was probed that egg shell membrane (ESM) which is a natural material has antibacterial and wound-healing characteristics [136]. 5Cu-BG/ESM was synthesized successfully, and results showed that 5Cu-BG/ESM films may be a potential source for wound healing and to avoid various bacterial infections [131]. Figure 11.6 shows the effect of undoped BG (Blank), pure ESM and Cu-BG/ESM on the bacterial growth and confirms that Cu-BG/ESM has the potential to combat bacterial infections.

An overview of the type of BGs, their clinical use, application and reasons that make them potent against different species of microbes is given in Table 11.2.

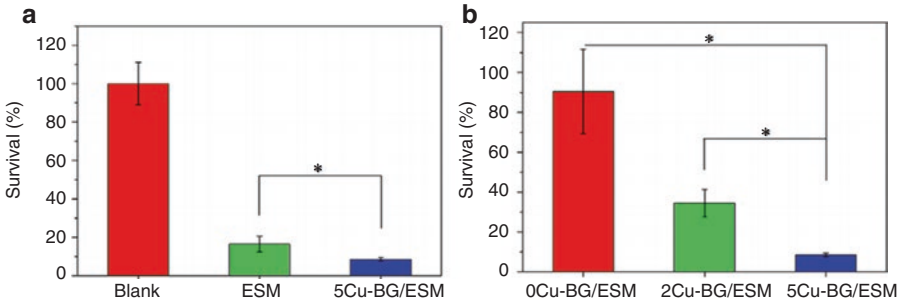

Fig. 11.6 Representing the antibacterial effect of Blank, ESM and Cu-BG/ESM on bacterial growth [131]

Table 11.2 An overview of the type of BGs, applications and their clinical use

No	Type of BGs	Application/clinical use	Bacterial species	Particle/pore size	Reason	Reference
1	Ag-doped BGs (SiO_2–CaO–P_2O_5–Ag_2O) 58S	Antibacterial	*E. Coli*	5–7 nm	High pH/Ag ion concentration	[87, 137]
2	GO doped BG (graphene oxide bioactive glass) ($Si(OC_2H_5)_4$, $Ca(NO_3)_2$ and $(C_2H_5)_3PO_4$,	Antibacterial	*S. aureus*	785 nm	High pH	[138]
3	BG-forsterite ($SiO_2CaOP_2O_5$, Mg_2SiO_4)	Antibacterial	*E. Coli*	10–16 nm	High pH	[16]
4	MMBG (SiO_2:CaO:P_2O_5:Fe_3O_4)	Drug delivery/ antibacterial	*S. aureus*	4.98 nm and 5.40 nm	F^- ion	[139]
			Staphylococcus epidermidis (*S. epidermidis*)			
5	BG-F (SiO_2–P_2O5–CaO–Na_2O–CaF_2)	Antibacterial	*Porphyromonas gingivalis* (*P. gingivalis*)	–	High pH	[140]
		Angiogenesis	*Aggregatibacter actinomycetemcomitans* (*A. actinomycetemcomitans*)			
6	BG-Sr (SiO_2-P_2O_5-CaO-Na_2O-SrO)	Antibacterial	*P. gingivalis*	–	Sr^{2+} concentration	[141]
		In vitro osteogenic	*A. actinomycetemcomitans*			
7	45S5	Antibacterial/wound healing	*E. coli*	0.02–0.06 μm	High pH	[80, 93, 125]
			S. aureus	90–710 μm		
			P. aeruginosa			
			S. sanguis			
			A. viscosus			

8	S53P4	Antibacterial/wound healing	*E. faecalis*	<45 μm	High pH and high Na and Si concentration	[10, 112]
			S. mutans			
			P. gingivalis			
			A. actinomycetemcomitans			
9	$CaPSiO_2$	Antibacterial	*S. epidermidis*	<45 μm	High Ca concentration	[142]
10	$76SiO_2$-22CaO-$2P_2O$	Antibacterial	*E. coli*	90-710 μm	High pH	[80, 142]
			S. aureus			
			P. aeruginosa			
11	Cu-BG/ESM	Antibacterial	*E. coli*	40–50 nm	Both Cu^{2+} ions and ESM	[131]
		Angiogenesis				

11.10 Conclusion

During the past decades, huge interest has been shown in the development of BGs including various ceramic materials for bone and dental repair as well as to overcome the bacterial infections that result due to the implantation of these materials in the living system. The major reason that lies behind this development is to increase life expectancy and the social obligations to provide a better quality of life. An escalating attention has been paid towards the use of BGs in bone tissue and dental repair, to combat different bone infections, and the development of new BGs having better potential to eradicate bacterial infections has led to the synthesis of novel BG materials.

The precise mechanisms of the antibacterial activity of BGs is still unknown; however, it is believed that various factors such as the chemical composition and concentration of BG; the high concentrations of Ca^{2+}, Na^{+} and Si^{4+} ions to be released from the BGs and especially high pH are the reasons of their antibacterial characteristics. These novel nanosized BGs have provoked the modern researchers to explore new applications of these glassy materials in biomedical engineering field particularly to make them more secure in context to bacterial infections. Their antibacterial effectiveness and clinical use however still require more perfection and must be validated both at in vivo and in vitro level.

References

1. Hench LL, Wilson J. An introduction to bioceramics, vol. 1. Singapore: World Scientific; 1993.
2. Aurégan J-C, Bégué T. Bioactive glass for long bone infection: a systematic review. Injury. 2015;46:S3–7.
3. Hu S, et al. Study on antibacterial effect of 45S5 Bioglass®. J Mater Sci Mater Med. 2009;20(1):281–6.
4. Rahaman MN, et al. Bioactive glass in tissue engineering. Acta Biomater. 2011;7(6): 2355–73.
5. Day RM. Bioactive glass stimulates the secretion of angiogenic growth factors and angiogenesis in vitro. Tissue Eng. 2005;11(5–6):768–77.
6. Donaruma LG. In: Williams DF, editor. Definitions in biomaterials. Amsterdam: Elsevier; 1987. 72 pp, 1988, Wiley Online Library.
7. Park J, Lakes RS. Biomaterials: an introduction. New York: Springer Science & Business Media; 2007.
8. Hench LL, et al. Bonding mechanisms at the interface of ceramic prosthetic materials. J Biomed Mater Res. 1971;5(6):117–41.
9. Kokubo T, Takadama H. How useful is SBF in predicting in vivo bone bioactivity? Biomaterials. 2006;27(15):2907–15.
10. Stoor P, Söderling E, Salonen JI. Antibacterial effects of a bioactive glass paste on oral microorganisms. Acta Odontol Scand. 1998;56(3):161–5.
11. Hench LL, Andersson O. Bioactive glasses. Adv Ser Ceram. 1993;1:41–62.
12. Leppäranta O, et al. Antibacterial effect of bioactive glasses on clinically important anaerobic bacteria in vitro. J Mater Sci Mater Med. 2008;19(2):547–51.

13. Arkudas A, et al. Evaluation of angiogenesis of bioactive glass in the arteriovenous loop model. Tissue Eng Part C Methods. 2013;19(6):479–86.
14. Välimäki V-V, Aro H. Molecular basis for action of bioactive glasses as bone graft substitute. Scand J Surg. 2006;95(2):95–102.
15. Coraça-Huber DC, et al. Efficacy of antibacterial bioactive glass S53P4 against S. Aureus biofilms grown on titanium discs in vitro. J Orthop Res. 2014;32(1):175–7.
16. Saqaei M, et al. Effects of adding forsterite bioceramic on in vitro activity and antibacterial properties of bioactive glass-forsterite nanocomposite powders. Adv Powder Technol. 2016;27:1922–32.
17. Andersson Ö, et al. Evaluation of the acceptance of glass in bone. J Mater Sci Mater Med. 1992;3(2):145–50.
18. Andersson OH, et al. Models for physical properties and bioactivity of phosphate opal glasses. Glastech Ber. 1988;61(10):300–5.
19. Gross UM, Strunz V. The anchoring of glass ceramics of different solubility in the femur of the rat. J Biomed Mater Res. 1980;14(5):607–18.
20. Li J, et al. In vitro biocompatibility study of calcium phosphate glass ceramic scaffolds with different trace element doping. Mater Sci Eng C. 2012;32(2):356–63.
21. Li R, Clark A, Hench L. An investigation of bioactive glass powders by sol-gel processing. J Appl Biomater. 1991;2(4):231–9.
22. Franks K, et al. Investigation of thermal parameters and crytallisation in a ternary CaO–Na 2 O–P 2 O 5-based glass system. Biomaterials. 2001;22(5):497–501.
23. Hench LL, Paschall H. Direct chemical bond of bioactive glass-ceramic materials to bone and muscle. J Biomed Mater Res. 1973;7(3):25–42.
24. Abbasi Z, et al. Bioactive glasses in dentistry: a review. J Dent Biomater. 2015;2(1):1–9.
25. Sakka S. Glasses and glass-ceramics from gels. J Non-Cryst Solids. 1985;73(1–3):651–60.
26. Brinker CJ, Scherer GW. Sol→ gel→ glass: I. Gelation and gel structure. J Non-Cryst Solids. 1985;70(3):301–22.
27. Laudisio G, Branda F. Sol–gel synthesis and crystallisation of 3CaO· 2SiO 2 glassy powders. Thermochim Acta. 2001;370(1):119–24.
28. Mortazavi V, et al. Antibacterial effects of sol-gel-derived bioactive glass nanoparticle on aerobic bacteria. J Biomed Mater Res A. 2010;94(1):160–8.
29. Greenspan D, Zhong J, LaTorre G. Evaluation of surface structure of bioactive glasses in-vitro. Bioceramics. 1995;8:477–82.
30. Sepulveda P, Jones JR, Hench LL. Characterization of melt-derived 45S5 and sol-gel–derived 58S bioactive glasses. J Biomed Mater Res. 2001;58(6):734–40.
31. Wasko MK, Borens O. Antibiotic cement nail for the treatment of posttraumatic intramedullary infections of the tibia: midterm results in 10 cases. Injury. 2013;44(8):1057–60.
32. Hake ME, et al. Local antibiotic therapy strategies in orthopaedic trauma: practical tips and tricks and review of the literature. Injury. 2015;46(8):1447–56.
33. Arias PP, et al. Activity of bone cement loaded with daptomycin alone or in combination with gentamicin or PEG600 against Staphylococcus epidermidis biofilms. Injury. 2015;46(2): 249–53.
34. Brunner TJ, Grass RN, Stark WJ. Glass and bioglass nanopowders by flame synthesis. Chem Commun. 2006;13:1384–6.
35. Brunner TJ, Grass RN, Stark WJ. Glass and bioactive glass nanopowders by flame synthesis. Eur Cells Mater. 2006;11:18.
36. Han J-K, et al. Synthesis of high purity nano-sized hydroxyapatite powder by microwave-hydrothermal method. Mater Chem Phys. 2006;99(2):235–9.
37. Kim W, Saito F. Sonochemical synthesis of hydroxyapatite from H 3 PO 4 solution with Ca (OH) 2. Ultrason Sonochem. 2001;8(2):85–8.
38. Sarkar SK, Lee BT. Synthesis of bioactive glass by microwave energy irradiation and its In-vitro biocompatibility. Bioceram Dev Appl. 2011;1:1–3.

39. Clark DE, Pantano Jr CG, Hench LL. Corrosion of glass. New York: Books for Industry and the Glass Industry; 1979.
40. Greenspan DC. Bioactive glass: mechanisms of bone bonding. Tandläkartidningen Årk. 1999;91(8):1–32.
41. Wallace K, et al. Influence of sodium oxide content on bioactive glass properties. J Mater Sci Mater Med. 1999;10(12):697–701.
42. Hench LL. A genetic theory of bioactive materials. In: Key engineering materials. Uetikon-Zuerich: Trans Tech Publ.; 2001.
43. González P, et al. Raman spectroscopic study of bioactive silica based glasses. J Non-Cryst Solids. 2003;320(1):92–9.
44. Vichery C, Nedelec J-M. Bioactive glass nanoparticles: from synthesis to materials design for miomedical applications. Materials. 2016;9(4):288.
45. Liu S, et al. The effect of submicron bioactive glass particles on in vitro osteogenesis. RSC Adv. 2015;5(49):38830–6.
46. Srivatsan T. Processing and fabrication of advanced materials, XVII: part 8: polymer-based composites and nano composites: volume two, vol. 2. New Delhi: IK International Pvt Ltd; 2009.
47. Gorustovich AA, et al. Osteoconductivity of strontium-doped bioactive glass particles: a histomorphometric study in rats. J Biomed Mater Res A. 2010;92(1):232–7.
48. Hench LL. Bioceramics. J Am Ceram Soc. 1998;81(7):1705–28.
49. Neel EAA, et al. Bioactive functional materials: a perspective on phosphate-based glasses. J Mater Chem. 2009;19(6):690–701.
50. Pan H, et al. Strontium borate glass: potential biomaterial for bone regeneration. J R Soc Interf. 2009:rsif20090504.
51. Khera RA, Iqbal M. Nanoscale bioactive glasses and their composites with biocompatible polymers. Chem Int. 2015;1(1):17–34.
52. Brink M, et al. Compositional dependence of bioactivity of glasses in the system Na2O-K2O-MgO-CaO-B2O3-P2O5-SiO2. J Biomed Mater Res. 1997;37(1):114–21.
53. Yamaguchi M, Oishi H, Suketa Y. Stimulatory effect of zinc on bone formation in tissue culture. Biochem Pharmacol. 1987;36(22):4007–12.
54. Du RL, et al. Characterization and in vitro bioactivity of zinc-containing bioactive glass and glass-ceramics. J Biomater Appl. 2006;20(4):341–60.
55. Beherei HH, Mohamed KR, Mahmoud AI. Preparation, bioactivity and antibacterial effect of bioactive glass/chitosan biocomposites. In: 13th international conference on biomedical engineering. Berlin/Heidelberg: Springer; 2009.
56. Saino E, et al. In vitro calcified matrix deposition by human osteoblasts onto a zinc-containing bioactive glass. Eur Cell Mater. 2011;21(2):59–72.
57. Tang Z-L, et al. Role of zinc in pulmonary endothelial cell response to oxidative stress. Am J Phys Lung Cell Mol Phys. 2001;281(1):L243–9.
58. Yamaguchi M, Inamoto K, Suketa Y. Effect of essential trace metals on bone metabolism in weanling rats: comparison with zinc and other metals' actions. Res Exp Med. 1986;186(5):337–42.
59. Oki A, et al. Preparation and in vitro bioactivity of zinc containing sol-gel–derived bioglass materials. J Biomed Mater Res A. 2004;69(2):216–21.
60. Courthéoux L, et al. Controlled bioactivity in zinc-doped sol-gel-derived binary bioactive glasses. J Phys Chem C. 2008;112(35):13663–7.
61. Bini M, et al. SiO2− P2O5− CaO glasses and glass-ceramics with and without ZnO: relationships among composition, microstructure, and bioactivity. J Phys Chem C. 2009;113(20):8821–8.
62. Hoppe A, Güldal NS, Boccaccini AR. A review of the biological response to ionic dissolution products from bioactive glasses and glass-ceramics. Biomaterials. 2011;32(11):2757–74.
63. Goh Y-F, et al. In-vitro characterization of antibacterial bioactive glass containing ceria. Ceram Int. 2014;40(1):729–37.

64. Garner J, Heppell P. Cerium nitrate in the management of burns. Burns. 2005;31(5):539–47.
65. Lin Y, Yang Z, Cheng J. Preparation, characterization and antibacterial property of cerium substituted hydroxyapatite nanoparticles. J Rare Earths. 2007;25(4):452–6.
66. Cai X, et al. Synergistic antibacterial zinc ions and cerium ions loaded α-zirconium phosphate. Mater Lett. 2012;67(1):199–201.
67. Aimei C, et al. Dissociation of outer membrane for *Escherichia coli* cell caused by cerium nitrate. J Rare Earths. 2010;28(2):312–5.
68. Singh RK, Srinivasan A. Apatite-forming ability and magnetic properties of glass-ceramics containing zinc ferrite and calcium sodium phosphate phases. Mater Sci Eng C. 2010;30(8):1100–6.
69. Zhang H, et al. Aqueous dispersed conducting polyaniline nanofibers: promising high specific capacity electrode materials for supercapacitor. J Power Sources. 2011;196(23): 10484–9.
70. Zhu L, et al. Antimicrobial activity of different copper alloy surfaces against copper resistant and sensitive salmonella enterica. Food Microbiol. 2012;30(1):303–10.
71. Ibrahim SA, Yang H, Seo CW. Antimicrobial activity of lactic acid and copper on growth of salmonella and *Escherichia coli* O157: H7 in laboratory medium and carrot juice. Food Chem. 2008;109(1):137–43.
72. Jaiswal S, McHale P, Duffy B. Preparation and rapid analysis of antibacterial silver, copper and zinc doped sol–gel surfaces. Colloids Surf B: Biointerfaces. 2012;94:170–6.
73. Chatterjee AK, Chakraborty R, Basu T. Mechanism of antibacterial activity of copper nanoparticles. Nanotechnology. 2014;25(13):135101.
74. El-Kady MF, et al. Laser scribing of high-performance and flexible graphene-based electrochemical capacitors. Science. 2012;335(6074):1326–30.
75. El-Kady AM, Ali AF. Fabrication and characterization of ZnO modified bioactive glass nanoparticles. Ceram Int. 2012;38(2):1195–204.
76. Goh YF, et al. Bioactive glass: an in-vitro comparative study of doping with nanoscale copper and silver particles. Int J Appl Glas Sci. 2014;5(3):255–66.
77. Sawai J. Quantitative evaluation of antibacterial activities of metallic oxide powders (ZnO, MgO and CaO) by conductimetric assay. J Microbiol Methods. 2003;54(2):177–82.
78. Prabhu M, et al. Preparation and characterization of silver-doped nanobioactive glass particles and their in vitro behaviour for biomedical applications. J Nanosci Nanotechnol. 2013;13(8):5327–39.
79. Bellantone M, Coleman NJ, Hench LL. Bacteriostatic action of a novel four-component bioactive glass. J Biomed Mater Res. 2000;51(3):484–90.
80. Bellantone M, Williams HD, Hench LL. Broad-spectrum bactericidal activity of Ag2O-doped bioactive glass. Antimicrob Agents Chemother. 2002;46(6):1940–5.
81. Fan F-Y, et al. Preparation and characterization of silver nanocrystals decorated mesoporous bioactive glass via synchrotron X-ray reduction. J Non-Cryst Solids. 2016;450:128–34.
82. Shi Z, et al. Facile fabrication and characterization of poly (tetrafluoroethylene)@ polypyrrole/nano-silver composite membranes with conducting and antibacterial property. Appl Surf Sci. 2012;258(17):6359–65.
83. Yang F-C, et al. Evaluation of the antibacterial efficacy of bamboo charcoal/silver biological protective material. Mater Chem Phys. 2009;113(1):474–9.
84. Pratten J, et al. In vitro attachment of Staphylococcus epidermidis to surgical sutures with and without Ag-containing bioactive glass coating. J Biomater Appl. 2004;19(1):47–57.
85. Blaker JJ, Boccaccini AR, Nazhat SN. Thermal characterizations of silver-containing bioactive glass-coated sutures. J Biomater Appl. 2005;20(1):81–98.
86. Blaker J, Nazhat S, Boccaccini A. Development and characterisation of silver-doped bioactive glass-coated sutures for tissue engineering and wound healing applications. Biomaterials. 2004;25(7):1319–29.
87. Balamurugan A, et al. An in vitro biological and anti-bacterial study on a sol–gel derived silver-incorporated bioglass system. Dent Mater. 2008;24(10):1343–51.

88. Efrima S, Bronk B. Silver colloids impregnating or coating bacteria. J Phys Chem B. 1998;102(31):5947–50.
89. Liau S, et al. Interaction of silver nitrate with readily identifiable groups: relationship to the antibacterialaction of silver ions. Lett Appl Microbiol. 1997;25(4):279–83.
90. Solioz M, Odermatt A. Copper and silver transport by CopB-ATPase in membrane vesicles of enterococcus hirae. J Biol Chem. 1995;270(16):9217–21.
91. Seuss S, Heinloth M, Boccaccini AR. Development of bioactive composite coatings based on combination of PEEK, bioactive glass and Ag nanoparticles with antibacterial properties. Surf Coat Technol. 2016;301:1–148.
92. El-Kady AM, et al. Synthesis, characterization and microbiological response of silver doped bioactive glass nanoparticles. Ceram Int. 2012;38(1):177–88.
93. Waltimo T, et al. Antimicrobial effect of nanometric bioactive glass 45S5. J Dent Res. 2007;86(8):754–7.
94. Gentleman E, et al. The effects of strontium-substituted bioactive glasses on osteoblasts and osteoclasts in vitro. Biomaterials. 2010;31(14):3949–56.
95. Brauer DS, et al. Bactericidal strontium-releasing injectable bone cements based on bioactive glasses. J R Soc Interf. 2012:rsif20120647.
96. Lewis A. Drug-device combination products: delivery technologies and applications. Boca Raton: Elsevier; 2009.
97. Schierholz J, et al. The antimicrobial efficacy of a new central venous catheter with long-term broad-spectrum activity. J Antimicrob Chemother. 2000;46(1):45–50.
98. Alkhraisat MH, et al. Loading and release of doxycycline hyclate from strontium-substituted calcium phosphate cement. Acta Biomater. 2010;6(4):1522–8.
99. Dabsie F, et al. Does strontium play a role in the cariostatic activity of glass ionomer?: Strontium diffusion and antibacterial activity. J Dent. 2009;37(7):554–9.
100. Guida A, et al. Preliminary work on the antibacterial effect of strontium in glass ionomer cements. J Mater Sci Lett. 2003;22(20):1401–3.
101. Boccaccini A, et al. Development and characterisation of silver-doped bioactive glass-coated sutures for tissue engineering and wound healing applications. Biomaterials. 2004;25(7–8): 1319–29.
102. Bunting S, et al. Bioresorbable glass fibres facilitate peripheral nerve regeneration. J Hand Surg (Br Eur). 2005;30(3):242–7.
103. Stanley HR, et al. Using 45S5 bioglass cones as endosseous ridge maintenance implants to prevent alveolar ridge resorption: a 5-year evaluation. Int J Oral Maxillofac Implants. 1997;12(1):95–105.
104. Kalmodia S, Molla AR, Basu B. In vitro cellular adhesion and antimicrobial property of SiO2–MgO–Al2O3–K2O–B2O3–F glass ceramic. J Mater Sci Mater Med. 2010;21(4): 1297–309.
105. Echezarreta-López M, Landin M. Using machine learning for improving knowledge on antibacterial effect of bioactive glass. Int J Pharm. 2013;453(2):641–7.
106. Zhang D, et al. Antibacterial effects and dissolution behavior of six bioactive glasses. J Biomed Mater Res A. 2010;93(2):475–83.
107. Chaloupka K, Malam Y, Seifalian AM. Nanosilver as a new generation of nanoproduct in biomedical applications. Trends Biotechnol. 2010;28(11):580–8.
108. Simchi A, et al. Recent progress in inorganic and composite coatings with bactericidal capability for orthopaedic applications. Nanomed Nanotechnol Biol Med. 2011;7(1):22–39.
109. Pye A, et al. A review of dental implants and infection. J Hosp Infect. 2009;72(2):104–10.
110. Campoccia D, Montanaro L, Arciola CR. The significance of infection related to orthopedic devices and issues of antibiotic resistance. Biomaterials. 2006;27(11):2331–9.
111. Waltimo T, et al. Fine-tuning of bioactive glass for root canal disinfection. J Dent Res. 2009;88(3):235–8.
112. Zehnder M, et al. Dentin enhances the effectiveness of bioactive glass S53P4 against a strain of enterococcus faecalis. Oral Surg Oral Med Oral Pathol Oral Radiol Endod. 2006;101(4): 530–5.

113. Misra SK, et al. Poly (3-hydroxybutyrate) multifunctional composite scaffolds for tissue engineering applications. Biomaterials. 2010;31(10):2806–15.
114. Gorriti MF, et al. In vitro study of the antibacterial activity of bioactive glass-ceramic scaffolds. Adv Eng Mater. 2009;11(7):B67–70.
115. Xie ZP, et al. In vivo study effect of particulate bioglass® in the prevention of infection in open fracture fixation. J Biomed Mater Res B Appl Biomater. 2009;90(1):195–201.
116. Day RM, Boccaccini AR. Effect of particulate bioactive glasses on human macrophages and monocytes in vitro. J Biomed Mater Res A. 2005;73(1):73–9.
117. Verrier S, et al. PDLLA/bioglass® composites for soft-tissue and hard-tissue engineering: an in vitro cell biology assessment. Biomaterials. 2004;25(15):3013–21.
118. Palza H, et al. Designing antimicrobial bioactive glass materials with embedded metal ions synthesized by the sol–gel method. Mater Sci Eng C. 2013;33(7):3795–801.
119. Prabhu M, et al. Synthesis, characterization and biological response of magnesium-substituted nanobioactive glass particles for biomedical applications. Ceram Int. 2013;39(2):1683–94.
120. Munukka E, et al. Bactericidal effects of bioactive glasses on clinically important aerobic bacteria. J Mater Sci Mater Med. 2008;19(1):27–32.
121. Prabhu M, et al. In vitro bioactivity and antimicrobial tuning of bioactive glass nanoparticles added with neem (*Azadirachta indica*) leaf powder. Biomed Res Int. 2014;2014:1–10.
122. Zhang D, et al. Factors controlling antibacterial properties of bioactive glasses. In: Key engineering materials. Uetikon-Zuerich: Trans Tech Publ.; 2007.
123. Zhang D, et al. Comparison of antibacterial effect of three bioactive glasses. In: Key engineering materials. Uetikon-Zuerich: Trans Tech Publ.; 2006.
124. Andersson Ö, Kangasniemi I. Calcium phosphate formation at the surface of bioactive glass in vitro. J Biomed Mater Res. 1991;25(8):1019–30.
125. Allan I, Newman H, Wilson M. Antibacterial activity of particulate bioglass® against supra- and subgingival bacteria. Biomaterials. 2001;22(12):1683–7.
126. Green SA. Complications of external skeletal fixation. Clin Orthop Relat Res. 1983;180: 109–16.
127. Sepulveda P, Jones J, Hench L. In vitro dissolution of melt-derived 45S5 and sol-gel derived 58S bioactive glasses. J Biomed Mater Res. 2002;61(2):301–11.
128. Seuss S, Lehmann M, Boccaccini AR. Alternating current electrophoretic deposition of antibacterial bioactive glass-chitosan composite coatings. Int J Mol Sci. 2014;15(7):12231–42.
129. Delben JRJ, et al. Synthesis and thermal properties of nanoparticles of bioactive glasses containing silver. J Therm Anal Calorim. 2009;97(2):433–6.
130. Biswas K, et al. Biological activities and medicinal properties of neem (*Azadirachta indica*). Curr Sci (Bangalore). 2002;82(11):1336–45.
131. Li J, et al. Preparation of copper-containing bioactive glass/eggshell membrane nanocomposites for improving angiogenesis, antibacterial activity and wound healing. Acta Biomater. 2016;36:254–66.
132. Wang Y, et al. Biological and bactericidal properties of Ag-doped bioactive glass in a natural extracellular matrix hydrogel with potential application in dentistry. Eur Cell Mater. 2015;29:342–55.
133. Turner NJ, et al. Xenogeneic extracellular matrix as an inductive scaffold for regeneration of a functioning musculotendinous junction. Tissue Eng A. 2010;16(11):3309–17.
134. Singelyn JM, et al. Catheter-deliverable hydrogel derived from decellularized ventricular extracellular matrix increases endogenous cardiomyocytes and preserves cardiac function post-myocardial infarction. J Am Coll Cardiol. 2012;59(8):751–63.
135. Marelli B, et al. Three-dimensional mineralization of dense nanofibrillar collagen – bioglass hybrid scaffolds. Biomacromolecules. 2010;11(6):1470–9.
136. Ahlborn G, Sheldon BW. Identifying the components in eggshell membrane responsible for reducing the heat resistance of bacterial pathogens. J Food Prot. 2006;69(4):729–38.
137. Zhu H, et al. Preparation and antibacterial property of silver-containing mesoporous 58S bioactive glass. Mater Sci Eng C. 2014;42:22–30.

138. Shih S.-J, et al. Investigation of bioactive and antibacterial effects of graphene oxide-doped bioactive glass. Adv Powder Technol. 2016;27(3):1013–20.
139. Liu Y-Z, et al. Drug delivery property, bactericidal property and cytocompatibility of magnetic mesoporous bioactive glass. Mater Sci Eng C. 2014;41:196–205.
140. Liu J, et al. Fluoride incorporation in high phosphate containing bioactive glasses and in vitro osteogenic, angiogenic and antibacterial effects. Dent Mater. 2016;32(10):e221–37.
141. Liu J, et al. Strontium-substituted bioactive glasses in vitro osteogenic and antibacterial effects. Dent Mater. 2016;32(3):412–22.
142. Vaahtio M, et al. Effect of ion release on antibacterial activity of melt-derived and sol-gel-derived reactive ceramics. In: Key engineering materials. Uetikon-Zuerich: Trans Tech Publ.; 2006.

Chapter 12
Development of URIST™ a Multiphasic rhBMP-2 Bone Graft Substitute

Sean A.F. Peel, Aileen J.J. Zhou, Hanje Chen, and Cameron M.L. Clokie

Abstract Recombinant human bone morphogenetic protein (BMP) containing implants can be as effective as autogenous bone grafts and have been approved clinically to stimulate spine fusion, repair of long bone non-unions and bone augmentation in the jaw.

BMP implants are expensive and are associated with complications including ectopic bone formation, inflammation and cancer due to the very high doses of BMP used. These high doses are required due to the inefficient burst release from the collagen carriers used. However, the use of traditional sustained release carriers to deliver BMP have not been successful.

We have developed a novel BMP carrier URIST which releases the BMP with an initial burst to promote mesenchymal cell recruitment followed by a sustained release. We have demonstrated in a series of non-clinical studies that URIST can produce more bone with less BMP than the currently approved collagen carrier. Further in a large animal model we demonstrate that URIST is safe and effective for alveolar ridge augmentation.

Keywords Bone graft substitute • rhBMP-2 • Bone morphogenetic protein • Biphasic calcium phosphate • Calcium sulphate dihydrate • Poloxamer P407 • Burst release • Sustained release • Multiphasic release

12.1 Background

It is estimated that over six million surgeries are performed worldwide annually to promote bone repair (Table 12.1). These surgeries include repair of fracture non-unions, joint fusions in the spine and elsewhere, bone defect repair and bone augmentation and are performed by a variety of clinicians including orthopaedic, spine, oral-maxillofacial and dental surgeons.

To be published in "Clinical Applications of Biomaterials: State-of-the-art progress, trends and novel approaches" Gurbinder Kaur (ed) Springer-Nature.

S.A.F. Peel, Ph.D. (✉) • A.J.J. Zhou, Ph.D. • H. Chen, M.Sc. • C.M.L. Clokie, DDS; Ph.D.
Induce Biologics Inc., Toronto, ON, Canada
e-mail: sean.peel@inducebiologics.ca

G. Kaur (ed.), *Clinical Applications of Biomaterials*,
DOI 10.1007/978-3-319-56059-5_12

Table 12.1 Number of procedures that could use bone grafts

Procedure	USA[a]	ROW[b]	World wide
Spine fusion	463,741	1,135,366	1,599,107
Other joint fusion	10,765	26,356	37,121
Fracture non-unions	33,325	81,589	114,914
Hip arthroplasty revisions[c]	66,100	162,810	229,310
Knee arthroplasty revisions[c]	100,100	245,072	345,172
Other joint arthroplasty revisions[c]	13,350	32,684	46,034
Other	55,550	136,002	191,552
Dental bone graft procedures[d]	1,180,000	2,888,966	4,068,966
Total			6,632,176

[a]The number of procedures for the USA were estimated using discharge data from the National Inpatient Sample (NIS), Healthcare Cost and Utilization Project (HCUP), Agency for Healthcare Research and Quality (https://hcupnet.ahrq.gov/ accessed 22-Jan-2017)
[b]An estimate for the number of procedures for the ROW (rest of the world) was estimated based on a market report that in 2013 29% of all orthopaedic and spine procedures were performed in the USA (Global Orthopedic Device Market, Kalorama Information 2015)
[c]The number of US arthroplasty revision procedures were estimated by multiplying the number of surgeries by 15% as an estimate of the number of revisions based on reported hip revision rates in the US, UK and Europe (Haddad FS Rayan F. *Orthopedics*. 2009 Sep;32(9))
[d]The number of dental bone graft procedures estimate uses the reported number of procedures performed in 2010 (US Market for Dental Bone Graft Substitutes, Dental Membranes and Tissue Engineering; iDATA Research Inc. 2010)

These surgeries often involve the implantation of a graft that will provide a scaffold for tissue ingrowth, maintain space and ideally promote the repair process by the addition of cells and/or signalling molecules.

12.1.1 Autograft

The surgeon's first choice as a graft material is autograft, bone harvested from elsewhere in the patient's body including the iliac crest, tibial crest, or fibula. However, the use of autograft requires additional surgical time and increases blood loss and recovery time by the patient. Significant complications associated with harvesting autograft include increased risk of fracture and infection at the donor site, nerve or vascular damage, significant prolonged pain and cosmetic defects such as scaring (Fig. 12.1) [1, 2]. Further there is a limited availability of bone that can be harvested, (especially in paediatric populations) and autografts can suffer from low viability and significant resorption. While a number of synthetic and allogenic materials have been used in bone grafting as bone void fillers for small defects they lack significant biological activity and cannot be used as an alternative to autograft [3, 4].

Fig. 12.1 Photograph of a scar produced following harvest of bone autograft. To harvest a fibular bone autograft an incision was made from just above the ankle to just below the knee, resulting in a large scar (photograph courtesy of Dr. Cameron Clokie)

12.1.2 Bone Morphogenetic Proteins and the First Generation rhBMP Implants

Bone morphogenetic proteins -2 (BMP-2) and -7 (BMP-7) are highly expressed during bone repair [5, 6] and have been shown to promote the chemotaxis and proliferation of mesenchymal stem cells and their differentiation into osteoblasts [7, 8]. This has led to the development of bone graft substitutes containing recombinant human BMP-2 (rhBMP-2) and recombinant human BMP-7 (rhBMP-7) which have been shown to be an effective alternative to autograft in numerous animal and clinical studies [9]. The rhBMP-2 implant INFUSE® (Medtronic) has been approved in the US, Europe, Canada and elsewhere as an alternative to autograft by for use in lumbar spinal fusion, long-bone non-union and for alveolar ridge and sinus augmentation (increasing bone height and width in the upper and lower jaw and sinuses) [10]. The rhBMP-7 implant OP-1™ (Stryker/Olympus) was approved in Europe, Canada, and Australia for the treatment of tibial non-unions [11]. However, OP-1 only received the much more limited humanitarian device exemption (HDE) by the US-FDA for revision posterolateral spine fusion and tibial non-union.

12.1.2.1 Challenges with the First Generation of rhBMP Implants

Recombinant human BMP (rhBMP) implants were rapidly adopted after their approval in 2001 and 2002, with approximately 25% of spinal fusions in the USA using rhBMP implants by 2008 [12]. However, significant complications have been reported including heterotopic bone formation, the creation of boney cysts, induction of autoantibodies and inflammation [12–14]. Concerns have also been raised

regarding the potential risk of cancer, following a pivotal clinical trial using AMPLIFY, a second generation rhBMP-2 implant that used a higher concentration (2.0 mg/mL vs 1.5 mg/mL) and higher overall rhBMP-2 dose (40 mg/mL vs 4.3–12 mg/mL) than INFUSE [15, 16]. A retrospective analysis of approximately 20,000 patients who underwent spinal fusions with the lower dose approved BMP implants found no significant increase in the risk of cancer [17] suggesting that any increased risk is linked to the higher dose.

Further, the price of rhBMP implants is very high and a systematic review of the clinical and cost effectiveness of rhBMPs commissioned by the NHS (UK) concluded that "*According to the results of economic evaluation, the use of BMP for spinal fusion is unlikely to be cost-effective*" [18]. This has significantly limited the use of rhBMP implants, especially outside of the USA. These high prices are related to the high cost of goods (primarily the rhBMP) which ultimately led to Olympus stopping the sale of OP-1 in 2014 [19].

The complications and high cost of rhBMP implants is due to the high concentrations of rhBMP used. While the concentration of rhBMP-2 used in INFUSE is 1.5 mg/mL in vitro studies show that cells are responsive to rhBMP-2 in the ng/mL range, reaching a maximum in the low μg/mL range (Fig. 12.2) leading to the conclusion that the doses used are up to 10,000 times higher than is physiological [21].

12.1.2.2 Burst Release of rhBMP from ACS Necessitates the Use of High Doses

The reason that high doses are required is that the rhBMPs are rapidly cleared from the implant site and are susceptible to proteolysis or inactivation. Therefore rhBMP-2 does not induce bone formation unless it is combined with a carrier, which delays loss of BMP from the implant site, ensuring an effective concentration remains at the implant site long enough to stimulate bone formation [22]. The rhBMP-2 implant INFUSE uses an absorbable collagen sponge (ACS) as the carrier. At the time of surgery, a solution of rhBMP-2 is soaked onto the sponge for 20–30 min prior to being implanted (Fig. 12.3).

The rhBMP-2 is rapidly released from the ACS in a "burst". In vitro approximately 80% of rhBMP-2 loaded onto ACS is released within 24 h, with the remaining released over the next few days (Fig. 12.4). In vivo studies using radiolabelled rhBMP-2 show that rhBMP-2 delivered using ACS is rapidly lost from the implant site with approximately 10% remaining after 6 days [23] and it was unknown how much of the remaining rhBMP-2 was intact or active. In comparison studies of expression of BMP-2 during bone repair indicates that BMP expression is stimulated within a matter of hours after injury and remains elevated throughout the inflammatory and repair phase of bone healing during which recruitment and differentiation of mesenchymal progenitors and the production of woven bone is occurring [6, 24]. Expression of BMP-2 and other BMPs returns to normal during the remodelling phase when the woven bone is replaced by lamellar bone. While in rats BMP-2 is elevated for 21 days, in rabbits BMP expression was shown to be

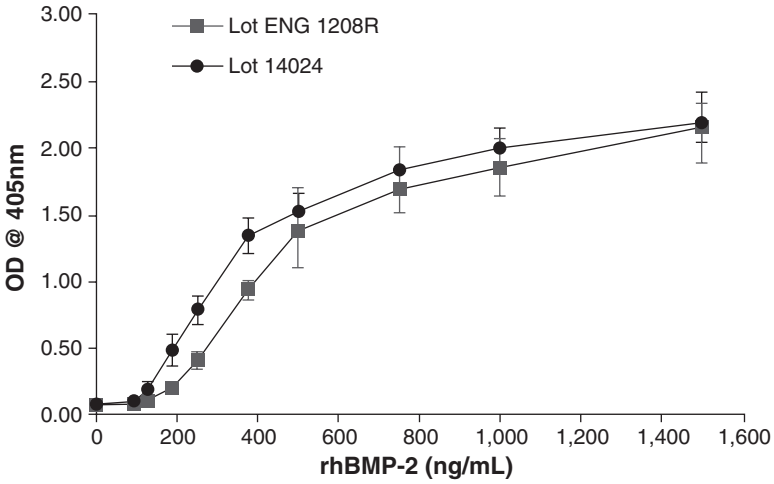

Fig. 12.2 C2C12 cell dose response to rhBMP-2. The concentration range over which cells were responsive to rhBMP-2 was assessed using the C2C12 cell based assay. C2C12 cells were seeded in 96 well plates overnight. The following day the media was removed and the test media with a varying concentration of rhBMP-2 from two different lots at concentrations from 50 to 1,500 ng/mL was added to the cells. Two days later the media was removed the cell were lysed and the alkaline phosphatase activity of the lysates was measured as described previously [20]

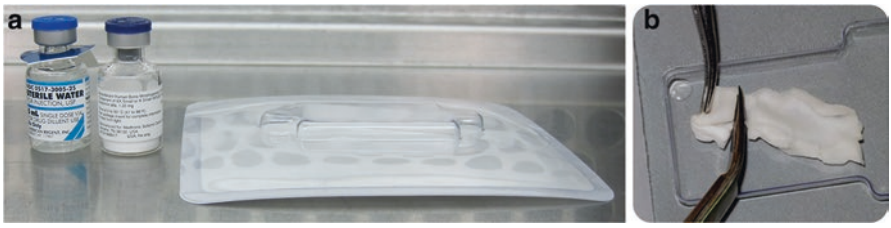

Fig. 12.3 Preparation of Medtronic's INFUSE® implant. Medtronic's rhBMP-2 implant INFUSE® comprises a vial of lyophilized rhBMP-2, a vial of water for injection and an absorbable collagen sponge (ACS) in a plastic tray (**a**) The water is added to the rhBMP-2 powder to produce a 1.5 mg/mL solution that is then applied to the ACS and left to soak for at least 20 min. After 20 min the ACS handles like wet kitchen towel. If it is squeezed liquid can be expelled from the sponge (**b**)

elevated for up to 10 weeks [25] and humans the repair phase is expected to take 16 weeks or longer [26, 27]. Therefore, ideally BMP should be maintained at an effective concentration at the healing site through-out at least the first 16 weeks. The only way to achieve this using an ACS carrier is to load very large amounts of rhBMP.

BMP activity is inhibited by the binding protein noggin. Studies have shown that noggin expression is rapidly upregulated, following placement of a BMP-2 implant, peaking around day 4 before declining [28], while in vitro studies suggest that the

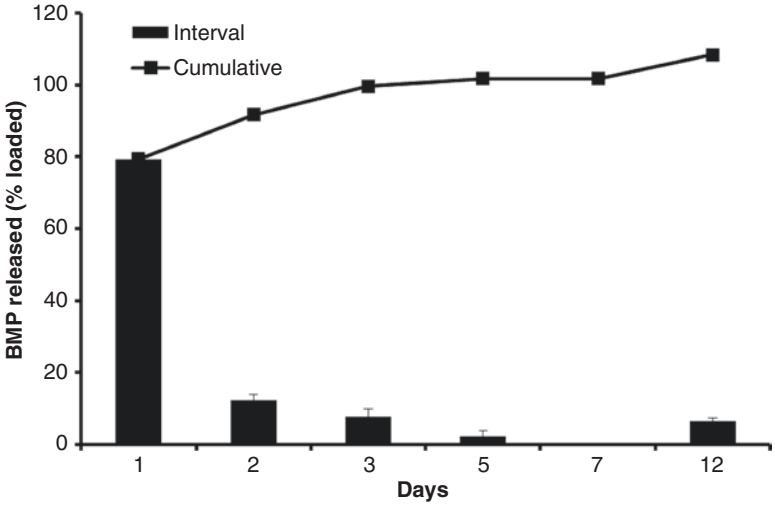

Fig. 12.4 rhBMP-2 release from ACS. 9.1 μg rhBMP-2 was soaked onto an absorbable collagen sponge for a minimum of 20 min before 1 mL of PBS+0.1% BSA was added and the samples were held at 37 °C. At each time point the PBS+BSA was removed and replaced with fresh solution. After 12 days all the samples were assayed for BMP-2 using an ELISA. Approximately 80% of the rhBMP-2 loaded was recovered after 1 day, and over 95% within 3 days

level of noggin expressed is proportional to the dose of rhBMP-2 [29]. Further it has been shown that inhibition of noggin expression in vivo enhances the amount of bone formed by rhBMP-2 implants [30]. Consequently, implants that release very high doses of rhBMP initially induce a very strong expression of noggin reducing the effectiveness of the implant.

For these reasons burst release carriers require very high doses of BMP to be effective.

12.1.3 Studies on Sustained Release Carriers

The polymer poly lactide-co-glycolide (PLGA) has been widely used for as a drug delivery system and can produce a variety of release profiles, including sustained release, based on the monomer ratio and molecular weight. We evaluated the potential of using a PLGA sustained release carrier OsteoScaff™ for delivery of rhBMP-2. While it produced a sustained release profile in vitro (Fig. 12.5), when we compared the amount of bone induced by rhBMP-2 delivered from OsteoScaff and ACS carriers, the OsteoScaff carrier produced less bone, even though the amount released was within the physiological effective range (Fig. 12.6).

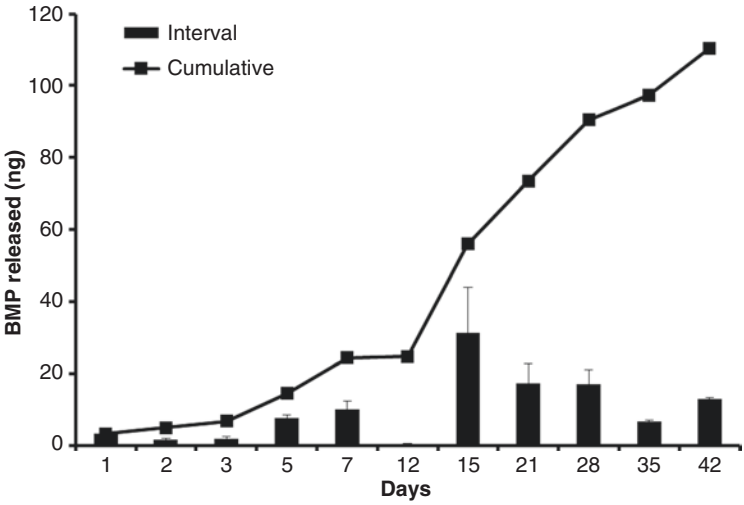

Fig. 12.5 BMP release from OsteoScaff™ and bone formed in vivo. OsteoScaff™ granules comprise a PLGA matrix within which is embedded small particles of calcium phosphate cement. The granules are coated with a thin layer of hydroxyapatite. The PLGA matrix was loaded with 9.1 μg of rhBMP-2 per 5 mg OsteoScaff. Granules were placed in sterile Epindorf tubes and 1 mL PBS with 0.1% BSA was added. The Epindorfs were gently shaken at 37 °C and at various times the PBS-BSA solution was removed and replaced with fresh PBS-BSA. The amount of rhBMP-2 released was measured by ELISA. Results showed that the granules produced a sustained release of 18 ng/mL per week with no burst over the duration of the study. By the end of the study only 1.2% of the total amount of rhBMP-2 loaded was recovered

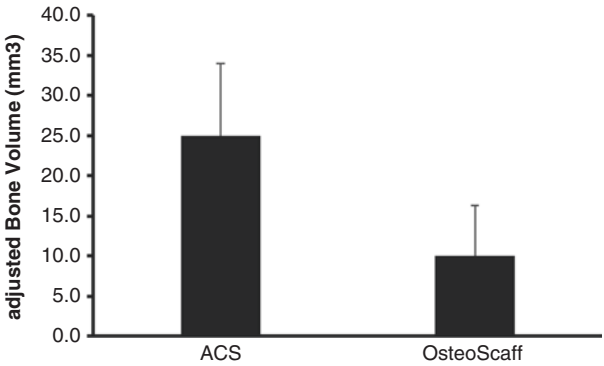

Fig. 12.6 Amount of bone formed by rhBMP-2 delivered from ACS or OsteoScaff™. OsteoScaff granules were prepared with rhBMP-2 aseptically as described in Fig. 12.6. Twenty-two milligram of OsteoScaff containing 40 μg of rhBMP-2 was placed into gelatin capsules. ACS was cut into pieces and placed into sterile Epindorf tubes and 40 μg of rhBMP-2 (1 mg/mL) was added to the sponges which were then placed into gelatin capsules. The mouse muscle pouch assay was used to asses the efficacy of the two carriers as described previously [20]. In brief the gelatin capsules were implanted into the hind limbs of male CD1 mice. After 28 days the mice were sacrificed and the amount of bone formed was assessed by microCT. To correct for the presence of the calcium phosphate the adjusted bone volume was calculated as described by Humber et al. [31]. While the total volume of the ossicles produced were similar the adjusted bone volume within the ossicles of in the OsteoScaff group was significantly less than with the ACS group

12.2 A Multiphasic Release System

When a BMP implant is placed in a bone defect the cell density will increase over time and must achieve a "critical cell density" for the implant to be effective [22]. As rhBMP-2 has been shown to be chemotactic for mesenchymal stem cells we investigated whether a carrier that released BMP with both an initial short release over a few days to recruit cells followed by a sustained release over several weeks to maintain an effective concentration would be more effective than ACS. We termed this a "multiphasic release system".

12.2.1 Device Design

The multiphasic release system was designed with four components; poloxamer P407 gel (P407), calcium sulphate dihydrate granules (CSD), biphasic calcium phosphate granules (BCP) and rhBMP-2. The CSD and BCP granules acted as an osteoconductive scaffold, supporting osteogenic tissue ingrowth, and as a volume filler. The rhBMP-2 was distributed between the other three components.

Poloxamer P407 (P407) is a block co-polymer of polyethylene and polypropylene, is relatively non-toxic and is listed as an inactive ingredient in numerous approved drug formulations [32, 33]. Gels of P407 exhibit reverse phase properties, becoming more viscous as temperatures increase. These gels can be combined with bone graft substitues to improve handling without impairing bone healing [34]. Gels have also been used to extend the release of drugs from minutes to hours and have been used to effectively deliver rhTGF-ß1 and BMP to promote bone repair [35–37].

In a series of preliminary studies, we screened various potential osteoconductive materials before deciding to focus on CSD and BCP (not shown). Bone graft substitutes comprising calcium sulphate, various calcium phosphates (hydroxyapatite, beta tricalcium phosphate) or their mixtures have been used clinically for many years. Calcium sulphate is biocompatible, osteoconductive and undergoes rapid resorption over 4–8 weeks in vivo without causing any significant inflammatory response [38]. This resorption may occur too quickly to adequately ensure space is maintained for bone ingrowth and consequently calcium sulphate has been combined with a variety of other materials to ensure sufficient scaffold remains during the healing period.

Calcium phosphate grafts have in many instances replaced calcium sulphate as they also are biocompatible, osteoconductive and do not elicit an inflammatory response, but their resorption rates are slower, varying depending on the form used. Hydroxyapatite (HAp) can take years to resorb, while beta tricalcium phosphate (bTCP) resorbs more rapidly. In one study when implanted in a bone defect after 24 weeks 5% of the HAp had resorbed while 55% of the bTCP had resorbed [39]. Often mixtures of hydroxyapaptite and beta tricalcium phosphate, which are called biphasic calcium phosphates (BCP), are used [40, 41].

A series of studies were performed to validate and refine the multiphasic release device design.

12.2.2 Study 1: Evaluation of rhBMP-2 Release from P407, BCP and CSD and Their Mixtures

To evaluate the release of rhBMP-2 from the various components and their mixtures we prepared samples as described in Tables 12.2 and 12.3.

12.2.2.1 Sample Preparation

All procedures were performed aseptically in a biological safety cabinet (BSC) to prevent contamination. The various amounts of scaffold material were weighed out and added to sterile Eppendorf tubes. Where the scaffold is a mixture of CSD and

Table 12.2 Materials used in studies

Acronym	Full name	Vendor	Description
ACS	Absorbable collagen sponge	Medtronic	From an INFUSE™ kit
BCP-1	Biphasic calcium phosphate-1	Citagenix	20/80 HAp/ß-TCP granules
			0.5–1 mm diameter
BCP-2	Biphasic calcium phosphate-2	Biomatlante	60/40 HAp/ß-TCP granules
			0.5–1 mm diameter
BMP	1 mg/mL rhBMP-2 in IFB	Induce Biologics	Mammalian cell produced
			>95% purity
CSD-1	Calcium sulphate dihydrate	Wright Medical	Osteoset pellets were prepared and ground and sieved to the desired size
			0.5–1 mm
CSD-2	Calcium sulphate dihydrate	Induce Biologics	Granules
			0.5–1 mm
ELISA kit	Quantikine BMP-2 ELISA	R&D Systems	
P407	25% poloxamer P407 gel	Induce Biologics	
IFB	Induce formulation buffer	Induce Biologics	
TPP tube	50 mL TPP tube	Mandel Scientific	Sterile polypropylene tube with 0.22 micron filter in lid

Table 12.3 Study design for rhBMP-2 release study

Group	Scaffold	Wt. (mg)	rhBMP-2 (µg)	P407 (µL)	*n*	Comments
1	CSD	10	25	None	3	
2	CSD	10	25	20	3	
3	CSD	10	25	None	3	
4	CSD	10	25	20	3	
5	CSD+BCP (2:1)	6.7+3.3	25	None	3	
6	CSD+BCP (2:1)	6.7+3.3	25	20	3	URIST™
7	None	–	25	20	3	Control
8	None	–	25	None	3	Control

Used CSD-2 granules produced by Induce Biologics Inc.
Used BCP-2 from Biomatlante (60/40 Hap/bTCP)

BCP, these were mixed bulk and then 10 mg of the mixture was weighed and added to the Eppendorf.

The desired amount of rhBMP-2 was added to each tube in laminar flow hood, sealed and held at room temperature for various periods before being frozen and lyophilized.

Prior to the study P407 gel was pipetted into the Epindorf tubes and mixed with the lyophilized powder to produce a putty.

All procedures were performed aseptically to maintain sterility.

12.2.2.2 Measuring BMP Release

One milliliter of sterile PBS+0.15% BSA was added to each sample. Samples were then sealed and placed in an incubator at 37 °C. At each collection time point (Day 1, 2, 3, 4, 7, 14, 21, 28, 42, 49) the samples were removed, the contents were allowed to settle and the supernatant was collected and centrifuged. Fresh PBS+BSA was added to the sample which was returned to the incubator and incubation continued at 37 °C.

Aliquots were taken from the supernatants and analyzed by ELISA per the manufacturer's instructions.

Results

The results are summarized in Table 12.4 and Figs. 12.7, 12.8, and 12.9.

The results showed that virtually 100% of rhBMP-2 was recovered from the buffer only group within 24 h and 100% was recovered from the P407 gel only group within 3 days.

The presence of CSD, BCP or their mixture greatly reduced the total amount of BMP released over the duration of the study. Addition of P407 gel to CSD, BCP or their mixture consistently reduced the release of BMP from the scaffold material on day 1 but increased it between days 7 and the end of the study.

The total amount of BMP released over the duration of the study (49 days) was consistently lower in groups where P407 had been added to a carrier containing CSD.

In the group that only contained BCP the total amount of BMP released over the first 7 days was lower when P407 was added, but over the remaining part of the study more BMP was released from the BCP when P407 was added.

Conclusions

The results indicated that:

Addition of P407 delays release of BMP-2, such that less BMP is released on day 1 and more is released at later timepoints;

Table 12.4 Total BMP released from each group

Group	Scaffold	P407	Total BMP released (μg)	SD (μg)
1	CSD	None	11.2	1.4
2	CSD	20 μl	8.4	0.5
3	BCP	None	9.7	0.8
4	BCP	20 μl	10.4	1.1
5	CSD+BCP	None	10.4	1.3
6	CSD+BCP	20 μl	7.8	0.5
7	None	20 μl	22.1	4.4
8	None	None	26.6	0.4

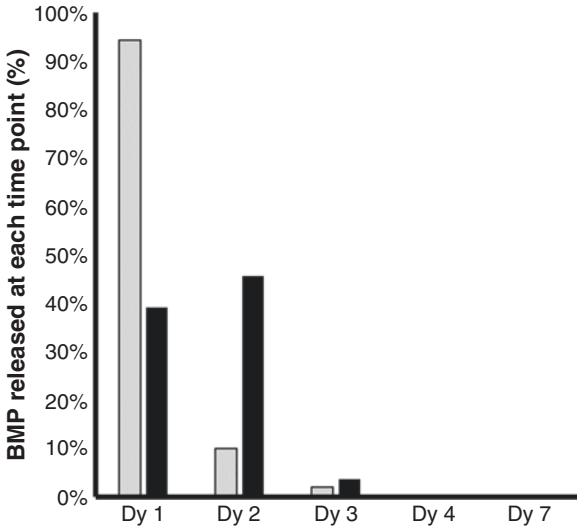

Fig. 12.7 rhBMP-2 release from P407 gel in vitro. A gel of Poloxamer 407 (P407) was prepared and was then stored at 2–8 °C until used. One milliliter of ice cold P407 was transferred to a sterile Epindorf tubes and a solution of 1 mg/mL rhBMP-2 was added to the P407 gel. The P407 was allowed to warm and gel. Following this 1 mL PBS containing 0.1% BSA was added. The Epindorfs were gently shaken at 37 °C and at various times the PBS-BSA solution was removed and replaced with fresh PBS-BSA. The amount of rhBMP-2 released was measured by ELISA. Results showed that gel released all of the rhBMP-2 over 3 days

The total amount of BMP-2 released from samples containing CSD, BCP or their mixtures was less than 50% over the period of the study;

The results demonstrated that the combination of CSD, BCP and P407 produced the desired multiphasic release profile where there is an initial more rapid release over the first 7 days (~25%) and then a smaller prolonged release over the remaining 42 days (~10%).

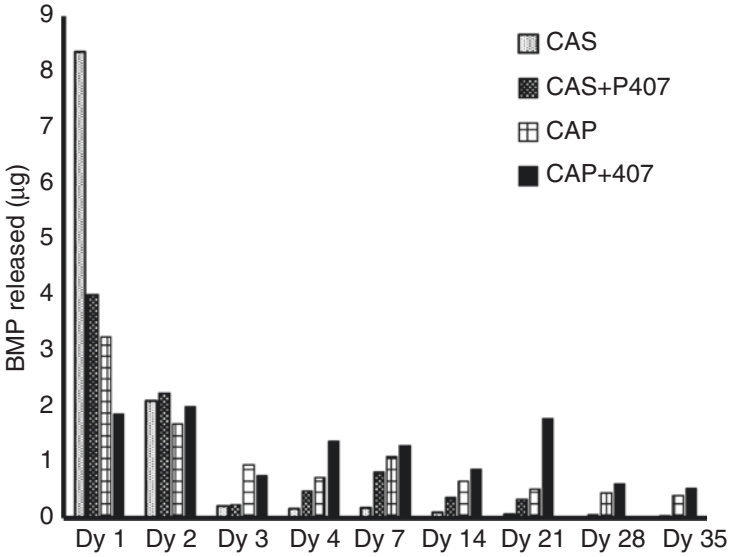

Fig. 12.8 BMP released from CSD, BCP with and without P407. With both CSD and BCP carriers the addition of P407 reduced the amount of BMP released on Day 1. From Day 4 on more BMP was released in the samples containing the P407

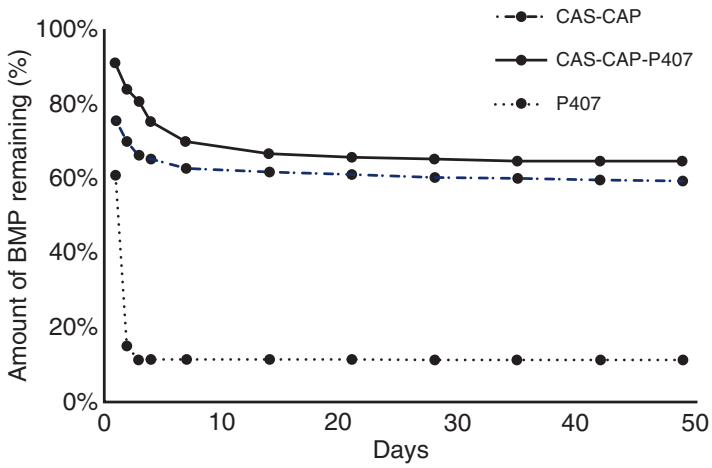

Fig. 12.9 Release of BMP from a mixture of CSD and BCP with or without P407. After an initial burst release of 20–30% of the rhBMP-2 over the first 7 days the CSD-BCP P407 implant maintained a sustained release over the remaining period of the study. The mixture of CSD-BCP-P407 released less rhBMP-2 over the duration of the study, than the CSD-BCP carrier alone

12.2.3 Study 2 Comparison of the Multiphasic Release Carrier to the Commercial ACS Carrier

To determine whether a multiphasic release carrier could be effective using less rhBMP-2 we compared the effect of CSD, BCP and their mixtures (all combined with P407) as a carrier for rhBMP-2 compared to ACS. The study design in summarized in Table 12.5. The ACS carrier received twice as much rhBMP-2 as the other carriers.

The osteoinductive activity of the various carriers was evaluated using the mouse muscle pouch assay as previously described [20]. The study was approved by the local animal care committee.

12.2.3.1 Sample Preparation

Sterile CSD granules (0.5–1.2 mm) were prepared by grinding sterile Osteoset pellets (3 mm diameter, Wright Medical) and sieving between 1.18 mm and 0.5 mm sieves. The ACS sponge was cut into pieces approximately 5 × 5 mm and placed in Epindorf capsules.

Purified recombinant hBMP-2 produced in CHO cells, was stored at −80 °C.

Poloxamer 407 (P407) gel was sterilized by autoclaving. The P407 gel was kept at 2–8 °C after sterilization.

BMP was lyophilized onto the CSD and BCP scaffolds as follows:

Table 12.5 Study design for comparison of the multiphasic release carriers

Group side a/b	Name	CSD (mg)	BCP (mg)	P407 (µl)	BMP (µg)	BMP distribution scaffold/P407	n
1a	ACS + BMP				80	Soak	12
1b	ACS				0	–	
2a	CSD(B)+P407	30	–	45	40	100/0	12
2b	CSD+P407	30		45	0	–	
3a	CSD(B)+P407(B)	30		45	40	70/30	12
4a	CSD(B)+P407(B)		30	45	40	70/30	12
4b	CSD+P407		30	45	0	–	
5a	2:1 CSD:BCP(B)+P407(B)	20	10	45	40	70/30	12
5b	2:1CSD:BCP+P407	20	10	45	0	–	
6a	2:1CSD:BCP(B)+P407(B)	20	10	45	40	90/10	12
7a	1:1CSD:BCP(B)+P407(B)	15	15	45	40	70/30	12
7b	1:1CSD:BCP+P407			45	0	–	
8a	1:1CSD:BCP(B)+P407(B)	15	15	45	40	90/10	12

Each mouse receives an rhBMP-2 containing implant on side a. Side b either received a matching control implant with no BMP or nothing

CSD calcium sulphate dihydrate, *BCP* biphasic calcium phosphate, *P407* poloxamer 407 gel, *(B)* rhBMP-2 associated with the material (CSD-1; BCP-1; CSD:BCP or P407)

The required amount of scaffold was weighed out and placed into a sterile Epindorf tube. The desired amount of rhBMP-2 was added to the scaffold and was held at room temperature for a fixed period prior to freezing. Once frozen the Epindorf tubes were placed in a lyophilizer and lyophilized overnight. All procedures were performed aseptically to maintain sterility.

P407 gel containing rhBMP-2 was prepared in bulk in sterile Epindorf tubes by adding the rhBMP-2 solution to the P407 gel. At the time of surgery the appropriate amount of P407 was pipetted onto the scaffold.

12.2.3.2 Surgery

INFUSE® implants were prepared at the time of surgery by adding BMP-2 solution (1.5 mg/mL) to the ACS in each Epindorf. The solution was allowed to soak for at least 20 min before implantation. At time of implantation the soaked ACS was placed into a sterile #5 gelatin capsule and placed in the muscle pouch as described below.

Samples where poloxamer was to be mixed with scaffold were prepared by pouring out the granules onto a sterile stainless steel tray. The poloxamer was kept on ice and the appropriate amount of poloxamer gel was applied by pipette to the gel. The scaffold and gel were mixed and then carefully placed into a gelatin capsule which was then placed in the muscle pouch.

Male CD-1 mice (approximately 22 gm) had intramuscular pouches formed in their biceps femoris muscle by blunt dissection. The bioimplant is then placed into the pouch. The skin was then pulled together and closed using Michel clips.

Each mouse received an rhBMP-2 containing implant one side and the contralateral side either received a matching control implant with no rhBMP-2 or nothing. The rhBMP-2 containing implant was placed on the right side in six mice and the left side in the other six mice of the group.

The mice were monitored daily. Originally the mice were to be euthanized after 28 days. However due to some implants forming so much bone that bridging occurred between the spine and the femur, which restricted the mice's mobility the mice were sacrificed after 17 days. Following sacrifice of the animals, the rear limbs were dissected out and fixed using 10% neutral buffered formalin.

12.2.3.3 Micro CT Analysis

The amount of bone formed was determined by micro CT (Fig. 12.10). Appropriate values were adjusted for the presence of calcium from the residual scaffold as previously described [31].

The region where the implant had been placed was imaged using a GE Healthcare eXplore Locus SP microCT scanner. The residual scaffold and any new mass that had formed around the implant in the muscle (collectively called an ossicle) was outlined to define the region of interest (ROI).

As the scaffold material was denser than the new bone it was possible to determine threshold values for new bone and scaffold separately by imaging multiple samples

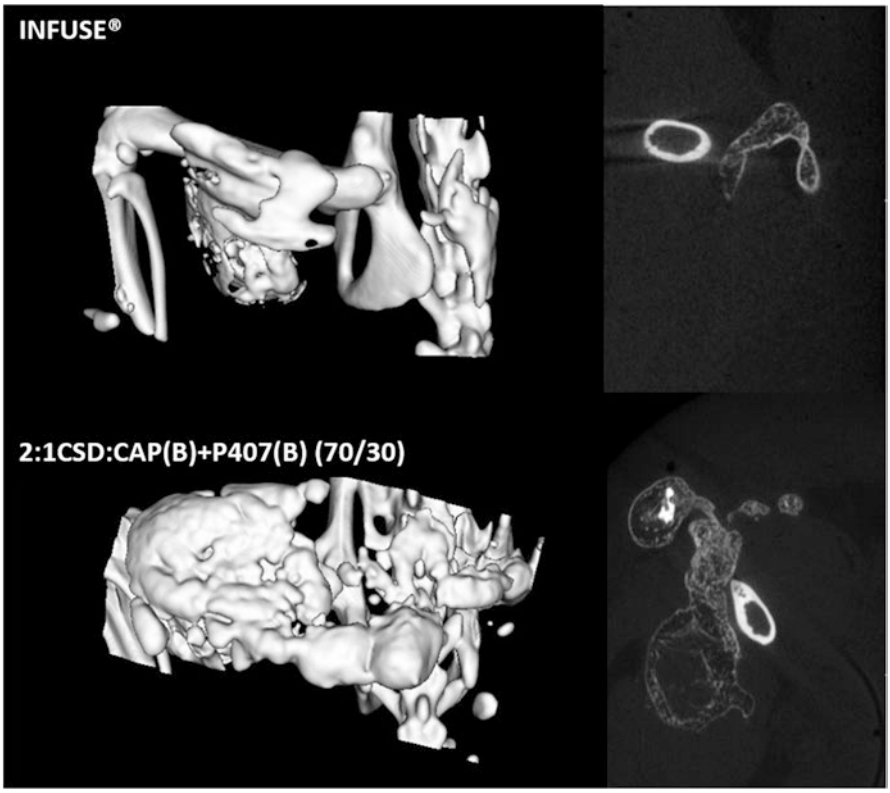

Fig. 12.10 Micro CT reconstructions and slice views. MicroCT images and 3D reconstructions show the formation of bone around the carriers. Sufficient bone was formed in the implants containing CSD to obscure the underlying skeleton. A representative 3D reconstruction of an INFUSE® sample and a 2:1 CAS:CAP(B)+P407(B) sample are shown. The images on the left side are the 3D reconstructions, those on the right side are a 2D slice. The bright white oval shapes in the 2D images are a cross section of the femur. INFUSE bioimplant produced a small volume of bone (ossicles) around the implant. The pelvic bones can be seen to the right and the lower leg bones to the left. The CSD-CAP+P407 bioimplant produced so much bone that it completely obscured the underlying skeleton

from each group and taking an average of the grey scale values. For the purpose of standardization the lowest scaffold threshold value obtained for a material (CSD) was used for all scaffolds, except the ACS which was assumed to contain no calcium and thus no correction was required. Similarly a single value for new bone was used.

Analyses were performed using the two threshold values. The upper threshold distinguished scaffold from bone and soft tissue, while the lower distinguished bone + scaffold from soft tissue. By subtracting the upper threshold values from the lower threshold values the values for bone only were determined. Seven different parameters were measured using the microCT. Table 12.6 describes the parameters obtained or derived.

Table 12.6 Micro CT parameters

Parameter	Abbreviation	Description	Threshold dependent
Total volume	TV	Total volume of ROI. Includes volume occupied by bone, scaffold and soft tissues	No
Bone volume	BV (SV)	Volume occupied by voxels with grey scale above threshold value in the ROI When using the upper threshold this would represent the scaffold volume When using the lower threshold this would be a measure of the bone+scaffold volume	Yes
Bone mineral content	BMC	Mineral content within the ROI. This is based on comparison of greyscale of all voxels in	No
Bone mineral density	BMD	BMC/TV	No
Bone volume mineral content	BV-MC (SV-MC)	Mineral content of tissue within the ROI with voxels greater than the threshold value (i.e. bone) When using the upper threshold this would represent the mineral content due to the scaffold	Yes
Bone volume Mineral density	BV-MD (SV-MD)	BV-MC/BV When using the upper threshold this would represent the mineral density of the scaffold	Yes
Bone volume fraction	BVF (SVF)	BV/TV The fraction of the total volume occupied by tissue with a grey scale greater than the threshold value When using the upper threshold this would represent the percentage of the ossicle occupied by scaffold	Yes
Derived parameters			
Adjusted bone volume	aBV	BV-SV	Yes
Adjusted BV mineral content	aBV-MC	(BV-MC) – (SV-MC)	Yes
Adjusted BV mineral density	aBV-MD	(aBV-MC)/aBV	Yes
Adjusted bone volume fraction	aBVF	aBV/TV	Yes

The two measures used to determine osteoinductive activity were total volume (TV) and adjusted bone volume (aBV) of the ROI.

12.2.3.4 Histological Analysis

Following micro CT analysis samples were decalcified in formic acid, embedded in wax, sectioned and stained with hematoxalyin and eosin for light microscopy (Figs. 12.11, 12.12, 12.13, 12.14).

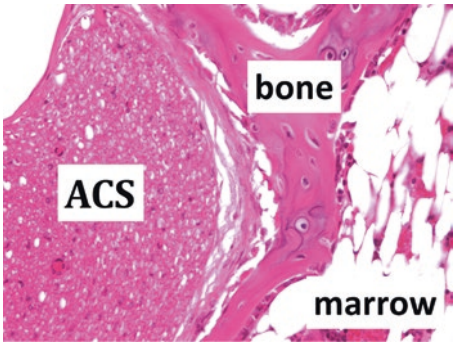

Fig. 12.11 Histological appearance of the INFUSE® implant. The ACS carrier formed ossicles of bone with a thin shell of bone surrounding the ACS carrier. The ACS was still visible and did not appear to allow any cellular infiltration within the body of the carrier. The bone often appeared to be woven or chondroid in appearance. Cartilage was also seen in some areas (not shown). Marrow was also present within the ossicle (Gp1A 40× original magnification)

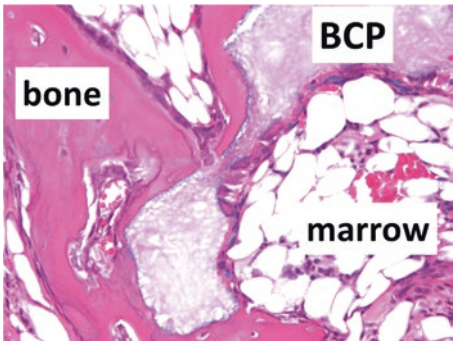

Fig. 12.12 Histological appearance of a BCP carrier implant. The BCP carrier produced ossicles with a thin shell of bone surrounding the biphasic calcium phosphate (BCP) carrier. Bone could be seen forming directly onto the surface of the BCP granules and through-out the carrier, with no fibrous tissue formation. Marrow was seen through-out the ossicle (Gp 4A 40× original magnification)

12.2.3.5 Statistical Analysis

As the ACS alone did not form ossicles that could be measured they were not included in any statistical analyses.

The microCT parameters were tested for normality and equal variance. Normally distributed data with equal variance was tested for significant differences using ANOVA. All other data was tested using ANOVA on RANKs. Post – Hoc testing was performed all pairwise using the Student-Newman-Keuls Method.

All statistical tests were performed using Sigma Stat v3.5.

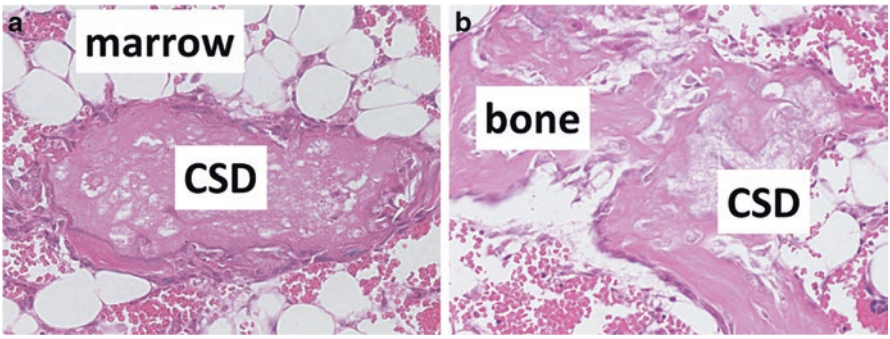

Fig. 12.13 Histological appearance of the CSD and CSB-BCP carrier implants. Similar to the BCP implants, CSD and CSD-BCP implants formed an ossicles with a thin shell of bone surrounding the carrier. Calcium sulphate dihydrate (CSD) granules could be seen, surrounded by marrow (**a**). Bone formed on the surface of the CSD granules and into the voids left as the CSD granules resorbed (**b**). The CSD granules resorb quickly, and some areas show only residual parts of the granules (Gp6a 40× original magnification)

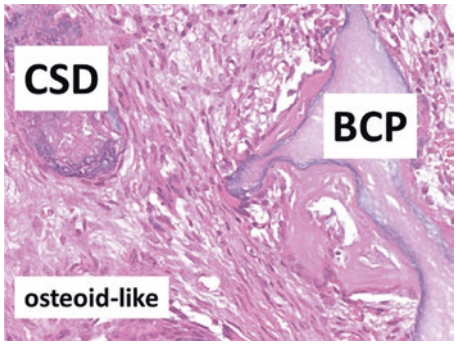

Fig. 12.14 Histological appearance showing both the BCP and CSD granules. This photograph shows an area where a more osteoid-like tissue was seen around the CSD and BCP granules (Gp 5a 40× original magnification)

Results and Analysis

All surgeries were uneventful and the mice recovered from the anesthesia quickly and were moving well.

12.2.3.6 Early Termination of Study Due to Impaired Hind Limb Mobility

After 14 days weeks it was noted that some mice were showing impaired mobility of the hind limbs. The worst case, where the hind limbs became immobilized, was sacrificed and scanned immediately by microCT. The microCT images showed a radiodense mass that appeared to fuse the femurs to the spine and pelvis. Other mice became progressively worse and all remaining mice were sacrificed 17 days after surgery.

12.2.3.7 MicroCT Analysis

The total volume and adjusted bone volume results and statistical analyses are summarized in Tables 12.7 and 12.8.

Table 12.7 Micro CT results: evaluation of multiphasic carriers

Group	Name	BMP distribution scaffold/P407	Total volume (mm^3)		aBV (mm^3)	
			Mean	SD	Mean	SD
1a	ACS(B) (Infuse)	Soak	200.6	94.1	75.4	62.6
1b	ACS		nd	nd	nd	nd
2a	CSD(B)+P407	100/0	270.7	52.2	115.4	34.0
2b	CSD+P407	–	164.6	57.9	68.8	27.4
3a	CSD(B)+P407(B)	70/30	384.6	68.1	163.3	39.0
4a	CAP(B)+P407(B)	70/30	299.1	104.3	101.3	35.7
4b	BCP+P407	–	90.6	81.1	23.6	13.8
5a	2:1 CSD:BCP(B)+P407(B)	70/30	336.5	125.8	129.8	45.8
5b	2:1CSD:BCP+P407	–	121.2	81.6	46.7	29.0
6a	2:1CSD:BCP(B)+P407(B)	90/10	259.2	45.1	114.1	41.7
7a	1:1CSD:BCP(B)+P407(B)	70/30	275.6	97.1	111.7	26.8
7b	1:1CSD:BCP+P407	–	137.9	53.5	67.0	23.4
8a	1:1CSD:BCP(B)+P407(B)	90/10	269.7	53.9	112.9	34.5
P value (ANOVA on RANKS)			<0.001		<0.001	

Table 12.8 Post hoc test for TV and aBV (comparison of BMP containing groups)

Comparison (TV)	$P < 0.05$	Comparison (aBV)	$P < 0.05$	
3a–TV vs 1aTV	Yes	3a- aBV vs 1a – aBV	Yes	
3a–TV vs 6a–TV	Yes	3a- aBV vs 4a – aBV	Yes	
3a–TV vs 7a–TV	Yes	3a- aBV vs 8a – aBV	Yes	
3a–TV vs 8a–TV	Yes	3a- aBV vs 7a – aBV	Yes	
3a–TV vs 2aTV	Yes	3a- aBV vs 6a – aBV	Yes	
3a–TV vs 4a–TV	Yes	3a- aBV vs 2a – aBV	Yes	
3a–TV vs 5a–TV	Yes	3a- aBV vs 5a – aBV	Yes	
5a–TV vs 1aTV	Yes	5a – aBV vs 1a – aBV	Yes	
5a–TV vs 6a–TV	Yes	5a – aBV vs 4a – aBV	Yes	
5a–TV vs 7a–TV	Yes			
5a–TV vs 8a–TV	Yes			
5a–TV vs 2aTV	Yes			
5a–TV vs 4a–TV	Yes			
2aTV vs 1aTV	Yes	2a – aBV vs 1a – aBV	Yes	
4a–TV vs 1aTV	Yes		4a – aBV vs 1a – aBV	Yes
6a–TV vs 1aTV	Yes		6a – aBV vs 1a – aBV	Yes
7a–TV vs 1aTV	Yes		7a – aBV vs 1a – aBV	Yes
8a–TV vs 1aTV	Yes		8a – aBV vs 1a – aBV	Yes

All pairwise multiple comparison procedures (Student-Newman-Keuls Method)

Total Volume

Comparison of ACS to multiphasic carriers The results showed that the multiphasic carriers produced ROI with a larger total volume than the ACS carrier, even though they had less rhBMP-2.

Effect of Distributing BMP between the granules and the P407 gel When BMP was distributed between the P407 gel and the CSD granules it produced larger ossicles than when all of the BMP was lyophilized onto the CSD. (Gp3a > Gp2a).

When using the 2:1 CSD:BCP granules more bone was formed when 70% was lyophilized onto the granules and 30% was in the P407gel than when 90% was lyophilized and 10% was in the gel. (Gp5a > Gp7a).

Effect of using CSD rather than BCP granules In groups with the same distribution of BMP between the granules and P407 we found that using CSD granules produced larger ossicles than BCP (Gp 3a > Gp 4a). When CSD was mixed with BCP groups with more than 50% CSD in the ratio formed the largest ossicles (Gp3a (100CSD) > 5a (67% CSD) > Gp 7a (50% CSD) = 4a (0% CSD).

Adjusted Bone Volume

Comparison of ACS to multiphasic carriers The ACS carriers produced a hollow shell of bone and the adjusted bone volume was significantly less than in the other groups.

Effect of Distributing BMP between the granules and the P407 gel When BMP was distributed between the P407 gel and the CSD granules it produced more bone than when all of the BMP was lyophilized onto the CSD. (Gp3a > Gp2a).

Effect of using CSD rather than BCP granules In groups with the same distribution of BMP between the granules and P407 we found that using CSD granules produced larger ossicles than BCP (Gp 3a > Gp 4a).

When CSD was mixed with BCP groups with more than 50% CSD in the ratio formed the largest ossicles (Gp3a (100CSD) > 5a (67% CSD) > 4a (0% CSD).

12.2.3.8 Histology

Tissue response to CSD and BCP granules Histological evaluation showed no signs of inflammation or fibrous encapsulation of the ACS, BCP or CSD, with bone being seen in direct contact with both the BCP and CSD granules.

While there was little/no indication of resorption or degradation of the BCP granules, the CSD granules were already showing signs of degradation, with the appearance of voids within the CSD granules.

Conclusions

Based on the results of this study implants using CSD:BCP granules as a carrier produced larger ossicles with more bone than the ACS implant, even though less rhBMP-2 was loaded.

Histological examination of the implants indicates that CSD had begun to degrade within 17 days, while BCP granules remain intact.

Implants that had a mixture of BCP and CSD granules produced the larger ossicles with more bone when the CSD ratio was increased.

Based on the rapid degradation of CSD granules observed histologically and the micro-CT results the 2:1 CSD:CAP mixture is considered the best scaffold of those tested for further evaluation. This design was named URIST™.

12.2.4 Evaluation of URIST Efficacy in a Dog Model

12.2.4.1 Aims and Objectives

This study was conducted to assess performance of URIST™ in the alveolar ridge of canines.

12.2.4.2 Experimental Design

This study was approved by the local animal care committee and was performed following Good Laboratory Practices (GLP).

Twenty-four (24) beagle dogs (12 male and 12 female) were split into two groups ($n = 6$ per group per sex). Group 1 evaluated the various treatments for socket preservation, and Group 2 evaluated the treatments when used for alveolar ridge augmentation.

In all 24 animals, both the left and right second molars (M2) and the left and right fourth premolars (PM4) of the mandible (lower jaw) were extracted (i.e. four teeth per jaw per animal).

Group 1: Socket Preservation Group(n = 12)

In all 12 animals of this group following tooth extraction the tooth extraction socket was filled with the various graft materials or was left unfilled.

6 animals

Side 1: One socket was left unfilled as a negative control, while the other was treated with autograft (bone harvested from the iliac crest of each dog) was used as a positive control.

Side 2: Both sockets were treated with URIST Putty (dose: 1 mg BMP per cc volume).

6 animals

Side 1: One socket was left unfilled, while the other was treated with autograft.

Side 2: Both sockets were treated with URIST Putty (dose: 0.5 mg BMP per cc).

Group 2: Ridge Augmentation Group(n = 12)

In all 12 animals in this group the buccal wall of the extraction socket was removed.

6 animals

Side 1: One socket was left unfilled, while the other was treated with autograft.

Side 2: Both sockets were treated with URIST Putty (dose: 1 mg BMP per cc).

6 animals

Side 1: One socket was left unfilled, while the other was treated with autograft.

Side 2: Both sockets were treated with URIST Putty (dose: 0.5 mg BMP per cc).

After 6 weeks (t = 6 weeks) bone cores were taken at the extraction sites and dental implants were placed.

12.2.4.3 Results

The surgical procedures were performed in all animals without incident and all animals recovered from the procedure without any problems.

The amount of URIST Putty placed in each site was estimated based on the weight of the putty that remained in the vials after use. 18 ± 3% was used per tooth socket for socket preservation, and 28 ± 5% was used per tooth for ridge augmentation. Therefore, the actual amount of BMP applied was approximately 0.1–0.2 mg for socket preservation and 0.15–0.3 mg for socket augmentation for the 0.5 mg and 1.0 mg BMP containing URIST implants respectively.

Approximately half of the animals experienced some bone reaction at the site of the extraction – this was considered a result of the tooth extraction and no differences were noted between sites treated with URIST or the controls.

Measurements of the Jaw

Jaw measurements were performed using a caliper, to estimate the alveolar ridge width at three levels from the bottom of the socket: apex (bottom), mid, and crest (top). The results of the crest width are summarized in Figs. 12.15 and 12.16.

In the socket preservation group, no significant difference was detected in the mid and apex width measurements among the groups, as bone loss typically begins at the crest level. The unfilled sockets showed a loss in crest width as expected. The crest width was maintained at the lower BMP dose and increased significantly at the higher dose compared to the unfilled sockets ($P < 0.001$) and the autograft-treated sockets ($P = 0.010$) (Two-way ANOVA with Holm-Sidak post-hoc test). Intermediate results were seen with the autogenous bone-treated sockets.

In the ridge augmentation group (where the buccal bone had been removed), there was some increase in crest width in the unfilled group, but the increase was significantly greater in the URIST-treated groups at both doses than the unfilled

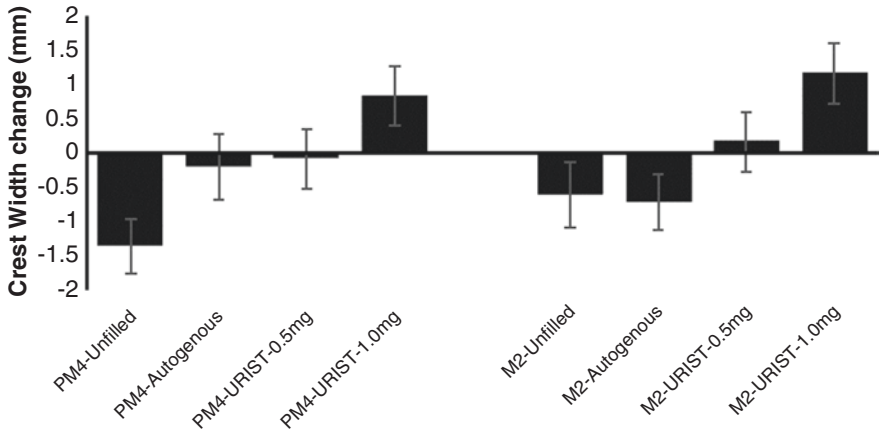

Fig. 12.15 Changes in crest width in the socket preservation group (mean ± SD). Sockets that did not receive a bone graft reduced in width over 6 weeks, while those grafted with autograft or URIST maintained or increased their width. PM4: *left* and *right* fourth premolars; M2: *left* and *right* second molars

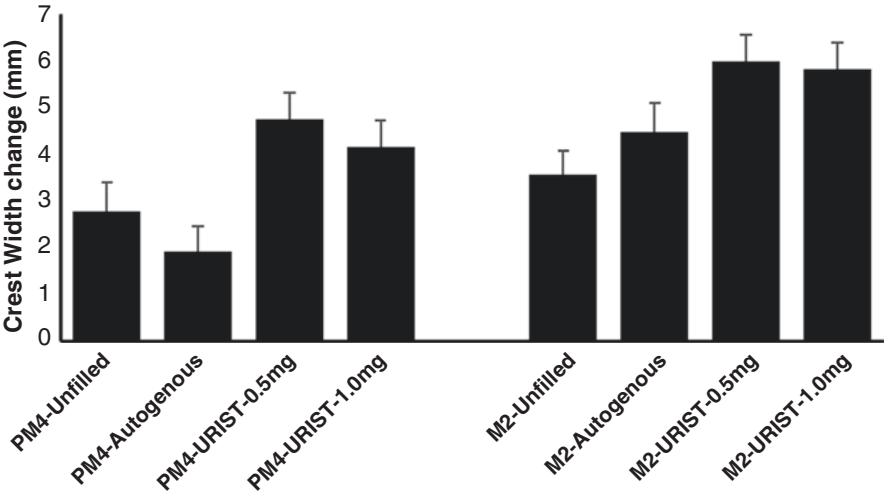

Fig. 12.16 Changes in crest width in the ridge augmentation group (mean ± SD). Sockets that did not receive a bone graft increased in width slightly however those grafted with URIST with both the high and low dose of rhBMP-2 produced significantly thicker jaw widths. PM4: *left* and *right* fourth premolars; M2: *left* and *right* second molars

(*P = 0.003* for URIST-0.5 mg, *P = 0.011* for URIST-1 mg), and autogenous sockets (*P = 0.002* for URIST-0.5 mg, *P = 0.010* for URIST-1 mg) (Two-way ANOVA with Holm-Sidak post-hoc test). Intermediate results were seen with the autogenous bone-treated sockets. Similar trends were also observed in the apex and mid ridge width measurements.

Histology of Bone Cores

The bone cores taken from the unfilled sockets, autogenous bone-treated sockets, and URIST-treated sockets were similar histologically for each of the parameters evaluated, including fibrous connective tissue, neovascularization, new woven bone formation, and new lamellar bone formation (Fig. 12.17). No significant inflammation or signs of infection were seen at any of the URIST-treated or control sites.

Each core from the URIST-treated sockets in both the socket preservation and ridge augmentation groups had a small amount of the test article material present, often with new woven bone around the test article.

12.2.4.4 Conclusions of the Efficacy Study

The results of this GLP study show that the URIST Putty was effective in (1) maintaining jaw dimensions when used for socket preservation, and (2) increasing jaw dimensions when used for ridge augmentation, showing statistically significantly better results than autograft and negative controls. Further, based on the bone core histology, URIST achieved this primarily through the stimulation of bone formation, rather than just having the graft material fill the space.

There were no major adverse effects associated with the use of URIST and the dogs appeared in good health throughout the study. Sufficient ridge dimensions were maintained or produced to allow for the placement of dental implants.

12.3 Discussion

The currently approved rhBMP-2 implant can be as effective as autogenous bone, however it requires very high doses of rhBMP-2 to be so, due to the rapid burst release of the rhBMP-2 from the absorbable collagen sponge. However, sustained release carriers such as PLGA also require very high doses and do not appear to be any better as a delivery system.

For bone graft substitutes to be an effective alternative to autogenous bone they need to provide not just a scaffold for bone repair, but also the signals to promote osteogenic tissue ingrowth and differentiation into osteoblasts.

BMP-2 not only induces the differentiation of osteoprogenitor cells into bone forming osteoblasts, it also is a chemoattractant and therefore can play a role in recruiting osteogenic cells. It has been proposed that success of BMP implants depends on obtaining a sufficient density osteoprogenitor cells at the implant site, and that a “high initial burst” of rhBMP-2 from ACS achieves this [42].

We hypothesized that a multiphasic delivery system that provides sufficient rhBMP-2 release initially to recruit cells, followed by sustained release of the remaining rhBMP-2 over a prolonged period would be require less rhBMP-2 to be effective than the current ACS implant.

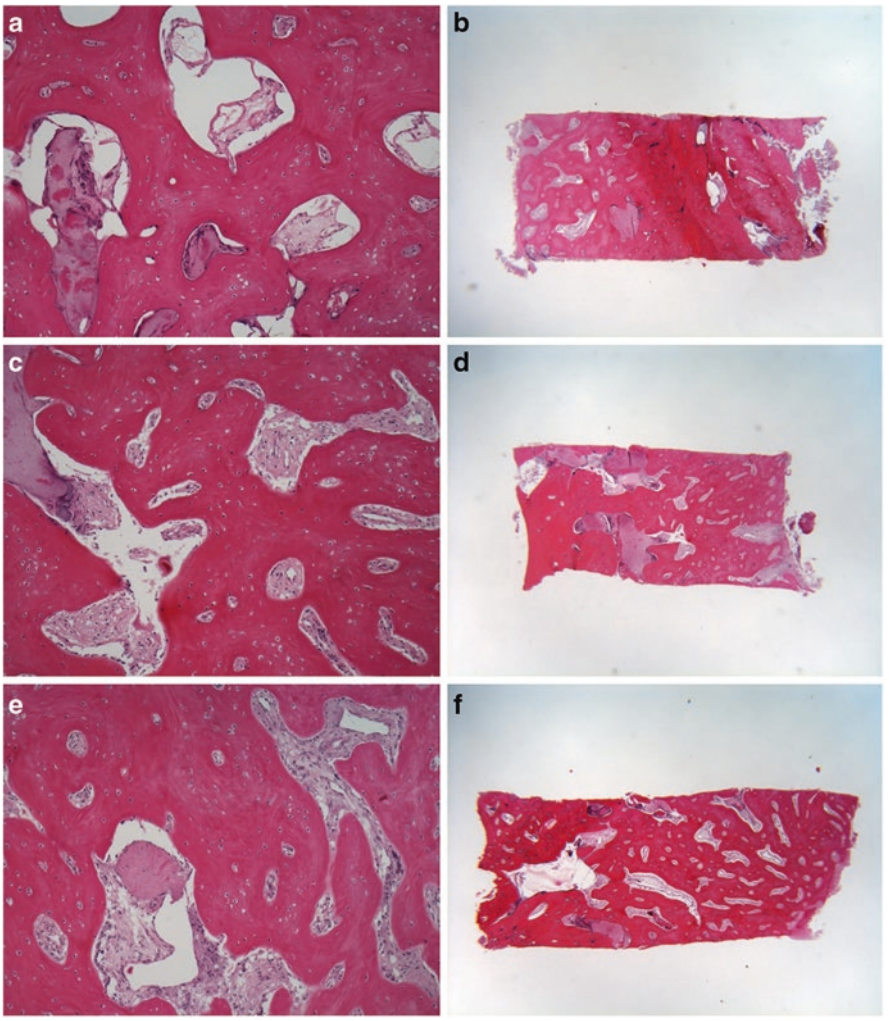

Fig. 12.17 Histology of bone cores from dog study. Hematoxylin and eosin stained sections of the unfilled (**a**, **b**), autograft filled (**c**, **d**), and URIST Putty filled (1 mg BMP) (**e**, **f**) bone cores taken at 100× (**a**, **c**, **e**) and 4× (**b**, **d**, **f**) magnification. All bone cores had a similar histological appearance

The results of the in vitro study demonstrated that combining P407 gel with CSD and or BCP granules produces such a multiphasic rhBMP-2 release profile in vitro. The mixture of P407 gel, CSD and BCP released approximately 25% of the loaded rhBMP-2 over the initial 7 days where it could act as a chemoattractant for mesenchymal stem cells, while the remaining BMP would be released more slowly in a sustained fashion.

While we did not measure the release of rhBMP-2 in vivo, it would be expected that the rhBMP-2 associated with the P407 gel would be completely released over

the first 3–5 days, rhBMP-2 associated with the surface of the CSD would be released as it degrades over the first 4–6 weeks and the rhBMP-2 associated with the surface of the BCP would be released as it degrades over the following months.

The mouse muscle pouch study clearly showed that even with half the amount of rhBMP-2 an implant that uses a mixture of CSD and BCP granules and P407 gel can produce 50% larger ossicles that contain twice as much bone as the currently approved ACS implant. This study also showed that it was important that some of the rhBMP-2 be incorporated into the P407, rather than having it all associated with the CSD and BCP granules and relying on release from the surface of the granules to produce the initial burst. This supports the hypothesis that sufficiently high amount of rhBMP-2 must be released initially to act effectively to recruit the osteoprogenitors.

While in the mouse muscle pouch study the rhBMP-2 was added directly to the P407 gel, we have determined that by varying the concentration of protein and the ratio of loading solution to scaffold we can vary the amount of protein that is associated with the surface of the CSD and BCP granules and the amount that remains unbound during lyophilization. This unbound protein would then be able to dissolve directly into the P407 gel when it is added prior to surgery, producing the same effect. This approach was used to prepare the implants used in the dog efficacy study.

The GLP efficacy study showed that the URIST implant was effective both in socket preservation (preventing bone loss following tooth extraction) and alveolar ridge augmentation (augmenting bone volume). URIST at both BMP doses was significantly better than autograft in the ridge augmentation group. This was somewhat surprising and may be due to using particulate autograft, without any membrane to assist its retention at the site. The amount of rhBMP-2 placed in the defects was estimated based on the amount of unused putty to be 0.1 and 0.15 mg for the low dose URIST preparation and 0.2 and 0.3 mg for the high dose URIST preparation for preservation and augmentation procedures respectively. By comparison a study on ridge augmentation in dogs using rhBMP-2-ACS implants used 0.86 mg rhBMP-2 [43], while the pivotal clinical trial using rhBMP-2 on ACS for ridge augmentation used 0.9 to 1.9 mg rhBMP-2 [44].

In conclusion, these studies supported our hypothesis that a multiphasic delivery carrier could be effective with lower doses of rhBMP-2 than the currently approved ACS carrier, and led to the design of an rhBMP-2 carrier that was a mixture of CSD and BCP granules with P407 gel (URIST™).

References

1. Dimitriou R, et al. Complications following autologous bone graft harvesting from the iliac crest and using the RIA: a systematic review. Injury. 2011;42(Suppl 2):S3–15.
2. Seiler 3rd JG, Johnson J. Iliac crest autogenous bone grafting: donor site complications. J South Orthop Assoc. 2000;9(2):91–7.
3. Sammarco VJ, Chang L. Modern issues in bone graft substitutes and advances in bone tissue technology. Foot Ankle Clin. 2002;7(1):19–41.
4. Szpalski M, Gunzburg R. Applications of calcium phosphate-based cancellous bone void fillers in trauma surgery. Orthopedics. 2002;25(5 Suppl):s601–9.
5. Rosen V. BMP-2 signalling in bone development and repair. Cytokine Growth Factor Rev. 2009;20:475–80.

6. Yu Y, et al. TGF-beta, BMPS, and their signal transducing mediators, Smads, in rat fracture healing. J Biomed Mater Res. 2002;60(3):392–7.
7. Li G, et al. rhBMP-2, rhVEGF(165), rhPTN and thrombin-related peptide, TP508 induce chemotaxis of human osteoblasts and microvascular endothelial cells. J Orthop Res. 2005;23(3):680–5.
8. Lee DH, et al. Chemotactic migration of human mesenchymal stem cells and MC3T3-E1 osteoblast-like cells induced by COS-7 cell line expressing rhBMP-7. Tissue Eng. 2006; 12(6):1577–86.
9. Lane JM. Bone morphogenic protein science and studies. J Orthop Trauma. 2005;19(10 Suppl):S17–22.
10. Khan SN, Lane JM. The use of recombinant human bone morphogenetic protein-2 (rhBMP-2) in orthopaedic applications. Expert Opin Biol Ther. 2004;4(5):741–8.
11. Giannoudis PV, Tzioupis C. Clinical applications of BMP-7: the UK perspective. Injury. 2005;36(Suppl 3):S47–50.
12. Cahill KS, et al. Prevalence, complications, and hospital charges associated with use of bone-morphogenetic proteins in spinal fusion procedures. JAMA. 2009;302(1):58–66.
13. Tannoury CA, An HS. Complications with the use of bone morphogenetic protein 2 (BMP-2) in spine surgery. Spine J. 2014;14(3):552–9.
14. Woo EJ. Recombinant human bone morphogenetic protein-2: adverse events reported to the manufacturer and user facility device experience database. Spine J. 2012;12(10):894–9.
15. Devine JG, et al. The use of rhBMP in spine surgery: is there a cancer risk? Evid Based Spine Care J. 2012;3(2):35–41.
16. Fu R, et al. Effectiveness and harms of recombinant human bone morphogenetic protein-2 in spine fusion: a systematic review and meta-analysis. Ann Intern Med. 2013;158(12):890–902.
17. Cooper GS, Kou TD. Risk of cancer after lumbar fusion surgery with recombinant human bone morphogenic protein-2 (rh-BMP-2). Spine (Phila Pa 1976). 2013;38(21):1862–8.
18. Garrison K, et al. Clinical effectiveness and cost-effectiveness of bone morphogenetic proteins in the non-healing of fractures and spinal fusion: a systematic review. Health Technol Assess. 2007;11(30):1.
19. Olympus Corporation. Olympus corporation announces plans to discontinue operations for its Biotechnology Division in the U.S. 2014: PR Newswire.
20. Barr T, et al. Comparison of the osteoinductivity of bioimplants containing recombinant human bone morphogenetic proteins 2 (Infuse) and 7 (OP-1). Oral Surg Oral Med Oral Pathol Oral Radiol Endod. 2010;109(4):531–40.
21. De Groot K. Carriers that concentrate native bone morphogentic protein in vivo. Tissue Eng. 1998;4(4):337–41.
22. Seeherman H, Wozney JM. Delivery of bone morphogenetic proteins for orthopedic tissue regeneration. Cytokine Growth Factor Rev. 2005;16(3):329–45.
23. Friess W, et al. Characterization of absorbable collagen sponges as rhBMP-2 carriers. Int J Pharm. 1999;187(1):91–9.
24. Xu SW, et al. Early period of fracture healing in ovariectomized rats. Chin J Traumatol. 2003;6(3):160–6.
25. Morone MA, et al. The Marshall R. Urist young investigator award. Gene expression during autograft lumbar spine fusion and the effect of bone morphogenetic protein 2. Clin Orthop Relat Res. 1998;351:252–65.
26. Ivaska KK, et al. Effect of fracture on bone turnover markers: a longitudinal study comparing marker levels before and after injury in 113 elderly women. J Bone Miner Res. 2007;22(8):1155–64.
27. Karladani AH, et al. The influence of fracture etiology and type on fracture healing: a review of 104 consecutive tibial shaft fractures. Arch Orthop Trauma Surg. 2001;121(6):325–8.
28. Nakamura Y, et al. Temporal and spatial expression profiles of BMP receptors and noggin during BMP-2-induced ectopic bone formation. J Bone Miner Res. 2003;18(10):1854–62.
29. Nakamura Y, et al. Expression profiles of BMP-related molecules induced by BMP-2 or -4 in muscle-derived primary culture cells. J Bone Miner Metab. 2005;23(6):426–34.
30. Takayama K, et al. RNA interference for noggin enhances the biological activity of bone morphogenetic proteins in vivo and in vitro. J Bone Miner Metab. 2009;27(4):402–11.

31. Humber CC, et al. Bone healing with an in situ-formed bioresorbable polyethylene glycol hydrogel membrane in rabbit calvarial defects. Oral Surg Oral Med Oral Pathol Oral Radiol Endod. 2010;109(3):372–84.
32. US Food and Drug Administration. Inactive ingredient database. 2016 [cited 2017 14 Jan]; Available from: http://www.accessdata.fda.gov/scripts/cder/iig/index.Cfm.
33. Dumortier G, et al. A review of poloxamer 407 pharmaceutical and pharmacological characteristics. Pharm Res. 2006;23:2709–28.
34. Zhou AJ, Clokie CM, Peel SA. Bone formation in algae-derived and synthetic calcium phosphates with or without poloxamer. J Craniofac Surg. 2013;24(2):354–9.
35. Issa JPM, et al. Bone healing process in critical-sized defects by rhBMP-2 using poloxamer gel and collagen sponge as carriers. Micron. 2008;39(1):17–24.
36. Clokie CML, Urist MR. Bone morphogenetic protein excipients: comparative observations on poloxamer. Plast Reconstr Surg. 2000;105:628–37.
37. Clokie CM, Bell RC. Recombinant human transforming growth factor beta-1 and its effects on osseointegration. J Craniofac Surg. 2003;14(3):268–77.
38. Thomas MV, Puleo DA. Calcium sulfate: properties and clinical applications. J Biomed Mater Res B Appl Biomater. 2009;88(2):597–610.
39. Lu J, et al. The biodegradation mechanism of calcium phosphate biomaterials in bone. J Biomed Mater Res. 2002;63(4):408–12.
40. Nery EB, et al. Tissue response to biphasic calcium phosphate ceramic with different ratios of HA/beta TCP in periodontal osseous defects. J Periodontol. 1992;63(9):729–35.
41. LeGeros RZ, et al. Biphasic calcium phosphate bioceramics: preparation, properties and applications. J Mater Sci Mater Med. 2003;14(3):201–9.
42. Li RH, Wozney JM. Delivering on the promise of bone morphogenetic proteins. Trends Biotechnol. 2001;19(7):255–65.
43. Sigurdsson TJ, et al. Bone morphogenetic protein-2 for peri-implant bone regeneration and osseointegration. Clin Oral Implants Res. 1997;8(5):367–74.
44. Fiorellini JP, et al. Randomized study evaluating recombinant human bone morphogenetic protein-2 for extraction socket augmentation. J Periodontol. 2005;76(4):605–13.

Chapter 13
Development and In Vitro Analysis of a New Biodegradable PLA/Hydroxyapatite (HAp) Composite for Biomedical Applications

Innocent J. Macha, Besim Ben-Nissan, Andy Choi, and Sophie Cazalbou

Abstract The development of new drugs or formulations for the treatments of different musculoskeletal disorders (MSDs) has now being a focus of pharmaceutical and scientific societies. Targeted and multidelivery of drug and key minerals to support bone repair and regeneration at the defect site, from flexible biodegradable devices at the rate within the therapeutic window, seem to be an effective strategy. However, the drug delivery vehicles available are neither flexible and degradable nor able to deliver both pharmaceutical drug and minerals effectively. The use of biodegradable polymer and bioceramic for composite development with enough flexibility and potential for slow in situ drug delivery for biomedical applications could be one of the real options to mitigate MSDs problem. In vitro analysis of the developed devices is a vital step towards clinical trial and commercialization of the implant. Different approach and results have been compared to draw guidelines for the development and testing of thin film composite applications as a slow drug delivery vehicle.

Keywords Polylacticacid • Hydroxyapatite • Biocomposite • Drug delivery • Antibiotics • in vitro analysis • Stem cells • Biofilms

I.J. Macha
Mechanical and Industrial Engineering, University of Dar es Salaam,
P.O Box 35131, Dar es Salaam, Tanzania

B. Ben-Nissan (✉) • A. Choi
Advanced Tissue Regeneration & Drug Delivery Group, School of Life Sciences,
University of Technology Sydney, Australia School of Life Sciences,
P.O. Box 123, Broadway, NSW 2007, Australia
e-mail: Besim.Ben-Nissan@uts.edu.au

S. Cazalbou
CIRIMAT Université de Toulouse, CNRS, INPT, UPS, ENSIACET,
4 allée Emile Monso, BP 44362, 31030 Toulouse cedex 4, France

G. Kaur (ed.), *Clinical Applications of Biomaterials*,
DOI 10.1007/978-3-319-56059-5_13

13.1 Introduction

The physical and emotional trauma the patients encounter due to adverse events associated with medical implant-tissue infections and clinical conventional therapies have raised a great concern in public health and become an economic burden for many countries. Despite the significant efforts that have been directed towards discovering new drugs or improving the clinical outcomes of current drugs and practices by using new formulations [1], needs for new and innovative solutions are huge. The use of biomaterials to address this problem is likely to provide scientists and biomedical field communities with a promising approach towards a solution. One of the advantages of biomaterials is the possibility to be designed to stimulate specific cellular responses at the molecular level. Biomaterials are grouped into three classes, bioinert, bioactive and bioresorbable, based on the reactions of biological systems to them when implanted. They can be modified in their molecular level to elicit specific interactions with cell integrins and thereby direct cell proliferation, differentiation and extracellular matrix production and organization. In addition, bioresorbable biomaterials can be designed to gradually degrade/dissolve and thus allow the release of bioactive elements (drugs, mineral ions) capable of promoting bone regeneration/repair and to avoid certain side effects related to surgery. These biomaterials are then replaced by the newly formed bone tissue.

Polymeric biomaterials form one of the most important material groups in biomedical engineering. They have a wide range of applications in drug delivery and wound healing as well. Synthetic polymers like α-hydroxy acids, which include poly(glycolic acid), poly(lactic acid) and their copolymers, polyanhydrides and naturally occurring polymers like chitosan and hyaluronan, have been extensively used in medical devices and the pharmaceutical industry. The propensity of some of the polymeric biomaterials to uptake and release active substances as the consequence of their degradation addresses the significant healthcare costs involved and the deaths associated with many clinical complications. Many attempts [2, 3] have been successfully made to incorporate drugs into implantable polymeric devices for a sustainable and controlled release. Though they cannot be directly subjected to load-bearing conditions, their role in improving people's life is significant huge while their potentials are not fully taped.

Ceramic biomaterials or bioceramics are the class of ceramics used in the biomedical field to repair and reconstruct the necrotic and damaged tissue of musculoskeletal systems [4]. Different classes of these materials are known based on their response to biological environment, for instance, alumina (Al_2O_3) and zirconia (ZrO_2) are termed bioinert, bioglass and glass ceramic are bioactive, while calcium phosphate ceramics (CPC) are classified as bioactive and bioresorbable. Though bioceramics are widely used as implants in orthopaedics, maxillofacial surgery and for dental implants, more developments are in progress for extending their applications and achieving improvements in their performance and reliability. Metal implants like titanium and its alloys have a long-term problem of loosening after being implanted, due to a lack of sufficient bioactivity on the surface over time [5]. Ben-Nissan [6, 7] developed solgel

crystalline nanocoatings of hydroxyapatite on different substrates of medical implants. Using hydroxyapatite, which is chemically similar to the mineral component of natural bone as a coating, has the added advantage that bioinert implant materials like titanium and cobalt chromium alloys and alumina can be given bioactive coatings with an improvement of their osteointegration.

Due to different properties of polymeric and ceramic biomaterials, it has been shown that their combination results into biomaterials with superior biological, physical and mechanical properties. It has been shown that the release of acidic degradation products from polymeric materials causes inflammatory reactions; thus the degradation products from ceramic biomaterials could possibly buffer the acidic products from polymers and reduce the significantly inflammatory effects. Usually ceramics are hard and brittle unlike polymers which are flexible and ductile. Different techniques for their combinations exist; however, one of the major challenges is the proper ratio and the method that will tailor and optimize the required properties for a specific applications, whether in tissue engineering or drug delivery due to poor interfacial bonding between ceramic particles and polymer matrix. To achieve excellent properties, surface modifications of bioceramics particles have been attempted using silane coupling agents, titanate and zirconates in order to improve interfacial bonding between inorganic particles and the polymer matrix [8].

13.2 Biodegradable Polylactic Acid as Composite Precursor

At present, PLA is one of the most promising polymeric clinical materials and has drawn a lot of attention from scientists and industrialists. Its synthesis methods and physical, mechanical, optical and biological properties have been extensively studied [9, 10]. Pure PLA is a semi-crystalline polymer with a glass transition temperature Tg of about 55 °C and melting point (Tm) of about 180 °C [11]. Polymers prepared from meso- or rac-lactide are in general amorphous, but by applying a stereo-selective catalyst, polymers having tacticity high enough for crystallization also have been obtained. The crystal structure of PLA was studied and reported to be the left-handed helix conformation for the α-form [12]. The solubility of PLA highly depends on the degree of crystallinity, polymer molar mass and other comonomer units present in the polymer. It has been reported that PLA is soluble in most organic solvents such as acetone, pyridine, ethyl lactate, tetrahydrofuran, xylene, ethyl acetate, dimethylsulfoxide, N,N-dimethylformamide and methyl ethyl ketone [11]. PLA is insoluble in water, alcohols (e.g. ethanol, propylene glycol) and unsubstituted hydrocarbons (e.g. hexane, heptanes). Lactic acid (2-hydroxypropionic acid) is a simple chiral molecule that exists as two enantiomers, L- and D-lactic acid, which differs in their effect on polarized light. The optically inactive D, L or mesoform is an equimolar (racemic) mixture of D(−) and L(+) isomers [13]. The stereochemistry and thermal history have direct influence on PLA crystallinity and, therefore, on its properties in general. PLA with PLLA content higher than 90% tends to be crystalline, while the lower optically pure is amorphous. Semi-crystalline

PLA has higher mechanical properties than the amorphous. The mechanical properties of PLA is reasonably good for a wide range of applications.

Within biomedical fields, PLA has been widely used for clinical implant materials, drug delivery systems and also as degradable scaffolds. PLA provides excellent clinical properties at relatively low cost, which increases its use in biomedical applications. Different medical devices have been developed using PLA from degradable sutures to membranes for wound dressings. Different properties can be easily tuned from the simple modifications of the physical structural properties of PLA. It has been shown that blending or copolymerizing PLA with either degradable or no-degradable biocompatible materials results in new products with the desired behaviour without compromising its biocompatibility, which consequently improves the quality and reduces the cost of production. Surface properties play an important role in both biocompatibility and bio-functionability of biomaterials hence its applications. Different surface modification strategies, such as physical, chemical, plasma and radiation-induced methods, have been employed to create desirable surface properties of PLA biomaterials [14]. Resorbable fixation can be used for both anterior and middle cranial base surgical approaches. Imola and Schramm in their study reported that bioresorbable fixation systems represent a major advance in paediatric craniomaxillofacial surgery [15].

13.3 Calcium Phosphate Materials from Marine Structures

On the other hand, calcium phosphate (CaP) materials have gained clinical acceptance for the past 40 years [16]. Hydroxyapatite [$Ca_{10}(PO_4)_6(OH)_2$, HAp] and β-tricalcium phosphate [$Ca_3(PO_4)_2$, β-TCP] are one of the most widely used synthetic materials (CaPs) in the areas of orthopaedic and dentistry for augmentation and bone substitution and repair due to their similarity with the mineral phase of bone. It is known that bone formation involves a series of complex events leading to mineralization of extracellular matrix proteins by cells with specific functions for maintaining the integrity of the bone [17]. The scientific and clinical communities agreed that bone apatite can be better described as carbonated calcium-deficient hydroxyapatites (CHA) and approximated by the formula: $(Ca,X)_{10}(PO_4,CO_3)_6(OH,Y)_2$ where X are cations (magnesium, sodium, strontium ions or lacunae) that can substitute for the calcium ions, and Y are anions (chloride, fluoride ions or lacunae) that can substitute for the hydroxyl group [18]. Theoretical composition of HAp is 39.68 wt% Ca, 18.45 wt% P; with Ca/P wt ratio of 2.151 and Ca/P molar ratio of 1.667. HAp is stable in a wide range of pH 4.4–8.0 and has higher stability in aqueous media than other calcium phosphate ceramics [19].

The use of synthetic materials in the biomedical field has been greatly successful for many years. Nevertheless the shaping processes used do not yet make it possible to obtain biosimilar materials to the bone or to its mineral phase. They are the result of a calculated compromise between chemical composition similar to that of bone, mechanical properties compatible with the host tissue and the presence of an inter-

connected porous network that promotes cellular invasion. Natural materials have superior biological and structural properties compared to synthetic materials, and they provide an abundant source of novel biomedical applications [20]. Calcium phosphates, specifically HAp and TCP, can be prepared from natural materials composed of calcium carbonate with a unique architecture such as sea coral [20], mussel [21], egg shells [22] and nacre *Venus verrucosa* [23] for biomedical applications. The high price of bioceramics in the market reflects the significant costs of raw materials that can easily be replaced by natural biogenic materials.

The potential applications of natural biogenic materials such as marine structures can be easily overlooked due to the environmental concerns. While it is true that a wide range of marine structures are limited and protected, similarly there are also a variety of materials that are abundantly available and are yet to be exploited for their possible use [24]. Previous work has shown that corals can be artificially grown as synthetic corals in specific areas and containers [25]. Among marine structures, coral mineral, which mainly consists of calcium carbonate in the forms of aragonite or calcite with trace elements of strontium, magnesium and sodium, has considerable success as the apatite precursors and bone graft materials [26]. Corals have a porous structure with pore size ranges from 150 to 500 μm, similar to cancellous bone and form chemical bonds with bone and soft tissue in vivo [20]. Kühne and his colleagues analysed osseous reactions in the rabbit femoral condyle to coralline hydroxyapatite bone substitutes of various pore sizes by radiology and histology [27]. Their results suggest that there was a substantial production of bone within the 500-micron pore size. In addition they concluded that the pore size of the coralline hydroxyapatite influenced the development of bone in the implants. It was further reported that the interaction of the primary osteons between the pores via the interconnections allows propagation of osteoblasts [28].

13.3.1 Conversion of Marine Structures (Coralline Materials) to Calcium Phosphates

A number of synthesis routes for calcium phosphates have been reported in the literature. The main two are the wet chemical and solid-state reaction methods. Other alternative methods like mechanochemical, electrospray, hydrothermal and microwave heating to mention just a few have been reported previously. Size reduction of coral particles is necessary before conversion in order to enhance surface area that will consequently reduce the conversion time. Figure 13.1 shows the morphology of coral before and after size reduction by ball mill.

Since micro-, meso- and nanopores present in normal coral, meso- and nanopores will still present in the particles after size reduction and play a big role on the loading active clinical agent into the materials. The conversion method that retains the microstructure of coral is more preferable for wide range of medical applications. It has been shown that both hydrothermal and mechanochemical techniques with ammonium phosphate solution produced HAp with morphologies of platelets similar to the

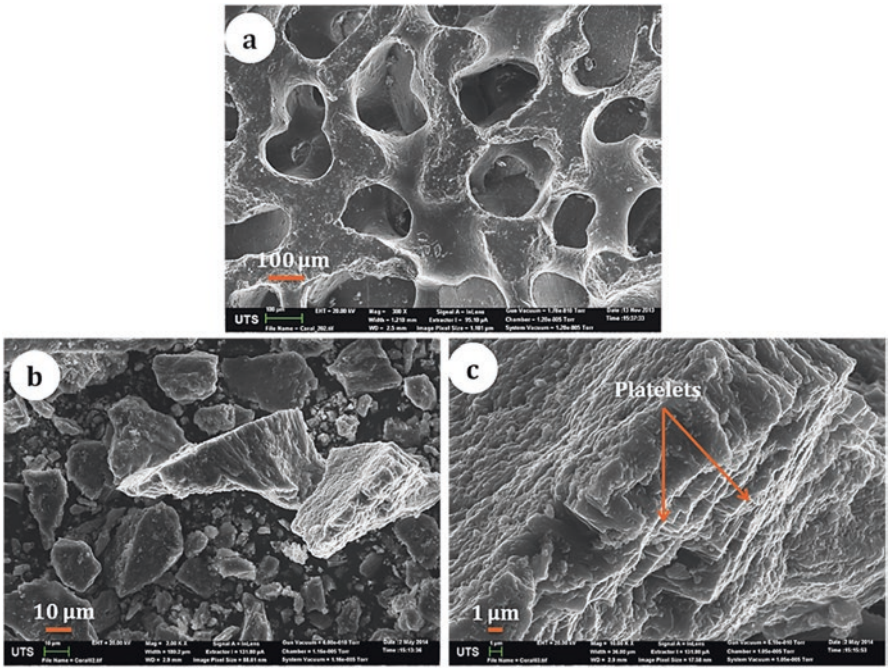

Fig. 13.1 SEM pictures showing the morphology of coral (**a**) before ball mill showing pores and interconnected pores, (**b**) after ball mill showing different particle sizes and (**c**) higher magnifications of (**b**) revealing platelets morphology of singer particle

original coral suggesting the solid-state topotactic ion exchange reaction mechanism [29]. On the other hand, with orthophosphoric phosphate solution, the reaction mechanism is suggested to be dissolution-recrystallization (Fig. 13.2).

Previous studies revealed that coral does not contain impurities that could be harmful to humans. It has been shown that there is no presence of any heavy metals in coralline materials. Previous analysis of coral on an imaging laser ablation inductively coupled plasma mass spectroscopy (LA-ICP-MS) [30] showed the presence of magnesium and strontium in HAp-derived coral, which are beneficial to the human body.

13.4 Biodegradable PLA/HAp Composites as Drug Delivery Systems

Tailoring better properties for drug release systems can be carefully achieved by the combination of more than two components to make composite systems. It has been shown that composite drug delivery systems composed of silica nanoparticles coated with β-TCP and bioactive glass showed high performance in the local and extremely sustained delivery of the bicomponent antitubercular drugs and excellent biocompatibility [31].

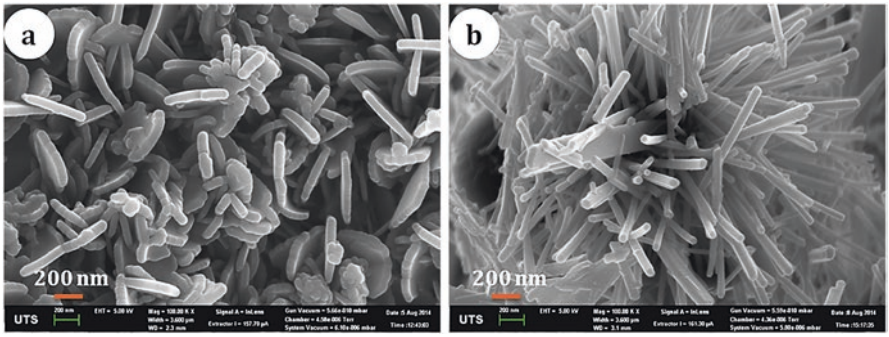

Fig. 13.2 SEM pictures showing the morphology of HAp mechanochemical converted coral by (**a**) ammonium phosphate solution, platelets morphology and (**b**) orthophosphoric phosphate solution, rod-like morphology

The most studied low molecular weight drugs incorporated in calcium phosphate are antibiotics, while osteoporotic, anticancer and other drugs have also been evaluated, showing in most cases profiles with burst release initially fitting the Higuchi model. It has been shown that these drugs remain active after their incorporation into the cements. However, given the dynamic nature of the setting process, and to approach the reality of the surgical room, it was suggested that it would be of interest to increase the number of release studies from unset drug containing cements [32].

Biodegradable PLA and PLGA (poly(D,L-lactic-co-glycolic acid)) polymer films loaded with gentamicin have been developed to serve as "coatings" for possible fracture fixation devices and prevent implant-associated infections. The use of biodegradable polymer films is advantageous due to their propensity to uptake and release antibiotics, as a consequence of their degradability. Although their drug release rates are high, they could be tailored to form biocomposites with different biodegradability rates by incorporating other materials. Biodegradable polymer-bioceramic composites would be ideal in this endeavour because of the bioactive nature of ceramic materials, which promote tissue growth. Incorporation of bioceramics derived from coral in the polymer improves not only controlled drug release but also bioactivity and tissue regeneration, especially in orthopaedic and maxillofacial applications. Investigations have shown that antibiotics have been ototoxic and nephrotoxic at high dosages. For most controlled release systems, the loaded dosages are usually high, and therefore the systemic exposure of antibiotic in blood and urine is the major safety concern. The use of HAp-derived coralline materials provides possibilities to control the release and hence avoid the toxic level of drugs.

Solution casting method is suggested to be the simplest method in production of PLA/HAp composite loaded with clinical active agents. The studies suggest that loading drugs into HAp particles and then using them for composite with biodegradable polymers as matrix produce films that are flexible and almost transparent suitable for biomedical applications. The amount of particulate matters in the composites can be controlled in order to control the amount of drug and flexibility of the resulting products. Moreover, there are few things that should be experimented or known before deciding

the amount of drug to be loaded into the devices. Minimum inhibitory concentration which is the lowest concentration of an antimicrobial agent that prevents visible growth of a microorganism in should be evaluated based on known protocols and used as the basis of the amount of drug to be loaded. For biodegradable polymer composites, degradation behaviour polymer is important on the release rate of drugs from these devices.

After loading the drug into devices, it is advised to evaluate any alteration or denaturation of drugs loaded in a polymer matrix. IR techniques can be used to evaluate any chemical modification by comparing the shifts of drugs in polymer matrix that should be consistent with IR shifts of these drugs before imbedded into the matrix. Other characteristics such as drug dissolution profiles, antibacterial efficacy test and morphological, chemical and biological properties should also be evaluated for any drug delivery device.

13.4.1 In Vitro Drug Release in Buffer Solutions

Drug release profiles from PLA/HAp composites could take place in different stages depending on the type of drug loaded. Several factors govern the release of drug from biodegradable drug delivery devices. Although most of drug delivery devices will have burst effect due to the surface-bound drugs that can be assimilated as the direct dissolution of drugs in buffer solution, the release stages after that are mainly governed by diffusion of drug from within the devices. In comparison, drug release from PLA film and from PLA/HAp composites behaves differently in their second stages of release. This step is driven by the internal diffusion of drugs impregnated within the matrix possibly in the porous part of the matrix generated during preparation. The release of gentamicin, for instance, from PLA/HAp, is preceded by a lag phase which occurs in the early hours of release. It is suggested that the presence of HAp within the matrix could in many ways hinder or slow down the release of drug through micropores unlike the release from PLA film alone. Generally, the release in this step is slower compared to the previous step due to the resistance imposed by narrow and small pores with the matrix and between matrix and particles.

For some drug such as bisphosphonate in PLA/HAp devices, their release profile terminated at stage three. At this stage there is pore growth due to both mass loss by polymer degradation and pore coalescence (micropores coalescing (or joining) to form mesopores). For the device containing HAp, the release amount in all stages is lower from the PLA film because drug diffusion is delayed by an induction time sufficient to allow nano- and micropores of HAp to coalesce and permit the passage of the macromolecular drug out from the occlusion through the microporated matrix [33]. Moreover, for PLA/HApBP, drug (BP) previously adsorbed on mineral particles is reported to have strong affinity to the nanocrystalline apatites with adsorption phenomena occurring at the surface of apatite crystals [34]. The affinity between drug and drug carrier plays an important role on controlling the dissolution rate. It can be carefully designed for a prolonged drug dissolution. The most important feature of this aspect is the kinetics of which drug dissolution pattern portrays.

13.4.2 Drug Release Kinetics

Drug release kinetics can be assessed using model-dependent methods in order to determine the release mechanisms involved during the drug release. There are a number of kinetic models available which describe the overall release of drug from the dosage forms. These models can be carefully selected and being used to fit the drug release data. For biodegradable drug release devices, it could be difficult to find a single empirical expression that describes all of the mechanisms involved in the release. However, it could sometimes be easier to use the model that describes only the mechanism of drug transport through the devices. It is worth to note that the combinations of kinetic model could be used for one drug in order to gain more information on the release mechanisms. Different drugs would have different release kinetics from the same device due to their different drug-device interactions.

For instance, the release of gentamicin from hydroxyapatite-PLA composites indicates that a number of different mechanisms might control the release. The release mechanisms comprise the mixture of diffusion, supercase II mechanism and other mechanisms of transport which control the drug release. On the other hand, the release of bisphosphonate (BP) drug from hydroxyapatite-PLA composite, but initially loaded into hydroxyapatite particles, displays a different kinetics. It has been highlighted that the strong affinity of BP molecules for the nanocrystalline apatite explains the retardation on the drug release due to the adsorption phenomena that occur at the surface of apatite crystals. Thus, BP molecules in contact with apatite crystals are exchanged with phosphate ions located in the reactive labile apatitic layer and cannot be spontaneously released without another anionic exchange or without the dissolution of the crystals.

Generally, there are many other factors that influence drug release kinetics in vivo that could not be considered during in vitro study. Some of these factors are biological parameters such as transport of drug via diffusion-convection, biological properties of tissue and arterial ultrastructure, hydrodynamic conditions at the implantation site and final biological response to drug delivery device.

13.5 Stem Cells Study

Different types of cells have been used in tissue engineering and in therapeutic strategies in cell therapy including stem cell transplantation. Stem cells are primarily used to understand the mechanisms by which natural or synthetic biomaterials are able to elicit a cellular response when implanted in vivo. Stem cells are different from other types of cells in the human body. They are capable of dividing and renewing themselves for an extended period of time. They are also unspecialized and can be differentiated into specialized cells.

There has been an increase in the number of researches on implantable biomaterials and their application in regenerative medicine. This has also created necessary

testing procedures to be undertaken using in vitro laboratory tests, according to ISO 10993 to avoid dangers for patients and unnecessary animal experiments. Cell compatibility of biomaterials involves three important stages, which are adhesion of cells on the surface, proliferation and finally differentiation. When biomaterial is implanted into a living body, rapidly the biomaterial is coated with a protein layer before the cells' attachment. Serum protein and various extracellular matrices (ECM) are involved such as fibronectin, fibrinogen, albumin and vitronectin [35]. The protein adsorption and conformation are partly influenced by the morphology of the biomaterial surface, which also influences the cell adhesion and proliferation process [36]. It has been reported that micro-/nano-surface topography has a direct impact on cell adhesion and proliferation with a micro-textured surface favouring the adhesion.

Apart from morphology, the chemical composition of the biomaterial surface has been suggested to play a significant role in the adhesion and proliferation of cells. Keselowsky and his co-workers [37] showed that the cell adhesion through integrin group of cell surface receptors depends on the conformation of adsorbed fibronectin. In their demonstration, they used a self-assembled monolayer of different functional groups such as OH, COOH, NH_2 and CH_3 termini, to create surfaces with different chemistry that are hydrophilic and neutrally charged, hydrophilic and acidic, hydrophilic and basic and hydrophobic, respectively. Their findings suggested that the adhesion strength of cell binding (as determined by a centrifugation assay) followed the trend: OH>COOH>NH_2>CH_3. They also found that specific gene expression of cells such as osteoblast, alkaline phosphatase enzyme activity and matrix mineralization showed the dependence on surface chemistry in which OH- and NH_2-terminated surfaces were more advantageous compared with COOH and CH_3 SAMs. Hydrophobic surfaces seem to cause denaturation of proteins and prevent the surface exposure to cell-binding groups responsible to cell adhesion. On the other hand, hydrophilic and neutrally charged surfaces induce the least extent of unfolding or denaturation, leading to a good cell adhesion on the fibronectin [38].

Synthetic polymeric biomaterials can only support cell adhesion and proliferation to a limited extent due to the lack of functional groups necessary for cell interaction [39]. When human adipose-derived stem cells (hADSC) were seeded on PLA and PLA/HAp composites for proliferation and attachment experiment, the results show abundant cell attachment on PLA/HAp and PLA/HApGM samples and none on PLA and PLAGM. This can be due to the fact that PLA has an alkyl pendant group (CH_3-) in its backbone, which makes the polymer more hydrophobic, and tends to denaturalize protein responsible for cell binding and adhesion. Gentamicin has NH_2- group, which with CH_3- on the polymer backbone reduces any chance for protein binding on the surface. This was evident because these samples (PLA and PLGM) do not show any cells on their surfaces. The addition of hydroxyapatite crystals in the organic matrix improves the bioactivity of the materials by changing the surface chemistry from hydrophobic to hydrophilic and neutrally charged with the presence of OH group, which favours binding of adhesive protein (vitronectin and fibronectin) and subsequently cellular interaction. Surface treatment could be employed to increase cell affinity on these surfaces such as exposure to plasma, coatings, corona discharge, ions and ultraviolet (UV) ozone. Moreover, specific functional groups can be covalently attached to biomaterial surfaces to enhance cell attachments.

13.6 Biofilm Study

Invasive medical devices are widely used in the medical field to replace and repair damaged tissue or for diagnostic purposes. A significant proportion of these devices, which are especially used in central venous catheters, neurosurgical ventricular shunts, implantable neurological stimulators, cochlear implants, intraocular lenses, heart valves, breast implants, ventricular assist devices, coronary stents, arthro-prostheses, fracture-fixation devices, inflatable penile implants and dental implants, is associated with medical device-associated infection [40]. Increasing evidence suggests that bacterial biofilm is the leading course of implants failure in device-associated infections, which also lead to significant morbidity and mortality [41]. It was reported that more than five million central venous catheters alone are implanted annually in the USA, of which 5–26 percentage lead to catheter-related infectious complication. It was estimated the clinical outcomes and costs associated with catheter-related bloodstream infections (CRBSIs) in four European countries [42]. Their results suggest that there are more than 1,000 deaths per year with an associated cost of €35–164 million per year, per country. Biofilm is a microbial-derived sessile community, characterized by cells that are irreversibly attached to a substratum or interface to each other, embedded in a matrix of extracellular polymeric substances that they have produced.

According to International Union of Pure and Applied Chemistry (IUPAC), biofilm is "an aggregate of microorganisms in which cells that are frequently embedded within a self-produced matrix of extracellular polymeric substance (EPS) adhere to each other and/or to a surface" [43]. The three-dimensional extracellular polymeric substances protect bacteria from the external environment so they become more resistant to antimicrobial stress and to the immune system. Treatment of biofilm is difficult after its formation; most of the contaminated devices have to be removed, as the only clinical alternative. An ideal option to deal with biofilm is the development of medical devices with surfaces or materials that prevent microbial surface adhesion or viability. In additional, the designing of medical devices with an antimicrobial agent could also serve as a strategy against biofilm formation. Antibiotics can be incorporated into the materials, coated, covalently bonded or loaded into the thin film that can be used to cover the implants resulting into either slow release of antibiotic or in contact killing without release of antibiotic. Another approach is to modify the surface of the medical device chemically or physically to render the surface microbial adhesion free. Chemical surface modifications have been mostly targeted on the hydrophobicity properties of the materials. One of the major challenges in designing and selection of materials for biofilm prevention and treatments is the lack of in-depth understanding of the mechanisms of bacterial adhesion.

Bacterial biofilms are protected from antibiotic killing. Poor diffusion and penetration of antibiotic through the biofilm contribute to the persistence of biofilm infections especially those associated with implanted devices [44]. A variety of reasons on microbial resistance to antimicrobial agents have been postulated. An increase in the depletion of oxygen and nutrients resulting in slow growth of bacteria, adaptive stress responses and formation of persistent cells is hypothesized to constitute a multilayered defence. The focus is directed towards disabling biofilm resistance, which may

enhance the ability of existing antibiotics to treat infections involving biofilms [45]. It has been reported that in most cases, biofilm can be prevented aggressively by antibiotic in their early stages and can also be treated by chronic suppressive therapy.

The major challenge associated with the use of antibiotics is ensuring retention of antibiotic release and activity for a prolonged period of time after post-operation. The use of biodegradable polymer – ceramic composite for prevention of bacterial infections associated with orthopaedic implants – would be an ideal approach. It was reported that the release of antimicrobial agent from PLA thin film composites sustained for more than 8 weeks [2]. *Pseudomonas aeruginosa* is regarded as an opportunistic pathogen causing indwelling device-related infections especially in catheters. *P. aeruginosa* infection is a leading cause of morbidity and mortality in cystic fibrosis (CF) patients. It was reported that the median survival age of a patient with CF in 2011 was predicted to be 36.8 years, a slight rise compared to 2010 [46]. *S. aureus* infection on the other hand causes serious infectious complications such as severe sepsis, septic thrombosis and/or severe deep-seated infections (endocarditis, osteomyelitis and other metastatic infections) [47].

In the biofilm study, biofilm image features taken by confocal laser scanning fluorescence microscopy (CLSM) and calculated by COMSTAT could be chosen to characterize biofilm development by bacterial strains on the surface of biomaterials. The variables such as biomass, average thickness, roughness coefficient and surface to biovolume ratio are used for interpretation of biological and physical characteristics of biofilm on the surfaces [48]. Biomass represents the overall volume of the biofilm and also provides an estimate of the biomass in the biofilm, average thickness provides a measure of the spatial size of the biofilm, roughness represents a measure of biofilm heterogeneity, and surface to biovolume ratio tells us how large a portion of the biofilm is exposed to the nutrient flow.

References

1. Li C, Zheng Y, Wang X, et al. J Cell Physiol. 2012;227:2805.
2. Macha IJ, Cazalbou S, Ben-Nissan B, Harvey KL, Milthorpe B. Mar Drugs. 2015;13:666. doi:10.3390/md13010666.
3. Macha IJ, Cazalbou S, Shimmon R, Ben-Nissan B, Milthorpe B. Development and dissolution studies of bisphosphonate (clodronate) containing hydroxyapatite/PLA biocomposites for slow drug delivery. J Tissue Eng Regen Med. 2015. doi: 10.1002/term.2066. [Epub ahead of print].
4. Hench LL. Bioceramics: from concept to clinic. J Am Ceram Soc. 1991;74(7):1487–510.
5. Suchanek W, Yoshimura M. J Mater Res. 1998;13:94. doi:10.1557/JMR.1998.0015.
6. Chai CS, Ben-Nissan B. J Mater Sci Mater Med. 1999;10:465.
7. Choi AH, Ben-Nissan B. Nanomedicine. 2007;2:51. doi:10.2217/17435889.2.1.51.
8. Macha IJ, Ben-Nissan B, Milthorpe B. Curr Nanosci. 2014;10:200.
9. Drumright RE, Gruber PR, Henton DE. Adv Mater. 2000;12:1841. doi:10.1002/1521-4095(200012)12:23<1841::aid-adma1841>3.0.co;2-e.
10. Liu P, Ouyang Y, Xiao R. International forum on biomedical textile materials, proceedings: 298. 2010.
11. Södergård A, Stolt M. Prog Polym Sci. 2002;27:1123. doi:10.1016/s0079-6700(02)00012-6.
12. De Santis P, Kovacs AJ. Biopolymers. 1968;6:299. doi:10.1002/bip.1968.360060305.
13. Gupta AP, Kumar V. Eur Polym J. 2007;43:4053. doi:10.1016/j.eurpolymj.2007.06.045.

14. Lasprilla AJR, Martinez GAR, Lunelli BH, Jardini AL, Filho RM. Biotechnol Adv. 2012;30:321. doi:10.1016/j.biotechadv.2011.06.019.
15. Peltola T, Jokinen M, Veittola S, Simola J, Yli-Urpo A. J Biomed Mater Res. 2001;54:579.
16. LeGeros RZ. Chem Rev. 2008;108:4742. doi:10.1021/cr800427g.
17. LeGeros RZ. Clin Orthop Relat Res. 2002:81.
18. LeGeros RZ. Calcium phosphate materials in restorative dentistry: a review. Adv Dent Res. 1988;2(1):164–80.
19. Best SM, Porter AE, Thian ES, Huang J. J Eur Ceram Soc. 2008;28:1319. http://dx.doi.org/10.1016/j.jeurceramsoc.2007.12.001
20. Ben-Nissan B. Curr Opin Solid State Mater Sci. 2003;7:283.
21. Macha IJ, Ozyegin LS, Chou J, Samur R, Oktar FN, Ben-Nissan B. J Aust Ceram Soc. 2013;49:122.
22. Macha IJ, Ozyegin LS, Oktar FN, Ben-Nissan B. J Aust Ceram Soc. 2015;51
23. Oktar F, Tuyel U, Demirkol N, et al. Artificial organs conference, FYROM, 2010 International Journal of Artificial Organs, (Special Issue). 2010.
24. Green DW, Ben-Nissan B. Biomimetic applications in regenerative medicine: scaffolds, transplantation modules, tissue homing device and stem cells. In: Tochilin V, Amiji M, editors. Handbook of materials for nanomedicine. Singapore: Pan Stanford Publishing Pte Ltd; 2010. p. 821–50.
25. Ben-Nissan B, Milev A, Vago R. Biomaterials. 2004;25:4971. doi:10.1016/j.biomaterials.2004.02.006.
26. Ben-Nissan B. MRS Bull. 2004;29:28.
27. Kuhne JH, Bartl R, Frisch B, Hammer C, Jansson V, Zimmer M. Acta Orthop Scand. 1994:65.
28. Heness G, Ben-Nissan B. Mater Forum. 2004;27:104.
29. Macha IJ, Boonyang U, Cazalbou S, et al. J Aust Ceram Soc. 2015;51:149.
30. Chou J, Valenzuela S, Green DW, et al. Nanomedicine. 2014;9:1131. doi:10.2217/nnm.13.116.
31. Zhu M, Wang H, Liu J, et al. Biomaterials. 2011;32:1986. doi:10.1016/j.biomaterials.2010.11.025.
32. Ginebra M-P, Canal C, Espanol M, Pastorino D, Montufar EB. Adv Drug Deliv Rev. 2012;64:1090. doi:10.1016/j.addr.2012.01.008.
33. Batycky RP, Hanes J, Langer R, Edwards DA. J Pharm Sci. 1997;86:1464. doi:10.1021/js9604117.
34. Pascaud P, Bareille R, Bourget C, Amedee J, Rey C, Sarda S. Biomed Mater. 2012;7:054108. doi:10.1088/1748-6041/7/5/054108.
35. Palacio ML, Bhushan B. Philos Trans Ser A Math Phys Eng Sci. 2012;370:2321. doi:10.1098/rsta.2011.0483.
36. Noh H, Vogler EA. Biomaterials. 2007;28:405. http://dx.doi.org/10.1016/j.biomaterials.2006.09.006
37. Garcia AJ, Keselowsky BG. Critical reviews in eukaryotic. Gene Exp. 2002;12:151.
38. Keselowsky BG, Collard DM, Garcia AJ. J Biomed Mater Res B. 2003;66:247. doi:10.1002/jbm.a.10537.
39. Alvarez-Barreto JF, Landy B, VanGordon S, Place L, DeAngelis PL, Sikavitsas VI. J Tissue Eng Regen Med. 2011;5:464. doi:10.1002/term.338.
40. Arciola CR, Campoccia D, Speziale P, Montanaro L, Costerton JW. Biomaterials. 2012;33:5967. http://dx.doi.org/10.1016/j.biomaterials.2012.05.031
41. Klevens RM, Edwards JR, Richards Jr CL, et al. Public Health Rep (Washington, DC: 1974). 2007;122:160.
42. Tacconelli E, Smith G, Hieke K, Lafuma A, Bastide P. J Hosp Infect. 2009;72:97. http://dx.doi.org/10.1016/j.jhin.2008.12.012
43. Vert M, Doi Y, Hellwich K-H, et al. Pure Appl Chem. 2012;84:34.
44. Stewart PS. Int J Med Microbiol. 2002;292:107. http://dx.doi.org/10.1078/1438-4221-00196
45. Hoiby N, Bjarnsholt T, Givskov M, Molin S, Ciofu O. Int J Antimicrob Agents. 2010;35:322. doi:10.1016/j.ijantimicag.2009.12.011.
46. Marshall BC, Hazl L. Cystic fibrosis patient registry annual data report. Bethesda: Cystic Fibrosis Foundation. 2011.
47. von Eiff C, Jansen B, Kohnen W, Becker K. Drugs. 2005;65:179.
48. Heydorn A, Nielsen AT, Hentzer M, et al. Microbiology. 2000;146(Pt 10):2395.

Chapter 14
Biomaterials for Cell Encapsulation: Progress Toward Clinical Applications

Gurbinder Kaur, Francesco Baino, John C. Mauro, Vishal Kumar, Gary Pickrell, Nammalwar Sriranganathan, and Steven Grant Waldrop

Abstract Cell microencapsulation is a technique to treat a wide range of diseases through the continuous and controlled delivery of therapeutic products. This technique can also treat multiple diseases in the absence of immunosuppression. Over the past few years, the quality of life of patients has improved remarkably as a direct result of microencapsulation technology, as this technology eliminates the requirement of an immunosuppressant. However, much additional research needs to be conducted in order to commercialize and clinically apply more widely this life-saving technology.

Keywords Encapsulation • Alginates • Chitosan • Microcapsules • Microcarriers • Immobilization • Polymer matrices

G. Kaur (✉)
School of Physics and Materials Science, Thapar University, Patiala, India
e-mail: gkapds@gmail.com

F. Baino
Institute of Materials Physics and Engineering, Applied Science and Technology Department (DISAT), Politecnico di Torino, Corso Duca degli Abruzzi 24, 10129 Torino, Italy

J.C. Mauro
Science and Technology Division, Corning Incorporated, Corning, NY 14831, USA

V. Kumar
Sri Guru Granth Sahib World University, FatehGarh Sahib, Punjab, India

G. Pickrell
Department of Material Science and Engineering, Holden Hall, Virginia Polytechnic Institute and State University, Blacksburg, VA 24060, USA

N. Sriranganathan • S.G. Waldrop
Department of Biomedical Sciences and Pathobiology, Virginia Polytechnic Institute and State University, Blacksburg, VA 24060, USA

G. Kaur (ed.), *Clinical Applications of Biomaterials*,
DOI 10.1007/978-3-319-56059-5_14

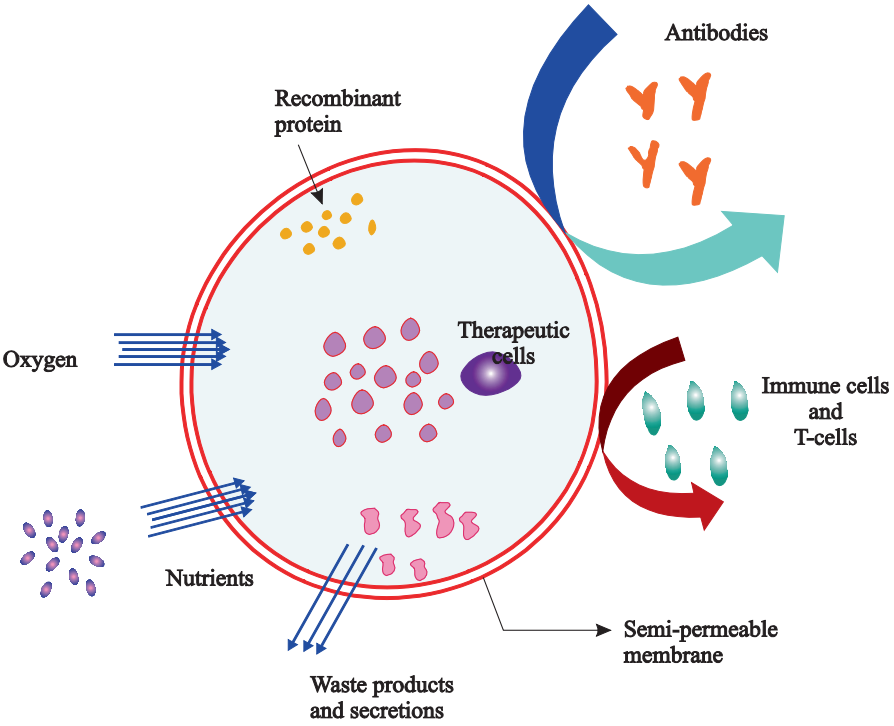

Fig. 14.1 Cell microencapsulation technology

14.1 What Is Microencapsulation?

With cell microencapsulation technology, a biologically active material within a polymeric matrix is surrounded by a semipermeable membrane designed in a way to circumvent any immune rejection [1–4]. This technology involves immobilization of cells within the semipermeable membrane. The purpose of the membrane is to protect the inner cells from the host immune system and from mechanical stress. Hence, the membrane facilitates the bidirectional diffusion of oxygen nutrients and waste products but restricts the access of external antibodies and immune cells, thereby preventing damage/destruction of the enclosed cells. Microencapsulation technology is beneficial from the host-patient cell response point of view, since this technology circumvents the need for immunosuppressants, which is an important issue to be considered with any organ transplant. This results in a reduction of side effects, and hence normal bodily functions are not compromised. Figure 14.1 gives the schematic of cell microencapsulation indicating the bidirectional flow of nutrients and other elements.

Cell microencapsulation allows various advantages over other medical techniques for transplantation [2–8]:

- The cells encapsulated are viable and release the therapeutic products continuously, allowing a prolonged duration of the treatment
- If the capsule sizes are smaller (100–500 μm), then they are in close contact with blood, and increased oxygen transfer causes long-term cell functionality.
- The implantation of nonhuman cells could be possible due to microencapsulation technology. Hence, due to the limited availability of donor time, promising results for nonhuman cell implantation can be obtained.
- Microcapsules possess high surface-to-volume ratio, which improves the bidirectional diffusion of oxygen and nutrients.
- The physical barrier provided by the encapsulation protects the premature degradation and metabolism of drugs.
- Microencapsulation minimizes systemic exposure and promotes tight control over the device.
- Primary/stem cells can be modified to express any desired protein in vivo without host genome modification.

Microencapsulation technology traces its origins back to 1933, when Bisceglie enclosed tumor cells in a polymer membrane that was then transplanted into a pig's abdominal cavity [9]. The results indicated no destruction of these cells by the immune system. The microencapsulation was put into practice in small animal models, immobilizing xenograft islet cells to aid the diabetes control. As a result of these promising results, microencapsulation technology has been applied for a wide variety of applications including hemophilia, renal failure, neurological/sensory disorders, diabetes, etc. Thus far, emphasis has been given primarily to the polymer science, polyelectrolyte selection, biocompatibility, characterization, toxicology, and cost issues for the microcapsule fabrication.

14.2 Microcapsules and Microcarriers

The microfabricated biomaterials such as microcapsules and microcarriers offer many advantages, including [10–15]:

- Multiple adhesive or morphogenic signals can be provided simultaneously from a micro-fabricated substrate.
- Recapitulation of the features of individual living cells existing in micro-nano-dimensions
- Separate analysis of multiple parameters governing cell-biomaterial interactions.

Microcapsules aim to isolate a mass of cells physically from the surrounding environment and confine them within a semipermeable polymeric membrane without using immunosuppressive agents. The immunosuppressive drugs can have

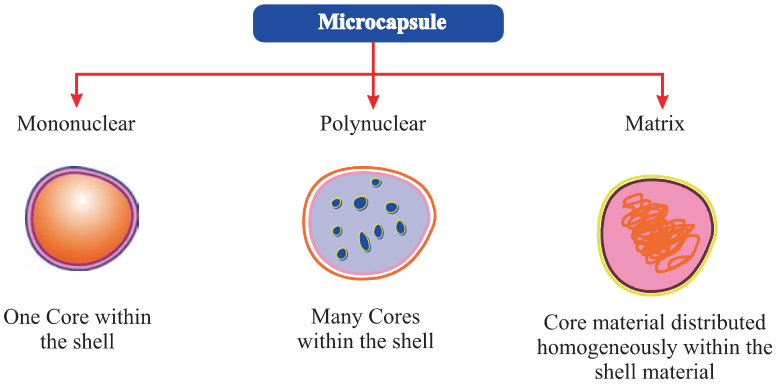

Fig. 14.2 Types of microcapsule

severe side effects and may lead to undesired complications such as failure of tumor surveillance and other infections. The membrane barrier of microcapsules acts as an artificial immunoprivileged site, shielding the therapeutic cells from host immune cells, thereby preventing graft destruction. The capsule environment supports cellular metabolism, proliferation, differentiation, and morphogenesis. The microcapsule can be classified into three different types as indicated in Fig. 14.2.

The core/shell configuration of the microcapsules can likewise be classified into three different types: matrix-core/shell, liquid-core/shell, and cells-core/shell microcapsule (Fig. 14.3) [16–21].

Many refinements of the structures listed in Fig. 14.3 have been attempted to yield a microcapsule with optimized performance.

The mechanical stability of the microcapsule must be taken into account to prevent its breakage due to osmotic and physical stress. The membrane wall thickness should be uniform to optimize the diffusion of molecules. The encapsulation technique should be sufficiently gentle to preserve the cell size and integrity. The method must also reproducibly ensure cell integrity and viability during implantation. The microcapsules prepared by the polyelectrolyte complexation of alginate with polycation poly(L-lysine) (PLL) has been extensively used for 3-D cell cultures, gene/cell therapy, and bioengineering [19, 22–29]. Biocompatible microcapsules with high mechanical stability and controlled size (approximately 30–60 μm) have been produced by cell immobilization technologies [10]. A spraying technique has been used to encapsulate stem cells and monocytes [30].

For the pancreatectomized canine allotransplantation experiments, five component/three membrane hybrid capsules are produced of sodium alginates, cellulose sulfate, poly(L-lysine (PLL), $CaCl_2$, and polymethylene-co-guanidine (PMCG) components, which yielded high immunoprotection without comprising the therapeutic product efflux and nutrients/oxygen influx [10, 23–27]. The conformal coating directly forms a barrier on cell mass and thus eliminates unused space in the microcapsule, thereby increasing the mass transport between cell mass and capsule exterior. Other approaches, where microcapsules are employed as microcarriers,

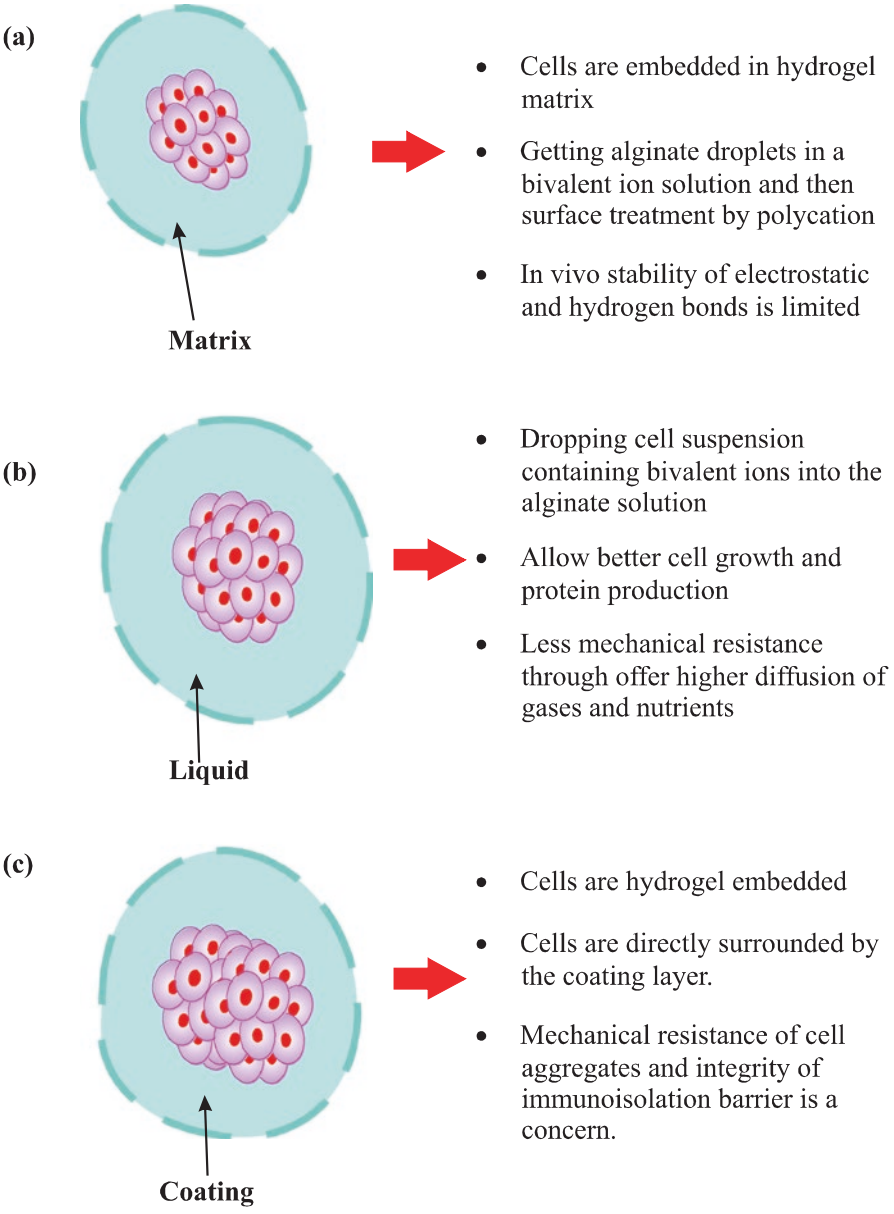

Fig. 14.3 Core/shell configuration of microcapsules: (**a**) matrix-core/shell, (**b**) liquid-core/shell, and (**c**) cells-core/shell microcapsules

have also been used (Fig. 14.4). The cells are absorbed on the biomaterial surface, which acts as a support matrix for the growth of adherent cells.

Many commercially available microcarriers are collagen-based (CULTISPHER; PERCELL), dextran-based (CYTODEX, GE HEALTHCARE), or polystyrene-based

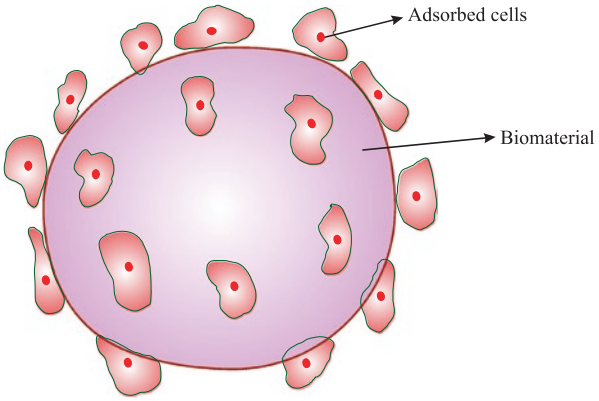

Fig. 14.4 Microcarriers for bone tissue engineering

(SOLOHILL ENGINEERING) gelatin microcarriers [31–34]. The critical points that should be considered while designing the microcarriers/microcapsule are listed in Fig. 14.5.

14.3 Cell Immobilization

Through cell immobilization, the cells can be kept in a distinct support/matrix, which allows exchange of the medium. Natural polymers, like alginate, chitosan, collagen, gelatin, cellulose, and starch, are commonly used as matrices for the cell immobilization. Synthetic polymers with porous surfaces that can trap and hold cells like polyethylene glycol (PEG) and polyvinyl chloride (PVC) are also used for the immobilization [33–35]. Glass, silica, ceramics, zeolites, and charcoal are the inorganic support matrices. The immobilization can be attained by encapsulation, copolymerization, entrapment, and adsorption as shown in Fig. 14.6.

For the adsorption process, low energy bonds such as van der Waals forces, hydrogen bonds, and ionic interactions are involved. The particle size for adsorption immobilization should be between 500 Å and 1 mm in diameter. The covalent bonding involves covalent bonds between the cell and the support. The common supports are proteins, cellulose, agarose, amino benzyl cellulose, porous glass, and silica. For the entrapment process, agar, gelatin, alginate, cellulose triacetate, and polyacrylamide are used as matrices to physically entrap the cells (the matrix shall be water soluble). For the copolymerization, the cross-linking between a group of cells via polyfunctional reagents occurs, and hence no matrix is required. The commonly used polyfunctional reagents are diazonium salt and glutaraldehyde. One widely investigated method involves enclosing the cells inside a semipermeable membrane through which exchange of nutrients and wastes occurs. Before the cell immobilization process, various factors should be considered, e.g., the cells shall not proliferate

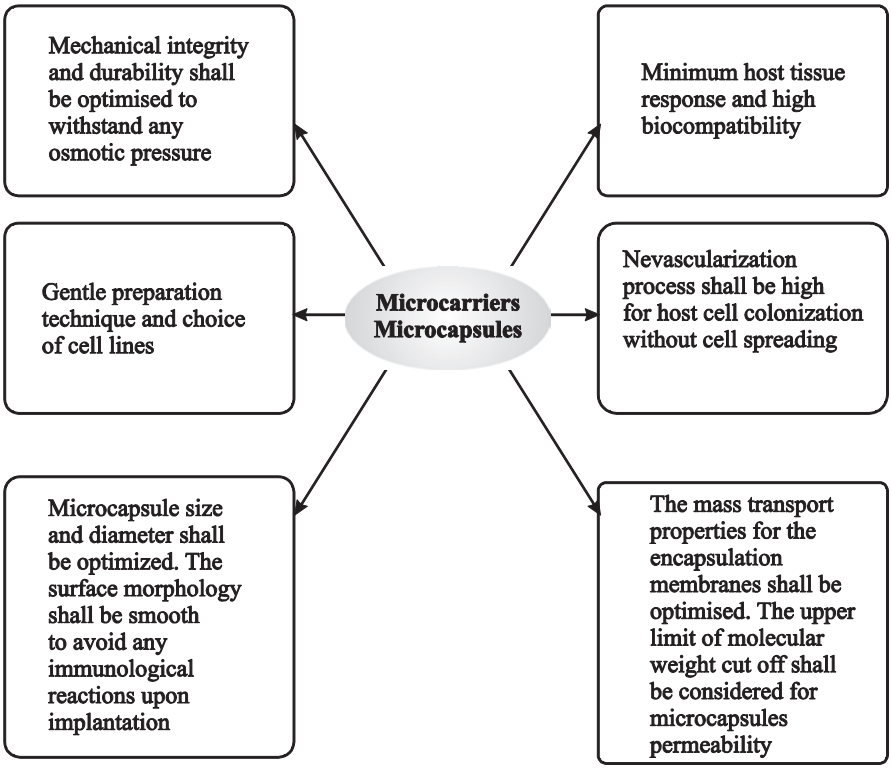

Fig. 14.5 Requirements for microcarriers/microcapsules

following encapsulation in order to maintain the efficiency and potential to deliver therapeutic agents for prolonged durations. Different cell sources along with the preferred encapsulating materials and their applications are given in Table 14.1. The cell sources should also be considered, for instance, whether they are allogeneic cells (cells obtained from other human beings), autologous cells (cells obtained from the patient's own body), and xenogeneic cells (cells obtained from another species such as pigs/primates). The xenogeneic cells can pose the risk of transmitting animal viruses, whereas autologous cells have limited availability.

Before the use of cell lines, they must be thoroughly checked and tested for viruses and tumorigenicity

14.4 Polymer Matrices for Encapsulation

Two geometries have been implied for the cell encapsulation, i.e., microcapsules and macrocapsules [10, 34–36]. Macrocapsules have higher surface-to-volume ratio, and more nutrients are required for the adequate diffusion of the nutrients.

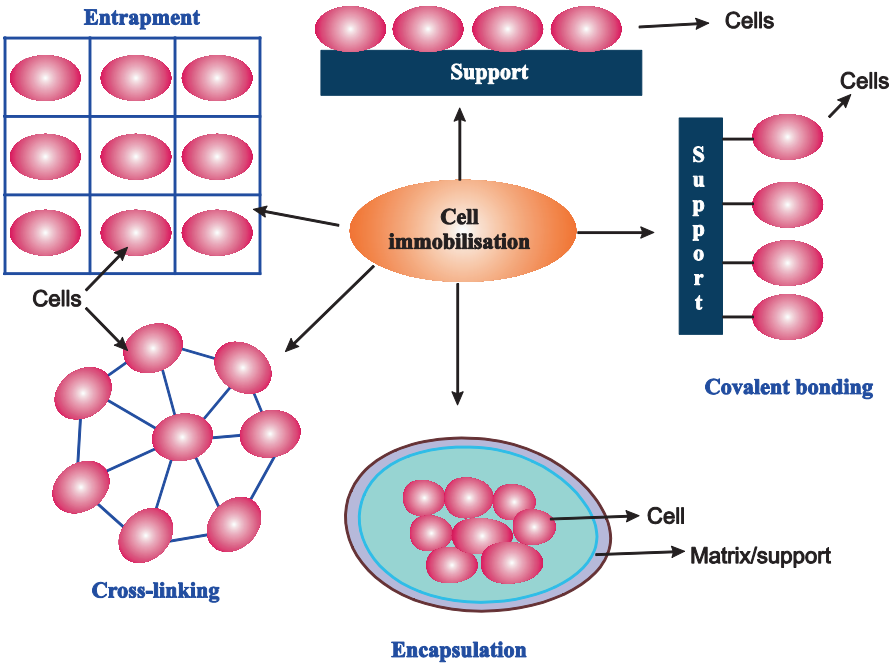

Fig. 14.6 Different cell immobilization techniques

Table 14.1 Cell sources for the cell immobilization [10, 17, 18, 30, 33–40]

Encapsulating material	Cell and applications
Alginate	Parathyroid cells ↔ artificial organs
	Chondrocytes ↔ bone and cartilage regeneration
	Bacteria ↔ urea elimination
	Kidney cells ↔ neurotrophic factors, hemophilia, and anti-angiogenesis
	Leydig cells ↔ hormone replacement
	Stem cells ↔ bone regeneration
	Myeloma cells ↔ hepatic growth factor
Alginate/chitosan	Tumor cells ↔ cancer, interleukins
Cellulose sulfate	Virus cells ↔ cancer
Alginate/agarose/acetate	Hybridoma cells ↔ antibody production
Alginate/HEMA-MMA	PC12 pheochromocytoma cells ↔ neurotransmitter
	Hepatocytes ↔ liver transplantation
	Ovary cells ↔ Fabry disease
	Fibroblasts ↔ epilepsy, metabolic deficiency
	Myoblasts ↔ cancer, neurotrophic factors
	Pancreatic islets ↔ diabetes

Macrocapsules can be intravascular or extravascular, and the intravascular devices offer advantage of being in close proximity to the blood, promoting the rapid exchange of therapeutic molecules and nutrients. Such macrocapsules have been researched extensively.

Many polymers have been introduced for encapsulation due to their biocompatibility, i.e., the material can reside inside the host body for prolonged durations with minimal inflammatory response. The polymer material should not interfere with the viability of the cells in the capsule. In addition to this, the polymers should not induce any host responses that interfere with the functionality of the encapsulated cells. The following section deals with the synthetic and natural polymers used for the encapsulation process.

14.4.1 Synthetic Polymers for Encapsulation

Synthetic polymers offer several advantages over natural polymers, as they can be easily tailored and can possess improved biocompatibility. For the encapsulation of pancreatic islets, kidney cells, and hepatocytes, the polymer encapsulation process may be associated with toxicity. Many polymers have been used for the encapsulation of cells like mesenchymal stem cells, osteoblasts, chondrocytes, and pancreatic islets. Poly(vinyl alcohol) (PVA), a thermoplastic polymer, has been used for the encapsulation of genetically engineered cells secreting neurotrophic factors and neurotransmitters for the treatment of Alzheimer's disease, Parkinson's disease, and Huntington's disease [41–47]. Polyacrylonitrile and poly(vinyl chloride) are the most commonly applied copolymers with PVA. Its most prominent application is the encapsulation of islets of Langerhans since 1977. PVA has low hydrophilicity, which makes it less susceptible to the cell adhesion in vivo. The cell adhesion can be increased by making PVA alginate-chitosan composites, which tend to overcome stability issues of homopolymers [34, 41–44]. Alginate and chitosan are natural polysaccharides used as supportive structural matrix for the PVA. To increase the biotolerability of the polymer, its surface is coated by polysaccharides or polyethylene glycol (PEG). After long-term application, the permeability of polyacrylonitrile and poly(vinyl chloride) (PAN-PVC) decreases interference with the cell survival. To improve the response of PAN-PVC, poly(ethylene oxide) (PEO) has been grafted on its surface, which increased the protein adsorption and also resulted in strong fibrotic responses against the grafts. PEG has been used for macro- and microencapsulation because it involves soft solvents.

The photopolymerization of PEG diacrylate prepolymers results in cell encapsulation. When PEG macromers terminating with acrylate or methacrylate groups are exposed to ultraviolet light, these groups undergo rapid cross-linking [48–62]. It has been reported that these capsules provide immunoprotection, but the pore size is so small that it hinders the nutrition intake [51–55]. PEG hydrogels are superior due to their short diffusion time scale and high water content. The protein adsorption on PEG surfaces is also small, attributed to the elastic restoring force and osmotic pressure

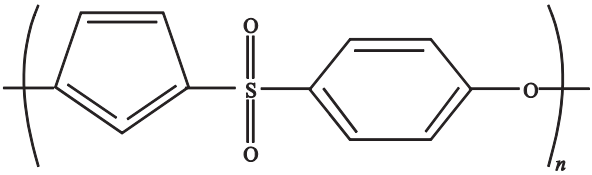

Fig. 14.7 Polymerization of dichlorophenyl sulfone with dihydroxydiphenyl sulfone yields poly(ether-sulfone) (PES)

generated by the PEG chains, which are noncompatible with the protein nucleus. However, the PEG networks can carry cytotoxic molecules into the capsules.

Polypropylene, a thermoplastic polymer, has been used for the macroencapsulation of human parathyroid cells, hepatocytes, OKT3 cells for secreting monoclonal antibodies, and WEHI-3B mouse cell lines [63–65]. Strong host responses against polypropylene have been observed, and hence there is a need to coat its surface with hydrophilic agents to increase the biocompatibility. Polyurethane (PU) and elastomer polymers have been used for the encapsulation of pancreatic islets and pituitary tissues. PU membranes are thinner than the PAN-PVC walls, which enhances the nutrient and oxygen transport [66, 67]. The drawback of using PU films is their biodegradability, leading to complete collapse and degradation of grafts causing its failure. The hydrophobic nature of PU can trigger the host response, and hence the PU membrane surface can be treated with hydrophilic reagents to decrease the surface energy. Poly(ether-sulfone) (Fig. 14.7), a thermoplastic polymer, is used in the form of hollow fibers for cell macroencapsulation applications [68, 69].

For the functional survival, the cells can be mixed with collagen/alginate before injecting them in PES hollow fibers. For vascular tissue formation, the open rough porous surface of polysulfone capillary yields suitable surface area. However, the center of PES microcapsule has limited nutrient and oxygen supply. To increase the biocompatibility of PES, its surface should be coated with silane or polyvinylpyrrolidone (PVP) [34].

Polyacrylates are also applied for the cell encapsulation, and the most commonly used acrylates are hydroxyethyl methylacrylate-methyl methacrylate (HEMA-MMA) and poly(hydroxyl ethyl methacrylate (PHEMA) [70–77]. Polyacrylates have been used for the microencapsulation of fibroblasts, human hepatoma cells, pancreatic islets, and PO12 cells. Polyacrylate capsules possess low membrane permeability for the nutrients. HEMA-based capsules do not possess enough adherence of cells within the intracapsular core, hence affecting the cell proliferation. To enhance the adhesion, the co-encapsulation of agarose/chitosan matrices has been done in the capsule core. PHEMA have low mechanical strength though it does not suffer from protein adsorption. The HEMA-MMA encapsulation has yielded promising results in vitro, but in vivo some important issues still persist: for example, fibrinogen and fibronectin deposits could be observed on the HEMA-MMA capsule surface.

Another sodium salt of polystyrene sulfonic acid, i.e., sodium polystyrene sulfate (PSS), has been used for the encapsulation of red blood cells (RBC) and pancreatic islets [78–81]. PSS is applied according to a layer-by-layer technique in combination with poly(diallyl-dimethyl ammonium chloride) (PDADMAC) and polyallylamine hydrochloride (PAH) (Fig. 14.8).

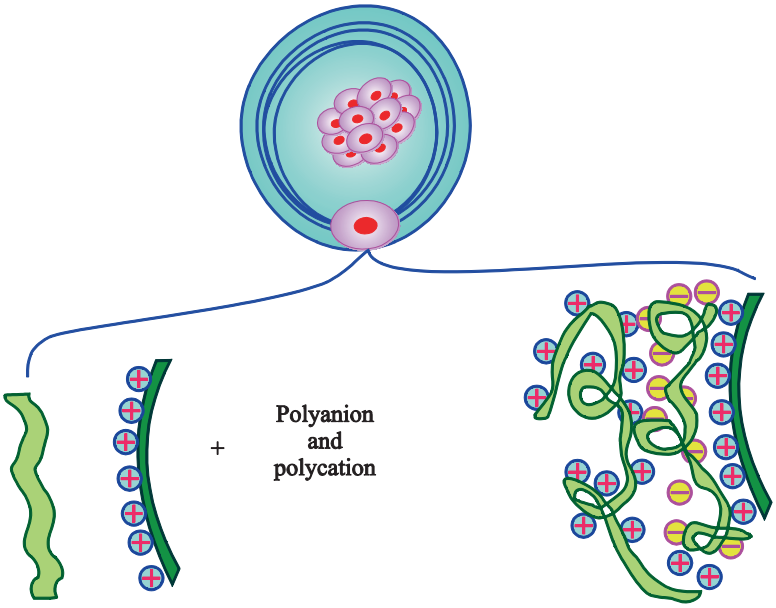

Fig. 14.8 Layer-by-layer technique for the capsule formation

Opposite charged polymers are adsorbed onto a charged surface, and immunoprotective and biocompatible layers are formed. Biocompatibility and mechanical strength are the primary issues to be addressed, but unwanted complement-activating effect is provoked by the sodium polystyrene surfaces.

14.4.2 Natural Polymers for Encapsulation

Polysaccharides are the most widely used materials for cell encapsulation due to their ability to form hydrogels and elicit minor host responses. Due to their potential viability, they have been regarded as the ideal candidates for the encapsulation. Table 14.2 lists some common materials used for cell encapsulation.

14.4.2.1 Alginates for Cell Encapsulation

Among natural polymers, alginates are the most promising candidates for cell microcapsule fabrication. Alginates are anionic polysaccharide composed of β-D-mannuronic (M blocks) and α-L-guluronic (G blocks) cross-linked with the regions of mixed sequences (MG blocks) [35, 48]. M-and-G block ratio is dependent on the sources of algae extraction. Alginates are also extracted from the *Azotobacter vinelandii* bacteria and several *Pseudomonas* species. In order to obtain pliable gels,

Table 14.2 Overview of polymeric materials used for cell encapsulation [42–81]

Material	Cell
HEMA-MMA	Pancreatic islets, human hepatoma cells and fibroblasts
Polydiallyl-dimethyl ammonium chloride (PDADMAC)	Red blood cells and pancreatic islets
Polyvinyl alcohol (PVA)	Islets of Langerhans, treatment of Parkinson's disease, Alzheimer's disease, and Huntington's disease
Polypropylene (PP)	Human parathyroid cells, hepatocytes, and OKT3 cells for secreting monoclonal antibodies
Collagen	Myoblasts
Polyethylene glycol (PEG)	Primary hepatocytes murine embryonic liver cells and condylar chondrocytes
Dextran	Human embryonic stem cells
Chitosan	Human periodontal ligament chondrocytes and fibroblasts
Agarose	Feline kidney cells and murine embryonic stem cells
Hyaluronic acid	Auricular chondrocytes
Polylactic glycolic acid	Bone marrow stromal cells

alginates with high mannuronic acid content are desired, whereas the guluronic acid content should be higher for getting more rigid structures. Alginate extraction and its contamination is the major concern, because raw alginates usually contain impurities like polyphenols, proteins, and endotoxins. Currently, many techniques are utilized to purify the alginates, though residual proteins are always present, which are optimum for the microcapsule biocompatibility. From the immunoprotection point of view, the alginate gels are too porous, and hence the cationic polymers of synthetic origin are used to coat alginate gels. Agarose, chitosan, PEG, cellulose sulfate, and glutaraldehyde have also been used to coat alginate gels in addition to the synthetic polymers like poly(L-ornithine) and poly(L-lysine). The coating layer shall be optimized to sustain the prolonged diffusion kinetics of therapeutic agents and nutrients. For instance, the poly(L-lysine) membrane should be ≤ 4 μm for encapsulation of the pancreatic islets, as the layer thickness directly influences the response toward glucose load. Other factors like pore size and mechanical strength shall also be optimized in addition to the coating thickness. PEG and charged derivatives of PEG such as polyoxyethylene bis(amine) and methoxypolyoxyethylene amine are also used to coat the alginates. The PEG derivatives contain amine groups, which interact with the negatively charged alginate on the microcapsule surface.

The encapsulation device protects the enclosed cellular tissue from the host's immune response, and hence the biocompatibility and biotolerability shall be very high [82–88]. Alginate composition also regulates properties like stability, permeability, and biocompatibility. High G block content in alginates is found to cause severe cell overgrowth, whereas high M alginates cause inflammatory response by stimulating monocytes to produce cytokines such as tumor necrosis factor (TNF), interleukin-1 (IL-1), and interleukin-6 (IL-6). High M-alginate transplantation produces M-alginate antibodies, whereas no such antibodies could be observed

Table 14.3 Alginate matrices for cell encapsulation [30, 36, 39–41, 82–89]

Material	Cell implantation site	Application
Alginate	Monocytes, mesenchymal stem cells, islets of Langerhans, neurine-derived adipose tissue stromal cells (peritoneal cavity, kidney capsule, muscle)	Bone regeneration, diabetes, muscle regeneration
Alginate	In vitro studies for Crandall-Reese Feline kidney cells	Increase in stability
Alginate	In vitro study of the bone-derived cells	Immobilization of substrate with cells
Alginate-chitosan	Chondrocytes, baby hamster kidney cells (subcutaneous space), and human osteoblast cells	Increased mechanical properties
Alginate-Agarose	Feline kidney cells in vitro studies	Subsieve size capsules
Alginate-PLL-alginate	Embryonic stem cells (peritoneal cavity), islets of Langerhans, myoblasts, EL-4, thymoma, chromaffin cells (subarachnoid space, subcutaneous space)	Chronic neuropathic pain, anemia, bone repair, and regeneration
Alginate-PLO-alginate	Islets of Langerhans and choroid plexus (brain, peritoneal cavity)	Neuroprotection and diabetes

when G-alginates were transplanted. It has also been reported that the majority of high G-alginate capsules are adherent to the abdominal cavity along with the inflammatory response, whereas the intermediate G-alginate capsules float freely in the peritoneal cavity. Table 14.3 lists common alginate matrices for cell encapsulation applications.

Alginate gels can be stabilized by the application of covalent cross-linking molecules by introducing aldehyde, hydroxyl, or phenol moieties. Alginate capsules are also prepared by the sol-gel techniques, where extrusion of an alginate solution containing therapeutic cells in a cross-linking solution consisting of divalent ions like Ba^{2+}, Sr^{2+}, and Ca^{2+} is performed. The affinity of alginates for divalent ions varies in order of $Mn^{2+} < Co^{2+}/Zn^{2+}/Ni^{2+} < Ca^{2+} < Sr^{2+} < Ba^{2+} < Cu^{2+} < Pb^{2+}$ [88]. Alginate gels can be modified by different peptides/proteins along with the polymer tailoring and extracellular matrix (ECM) sequence. By tailoring the polymers, the cell proliferation and differentiation can be controlled. Arginine-glycine-aspartic acid (RGD) is the most commonly employed fibronectin-derived peptide, which is present in ECM. The in vivo long-term functionality of the encapsulated myoblast cells can be promoted by biomimetic cell-hydrogel capsules.

14.4.2.2 Chitosan for Cell Encapsulation

Chitosan is found in crustacean shells, mollusks, insects, and fungi. Chitosan degrades via enzymatic hydrolysis and has hydrophilic nature. Chitosan does not exhibit fibrous encapsulation upon implantation nor does it induce inflammatory

response inside the human body. Chitosan has been used for drug delivery applications, wound dressings, dermal substitutions, and implants. Chitosan has been used for microencapsulation applications as a polymer matrix for the encapsulation of fibroblasts, cardiomyocytes, hepatocytes, R208F cells, human bone marrow stromal cells, and PC12 cells [90–97]. Chitosan has a strong affinity for polyanions and contains reactive hydroxyl and amino acid groups. The high solubility of N-acetylated chitosan in water and aqueous solutions also makes it an interesting candidate for various biological applications. If the concentration of N-acetylated chitosan is increased, then a decrease in permeability and increase in mechanical strength is observed. Chitosan-alginate matrices have been used for the pancreatic islets in streptozotocin (STZ)-induced diabetic mice. However, the applications of chitosan are limited due to their low mechanical strength, and hence they are usually combined with other materials like agarose/cellulose and gelatin to form a polymer matrix with enhanced properties.

14.4.2.3 Cellulose for Cell Encapsulation

Cellulose is one of the most abundant polysaccharides present in nature without any branching or substitutional group. Cellulose is the predominant structural component of the primary cell wall of oomycetes, algae, and green plants. Cellulose is enzymatically degradable, but its degradation is limited in humans and animals due to the absence of the hydrolase enzyme. The formula of cellulose is $(C_6H_{10}O_5)n$ and consists of β(1–4) linked D-glucose monomer units. Though cellulose is insoluble in water and organic solvents, its derivatives like carboxymethyl cellulose (CMC) and sodium cellulose sulfate (NaCS) are water soluble. CMC contains carboxymethyl groups attached to some hydroxyl groups of glucose backbone. NaCS is the ester derivative of cellulose and can be obtained when cellulose reacts with sulfuric acid or sulfur-containing reagents. Cellulose sulfate-poly(diallyldimethylammonium chloride) capsules have been used to deliver monoclonal antibodies into the bloodstream of mice. Poly(diallyldimethylammonium chloride) is a polycation, whereas cellulose sulfate is a polyanion, and their microcapsules are mechanically stronger when produced via interfacial polyelectrolyte complexation.

Cellulose has been used for encapsulating hybridoma cells, embryonic kidney cells, insulin-producing cell lines, and cytotoxic epithelial cells [35, 98–100]. The chondrocytes have been encapsulated by thermosensitive CMC/Chitosan hydrogels. The high-viscosity CMC/chondroitin sulfate chitosan has mechanical strength and permeability properties similar to those of the alginate-poly(L-lysine) capsules. For the encapsulation of feline kidney cells, CMC with phenol groups has been applied to produce microcapsules in the range of 60–220 μm. Inflammatory response against cellular tissues has also been reported such as fibrous capsulation reaction after 15 days of implantation in mice. Before commercialization of cellulose-based microcapsules, issues like cytocompatibility and the response of host tissue must be resolved.

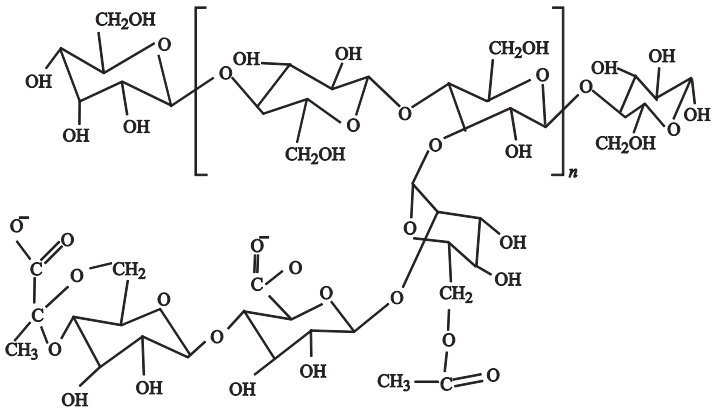

Fig. 14.9 Structure of xanthan consisting of glucose units, mannose, and glucuronic acid units

14.4.2.4 Other Polymers for Cell Encapsulations

Collagen, agarose, and xanthan are among other polymers used for the cell microencapsulation [101–108]. Collagen is found in abundance in mammalian connective tissues, especially in skin and musculoskeletal tissues.

Types I, II, III, and IV are the most common human collagen proteins among 29 types of collagen found inside the human body. Due to abundance in nature and high biocompatibility/biodegradability, collagen has been extensively used in cell immobilization. Collagen can be easily processed in the form of films, sponges, and injectable cell immobilization carriers. Collagen has found applications in macroporous scaffolds, cell encapsulation, and cellular distribution control for immunoisolated devices. Over 90% of collagen is type I, and it is commonly used for the cell encapsulation because it does not initiate strong host response or allergic reactions. Collagen has been used for encapsulating fibroblasts, hepatocytes, and stem cells.

The durability of collagen capsules can be increased by producing an inner core of collagen with an outer shell of tetrapolymer of 2-hydroxy-ethyl methylacrylate (HEMA), methyl methacrylates (MMA), and methacrylic acid (MAA). Collagen cross-linking with glutaraldehyde has also been performed to improve the mechanical properties and stability of the capsules. However, the inflammatory response and limited biotolerability of glutaraldehyde makes it non-applicable for long-term biomedical goals.

Xanthan, a natural polysaccharide obtained from the bacterial coating of xanthomonas campestris, has been used for encapsulating chondrocytes. The structure of xanthan consists of (1→4)-β-D-glucose units with end chains of β-D-glucuronic acid, β-D-mannose and side chains of D-(1→4), and β-D-(1→2) linkages as shown in Fig. 14.9.

Xanthan has shown stable characteristics for change in pH, media, and temperature, which is highly desirable as biomaterials should have tendency to withstand the

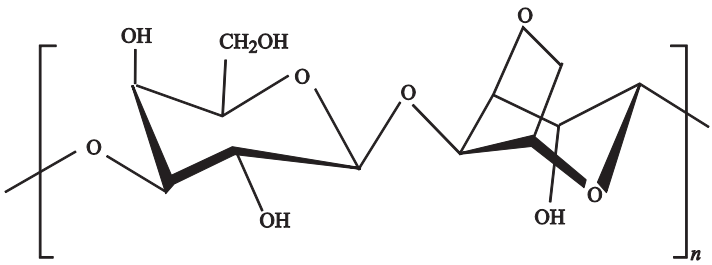

Fig. 14.10 Structure of agarose polysaccharides

temperature and media changes. Another agar-derived polysaccharide, agarose, which is similar to alginates, has been used for the cell encapsulation. Agarose consists of 3,6-anhydro-L-galacto-pyranosyl and β-D-galactopyranosyl, which are coupled through 1→3 binding as depicted in Fig. 14.10. Agarose has been used for the encapsulation of insulinoma cells, kidney cells, hybridoma cells, and fibroblasts.

By varying the agarose concentration to form the gels, the immunoprotective properties can be tailored, and the addition of only 5% agarose yields immunoprotective capsules. Agarose-encapsulated PCl2 cells delivered dopamine for almost 5 weeks after transplantation without immune rejection. When agarose microcapsules are coated with polyacrylamide, they show impermeability for antibodies but triggered host responses that interfered with the functional survival of islets. Upon coating agarose surface with carboxymethyl cellulose, the biotolerability of the capsules is enhanced. Superior functionality of rat pancreatic islets was observed for collagen-agarose microbeads compared to the agarose alone. With agarose, toxicity remains an issue, as it cannot provide 100% impermeability to the entry of deleterious molecules and can also have unavoidable impurities. Hence, finding a pure source of agarose remains an open challenge. The microcapsules composed of 5% agarose/5% polystyrene sulfonic acid freely float in the peritoneal cavity, but the one with 10% polystyrene sulfonic acid (PSS) are surrounded by adipose tissue indicating the host tissue response against agarose/PSS implantation.

14.5 Cell Encapsulation Technology in Therapeutic Applications

Cell encapsulation technology has been widely investigated for cancer treatment, gene disorders, and the development of artificial organs (Table 14.4).

The treatment of Mendelian disorders such as hemophilia, dwarfism, etc., is now possible with the encapsulation technology. Kidney failure, diabetes, and cancer have been some of the most widespread diseases across the globe. Cell encapsulation has opened new avenues for the treatment of such pathologies, which were known to be incurable from decades.

Table 14.4 Applications of cell encapsulation technology [109–113]

Disorder	Microencapsulation application
Anemia	C_2G_2 myoblasts enclosed in PES hollow fibers (C_2G_2 secrete erythropoietin)
Dwarfism	C_2G_2 myoblasts in alginate-poly-L-lysine-alginate (APA) microcapsules
Diabetes	Islet immobilization especially in alginate microcapsules
Hemophilia	C_2G_2 myoblasts in APA microcapsule
Hypoparathyroidism	Parathyroid tissue in barium chloride hardened alginate capsules
Adenosine deaminase (ADA) deficiency	ADA expressing fibroblasts encapsulated in APA capsules
Kidney failure	E. coli strain transfected with gene encoding Klebsiella aerogenes urease

14.5.1 Cell Encapsulation in Treating Diabetes

Diabetes mellitus results from defects in insulin secretion and is characterized by hyperglycemia [35, 114–120]. For insulin-dependent diabetes mellitus patients, the transplantation of islets of Langerhans has been studied as an effective method. The "Edmonton protocols" based on the use of human islets from cadaveric donors has been a breakthrough for the patients suffering from type I diabetes (TID). Nevertheless, the need for lifelong immunosuppression and limited availability of human tissues pose barriers for the use of this technology for the treatment of patients suffering from TID. TID epipathogenesis involves autoimmune β-cell selective killing by autoreactive CD4 clones via a complex chain of proapoptotic and pro-inflammatory molecules. The use of insulin is virtually the only treatment for diabetes TID patients. However, insulin therapy has disadvantages like blood glucose level brittleness and the inability to mimic the stimulus-coupled insulin secretory kinetics of β cells under physiological environment. Cell encapsulation technology has been the focus of research groups for the transplantation of pancreatic islets in TID patients. Clinical islet transplantation (TX) has been pursued in lieu of whole pancreatic graft to avoid the high morbidity associated with such a large surgery. Lim and coworkers [19] devoted their research toward the implantation of microencapsulated xenograft islet cells into rats and found positive outcomes for the diabetes treatment. Agarose, chitosan, sodium cellulose sulfate, alginate, PEG, and acrylates have been among the prominent polymers used for the islet encapsulation. The safety and outcomes of alginate-encapsulated porcine islets in a nonhuman primate model (monkeys) of streptozotocin-induced diabetes yielded reduced insulin requirement for the islet transplanted monkeys, while the disease worsened for the control animals.

Tuch and coworkers [121] transplanted human islets encapsulated in barium alginate microcapsules intraperitoneally without immunosuppression inside four TID

patients (no detectable C-peptide). C-peptide was detected 1 day after implantation, although it became undetectable 1–4 weeks post-implantation. The insulin and blood glucose requirement decreased, and no significant alteration is glycemic control was observed. After 16 months of implantation, the laparoscopy and biopsy were performed on the four patients. The capsules were found scattered throughout the peritoneal cavity and also attached to spleen, kidney, and parietal peritoneum. Biopsy also revealed that the capsules were surrounded by fibrous tissue with thin-walled capillaries along with the histiocytic response. Ischemic necrosis/inflammation initiated by the fibrinogen enclosing capsule surface could possibly have caused graft failure.

The clinical potential of PEGylation/immunosuppressant with low doses of cyclosporine A was studied in a rodent model, and normal blood glucose responsiveness and hormone synthesis could be obtained 1 year after implantation [38]. Phase I/II clinical trials by Novocell for the encapsulated human islet allograft implanted into subcutaneous site follow this procedure. A research group at the University of Perugia has studied the long-term stability of encapsulated human islet xenogeneic transplantation. The three main objectives of this research work were to study xenogeneic islet transplantation (T_x)-related adverse reaction, host sensitization toward grafted encapsulated islet cell antigens, and T_x-directed immune reactivity. The grafting was done intraperitoneally under ultrasound guidance/anesthesia, and no inflammation, immune sensitization, or adverse reactions could be seen. The morphologically intact functional islets upon static incubation with glucose were considered as donor islets and underwent microencapsulation prior to the xenogeneic islet transplantation (Fig. 14.11a, b).

Decline of exogenous daily insulin was observed for all the patients along with detection of C-peptide level. No anti-MHC class I–II, islet cell antibodies, or anti-GAD65 antibodies could be detected after a 5-year implantation for the patients. Only one patient complained of superficial abdominal discomfort almost near to 5 years postoperatively. A small palpable mass was observed resembling a cyst-like formation (≈3 cm) near the fascia of anterior rectus muscle of the patient. Under local anesthesia, the patient underwent surgery removing this cyst-like mass. The cyst had capsules that were intact and contained necrotic debris, which was once viable human islet. Living cell technologies (LCT) collaborated their work with the University of Perugia in 1929 and performed several experimental trials on the primates and rodents. The biocompatibility of microencapsulated neonatal pig islets in an alginate matrix in nondiabetic monkeys was observed. LCT launched a phase I/IIa study of neonatal insulin-producing porcine pancreatic islet cells (DIABCELL®) in Moscow (2007). After 18–96 weeks of transplantation, no marked adverse effects could be seen in seven patients with insulin-dependent diabetes after receiving one to three implants of DIABCELL®. Phase IIb clinical trials are underway is Argentina and New Zealand after the successful completion of clinical trials in Russia. The approach of LCT has been criticized by the International Xenotransplantation Association and regarded as risky and premature. The biocompatibility, hypoxia, and immunoprotection remain the potential issue for the islet encapsulation process. A new method of islet encapsulation using a layer of HEK293 living cells has

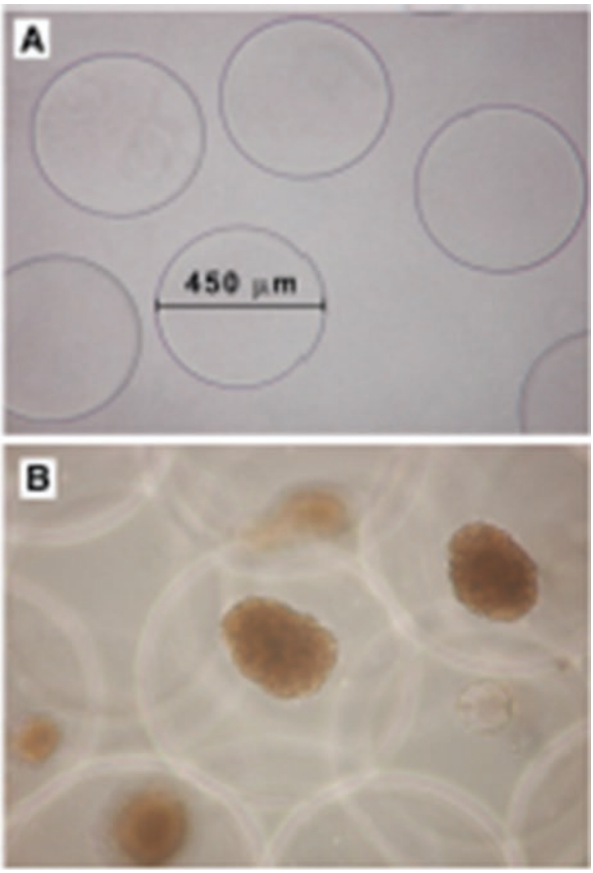

Fig. 14.11 Transplantation of (**a**) empty capsules obtained at the end of the procedure and (**b**) human islet-containing microcapsules [38]

been used (Fig. 14.12). Hamster islets were modified with biotin-PEG-lipid and immobilized with streptavidin-immobilized HEK293 cells. HEK293 cells were immobilized on the surface of the islets and cultured on a nontreated dish in Medium 199 at 37 °C. Glucagon-like peptide I features a strategy to modify PEG hydrogels thereby enhancing the islet efficiency. Though all these approaches have potential favorable outcomes, clinical trials must be administered carefully before advancing with this technology.

14.5.2 Cell Encapsulation in Neurological Sensory Disorders

Loss of neurons and glial cells in the brain or spinal cord causes neurological disorders [112, 123–130]. Cell encapsulation therapies have also been developed as potential treatment for a variety of neurological disorders. The cell encapsulation can deliver neurotrophins that help neurons to survive. The blood-brain barrier

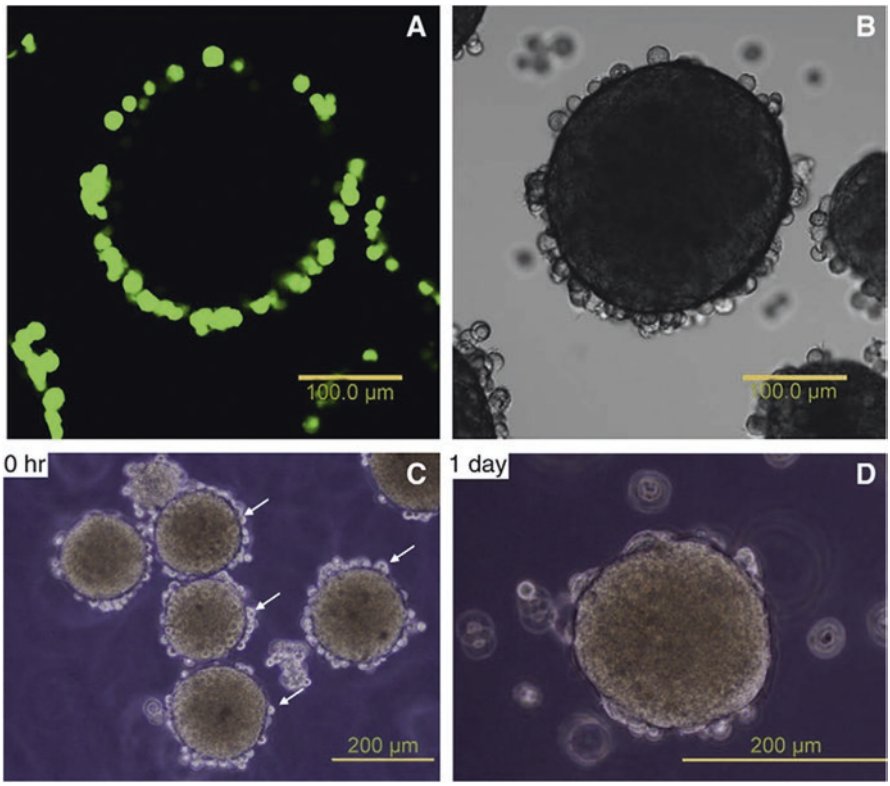

Fig. 14.12 (**a**, **b**) Confocal laser scanning and differential interference microscope images of surface-modified cells and islets. The HEK293 cells were labeled with CellTracker®. (**c**, **d**) Phase-contrast microscopy of HEK293 cell-immobilized islets in culture at 0 and 1 days. *Arrows* indicate immobilized HEK293 cells [122]

(BBB) limits the delivery of molecules to the brain, and hence several strategies have been used for the targeted delivery of drugs. Gene therapy approaches, biomaterial-based drug delivery, direct brain infusion, and cell encapsulation are the prominent techniques used for the treatment of brain disorders and central nervous system (CNS) diseases. In gene therapy approaches, a viral vector-containing gene is injected into the brain to initiate the neuron to produce factors. The treatment cannot be stopped once the virus in injected, and by no means the gene expression can be localized. Drug delivery approaches provide sustained drug release but cannot provide long-term delivery for the chronic CNS diseases. As to the direct infusion techniques, an invasive technique is used, where a catheter is implanted into the brain and is attached to the pump for controlling infusion rate and timing. This technique can cause blockage of protein functions by immunological responses and the pumps are prone to the leakage. Cell encapsulation technology remains the ideal choice for the clinical applications because it allows the use of allo- and xenografts without immunosuppression providing neurochemical diffusion and cell viability.

Cell encapsulation technology provides the advantage of configuration removal and replacement of the cells. In addition to this, a greater spread of proteins is obtained throughout the target region, due to the usage of multiple cell implants.

Common neurological disorders include Parkinson's disease, Alzheimer's disease, epilepsy, Huntington's disease, amyotrophic lateral sclerosis, and chronic pain [112, 123–130] (Fig. 14.13). Chronic neurodegenerative disease requires long-term treatment, and hence the sustained release of therapeutic molecules is needed. Choroid plexus is one of the sources of transplantable cells due to its imperative role in cerebrospinal fluid production along with the maintenance of extracellular fluid concentrations. Alginate-based encapsulation systems have been developed for the delivery of neurotropic factors in the rodent and primate models for the treatment of Huntington's disease.

For the treatment of Parkinson's disease, oral administration of levodopa, a precursor of dopamine, is used for the replacement of lost dopaminergic neurons. However, levodopa has undesirable side effects, and hence its administration shall be regulated.

Chromaffin cells or pheochromocytoma cell line PC12 have been encapsulated in hollow fibers, poly(acrylonitrile-co-vinyl chloride) polymers, or poly(L-lysine)-coated alginate capsules [131, 132]. The implants effectively increased the efficiency of levodopa over weeks. A new drug delivery system using gelatin microcarriers (Spheramine) has been tested for the treatment of Parkinson's disease. The system consists of an active component of cultured human retinal pigment epithelial (hRPE) cells attached to the cross-linked porcine gelatin micro carrier, and no immunosuppression was required as the hRPE was isolated from the postmortem of human eye tissue. The preclinical efficiency of the hRPE cells was determined by the animal model of unilateral 6-hydroxy dopamine (6–OHDA) lesioned rats and hemiparkinsonian *Macaca mulatta* monkey. The pathogenesis of Parkinson's disorder is linked to the neurotrophin deficiencies and hence the delivery of glial cell-derived neurotrophic factor (GDNF), and brain-derived neurotrophic factor (BDNF) has been investigated via intracerebral and intrathecal injection. Phase I and II clinical trials were conducted for the delivery of GDNF via a mechanical pump intracerebroventricularly. No positive results could be observed from the phase I clinical trials, and then a second trial was conducted in 34 patients with half of the patients receiving placebo reception and the other one administered with GDNF. Despite the increased dopamine uptake in the putamen, no significant behavioral changes were observed for the treated patients, which clearly signify the importance of GDNF method. Baby hamster kidney (BHK) cells were genetically modified for the secretion of nerve growth factor (NGF). A significant recovery from the rotational behavior could be observed for the rats receiving adrenal medulla with intrastriatal NGF-secreting cells as compared to the rats receiving adrenal medulla alone. Co-grafting of human embryonic dopaminergic neurons with encapsulated GDNF-secreting C2C12 cells enhanced fiber growth.

NGF has also been investigated for the treatment of Alzheimer's disease due to its potent target-derived trophic and tropic effects on the cholinergic basal forebrain neurons [133, 134]. NGF-secreting BHK cells prevented the cholinergic neuron loss

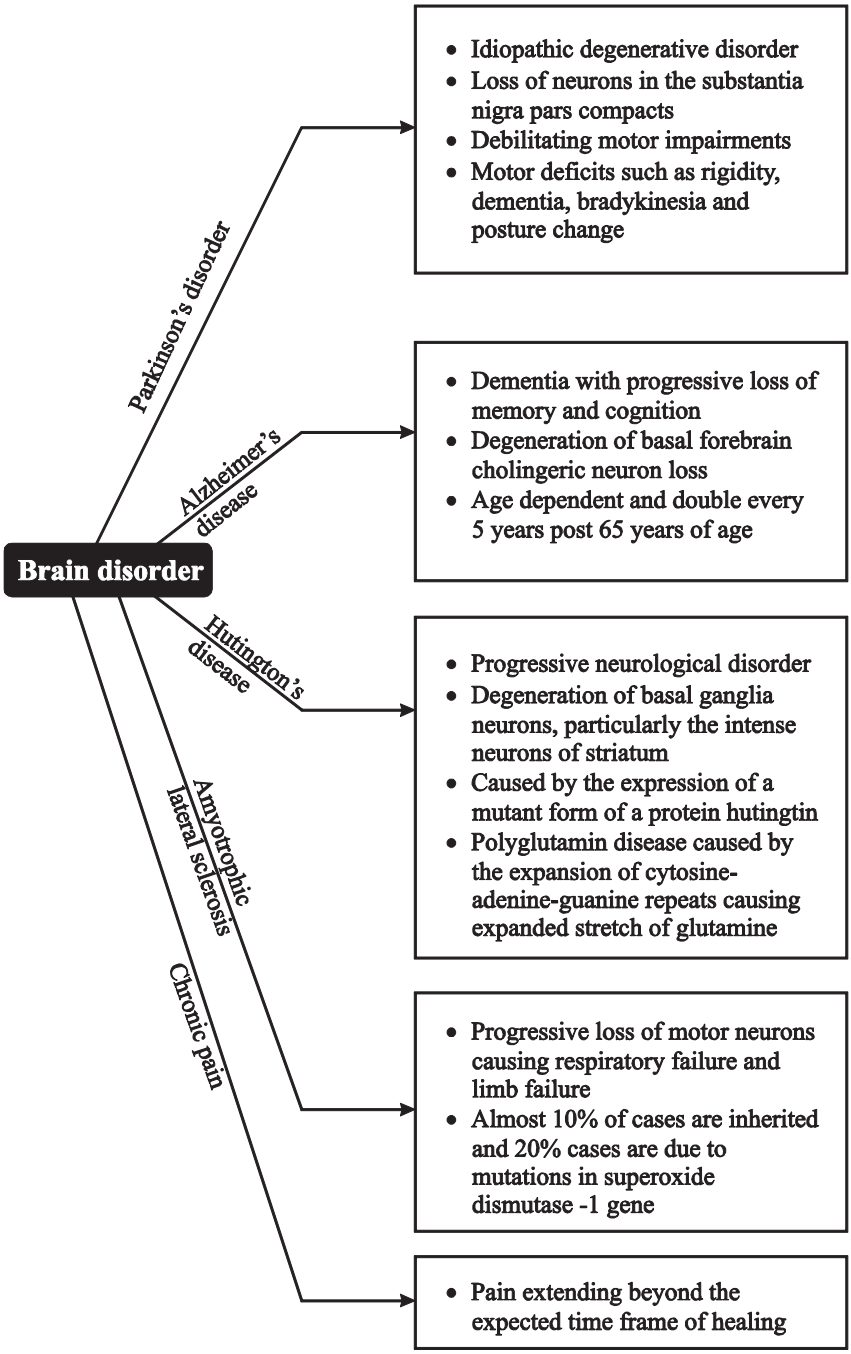

Fig. 14.13 Commons neurodegenerative diseases

following the aspiration of fornix. The mesenchymal stem cells expressing glucagon-like peptide were evaluated for Alzheimer's disease in a double transgenic murine model and the result depicted reduction in A-beta-induced toxicity in vitro along with the neuroprotective and anti-inflammatory properties. In the Alzheimer's disease, BDNF levels are depressed, which can be regarded as the lack of BDNF associated with the neurons containing neurofibrillary tangles. Ciliary neurotrophic factor (CNTF) and GLP-1 have also been tested for the Alzheimer's disease therapy. Alginate microcapsule containing myoblasts to secrete CNTF were implanted intracerebroventrically into mice with the mutant amyloid precursor protein, and significant improvement in the cognitive function could be observed. Human bone marrow-derived stem cells transfected with BLP-1, encapsulated in alginate, and implanted intracerebroventrically into a transgenic mouse model reduced the amyloid deposition and induced suppression of the inflammatory response.

For the treatment of injured spinal cord, the genetically engineered cells immobilized the growth factor producing fibroblasts [125–127]. The injured spinal cord of adult Sprague-Dawley rats could be treated by the genetically modified fibroblasts, and locomotor function was observed to be revived. BDNF-producing fibroblasts encapsulated in alginate poly(L-ornithine) microcapsules, implanted in spinal cord injury murine model, indicated recovery of hind limb and forelimb. The detection of Huntington's disease can be done via genetic testing for the mutant gene (Huntington gene). CNTF and NGF are the commonly used neurotrophic factors for the treatment of Huntington's disease. CNTF protects the striatal neurons that die in Huntington's disease, and it crosses blood-brain barrier poorly; hence, it shall be delivered directly to the brain. When NGF- and CNTF-producing cells were implanted in the quinofinic acid model of Huntington's disease, then a reduction of lesion size was observed. In addition to this, the behavioral aspect indicated improved learning behavior and memory tasks. Phase I clinical trials performed on six patients using capsules loaded with cells transfected to secrete CNTF revealed positive electro-physical changes in three patients, thus indicating improved neural circuit function.

CNTF, vascular endothelial growth factor (VEGF), and GDNF have revealed potential in superoxide dismutase-1 (SOD-1) mutant rats and mice as models of amyotrophic lateral sclerosis (ALS). Upon intraperitoneal or intracerebroventricular implantation of VEGF in rodents, prevention of motor neuron degeneration and prolonged survival of SOD-1 mutant was observed. Disorders like chronic pain can be cured naturally using adrenal chromaffin cells, because they secrete peptides-less enkephalin, adrenaline, and catecholamines. The encapsulation of chromaffin cells has been investigated in a rat model for the treatment of chronic pain. Phase I clinical trial was conducted on patients suffering from chronic pain. Bovine chromaffin cells in alginate contained in poly(acrylonitrile-co-vinyl chloride) were implanted in the patients. No cellular growth on the surface of capsules could be observed, and pain relief was reported. Sensory diseases like visual and hearing losses could also be treated by the encapsulation technology. Hearing loss usually occurs when the cochlear hair cell is damaged, and visual losses often involve retinal degeneration (retinitis pigmentosa) and age-related macular degeneration. Retinitis pigmentosa

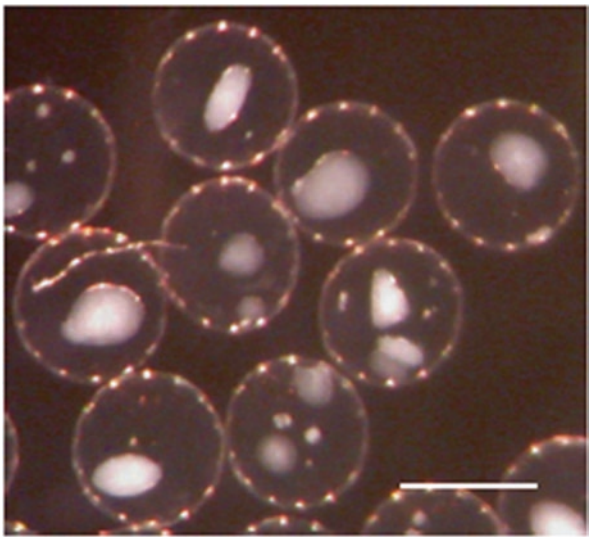

Fig. 14.14 BDNF-secreting Schwann cells encapsulated in alginate microcapsules [109]

involves death of photoreceptors in retina periphery, whereas age-related macular degeneration involves the accumulation of waste products in the macula or leakage of blood/fluid in the retina causing inflammation and vision impairment.

In sensorineural hearing loss, auditory neurons undergo progressive degeneration leading to neuronal loss after deafness. Genetically-modified Schwann cells secreting BDNF have shown to enhance the auditory neuron survival in vitro [109]. In vivo testing of BDNF-secreting Schwann cells encapsulated in PLL-coated alginate capsules was done by implanting them into deafened guinea pig cochleae (Fig. 14.14).

No adverse reaction was observed in these cells, and auditory neuron survival was enhanced.

14.5.3 Cell Encapsulation in Cancer Therapy

Cancer and tumors have been the cause of high mortality rate across the globe and thus need immediate attention [113, 135–138]. Brain tumors can be from meninges, sellar region, neuroepithelial origin, or cranial nerves. The commonly occurring tumors belong to glioma group because of their resemblance to the glial support cells of oligodendrocytes, brain, and astrocytes. The glial tumors are categorized as type I–IV depending upon their malignancy stages in the patients. Stage IV is the most dangerous malignant tumor, and the time frame from diagnosis to death is almost 14 months. By contrast enhancement imaging of the magnetic resonance imaging (MRI), the blood-brain barrier disruption and neovascularization can be detected. Chemotherapy and radiation therapy are the common treatments for the

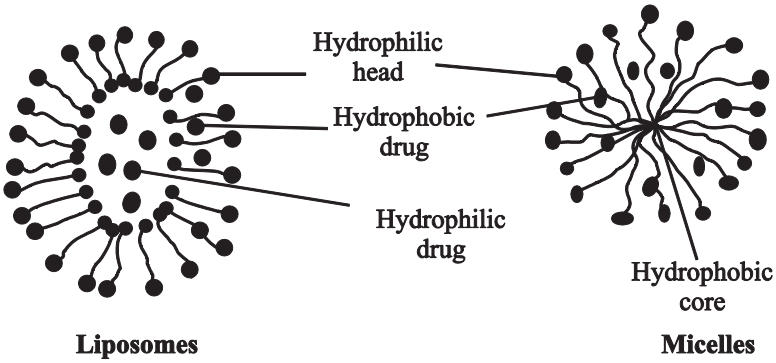

Fig. 14.15 Schematic of liposomes and micelles [113, 135–138]

glioblastomas, but even after using these treatments, the survival rate remains <10%. In addition to this, these treatments are very expensive and painful, and the side effects have a prolonged effect. Therefore, new technologies like targeted molecular therapies, immune-based therapies, and encapsulation technologies are being investigated. The blood-brain barrier (BBB) hampers the drug delivery to the brain. BBB is a structure composed of pericytes and brain endothelial cells, which regulates and protects healthy brain from the blood noxious factors and also hinders drug delivery in the affected brain area. The tumor core of gliomas contains leaky blood vessels and the "non-enhancing lesion" is largely regulated by the BBB. Another cause of drug delivery hindrance is the diffusion of agents from blood to the high interstitial pressure containing tumors. To deliver the appropriate chemotherapeutics to the tumor site, different nanocarriers like liposomes, micelles, and polymeric nanoparticles have proven to be promising drug delivery vehicles. Liposomes are spherical structures, artificially prepared and made of lipid bilayers consisting of natural/synthetic cholesterol and phospholipids (cholesterol-phospholipid ratio regulates the drug release kinetics) as shown in Fig. 14.15. In contrast to this, the formation of micelles occurs when amphiphiles (with both hydrophobic and hydrophobic character) are placed in water. The micelles core is hydrophobic serving as a depot for poorly water-soluble drugs, whereas the outer shell is hydrophilic protecting the encapsulated drugs (Fig. 14.15).

A list of anticancer drugs along with their carriers and specific applications is reported in Table 14.5.

Polymer nanoparticles, such as gelatin, alginate and chitosan, PLA, PLGA, polyphosphazenes, and polyanhydrides, are used for the anticancer drug adsorption, entrapping, and encapsulation. Cell encapsulation is useful for the aggressive gliomas, as the recurrence of gliomas can be delayed by the implantation of encapsulated cells in the exact site affected by the tumor. Table 14.6 lists the common cancers and their treatment using encapsulation technology. Alginate capsules secreting anti-angionenic peptide endostatin yielded survival benefit in the immunocompetent BT4C rat brain tumor model. The presence of endostatin in the

Table 14.5 List of drugs with micellar and liposomal carriers for the tumor treatment

Drug	Carrier and application
Doxorubicin hydrochloride	Liposomal doxorubicin for treating children with refractory solid tumors
PEGylated doxorubicin	Dose limiting toxicity of PEG-DOX in liposomal carriers
Paclitaxel loaded polymeric micelle (Genexol-PM)	Treating patients with recurrent breast cancer. Genexol-PM is also used for the treatment of ureter and bladder cancer
NK 10 (paclitaxel)	Paclitaxel incorporating micelle nanoparticle for the patient with metastatic or recurrent breast cancer
Vincristine sulfate	Liposome drug for the treatment of malignant cancer in children who could not respond to standard treatment
Cytarabine	Liposomal drug for the whole brain therapy of patients with leptomeningeal metastasis from malignant melanoma
	Liposomal drug used in investigating the effectiveness of depoCyt drug for neoplastic meningitis
	Liposomal cytarabine + methotrexate for treating patients CNS metastases from metastatic breast cancer

Table 14.6 Cancer treatment using encapsulation technology [113, 135–138]

Cancer type	Cell line	Encapsulation model
Leukemia	Anti-Pl5E antibody producing hybridoma cells encapsulated in alginates	Intraperitoneal injection in tumor-bearing mice
Pancreatic cancer	Genetically modified allogeneic cells (expressing P450 enzyme)	Clinical trials in patients with pancreatic cancer
Colon cancer	Inducible nitric oxide synthase expressing murine interlukin-12	Xenograft nude mouse model
Ovarian cancer	Inducible nitric oxide synthase over expressing cells	Xenograft nude mouse model
Glioblastoma	Baby hamster kidney expressing human endostatin	Mouse xenograft model
	Encapsulated human fetal kidney 293-Epstein-Barr virus nuclear antigen	Intracerebral implantation in rats
	Psi 2-VIK cells encapsulated in microporous polyether-sulfone	Striatum of C6 glioblastoma bearing rats

cerebrospinal fluid confirmed the distribution of therapeutic agents throughout the brain via intraparenchymal transplants.

Poly(lactic acid)-encapsulated IL-12 and TNF-α have been implanted intratumorally in a fibrosarcoma model (MCA205 cell line). Though antitumor immune response was observed, multiple capsules were required for the sustained delivery. Genetically modified C_2C_{12} myoblasts secreting cytokine and immobilized microcapsule were implanted in tumor-bearing mice for the sustained release of IL-2. Prolonged survival of animals was observed though treatment of tumor was slow. Tumor growth can also be inhibited by controlling angiogenesis, as tumor growth depends on the formation of new blood vessels. Endostatin is one of the most

potent antiangiogenic drug, which can induce apoptosis in tumor cells. Human endostatin-secreting Chinese hamster ovary cells encapsulated in alginate-poly(L-lysine)-alginate microcapsules were implanted in B16 melanoma-infected mice. The subcutaneous growth of melanoma was significantly inhibited upon the intraperitoneal implantation of these microencapsulated cells. Chemotherapeutic agents or prodrugs can also be activated by the use of encapsulated cells over expressing enzymes. One such example is the overexpression of cytochrome P450 enzyme by genetically modified feline kidney epithelial cells encapsulated in cellulose sulfate upon its implantation into xenograft tumors. It was followed by multiple administration of prodrug ifosfamide, a chemotherapeutic which is activated by cytochrome P450 enzyme. After this combined therapy, some mice even got complete rid of tumor.

14.6 Future Scope

Cell microencapsulation technology holds great promise for the treatment of a wide variety of diseases, since this technology allows the controlled, continuous release of drugs while suppressing the body's immunoresponse. However, several challenges must be overcome before this technology can be adopted for widespread clinical applications. These challenges include ensuring consistent performance and safety of the microencapsulation therapy, as well as developing scaled-up manufacturing technologies that can ensure purity and sufficiently low-cost microcapsule production. Other challenges include ensuring that cell reproduction is controlled to maintain consistent drug delivery over a long period of time. The initial culture and storage of suitable cells for microencapsulation therapy is another concern that must be addressed. Finally, with the diverse range of diseases that can be targeted through microencapsulation technology, specialized microcapsules will need to be developed. Continued research in all of these areas will enable the progress necessary to invent and implement new and effective microencapsulation-based therapies for diabetes, cancer, heart diseases, and many other diseases afflicting large populations of people.

References

1. Chang TMS. Semipermeable microcapsules. Science. 1964;146:524–5.
2. Chick WL, et al. Beta cell culture on synthetic capillaries: an artificial endocrine pancreas. sScience. 1975;187:847–84.
3. Sun YL, et al. Normalization of diabetes in spontaneously diabetic cynomologous monkeys by xenografts of microencapsulated porcine islets without immunosuppression. J Clin Invest. 1996;98:1417–22.
4. Orive G, Hernández RM, Rodríguez Gascón A, Calafiore R, Chang TMS, De Vos P, … Pedraz JL. History, challenges and perspectives of cell microencapsulation. Trends Biotechnol. 2004;22(2):87–92. http://doi.org/10.1016/j.tibtech.2003.11.004.

5. Murua A, Portero A, Orive G, Hernández RM, de Castro M, Pedraz JL. Cell microencapsulation technology: towards clinical application. J Control Release. 2008;132(2):76–83. http://doi.org/10.1016/j.jconrel.2008.08.010.
6. Orive G, et al. Microencapsulation of an anti VE-cadherin antibody secreting 1B5 hybridoma cells. Biotechnol Bioeng. 2001;76:285–94.
7. Sharkawy AA, et al. Engineering the tissue which encapsulates subcutaneous implants. Diffusion properties. J Biomed Mater Res. 1997;37:401–12.
8. Hunkeler D, et al. Objectively assessing bioartificial organs. Ann N Y Acad Sci. 2001;944:456–71.
9. Bisceglie V. Uber die antineoplastische immunitat; heterologe Einpflnzung von Tumoren in Huhner-embryonen. Ztschr Krebsforsch. 1933;40:122–40.
10. Hernández RM, Orive G, Murua A, Pedraz JL. Microcapsules and microcarriers for in situ cell delivery. Adv Drug Deliv Rev. 2010;62(7–8):711–30. http://doi.org/10.1016/j.addr.2010.02.004.
11. Kulig KM, Vacanti JP. Hepatic tissue engineering. Transpl Immunol. 2004;12:303–10.
12. Street CN, Rajotte RV, Korbutt GS. Stem cells: a promising source of pancreatic islets for transplantation in type 1 diabetes. Curr Top Dev Biol. 2003;58:111–36.
13. Orive G, de Castro M, Ponce S, Hernández RM, Gascón AR, Bosch M, Alberch J, Pedraz JL. Long-term expression of erythropoietin from myoblasts immobilized in biocompatible and neovascularized microcapsules. Mol Ther. 2005;12:283–9.
14. Caruso F. Hollow capsule processing through colloidal templating and selfassembly. Chemistry. 2000;6:413–9.
15. Li RH. Materials for immunoisolated cell transplantation. Adv Drug Deliv Rev. 1998;33:87–109.
16. Qiu C, Chen M, Yan H, Wu HK. Generation of uniformly sized alginate microparticles for cell encapsulation by using a soft-lithography approach. Adv Mater. 2007;19:1603–7.
17. Murua A, de Castro M, Orive G, Hernández RM, Pedraz JL. In vitro characterization and in vivo functionality of erythropoietin-secreting cell immobilized in alginate–poly-L-lysine–alginate microcapsules. Biomacromolecules. 2007;8:3302–7.
18. Orive G, Hernandez RM, Gascon AR, Pedraz JL. Challenges in cell encapsulation. In: Nedovic V, Willaert R, editors. Applications of cell immobilization biotechnology, vol. 8B. Dordrecht: Springer; 2005. p. 185–96.
19. Lim F, Sun AM. Microencapsulated islets as bioartificial endocrine pancreas. Science. 1980;210:908–10.
20. Consiglio S, Martino D, Dolcetta G, Cusella M, Conese S, Marchesini G, Benaglia L, Wrabetz A, Orlacchio N, Déglon P, Aebischer GM, Severini C. Bordignon, metabolic correction in oligodendrocytes derived from metachromatic leukodystrophy mouse model by using encapsulated recombinant myoblasts. J Neurol Sci. 2007;255:7–16.
21. Whitesides GM. The origins and the future of microfluidics. Nature. 2006;442:368–73.
22. Antosiak-Iwańska M, Sitarek E, Sabat M, Godlewska E, Kinasiewicz J, Weryński A. Isolation, banking, encapsulation and transplantation of different types of Langerhans islets. Pol Arch Med Wewn. 2009;119:311–6.
23. Stover NP, Watts RL. Spheramine for treatment of Parkinson's disease. Neurotherapeutics. 2008;5:252–9.
24. Orive G, Tam SK, Pedraz JL, Hallé JP. Biocompatibility of alginate–poly-Llysine microcapsules for cell therapy. Biomaterials. 2006;20:3691–700.
25. Benoit DS, Schwartz MP, Durney AR, Anseth KS. Small functional groups for controlled differentiation of hydrogel-encapsulated human mesenchymal stem cells. Nat Mater. 2008;7:816–82.
26. Falk S, Zhang SJ. Sherman, pigment epithelium derived factor (PEDF) is neuroprotective in two in vitro models of Parkinson's disease. Neurosci Lett. 2009;458:49–52.
27. Tatard VM, Venier-Julienne MC, Saulnier P, Prechter E, Benoit JP, Meneia P, Montero-Menei CN. Pharmacologically active microcarriers: a tool for cell therapy. Biomaterials. 2005;26:3727–37.

28. Sommar P, Pettersson S, Ness C, Johnson H, Kratz G, Junker JPE. Engineering three-dimensional cartilage- and bonelike tissues using human dermal fibroblasts and macroporous gelatine microcarriers. J Plast Reconstr Aesthet Surg. 2010;63:1036–46.
29. Sun ZJ, Lu GJ, Li SY, Yu WT, Wang W, Xie YB, Ma X. Differential role of microenvironment in microencapsulation for improved cell tolerance to stress. Appl Microbiol Biotechnol. 2007;75:1419–27.
30. Herrero EP, Martín del Valle EM, Galán MA. Immobilization of mesenchymal stem cells and monocytes in biocompatible microcapsules to cell therapy. Biotechnol Prog. 2007;23: 940–5.
31. Chevallay B, Herbage D. Collagen-based biomaterials as 3D scaffold for cell cultures: applications for tissue engineering and gene therapy. Med Biol Eng Comput. 2000;38:211–8.
32. Rosenblatt J, Devereux B, Wallace DG. Injectable collagen as a pH-sensitive hydrogel. Biomaterials. 1994;15:985–95.
33. Senuma Y, Franceschin S, Hilborn JG, Tissieres P, Bisson I, Frey P. Bioresorbable microspheres by spinning disk atomization as injectable cell carrier: from preparation to in vitro evaluation. Biomaterials. 2000;21:1135–44.
34. De Vos P, Lazarjani HA, Poncelet D, Faas MM. Polymers in cell encapsulation from an enveloped cell perspective. Adv Drug Deliv Rev. 2014;67–68:15–34. http://doi.org/10.1016/j.addr.2013.11.005.
35. Scharp DW, Marchetti P. Encapsulated islets for diabetes therapy: history, current progress, and critical issues requiring solution. Adv Drug Deliv Rev. 2014;67–68:35–73. http://doi.org/10.1016/j.addr.2013.07.018.
36. Orive G, Gascón AR, Hernández RM, Igartua M, Pedraz JL. Cell microencapsulation technology for biomedical purposes: novel insights and challenges. Trends Pharmacol Sci. 2003;24(5):207–10. http://doi.org/10.1016/S0165-6147(03)00073-7.
37. Rokstad AMA, Lacík I, de Vos P, Strand BL. Advances in biocompatibility and physicochemical characterization of microspheres for cell encapsulation. Adv Drug Deliv Rev. 2014;67–68:111–30. http://doi.org/10.1016/j.addr.2013.07.010.
38. Calafiore R, Basta G. Clinical application of microencapsulated islets: actual prospectives on progress and challenges. Adv Drug Deliv Rev. 2014;67–68:84–92. http://doi.org/10.1016/j.addr.2013.09.020.
39. Abbah SA, Lu WW, Chan D, Cheung KMC, Liu WG, Zhao F, Li ZY, Leong JCY, Luk KDK. In vitro evaluation of alginate encapsulated adipose-tissue stromal cells for use as injectable bone graft substitute. Biochem Biophys Res Commun. 2006;347:185–91.
40. Maguire T, Davidovich AE, Wallenstein EJ, Novik E, Sharma N, Pedersen H, Androulakis IP, Schloss R, Yarmush M. Control of hepatic differentiation via cellular aggregation in an alginate microenvironment. Biotechnol Bioeng. 2007;98:631–44.
41. Dulieu C, Bazile D. Influence of lipid nanocapsules composition on their aptness to freeze-drying. Pharm Res. 2005;22:285–92.
42. Iwata H, Amemiya H, Hayashi R, Fujii S, Akutsu T. The use of photocrosslinkable polyvinyl alcohol in the immunoisolation of pancreatic islets. Transplant Proc. 1990;22:797–9.
43. Hymer WC, Wilbur DL, Page R, Hibbard E, Kelsey RC, Hatfield JM. Pituitary hollow fiber units in vivo and in vitro. Neuroendocrinology. 1981;32:339–49.
44. Qi Z, Shen Y, Yanai G, Yang K, Shirouzu Y, Hiura A, Sumi S. The in vivo performance of polyvinyl alcohol macro-encapsulated islets. Biomaterials. 2010;31:4026–31.
45. Winn SR, Lindner MD, Lee A, Haggett G, Francis JM, Emerich DF. Polymer-encapsulated genetically modified cells continue to secrete human nerve growth factor for over one year in rat ventricles: behavioral and anatomical consequences. Exp Neurol. 1996;140:126–38.
46. Vrana NE, O'Grady A, Kay E, Cahill PA, McGuinness GB. Cell encapsulation within PVA-based hydrogels via freeze-thawing: a one-step scaffold formation and cell storage technique. J Tissue Eng Regen Med. 2009;3:567–72.
47. Qi M, Gu Y, Sakata N, Kim D, Shirouzu Y, Yamamoto C, Hiura A, Sumi S, Inoue K. PVA hydrogel sheet macroencapsulation for the bioartificial pancreas. Biomaterials. 2004;25: 5885–92.

48. Kaur G. Biaoctive glasses:potential biomaterials for future therapy. Heidelberg: Springer; 2017.
49. Zalipsky S, Mullah N, Harding JA, Gittelman J, Guo L, DeFrees SA. Poly(ethylene glycol)-grafted liposomes with oligopeptide or oligosaccharide ligands appended to the termini of the polymer chains. Bioconjug Chem. 1997;8:111–8.
50. Lutolf MP, Hubbell JA. Synthetic biomaterials as instructive extracellular microenvironments for morphogenesis in tissue engineering. Nat Biotechnol. 2005;23:47–55.
51. Nguyen KT, West JL. Photopolymerizable hydrogels for tissue engineering applications. Biomaterials. 2002;23:4307–14.
52. Hubbell JA, Pathak CP, Sawhney AS, Desai NP, Hossainy SFA. Gels for encapsulation of biological materials. US Patent US 5801033 A, CA, USA, 2004.
53. Chang SJ, Lee CH, Hsu CY, Wang YJ. Biocompatible microcapsules with enhanced mechanical strength. J Biomed Mater Res A. 2002;59:118–26.
54. Nuttelman CR, Rice MA, Rydholm AE, Salinas CN, Shah DN, Anseth KS. Macromolecular monomers for the synthesis of hydrogel niches and their application in cell encapsulation and tissue engineering. Prog Polym Sci. 2008;33:167–79.
55. Andrade JD, Hlady V. Plasma protein adsorption: the big twelve. Ann N Y Acad Sci. 1987;516:158–72.
56. Sabnis A, Rahimi M, Chapman C, Nguyen KT. Cytocompatibility studies of an in situ photopolymerized thermoresponsive hydrogel nanoparticle system using human aortic smooth muscle cells. J Biomed Mater Res A. 2009;91:52–9.
57. Cellesi F, Tirelli N, Hubbell JA. Towards a fully-synthetic substitute of alginate: development of a new process using thermal gelation and chemical crosslinking. Biomaterials. 2004;25:5115–24.
58. Cellesi F, Tirelli N. A new process for cell microencapsulation and other biomaterial applications: thermal gelation and chemical cross-linking in “tandem”. J Mater Sci Mater Med. 2005;16:559–65.
59. Lin CC, Metters AT, Anseth KS. Functional PEG–peptide hydrogels to modulate local inflammation induced by the pro-inflammatory cytokine TNFalpha. Biomaterials. 2009;30:4907–14.
60. Cruise GM, Scharp DS, Hubbell JA. Characterization of permeability and network structure of interfacially photopolymerized poly(ethylene glycol) diacrylate hydrogels. Biomaterials. 1998;19:1287–94.
61. Sawhney AS, Pathak CP, Hubbell JA. Interfacial photopolymerization of poly(ethylene glycol)-based hydrogels upon alginate–poly(L-lysine) microcapsules for enhanced biocompatibility. Biomaterials. 1993;14:1008–16.
62. Jang JY, Lee DY, Park SJ, Byun Y. Immune reactions of lymphocytes and macrophages against PEG-grafted pancreatic islets. Biomaterials. 2004;25:3663–9.
63. Lamberton P, Lipsky M, McMillan P. Use of semipermeable polyurethane hollow fibers for pituitary organ culture. In Vitro Cell Dev Biol. 1988;24:500–4.
64. Kim YT, Hitchcock R, Broadhead KW, Messina DJ, Tresco PA. A cell encapsulation device for studying soluble factor release from cells transplanted in the rat brain. J Control Release. 2005;102:101–11.
65. Seymour RB, Kauffman GB. Polyurethanes: a class of modern versatile materials. J Chem Educ. 1992;69:909–14.
66. Takebe K, Shimura T, Munkhbat B, Hagihara M, Nakanishi H, Tsuji K. Xenogeneic (pig to rat) fetal liver fragment transplantation using macrocapsules for immunoisolation. Cell Transplant. 1996;5:S31–3.
67. Granicka LH, Kawiak JW, Glowacka E, Werynski A. Encapsulation of OKT3 cells in hollow fibers. ASAIO J. 1996;42:M863–6.
68. Petersen P, Lembert N, Stenglein S, Planck H, Ammon HP, Becker HD. Insulin secretion from cultured islets encapsulated in immuno- and virus-protective capillaries. Transplant Proc. 2001;33:3520–2.
69. Deglon N, Heyd B, Tan SA, Joseph JM, Zurn AD, Aebischer P. Central nervous system delivery of recombinant ciliary neurotrophic factor by polymer encapsulated differentiated C2C12 myoblasts. Hum Gene Ther. 1996;7:2135–46.

70. Ronel SH, D'Andrea MJ, Hashiguchi H, Klomp GF, Dobelle WH. Macroporous hydrogel membranes for a hybrid artificial pancreas. I. Synthesis and chamber fabrication. J. Biomed Mater Res A. 1983;17:855–64.
71. Sefton MV, May MH, Lahooti S, Babensee JE. Making microencapsulation work: conformal coating, immobilization gels and in vivo performance. J Control Release. 2000;65:173–86.
72. Fleming AJ, Sefton MV. Viability of hydroxyethyl methacrylate–methyl methacrylate-microencapsulated PC12 cells after omental pouch implantation within agarose gels. Tissue Eng. 2003;9:1023–36.
73. Gharapetian H, Davies NA, Sun AM. Encapsulation of viable cells within polyacrylate membranes. Biotechnol Bioeng. 1986;28:1595–600.
74. Sugamori ME, Sefton MV. Microencapsulation of pancreatic islets in a water insoluble polyacrylate. ASAIO Trans. 1989;35:791–9.
75. Lahooti S, Sefton MV. Methods for microencapsulation with HEMA–MMA. Methods Mol Med. 1999;18:331–48.
76. Wells GD, Fisher MM, Sefton MV. Microencapsulation of viable hepatocytes in HEMA–MMA microcapsules: a preliminary study. Biomaterials. 1993;14:615–20.
77. Uludag H, Sefton MV. Metabolic activity of CHO fibroblasts in HEMA–MMA microcapsules. Biotechnol Bioeng. 1992;39:672–8.
78. Sukhorukov GB, Donath E, Moya S, Susha AS, Voigt A, Hartmann J, Mohwald H. Microencapsulation by means of step-wise adsorption of polyelectrolytes. J Microencapsul. 2000;17:177–85.
79. Georgieva R, Moya S, Donath E, Baumler H. Permeability and conductivity of red blood cell templated polyelectrolyte capsules coated with supplementary layers. Langmuir. 2004;20:1895–900.
80. Brown LF, Detmar M, Claffey K, Nagy JA, Feng D, Dvorak AM, Dvorak HF. Vascular permeability factor/vascular endothelial growth factor: a multifunctional angiogenic cytokine. EXS. 1997;79:233–69.
81. Krol S, del Guerra S, Grupillo M, Diaspro A, Gliozzi A, Marchetti P. Multilayer nanoencapsulation. New approach for immune protection of human pancreatic islets. Nano Lett. 2006;6:1933–9.
82. Wee S, Gombotz WR. Protein release from alginate matrices. Adv Drug Deliv Rev. 1998;31:267–85.
83. Bruni S, Chang TM. Hepatocytes immobilised by microencapsulation in artificial cells: effects on hyperbilirubinemia in Gunn rats. Biomater Artif Cells Artif Organs. 1989;17:403–11.
84. Teramura Y, Oommen OP, Olerud J, Hilborn J, Nilsson B. Microencapsulation of cells, including islets, within stable ultra-thin membranes of maleimideconjugated PEG-lipid with multifunctional crosslinkers. Biomaterials. 2013;34:2683–93.
85. Lanza RP, Ecker D, KÅhtreiber WM, Staruk JE, Marsh J, Chick WL. A simple method for transplanting discordant islets into rats using alginate gel spheres. Transplantation. 1995;59:1485–7.
86. Fu XW, Sun AM. Microencapsulated parathyroid cells as a bioartificial parathyroid. In vivo studies. Transplantation. 1989;47:432–5.
87. Stokke BT, Smidsroed O, Bruheim P, Skjaak-Braek G. Distribution of urinate residues in alginate chains in relation to alginate gelling properties. Macromolecules. 1991;24:4637–45.
88. Morch YA, Donati I, Strand BL, Skjak Braek G. Effect of Ca2+, Ba2+, and Sr2+ on alginate microbeads. Biomacromolecules. 2006;7:1471–80.
89. Sobol M, Bartkowiak A, de Haan B, de Vos P. Cytotoxicity study of novel water-soluble chitosan derivatives applied as membrane material of alginate microcapsules. J Biomed Mater Res A. 2013;101:1907–14.
90. Zhu JH, Wang XW, Ng S, Quek CH, Ho HT, Lao XJ, Yu H. Encapsulating live cells with water-soluble chitosan in physiological conditions. J Biotechnol. 2005;117:355–65.

91. Haque T, Chen H, Ouyang W, Martoni C, Lawuyi B, Urbanska AM, Prakash S. In vitro study of alginate-chitosan microcapsules: an alternative to liver cell transplants for the treatment of liver failure. Biotechnol Lett. 2005;27:317–22.
92. Karle P, Muller P, Renz R, Jesnowski R, Saller R, von Rombs K, Nizze H, Liebe S, Gunzburg WH, Salmons B, Lohr M. Intratumoral injection of encapsulated cells producing an oxazaphosphorine activating cytochrome P450 for targeted chemotherapy. Adv Exp Med Biol. 1998;451:97–106.
93. Kubota N, Tatsumoto N, Sano T, Toya K. A simple preparation of half N-acetylated chitosan highly soluble inwater and aqueous organic solvents. Carbohydr Res. 2000;324:268–74.
94. Gupta S, Kim SK, Vemuru RP, Aragona E, Yerneni PR, Burk RD, Rha CK. Hepatocyte transplantation: an alternative system for evaluating cell survival and immunoisolation. Int J Artif Organs. 1993;16:155–63.
95. Lee BR, Lee KH, Kang E, Kim DS, Lee SH. Microfluidic wet spinning of chitosan-alginate microfibers and encapsulation of HepG2 cells in fibers. Biomicrofluidics. 2011;5:22208.
96. Ruel-Gariepy E, Leclair G, Hildgen P, Gupta A, Leroux JC. Thermosensitive chitosan-based hydrogel containing liposomes for the delivery of hydrophilic molecules. J Control Release. 2002;82:373–83.
97. Dautzenberg H, Schuldt U, Grasnick G, Karle P, Muller P, Lohr M, Pelegrin M, Piechaczyk M, Rombs KV, Gunzburg WH, Salmons B, Saller RM. Development of cellulose sulfate-based polyelectrolyte complex microcapsules for medical applications. Ann N Y Acad Sci. 1999;875:46–63.
98. Stadlbauer V, Stiegler PB, Schaffellner S, Hauser O, Halwachs G, Iberer F, Tscheliessnigg KH, Lackner C. Morphological and functional characterization of a pancreatic beta-cell line microencapsulated in sodium cellulose sulfate/ poly(diallyldimethylammonium chloride). Xenotransplantation. 2006;13:337–44.
99. Weber W, Rinderknecht M, Daoud-El Baba M, de Glutz FN, Aubel D, Fussenegger M. CellMAC: a novel technology for encapsulation of mammalian cells in cellulose sulfate/ pDADMAC capsules assembled on a transient alginate/Ca2+ scaffold. J Biotechnol. 2004;114:315–26.
100. Schaffellner S, Stadlbauer V, Stiegler P, Hauser O, Halwachs G, Lackner C, Iberer F, Tscheliessnigg KH. Porcine islet cells microencapsulated in sodium cellulose sulfate. Transplant Proc. 2005;37:248–52.
101. Yang H, Zhao K, Ye Y, Deng S. Study of macroencapsulated islet xenografts for treatment of diabetes in mice. Hua Xi Yi Ke Da Xue Xue Bao. 1998;29:132–5.
102. Scheirer W, Nilsson K, Merten OW, Katinger HW, Mosbach K. Entrapment of animal cells for the production of biomolecules such as monoclonal antibodies. Dev Biol Stand. 1983;55:155–61.
103. Jain K, Yang H, Cai BR, Haque B, Hurvitz AI, Diehl C, Miyata T, Smith BH, Stenzel K, Suthanthiran M, et al. Retrievable, replaceable, macroencapsulated pancreatic islet xenografts Long-term engraftment without immunosuppression. Transplantation. 1995;59: 319–24.
104. Yin C, Chia SM, Quek CH, Yu H, Zhuo RX, Leong KW, Mao HQ. Microcapsules with improved mechanical stability for hepatocyte culture. Biomaterials. 2003;24:1771–80.
105. Lahooti S, Sefton MV. Microencapsulation of normal and transfected L929 fibroblasts in a HEMA–MMA copolymer. Tissue Eng. 2000;6:139–49.
106. Wu FJ, Friend JR, Lazar A, Mann HJ, Remmel RP, Cerra FB, Hu WS. Hollow fiber bioartificial liver utilizing collagen-entrapped porcine hepatocyte spheroids. Biotechnol Bioeng. 1996;52:34–44.
107. Vendruscolo CW, Andreazza IF, Ganter JL, Ferrero C, Bresolin TM. Xanthan and galactomannan (from M. scabrella) matrix tablets for oral controlled delivery of theophylline. Int J Pharm. 2005;296:1–11.
108. Mendes AC, Baran ET, Pereira RC, Azevedo HS, Reis RL. Encapsulation and survival of a chondrocyte cell line within xanthan gum derivative. Macromol Biosci. 2012;12:350–9.

109. Zanin MP, Pettingill LN, Harvey AR, Emerich DF, Thanos CG, Shepherd RK. The development of encapsulated cell technologies as therapies for neurological and sensory diseases. J Control Release. 2012;160(1):3–13. http://doi.org/10.1016/j.jconrel.2012.01.021.
110. Hasse C, Zielke A, Klöck G, Schlosser A, Barth P, Zimmermann U, … Rothmund M. Amitogenic alginates: key to first clinical application of microencapsulation technology. World J Surg. 1998;22(7):659–65. http://doi.org/10.1007/s002689900449.
111. Giri J, Li WJ, Tuan RS, Cicerone MT. Stabilization of proteins by nanoencapsulation in sugar-glass for tissue engineering and drug delivery applications. Adv Mater. 2011;23(42):4861–7. http://doi.org/10.1002/adma.201102267.
112. Emerich DF, Orive G, Thanos C, Tornoe J, Wahlberg LU. Encapsulated cell therapy for neurodegenerative diseases: from promise to product. Adv Drug Deliv Rev. 2014;67–68:131–41. http://doi.org/10.1016/j.addr.2013.07.008.
113. Bhujbal SV, de Vos P, Niclou SP. Drug and cell encapsulation: alternative delivery options for the treatment of malignant brain tumors. Adv Drug Deliv Rev. 2014;67–68:142–53. http://doi.org/10.1016/j.addr.2014.01.010.
114. Downing R. Historical review of pancreatic islet transplantation. World J Surg. 1984;8:137–42.
115. Papaspyros NS. The history of diabetes mellitus. Stuttgart: George Thieme Verlag; 1964.
116. Sorenson RL. Isolation of an insulin secretion granule rich fraction from rat islets. Anat Rec. 1968;160:498.
117. Scharp DW, Kemp CB, Knight MJ, Ballinger WF, Lacy PE. The use of Ficoll in the preparation of viable islets of Langerhans fromthe rat pancreas. Transplantation. 1973;16:686–9.
118. Moskalewski S. Isolation and culture of the islets of Langerhans of the Guinea pig. Gen Comp Endocrinol. 1965;5:342–53.
119. Lacy PE, Kostianovsky M. Method for the isolation of intact islets of Langerhans from the rat pancreas. Diabetes. 1967;16:35–9.
120. Ballinger WF, Lacy PE. Transplantation of intact pancreatic islets in rats. Surgery. 1972;72:175–86.
121. Tuch BE, Keogh GW, Williams LJ, Wu W, Foster JL, Vaithilingam V, Philips R. Safety and viability of microencapsulated human islets transplanted into diabetic human. Diabetes Care. 2009;32:1887–9.
122. Teramura Y, Iwata H. Islet encapsulation with living cells for improvement of biocompatibility. Biomaterials. 2009;30:2270–5.
123. Garcia P, Youssef I, Utvik JK, Florent-Béchard S, Barthélémy V, Malaplate-Armand C, Kriem B, Stenger C, Koziel V, Olivier JL, Escanye MC, Hanse M, Allouche A, Desbène C, Yen FT, Bjerkvig R, Oster T, Niclou SP, Pillot T. Ciliary neurotrophic factor cell-based delivery prevents synaptic impairment and improves memory in mouse models of Alzheimer's disease. J Neurosci. 2010;30:7516–27.
124. Spuch C, Antequera D, Portero A, Orive G, Hernández RM, Molina JA, Bermejo-Pareja F, Pedraz JL, Carro E. The effect of encapsulated VEGF-secreting cells on brain amyloid and behavioral impairment in amouse model of Alzheimer's disease. Biomaterials. 2010;31:5608–18.
125. Emerich DF, Lindner MD, Winn SR, Chen E, Frydel B, Kordower JH. Implants of encapsulated human CNTF-producing fibroblasts prevent behavioral deficits and striatal degeneration in a rodent model of Huntington's disease. J Neurosci. 1996;1:5168–81.
126. Emerich DF, Cain CK, Greco C, Saydoff JA, Hu Z-Y, Liu H, Lindner MD. Cellular delivery of human CNTF prevents motor and cognitive dysfunction in a rodent model of Huntington's disease. Cell Transplant. 1997;6:249–66.
127. Emerich DF, Winn SR, Hantraye PM, Peschanski M, Chen E, Chu Y, McDermott P, Baetge EE, Kordower JH. Protective effects of encapsulated cells producing neurotrophic factor CNTF in a monkey model of Huntington's disease. Nature. 1997;386:395–9.
128. Lindvall O, Wahlberg LU. Encapsulated cell biodelivery of GDNF: a novel clinical strategy for neuroprotection and neuroregeneration in Parkinson's disease? Exp Neurol. 2008;209:82–8.

129. Zheng JS, Tang LL, Zheng SS, Zhan RY, Zhou YQ, Goudreau J, Kaufman D, Chen AF. Delayed gene therapy of glial cell line-derived neurotrophic factor is efficacious in a rat model of Parkinson's disease. Brain Res Mol Brain Res. 2005;134:155–61.
130. Gash DM, Zhang Z, Ovadia A, Cass WA, Yi A, Simmerman L, Russell D, Martin D, Lapchak PA, Collins F, Hoffer BJ, Gerhardt GA. Functional recovery in parkinsonian monkeys treated with GDNF. Nature. 1996;380:252–5.
131. Tresco PA, Winn SR, Aebischer P. Polymer encapsulated neurotransmitter secreting cells: potential treatment for Parkinson's disease. ASAIO. 1992;38:17–23.
132. Tresco PA, Winn SR, Jaeger CB, Greene LA, Aebischer P. Polymer-encapsulated PC12 cells: long-term survival and associated reduction in lesioned-induced rotational behavior. Cell Transplant. 1992;1:255–64.
133. Emerich DF, Winn SR, Harper J, Hammang JP, Baetge EE, Kordower JH. Implants of polymer-encapsulated human NGF-secreting cells in the nonhuman primate: rescue and sprouting of degenerating cholinergic basal forebrain neurons. J Comp Neurol. 1994;349: 148–64.
134. Winn SR, Hammang JP, Emerich DF, Lee A, Palmiter RD, Baetge EE. Polymer-encapsulated cells genetically modified to secrete human nerve growth factor promote the survival of axotomized septal cholinergic neurons. Proc Natl Acad Sci U S A. 1994;91:2324–8.
135. Lee J-L, Ahn J-H, Park SH, Lim HY, Kwon JH, Ahn S, et al. Phase II study of a cremophor-free, polymeric micelle formulation of paclitaxel for patients with advanced urothelial cancer previously treated with gemcitabine and platinum. Investig New Drugs. 2012;k30:1984–90.
136. Saif MW, Podoltsev NA, Rubin MS, Figueroa JA, Lee MY, Kwon J, et al. Phase II clinical trial of paclitaxel loaded polymeric micelle in patients with advanced pancreatic cancer. Cancer Investig. 2010;28:186–94.
137. Read TA, Sorensen DR, Mahesparan R, Enger PO, Timpl R, Olsen BR, et al. Local endostatin treatment of gliomas administered by microencapsulated producer cells. Nat Biotechnol. 2001;19:29–34.
138. Terzis AJA, Niclou SP, Rajcevic U, Danzeisen C, Bjerkvig R. Cell therapies for glioblastoma. Expert Opin Biol Ther. 2006;6:739–49.

Index

A
Absorbable collagen sponge (ACS), 386
ACB-BAG graft, 349
Activated partial thromboplastin time (APTT), 20
Adipose-derived stem cells (ADSCs), 7
Agarose polysaccharides, 440
Ag-substituted biomaterials, 365
Alginates, 435–437
Allografts, 338
Alumina (Al_2O_3), 412
Alzheimer's disease, 445
3-Aminopropyltriethoxysilane (APTES), 51
Amorphous calcium phosphate (ACP), 26
Amorphous solid, 38
Amyotrophic lateral sclerosis (ALS), 447
Angiogenesis
  bioactive glasses, 13
  45S5 Bioglass®, 13–15
  CAM, 16, 17
  endothelial cell proliferation, 16
  factors, 13
  hard-soft tissue interfaces, 13
  in vitro/in vivo effects, 14
  ionic dissolution products, 16
  malignant tumors/cancer, 13
  neovascularization, 13, 18
  PDLLA/glass composites, 18
  VEGF, 14, 15
Anterior cervical corpectomy and fusion (ACCF), 83
Antibiotics, 302–304
Anti-inflammatory drugs, 304
Antitumour drug, 233
Apatite cements, 97
Apatite/wollastonite (A/W) glass-ceramic coating, 11
Apatite-based glass-ceramics, 322–324
Apatite-mullite glass-ceramics, 329, 330
APTS-BG-MA, 51
Autogenous bone graft
  calvarium, 338
Autograft, 384–385

B
Baby hamster kidney (BHK), 445
Bactericidal action, 365
BAG-poly-L/DL-lactide 70/30 composites, 345
BDNF-secreting Schwann cells, 448
Beta-tricalcium phosphate (β-TCP), 66, 390
  advantages, 66
  bone graft material, 68–70
  bone substitutes/fillers, 68–71
  carrier material, 71–73
  drug delivery, 71–74
  implants, 74
Bioactive dental glass-ceramics (BDGCs), 316
Bioactive glasses (BAGs), 2, 3, 339, 362–366
  and angiogenesis, 13–18
  antibacterial effect, 373
  antibacterial properties, 358
  antibiotics, 302–304
  anti-inflammatory drugs, 304
  applications, 366, 367
  BG20F, 369
  biomaterials, 35
  bone tissue regeneration, 25–26
  bone tissue repair, 11–13

G. Kaur (ed.), *Clinical Applications of Biomaterials*,
DOI 10.1007/978-3-319-56059-5

Bioactive glasses (BAGs) (*cont.*)
composites
advantages, 345
BAG, 345
BDDMA, 346
with ceramic, 347–349
concentration, 345
disadvantages, 345
extrusion process, 344
with other materials, 349–350
pBisGMA-pTEGDMA, 347
phases, 344
PMMA, 345
pore size, 346
protein adsorption, 346
resin matrix, 347
solid-liquid phase separation, 345
solvent casting, 344
composition, 367–369
dental materials, 8–9
dissolution behaviour, 370
drawbacks, 359
drug delivery, 298–301
glass ceramic materials, 358
glass structure, 37–40
HCA, 36
intrabony defects, 343
maxillofacial area, 343
mechanism, 36, 361–362
methods, 366
morphology, 369–370
natural organic substance, 372–376
ophthalmology, 9–11
orbital floor repair, 10
osteoblast cells, 37
osteoconductive and angiogenic, 358
particle size and surface area, 372
pH, 368, 370–372
physical chemical properties, 294–297
physiological properties, 344
polymer composites, 293, 345
precautions, 358
properties
cerium, 364
copper, 364
silver, 365–366
strontium, 366
zinc, 363–364
S53P4, 343
shaping and flexibility, 344
silica-rich layer, 37
silicate-based materials, 358
Si–OH groups, 37
stages, interfacial reactions, 36
types, 374–375
borate, 363
phosphate, 362–363
silicate, 362
wound healing, 18–25
Bioactive metallic ions, 233
Bioceramics, 2, 3, 66, 229, 290, 291
Bioceramics of $CaPO_4$
biological properties and in vivo behavior
bioactivity, 167–170
biodegradation, 165–166
cellular response, 170–172
interactions with tissues and host, 161, 162
osteoinduction, 163–164
biomedical applications, 147–160
$CaPO_4$ deposits (coatings, films and layers), 156–158
functionally graded bioceramics, 158–160
self-setting (self-hardening) formulations, 155–156
chemical composition and preparation, 128–130
electric/dielectric and piezoelectric properties, 138–139
forming and shaping, 130–132
history, 128–135
in tissue engineering, 143–144, 172–180
scaffolds and their properties, 173–177
mechanical properties, 135–138
non-biomedical applications, 172
porosity, 140–147
possible transparency, 139–140
registered commercial trademarks, 148–154
scaffolds, 177–179
sintering and firing, 132–135
Biocompatibility, 290, 293, 295
Biodegradable polylactic acid, 413–414
Biofilm, 421–422
Bioglass® 45S5, 2
Biological functionalization, 52–54
Biological safety cabinet (BSC), 391
Biomaterials, 2, 125, 127, 128
bone filling, 302
bone substitute, 302
ceramic, 290
orthopedic implants, 302
polymeric, 290
Biomedical applications, 229
Biomimetic approach, 243
Biomimetic processing, 229
Bioresorption of CPCs, 113, 114

Biphasic calcium phosphate (BCP), 390, 399
Bisphosphonate (BP), 419
Blood-brain barrier (BBB), 443–444, 449
Bone autograft, 385
Bone healing, 11
Bone morphogenetic protein-2 (BMP-2), 74
Bone regeneration, 305, 306
BoneSource® BVF Preparation, 107–109
Borate bioactive glasses, 38–40
Bovine aortic endothelial cells (BAECs), 15
Brain tumors, 448
Brain-derived neurotrophic factor (BDNF), 445
Brushite cements, 98
Buffer solutions, 418

C
C2C12 cell dose, 387
Calcium orthophosphates, 126
Calcium phosphate, 232–233, 414–416
Calcium phosphate cements (CPCs), 105–109, 116–118
  advantages and disadvantages, 115–116
  apatite, 97
  applications, 119
  bone cements, 92
  bone substitute, 92
  brushite, 98
  β-Tricalcium phosphate, 93
  cohesion, 104
  cohesion time, 103
  compounds, 93
  DCPA, 93
  DCPD, 93
  dental cement, 92
  effect of process parameters, 114, 115
  FDA, 92
  formulations, 95
  Gillmore apparatus, 101–103
  hydroxyapatite (HA), 92
  implantation, 103
  medical applications (*see* Medical applications, CPCs)
  mixing, 118
  paste, 103
  properties, 94–95
  protocol (*see* Cement preparation protocol)
  quantitative tests, 103
  setting process, 95–96
  Setting Process Phases, 104–105
  Setting Time, 99–103
  solubility, CPs, 94
  Static disintegration test, 104
  structure, 118
  synthetic hydroxyapatite (HA), 92
  Tetracalcium phosphate (TTCP), 93
  Vicat apparatus, 101
  Vicat needle, 100
  washed-out sediment, 103
Calcium phosphate ceramics (CPC), 6
Calcium sulphate dihydrate (CSD), 400
Cancer treatment, 306
CaO-rich bioactive glass (BGCa/Mix), 7
Carboxymethyl cellulose (CMC), 438
Catheter-related bloodstream infections (CRBSIs), 421
Cell encapsulation
  agarose, 440
  applications, 441
  cancer therapy, 448–451
  diabetes, 441–443
  human collagen proteins, 439
  macrocapsules, 431
  Mendelian disorders, 440
  microcapsules, 431
  natural polymers
    alginates, 435–437
    cellulose, 438
    chitosan, 437–438
    materials, 436
  neurological sensory disorders, 443–448
  synthetic polymers, 433–435
  Xanthan, 439
Cell immobilization, 430–432
Cell microencapsulation technology, 426–427
Cement preparation protocol
  bioresorption, 113, 114
  BoneSource® BVF Preparation, 107–109
  HydroSet preparation, 106, 108
  injectability, 109–111
  mechanical properties, 112–113
  mixing process, 105
  porosity, 111–112
Ceramics, 127
  bioactive glass, 339
  fabrication, 348
  materials, 127
  technology, 228
Cerium (Ce), 364
Chinese hamster ovary (CHO) cells, 74
Chitosan, 437–438
Chorioallantoic membrane (CAM), 16
Choroid plexus, 445
Chromaffin cells, 445
Chronic neurodegenerative disease, 445
ChronOS™ Inject Bone Void Filler, 105
Ciliary neurotrophic factor (CNTF), 447
Cobalt, 49–50

Cohesion time (CT), 103
Commercial apatite CPCs, 97
Commercial brushite CPCs, 98
Commercial CPCs, 116
Conjunctival or corneal epithelium, 11
Controlled release
  drug delivery, 288
  injections, 289
  phosphate-buffered saline, 306
  pills, 289
  specificity, 290
  zero-order, 288
Copper (Cu), 47, 48, 364
Coral exoskeletons, 246, 247
CP ceramics, 113
CPCs. *See* Calcium phosphate cements (CPCs)
CpG and polyinosinic-polycytidylic acid, 235
Craniectomy, 338
Craniofacial implant material, 343
Cranioplasty, 338
  advantages, 339
  craniofacial bone substitute, 339
  craniofacial implant material, 339, 343
  disadvantages, 339
  evolution, 339–341
  functionalities, 338
  graft material, 339
  history, 339, 340
  infection, 338
  mechanical properties, 342–343
  origin, 341–342
  procedure, 338
  reconstruction, 338
  shape, 341–342
  size, 341–342
Craniotomy, 338
Cu-doped microfibers, 23
Cytocompatibility, 7

D
Dendritic cells, 235
Dental
  compositions, 317
  glass-ceramics, 316
  mechanical properties, 318
  survival rates, 324–325
Diabetes mellitus, 441–443
Diatoms, 245
Dichlorophenyl sulfone, 434
1,2-Dimyristoyl-sn-glycero-3-phosphate (DMPA), 241
1,2-Dimyristoyl-sn-glycero-3-phosphocholine (DMPC), 241
Drug delivery, 290–293
  and bioactive molecules, 288
  bond rearrangement, 290
  concentration, 288
  definition, 289
  degradation rate, 288
  materials
    bioactive glass, 293
    ceramics, 290, 291
    polymers, 291–292
  mechanisms, 289
  nonresponsive mechanisms, 289
  pharmaceutical science, 287
  therapeutic window, 289
Drug delivery systems
  ability and efficacy, 239
  amphipathic molecule bearing, 241
  aspirin, 238
  biomaterials, 230
  biomedical systems, 239
  biomimetic approach, 237
  blood plasma, 230
  bone regeneration systems, 240
  bone stimulatory drug, 248–249
  β-Tri-Calcium Phosphate, 250
  calcium phosphate, 248
  cancer chemotherapy, 236
  cancer treatment, 236
  controlled mineralisation technology, 236
  coral exoskeletons, 246–247
  coral sources and purity, 247
  gentamicin against MRSA, 249–250
  heparin/$CaCO_3$/calcium phosphate, 237
  hyaluronic acid, 237
  immunocompetent murine model, 237
  indomethacin, 241
  interwoven cellular and molecular ecosystem, 230
  liposome encapsulation, 240
  liposomes, 240
  marine invertebrates, 231
  metallic ions, 239
  methazolamide, 238
  morphology, 236
  MTT assay, 237
  nanocoatings, 239
  nano-HAp, 240
  nanostructured materials, 239
  nucleation process, 240
  polymeric macromolecules/non-ionic surfactant, 240
  porous silica-calcium phosphate nanocomposites, 237
  properties, 231–232

scaffold-based tissue engineering, 230
siRNA and pDNA, 240
spherical nanoparticles, 236
thioredoxin 1 (TrxA), 238
tissue-promoting proteins, 231
Drug delivery, mesoporous bioactive glasses
consequences, 278
drug release pattern, 278
extracorporeal physical stimuli, 279
ionic dissolution products, 275, 276
local delivery, 272
local drug delivery and tissue engineering, 273–274
molecule release, 277–278
nanodelivery systems, 279
organoalkoxysilane molecules, 279
properties, 278
scaffolds, 273
systemic delivery, 272
Drug release kinetics, 419

E
Edmonton protocols, 441
E-glass fibre bundles, 346
Electrochemical impedance spectroscopy (EIS), 74
Electro-spinning technique, 18
Enamel matrix protein derivative (EMD), 349
Endostatin, 450
Enzyme-linked immunosorbent assay (ELISA), 15
Extracellular matrices (ECM), 12, 420

F
Fibroblast growth factor (FGF), 13
Fibronectin, 53, 54
Flame synthesis method, 360
Fluorcanasite ($Ca_5Na_4K_2Si_{12}O_{30}F_4$), 328, 329
Fluoride ions, 43
Fluorrichterite glass-ceramics, 325–328
Fourier transform infrared spectroscopy (FTIR), 68
Functionally gradient materials (FGMs), 158

G
Gelatin-coated bioactive glass, 300
Gene delivery, 234–235
Gentamicin, 249–250, 308
Glass-ceramic
CAD/CAM dental restorations, 315
dental materials, 313
dental technicians, 314
lost-wax casting, 314
management fields, 314
optical properties, 316
polycrystalline materials, 314
research, 316
residual glassy phase, 315
restoration, 314
stages, 314
viscous liquid, 315
Glial cell-derived neurotrophic factor (GDNF), 445
Glial tumors, 448
Good Laboratory Practices (GLP), 403
Gram-negative organisms, 358
Gram-positive organisms, 358
Guided tissue regeneration (GTR), 347

H
Hamster islets, 443
Hank's balanced salt solution (HBSS), 16
HEK293 cells, 444
Hematoxylin, 407
High-performance liquid chromatography (HPLC), 71
Host tissue interface, 2
Hot isostatic pressing, 228
Hot pressing (HP), 228
Human fetal osteoblastic cells (hFOB), 25
Human microvascular endothelial cells (HMVEC), 15
Human retinal pigment epithelial (hRPE) cells, 445
Human umbilical vein endothelial cells (HUVECs), 16
Humanitarian device exemption (HDE), 385
Huntington's disease, 447
Hydrothermal conversion method, 251
Hydroxyapatite (HAp), 7, 66, 229
advantages, 75
bioactive glasses, 341
B-n-HAp ceramics, 76
bone substitutes/fillers, 80–86
bone tissue, 74
cell adhesion and proliferation, 76
ceramics, 75
drug delivery, 77–79
implants, 77–82
minerals, 348
P_2O_5-base bioactive glass, 348
XRD spectrum, 74, 75
Hydroxyapatite/bioactive glass scaffolds, 4
Hydroxycarbonate apatite (HCA), 36, 37

hydroxyethyl methylacrylate-methyl methacrylate (HEMA-MMA), 434
Hypoxia-inducible factor (HIF), 23
Hypoxia-inducible factor-1 (HIF-1), 49

I
Ibuprofen, 308
Implant-related osteomyelitis (IRO), 71
Inductively coupled plasma mass spectroscopy (ICP), 248
Injectability, CPCs, 109–111
Injectable biomedical glasses, 13
International Union of Pure and Applied Chemistry (IUPAC), 421
International Xenotransplantation Association, 442
Ion-doped bioactive silicate glasses
  acidic or basic catalysts, 42
  cobalt-doped, 49–50
  copper-doped, 47–48
  fluor-doped, 42–43
  gelation process, 42
  magnesium-doped, 43–45
  melt-quenching and sol-gel processes, 40, 41
  metallic dopants, 40
  silver-doped, 46–47
  strontium-doped, 45–46
  trace elements, 40
  zinc-doped, 48–49

L
Layer-by-layer technique, 435
Leucite glass-ceramics, 319, 320
Lipofectamine 2000 method, 235
Liposomes, 449
Liposomes and micelles, 449, 450
Lithium disilicate (LS2), 320–322
Lithium zirconium silicate glass-ceramic, 324
Lithography, 145
Living cell technologies (LCT), 442

M
Macrocapsules, 431
Macroporosity, 3
Magnesium, 43
Marine exoskeletons, 251
Marine material
  aquatic organisms, 241
  biomimetic approach, 243
  bone morphogenesis, 242
  coralline apatites and coral skeletons, 242
  proteins and biopolymers, 242
  synthetic implants, devices and prosthetics, 243–246
  transformative self-assembly and non-equilibrium chemistry, 242
Marine structures, 415–417
Matrix metallic proteinase (MMP) inhibition, 13
Mechanical properties
  bone, 341
  cranial bone, 342–343
  substitute, 339
Mechanism of formation of mesoporous silica
  complex structures, 264
  development of uniform mesopores, 265
  honeycomb-like porous structure, 264
  monodispersed mesoporous silica spheres, 266
  particles, 264
  SEM images, 267
  tetramethylorthosilicate (TMOS), 265
  TMOS, 266
  transmission electron micrograph (TEM) image, 265
  wrinkled particles, 266, 267
Medical applications, CPCs
  craniofacial, 117
  delivery of drugs, 118
  dental, 117
  osteoporotic, 118
  vertebral fractures, 116
Medtronic's INFUSE® implant, 387
Melt-quenching method, 41, 359
Mendelian disorders, 440
Mesenchymal stem cells (MSCs), 44, 71, 235
Mesoporous bioactive glass (MBG), 26, 46, 50–52, 260, 264–266, 272–280, 299
  bioactive material, 268
  bioactivity, 268, 271–272
  biomedical field, 280
  delivery of therapeutics, 280
  drug delivery (*see* Drug delivery, mesoporous bioactive glasses)
  fixation, 258
  gel glasses, 269
  in vitro and in vivo drug-delivery properties, 280
  IUPAC definition, 259
  lifetime special care, 258
  materials, 259
  MCM-41, 259
  orthopedic prostheses, 258
  research activity, 259

S46P0 and bone interface, 270
SEM/EDX outcomes, 269
silica (*see* Mechanism of Formation of Mesoporous Silica)
structure, MCM-41, 261
structure, MCM-48, 261
synthesis (*see* Synthesis of mesoporous glasses)
Methicillin-resistant *Staphylococcus aureus* (MRSA), 71, 249–250, 368
Mica-based glass-ceramics, 316
Micro CT parameters, 398
Micro CT reconstructions, 397
Microcapsules, 427–431
Microcarriers, 427–431
Microwave-based approach, 361
Minimum effective concentration (MEC), 288
Minimum toxic concentration (MTC), 288
Mitogen-activated protein kinase (MAPK), 16
Multifunctional drug delivery systems, 308
Multiphasic carriers, 401
Multiphasic release carriers, 395
Multiphasic release system, 395–400, 402
ACS
histological analysis, 398
impaired hind limb mobility, 400
micro CT analysis, 396–398
mouse muscle pouch assay, 395
sample preparation, 395–396
statistical analysis, 399–400
surgery, 396
BMP release, 392–393
device design, 390
histology, 402–403
microCT analysis
adjusted bone volume, 402
total volume, 402
P407 gel, 392
rhBMP-2, 390

N
Nanoceramics, 229
Nanocomposite, 229, 230
Nanodrug delivery systems, 234
Nanogels, 230
Nano-hydroxyapatite (nano-HAp) systems, 230
Nanosized bioactive glass (nBG), 23
Nanostructured material, 228
Natural hydroxyapatite, 232
Natural-born lithographers, 245
Nerve growth factor (NGF), 445
Neurological sensory disorders
direct infusion techniques, 444
GDNF, 445
Huntington's disease, 445
neurodegenerative diseases, 446
neurotrophins, 443
NGF, 445

O
Ophthalmology, 9, 10
Organic–inorganic hybrid materials, 27
Orthopedics
biomaterials and manufacturing techniques, 66
natural bone matrix, 66
Ossification of the posterior longitudinal ligament (OPLL), 83
Osteoconductive materials, 362
Osteoinduction, 163–166
Osteoporosis, 305, 306
Osteoproductive materials, 362
OsteoScaff™, 389

P
Parkinson's disease, 445
Pharmacokinetics, 298
Pheochromocytoma cell line, 445
Phosphate bioactive glasses, 40
Phosphate-buffered saline (PBS), 300
Phosphate-buffered solution (PBS), 20
PLA/HAp composite
biomaterials, 412, 413
ceramic biomaterials, 412
clinical complications, 412
combinations, 413
crystalline nanocoatings, 413
drug delivery systems, 416–419
implant-tissue infections, 412
polymeric biomaterials, 412
Plasmid DNA (pDNA), 234, 240
Platelet-rich plasma (PRP), 349
Poloxamer P407 (P407), 390, 393
Poly lactide-co-glycolide (PLGA), 388
Poly(diallyldimethylammonium chloride), 438
poly(hydroxyl ethyl methacrylate (PHEMA), 434
Poly(vinyl alcohol) (PVA), 433
Polyacrylates, 434
Polycation poly(L-lysine) (PLL), 428
Polyethylene glycol (PEG), 241
Polyglycolic acid (PGA), 68
Poly-L-lactic acid, 301

Polymer composites, 293
Polymeric macromolecules, 233
Polymers, 291, 292
Polymethyl methacrylate (PMMA), 339
Polypropylene, 434
Polysaccharides, 435
Polysaccharides or polyethylene glycol (PEG), 433
Polyvinylpyrrolidone (PVP), 434
Porosity, 140, 142, 145–147
Porosity, CPCs, 111–112
Porous bioceramics, 145
Porous stoichiometric hydroxyapatite, 53
Post hoc test, TV and aBV, 401
Protamine sulphate, 235
Protein delivery, 235–236
Prothrombin time (PT), 20

R
Recombinant human BMP (rhBMP)
  ACS, 386–388
  first generation, 385–386
Restorative dental glass-ceramics (RDGCs), 316
Retinitis pigmentosa, 447
rhBMP-2
  autogenous bone, 406
  BMP, 393
  bone grafts, 384
  CSD and BCP granules, 407, 408
  design, 391
  GLP efficacy, 408
  lyophilization, 408
  materials, 391
  multiphasic delivery system, 406
  osteoblasts, 406
  URIST, 408
Ridge augmentation group, 404, 405

S
45S5 Bioglass®, 4, 26
S53P4 glass, 9
Scanning electron microscopy (SEM), 66, 68
Self-assembly mechanism, 229
Setting Time, CPCs, 99–103
58S glass (SGBG-58S), 21
Silanization, 50–52
Silicate glasses, 38
Silver (Ag), 46–47, 365–366
Simulated body fluid (SBF), 36, 169
Simvastatin, 248–249
Small interfering ribonucleic acid (siRNA), 234
Small interfering RNA (siRNA), 240
Socket preservation group, 403, 405
Sodium cellulose sulfate (NaCS), 438
Sol-gel method, 41, 42, 360
Sol-gel processing, 228, 244
Solvent casting/particulate leaching (SCPL), 344
Stem cells, 419–420
Strontium (Sr), 45, 366
Superoxide dismutase-1 (SOD-1) mutant, 447
Sustained Release, 288, 295, 298, 300, 302, 308
Sustained release carriers, 388–390
Synthesis of mesoporous glasses
  bioactive, 264
  $CaO\text{-}SiO_2\text{-}P_2O_5$, 264
  evaporation-induced self-assembly (EISA) process, 262
  formation of MCM41, 261
  liquid crystal templating mechanism, 260
  M41S materials, 262
  MCM-41 structure, 260
  MCM-48 structure, 261
  polycondensation reactions, 260
  Santa Barbara Amorphous (SBA)-type materials, 262
  silica nanoparticles, 262
  silicatic framework, 260
  sol–gel process, 260
  surfactant/TEOS, 264
Synthetic apatites, 232
Synthetic materials, 338, 340

T
3-D Porous Scaffolds
  angiogenic and osteoinductive molecules, 6
  bioceramic and bioactive glass, 5
  biopolymers, 7
  cell viability and ALP activity, 7
  ceramic/polymer composite scaffolds, 4, 5
  drug release mechanisms, 8
  efficient delivery system, 6
  IDMC, 7
  inorganic bioactive particles, 7
  Korsmeyer–Peppas, Higuchi and Hixon–Crowell models, 8
  materials, 4
  microporosity and nanotopography, 6
  osteoconduction, 6
  osteoinduction, 5, 6
  osteointegration, 6

PCL-based scaffolds, 7
polymers, 7
SEM images, 5
synthetic bioresorbable polyesters, 4
3D printing methods, 243
3-D scaffolds, 3
Tissue engineering, 3
Tissue/implant interface interactions, 229
Tissue-implant interactions, 244
Titanium (Ti)-based Küntscher nails (K-nails), 80
Total hip arthroplasty (THA), 80
Transforming growth factor beta-1 (TGF-β1), 235
β-Tri-Calcium Phosphate, 250
Tri-calcium phosphates (TCP), 248
Turku Clinical Biomaterials Centre, 347
Two-step sintering (TSS), 135
Type I diabetes (TID), 441

U
Unidirectional porous hydroxyapatite (UDPHAp), 83
URIST efficacy
aims and objectives, 403
bone cores, 406
experimental design, 403–404
GLP study, 406
Jaw measurements, 404–405
socket preservation, 404
US food and drug administration (FDA), 359

V
Vascular endothelial growth factor (VEGF), 13

W
Wet chemical processing techniques, 228
Wound healing
3Cu–BG microfibers, 25
bioactive glasses, 18
cell proliferation, 21
Chinese herbal medicine, 21
connexin 43 (C×43), 22
cottony fibrous bioactive borate glass, 19
electro-spinning technique, 18
G/C-xBG, 20
HE staining, 24
HUVECs, 22
hydroxyapatite conversion and cell-glass interactions, 21
KDR protein expression, 23
keratinocyte/fibroblast proliferation, 22
SGBG – 58S, 21
VEGF and bFGF, 23

X
Xanthan, 439
Xenograft tumour model, 234
Xenografts, 338
Xerogel, 42
X-ray diffraction (XRD), 66
X-ray photoelectron spectroscopy, 236

Y
Yunnan Baiyao ointments, 21

Z
Zinc (Zn), 48–49, 250, 363–364
Zirconia (ZrO_2), 412